ACR Announcements

AMERICAN COLLEGE OF RHEUMATOLOGY
2200 Lake Boulevard NE, Atlanta, Georgia 30319-5312
www.rheumatology.org

ACR 2021 State-of-the-Art Clinical Symposium

Join your rheumatology colleagues in this year's State-of-the-Art Clinical Symposium (SOTA) being held virtually on April 9–11. During SOTA weekend, the SOTA speakers and moderators will deliver exceptional scientific content in areas ranging from therapeutic developments, recent research findings, and scientific advances, in an environment conducive to dialogue and networking. Register for early-bird rates by March 31; register for standard rates after March 31. Visit www.rheumatology.org/Learning-Center/Educational-Activities to learn more and register.

ACR 2021 Pediatric Rheumatology Symposium

Join your pediatric colleagues from across the country in this year's Pediatric Rheumatology Symposium (PRSYM) being held virtually May 19–22. This unique symposium will provide you with the most up-to-date, practical clinical information and basic science knowledge on the diagnosis and management of pediatric patients with rheumatic diseases and immune disorders. Visit www.rheumatology.org/Learning-Center/Educational-Activities to learn more and register.

Nominations for ACR Awards of Distinction and Masters Due May 17

The ACR has many Awards of Distinction, including the Presidential Gold Medal. Members who wish to nominate a colleague or mentor for an Award of Distinction must complete the online form at www.rheumatology.org by May 17, 2021. The nomination process includes a letter of nomination, 2 additional letters of recommendation, and a copy of the nominee's curriculum vitae. Recognition as a Master of the American College of Rheumatology is one of the highest honors the ACR bestows. The designation of Master is conferred on ACR members age 65 or older who have made outstanding contributions to the field of rheumatology through scholarly achievements and/or service to their patients, students, and the profession. To nominate someone for a Master designation, members must complete the online nomination form at www.rheumatology.org and include a letter of nomination, 2 supporting letters from voting members of the ACR, and the nominee's curriculum vitae. Nominees for ACR Master must have reached the age of 65 before October 1, 2021.

ACR Invites Nominations for Volunteer Positions

The ACR encourages all members to participate in forming policy and conducting activities by assuming positions of leadership in the organization. Positions are available in all areas of the work of the American College of Rheumatology and the Rheumatology Research Foundation. Please visit www.rheumatology.org for information about nominating yourself or a colleague for a volunteer position with the College. The deadline for volunteer nominations is May 17, 2021. Letters of recommendation are not required but are preferred.

Arthritis & Rheumatology

An Official Journal of the American College of Rheumatology
www.arthritisrheum.org and wileyonlinelibrary.com

Cover design: Todd Machen

This journal is printed on acid-free paper.

Arthritis & Rheumatology

An Official Journal of the American College of Rheumatology
www.arthritisrheum.org and wileyonlinelibrary.com

VOLUME 73 • April 2021 • NO. 4

Cover image: The figure on the cover depicts SARS–CoV-2 infection inducing both innate and adaptive immune activation that leads to the hallmark clinical features of multisystem inflammatory syndrome in children (MIS-C), including fever, conjunctival injection, rash, gastrointestinal symptoms, cardiac dysfunction, coronary artery aneurysms, and endothelial activation. This issue of *Arthritis & Rheumatology* includes version 2 of the American College of Rheumatology's MIS-C and COVID-19–Related Hyperinflammation Task Force guidance on the management of MIS-C associated with SARS–CoV-2 and hyperinflammation in COVID-19 (Henderson et al, pages e13–e29). The image was created by Jacqueline V. Behrens with input from the Task Force.

In this Issue

Highlights from this issue of *A&R* | By Lara C. Pullen, PhD

Multimorbidity in Antineutrophil Cytoplasmic Antibody–Associated Vasculitis

Rheumatologists consider antineutrophil cytoplasmic antibody–associated vasculitis (AAV) to be a chronic, relapsing condition. For many chronic diseases such as cardiovascular disease or chronic kidney disease, multimorbidity is the rule rather than the exception. In this issue, Sarica et al (p. 651) report the results of the first study to describe longitudinal trends in the incidence of multimorbidity in AAV patients and calculate the health care expenditure attributable to multimorbidity. The researchers observed that the highest proportional risk in AAV patients was for osteoporosis. Their analysis of a large national cohort from Scotland reinforces the importance of holistic care in patients with AAV.

p. 651

The study included 543 patients with AAV and 2,672 matched general population controls, whom the investigators followed for a median of 5.1 years. Eligible patients with AAV were diagnosed between 1997 and 2017, and the researchers retrieved linked morbidity and health care expenditure data from a UK national hospitalization repository and from published national cost data. They defined multimorbidity as the development of ≥2 disorders. The team analyzed prespecified morbidities, individually and together, for risks and associations over time using modified Poisson regression, discrete interval analysis, and chi-square test for trend.

After 1 year, 23.0% of AAV patients and 9.3% of controls had developed multimorbidity, and after 10 years, 37.0% of AAV patients and 17.3% of controls had developed multimorbidity. The researchers thus found that while AAV patients were more likely to develop individual morbidities at all time points, multimorbidity was most often diagnosed <2 years after diagnosis of AAV. They concluded from this that these initial 2 years might represent a critical opportunity for early screening of patients with AAV. Multimorbidity in AAV patients was associated with disproportionate increases in health care expenditures, with those expenditures highest for AAV patients with ≥3 morbidities. In comparison to AAV patients with no morbidities, the development of multimorbidity in AAV patients was associated with a 2–4-fold increase in total health care expenditure, with a 3–5-fold increase in inpatient health care expenditure.

Dual-Energy Computed Tomography Ineffective at Identifying Early Calcium Crystal Deposition

Although rheumatologists are now beginning to use dual-energy computed tomography (DECT) to detect calcium pyrophosphate deposition (CPPD), a question remains as to whether early calcium crystal deposition alters DECT attenuation characteristics in menisci and articular cartilage prior to the appearance of detectable chondrocalcinosis by conventional CT. In this issue, Budzik et al (p. 687) describe their efforts to assess the ability of DECT to identify this early calcium crystal deposition. They report that, while DECT has the potential to characterize knee intraarticular mineralization, it cannot yet accurately identify early calcium crystal deposition that is not visible as chondrocalcinosis on conventional CT.

p. 687

The investigators found that in both menisci and articular cartilage, and for all 5 DECT attenuation parameters, calcified regions of interest (ROIs) in CPPD patients showed significantly higher values than those in controls. Conversely, noncalcified ROIs in CPPD patients were comparable to those in controls. Ultimately, while specific DECT parameters yielded good accuracy in differentiating calcified ROIs in CPPD patients from those in controls, DECT failed to distinguish between noncalcified ROIs in CPPD patients and controls. The authors concluded that the main potential clinical utility of DECT in calcium crystal–associated rheumatic and musculoskeletal diseases is in characterizing larger/higher-concentration crystal aggregates, rather than in lowering the detection limit for early/lower-concentration calcium crystal deposition not visible with conventional CT.

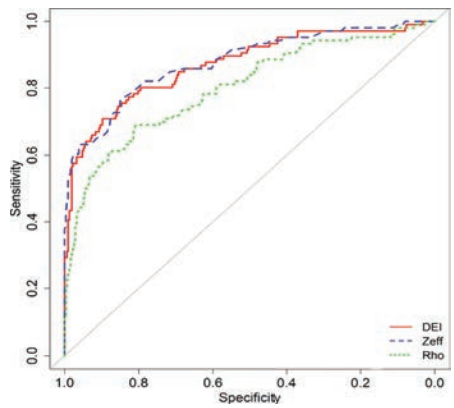

Figure 1. Receiver operating characteristic curves showing the diagnostic accuracy of dual-energy index (DEI), effective atomic number (Z_{eff}), and electron density (rho) in differentiating calcified meniscal ROIs in patients with CPPD from ROIs in controls. DEI and Z_{eff} both outperformed rho and exhibited comparable diagnostic performances.

Sustained Remission of Granulomatosis with Polyangiitis

Rheumatologists seek sustained remission off-therapy (SROT) for their patients with granulomatosis with polyangiitis (GPA), and many see it as an indicator of a potential "cure" or its first surrogate marker. In this issue, Puéchal et al (p. 641) report that after conventional therapies, only 7% of GPA patients had reached SROT at 10 years postdiagnosis. While the investigators were unable to find any baseline vasculitis characteristics that distinguished patients who achieved/maintained SROT from those who experienced disease relapse and/or continued to receive glucocorticoids (GCs) or immunosuppressant therapy, they did find that patients with SROT had received more intensive induction therapy and rituximab maintenance therapy more frequently than those who did not achieve SROT.

p. 641

The researchers evaluated 795 patients with GPA. At 3 years postdiagnosis, they compared 92 GPA patients with SROT to 342 control subjects who had experienced disease relapse and/or were still receiving GCs or immunosuppressants. Although they found no baseline differences between the 2 populations, patients with SROT had more frequently received intravenous cyclophosphamide as induction therapy compared to controls and had a higher median number of infusions. When the researchers examined the patients at 5 years postdiagnosis, they again saw no baseline differences between groups but found that patients with SROT at 5 years postdiagnosis had received more cyclophosphamide infusions compared to controls. In addition, more patients with SROT had received rituximab maintenance therapy than controls at 3 years and 5 years postdiagnosis. While 20% of patients had reached SROT at 3 years, this number decreased to 7% (of the 74 patients with 10-year follow-up data) at 10 years postdiagnosis.

Journal Club

A monthly feature designed to facilitate discussion on research methods in rheumatology.

In Utero and Early Life Exposure to the Great Chinese Famine and Risk of Rheumatoid Arthritis in Adulthood

VanEvery et al. *Arthritis Rheumatol.* 2021;87:596–603

In utero and early life adversity—including famine, natural disasters, and war—have previously been associated with increased risk of chronic diseases that involve systemic inflammation, such as cardiovascular disease and type 2 diabetes mellitus. However, little is known about the long-term impact of these stressors on autoimmunity, or specifically on rheumatoid arthritis (RA) risk. As climate change, war, and global pandemics continue to cause food insecurity and early life malnutrition, it is important to understand the long-term effects of early life famine and adversity exposure.

VanEvery and colleagues used a cohort of ~100,000 participants from the ongoing Kailuan Study, including those born before, during, and after the Great Chinese Famine of 1959–1961, to examine whether in utero or early childhood exposure to famine was associated with an increased risk of RA in adulthood. This analysis consisted of logistic regression with adjustment for confounders (sex, C-reactive protein, metabolic characteristics, alcohol consumption, smoking behavior, hypertension, and diabetes), which was used to calculate the odds ratio and 95% confidence interval of RA, according to famine exposure status (exposed in utero, exposed between ages 0 and 3 years, exposed between ages 3 and 6 years, or exposed at age 6 years or older), compared to participants born after 1961 (i.e., not exposed to famine).

Questions

1. **Why is it difficult (ethically, logistically, statistically) to study the impact of early life/in utero adverse events on later life health outcomes in humans?**
2. **The current study used a natural experiment design. Could an experimental design, e.g., a randomized clinical trial, be used to investigate the impact of early life adversity?**
3. **What is currently known about early life exposures and RA risk?**
4. **Do you think other adverse events in early life (neglect or abuse) would have a similar, smaller, or larger impact on RA risk in adulthood?**
5. **Why do you think the impact of famine exposure on RA risk is larger in the first 3 years of life than it is in older age?**

Clinical Connections

Interleukin-7/Interferon Axis Drives T Cell and Salivary Gland Epithelial Cell Interactions in Sjögren's Syndrome

Rivière et al, *Arthritis Rheumatol* 2021;87:631–641

CORRESPONDENCE
Gaetane Nocturne, MD, PhD: gaetane.nocturne@aphp.fr

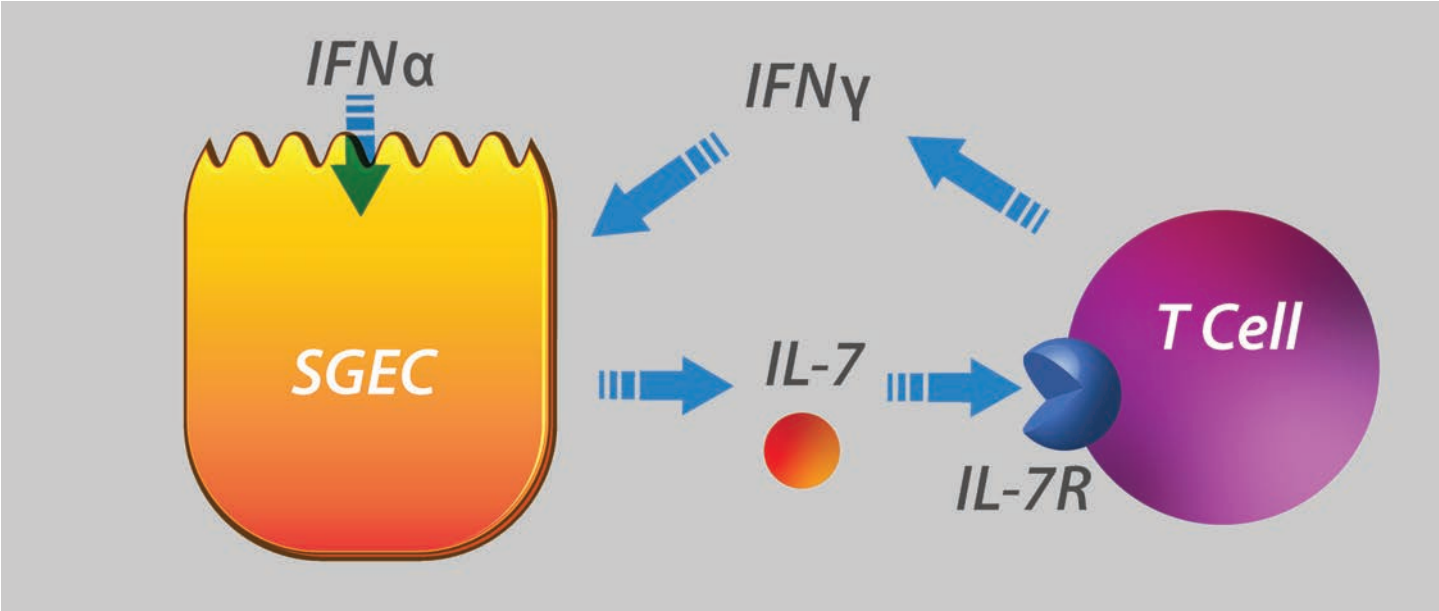

SUMMARY

Primary Sjögren's syndrome (SS) is a systemic autoimmune disease characterized by an infiltration of exocrine glands, notably salivary and lachrymal glands leading to dryness. In addition, patients suffer from fatigue and pain in one-third of the cases of systemic involvement. An interferon (IFN) signature involving type I and type II IFNs is detected in the majority of patients. Several lines of evidence support the pathogenic role of salivary gland epithelial cells (SGECs) in primary SS; these cells are the target of the disease but also participate in its amplification. In their study, Rivière et al demonstrate that SGECs stimulated by IFNs are able to produce interleukin-7 (IL-7), a key cytokine for the activation of T cells. In turn, T cells produce IFNγ, which leads to a vicious circle of amplification. Interestingly, using a monoclonal antibody that targets IL-7 receptor (IL-7R) allows the IFN signature to be decreased, highlighting the potential therapeutic interest in this new pathway in primary SS.

KEY POINTS

- SGECs stimulated by IFN are able to produce IL-7 that in turn activate T cell lymphocytes.
- SGECs promote a pathogenic IFN/IL-7 amplification loop in primary SS.
- Targeting the IL-7 pathway with a monoclonal anti–IL-7R reduces IFN signatures and may be a promising therapeutic approach in primary SS.

Large-Scale Characterization of Systemic Sclerosis Serum Protein Profile: Comparison to Peripheral Blood Cell Transcriptome and Correlations With Skin/Lung Fibrosis

Bellocchi et al, *Arthritis Rheumatol* 2021;87:660–670

CORRESPONDENCE
Shervin Assassi, MD, MS: shervin.assassi@uth.tmc.edu

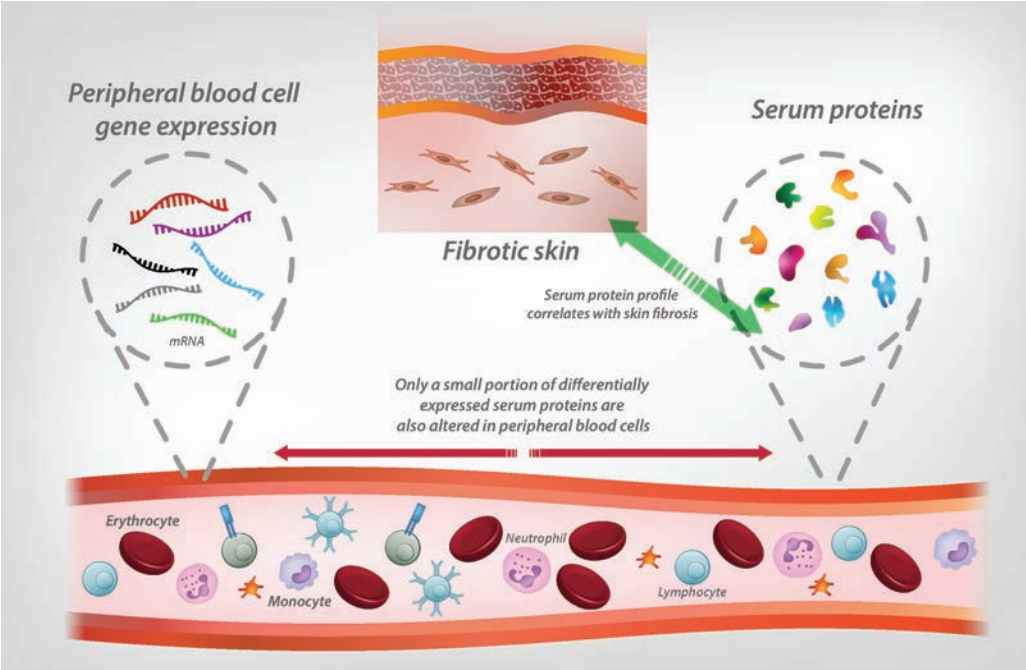

KEY POINTS

- The serum protein profile in SSc is distinct and enriched for fibrotic as well as immune cell homing pathways.
- Rather than being a mere reflection of peripheral blood cell gene expression dysregulations, serum protein profile can serve as a window to disease severity and molecular dysregulations in the diseased tissue in systemic sclerosis.

SUMMARY

Proteins are in closer proximity to disease pathogenesis than findings at the DNA or RNA level, and serum samples are more readily accessible than diseased tissue such as the skin or lungs. Bellocchi et al investigated the correlation of serum proteins with systemic sclerosis (SSc) fibrotic features.

To characterize the molecular profile of SSc, a large panel of proteins was examined in the serum of individuals with diffuse cutaneous SSc who were not receiving immunosuppressive agents. Furthermore, the serum proteins were compared to gene expression profiles of concurrently collected peripheral blood.

Compared to matched controls, individuals with SSc had a distinct serum protein profile that correlated with the extent of skin involvement and showed an enrichment for fibrotic and immune cell homing pathways.

Only a small portion (15.5%) of differentially expressed serum proteins was also differentially expressed in the concurrently collected peripheral blood gene expression profile, supporting the notion that differential expression for most serum proteins in SSc is likely to originate outside the peripheral blood cells.

Arthritis & Rheumatology
Vol. 73, No. 4, April 2021, pp 551–552
DOI 10.1002/art.41636

American College of Rheumatology
Empowering Rheumatology Professionals

IN MEMORIAM

Raphael J. DeHoratius, MD, 1942–2020

Raphael J. DeHoratius, MD passed away on November 26, 2020, at the age of 78, at home with his long-time companion, Elizabeth Grace. He is also survived by 3 daughters Nicole DeHoratius (Dieter Cohrs), Danielle DeHoratius, and Gabriel Koons, and 6 grandchildren. Ralph grew up in Philadelphia as the oldest child of Pasquale and Edith DeHoratius. He attended St. Joseph's University and then obtained his medical degree from Jefferson Medical College of Thomas Jefferson University. He completed his internal medicine training at the University of New Mexico in Albuquerque and continued in rheumatology under the tutelage of Dr. Ralph Williams. He remained at the University of New Mexico as a faculty member before serving 2 years in the Air Force in Wichita, Kansas. In 1976 he returned to Thomas Jefferson University Hospital, joining the Division of Rheumatology.

In his early career, Ralph was involved in scientific investigations of rheumatoid arthritis and systemic lupus erythematosus; along the way, he published more than 60 manuscripts. Over time he focused on patient care and teaching. In the 1970s there were not many rheumatologists involved in taking care of patients with lupus. Ralph's strong interest in lupus attracted a large practice of patients with the disease, and he established the Lupus Center at Thomas Jefferson University Hospital. He worked closely with the local chapter of the Arthritis Foundation. As well, he established a local chapter of the Lupus Foundation of America, working with Goldie and Eddie Simon, whose daughter had succumbed to lupus. This chapter became one of the most successful chapters in the country. By the late 1970s and early 1980s Ralph had established himself as one of the leading experts in the field of lupus. He was also a gifted teacher and over the years trained many rheumatology fellows, internal medicine residents, and medical students.

Ralph remained at Thomas Jefferson University Hospital until 1982, at which time he had become a Professor of Medicine. In 1982 he moved across town in Philadelphia to Hahnemann University to become Director of the Division of Clinical Immunology and Rheumatology. He remained at Hahnemann University for 10 years before returning to Thomas Jefferson. The last part of his career was spent in industry, working for Johnson & Johnson.

Over his career, Ralph was very active in the American College of Rheumatology, serving on several committees and subcommittees including the Undergraduate Education Subcommittee, Graduate Education Subcommittee, Annual Meeting Program Committee, and Annual Meeting Planning Committee. He

was also a great supporter of the ACR Research and Education Foundation (now the Rheumatology Research Foundation). His involvement with the ACR culminated in his being named the 66th President of the College in 2002.

I met Ralph in 1981 at Thomas Jefferson University, when I was second-year internal medicine resident doing an elective rotation in rheumatology. Ralph was one of the mentors who cemented my decision to pursue a rheumatology career. Our paths separated, but we kept in touch. Ralph went to Hahnemann University, and I continued with my rheumatology fellowship at Thomas Jefferson. I ran into Ralph at the ACR Annual Meeting in New Orleans in 1986, while I was looking for my first job. As luck would have it, he was looking for a new faculty member. He became my first boss and also my mentor for the early part of my career at Hahnemann. Our paths separated again in 1992 when Ralph returned to Thomas Jefferson and I moved on to Einstein Medical Center in Philadelphia. Even when we were at different institutions, Ralph continued to advise me about clinical as well as administrative issues, as I was now the head of a division. I last saw Ralph at the ACR Annual Meeting in Atlanta in 2019. He had retired, and he told me that this would be his last meeting.

Ralph DeHoratius was an outstanding clinician and physician with incredible clinical instincts. His patients followed him around the city from institution to institution for their care, many coming from great distances to see him. It was during my time working with him at Hahnemann University, seeing many lupus patients and receiving his counsel on their care, that I became an expert in lupus. His patients were devoted to him. After he left clinical practice a number of them came to me for follow-up, and we always shared a good Ralph story.

I want to relay a story about one of Ralph's patients, which I think shows the kind of physician he was. On a Friday at about noon, one of Ralph's patients was added to my schedule, as he was out of town. After reviewing her (paper) chart, I entered the room and introduced myself. This was a young woman with lupus who was being treated with moderate doses of prednisone and an immunosuppressive agent. She had a fever of 104°F, shortness of breath, and chest pain. I was concerned about pleuritis or pericarditis and of course, infection. After I introduced myself she told me that she would rather wait to see Dr. DeHoratius. I told her that he would be back on Monday. She actually thought about coming back on Monday, but I believe she was feeling so poorly that she knew this could not wait. After my evaluation, I knew she had pericarditis and called the cardiology service. When I explained to her that they were going to take her for pericardiocentesis, she asked that I stay with her during the procedure; she was frightened without Dr. DeHoratius. I watched the cardiothoracic surgeons drain about 1,000 ml of pericardial fluid.

To me, the devotion of this patient to Ralph was amazing. He had many patients in his practice who felt this way. They really loved him. Over time as my practice grew, I had many patients with similar devotion to me, which is very rewarding. Over the years, I realized that Ralph DeHoratius had taught me how to be a doctor.

Lawrence H. Brent, MD
Temple University
Philadelphia, PA

Arthritis & Rheumatology
Vol. 73, No. 4, April 2021, pp 553–565
DOI 10.1002/art.41587

American College of Rheumatology
Empowering Rheumatology Professionals

EXPERT PERSPECTIVES ON CLINICAL CHALLENGES

Expert Perspective: Immune Checkpoint Inhibitors and Rheumatologic Complications

Laura C. Cappelli and Clifton O. Bingham III

Rheumatologists increasingly receive consults for patients treated with immune checkpoint inhibitors (ICIs) for cancer. ICIs can cause inflammatory syndromes known as immune-related adverse events (IRAEs). Several rheumatic IRAEs have been reported, including inflammatory arthritis, polymyalgia rheumatica, and myositis. For patients who present with musculoskeletal symptoms while receiving ICI therapy, it is important to have an algorithm for evaluation. The differential diagnosis includes a range of musculoskeletal syndromes, such as crystalline arthritis, mechanical issues, and osteoarthritis, in addition to IRAEs. After diagnosing a rheumatic IRAE, rheumatologists must work with the patient and the oncologist to form a treatment plan. Treatment of IRAEs is guided by severity. Evidence for management is limited to observational studies. Inflammatory arthritis and polymyalgia rheumatica are treated with nonsteroidal antiinflammatory drugs in mild cases, glucocorticoids for moderate-to-severe cases, and sometimes require other disease-modifying antirheumatic drugs. Myositis due to ICIs can be accompanied by myocarditis or myasthenia gravis. Glucocorticoids and withholding the ICI are usually required to treat myositis; some patients with severe myositis require intravenous immunoglobulin or plasmapheresis. Further research is needed to optimize treatment of IRAEs that does not compromise the antitumor effect of ICIs.

Clinical challenge

You receive a consult from a local oncologist. A 65-year-old man with a history of knee osteoarthritis (OA) who had previously undergone total joint arthroplasty of the left knee and is being treated with nivolumab (anti–programmed death 1 [anti–PD-1] monoclonal antibody) for non–small cell lung cancer has new symptoms of severe aching in his arms and legs, with limited mobility. The oncologist does not localize symptoms to the joints and/or muscles but notes that the patient is having trouble doing chores around the house such as cleaning and cooking.

Background

Cancer immunotherapy has been a substantial breakthrough for treating patients with a variety of malignancies. The most commonly used class of cancer immunotherapy, immune checkpoint inhibitors (ICIs), block immune regulatory interactions and allow for increased T cell activation and an antitumor immune response (1–3). Currently approved ICIs block CTLA-4, PD-1, or programmed death ligand 1 (PD-L1), but investigations focusing on a variety of other positive and negative regulatory targets are underway (4). ICIs are used for an ever-expanding list of tumor types. Initially, they were used only in advanced-stage cancer, but now adjuvant therapy in melanoma (5) is approved, and neoadjuvant therapy has shown efficacy for non–small cell lung cancer (6). ICIs first came to the attention of rheumatologists in the mid-2010s due to their side effect profile. ICIs can cause inflammatory adverse events, termed immune-related adverse events (IRAEs), likely due to non–tumor-specific immunologic activation. IRAEs can affect nearly any tissue type including the skin, gastrointestinal tract, nervous system, lungs, endocrine organs, and musculoskeletal structures (7). Some IRAEs, such as dermatitis and thyroid disease, are common and not life-threatening, while others, such as myocarditis, are uncommon but often fatal (8). Many IRAEs share similarities with classic autoimmune diseases, but there are key differences in clinical presentations, treatment, and long-term outcomes (9).

Dr. Cappelli's work was supported by the National Institute of Arthritis and Musculoskeletal and Skin Diseases, NIH (grant K23-AR-075872).

Laura C. Cappelli, MD, MHS, Clifton O. Bingham III, MD: Johns Hopkins School of Medicine, Baltimore, Maryland.

Drs. Cappelli and Bingham have received research support from Bristol Myers Squibb.

Address correspondence to Laura C. Cappelli, MD, MHS, 5501 Hopkins Bayview Circle, Suite 1B1, Baltimore, MD 21224. Email: lcappel1@jhmi.edu.

Submitted for publication August 25, 2020; accepted in revised form November 5, 2020.

Rheumatic IRAEs were not acknowledged as early in the history of ICIs as some other IRAEs, but are increasingly noted. IRAEs with phenotypes similar to rheumatoid arthritis (RA), spondyloarthritis, polymyalgia rheumatica (PMR), giant cell arteritis (GCA), myositis, antineutrophil cytoplasmic antibody–associated vasculitis, scleroderma, and other rheumatic diseases have been described (10). Epidemiologic data remain limited, particularly for rare IRAEs like vasculitis and scleroderma. Inflammatory arthritis, however, may occur in 3–7% of patients treated with ICIs (11,12). More than 40% of oncology patients are eligible for treatment with ICIs; thus, the number of patients who may experience rheumatic IRAEs from ICI treatment is substantial (13). Studies have yet to define risk factors for development of specific rheumatic IRAEs. IRAEs are generally more common in patients treated with combination anti–PD-1/anti–CTLA-4 blockade than those treated with monotherapies (14). Certain IRAEs, such as rash, colitis, and hypophysitis, are more common with CTLA-4 blockade, while pneumonitis and hypothyroidism are more common with PD-1 blockade (15). Rheumatic IRAEs may persist after cessation of ICI therapy, as seen in inflammatory arthritis (16). Persistence of inflammatory arthritis has been associated with combination ICI therapy regimens, longer duration of ICI therapy, and having multiple IRAEs (16).

Treatment of IRAEs is complicated by the coexistence of cancer and the goal of immunologic activation against the tumor. Physicians must balance relieving inflammation in the organ affected by the IRAE with not impairing the antitumor response to ICI. Treatment of IRAEs usually starts with glucocorticoids and may require withholding ICI therapy. On a positive note, IRAEs seem to be a positive prognostic factor for tumor response in different types of tumor (17).

The clinical scenario above highlights several issues that arise in referrals for suspected rheumatic IRAEs. Non-rheumatology providers may not be familiar with musculoskeletal and neurologic examinations or with associated symptoms that can accompany inflammatory arthritis, PMR/GCA, myositis, or other rheumatic syndromes. This issue is further complicated in the era of coronavirus disease 2019, when telemedicine makes physical examinations more difficult or impossible for certain maneuvers. Also, patients with cancer are often older adults and may have comorbidities, such as OA, that complicate the picture. As a result, rheumatologists must consider a broad differential diagnosis for patients receiving ICIs, as we will detail in the next section.

Approach

History. An important first step is to determine whether the patient's symptoms are related to ICI therapy. This is a key branch point in our evaluation algorithm (Figure 1). Establishing a temporal relationship can usually be accomplished by history and careful review of the medical record, including primary care and oncology notes. If symptoms were present before ICI therapy, the patient should be assessed for an underlying autoimmune or mechanical issue based on history and physical examination.

It is important to remember, however, that patients can have injuries and other mechanical issues unrelated to ICI therapy during their treatment. Even if the symptoms clearly started while receiving ICI therapy, physicians should consider a full differential diagnosis. There are reports of patients experiencing "activated OA," with more pain and swelling at joints previously affected by OA (11,18). Crystalline arthritis, particularly calcium pyrophosphate disease (19,20), was also reported in patients being treated with ICIs. We ask patients about all past musculoskeletal, inflammatory, and autoimmune diagnoses, with particular attention to prior injuries and surgeries, OA, and crystalline arthritis. Information on any trauma or change in physical activity preceding the symptoms should be elicited. Family history may be helpful. If there is a significant history of autoimmunity in the family, the patient may have an underlying autoimmune disease that is unmasked, or they may be more likely to develop IRAEs. The stage of the patient's cancer and how well they are responding to treatment may also suggest whether metastatic disease could be causing symptoms (21).

For patients in whom an IRAE is suspected and no alternate cause of symptoms is found, determining the type of IRAE is the next step. Pain may be present in the joints in inflammatory arthritis or PMR or in the muscles/fascia in myositis or eosinophilic fasciitis due to ICIs. Fatigue may be present in rheumatic IRAEs, but has also been seen in endocrine IRAEs and in ICI-treated patients without a defined IRAE (22). Weakness could reflect myositis but also myasthenia gravis, neuropathy, or untreated thyroid disease, all of which can occur as IRAEs.

Taking note of the ICI regimen and whether the patient has experienced nonrheumatic IRAEs can be clarifying. As mentioned above, combination CTLA-4/PD-1 blockade typically has the highest rate of IRAEs, so a high level of suspicion should be maintained in patients receiving these treatment regimens. In studies of inflammatory arthritis as an IRAE, ≥50% of patients experienced additional IRAEs (18). For patients with suspected myositis, history should also be evaluated to identify symptoms of myasthenia or myocarditis, as these IRAEs can accompany each other (23,24).

Finally, IRAEs may present after ICI therapy cessation (25). For patients who have received ICIs in the last 1–2 years, IRAEs remain part of the differential diagnosis.

Physical examination. When possible, patients should be evaluated in person so a full physical examination can be performed. Musculoskeletal and neurologic examinations are critical. If the patient has significant peripheral synovitis and/or enthesitis, dactylitis, or bursitis, then inflammatory arthritis is the most likely diagnosis. In PMR, many patients lack peripheral inflammatory arthritis, though there are more reports of peripheral arthritis in PMR associated with ICIs than in the traditional disease (18). Patients with PMR may have limited range of motion in the hips

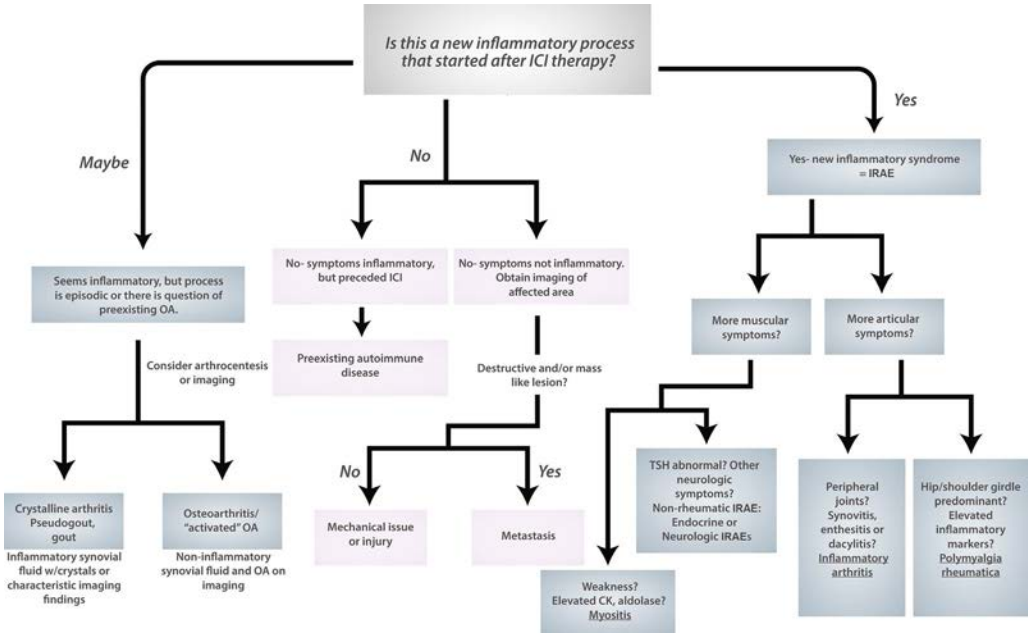

Figure 1. Approach to differential diagnosis for musculoskeletal symptoms in patients receiving immune checkpoint inhibitor (ICI) therapy for cancer. Key branch points indicate whether symptoms are temporally related to ICI therapy and whether there is a persistent inflammatory syndrome present. If a patient has a new inflammatory syndrome that has only started since beginning ICI therapy, this is an immune-related adverse event (IRAE). An in-depth history and physical examination can localize the problem to muscles and joints. From there, a diagnosis of inflammatory arthritis, polymyalgia rheumatica, or myositis can be made. Alternatively, patients may experience weakness and/or muscle pain in endocrine IRAEs, such as thyroiditis, or neurologic IRAEs, such as myasthenia gravis. Patients who do not have a new inflammatory process may have a preexisting autoimmune disease or a noninflammatory musculoskeletal condition. In patients with noninflammatory musculoskeletal conditions, imaging is important to evaluate for metastasis. Finally, there are relatively common conditions, including crystalline arthritis and osteoarthritis (OA), that may be related to ICI therapy but are not as clearly IRAEs. TSH = thyroid-stimulating hormone; CK = creatine kinase.

and shoulders, or tenderness to palpation. A strength examination of the proximal and distal muscles can help determine whether myositis is present. A neurologic examination should also evaluate for possible signs of myasthenia gravis, such as ptosis, and signs of bulbar weakness. The physician should assess for signs of myocarditis, such as tachycardia, arrhythmia, or volume overload. Noting other IRAEs, such as rashes, dry mouth, or dry eyes, can also be helpful.

Diagnostic testing. Laboratory testing may reveal an elevated erythrocyte sedimentation rate (ESR) and/or C-reactive protein (CRP) level in inflammatory arthritis, PMR, or myositis. If inflammatory markers are elevated, they can be followed up for improvement with treatment of the IRAE. In the context of myositis as an IRAE, creatine kinase levels were shown to be elevated (1,000 to >15,000 units/liter [26]). Troponin should also be checked given the overlap of myocarditis with myositis. Autoantibodies are sometimes present in rheumatic IRAEs but at much lower rates than in traditional rheumatic diseases. In a systematic review, <10% of patients with inflammatory arthritis due to ICIs were rheumatoid factor positive or anti–cyclic citrullinated peptide (anti-CCP) positive (18). Similarly, the majority of patients with myositis caused by ICIs did not have myositis-specific autoantibodies (26). There have been reports, however, of anti–striated muscle antibodies and anti–acetylcholine receptor (anti-AChR) antibodies in patients with ICI-induced myositis (27,28). If myositis or myasthenia gravis is suspected, testing for anti-AChR antibodies is reasonable.

Joint fluid aspiration in inflammatory arthritis has shown white blood cell counts >1,000 cells/ml, with a neutrophil predominance (29,30). Synovial fluid analysis can be helpful in confirming inflammatory arthritis or assessing for crystalline disease, and should be performed when possible.

Ultrasound can demonstrate objective evidence of inflammatory arthritis, including synovitis detected by Doppler signal, tenosynovitis, and enthesophytes (30). Magnetic resonance imaging (MRI) may show synovitis, tenosynovitis, bone marrow edema, and erosions (31). In PMR, ultrasound may show subdeltoid and subacromial bursitis, trochanteric bursitis, or biceps tenosynovitis (32,33). Ultrasound and MRI may also suggest other diagnoses, such as crystalline arthritis, OA, and noninflammatory musculoskeletal conditions.

If myositis is suspected, electromyography (EMG), MRI, and muscle biopsy may be used to support the diagnosis. As in traditional forms of myositis, EMGs show a myopathic pattern, which may demonstrate abnormal spontaneous activity (irritable myopathy) (26). MRI can show muscle and/or fascial

Table 1. Studies on epidemiology, evaluation, and management of rheumatic IRAEs*

Author, year (ref.)	Study population	n	Results	Comments
IA				
Braaten et al, 2020 (16)	Patients with ICI-induced IA with ≥1 follow-up visit after ICI cessation	60	Risk factors for persistent IA after ICI cessation: longer-duration ICI, combination ICI therapy; persistent IA may be associated with better tumor response; no worse tumor prognosis in patients treated with DMARDs/biologics (MTX, LEF, SSA, HCQ, TNFi)	Biased toward patients surviving long enough to have follow-up after ICI cessation and patients engaged in rheumatology care (likely more severe IA)
Kim et al, 2017 (47)	Patients with ICI-induced IA treated with TCZ	3	All patients had symptomatic improvement of IA; 1 patient had durable antitumor response while receiving TCZ for 18 months	All 3 patients had melanoma; difficult to draw conclusions regarding any effect on tumor response from only 3 patients
Subedi et al, 2020 (31)	ICI-treated patients referred for rheumatology consult for IA	8	Tenosynovitis and synovitis of wrists and hands most common; also saw bone marrow edema and erosions in 3 patients	Retrospective review; MRI may identify those with high-risk IA, larger prospective study needed
Roberts et al, 2019 (45)	Patients with ICI-induced IA treated with HCQ first-line	11	Only 1 patient needed MTX, none required biologics; 5 patients received GCs for IA or other IRAEs in addition; 7 patients had resolution of joint pain	Small sample size, but HCQ was safe and effective in this population; deserves additional study given favorable safety profile of HCQ
Buder-Bakhaya et al, 2018 (11)	Patients treated with pembrolizumab or nivolumab (with our without ipilimumab) for metastatic cutaneous malignancy	26 (arthralgia)	Arthralgia was common (13%); arthritis was present in 5–7.6%, depending on whether activated OA was counted as IA; 40% with arthritis needed GCs and 20% needed other immunosuppression	Arthralgia can be managed with NSAIDs, while those with objective evidence of IA more often needed GCs; raises question about how to classify those with known OA and synovitis using imaging, in the setting of ICI
Cappelli et al, 2018 (44)	Patients with ICI-induced IA treated with anti–PD-1/PD-L1 monotherapy or anti–PD-1/anti-CTLA-4 combination therapy	30	Combination therapy: more likely to present with knee arthritis, to have higher CRP, and to have other IRAEs; TNFi- and MTX-treated patients with prior tumor response had no tumor progression	Because this was an earlier study (less recognition of IA as an IRAE) and because all patients were referred to a rheumatologist, likely represents more severe IA (80% needed GCs); follow-up time only up to 16 months for evaluating tumor response
IA and PMR				
Ghosh et al, 2020 (18)	Patients with IA or PMR due to ICI therapy	294 (IA), 78 (PMR)	Median time to onset of arthritis 4 months; polyarthritis most common joint involvement pattern; <10% positive for RF or anti-CCP; 45% needed additional immunomodulatory therapy beyond steroids	SLR of observational studies, including case reports; incomplete data for arthritis joint patterns, serologies, and arthritis outcomes based on what was included in the primary studies; most recent SLR focused on arthritis
Belkhir et al, 2017 (75)	Patients with seropositive (RF or anti-CCP) IA or PMR after ICI therapy	4 (PMR), 6 (RA)	In patients with RA, 5 of 6 needed steroids, 3 needed DMARDs; PMR steroid dosing: prednisone 20–60 mg/day	Small case series; seropositive patients are minority in ICI-induced IA; 2 of 3 patients with pre-ICI serum already had anti-CCP
PMR				
Calabrese et al, 2019 (32)	Patients with PMR due to ICI therapy	20 (case series), 29 (SLR)	Case series and SLR; 94% received GCs (prednisone 7.5–60 mg/day); in case series, 30% of patients had normal inflammatory markers	Attempted to evaluate for EULAR/ACR classification criteria but incomplete data for many cases in the SLR; whether traditional classification criteria should be used for ICI-induced disease remains a question
Van der Geest et al, 2020 (33)	Patients with PMR due to ICI therapy	6	Imaging study, 6 with US and 5 with PET; uptake on PET in shoulders, hip joints, greater trochanters, sternoclavicular joints, and interspinous bursae	Small number of patients, but useful concept given that many oncology patients regularly have PET scans for tumor evaluation

(Continued)

Table 1. (*Cont'd*)

Author, year (ref.)	Study population	n	Results	Comments
Myositis				
Touat et al, 2018 (26)	Patients with metastatic cancer and myositis due to ICIs	10	Heterogeneity in muscle involvement: proximal pattern most common but some with ocular/bulbar/neck primarily; GCs: IV methylprednisolone 1–1,000 mg/kg used for treatment; 3 patients needed IVIG or PE	Small number of patients, but many had EMG and muscle biopsy data, which are useful in describing ICI-induced myositis
Matas-Garcia et al, 2020 (23)	Patients receiving ICI with biopsy-proven inflammatory myopathy	9	Some muscle necrosis in all 9 patients, perimysial/perivascular inflammatory infiltrate more common than endomysial inflammatory infiltrate; IV prednisone 0.5–2,000 mg/kg/day, with 5 needing IVIG	Small number of patients, but helpful data on biopsy characteristics, treatments, and outcomes in biopsy-proven myositis
>1 IRAE (epidemiology, cancer outcomes)				
Richter et al, 2019 (76)	Retrospective single-center study of ICI-treated patients	43 (rheumatic IRAE)	2% of ICI-treated patients developed IA; 71% of those with rheumatic IRAE needed immunosuppression; only 12% required ICI discontinuation; 2 patients died of myositis	Likely underestimates prevalence of rheumatic IRAE, particularly mild; IA most common rheumatic IRAE
Allenbach et al, 2020 (8)	Rheumatic IRAE reported to WHO pharmacovigilance database	465 (myositis), 606 (IA), 76 (PMR)	Fatality rate for myositis 24%; arthritis and myositis more common in those treated with ICI combination therapy	WHO database requires active reporting, so likely biased toward more severe events; no available laboratory or imaging data to confirm diagnoses
Kostine et al, 2018 (12)	Patients who received ICIs at a single center	524 (total), 9 (IA), 11 (PMR)	19 patients required GCs, 2 required MTX; patients with rheumatic IRAEs had higher tumor response than those without	Only those referred to rheumatology were diagnosed as having rheumatic IRAE, likely biased toward more severe disease; collected in 2015–2017, when less awareness of rheumatic IRAEs
Angelopoulou et al, 2020 (53)	Literature review of musculoskeletal IRAEs	209 (IA), 51 (myositis), 44 (PMR)	Prevalence rate of musculoskeletal IRAEs of 6% in prospective studies; 70% of patients needed GCs, and 18% were treated with DMARDs	Question about search technique, given fewer cases found than in prior SLRs

* IRAEs = immune-related adverse events; IA = inflammatory arthritis; ICI = immune checkpoint inhibitor; DMARDs = disease-modifying antirheumatic drugs; MTX = methotrexate; LEF = leflunomide; SSA = sulfasalazine; HCQ = hydroxychloroquine; TNFi = tumor necrosis factor inhibitor; TCZ = tocilizumab; MRI = magnetic resonance imaging; GCs = glucocorticoids; OA = osteoarthritis; NSAIDs = nonsteroidal antiinflammatory drugs; anti–PD-1 = anti–programmed death 1; = anti–PD-L1 = anti–programmed death ligand 1; CRP = C-reactive protein; PMR = polymyalgia rheumatica; RF = rheumatoid factor; anti-CCP = anti–cyclic citrullinated peptide; SLR = systematic literature review; RA = rheumatoid arthritis; EULAR = European League Against Rheumatism; ACR = American College of Rheumatology; US = ultrasound; PET = positron emission tomography; IVIG = intravenous immunoglobulin; PE = plasma exchange; EMG = electromyogram; WHO = World Health Organization.

inflammation (34). Myofascial inflammation was actually more common than synovitis according to one MRI study of patients receiving ICIs who had musculoskeletal symptoms, so it should be considered when there is pain around the joint rather than centered on the joint (34). Muscle biopsies have shown 2 major patterns: endomysial lymphocytic inflammation and perivascular macrophagic infiltration, both of which can be accompanied by necrosis (23,26,35,36).

Managing rheumatic IRAEs. When the diagnosis of a rheumatic IRAE is confirmed, there are several questions that rheumatologists should consider. First, the plan for future oncology treatment should be determined. This may greatly influence how non–life-threatening IRAEs are managed. If ICI treatment is going to be stopped, there may be more flexibility in terms of immunosuppression. If chemotherapy or targeted agents are to be started, this needs to be considered in treatment decision-making. If the ICI will be continued or restarted, the acceptable dose of concurrent glucocorticoids should be discussed with the treating oncologist. Next, having a conversation with the patient about his or her goals with IRAE treatment is crucial. Patients have different perspectives based on personal values and cancer prognosis that may affect how aggressive they wish to be in treating IRAEs (37).

The approaches to managing inflammatory arthritis and PMR are similar. Glucocorticoids are first-line therapy for those who do not improve with nonsteroidal antiinflammatory drugs (NSAIDs) and/or intraarticular steroid injections. For those in

whom steroids cannot be tapered or in whom steroid-sparing agents are required, ICIs are often withheld or stopped. For those in whom steroids can be tapered or who have symptomatic control with prednisone 10 mg/day or equivalent, ICIs may be administered concurrently at the discretion of the oncologist. Steroid-sparing agents have included hydroxychloroquine (HCQ), sulfasalazine, methotrexate (MTX), tumor necrosis factor inhibitors (TNFi), and interleukin-6 receptor (IL-6R) inhibitors.

Myositis can be life-threatening and therefore requires a different approach. The ICI is almost always withheld if not discontinued when myositis is diagnosed. Hospitalized patients may receive a higher dose of intravenous (IV) steroids, while outpatients may start prednisone 1 mg/kg or equivalent. Treatment options are discussed in more detail below.

Evidence for treatment

The evidence for evaluation and treatment of rheumatic IRAEs is primarily derived from prospective and retrospective cohort studies, case series, and case reports (Table 1). There are a few systematic reviews that have combined the observational data, but the limited quality of some primary data should be considered when interpreting these studies.

General principles of treating IRAEs and of oncology guidelines. It is important to understand how referring oncologists conceptualize IRAE management and treatment. The Common Terminology Criteria for Adverse Events (CTCAE) is used to assess the severity of AEs in oncology clinical trials and serves as the measure of severity in management and treatment guidelines (38). For rheumatic/musculoskeletal IRAEs, the CTCAE has several limitations. For example, to have arthritis of grade 3 severity, patients must be hindered in performing their self-care activities of daily living or have irreversible joint damage. Having a CTCAE grade 3 or higher is often classified as a "severe" IRAE, so musculoskeletal IRAEs do not often meet this criterion. Several organizations publish guidelines for the evaluation and management of IRAEs, including the American Society of Clinical Oncologists (39), the European Society for Medical Oncology (40), the National Comprehensive Cancer Network (NCCN; 41), and the Society for Immunotherapy of Cancer (42). Most of these guidelines are developed according to expert consensus. The NCCN guidelines are updated, based on literature review, every 6 months. We have collated recommendations from all 4 major oncology guidelines into a general algorithm, so rheumatologists can understand what oncologists are referencing when managing inflammatory arthritis, PMR, and myositis (Figures 2–4). The European League Against Rheumatism has also published a document of overarching principles to guide diagnosis and management of rheumatic IRAEs (43). Similar to oncology guidelines, this is based on expert consensus.

Inflammatory arthritis. Some patients with mild symptoms will need only NSAIDs or an intraarticular steroid injection for treatment. Generally, patients presenting to rheumatologists

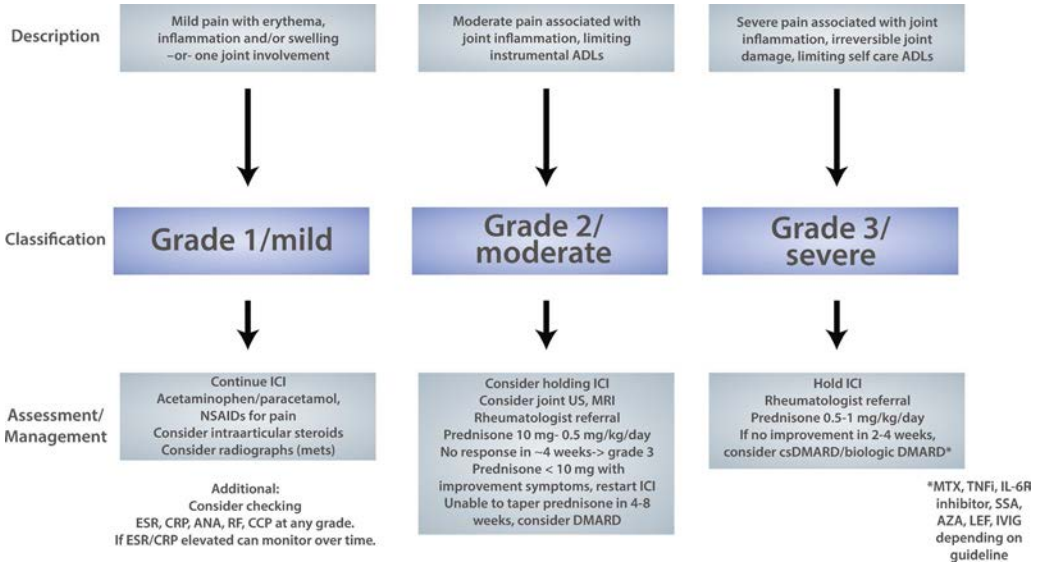

Figure 2. Composite oncology evaluation/treatment algorithm for musculoskeletal immune-related adverse events (IRAEs), based on the American Society of Clinical Oncology/National Comprehensive Cancer Network/European Society for Medical Oncology/Society for the Immunotherapy of Cancer guidelines for inflammatory arthritis. Severity (grade) of the IRAE is determined by the severity of symptoms and effect on daily function. Different evaluation and management strategies are recommended based on grade. ADLs = activities of daily living; ICI = immune checkpoint inhibitor; NSAIDs = nonsteroidal antiinflammatory drugs; ESR = erythrocyte sedimentation rate; CRP = C-reactive protein; ANA = antinuclear antibody; RF = rheumatoid factor; CCP = cyclic citrullinated peptide; US = ultrasound; MRI = magnetic resonance imaging; csDMARD = conventional synthetic disease-modifying antirheumatic drug; MTX = methotrexate; TNFi = tumor necrosis factor inhibitor; IL-6R = interleukin-6 receptor; SSA = sulfasalazine; AZA = azathioprine; LEF = leflunomide; IVIG = intravenous immunoglobulin.

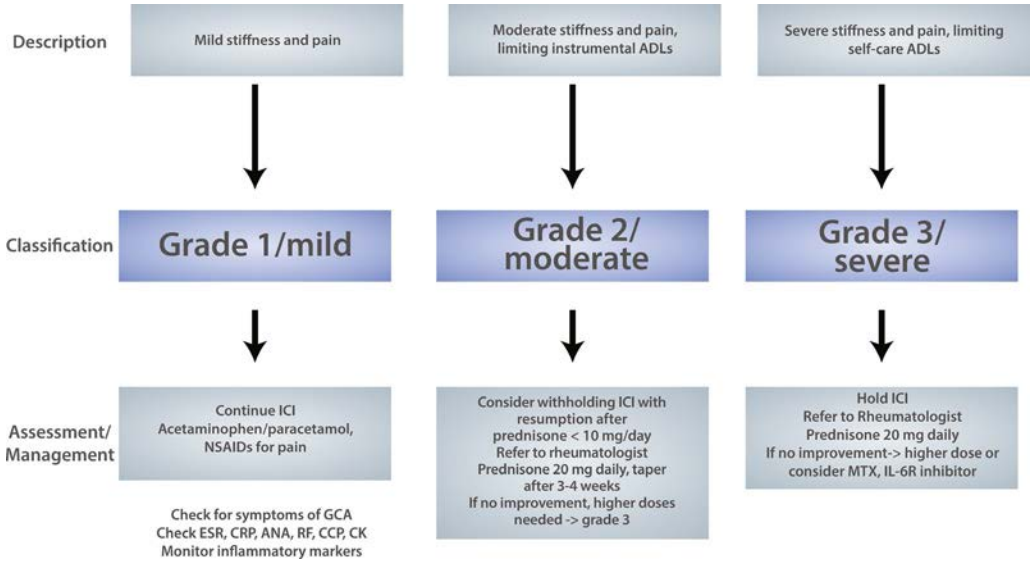

Figure 3. Composite oncology evaluation/treatment algorithm for musculoskeletal IRAEs, based on the American Society of Clinical Oncology/ National Comprehensive Cancer Network guidelines for polymyalgia rheumatica. Severity (grade) of the IRAE is determined by the severity of symptoms and effect on daily function. GCA = giant cell arteritis; CK = creatine kinase (see Figure 2 for other definitions).

for inflammatory arthritis will require systemic glucocorticoids for grade 2 symptoms (Figure 2). In one systematic review, 74% of patients with inflammatory arthritis were treated with systemic glucocorticoids (18) (Table 1). The reported dosing of glucocorticoids ranged from 5–20 mg/day of prednisone, or equivalent, to >1 mg/kg of prednisone (11,44). The length of a steroid taper is variable, due to heterogeneity in the severity of ICI-induced inflammatory arthritis. Some patients continued to receive ICIs while others stopped. Even among those who discontinue ICIs, >40% may still have symptoms 6 months after cessation (16) (Table 1).

MTX has commonly been used as a conventional synthetic disease-modifying antirheumatic drug (csDMARD) to treat ICI-induced inflammatory arthritis, particularly in patients with grade 2 symptoms in whom steroids cannot be tapered, or those with grade 3 symptoms (18) (Figure 2). Some oncologists have cited the approved lung cancer treatment regimen of pemetrexed (a chemotherapy agent similar to MTX) combined with pembrolizumab and carboplatin as a reason they are comfortable with MTX not impairing tumor response to ICI.

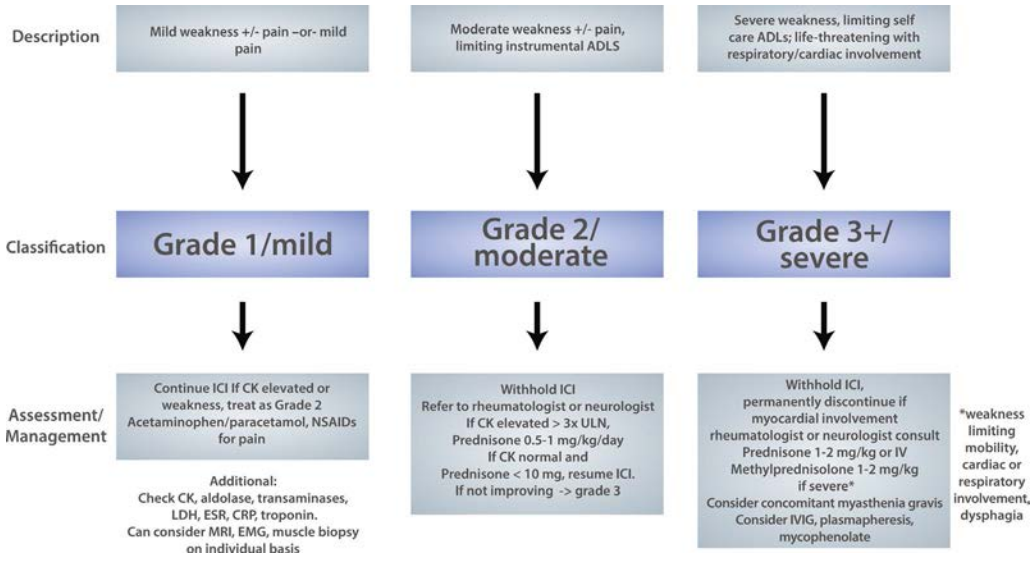

Figure 4. Composite oncology evaluation/treatment algorithm for musculoskeletal IRAEs, based on the American Society of Clinical Oncology/ National Comprehensive Cancer Network guidelines for myositis. Severity (grade) of the IRAE is determined by the severity of symptoms and effect on daily function. CK = creatine kinase; LDH = lactate dehydrogenase; EMG = electromyogram; ULN = upper limit of normal (see Figure 2 for other definitions).

HCQ has also been used as a steroid-sparing agent. In one Canadian study of patients with ICI-induced inflammatory arthritis (n = 11); HCQ was used early in the disease course, with good symptomatic control in the majority of patients (45). For patients with mild but persistent symptoms, HCQ could be a potential treatment. Sulfasalazine and leflunomide have also been used, but less commonly.

TNFi are the most commonly used class of biologic DMARDs. Infliximab was used early in ICI therapy to treat ipilimumab-induced colitis. Short-term use of infliximab (1–3 doses) has been shown not to affect tumor response in melanoma (46). Adalimumab, etanercept, and infliximab have been used to treat ICI-induced inflammatory arthritis (16,18) (Figure 2).

A small case series of 3 patients with inflammatory arthritis treated with tocilizumab (TCZ) was published in 2017 (47). One patient in this series continued to receive TCZ along with ICI therapy. Administering biologic DMARDs concurrently with ICIs was initially avoided but has become a more common practice. Recent data show successful colitis treatment with infliximab without discontinuing the ICI (48).

Due to limited numbers, data on tumor progression and csDMARD/biologic DMARD use are primarily analyzed by grouping drugs of different mechanisms together. In one study of 60 patients, there was no difference in tumor outcomes in those who required csDMARDs/biologic DMARDs and those who did not (16).

The data are even more limited regarding biologics beyond TNFi and IL-6R inhibitors. There is a case report of tumor progression with secukinumab when used for psoriasis (49), while another case of pembrolizumab-induced psoriasis was treated successfully in this way without progression (50). Apremilast has been successfully used in a patient with psoriatic arthritis (51) and in patients with psoriasis (52).

PMR. There are limited data on the management of PMR as an IRAE. In a systematic literature review of musculoskeletal IRAEs that included "polymyalgia rheumatica" in the search terms, only 78 patients were found in the published literature (18); another literature review showed 44 cases (53) (Table 1). The mainstay of treatment is glucocorticoids (required in 94% of patients in one study [32]). Dosing of steroids has differed somewhat from that in traditional PMR (Figure 3). Of 46 patients who needed steroids in one study, 17 of them (37%) required >20 mg/day of prednisone for symptomatic control. Dosing of glucocorticoids up to 60 mg/day has been reported (32).

Experience with steroid-sparing agents in ICI-induced PMR is even more limited. In one study, 5 of 49 patients needed additional immunosuppression (32). Two were treated with TCZ, and the 3 others were treated with MTX or HCQ. A patient with ICI-induced PMR being treated with infliximab has also been reported (54).

Myositis. Glucocorticoids are the first-line therapy for ICI-induced myositis. Initial dosing can range from 0.5 mg/kg/day of prednisone to 2,000 mg of IV methylprednisolone (23,26). Myositis is a clinical scenario in which initial aggressive therapy with high-dose immunosuppression is often indicated. With inflammatory arthritis and PMR, there is not the same risk of death or rapid morbidity, so a step-up approach is more commonly used in myositis (Figure 4).

IV immunoglobulin (IVIG) has been used in ICI-induced myositis (23,26) (Table 1). IVIG has also been used successfully for other IRAEs, such as myasthenia gravis (55), limbic encephalitis (56), pure red cell aplasia (57), and immune-mediated thrombocytopenia (58).

Case reports and series have described plasmapheresis (plasma exchange [PE]) for severe myositis and for patients with myasthenia and/or myocarditis overlap (23,26,59). Outcomes have been variable with the use of PE, with some patients making a recovery and others dying of respiratory failure despite PE. IVIG or PE is also used when there is myasthenia overlap.

When patients have myocarditis in addition to myositis, additional therapies have been attempted. TCZ was used successfully in 1 case of myositis/myocarditis overlap refractory to glucocorticoids (60). Abatacept has also been used in this scenario (61).

Managing preexisting autoimmune disease during ICI therapy. Patients with preexisting autoimmune diseases were excluded from the original clinical trials evaluating ICIs. However, with many regimens now approved as standard of care, patients with both autoimmune disease and cancer are increasingly receiving ICIs in clinical practice. Several retrospective studies and systematic literature reviews of observational studies have evaluated flares and de novo IRAEs in patients with preexisting autoimmune disease (Table 2). Overall, patients with preexisting autoimmune disease can generally be treated with ICIs and do not have AEs severe enough to require ICI treatment cessation. Approximately 40–50% of patients with autoimmune disease will experience a flare (62–64). It is important to note that these data are based primarily on patients with psoriasis, rheumatoid arthritis, and psoriatic arthritis and not vasculitis, scleroderma, or systemic lupus erythematosus. For more severe multisystem autoimmune diseases, the safety profile is less clear. The rate of flare may be higher with anti–PD-1/PD-L1 agents, while de novo IRAEs may be higher with anti–CTLA-4 agents (63). Most studies combine autoimmune diseases of all types, including those limited to 1 organ, such as psoriasis and autoimmune thyroid disease. One study of RA patients (n = 22) demonstrated that flares commonly occurred (in 55% of patients), but only 1 patient had to discontinue ICIs due to a flare or AE (65).

The question of how to manage preexisting autoimmune disease with steroids or other forms of immunosuppression is still under debate. There are data that suggest that immunosuppression with steroids or steroid-sparing immunosuppression at the start of ICI treatment is associated with worsened

Table 2. Studies on evaluation and management of preexisting autoimmune disease during ICI therapy*

Author, year (ref.)	Study population	n	Results	Comments
Tison et al, 2019 (64)	Patients with preexisting autoimmune disease treated with ICI for cancer	112	Most common diagnoses: psoriasis/PsA, RA, IBD; flares in 47%, other IRAEs in 42%; shorter progression-free survival in those who were receiving immunosuppressive therapy at ICI start	Multicenter retrospective study from France; raises concerns about effect of immunosuppression on tumor response
Efuni et al, 2020 (65)	RA patients treated with ICI for cancer	22	Flares in 55%, other IRAEs in 32%, mostly managed with steroids; only 1 patient discontinued ICI	Retrospective review, but encouraging for successful treatment of RA patients with ICIs
Abdel-Wahab et al, 2018 (63)	Patients with preexisting autoimmune disease treated with ICI for cancer	123	Psoriasis/PsA and RA most common diagnoses; more flares with anti–PD-1/PD-L1 agents, more de novo IRAEs with ipilimumab; 17% of patients discontinued ICI due to flare or IRAEs	SLR that included case reports; caution in interpreting numerical values for flare as likely biased toward more flares/IRAEs in case reports
Danlos et al, 2018 (77)	Patients from registry for those treated with anti–PD-1 who had preexisting autoimmune disease	45	Vitiligo and psoriasis most common diagnoses; <15% of patients receiving immunomodulatory therapy at ICI start	Not many patients with systemic autoimmune disease or receiving immunosuppressive therapy at start of ICI, so not applicable to many patients with rheumatic diseases
Menzies et al, 2017 (62)	Patients with preexisting autoimmune disease or prior severe IRAE treated with anti–PD-1 for melanoma	52 (preexisting autoimmune disease)	RA most common diagnosis (n = 13); 38% receiving immunosuppressive therapy at start of ICI; 38% had flare, 29% had de novo IRAEs; lower tumor response rate if receiving immunosuppressive therapy at ICI start	With small numbers of each autoimmune disease and heterogeneity, difficult to interpret tumor response data
Johnson et al, 2016 (78)	Patients with preexisting autoimmune disease treated with ipilimumab for melanoma	30	RA, psoriasis, and IBD most common diagnoses; 13 patients were receiving steroids or csDMARDs at start of ICI; 50% had flare and/or IRAEs	Small numbers of each autoimmune disease; ipilimumab monotherapy now uncommon since newer agents/regimens approved

* PsA = psoriatic arthritis; IBD = inflammatory bowel disease; csDMARDs = conventional synthetic disease-modifying antirheumatic drugs (see Table 1 for other definitions).

tumor response (64,66). Given the concern over affecting tumor response and the lack of data on the effects of specific agents, minimizing the amount of immunosuppression at the time of start of ICI treatment, and treating flares with short courses of steroids as needed, is a reasonable approach.

Discussion

Returning to our initial case, the 65-year-old man who developed new musculoskeletal symptoms during ICI treatment presents to your clinic for an appointment. On further history, he tells you that he started having symptoms ~6 months after ICI therapy started. First, his right knee was sore, and it was difficult to kneel due to stiffness and pain in the knee. He initially ignored this symptom, since he had experienced pain in his left knee before his joint replacement. Next, his ankles became painful and swollen. Finally, he developed stiffness and pain in his metacarpophalangeal and proximal interphalangeal joints, which impaired his grip and fine motor tasks. The hand symptoms, which have limited his ability to use buttons and dress himself, prompted him to reach out to his oncologist. It has been ~11 months since he received his first dose of ICI therapy. On examination, he shows synovitis of the small joints of the hands and ankles and bilateral knee effusions, with some warmth, along with right knee crepitus. He exhibits no decrease in strength. Laboratory reports show elevated ESR and CRP level, and he is negative for rheumatoid factor and anti-CCP antibodies. He is diagnosed as having inflammatory arthritis caused by ICI therapy. You have a discussion with his oncologist, who plans to withhold the next dose of ICI, and a tapering prednisone regimen is started at 40 mg/day. When the prednisone is tapered to 15 mg/day, however, symptoms return. Methotrexate is started as a steroid-sparing agent, with plans by his oncologist to restart ICI therapy when the inflammatory arthritis is stable.

IRAEs represent a new group of multisystem inflammatory disorders that rheumatologists will encounter for the foreseeable future. The patient described here could have had inflammatory arthritis, PMR, or myositis/fasciitis caused by the ICI treatment, depending on further history and physical examination. Currently, however, there are limited prospective data and no data from randomized clinical trials to guide management of all of these rheumatic IRAEs.

Before trials for management of rheumatic IRAEs can commence, there must be an agreed-upon taxonomy for types of IRAEs and an understanding of different phenotypes within categories. Additionally, the CTCAE used by oncologists to classify and grade IRAEs could be improved to better reflect rheumatic IRAEs and their impact on patients. As new types of immunotherapy and combination regimens are tested and approved, new IRAEs may be discovered, and improving the ability for signal detection by oncologists is important.

A first priority is high-quality prospective observational studies. These studies can provide insight into how to define rheumatic IRAEs for trial inclusion and what indices can be used to monitor disease activity and response to therapeutics. It may be that existing outcome measures from traditional rheumatic diseases are useful in IRAEs, but this has not been systematically studied.

Once case definitions and outcome measures are defined, clinical trials can begin to address several questions that arise in the treatment of IRAEs. The first question deals with the dosing of initial steroids and whether we should aim to increase the dose in the event of a lack of response, or decrease the dose as induction. Right now, it is unclear which will lead to lower cumulative steroid dosing and whether short-term higher-dose steroids have a different immunologic effect on tumor response than longer-term low-dose steroids. Types of immunosuppression beyond glucocorticoids have been adopted from treatments for traditional rheumatic disease, such as RA and dermatomyositis, and applied to similar IRAEs. Additional clinical research priorities for ICI-induced inflammatory arthritis, PMR, and myositis are outlined in Table 3.

One trial, NIVO-AID, conducted by the Cancer Therapeutics Evaluation Program, a part of the National Cancer Institute, is evaluating the use of nivolumab for patients with solid tumors and underlying autoimmune diseases (ClinicalTrials.gov identifier: NCT03656627). To our knowledge, there are no active trials specifically evaluating treatments for rheumatic IRAEs.

Table 3. Key clinical research questions for rheumatic IRAEs*

Research area and key clinical research questions
Rheumatic IRAEs (general)
Should GCs be started at a high dose with a taper, or started at a low dose with step-up therapy?
How early should csDMARDs and biologic DMARDs be utilized in treatment?
Do all rheumatic IRAEs have the possibility of becoming chronic processes or is this unique to IA?
IA
What are the phenotypes of IA, and do they correlate with response to particular treatments and cancer prognosis?
What is the role of OA in IA due to ICIs? Can an increase in OA pain be caused by ICIs, and does this represent a new process?
What imaging modality is most sensitive and specific for IA due to ICIs?
PMR
What is the optimal starting GC dose, and does it differ from traditional PMR?
Should patients with PMR-like symptoms and peripheral synovitis be classified as having PMR or IA?
What is the prevalence of GCA in those who develop PMR from ICIs?
Myositis
What is the optimal evaluation for patients with suspected myositis (e.g., EMG, MRI, muscle biopsy)?
What is the best starting dose for GCs?
What is the optimal steroid-sparing agent?
In which cases is it safe to rechallenge patients with ICIs?
Are there risk factors present in myositis before ICI therapy is started? If so, should patients with these risk factors have enhanced monitoring?

* csDMARDs = conventional synthetic disease-modifying antirheumatic drugs; GCA = giant cell arteritis (see Table 1 for other definitions).

It is critical to define the biology of IRAEs, which may allow for risk stratification at ICI treatment initiation and inform therapeutic choices guided by mechanism. Given the diversity of IRAEs in terms of presentation, severity, and response to treatments, the pathogenesis of IRAEs is likely heterogeneous. Limited data have been published on particular IRAEs that may be relevant to pathogenesis. For example, genetic studies in insulin-dependent diabetes mellitus associated with ICIs, and in inflammatory arthritis, suggest there may be similar HLA associations (67,68). Interestingly, particular HLA haplotypes have also been associated with better or worse tumor response to ICIs (69). Perturbations in the microbiome have been linked to development of colitis as an IRAE (70). Elevated baseline levels of IL-17 have also been associated with development of severe colitis (71). An intriguing question relevant to pathogenesis is why there have been minimal cases of lupus-like syndromes with IRAEs. Drug-induced lupus is a well-described entity and can be associated with many medications. Thus far, cutaneous forms of lupus, most commonly subacute cutaneous lupus, are described in association with ICIs, but systemic lupus is less frequently described as such (72–74).

Ultimately, high-quality clinical data collection coupled with translational science will allow patients with rheumatic IRAEs to be treated effectively. Until more data are available, discussing the limitations of our knowledge with referring oncologists and patients will allow for shared decision-making in managing IRAEs.

AUTHOR CONTRIBUTIONS

Drs. Cappelli and Bingham drafted the article, revised it critically for important intellectual content, and approved the final version to be published.

REFERENCES

1. Pardoll DM. The blockade of immune checkpoints in cancer immunotherapy [review]. Nat Rev Cancer 2012;12:252–64.
2. Topalian SL, Drake CG, Pardoll DM. Immune checkpoint blockade: a common denominator approach to cancer therapy. Cancer Cell 2015;27:450–61.
3. Wei SC, Duffy CR, Allison JP. Fundamental mechanisms of immune checkpoint blockade therapy. Cancer Discov 2018;8:1069–86.
4. Qin S, Xu L, Yi M, Yu S, Wu K, Luo S. Novel immune checkpoint targets: moving beyond PD-1 and CTLA-4 [review]. Mol Cancer 2019;18:155.
5. Baetz TD, Fletcher GG, Knight G, McWhirter E, Rajagopal S, Song X, et al. Systemic adjuvant therapy for adult patients at high risk for recurrent melanoma: a systematic review. Cancer Treat Rev 2020;87:102032.
6. Forde PM, Chaft JE, Smith KN, Anagnostou V, Cottrell TR, Hellmann MD, et al. Neoadjuvant PD-1 blockade in resectable lung cancer. N Engl J Med 2018;378:1976–86.
7. Postow MA, Sidlow R, Hellmann MD. Immune-related adverse events associated with immune checkpoint blockade. N Engl J Med 2018;378:158–68.
8. Allenbach Y, Anquetil C, Manouchehri A, Benveniste O, Lambotte O, Lebrun-Vignes B, et al. Immune checkpoint inhibitor-induced myositis, the earliest and most lethal complication among rheumatic and musculoskeletal toxicities [review]. Autoimmun Rev 2020: 102586.
9. Calabrese LH, Calabrese C, Cappelli LC. Rheumatic immune-related adverse events from cancer immunotherapy [review]. Nat Rev Rheumatol 2018;14:569–79.
10. Cappelli LC, Gutierrez AK, Bingham CO III, Shah AA. Rheumatic and musculoskeletal immune-related adverse events due to immune checkpoint inhibitors: a systematic review of the literature. Arthritis Care Res (Hoboken) 2017;69:1751–63.
11. Buder-Bakhaya K, Benesova K, Schulz C, Anwar H, Dimitrakopoulou-Strauss A, Weber TF, et al. Characterization of arthralgia induced by PD-1 antibody treatment in patients with metastasized cutaneous malignancies. Cancer Immunol Immunother 2018;67:175–82.
12. Kostine M, Rouxel L, Barnetche T, Veillon R, Martin F, Dutriaux C, et al. Rheumatic disorders associated with immune checkpoint inhibitors in patients with cancer—clinical aspects and relationship with tumour response: a single-centre prospective cohort study. Ann Rheum Dis 2018;77:393–8.
13. Haslam A, Prasad V. Estimation of the percentage of US patients with cancer who are eligible for and respond to checkpoint inhibitor immunotherapy drugs. JAMA Netw Open 2019;2:e192535.
14. Chai QQ, Du JY, Zhu J, Wu B. The differences in the safety and tolerability of immune checkpoint inhibitors as treatment for non-small cell lung cancer and melanoma: network meta-analysis and systematic review. Front Pharmacol 2019;10:1260.
15. Khoja L, Day D, Chen TW, Siu LL, Hansen AR. Tumour- and class-specific patterns of immune-related adverse events of immune checkpoint inhibitors: a systematic review. Ann Oncol 2017;28: 2377–85.
16. Braaten TJ, Brahmer JR, Forde PM, Le D, Lipson EJ, Naidoo J, et al. Immune checkpoint inhibitor-induced inflammatory arthritis persists after immunotherapy cessation. Ann Rheum Dis 2020;79:332–8.
17. Xing P, Zhang F, Wang G, Xu Y, Li C, Wang S, et al. Incidence rates of immune-related adverse events and their correlation with response in advanced solid tumours treated with NIVO or NIVO+IPI: a systematic review and meta-analysis. J Immunother Cancer 2019;7:341.
18. Ghosh N, Tiongson MD, Stewart C, Chan KK, Jivanelli B, Cappelli L, et al. Checkpoint inhibitor-associated arthritis: a systematic review of case reports and case series. J Clin Rheumatol 2020. E-pub ahead of print.
19. Kim ST, Bittar M, Kim HJ, Neelapu SS, Zurita AJ, Nurieva R, et al. Recurrent pseudogout after therapy with immune checkpoint inhibitors: a case report with immunoprofiling of synovial fluid at each flare. J Immunother Cancer 2019;7:126.
20. Corominas H, Badlissi F, Shmerling RH. Crystal-induced oligoarthritis triggered by pembrolizumab, an immune checkpoint inhibitor [letter]. Joint Bone Spine 2018;85:647–8.
21. Albayda J, Bingham CO III, Shah AA, Kelly RJ, Cappelli L. Metastatic joint involvement or inflammatory arthritis? A conundrum with immune checkpoint inhibitor-related adverse events. Rheumatology (Oxford) 2018;57:760–2.
22. Cortellini A, Vitale MG, de Galitiis F, di Pietro FR, Berardi R, Torniai M, et al. Early fatigue in cancer patients receiving PD-1/PD-L1 checkpoint inhibitors: an insight from clinical practice. J Transl Med 2019;17:376.
23. Matas-García A, Milisenda JC, Selva-O'Callaghan A, Prieto-González S, Padrosa J, Cabrera C, et al. Emerging PD-1 and PD-1L inhibitors-associated myopathy with a characteristic histopathological pattern [review]. Autoimmun Rev 2020;19:102455.
24. Jeyakumar N, Etchegaray M, Henry J, Lelenwa L, Zhao B, Segura A, et al. The terrible triad of checkpoint inhibition: a case report of myasthenia gravis, myocarditis, and myositis induced by cemiplimab in a patient with metastatic cutaneous squamous cell carcinoma. Case Reports Immunol 2020;2020:5126717.

25. Couey MA, Bell RB, Patel AA, Romba MC, Crittenden MR, Curti BD, et al. Delayed immune-related events (DIRE) after discontinuation of immunotherapy: diagnostic hazard of autoimmunity at a distance. J Immunother Cancer 2019;7:165.
26. Touat M, Maisonobe T, Knauss S, Salem OB, Hervier B, Auré K, et al. Immune checkpoint inhibitor-related myositis and myocarditis in patients with cancer. Neurology 2018;91:e985–94.
27. Shah M, Tayar JH, Abdel-Wahab N, Suarez-Almazor ME. Myositis as an adverse event of immune checkpoint blockade for cancer therapy. Semin Arthritis Rheum 2019;48:736–40.
28. Mammen AL, Rajan A, Pak K, Lehky T, Casciola-Rosen L, Donahue RN, et al. Pre-existing antiacetylcholine receptor autoantibodies and B cell lymphopaenia are associated with the development of myositis in patients with thymoma treated with avelumab, an immune checkpoint inhibitor targeting programmed death-ligand 1 [letter]. Ann Rheum Dis 2019;78:150–2.
29. Cappelli LC, Gutierrez AK, Baer AN, Albayada J, Manno RL, Haque U, et al. Inflammatory arthritis and sicca syndrome induced by nivolumab and ipilimumab. Ann Rheum Dis 2017;76:43–50.
30. Albayda J, Dein E, Shah AA, Bingham CO III, Cappelli L. Sonographic findings in inflammatory arthritis secondary to immune checkpoint inhibition: a case series. ACR Open Rheumatol 2019;1:303–7.
31. Subedi A, Williams SG, Yao L, Maharjan S, Strauss J, Sharon E, et al. Use of magnetic resonance imaging to identify immune checkpoint inhibitor-induced inflammatory arthritis. JAMA Netw Open 2020;3:e200032.
32. Calabrese C, Cappelli LC, Kostine M, Kirchner E, Braaten T, Calabrese L. Polymyalgia rheumatica-like syndrome from checkpoint inhibitor therapy: case series and systematic review of the literature. RMD Open 2019;5:e000906.
33. Van der Geest KS, Sandovici M, Rutgers A, Hiltermann TJ, Oosting SF, Slart RH, et al. Imaging in immune checkpoint inhibitor-induced polymyalgia rheumatica. Ann Rheum Dis 2020. E-pub ahead of print.
34. Daoussis D, Kraniotis P, Filippopoulou A, Argiriadi R, Theodoraki S, Makatsoris T, et al. An MRI study of immune checkpoint inhibitor-induced musculoskeletal manifestations myofasciitis is the prominent imaging finding. Rheumatology (Oxford) 2020;59:1041–50.
35. Vermeulen L, Depuydt CE, Weckx P, Bechter O, van Damme P, Thal DR, et al. Myositis as a neuromuscular complication of immune checkpoint inhibitors. Acta Neurol Belg 2020;120:355–64.
36. John S, Antonia SJ, Rose TA, Seifert RP, Centeno BA, Wagner AS, et al. Progressive hypoventilation due to mixed $CD8^+$ and $CD4^+$ lymphocytic polymyositis following tremelimumab-durvalumab treatment. J Immunother Cancer 2017;5:54.
37. Cappelli LC, Grieb SM, Shah AA, Bingham CO III, Orbai AM. Immune checkpoint inhibitor-induced inflammatory arthritis: a qualitative study identifying unmet patient needs and care gaps. BMC Rheumatol 2020;4:32.
38. US Department of Health and Human Services. National Institutes of Health. National Cancer Institute. Common Terminology Criteria for Adverse Events (CTCAE) version 5.0. 2017. URL: https://ctep.cancer.gov/protocolDevelopment/electronic_applications/docs/CTCAE_v5_Quick_Reference_8.5x11.pdf.
39. Brahmer JR, Lacchetti C, Schneider BJ, Atkins MB, Brassil KJ, Caterino JM, et al. Management of immune-related adverse events in patients treated with immune checkpoint inhibitor therapy: American Society of Clinical Oncology clinical practice guideline. J Clin Oncol 2018;36:1714–68.
40. Haanen J, Carbonnel F, Robert C, Kerr KM, Peters S, Larkins J, et al. Management of toxicities from immunotherapy: ESMO clinical practice guidelines for diagnosis, treatment and follow-up. Ann Oncol 2017;28 Suppl:iv119–42.
41. Thompson JA, Schneider BJ, Brahmer J, Andrews S, Armand P, Bhatia S, et al. Management of immunotherapy-related toxicities, version 1.2019. J Natl Compr Canc Netw 2019;17:255–89.
42. Puzanov I, Diab A, Abdallah K, Bingham CO III, Brogdon C, Dadu R, et al. Managing toxicities associated with immune checkpoint inhibitors: consensus recommendations from the Society for Immunotherapy of Cancer (SITC) Toxicity Management Working Group. J Immunother Cancer 2017;5:95.
43. Kostine M, Finckh A, Bingham CO III, Visser K, Leipe J, Schulze-Koops H, et al. EULAR points to consider for the diagnosis and management of rheumatic immune-related adverse events due to cancer immunotherapy with checkpoint inhibitors. Ann Rheum Dis 2020. E-pub ahead of print.
44. Cappelli LC, Brahmer JR, Forde PM, Le DT, Lipson EJ, Naidoo J, et al. Clinical presentation of immune checkpoint inhibitor-induced inflammatory arthritis differs by immunotherapy regimen. Semin Arthritis Rheum 2018;48:553–7.
45. Roberts J, Smylie M, Walker J, Basappa NS, Chu Q, Kolinsky M, et al. Hydroxychloroquine is a safe and effective steroid-sparing agent for immune checkpoint inhibitor-induced inflammatory arthritis. Clin Rheumatol 2019;38:1513–9.
46. Horvat TZ, Adel NG, Dang TO, Momtaz P, Postow MA, Callahan MK, et al. Immune-related adverse events, need for systemic immunosuppression, and effects on survival and time to treatment failure in patients with melanoma treated with ipilimumab at Memorial Sloan Kettering Cancer Center. J Clin Oncol 2015;33:3193–8.
47. Kim ST, Tayar J, Trinh VA, Suarez-Almazor M, Garcia S, Hwu P, et al. Successful treatment of arthritis induced by checkpoint inhibitors with tocilizumab: a case series. Ann Rheum Dis 2017;76:2061–4.
48. Badran YR, Cohen JV, Brastianos PK, Parikh AR, Hong TS, Dougan M. Concurrent therapy with immune checkpoint inhibitors and TNFα blockade in patients with gastrointestinal immune-related adverse events. J Immunother Cancer 2019;7:226.
49. Esfahani K, Miller WH Jr. Reversal of autoimmune toxicity and loss of tumor response by Interleukin-17 blockade. N Engl J Med 2017;376:1989–91.
50. Monsour EP, Pothen J, Balaraman R. A novel approach to the treatment of pembrolizumab-induced psoriasis exacerbation: a case report. Cureus 2019;11:e5824.
51. Nigro O, Pinotti G, Gueli R, Grigioni E, de Santis M, Ceribelli A, et al. Psoriatic arthritis induced by anti-PD1 and treated with apremilast: a case report and review of the literature. Immunotherapy 2020;12:549–54.
52. Fattore D, Annunziata MC, Panariello L, Marasca C, Fabbrocini G. Successful treatment of psoriasis induced by immune checkpoint inhibitors with apremilast [letter]. Eur J Cancer 2019;110:107–9.
53. Angelopoulou F, Bogdanos D, Dimitroulas T, Sakkas L, Daoussis D. Immune checkpoint inhibitor-induced musculoskeletal manifestations [review]. Rheumatol Int 2020. E-pub ahead of print.
54. Calabrese C, Kirchner E, Kontzias K, Velcheti V, Calabrese LH. Rheumatic immune-related adverse events of checkpoint therapy for cancer: case series of a new nosological entity. RMD Open 2017;3:e000412.
55. Safa H, Johnson DH, Trinh VA, Rodgers TE, Lin H, Suarez-Almazor ME, et al. Immune checkpoint inhibitor related myasthenia gravis: single center experience and systematic review of the literature. J Immunother Cancer 2019;7:319.
56. Chung M, Jaffer M, Verma N, Mokhtari S, Ramsakal A, Peguero E. Immune checkpoint inhibitor induced anti-glutamic acid decarboxylase 65 (anti-GAD 65) limbic encephalitis responsive to intravenous immunoglobulin and plasma exchange. J Neurol 2020;267:1023–5.
57. Isoda A, Miyazawa Y, Tahara K, Mihara M, Saito A, Matsumoto M, et al. Pembrolizumab-induced pure red cell aplasia successfully treated with intravenous immunoglobulin. Intern Med 2020;59:2041–5.

58. Shiuan E, Beckermann KE, Ozgun A, Kelly C, McKean M, McQuade J, et al. Thrombocytopenia in patients with melanoma receiving immune checkpoint inhibitor therapy. J Immunother Cancer 2017;5:8.
59. Xing Q, Zhang ZW, Lin QH, Shen LH, Wang PM, Zhang S, et al. Myositis-myasthenia gravis overlap syndrome complicated with myasthenia crisis and myocarditis associated with anti-programmed cell death-1 (sintilimab) therapy for lung adenocarcinoma. Ann Transl Med 2020;8:250.
60. Doms J, Prior JO, Peters S, Obeid M. Tocilizumab for refractory severe immune checkpoint inhibitor-associated myocarditis [letter]. Ann Oncol 2020;31:1273–5.
61. Salem JE, Allenbach Y, Vozy A, Brechot N, Johnson DB, Moslehi JJ, et al. Abatacept for severe immune checkpoint inhibitor-associated myocarditis. N Engl J Med 2019;380:2377–9.
62. Menzies AM, Johnson DB, Ramanujam S, Atkinson VG, Wong AN, Park JJ, et al. Anti-PD-1 therapy in patients with advanced melanoma and preexisting autoimmune disorders or major toxicity with ipilimumab. Ann Oncol 2017;28:368–76.
63. Abdel-Wahab N, Shah M, Lopez-Olivo MA, Suarez-Almazor ME. Use of immune checkpoint inhibitors in the treatment of patients with cancer and preexisting autoimmune disease: a systematic review. Ann Intern Med 2018;168:121–30.
64. Tison A, Quéré G, Misery L, Funck-Brentano E, Danlos FX, Routier E, et al. Safety and efficacy of immune checkpoint inhibitors in patients with cancer and preexisting autoimmune disease: a nationwide, multicenter cohort study. Arthritis Rheumatol 2019;71:2100–11.
65. Efuni E, Cytryn S, Boland P, Niewold TB, Pavlick A, Weber J, et al. Risk of toxicity after initiating immune checkpoint inhibitor treatment in patients with rheumatoid arthritis. J Clin Rheumatol 2020. E-pub ahead of print.
66. Arbour KC, Mezquita L, Long N, Rizvi H, Auclin E, Ni A, et al. Impact of baseline steroids on efficacy of programmed cell death-1 and programmed death-ligand 1 blockade in patients with non-small-cell lung cancer. J Clin Oncol 2018;36:2872–8.
67. Cappelli LC, Dorak MT, Bettinotti MP, Bingham CO, Shah AA. Association of HLA-DRB1 shared epitope alleles and immune checkpoint inhibitor-induced inflammatory arthritis. Rheumatology (Oxford) 2019;58:476–80.
68. De Filette JM, Pen JJ, Decoster L, Vissers T, Bravenboar B, van der Auwera B, et al. Immune checkpoint inhibitors and type 1 diabetes mellitus: a case report and systematic review. Eur J Endocrinol 2019;181:363–74.
69. Chowell D, Morris LG, Grigg CM, Weber JK, Samstein RM, Makarov V, et al. Patient HLA class I genotype influences cancer response to checkpoint blockade immunotherapy. Science 2018;359:582–7.
70. Chaput N, Lepage P, Coutzac C, Soularue E, Roux KL, Monot C, et al. Baseline gut microbiota predicts clinical response and colitis in metastatic melanoma patients treated with ipilimumab. Ann Oncol 2017;28:1368–79.
71. Tarhini AA, Zahoor H, Lin Y, Malhotra U, Sander C, Butterfield LH, et al. Baseline circulating IL-17 predicts toxicity while TGF-β1 and IL-10 are prognostic of relapse in ipilimumab neoadjuvant therapy of melanoma. J Immunother Cancer 2015;3:39.
72. Michot JM, Fusellier M, Champiat S, Velter C, Baldini C, Voisin AL, et al. Drug-induced lupus erythematosus following immunotherapy with anti-programmed death-(ligand) 1 [letter]. Ann Rheum Dis 2019;78:e67.
73. Shao K, McGettigan S, Elenitsas R, Chu EY. Lupus-like cutaneous reaction following pembrolizumab: an immune-related adverse event associated with anti-PD-1 therapy. J Cutan Pathol 2018;45:74–7.
74. Liu RC, Sebaratnam DF, Jackett L, Kao S, Lowe PM. Subacute cutaneous lupus erythematosus induced by nivolumab [letter]. Australas J Dermatol 2018;59:e152–4.
75. Belkhir R, Le Burel S, Dunogeant L, Marabelle A, Hollebecque A, Besse B, et al. Rheumatoid arthritis and polymyalgia rheumatica occurring after immune checkpoint inhibitor treatment. Ann Rheum Dis 2017;76:1747–50.
76. Richter MD, Crowson C, Kottschade LA, Finnes HD, Markovic SN, Thanarajasingam U. Rheumatic syndromes associated with immune checkpoint inhibitors: a single-center cohort of sixty-one patients. Arthritis Rheumatol 2019;71:468–75.
77. Danlos FX, Voisin AL, Dyevre V, Michot JM, Routier E, Taillade L, et al. Safety and efficacy of anti-programmed death 1 antibodies in patients with cancer and pre-existing autoimmune or inflammatory disease. Eur J Cancer 2018;91:21–9.
78. Johnson DB, Sullivan RJ, Ott PA, Carlino MS, Khushalani NI, Ye F, et al. Ipilimumab therapy in patients with advanced melanoma and preexisting autoimmune disorders. JAMA Oncol 2016;2:234–40.

American College of Rheumatology
Empowering Rheumatology Professionals

Arthritis & Rheumatology
Vol. 73, No. 4, April 2021, pp 566–567
DOI 10.1002/art.41599

EDITORIAL

Consequences of a Great Crisis on Chronic Diseases: How Childhood Exposures May Shape Future Health

Jason J. Lee[1] and Zumin Shi[2]

History, as the saying goes, repeats itself. And, during these historical coronavirus disease 2019 (COVID-19) pandemic times, a rheumatologist may wonder—what does the COVID-19 pandemic mean for rheumatology patients (1)? No one knows for sure, of course. But, if history really does repeat itself, infants and toddlers worldwide may be at risk. In this issue of *Arthritis & Rheumatology*, VanEvery et al examine the association between early life exposure to a prolonged crisis and future risk of rheumatoid arthritis (RA) (2). Specifically, the authors analyze data collected from adult participants enrolled in the Kailuan Study in China who were exposed to the Great Chinese Famine (1959–1961) during early life.

Major historical crises, notwithstanding their obvious tragedies, provide the medical community opportunities to study the relationships between environmental stressors and disease. In fact, previous studies of natural disasters, including other famines around the world, have established a link between exposures to crises and chronic diseases such as diabetes, obesity, metabolic syndrome, and even osteoarthritis (3–5). These studies are often able to examine a large population over time, as is the case for the Kailuan Study cohort of over 101,510 participants. Interestingly, the authors were able to show that early life exposure to the Great Chinese Famine from 1959 to 1961, including in utero exposures, independently increased the risk of RA development later in life, especially in those who were exposed between ages 0 and 3 years (multivariate adjusted odds ratio 4.53). The increased risk of RA was the same among seropositive patients and seronegative patients, and there were no interactions observed between famine exposure and smoking or obesity on the risk of developing RA.

The impact of nutrition on health and chronic disease has been examined for many years across all major fields of research. Indeed, various metabolic pathways have linked nutritional precursors like NAD to sirtuins and aging that may have major implications for age-related phenotypes like osteoarthritis (6,7). Some have even linked early life exposure to famines with epigenetic changes that manifest as chronic disease later in life (8), while others have investigated the link between nutrition and chronic disease from the microbiome perspective (9). Therefore, any alterations in diet, including a lack of proper nutrition, are worth investigating, and future research endeavors that study the interactions between metabolism and immune homeostasis appear promising.

Now, while the observed association between early life nutrition and chronic diseases like RA are indeed intriguing, if not frightening for young parents, these studies require careful interpretation. For instance, it has been noted that studies involving the Kailuan Study database may require additional attention to appropriate controls when analyzing the link between famine exposure and chronic disease (10). In the study by VanEvery and colleagues, the authors control for age-related discrepancies by adjusting for age under 40 years and still discovered significant findings. Also, despite the large cohort of registered participants, the actual number of participants from a severe famine region was small, thereby limiting the statistical power of the study.

Furthermore, despite the historical context of a 3-year famine, famine exposure and nutritional exposure must not be confused. In the study by VanEvery and colleagues, and others like it, early life data such as birth weight and diet, which affirms the early life nutritional status of affected individuals, are not readily available. Therefore, any nutritional inferences are circumstantial at best. In fact, bearing in mind that the study population mostly consisted of participants from less-severe famine regions, one must remember that the Great Chinese Famine was not only a problem of food supply, but also one of "entitlement" and food distribution among various socioeconomic groups (11). Therefore, socioeconomic confounders also need to be considered.

Other significant confounders of famine-era studies include further environmental exposures that may have caused great impact on health outcomes of disease. For example, the time period of The Great Famine was also a time when the People's Republic of China heavily endorsed and enforced The Great Leap policies, which emphasized not only grain farming, but also industrial steel production in the general population (12). Heavy metal exposure during this time was the greatest from 1959 to 1960.

[1]Jason J. Lee, MD, FRCPC: Western University, London, Ontario, Canada; [2]Zumin Shi, MD, PhD: Qatar University, Doha, Qatar.

No potential conflicts of interest relevant to this article were reported.

Address correspondence to Jason J. Lee, MD, 268 Grosvenor St., P.O Box 5777, London, Ontario N6A 4V2, Canada. Email: jlee2454@uwo.ca.

Submitted for publication October 30, 2020; accepted in revised form November 24, 2020.

Environmental exposures, such as heavy metals, are a known risk factor for developing RA (13), which further limits any nutritional inferences with regard to famine-era exposure and RA risk. Indeed, it has been shown that nutritional deprivation is not the only way that the immune system is altered during a famine or crisis, but exposure to stress in general may be a contributing factor. For example, stress in expectant mothers increases the risk of asthma in affected children, possibly related to altered glucocorticoid responses (14).

Based on these findings, several questions need to be answered. First, it is important to know whether famine modifies the association between RA and other health outcomes. It has been shown that Chinese famine exposure exacerbated the association between hypertension and cardiovascular disease (15). It is equally important to identify factors modifying the relationship between famine exposure and RA. Second, if the underlying mechanisms of RA are different for those exposed to famine than for those who were not exposed to famine, should the treatment and management also be different?

This historical examination of exposure to crisis in early life and future health risk is particularly relevant today. No matter what the single most important risk factor was at the time of crisis exposure, whether it be nutrition or otherwise, numerous studies of this kind have shown that early life exposure to historically stressful events increases the risk of chronic diseases like RA. Therefore, it is even more imperative for future prospective studies to identify modifiable risk factors and intervene before it is too late for future generations. Otherwise, history will indeed repeat itself.

AUTHOR CONTRIBUTIONS

Drs. Lee and Shi drafted the article, revised it critically for important intellectual content, and approved the final version to be published.

REFERENCES

1. Pope JE. What does the COVID-19 pandemic mean for rheumatology patients? [review]. Curr Treatm Opt Rheumatol 2020. E-pub ahead of print.
2. VanEvery H, Yang W, Olsen N, Zhang X, Shu R, Lu B, et al. In utero and early life exposure to the Great Chinese Famine and risk of rheumatoid arthritis in adulthood. Arthritis Rheumatol 2021;73: 596–603.
3. Lumey LH, Khalangot MD, Vaiserman AM. Association between type 2 diabetes and prenatal exposure to the Ukraine famine of 1932–33: a retrospective cohort study. Lancet Diabetes Endocrinol 2015;3:787–94.
4. Zhou J, Zhang L, Xuan P, Fan Y, Yang L, Hu C, et al. The relationship between famine exposure during early life and body mass index in adulthood: a systematic review and meta-analysis. PLoS One 2018;13:e0192212.
5. Wang Z, Zou Z, Dong B, Ma J, Arnold L. Association between the Great China Famine exposure in early life and risk of arthritis in adulthood. J Epidemiol Community Health 2018;72:790–5.
6. Dvir-Ginzberg M, Mobasheri A, Kumar A. The role of sirtuins in cartilage homeostasis and osteoarthritis. Curr Rheumatol Rep 2016;18:43.
7. Borradaile NM, Pickering JG. NAD(+), sirtuins, and cardiovascular disease. Curr Pharm Des 2009;15:110–7.
8. Zimmet P, Shi Z, El-Osta A, Ji L. Epidemic T2DM, early development and epigenetics: implications of the Chinese Famine [review]. Nat Rev Endocrinol 2018;14:738–46.
9. Shi Z. Gut microbiota: an important link between Western diet and chronic diseases [editorial]. Nutrients 2019;11:2287.
10. Li C, Lumey LH. Exposure to the Chinese famine of 1959–61 in early life and long-term health conditions: a systematic review and meta-analysis. Int J Epidemiol 2017;46:1157–70.
11. Lin JY, Yang DT. Food availability, entitlements and the Chinese famine of 1959–61. Economic J (London) 2000;110:136–58.
12. Yang DT. China's agricultural crisis and famine of 1959–1961: a survey and comparison to Soviet famines. Comp Econ Stud 2008;50:1–29.
13. Vihlborg P, Bryngelsson IL, Andersson L, Graff P. Risk of sarcoidosis and seropositive rheumatoid arthritis from occupational silica exposure in Swedish iron foundries: a retrospective cohort study. BMJ Open 2017;7:e016839.
14. Douros K, Moustaki M, Tsabouri S, Papadopoulou A, Papadopoulos M, Priftis KN. Prenatal maternal stress and the risk of asthma in children [review]. Front Pediatr 2017;5:202.
15. Shi Z, Nicholls SJ, Taylor AW, Magliano DJ, Appleton S, Zimmet P. Early life exposure to Chinese famine modifies the association between hypertension and cardiovascular disease. J Hypertens 2018;36:54–60.

American College of Rheumatology
Empowering Rheumatology Professionals

Arthritis & Rheumatology
Vol. 73, No. 4, April 2021, pp 568–575
DOI 10.1002/art.41572

Associations of Antibodies Targeting Periodontal Pathogens With Subclinical Coronary, Carotid, and Peripheral Arterial Atherosclerosis in Rheumatoid Arthritis

Jon T. Giles,[1] Jesper Reinholdt,[2] Felipe Andrade,[3] and Maximilian F. Konig[3]

Objective. Both periodontal disease and cardiovascular disease (CVD) are overrepresented in rheumatoid arthritis (RA). This study was undertaken to investigate the contribution of periodontal pathogens to CVD in RA.

Methods. RA patients underwent assessments of coronary artery calcification (CAC), carotid intima-media thickness and plaque, and ankle–brachial index via computed tomography, ultrasound, and Doppler ultrasound, respectively. Sera were assayed for antibodies targeting *Porphyromonas gingivalis* (Pg), *Aggregatibacter actinomycetemcomitans* serotype B (Aa), and Aa-derived leukotoxin A (LtxA). Associations of antibodies against these periodontal pathogens with measures of atherosclerosis were explored using generalized linear models.

Results. Among 197 RA patients, anti-Pg was detected in 72 patients (37%), anti-Aa in 41 patients (21%), and anti-LtxA in 84 patients (43%). Adjusting for relevant confounders and reported tooth loss, the mean CAC score was 90% higher in those with anti-Aa and/or anti-LtxA compared with those without either antibody (19 units versus 10 units; $P = 0.033$). The adjusted odds of CAC ≥100 units were 2.23-fold higher in those with anti-Aa and/or anti-LtxA compared with those without either antibody ($P = 0.040$). Anti-Aa and/or anti-LtxA seropositivity was significantly associated with all other assessed measures of atherosclerosis except carotid plaque. Anti-Pg was not associated with any measure of atherosclerosis. Higher swollen joint count was associated with CAC exclusively in the group with anti-Aa and/or anti-LtxA.

Conclusion. Immunoreactivity against Aa and/or its major virulence factor LtxA was associated with atherosclerosis in multiple vascular beds of RA patients and amplified the effect of swollen joints on coronary atherosclerosis, suggesting a role for treatment/prevention of periodontal disease in the prevention of CVD in RA.

INTRODUCTION

The burden of atherosclerotic cardiovascular disease (CVD) is greater in individuals with rheumatoid arthritis (RA) compared with those without RA (1). In addition to traditional CVD risk factors, a number of RA-associated factors, including seropositivity, RA duration, and measures of articular and systemic inflammation, have been associated with atherosclerotic burden (2–4). However, these factors do not account for all of the excess risk, suggesting that other mechanisms may contribute.

Periodontal disease and the bacterial pathogens that cause periodontitis are potential contributors to atherosclerotic CVD in RA. Periodontal disease is associated with both RA (5) and atherosclerosis (6), and links between the two have been proposed. In particular, pathogenic microbiota in the subgingival biofilm in periodontitis have been associated with systemic inflammation and immunoactivation (7). One such bacterial pathogen, *Porphyromonas gingivalis* (Pg), expresses numerous virulence factors that modulate host immune defenses, leading to overgrowth of oral commensal bacteria, which subsequently leads to inflammatory destruction of periodontal tissue (8). Gingival ulceration enables translocation of Pg into systemic circulation, which invades endothelial cells and leads to dysfunction. Moreover, locally produced proinflammatory cytokines and bacterial

The content of this paper is solely the responsibility of the authors and does not represent the official views of the NIH.

Supported by the Jerome L. Greene Foundation and the NIH (National Institute of Arthritis and Musculoskeletal and Skin Diseases grants AR-050026-01, T32-AR-048522-16A1, and R01-AR-069569).

[1]Jon T. Giles, MD, MPH: Columbia University Vagelos College of Physicians and Surgeons, New York, New York; [2]Jesper Reinholdt, PhD: Aarhus University, Aarhus, Denmark; [3]Felipe Andrade, MD, PhD, Maximilian F. Konig, MD: Johns Hopkins University, Baltimore, Maryland.

No potential conflicts of interest relevant to this article were reported.

Address correspondence to Jon T. Giles, MD, MPH, Columbia University College of Physicians and Surgeons, Division of Rheumatology, 630 West 168th Street, Physicians & Surgeons Building, Suite 3-450, New York, NY 10032. Email: jtg2122@columbia.edu.

Submitted for publication March 7, 2020; accepted in revised form October 27, 2020.

products (e.g., Pg lipopolysaccharide) can circulate and induce an acute-phase response (8,9). A second periodontitis-associated pathogen, *Aggregatibacter actinomycetemcomitans* (Aa), produces a highly virulent exotoxin with leukotoxic potential (leukotoxin A [LtxA]). The binding of LtxA to lymphocytes, neutrophils, and macrophages causes pyroptosis and activation of the inflammasome, releasing inflammatory cytokines and inducing secondary immunoactivation (10). Aa-derived LtxA is also a potent inducer of leukotoxic hypercitrullination (LTH) in neutrophils that is not caused by other periodontal pathogens (11,12). Moreover, RA sera contain autoantibodies directed against citrullinated autoantigens generated during LtxA-induced LTH (11).

Both pathogens have been implicated in atherogenesis. Microbial nucleic acids from both have been isolated from atheroma samples (13). Aa-associated LtxA induces the up-regulation of vascular adhesion molecules on endothelial cells (14), and atherosclerosis-prone mice infected with Aa have demonstrated up-regulation of vascular adhesion molecules, higher expression of inflammatory cytokines and chemokines in the wall of the aorta, and higher atherosclerotic plaque burden compared with uninfected mice (15). Multiple observational studies have linked periodontal disease and its associated pathogens, independently, with measures of subclinical atherosclerosis and CVD events (16), although causality remains questioned.

Considering these potential associations, we assessed immunoreactivity against Pg, Aa serotype B, and Aa-associated LtxA, and explored their associations with measures of atherosclerosis in the coronary, carotid, and peripheral arterial circulation, in RA patients. We hypothesized that RA patients with immunoreactivity against periodontal pathogens would demonstrate a greater burden of atherosclerosis in multiple vascular beds compared with those without such immunoreactivity.

PATIENTS AND METHODS

Patients. Participants were enrolled in the Evaluation of Subclinical Cardiovascular disease and Predictors of Events in RA (ESCAPE RA), a prospective cohort study investigating subclinical CVD in RA, previously described in detail (17,18). Patients met the 1987 American College of Rheumatology RA classification criteria (19) and were 45–84 years of age without known prior CVD events. Enrollment occurred between 2004 and 2006. All patients provided written informed consent prior to participation. The study was approved by the institutional review boards of the Johns Hopkins Medical Center and Columbia University Medical Center. Patient input was not directly involved in the design or conduct of the study.

Imaging of subclinical atherosclerosis. Coronary artery calcification (CAC) was measured with multidetector-row computed tomography as previously described (17), using the method described by Agatston et al (20). Scoring was conducted in a blinded manner with regard to group allocation and clinical characteristics. Carotid imaging was performed as previously described (18) and involved measures in the common carotid artery (CCA), internal carotid artery (ICA), and the carotid bulb. Carotid plaques were localized to the ICA and bulb and were defined as maximal focal protrusion into the lumen with reduction in the lumen diameter of >25%. Baseline and follow-up scans were reanalyzed concurrently by a single reader who was aware of the temporal ordering but unaware of clinical characteristics. The ankle–brachial index (ABI) was calculated as the ratio of the highest Doppler ultrasound–detected blood pressure of either the dorsalis pedis artery or posterior tibial artery, divided by the highest arm blood pressure, as previously described (21).

Sociodemographic characteristics and CVD risk factors. Demographic data and smoking history were obtained by self-reporting. Current use and dosage of medications were ascertained from prescription bottles. Body mass index (BMI) was calculated. Patients self-reported the current number of missing teeth.

Insulin resistance was evaluated using the homeostatic model assessment (HOMA) for insulin resistance index from the HOMA2 model (22). Hypertension was defined as systolic blood pressure ≥140 mm Hg, diastolic blood pressure ≥90 mm Hg, or antihypertensive medication use. Diabetes mellitus was defined as a fasting serum glucose level ≥126 mg/dl or antidiabetic medication use.

RA disease characteristics. Forty-four joints were examined by a trained assessor. RA disease duration was assessed from the self-reported date of diagnosis. RA disease activity was calculated with the Disease Activity Score in 28 joints using the C-reactive protein level (DAS28-CRP) (23). Current and past use of glucocorticoids and disease-modifying antirheumatic drugs was queried by detailed examiner-administered questionnaires. The Stanford Health Assessment Questionnaire (24) was used to assess disability related to common activities. Single-view anteroposterior radiographs of the hands and feet were scored, using the Sharp/van der Heijde method (25), by a trained radiologist.

Laboratory assessments. IgG antibodies against Aa strain HK1651 (serotype B), Pg strain W83, and purified LtxA were previously assessed in serum by enzyme-linked immunosorbent assay (ELISA). Anti-LtxA positivity was also confirmed by immunoprecipitation (11). High-sensitivity CRP and interleukin-6 were measured as previously described (26). Plasma lipids and glucose were measured by standard assays; low-density lipoprotein (LDL) cholesterol was estimated using the Friedewald equation. Rheumatoid factor (RF) and anti–cyclic citrullinated peptide antibodies were assessed by ELISA (seropositivity ≥40 units and ≥60 units, respectively). HLA alleles bearing the "shared epitope" were investigated by DRB1 sequencing as previously described (18).

Table 1. Patient characteristics according to the presence or absence of anti-Aa and/or anti-LtxA antibodies*

	Total (n = 197)	Negative for anti-Aa and anti-LtxA (n = 105)	Positive for anti-Aa and/or anti-LtxA (n = 92)
Age, mean ± SD years	59 ± 9	58 ± 8	61 ± 9
Male	79 (42)	40 (38)	39 (42)
White†	168 (85)	96 (91)	82 (78)
Any college	148 (76)	78 (74)	70 (77)
BMI, mean ± SD kg/m^2	28.5 ± 5.3	28.6 ± 5.0	28.3 ± 5.7
Ever smoking	116 (59)	64 (61)	52 (57)
Current smoking	23 (12)	9 (9)	14 (15)
Diabetes mellitus	12 (6)	6 (6)	6 (6)
Hypertension	105 (54)	55 (53)	50 (54)
Total cholesterol, mean ± SD mg/dl	194 ± 37	196 ± 34	192 ± 40
LDL cholesterol, mean ± SD mg/dl	116 ± 30	115 ± 29	116 ± 32
HDL cholesterol, mean ± SD mg/dl	54 ± 18	56 ± 20	52 ± 17
Triglycerides, mean (range) mg/dl	104 (68–149)	98 (74–151)	109 (66–144)
Current lipid-lowering medication	35 (15)	21 (20)	14 (15)
HOMA-IR, mean (range)	0.8 (0.5–1.4)	0.7 (0.5–1.35)	0.95 (0.55–1.4)
GFR, mean ± SD ml/minute	88 ± 22	89 ± 22	87 ± 23
Homocysteine, mean (range) μmoles/liter	9.0 (7.5–10.6)	8.9 (7.5–10.4)	9.2 (7.5–11.1)
RA duration, mean (range) years	9 (5–17)	10 (4–17)	8 (5–18)
RF ≥40 units‡	130 (66)	60 (57)	70 (76)
Anti-CCP ≥60 units	140 (71)	72 (69)	68 (74)
Any shared epitope alleles	136 (70)	74 (70)	62 (69)
DAS28-CRP, mean (range)	3.6 (2.9–4.3)	3.6 (2.9–4.4)	3.7 (2.9–4.3)
SJC (of 42 joints), mean (range)	7 (3–10)	7 (3–11)	6 (3–10)
TJC (of 44 joints), mean (range)	6 (2–13)	6 (2–13)	6 (2–12)
CRP, mean (range) mg/dl	2.6 (1.1–7.6)	2.8 (1.1–7.0)	2.4 (1.2–7.9)
IL-6, mean (range) pg/ml	3.9 (1.8–8.2)	3.7 (1.6–8.1)	4.3 (1.8–8.4)
HAQ, mean (range)	0.62 (0.12–1.25)	0.62 (0.12–1.25)	0.75 (0.12–1.50)
Total mSvdH score, mean (range)	8 (0–42)	7 (0–36)	11 (1–52)
Current prednisone	76 (39)	44 (42)	32 (35)
Cumulative prednisone dose, mean (range) gm	3.1 (0–9.5)	3.2 (0–10.1)	2.9 (0–8.7)
Nonbiologic DMARDs	165 (84)	90 (86)	75 (82)
MTX	125 (63)	64 (61)	61 (66)
HCQ	47 (24)	29 (28)	18 (20)
Biologic DMARDs	90 (46)	54 (51)	36 (40)
TNFi	86 (44)	52 (50)	34 (37)
Anti-Pg–positive§	72 (37)	31 (30)	41 (45)
No. of missing teeth¶			
None	34 (18)	24 (24)	10 (12)
1–9	119 (65)	62 (61)	57 (70)
10–31	17 (9)	6 (6)	11 (13)
32	14 (8)	9 (9)	4 (5)

* Except where indicated otherwise, values are the number (%) of patients. BMI = body mass index; LDL = low-density lipoprotein; HDL = high-density lipoprotein; HOMA-IR = homeostatic model assessment for insulin resistance; GFR = glomerular filtration rate; RA = rheumatoid arthritis; RF = rheumatoid factor; anti-CCP = anti–cyclic citrullinated peptide; DAS28-CRP = Disease Activity Score in 28 joints using the C-reactive protein level; SJC = swollen joint count; TJC = tender joint count; IL-6 = interleukin-6; HAQ = Health Assessment Questionnaire; mSvdH = modified Sharp/van der Heijde; DMARDs = disease-modifying antirheumatic drugs; MTX = methotrexate; HCQ = hydroxychloroquine; TNFi = tumor necrosis factor inhibitor; anti-Pg = anti–*Porphyromonas gingivalis*.
† $P = 0.009$ for patients positive for anti–*Aggregatibacter actinomycetemcomitans* (anti-Aa) and/or anti–leukotoxin A (anti-LtxA) versus patients negative for anti-Aa and anti-LtxA.
‡ $P = 0.005$ for patients positive for anti-Aa and/or anti-LtxA versus patients negative for anti-Aa and anti-LtxA.
§ $P = 0.029$ for patients positive for anti-Aa and/or anti-LtxA versus patients negative for anti-Aa and anti-LtxA.
¶ $P = 0.042$ for patients positive for anti-Aa and/or anti-LtxA versus patients negative for anti-Aa and anti-LtxA (data available for 184 patients).

Statistical analysis. Exposure to leukotoxic Aa strains was defined as having either anti-Aa or anti-LtxA. Exposure to leukotoxic Aa strains other than serotype B strains was captured in those who were seropositive for anti-LtxA but seronegative for anti-Aa HK1651 (ATCC 700685). Variables were examined according to the presence or absence of immunoreactivity against Aa and/or LtxA and Pg using *t*-tests for normally distributed continuous variables, the Kruskal-Wallis

test for non-normally distributed variables, and the chi-square goodness-of-fit test or Fisher's exact test, as appropriate, for categorical variables. The association of anti-Aa and/or anti-LtxA seropositivity with CAC, normally transformed as natural log (CAC + 1), was explored using multivariable linear regression, first in a crude model with anti-Aa and/or anti-LtxA positivity as the only covariate. Next, variables associated with CAC at the $P < 0.20$ level from univariate models were modeled. A reduced model was derived by excluding noncontributory covariates using Akaike's information criterion for nested models.

An additional sensitivity analysis included the number of reported missing teeth in order to ensure that observed associations of anti-Aa and/or anti-LtxA and CAC from prior models were not confounded by the presence of oral diseases, including periodontal disease and other causes of tooth loss. The normality assumption required for linear regression was tested using the Shapiro-Wilk test on the studentized residuals. Similar modeling was used for the other atherosclerosis outcomes, except for logistic regression for CAC >0 units, CAC ≥100 units, and carotid plaque presence. The intima-medial thickness (IMT) of the CCA (CCA-IMT) and the ICA (ICA-IMT) also required log transformation. The same models were repeated with anti-Pg as the covariate of interest. For all models, adjusted means and frequencies and their associated 95% confidence intervals were derived and graphed according to immunoreactivity against periodontal pathogens, with back transformation as appropriate. Next, we explored whether anti-Aa and/or anti-LtxA status modified the associations of other covariates with atherosclerosis outcomes by introducing anti-Aa and/or anti-LtxA × covariate interaction terms into the models, with *P* values for interaction terms derived using analysis of covariance. Stata SE 16 was used. A significance level of $\alpha \leq 0.05$ (2-tailed) was used throughout.

RESULTS

Patient characteristics. Among the 197 RA patients evaluated, anti-Aa serotype B was detected in 41 patients (21%), while anti-LtxA was detected in 84 patients (43%). Only 8 patients with anti-Aa were seronegative for anti-LtxA. Anti-Pg was detected in 72 patients (37%). Baseline characteristics according to anti-Aa and/or anti-LtxA status are summarized in Table 1. Those with anti-Aa and/or anti-LtxA were a mean 3 years older than those without anti-Aa and/or anti-LtxA and were significantly less likely to be white. Those with anti-Aa and/or anti-LtxA did not differ significantly on other lifestyle characteristics, CVD risk factors, or RA disease features, with the exception of a significantly higher prevalence of RF seropositivity in patients with anti-Aa and/or anti-LtxA compared to those without. Those with anti-Aa and/or anti-LtxA were significantly more likely to be anti-Pg seropositive and have more reported tooth loss.

Association of atherosclerosis with anti-Aa and anti-LtxA in RA but not with anti-Pg. The univariate associations of Aa-directed, LtxA-directed, and Pg-directed serologic status with measures of coronary, carotid, and peripheral arterial atherosclerosis are summarized in Table 2. The median CAC score was 30 units higher among those with anti-Aa and/or anti-LtxA compared with those without ($P = 0.046$). Likewise, the prevalence of any CAC or having a CAC of ≥100 units was higher among those with anti-Aa and/or anti-LtxA. Similarly, both the median CCA-IMT and ICA-IMT, but not the frequency of carotid plaque, were significantly higher for those with anti-Aa and/or anti-LtxA. For peripheral arteries, median ABI was significantly lower among RA patients with anti-Aa and/or anti-LtxA. In contrast, anti-Pg was not significantly associated with any measure of atherosclerosis.

Table 2. Crude associations of antibodies against periodontal pathogens with measures of coronary, carotid, and peripheral atherosclerosis*

	Negative for anti-Aa and anti-LtxA (n = 105)	Positive for anti-Aa and/or anti-LtxA (n = 92)	*P*	Negative for anti-Pg (n = 125)	Positive for anti-Pg (n = 71)	*P*
CAC						
CAC score, median (IQR) units	0 (0–134)	30 (0–215)	0.046	3 (0–161)	5 (0–202)	0.71
CAC score >0 units, no. (%)	50 (48)	56 (62)	0.041	66 (53)	40 (57)	0.56
CAC score ≥100 units, no. (%)	31 (30)	38 (42)	0.064	43 (34)	26 (37)	0.70
Carotid ultrasound						
CCA-IMT, median (IQR) mm	0.80 (0.74–0.88)	0.85 (0.76–0.94)	0.020	0.81 (0.73–0.90)	0.85 (0.76–0.94)	0.11
ICA-IMT, median (IQR) mm	1.02 (0.81–1.41)	1.22 (0.86–1.61)	0.042	1.13 (0.84–1.51)	1.07 (0.84–1.65)	0.74
Plaque, no. (%)	19 (18)	23 (26)	0.21	26 (21)	16 (23)	0.74
ABI, median (IQR)	1.18 (1.10–1.26)	1.13 (1.05–1.21)	0.035	114 (1.07–1.24)	1.16 (1.06–1.22)	0.93

* CAC = coronary artery calcification; IQR = interquartile range; CCA = common carotid artery; IMT = intima-medial thickness; ICA = internal carotid artery; ABI = ankle–brachial index (see Table 1 for other definitions).

Table 3. Multivariable indicators of log (CAC + 1)*

	Model 1		Model 2		Model 3		Model 4	
	β	*P*	β	*P*	β	*P*	β	*P*
Positive for anti-Aa and/or anti-LtxA	0.76	0.049	0.68	0.036	0.64	0.033	0.72	0.023
Age, per year	–	–	0.12	<0.001	0.12	<0.001	0.11	<0.001
Male sex	–	–	1.76	<0.001	1.86	<0.001	1.85	<0.001
White ethnicity	–	–	0.17	0.72	–	–	–	–
Ever smoking	–	–	0.68	0.044	0.68	0.035	0.83	0.019
Current smoking	–	–	−0.33	0.52	–	–	–	–
BMI, per kg/m^2	–	–	0.058	0.11	0.049	0.092	0.038	0.23
Diabetes mellitus	–	–	0.57	0.44	–	–	–	–
SBP, per mm Hg	–	–	−0.0075	0.44	–	–	–	–
Antihypertensive medication use	–	–	0.49	0.16	–	–	–	–
HDL cholesterol, per mg/dl	–	–	−0.0020	0.87	–	–	–	–
Log triglycerides	–	–	0.62	0.057	0.53	0.056	0.69	0.020
Statin use	–	–	1.11	0.011	1.14	0.005	1.21	0.004
GFR, per ml/minute	–	–	0.0062	0.56	–	–		
Log homocysteine	–	–	0.46	0.50	–	–		
RA duration, per year	–	–	0.042	0.009	0.037	0.011	0.041	0.010
RF >40 units	–	–	0.19	0.61	–	–		
SJC, per joint	–	–	0.052	0.11	0.068	0.024	0.074	0.021
Log CRP level	–	–	0.039	0.76	–	–	–	–
HCQ use	–	–	−0.16	0.68	–	–	–	–
Biologic medication use	–	–	0.20	0.53	–	–	–	–
No. of missing teeth								
None	–	–	–	–	–	–	Referent	–
1–9	–	–	–	–	–	–	0.12	0.78
10–31	–	–	–	–	–	–	0.085	0.90
32	–	–	–	–	–	–	–	–

* CAC = coronary artery calcification; SBP = systolic blood pressure (see Table 1 for other definitions).

Association of atherosclerosis with anti-Aa and anti-LtxA after adjustment for potential confounders. Seropositivity for anti-Aa and/or anti-LtxA remained significantly associated with CAC in models adjusted for all of the characteristics associated with CAC in univariate models (Table 3; model 2) and in a reduced model (Table 3; model 3). Here, the magnitude of the independent association of anti-Aa and/or anti-LtxA seropositivity with CAC was equivalent to ~5 years increment in age or ever having smoked. In model 3, longer RA duration and higher swollen joint counts were both significantly associated with CAC. After adjustment for age, sex, ever smoking, BMI, triglyceride level, statin use, RA duration, and swollen joint count, the adjusted mean CAC score was 90% higher in the group with anti-Aa and/or anti-LtxA compared to the group without (19 units versus 10 units; $P = 0.033$) (Figure 1A). With adjustment for these same covariates, anti-Aa and/or anti-LtxA seropositivity was significantly associated with CAC >0 units (Figure 1B), CAC ≥100 units (Figure 1C), and CCA-IMT (Figure 2A), and was inversely associated with ABI (Figure 2C). The association of anti-Aa and/or anti-LtxA seropositivity with ICA-IMT was higher, but not quite statistically significant, after adjustment (Figure 2B). Reported tooth loss was not associated with CAC and did not modify the association of anti-Aa and/or anti-LtxA with CAC when comodeled (Table 3; model 4).

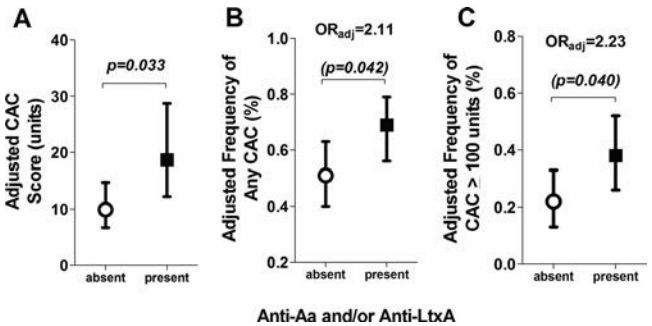

Figure 1. Associations between anti–*Aggregatibacter actinomycetemcomitans* (anti-Aa) and/or anti–leukotoxin A (anti-LtxA) antibodies and measures of coronary atherosclerosis, including adjusted coronary artery calcification (CAC) score (**A**), frequency of any CAC (**B**), and frequency of a CAC score >100 units (**C**). Data were adjusted for age, sex, smoking history, body mass index, triglycerides, statin use, rheumatoid arthritis duration, and swollen joint count. Bars show the mean and 95% confidence interval. OR$_{adj}$ = adjusted odds ratio.

Association of swollen joints with coronary atherosclerosis only in RA patients positive for anti-Aa and/or anti-LtxA. Next, we studied whether seropositivity for anti-Aa and/or anti-LtxA modified the associations of any other characteristics associated with atherosclerosis (Supplementary Table 1, on the *Arthritis & Rheumatology* website at http://onlinelibrary.wiley.com/doi/10.1002/art.41572/abstract). Among the characteristics associated with measures of atherosclerosis, only the

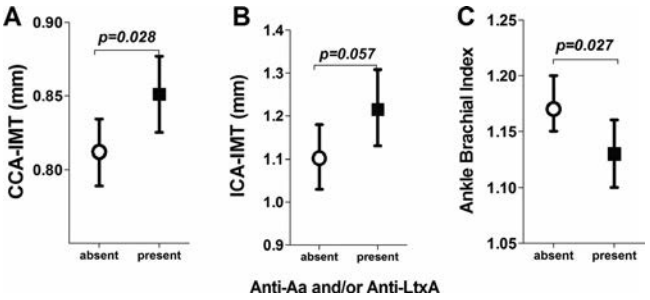

Figure 2. Associations between anti-Aa and/or anti-LtxA antibodies and measures of carotid and peripheral arterial atherosclerosis, including common carotid artery intima-media thickness (CCA-IMT) (**A**), internal carotid artery IMT (**B**), and ankle–brachial index (**C**). Data were adjusted for age, sex, smoking history, body mass index, triglycerides, statin use, rheumatoid arthritis duration, and swollen joint count. Bars show the mean and 95% confidence interval. See Figure 1 for other definitions.

association of swollen joint count with CAC differed according to anti-Aa and/or anti-LtxA status, such that higher swollen joint count was strongly associated with higher CAC score (Figure 3A) and with higher frequency of CAC ≥100 units (Figure 3B) among those seropositive for anti-Aa and/or anti-LtxA. The association was not linear, as the inflection of the association of swollen joints with CAC occurred at ~7 or 8 swollen joints (Figure 3). In contrast, a higher number of swollen joints was not associated with CAC among those without anti-Aa and anti-LtxA.

A significant interaction was also observed when the DAS28 was modeled instead of swollen joint count; however, substitution of tender joint count or CRP did not show an interaction with anti-Aa and/or anti-LtxA status (data not shown), suggesting that the association of the DAS28 with measures of CAC among those with anti-Aa and/or anti-LtxA was due to swollen joint count and not the other components of the DAS28 score. This modification

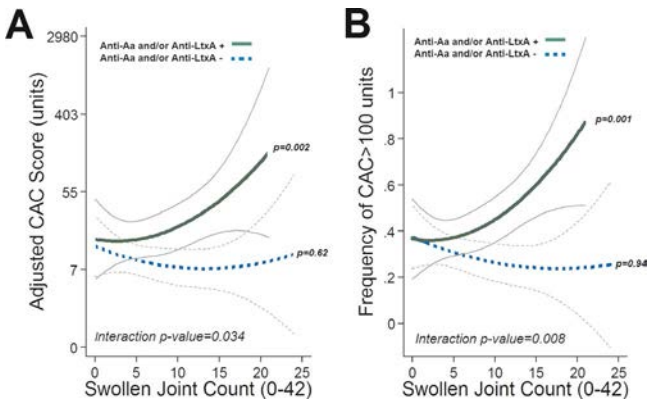

Figure 3. Differential association between swollen joint count and measures of coronary atherosclerosis, including adjusted CAC score (**A**) and frequency of a CAC score >100 units (**B**), according to the anti-Aa and/or anti-LtxA antibody status. Data were adjusted for age, sex, smoking history, body mass index, triglycerides, statin use, rheumatoid arthritis duration, and swollen joint count. Quadratic fit lines and 95% confidence intervals are shown. See Figure 1 for definitions.

was observed only for CAC and not for measures of carotid or peripheral arterial atherosclerosis (data not shown). The associations of anti-Aa and/or anti-LtxA with the atherosclerosis outcomes did not differ according to anti–citrullinated protein antibody (ACPA) or shared epitope status (data not shown).

DISCUSSION

To our knowledge, this is the first study linking atherosclerosis burden in RA with immunoreactivity against common periodontal pathogens. RA patients with serologic evidence of Aa exposure by either anti-Aa or its leukotoxin (LtxA) had significantly higher levels of CAC (a surrogate for coronary atherosclerosis), thicker carotid IMT (a surrogate for carotid atherosclerosis), and lower ABI (a surrogate for peripheral arterial atherosclerosis), even after adjustment for relevant confounders. Importantly, seropositivity for anti-Pg was not associated with any measure of atherosclerosis. Interestingly, an association of higher swollen joint count with CAC was observed only in the subgroup who were seropositive for anti-Aa and/or anti-LtxA.

Multiple studies have established a link between periodontal disease and RA. In a recent meta-analysis (5), the frequency of periodontitis was 13% higher in RA patients than in non-RA controls. Both anti-Aa and anti-Pg were more prevalent in RA patients compared with controls in certain studies (11,27,28), with some (but not all) demonstrating correlations with ACPA and disease activity (27). Anti-Pg levels were higher among patients at risk of developing RA compared with those not at risk (29), and levels correlated with RA-associated antibodies. In a smaller study that included periodontal sampling, the abundance of Pg at both healthy and inflamed periodontal sites was significantly higher among ACPA-positive individuals at risk of developing RA, compared with healthy controls (30). However, Aa abundance was not significantly higher, although differences may have been affected by the small sample size of the study (n = 48 at-risk subjects and n = 32 controls), ethnicity (31), and restriction of Aa to nonperiodontal oral reservoirs (31). Taken together, findings from these studies provide some argument for an increased prevalence of periodontitis and periodontitis-associated pathogens in RA and circumstantial links to disease risk and severity.

Periodontitis has been linked to atherosclerosis in the general population (16). CVD events were higher among those with periodontitis (32), and carotid atherosclerosis was linked to severe periodontitis (33). DNA from periodontal pathogens, including Aa and Pg, was isolated from atheroma in several (13) (but not all [34]) studies, particularly among those with chronic advanced periodontitis. Across several studies of atherosclerosis-prone mice (15), intravenous inoculation with Aa was associated with endothelial invasion and activation, LDL oxidation, Toll-like receptor activation, up-regulation of inflammatory cytokines and chemokines, and promotion of macrophage foam cell formation. In one study, Pg was associated with promotion of

plaque rupture through up-regulation of metalloproteinases (35). Colhoun et al reported that high levels of circulating anti-Aa and anti-Pg were associated with higher CAC scores (36), an association primarily observed among the subgroup with diabetes, suggesting interaction with other CVD risk factors. RA has been described as a diabetes equivalent for risk of CVD and may represent a population in which the effect of periodontal pathogens on atherogenesis is heightened.

In the present study, we did not observe an association of anti-Pg with any measure of atherosclerosis, which could indicate specificity in the effect related to only Aa in RA. This finding could also be unique to the cohort studied and thus requires confirmation in other cohorts. However, anti-Pg was as prevalent as anti-Aa in our sample and did not confound any of the associations of anti-Aa and/or anti-LtxA with measures of atherosclerosis when comodeled.

We also observed that higher swollen joint counts were associated with CAC only among RA patients with reactivity against Aa or LtxA. This interaction suggests that Aa infection may create a permissive environment for the inflammatory features of RA to contribute to atherogenesis, and it raises the possibility that anti-Aa status could be used to identify a subgroup of RA patients for whom aggressive control of synovitis may lead to a lower rate of atherosclerosis progression. Importantly, the interaction was specific to swollen joints and did not extend to tender joint count or circulating CRP. The mechanism underlying this interaction is unclear and warrants additional study. However, other types of effect modification in which anti-Aa status appeared to create a permissive environment for RA features have been noted in prior studies, where HLA–DRB1 shared epitope alleles were associated with higher levels of ACPA only among RA patients with anti-Aa (11,37), although such conditional associations have not been observed in all studies (28).

Our study has several notable strengths and weaknesses. Among the strengths, it is the first study of the association of periodontal pathogens with CVD in RA. Additionally, we measured atherosclerosis in multiple vascular beds, with confirmation of associations across vascular territories. Among the weaknesses, the cross-sectional design does not allow for firm conclusions regarding causality to be made. Since the point of seroconversion to reactivity against the periodontal pathogens was unknown, cumulative exposure could not be assessed. Because other periodontal pathogens may also contribute to atherogenesis, it is not clear whether any of the observed associations were specific to Aa or to the confounding effects of an unmeasured correlated causal factor. However, the finding that anti-Pg was not associated with atherosclerosis suggests that the associations of Aa with measures of atherosclerosis were not strongly confounded by other periodontal pathogens, though the possibility of confounding by other periodontal pathogens is not fully excluded. Finally, since we did not compare these associations in a group without RA, we cannot assert that our findings are specific to RA.

In summary, RA patients with evidence of exposure to Aa but not Pg had higher levels of atherosclerosis across multiple vascular beds independent of other CVD risk factors. The association of swollen joints with coronary atherosclerosis was restricted to RA patients with seroreactivity to anti-Aa and/or anti-LtxA. Although speculative, these findings suggest that assessing immunity against Aa may predict CVD in RA patients and that Aa-exposed patients may be appropriate for heightened CVD screening and primary prevention. However, confirmation in additional cohorts and studies demonstrating prediction and clinical utility are required before Aa immunoreactivity can be considered appropriate for clinical practice. At minimum, our study provides evidence that mechanistic studies assessing the links between periodontitis and CVD in RA are warranted.

ACKNOWLEDGMENT

We are grateful to Dr. Joan Bathon for access to data and samples from the ESCAPE RA cohort.

AUTHOR CONTRIBUTIONS

All authors were involved in drafting the article or revising it critically for important intellectual content, and all authors approved the final version to be published. Dr. Giles had full access to all of the data in the study and takes responsibility for the integrity of the data and the accuracy of the data analysis.

Study conception and design. Giles, Reinholdt, Andrade, Konig.
Acquisition of data. Giles, Reinholdt, Andrade, Konig.
Analysis and interpretation of data. Giles, Reinholdt, Andrade, Konig.

REFERENCES

1. Avina-Zubieta JA, Thomas J, Sadatsafavi M, Lehman AJ, Lacaille D. Risk of incident cardiovascular events in patients with rheumatoid arthritis: a meta-analysis of observational studies. Ann Rheum Dis 2012;71:1524–9.
2. Chung CP, Oeser A, Raggi P, Gebretsadik T, Shintani AK, Sokka T, et al. Increased coronary-artery atherosclerosis in rheumatoid arthritis: relationship to disease duration and cardiovascular risk factors. Arthritis Rheum 2005;52:3045–53.
3. Karpouzas GA, Malpeso J, Choi TY, Li D, Munoz S, Budoff MJ. Prevalence, extent and composition of coronary plaque in patients with rheumatoid arthritis without symptoms or prior diagnosis of coronary artery disease. Ann Rheum Dis 2014;73:1797–804.
4. Giles JT, Post WS, Blumenthal RS, Polak J, Petri M, Gelber AC, et al. Longitudinal predictors of progression of carotid atherosclerosis in rheumatoid arthritis. Arthritis Rheum 2011;63:3216–25.
5. Fuggle NR, Smith TO, Kaul A, Sofat N. Hand to mouth: a systematic review and meta-analysis of the association between rheumatoid arthritis and periodontitis. Front Immunol 2016;7:80.
6. Mustapha IZ, Debrey S, Oladubu M, Ugarte R. Markers of systemic bacterial exposure in periodontal disease and cardiovascular disease risk: a systematic review and meta-analysis. J Periodontol 2007;78:2289–302.
7. Silva N, Abusleme L, Bravo D, Dutzan N, Garcia-Sesnich J, Vernal R, et al. Host response mechanisms in periodontal diseases [review]. J Appl Oral Sci 2015;23:329–55.
8. How KY, Song KP, Chan KG. Porphyromonas gingivalis: an overview of periodontopathic pathogen below the gum line [review]. Front Microbiol 2016;7:53.
9. Amar S, Engelke M. Periodontal innate immune mechanisms relevant to atherosclerosis [review]. Mol Oral Microbiol 2015; 30:171–85.

10. Shenker BJ, Ojcius DM, Walker LP, Zekavat A, Scuron MD, Boesze-Battaglia K. Aggregatibacter actinomycetemcomitans cytolethal distending toxin activates the NLRP3 inflammasome in human macrophages, leading to the release of proinflammatory cytokines. Infect Immun 2015;83:1487–96.
11. Konig MF, Abusleme L, Reinholdt J, Palmer RJ, Teles RP, Sampson K, et al. Aggregatibacter actinomycetemcomitans-induced hypercitrullination links periodontal infection to autoimmunity in rheumatoid arthritis. Sci Transl Med 2016;8:369ra176.
12. Konig MF, Andrade F. A critical reappraisal of neutrophil extracellular traps and NETosis mimics based on differential requirements for protein citrullination. Front Immunol 2016;7:461.
13. Haraszthy VI, Zambon JJ, Trevisan M, Zeid M, Genco RJ. Identification of periodontal pathogens in atheromatous plaques. J Periodontol 2000;71:1554–60.
14. Dietmann A, Millonig A, Combes V, Couraud PO, Kachlany SC, Grau GE. Effects of Aggregatibacter actinomycetemcomitans leukotoxin on endothelial cells. Microb Pathog 2013;61–2:43–50.
15. Zhang T, Kurita-Ochiai T, Hashizume T, Du Y, Oguchi S, Yamamoto M. Aggregatibacter actinomycetemcomitans accelerates atherosclerosis with an increase in atherogenic factors in spontaneously hyperlipidemic mice. FEMS Immunol Med Microbiol 2010;59:143–51.
16. Lockhart PB, Bolger AF, Papapanou PN, Osinbowale O, Trevisan M, Levison ME, et al. Periodontal disease and atherosclerotic vascular disease: does the evidence support an independent association? A scientific statement from the American Heart Association. Circulation 2012;125:2520–44.
17. Giles JT, Szklo M, Post W, Petri M, Blumenthal RS, Lam G, et al. Coronary arterial calcification in rheumatoid arthritis: comparison to the multi-ethnic study of atherosclerosis. Arthritis Res Ther 2009;11:R36.
18. Kobayashi H, Giles JT, Polak JF, Blumenthal RS, Leffell MS, Szklo M, et al. Increased prevalence of carotid artery atherosclerosis in rheumatoid arthritis is artery-specific. J Rheumatol 2010;37:730–9.
19. Arnett FC, Edworthy SM, Bloch DA, McShane DJ, Fries JF, Cooper NS, et al. The American Rheumatism Association 1987 revised criteria for the classification of rheumatoid arthritis. Arthritis Rheum 1988;31:315–24.
20. Agatston AS, Janowitz WR, Hildner FJ, Zusmer NR, Viamonte M, Detrano R. Quantification of coronary-artery calcium using ultrafast computed-tomography. J Am Coll Cardiol 1990;15:827–32.
21. Allison MA, Criqui MH, McClelland RL, Scott JM, McDermott MM, Liu K, et al. The effect of novel cardiovascular risk factors on the ethnic-specific odds for peripheral arterial disease in the Multi-Ethnic Study of Atherosclerosis (MESA). J Am Coll Cardiol 2006;48:1190–7.
22. Wallace TM, Levy JC, Matthews DR. Use and abuse of HOMA modeling [review]. Diabetes Care 2004;27:1487–95.
23. Prevoo ML, van 't Hof MA, Kuper HH, van Leeuwen MA, van de Putte LB, van Riel PL. Modified disease activity scores that include twenty-eight–joint counts: development and validation in a prospective longitudinal study of patients with rheumatoid arthritis. Arthritis Rheum 1995;38:44–8.
24. Fries JF, Spitz PW, Kraines RG, Holman HR. Measurement of patient outcome in arthritis. Arthritis Rheum 1980;23:137–45.
25. Van der Heijde D. How to read radiographs according to the Sharp/van der Heijde method. J Rheumatol 2000;27:261–3.
26. Nettleton JA, Steffen LM, Mayer-Davis EJ, Jenny NS, Jiang R, Herrington DM, et al. Dietary patterns are associated with biochemical markers of inflammation and endothelial activation in the Multi-Ethnic Study of Atherosclerosis (MESA). Am J Clin Nutr 2006;83:1369–79.
27. Mikuls TR, Payne JB, Yu F, Thiele GM, Reynolds RJ, Cannon GW, et al. Periodontitis and Porphyromonas gingivalis in patients with rheumatoid arthritis. Arthritis Rheumatol 2014;66:1090–100.
28. Volkov M, Dekkers J, Loos BG, Bizzarro S, Huizinga TW, Praetorius HA, et al. Comment on "Aggregatibacter actinomycetemcomitans-induced hypercitrullination links periodontal infection to autoimmunity in rheumatoid arthritis" [letter]. Sci Transl Med 2018;10:eaan8349.
29. Mikuls TR, Thiele GM, Deane KD, Payne JB, O'Dell JR, Yu F, et al. Porphyromonas gingivalis and disease-related autoantibodies in individuals at increased risk of rheumatoid arthritis. Arthritis Rheum 2012;64:3522–30.
30. Mankia K, Cheng Z, Do T, Hunt L, Meade J, Kang J, et al. Prevalence of periodontal disease and periodontopathic bacteria in anti–cyclic citrullinated protein antibody–positive at-risk adults without arthritis. JAMA Netw Open 2019;2:e195394.
31. Fine DH, Markowitz K, Furgang D, Fairlie K, Ferrandiz J, Nasri C, et al. Aggregatibacter actinomycetemcomitans and its relationship to initiation of localized aggressive periodontitis: longitudinal cohort study of initially healthy adolescents. J Clin Microbiol 2007;45:3859–69.
32. Fedele S, Sabbah W, Donos N, Porter S, D'Aiuto F. Common oral mucosal diseases, systemic inflammation, and cardiovascular diseases in a large cross-sectional US survey. Am Heart J 2011;161:344–50.
33. Beck JD, Elter JR, Heiss G, Couper D, Mauriello SM, Offenbacher S. Relationship of periodontal disease to carotid artery intima-media wall thickness: the Atherosclerosis Risk in Communities (ARIC) study. Arterioscler Thromb Vasc Biol 2001;21:1816–22.
34. Ott SJ, El Mokhtari NE, Musfeldt M, Hellmig S, Freitag S, Rehman A, et al. Detection of diverse bacterial signatures in atherosclerotic lesions of patients with coronary heart disease. Circulation 2006;113:929–37.
35. Kuramitsu HK, Qi M, Kang IC, Chen W. Role for periodontal bacteria in cardiovascular diseases. Ann Periodontol 2001;6:41–7.
36. Colhoun HM, Slaney JM, Rubens MB, Fuller JH, Sheiham A, Curtis MA. Antibodies to periodontal pathogens and coronary artery calcification in type 1 diabetic and nondiabetic subjects. J Periodontal Res 2008;43:103–10.
37. Konig MF, Giles JT, Teles RP, Moutsopoulos NM, Andrade F. Response to comment on "Aggregatibacter actinomycetemcomitans-induced hypercitrullination links periodontal infection to autoimmunity in rheumatoid arthritis" [letter]. Sci Transl Med 2018;10:eaao3031.

American College of Rheumatology
Empowering Rheumatology Professionals

Arthritis & Rheumatology
Vol. 73, No. 4, April 2021, pp 576–586
DOI 10.1002/art.41554

Distinct Expression of Coinhibitory Molecules on Alveolar T Cells in Patients With Rheumatoid Arthritis–Associated and Idiopathic Inflammatory Myopathy–Associated Interstitial Lung Disease

Maho Nakazawa,[1] Katsuya Suzuki,[1] Masaru Takeshita,[1] Jun Inamo,[1] Hirofumi Kamata,[1] Makoto Ishii,[1] Yoshitaka Oyamada,[2] Hisaji Oshima,[2] and Tsutomu Takeuchi[1]

Objective. To identify immunologic factors in the lungs of patients with rheumatoid arthritis–associated interstitial lung disease (RA-ILD) and patients with idiopathic inflammatory myopathy–associated ILD (IIM-ILD) and to examine their pathologic mechanisms.

Methods. Eleven patients with RA-ILD, 16 with IIM-ILD, 6 with drug-induced ILD (DI-ILD), and 8 healthy controls were enrolled. Peripheral blood (PB) and bronchoalveolar lavage (BAL) fluid were immunophenotyped by flow cytometry. Alveolar macrophages (AMs) were analyzed by coculture assay with PB naive CD4+ T cells from healthy individuals and RNA sequencing.

Results. Several coinhibitory molecules were coexpressed on BAL fluid T cells (CTLA-4, programmed death 1 [PD-1], T cell immunoglobulin and mucin domain–containing protein 3 [TIM-3], and lymphocyte activation gene 3 protein, from most to least), whereas only PD-1 was expressed on PB T cells. CTLA-4+PD-1+CD4+ T cells were characteristic of RA-ILD, whereas CTLA-4+PD-1+TIM-3+CD8+ T cells were characteristic of IIM-ILD. BAL fluid PD-1+CD4+ T cells rarely expressed CXCR5, but their levels correlated with levels of plasmablasts and plasma cells ($\rho = 0.57$, $P = 0.006$), indicating that most of them would be considered peripheral helper T cells. In coculture experiments, AMs from patients with RA-ILD and IIM-ILD induced more PD-1 and TIM-3 on T cells ($P < 0.05$), suggesting that coinhibitory molecule expression on BAL fluid T cells was partly due to AMs. RNA sequencing showed significant down-regulation of PD ligand 1/2 genes in AMs from patients with RA-ILD compared to those with DI-ILD.

Conclusion. We have identified differences in coinhibitory molecule expression between patients with RA-ILD and those with IIM-ILD. PD-1 on T cells in RA-ILD and TIM-3 on CD8+ T cells in IIM-ILD might be key factors in the disease process. Evaluation of coinhibitory molecules on BAL fluid T cells could be clinically useful.

INTRODUCTION

Interstitial lung disease (ILD) is a common extraarticular manifestation of rheumatoid arthritis (RA), occurring in ~10–30% of patients (1). It is also the most common nonmusculoskeletal manifestation of idiopathic inflammatory myopathy (IIM), including polymyositis, dermatomyositis, and clinically amyopathic dermatomyositis, in which it has been demonstrated in 25–75% of patients (2). Since RA-associated ILD (RA-ILD) and IIM-associated ILD (IIM-ILD) have high mortality rates, elucidating their etiology and identifying treatment strategies is important (2–4). Although serum biomarkers associated with RA-ILD and IIM-ILD have been

Supported by intramural research funding from Keio University School of Medicine and the National Tokyo Medical Center.

[1]Maho Nakazawa, MD, Katsuya Suzuki, MD, PhD, Masaru Takeshita, MD, PhD, Jun Inamo, MD, Hirofumi Kamata, MD, PhD, Makoto Ishii, MD, PhD, Tsutomu Takeuchi, MD, PhD: Keio University School of Medicine, Tokyo, Japan; [2]Yoshitaka Oyamada, MD, PhD, Hisaji Oshima, MD, PhD: National Hospital Organization Tokyo Medical Center, Tokyo, Japan.

Dr. Suzuki has received consulting fees, speaking fees, and/or honoraria from AbbVie, Astellas, Bristol Myers Squibb, Eisai, Eli Lilly, Kissei, Fujifilm Medical Systems, Janssen, Shionogi Pharmaceuticals, Pfizer, and UCB (less than $10,000 each) and from Chugai Pharmaceutical, Mitsubishi Tanabe, Ono Pharmaceutical, Diaichi Sankyo, and Takeda Pharmaceutical (more than $10,000 each). Dr. Takeuchi has received consulting fees, speaking fees, and/or honoraria from AYUMI Pharmaceutical, Gilead, GlaxoSmithKline, Sanofi, Taiho Pharmaceutical, Diaichi Sankyo, Taisho Pharmaceutical, Eli Lilly, Novartis, Boehringer Ingelheim, Nippon Kayaku, Pfizer, Bristol Myers Squibb, Janssen, and UCB (less than $10,000 each) and from Astellas, Asahi Kasei Pharma, AbbVie, Eisai, Chugai Pharmaceutical, and Mitsubishi Tanabe (more than $10,000 each). No other disclosures relevant to this article were reported.

Address correspondence to Tsutomu Takeuchi, MD, PhD, Keio University School of Medicine, Division of Rheumatology, Department of Internal Medicine, 35 Shinanomachi, Shinjuku-ku, Tokyo, Japan. Email: tsutake@z5.keio.jp.

Submitted for publication March 26, 2020; accepted in revised form October 6, 2020.

identified, available evidence from bronchoalveolar lavage (BAL) fluid cellular analysis is limited (4–8). The BAL fluid CD4:CD8 ratio and cell profiles have been helpful in diagnosis of some ILDs (9–11). However, for RA-ILD and IIM-ILD, no specific BAL fluid findings have been established, and diagnostic effectiveness of BAL fluid is low. Although alveolar macrophages (AMs) and T cells are considered to be key factors in ILD (12), no comprehensive understanding of the roles of these cells has yet been obtained.

T cell activation is regulated by a T cell receptor (TCR) and cosignaling receptors, costimulatory molecules, and coinhibitory molecules (13). Costimulatory molecules are expressed on naive T cells, and after TCR stimulation, coinhibitory molecules are expressed to prevent excessive T cell activation.

Programmed death 1 (PD-1) has been identified as a receptor inducing cell death; its ligands are PD ligand 1 (PD-L1) and PD-L2 (14,15). Previous studies have demonstrated increased PD-1 expression at the site of inflammatory diseases, such as salivary gland tissues in primary Sjögren's syndrome, the lamina propria in ulcerative colitis, and synovial fluid in RA (16–18). Recently, it was demonstrated that PD-1^{high}CXCR5– peripheral helper T (Tph) cells in RA synovium have a B cell helper function (19). T cell immunoglobulin and mucin domain–containing protein 3 (TIM-3), another coinhibitory molecule, was identified as a negative regulator of Th1 immunity (20). The binding of galectin-9, one of its ligands, to TIM-3 negatively regulates T cells, similar to the effects observed with binding of PD-L1 to PD-1 (20–22). Treatment with TIM-3 blocking antibody causes experimental autoimmune encephalomyelitis (EAE), and galectin-9 injection ameliorates EAE (20–22). Another coinhibitory molecule, lymphocyte activation gene 3 protein (LAG-3), was identified as a surface marker on interleukin-10–secreting CD4+ type 1 Treg cells; its ligand is major histocompatibility complex class II (23). During chronic viral infection in mice, LAG-3 blockade controls the infection, suggesting that LAG-3 contributes to CD8+ T cell exhaustion (24). Therefore, LAG-3 is considered an immune

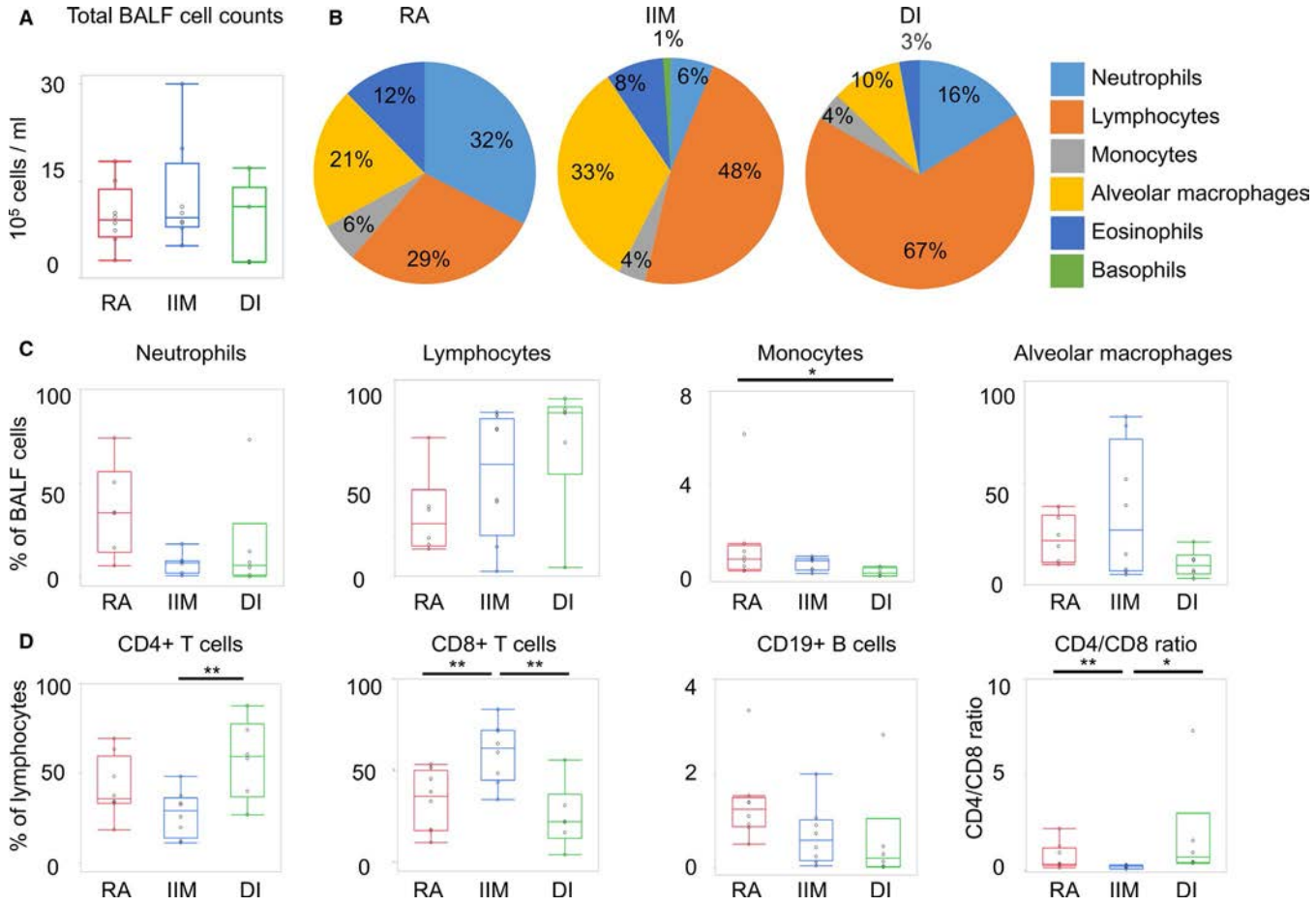

Figure 1. Cellular analysis of bronchoalveolar lavage fluid (BALF) from patients with rheumatoid arthritis–associated interstitial lung disease (RA-ILD) (n = 8), idiopathic inflammatory myopathy–associated ILD (IIM-ILD) (n = 8), and drug-induced ILD (DI-ILD) (n = 6). **A**, Total BAL fluid cell counts. **B**, Mean percentages of the different cell types assessed in BAL fluid. **C**, Percentages of neutrophils, lymphocytes, monocytes, and alveolar macrophages among total BAL fluid cells. **D**, Percentages of CD4+ T cells, CD8+ T cells, and CD19+ B cells, and CD4:CD8 cell ratios. In **A**, **C**, and **D**, data are presented as box plots, where the boxes represent the interquartile range, the lines within the boxes represent the median, and the lines outside the boxes represent the minimum and maximum values excluding outliers. Each circle represents an individual subject. * = $P < 0.05$; ** = $P < 0.01$, by Kruskal-Wallis test.

regulator. CTLA-4 is also an essential negative regulator of T cells, and shares the ligands CD80 and CD86 with CD28, one of the most important costimulatory molecules on T cells (25). CTLA-4 is overexpressed on RA synovial T cells (26).

Although several coinhibitory molecules have been described as noted above, there have been few studies on BAL fluid T cells. We speculated that these coinhibitory molecules are expressed on T cells in the lungs of patients with ILD since they receive frequent antigen stimulation in this disease, and that they may be involved in pathologic mechanisms of RA-ILD and IIM-ILD. In the present study we performed detailed immunophenotyping of BAL fluid T cells, particularly with regard to coinhibitory molecules, and identified distinct differences between diseases.

PATIENTS AND METHODS

Detailed methods are described in the supplementary text (on the *Arthritis & Rheumatology* website at http://onlinelibrary.wiley.com/doi/10.1002/art.41554/abstract). Patients with RA-ILD, IIM-ILD, or drug-induced ILD (DI-ILD) who attended Keio University Hospital or National Tokyo Medical Center were included. Characteristics of the patients and healthy control subjects in each analysis are shown in Supplementary Tables 1–5 (http://onlinelibrary.wiley.com/doi/10.1002/art.41554/abstract). Some sample donors overlapped between cohorts used for different experiments. Fresh cells from BAL fluid and peripheral blood (PB) were thoroughly immunophenotyped. (Supplementary Table 6, (http://onlinelibrary.wiley.com/doi/10.1002/art.41554/abstract). AMs were sorted from BAL fluid with an Aria III flow cytometer (BD Biosciences). AMs from patients with RA-ILD, IIM-ILD, and DI-ILD were analyzed by coculture assay with PB CD4+ naive T cells and RNA sequencing. The transcriptome data are available at the GEO database. The accession code is GSE142540. All custom computer codes in the generation or processing of the described data are available upon reasonable request.

RESULTS

Immunophenotyping of BAL fluid and PB. We immunophenotyped BAL fluid cells from patients with RA-ILD (n = 8), IIM-ILD (n = 8), and DI-ILD (n = 6). Baseline patient characteristics are shown in Supplementary Table 1 (http://onlinelibrary.wiley.com/doi/10.1002/art.41554/abstract). Total BAL fluid cell numbers did not differ significantly among the 3 groups (Figure 1A). Neutrophil and lymphocyte numbers were increased in patients with RA-ILD, and lymphocyte numbers were increased in patients with IIM-ILD and DI-ILD (Figure 1B), whereas >85% of BAL fluid cells from healthy individuals have been reported to be AMs (7). The CD4:CD8 ratio was significantly reduced in IIM-ILD patients (median 0.6 [interquartile range 0.2–0.8]), compared to 0.9 (interquartile range 0.7–3.5) in those with RA-ILD (Figure 1D).

We analyzed subpopulations of T cells and B cells from the BAL fluid of patients with RA-ILD, IIM-ILD, and DI-ILD and compared them to those in the PB of patients with RA-ILD (n = 8) and IIM-ILD (n = 13) and healthy controls (n = 8) (Figure 2). The majority of BAL fluid CD4+ and CD8+ T cells were effector memory T (Tem) cells, and naive T cells were almost absent (Figure 2A). Although there was no difference between groups in the Th1, Th17, Th1/17, and follicular helper T (Tfh) cell populations in either BAL fluid or PB (Figure 2A), the proportion of BAL fluid Treg cells was higher in IIM-ILD patients than in those with RA-ILD and DI-ILD. We further examined Treg cell subpopulations (Supplementary Figures 1 and 2, http://onlinelibrary.wiley.com/doi/10.1002/art.41554/abstract) and found that the subpopulation that was higher in patients with IIM-ILD than those with DI-ILD was Fr III, which does not have suppressive functions (27). We also examined CD28, CD69, and CXCR6 expression on T cells to investigate their activation status (Supplementary Figure 3, http://onlinelibrary.wiley.com/doi/10.1002/art.41554/abstract). BAL fluid T cells expressed all 3 molecules, whereas PB T cells expressed only CD28. In BAL fluid CD8+ T cells from patients with IIM-ILD, CD28 levels were low and CD69 levels were high, indicating that CD8+ T cells were highly activated in the lungs of these patients.

The subpopulations of B cells in the BAL fluid were also different from those in PB, with lower levels of naive cells and higher levels of preswitch memory cells, plasmablasts, and plasma cells in BAL fluid. Levels of plasma cells in BAL fluid and levels of plasmablasts and plasma cells in PB were significantly increased in patients with RA-ILD compared to patients with DI-ILD and heathy controls (Figure 2B). The proportion of BAL fluid monocytes was higher in RA-ILD than in DI-ILD (Figure 1C). The major subpopulation of monocytes in both BAL fluid and PB was classic monocytes, and nonclassic monocytes were almost absent in BAL fluid (Supplementary Figure 4, http://onlinelibrary.wiley.com/doi/10.1002/art.41554/abstract).

Next, we examined the surface expression of coinhibitory molecules PD-1, TIM-3, LAG-3, and CTLA-4 on T cells (Figure 2C). Regardless of the disease, coinhibitory molecule expression was high in BAL fluid, with CTLA-4 showing the highest expression, followed in order by PD-1, TIM-3, and LAG-3. While coinhibitory molecules other than PD-1 were rarely expressed on PB T cells, they were highly expressed on BAL fluid T cells. We compared coinhibitory molecule expression between BAL fluid and PB in 5 RA-ILD and 5 IIM-ILD patients (Supplementary Figure 5, http://onlinelibrary.wiley.com/doi/10.1002/art.41554/abstract). CTLA-4, PD-1, and TIM-3 were more highly expressed on BAL fluid T cells than on PB T cells, and there was no correlation between the rate of coinhibitory molecule positivity in BAL fluid T cells and the rate in PB T cells, which suggested that coinhibitory molecules must be evaluated on BAL fluid T cells.

We found that expression of PD-1, TIM-3, and LAG-3 on CD4+ T cells and of PD-1 and TIM-3 on CD8+ T cells was higher in BAL fluid from patients with RA-ILD than in that from patients

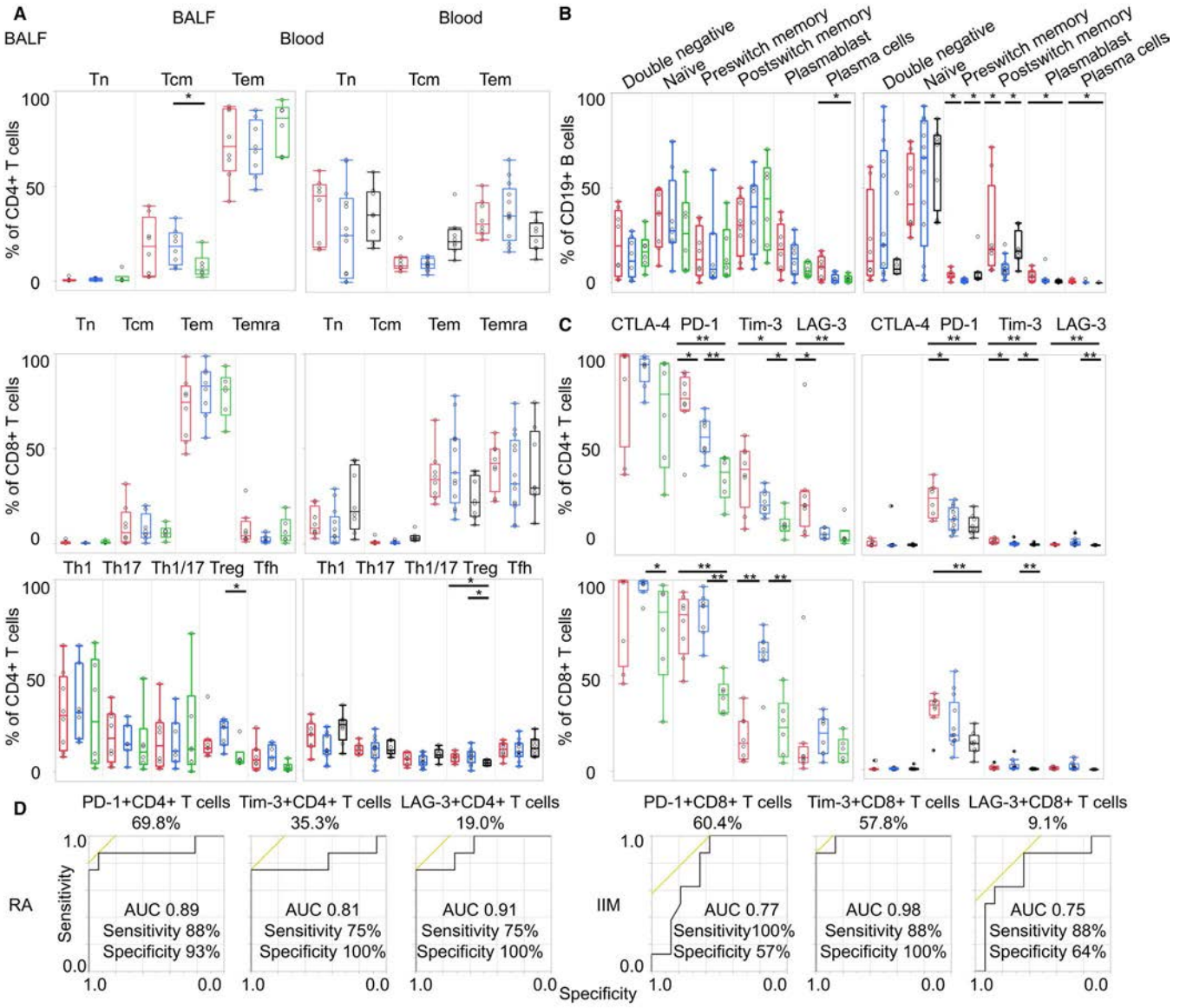

Figure 2. **A–C**, Immunophenotyping of T cell and B cell subpopulations in bronchoalveolar lavage fluid (BALF) cells from patients with rheumatoid arthritis–associated interstitial lung disease (RA-ILD) (red; n = 8), idiopathic inflammatory myopathy–associated ILD (IIM-ILD) (blue; n = 8), and drug-induced ILD (DI-ILD) (green; n = 6) (left) and in peripheral blood cells from patients with RA-ILD (red; n = 8) and IIM-ILD (blue; n = 13) and from healthy controls (black; n = 8) (right). **A**, Percentages of naive (Tn), central memory (Tcm), and effector memory (Tem) CD4+ T cells among CD4+ T cells, percentages of naive, Tcm, Tem, and CD45RA+ memory (Temra) CD8+ T cells among CD8+ T cells, and percentages of Th1, Th17, Th1/17, Treg, and follicular helper (Tfh) CD4+ T cells among CD4+ T cells. **B**, Percentages of B cell subsets. **C**, Percentages of CD4+ and CD8+ T cells positive for the coinhibitory molecules CTLA-1, programmed death 1 (PD-1), T cell immunoglobulin and mucin domain–containing protein 3 (TIM-3), and lymphocyte activation gene 3 protein (LAG-3). Data are presented as box plots, where the boxes represent the interquartile range, the lines within the boxes represent the median, and the lines outside the boxes represent the minimum and maximum values excluding outliers. Each circle represents an individual subject. * = $P < 0.05$; ** = $P < 0.01$, by Kruskal-Wallis test. **D**, Cutoff levels for the rate of PD-1, TIM-3, and LAG-3 positivity in CD4+ T cells associated with RA-ILD and for the rate of PD-1, TIM-3, and LAG-3 positivity in CD8+ T cells associated with IIM-ILD, by receiver operating characteristic area under the curve (AUC) analysis.

with DI-ILD. Additionally, expression of PD-1 and TIM-3 on CD4+ T cells and of CTLA-4, PD-1, and TIM-3 on CD8+ T cells was higher in BAL fluid from patients with IIM-ILD than in that from patients with DI-ILD. Therefore, we calculated the cutoff values for coinhibitory molecules that were more highly expressed in the RA-ILD and IIM-ILD groups than in the other 2 groups, by receiver operating characteristic analysis (Figure 2D). The cutoff values for PD-1, TIM-3, and LAG-3 positivity in CD4+ T cells associated with RA-ILD were 69.8%, 35.3%, and 19.0%, respectively, and the cutoff values for PD-1, TIM-3, and LAG-3 positivity in CD8+ T cells associated with IIM-ILD were 60.4%, 57.8%, and 9.1%, respectively.

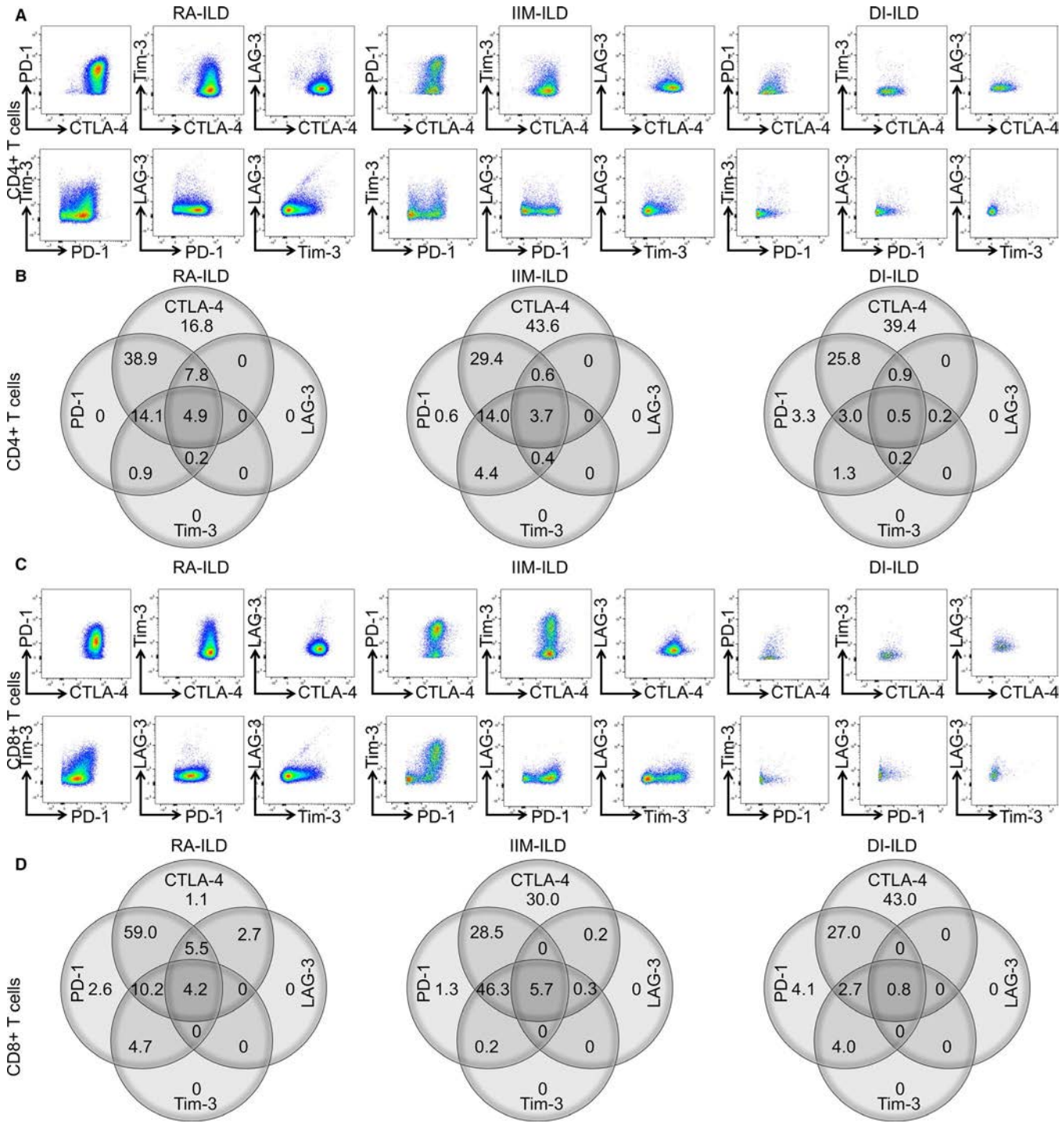

Figure 3. Coexpression of coinhibitory molecules on BAL fluid T cells. **A** and **C**, Two-dimensional plots of the coexpression of coinhibitory molecules on BAL fluid CD4+ T cells (**A**) and CD8+ T cells (**C**) from the RA-ILD group (n = 8), the IIM-ILD group (n = 8), and the DI-ILD group (n = 6). **B** and **D**, Venn diagrams showing the mean percentages of coinhibitory molecule–coexpressing CD4+ T cells (**B**) and CD8+ T cells (**D**). See Figure 2 for definitions.

Expression of coinhibitory molecules other than PD-1 on PB T cells was low, but somewhat increased in RA-ILD and IIM-ILD. Therefore, we examined their changes in response to treatment (Supplementary Figure 6, http://onlinelibrary.wiley.com/doi/10.1002/art.41554/abstract). The frequency of PD-1+ and TIM-3+ CD4+ T cells was significantly decreased after glucocorticoid treatment for ILD. We next investigated correlations between expression of these markers on BAL fluid T cells and clinical data (Supplementary Figure 7, http://onlinelibrary.wiley.com/doi/10.1002/art.41554/abstract). In RA-ILD, the proportion

of BAL fluid TIM-3+CD4+ T cells correlated positively with the 28-joint Disease Activity Score using the C-reactive protein level (28) and the Clinical Disease Activity Index (29) and negatively with diffusing capacity for carbon monoxide.

Next, we examined coinhibitory molecule expression on T cell subsets relative to differentiation stage (Supplementary Figure 8, http://onlinelibrary.wiley.com/doi/10.1002/art.41554/abstract). These markers were expressed on central memory T (Tcm) and Tem cells to the same extent, and rarely expressed on naive T cells. In each disease, the expression pattern of these molecules on Tcm and Tem cells was similar to that in CD4+ and CD8+ T cells overall. We further examined, in the RA-ILD group, whether there were differences in coinhibitory molecule expression according to computed tomography pattern or treatment and found no significant differences between nonspecific interstitial pneumonia and organizing pneumonia patterns or between treated and treatment-naive patients (Supplementary Figure 9, http://onlinelibrary.wiley.com/doi/10.1002/art.41554/abstract).

Coexpression of coinhibitory molecules on BAL fluid T cells. We next investigated the coexpression of coinhibitory molecules on BAL fluid T cells. Representative plots and the mean percentages of coinhibitory molecule coexpression are shown in Figure 3. Some CTLA-4+ T cells expressed PD-1, TIM-3, and LAG-3; some PD-1+ T cells expressed TIM-3 and LAG-3; and some TIM-3+ T cells expressed LAG-3. There were few other combinations. These findings further suggested that the frequency of expression of these coinhibitory molecules, from most to least, is CTLA-4 followed by PD-1, then TIM-3, then LAG-3. In RA-ILD, most BAL fluid CD4+ and CD8+ T cells were CTLA-4+PD-1+ (Figures 3B and D), whereas in IIM-ILD, most CD4+ T cells were CTLA-4+PD-1+ and most CD8+ T cells were CTLA-4+PD-1+TIM-3+. We further compared the coinhibitory molecule positivity rate between CD4+ and CD8+ T cells in individual patients (Supplementary Figure 10, http://onlinelibrary.wiley.com/doi/10.1002/art.41554/abstract). PD-1 and CTLA-4 were similarly expressed on CD4+ and CD8+ T cells from patients with

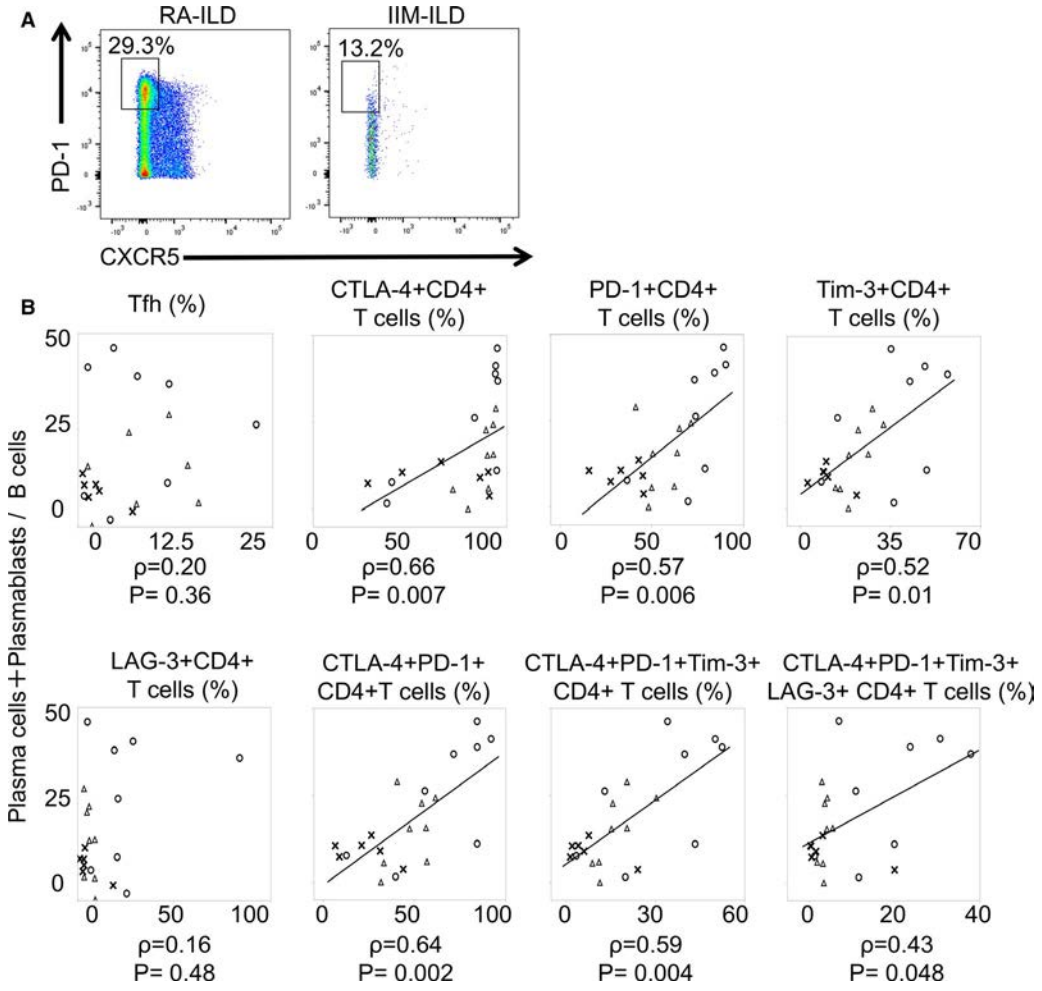

Figure 4. Correlation of T cell subsets with plasmablasts and plasma cells in BAL fluid. **A**, Representative plots of PD-1 and CXCR5 expression on BAL fluid CD4+ T cells from patients with RA-ILD and IIM-ILD. **B**, Correlation of total plasmablast and plasma cell levels with levels of Tfh cells and of coinhibitory molecule–positive CD4+ T cells from patients with RA-ILD (circles; n = 8), IIM-ILD (triangles; n = 8), and DI-ILD (times signs; n = 6), by Spearman's correlation test. See Figure 2 for definitions.

RA-ILD, whereas only TIM-3 was similarly expressed on CD4+ and CD8+ T cells from patients with IIM-ILD, and only CTLA-4 was similarly expressed on CD4+ and CD8+ T cells from those with DI-ILD.

Tph cells in the BAL fluid. Proportions of plasma cells and PD-1+CD4+ T cells were increased in the BAL fluid of patients with RA-ILD, whereas the proportion of Tfh cells did not differ by disease. Since we considered that PD-1+CD4+ T cells might be Tph cells, we additionally examined coexpression of PD-1 and CXCR5 on BAL fluid CD4+ T cells. Although the sample number was small, we observed that PD-1+CD4+ T cells rarely expressed CXCR5 (Figure 4A). We next examined correlation of coinhibitory molecule–positive CD4+ T cells with plasmablast and plasma cell populations (Figure 4B). In multiple coinhibitory molecule–coexpressing CD4+ T cells there was a correlation with these populations, whereas in multiple coinhibitory molecule–coexpressing CD8+ T cells there was not (Supplementary Figure 11A, http://onlinelibrary.wiley.com/doi/10.1002/art.41554/abstract). Analysis by disease type showed that the presence of CTLA-4+ and PD-1+ CD4+ T cells in RA-ILD and of TIM-3+ CD4+ T cells in IIM-ILD correlated with plasmablast and plasma cell populations, whereas there was no correlation in DI-ILD (Supplementary Figure 11B). In addition, the presence of PD-1+ and TIM3+ CD4+ T cells correlated with rheumatoid factor (RF) titer in RA-ILD (Supplementary Figure 11C).

AM–T cell cocultures. Next, to evaluate the effect of AMs, the major antigen-presenting cells in the lung, on coinhibitory molecule expression on T cells, we cocultured AMs with PB CD4+ naive T cells (Figure 5A). AMs were isolated from BAL fluid from patients with RA-ILD (n = 3), IIM-ILD (n = 4), and DI-ILD (n = 3). To clarify whether AM has effects other than TCR stimulation, and to compensate for interexperimental variations, we used anti-CD3/CD28 beads as controls for TCR stimulation in each experiment. Representative results

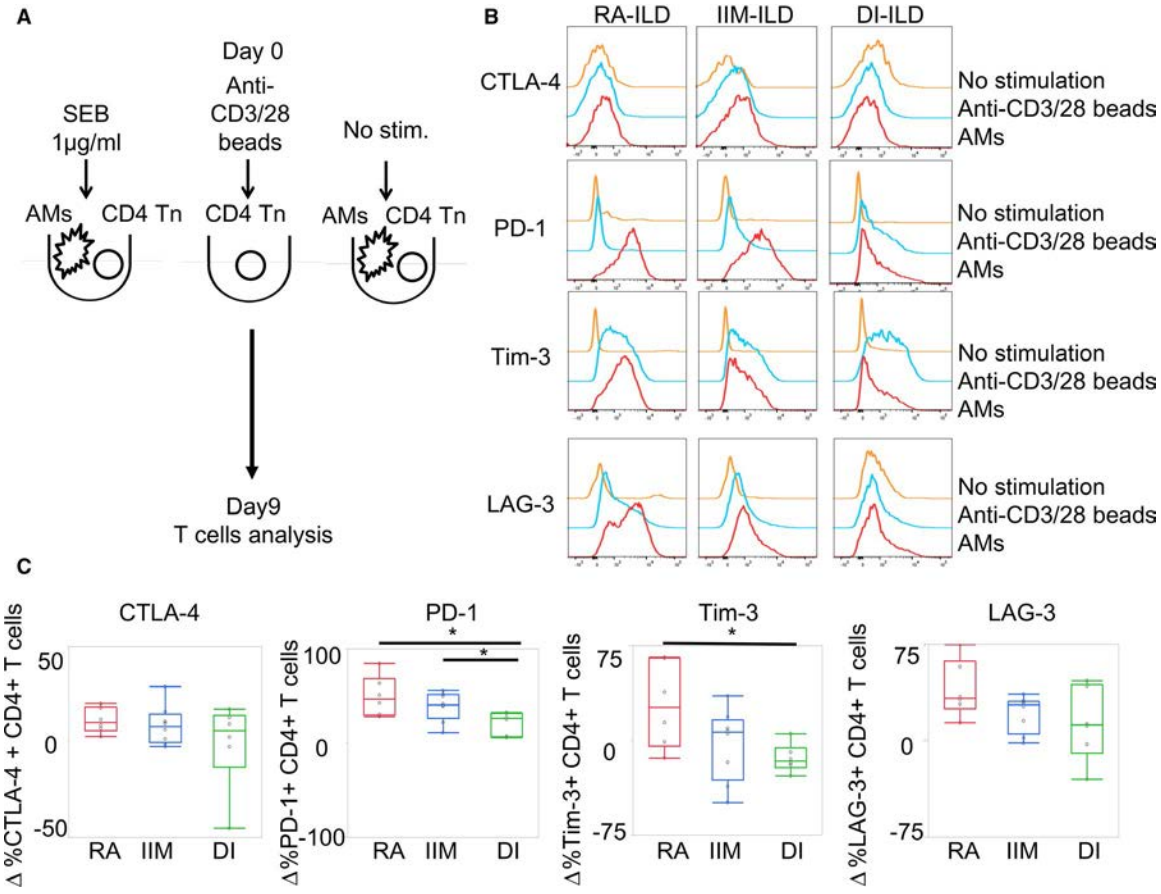

Figure 5. Coinhibitory molecule expression on peripheral blood CD4+ naive T cells cocultured with alveolar macrophages (AMs) isolated from the BAL fluid of patients with RA-ILD (n = 3), IIM-ILD (n = 4), and DI-ILD (n = 3). **A**, Schematic description of the coculture experiment. **B**, Representative expression of CTLA-4, PD-1, TIM-3, and LAG-3 on CD4+ T cells cultured with AMs from the 3 groups (red), cultured with anti-CD3/CD28 beads (blue), or not stimulated (No stim.) (yellow). **C**, Δ% of coinhibitory molecule expression in the 3 groups. Data are presented as box plots, where the boxes represent the interquartile range, the lines within the boxes represent the median, and the lines outside the boxes represent the minimum and maximum values excluding outliers. Each circle represents an individual subject. * = $P < 0.05$ by Kruskal-Wallis test. SEB = staphylococcal enterotoxin B (see Figure 2 for other definitions).

are shown in Figure 5B. In addition to TCR stimulation, AMs induced higher expression of coinhibitory molecules on T cells. Therefore, we examined the difference between the expression of coinhibitory molecules after coculture with AMs and the expression after stimulation with anti-CD3/CD28 beads; Δ% was calculated as (% of marker-positive cells cocultured with AMs) – (% of marker-positive cells stimulated with anti-CD3/28 beads). PD-1 and TIM-3 expression induced by AMs from patients with RA-ILD and PD-1 expression induced by AMs from patients with IIM-ILD were greater than the expression observed in patients with DI-ILD (Figure 5C), suggesting that PD-1 and TIM-3 expression on CD4+ T cells is partly due to AMs.

Transcriptional comparison of AMs. To examine the differences in AMs by disease, we performed transcriptome analysis of AMs from patients with RA-ILD (n = 5), IIM-ILD (n = 6), and DI-ILD (n = 5). By principal components analysis, the samples were not distinguished by disease (Figure 6A). This might be because AMs from patients with RA-ILD, IIM-ILD, or DI-ILD were activated to some extent. Next, we examined differential expression of genes between diseases. Compared to DI-ILD, 386 genes were differentially expressed in RA-ILD (151 up-regulated and 235 down-regulated) and 358 were differentially expressed in IIM-ILD (190 up-regulated and 268 down-regulated) (Supplementary data 1 and 2; see Supplementary text on the *Arthritis & Rheumatology*

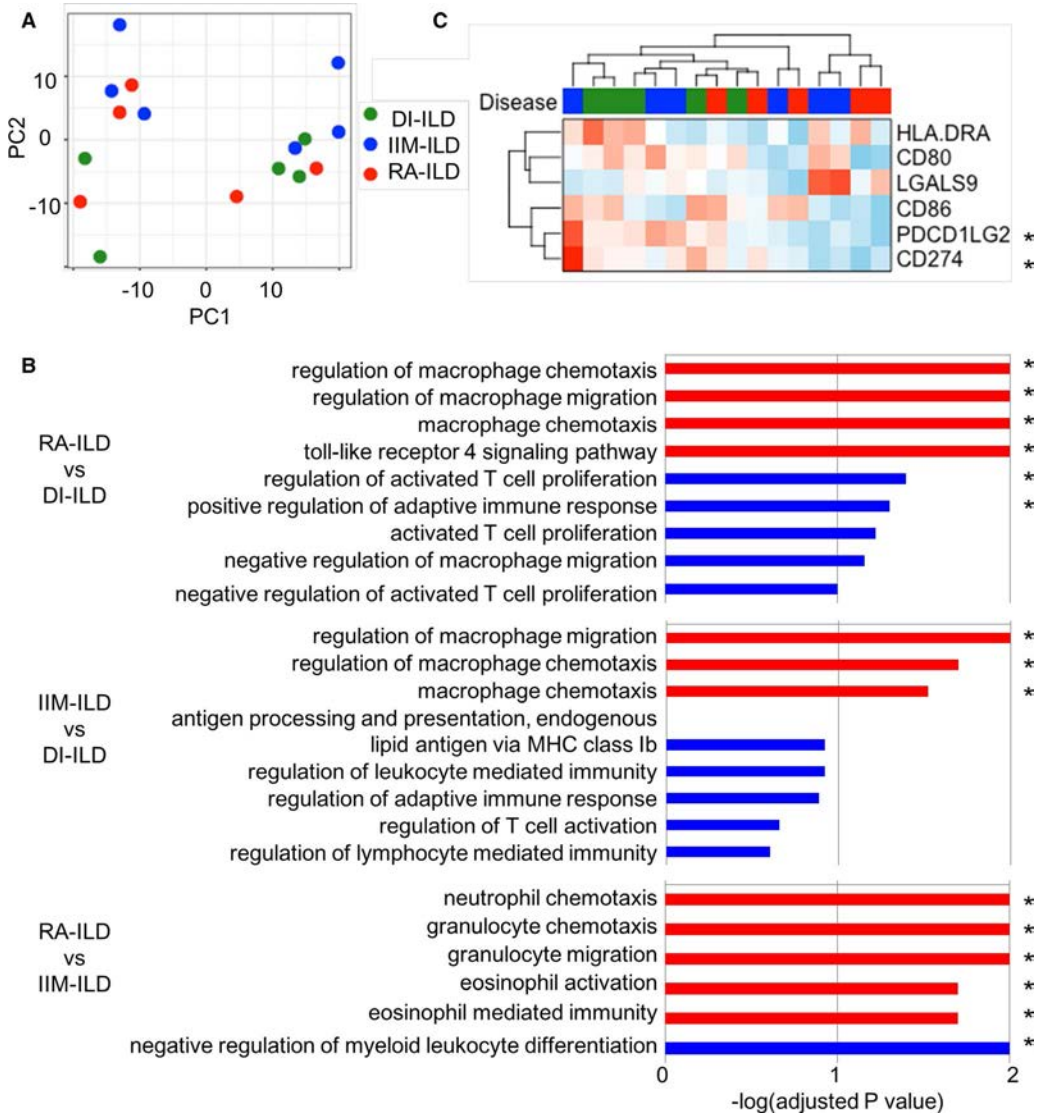

Figure 6. Transcriptome analysis of alveolar macrophages from patients with RA-ILD (red in **A** and **C**; n = 5), IIM-ILD (blue in **A** and **C**; n = 6), and DI-ILD (green in **A** and **C**; n = 5). **A**, Principal components (PC) analysis. **B**, Enriched pathways, determined according to differential gene expression between RA-ILD and DI-ILD, between IIM-ILD and DI-ILD, or between RA-ILD and IIM-ILD. Red bars indicate up-regulated genes and blue bars indicate down-regulated genes. Pathways are shown with the logarithm of the *P* value (Bonferroni corrected) based on hypergeometric distribution. * = corrected $P < 0.05$. **C**, Hierarchical clustering analysis. Rows correspond to genes (red indicates up-regulated and blue indicates down-regulated) and columns correspond to samples. * = $P < 0.05$ and an absolute log fold change of >1.2. MHC = major histocompatibility complex (see Figure 2 for other definitions).

website at http://onlinelibrary.wiley.com/doi/10.1002/art.41554/abstract). There were 366 genes that were differentially expressed in RA-ILD compared to IIM-ILD (229 up-regulated and 137 down-regulated [Supplementary data 3; see Supplementary text]). Figure 6B shows the top 5 pathways as determined by Gene Ontology enrichment analysis (Supplementary data 4–6; see Supplementary text). Macrophage chemotaxis–related pathways were up-regulated in RA-ILD and IIM-ILD compared to DI-ILD. In RA-ILD, the Toll-like receptor 4 signaling pathway was up-regulated, and regulation of activated T cell proliferation and positive regulation of adaptive immune response were down-regulated, compared to DI-ILD, which is suggestive of a proinflammatory status of AMs in RA-ILD.

To examine the interaction between AMs and T cells, we focused on the ligands of these coinhibitory molecules. As shown in Figure 6C, some ligands of the coinhibitory molecules were down-regulated in RA-ILD and IIM-ILD compared to DI-ILD. In particular, *CD274* and *PDCD1LG2*, genes for PD-L1/2, were significantly down-regulated in RA-ILD compared to DI-ILD, suggesting that inflammation may not be controlled even if PD-1 is highly expressed on T cells in RA-ILD. Neutrophil-related pathways were enriched in RA-ILD compared to IIM-ILD (Figure 6B), implying that AMs in RA-ILD cause neutrophilic inflammation as shown in Figure 1B.

DISCUSSION

In the present study we performed detailed immunophenotyping of BAL fluid T cells from patients with RA-ILD and IIM-ILD. Based on the expression rates and coexpression patterns, we demonstrated that coinhibitory molecules are expressed on BAL fluid T cells, in the order of CTLA-4, PD-1, TIM-3, and LAG-3 from most to least. In RA-ILD, PD-1+ and TIM-3+ CD4+ T cells in BAL fluid were increased. PD-1+CD4+ T cell populations correlated with differentiated B cells, and TIM-3+CD4+ T cell populations correlated with ILD severity and RF titer. In contrast, in IIM-ILD, activated CD8+ T cells were increased, and they coexpressed CTLA-4, PD-1, and TIM-3. Moreover, we showed that BAL fluid PD-1+CD4+ T cells can be considered Tph cells. Our coculture results demonstrated that expression of PD-1 and TIM-3 is partly due to AMs. Transcriptome analysis of AMs showed that *CD274* and *PDCD1LG2* were significantly down-regulated in AMs from patients with RA-ILD compared to those with DI-ILD. To our knowledge, this is the first detailed evaluation of coinhibitory molecule expression on lung T cells from patients with RA-ILD and IIM-ILD.

Surface coinhibitory molecule expression was higher on BAL fluid T cells than on PB T cells in RA-ILD and IIM-ILD. Naive T cells circulate in the blood until they encounter an antigen and differentiate into Tem cells; peripheral Tem cells then migrate to sites of inflammation. Indeed, Tem cells have been observed at other RA lesions, such as synovial membrane, and coinhibitory molecules are highly expressed on them (18,30–33). In RA-ILD, bronchus-associated lymphoid tissue helps immediate immune responses (34), and strong TCR stimulation has been reported to up-regulate CTLA-4, TIM-3, and PD-1 expression (35,36). Our results suggest that T cells are frequently stimulated by antigens in the lungs and express coinhibitory molecules.

Although expression of coinhibitory molecules on BAL fluid T cells is high, there are some differences. First, CTLA-4 was expressed on most BAL fluid T cells regardless of disease type, whereas the expression of PD-1, TIM-3, and LAG-3 on BAL fluid T cells was increased in RA-ILD and IIM-ILD. CTLA-4 is expressed on T cells at the priming phase, whereas PD-1 is expressed on antigen-specific effector T cells at the effector phase (36,37). PD-1 expression is considered to be induced by a specific immune response.

Second, PD-1 was highly expressed on BAL fluid T cells and also expressed on PB T cells in both RA-ILD and IIM-ILD. Our results suggest that BAL fluid PD-1+CD4+ T cells might be Tph cells, because they rarely express CXCR5, and they positively correlate with plasmablasts and plasma cell levels and RF titer in RA-ILD. This population may promote autoantibody production in the lungs and be pathogenetic in RA-ILD. Moreover, PD-1 ligands were found to be down-regulated in AMs from RA-ILD patients by transcriptome analysis, indicating that inflammation may not be regulated through the PD-1 and PD-L pathway in RA-ILD. Previous studies have revealed that blocking antibodies against PD-1 cause autoimmune disease and increased PD-L expression ameliorates autoimmune disease (37). Therefore, increased PD-L expression might be a treatment target in RA-ILD.

Third, TIM-3 expression on CD8+ T cells is characteristic of IIM-ILD. In IIM-ILD, expression of PD-1, TIM-3, and LAG-3 was more frequently observed on CD8+ T cells than on CD4+ T cells, whereas expression levels of other coinhibitory molecules were almost the same in CD4+ and CD8+ T cells from the same individual. Moreover, total CD8+ T cell and CD69+CD8+ T cell populations in the BAL fluid were increased, and CD28+CD8 T cells were decreased, in IIM-ILD, indicating that CD8+ T cells might be a key factor in the disease process. The effect of TIM-3 on macrophages is controversial (20,38), and further study is needed to clarify this.

Fourth, LAG-3 expression was significantly increased on CD4+ T cells from patients with RA-ILD, but was observed the least frequently among the 4 coinhibitory molecules. This may be because LAG-3 is associated with T cell exhaustion, which occurs less frequently in immunologically active lung lesions.

This detailed immunophenotyping analysis of BAL fluid is potentially useful for the diagnosis and assessment of disease activity in ILD associated with connective tissue diseases, although this has not yet been definitively established. In particular, our finding of higher expression of PD-1 and TIM-3 on T cells in RA-ILD and IIM-ILD than DI-ILD suggests differences in immunopathogenesis, and thus would be helpful for identification of the important cell populations in each disease. All samples in the present study were from patients with a definite clinical diagnosis, and

further study of other ILDs is needed to establish whether BAL fluid analysis is useful for differential diagnosis among patients with ILD of undiagnosed origin. Moreover, in RA-ILD, TIM-3 expression was associated with ILD severity. Evaluating coinhibitory molecule expression on T cells may thus help predict the severity of RA-ILD.

The study has some limitations. First, because of difficulty in collecting patients with these rare diseases, the sample size was small and treatment history varied. Since we could not collect BAL fluid from healthy subjects, we enrolled patients with DI-ILD as a disease control. As shown by CTLA-4 expression and AM transcriptome analysis, BAL fluid cells from patients with DI-ILD seemed to be activated to some extent. Second, we did not examine the antigen specificity of T and B cells; however, single-cell analysis of BAL fluid T and B cells is planned. When the antigens at the lungs are determined in the future, antigen specificity will be clarified. Additionally, to identify differences among diseases at the molecular level, genetic analysis including single-nucleotide polymorphism studies and surface antigen assessment by mass cytometry might be useful.

In conclusion, we report the first detailed immunophenotyping of BAL fluid cells from patients with a definite clinical diagnosis of RA-ILD or IIM-ILD. We identified subsets that could be related to RA-ILD and IIM-ILD pathogenesis. Analysis of coinhibitory molecules may facilitate the formulation of treatment strategies to specifically control T cell activation in these diseases.

AUTHOR CONTRIBUTIONS

All authors were involved in drafting the article or revising it critically for important intellectual content, and all authors approved the final version to be published. Dr. Nazakawa had full access to all of the data in the study and takes responsibility for the integrity of the data and the accuracy of the data analysis.

Study conception and design. Nakazawa, Suzuki, Takeshita, Takeuchi.
Acquisition of data. Nakazawa, Suzuki, Takeshita, Kamata, Ishii, Oyamada, Oshima, Takeuchi.
Analysis and interpretation of data. Nakazawa, Suzuki, Takeshita, Inamo, Takeuchi.

REFERENCES

1. Olson AL, Swigris JJ, Sprunger DB, Fischer A, Fernandez-Perez ER, Solomon J, et al. Rheumatoid arthritis-interstitial lung disease-associated mortality. Am J Respir Crit Care Med 2011;183:372–8.
2. Hallowell RW, Ascherman DP, Danoff SK. Pulmonary manifestations of polymyositis/dermatomyositis. Semin Respir Crit Care Med 2014;35:239–48.
3. Young A, Koduri G, Batley M, Kulinskaya E, Gough A, Norton S, et al. Mortality in rheumatoid arthritis: increased in the early course of disease, in ischaemic heart disease and in pulmonary fibrosis. Rheumatology (Oxford) 2007;46:350–7.
4. Chen J, Doyle TJ, Liu Y, Aggarwal R, Wang X, Shi Y, et al. Biomarkers of rheumatoid arthritis–associated interstitial lung disease. Arthritis Rheumatol 2015;67:28–38.
5. Bonella F, Costabe U. Biomarkers in connective tissue disease-associated interstitial lung disease. Semin Respir Crit Care Med 2014;35:181–200.
6. Doyle TJ, Patel AS, Hatabu H, Nishino M, Wu G, Osorio JC, et al. Detection of rheumatoid arthritis-interstitial lung disease is enhanced by serum biomarkers. Am J Respir Crit Care Med 2015;191:1403–12.
7. Meyer KC, Raghu G, Baughman RP, Brown KK, Costabel U, du Bois RM, et al. An official American Thoracic Society clinical practice guideline: the clinical utility of bronchoalveolar lavage cellular analysis in interstitial lung disease. Am J Respir Crit Care Med 2012;185:1004–14.
8. Mimori T, Nakashima R, Hosono Y. Interstitial lung disease in myositis: clinical subsets, biomarkers, and treatment. Curr Rheumatol Rep 2012;14:264–74.
9. Kantrow SP, Meyer KC, Kidd P, Raghu G. The CD4/CD8 ratio in BAL fluid is highly variable in sarcoidosis. Eur Respir J 1997;10:2716–21.
10. Trentin L, Migone N, Zambello R, di Celle PF, Aina F, Feruglio C, et al. Mechanisms accounting for lymphocytic alveolitis in hypersensitivity pneumonitis. J Immunol 1990;145:2147–54.
11. Allen JN, Davis WB, Pacht ER. Diagnostic significance of increased bronchoalveolar lavage fluid eosinophils. Am Rev Respir Dis 1990;142:642–7.
12. Holt PG, Strickland DH, Wikström ME, Jahnsen FL. Regulation of immunological homeostasis in the respiratory tract [review]. Nat Rev Immunol 2008;8:142–52.
13. Chen L, Flies DB. Molecular mechanisms of T cell co-stimulation and co-inhibition [review]. Nat Rev Immunol 2013;13:227–42.
14. Ishida Y, Agata Y, Shibahara K, Honjo T. Induced expression of PD-1, a novel member of the immunoglobulin gene superfamily, upon programmed cell death. EMBO J 1992;11:3887–95.
15. Nishimura H, Okazaki T, Tanaka Y, Nakatani K, Hara M, Matsumori A, et al. Autoimmune dilated cardiomyopathy in PD-1 receptor-deficient mice. Science 2001;291:319–22.
16. Bolstad AI, Eiken HG, Rosenlund B, Alarcón-Riquelme ME, Jonsson R. Increased salivary gland tissue expression of Fas, Fas ligand, cytotoxic T lymphocyte–associated antigen 4, and programmed cell death 1 in primary Sjögren's syndrome. Arthritis Rheum 2003;48:174–85.
17. Kanai T, Totsuka T, Uraushihara K, Makita S, Nakamura T, Koganei K, et al. Blockade of B7–H1 suppresses the development of chronic intestinal inflammation. J Immunol 2003;171:4156–63.
18. Hatachi S, Iwai Y, Kawano S, Morinobu S, Kobayashi M, Koshiba M, et al. CD4+ PD-1+ T cells accumulate as unique anergic cells in rheumatoid arthritis synovial fluid. J Rheumatol 2003;30:1410–9.
19. Rao DA, Gurish MF, Marshall JL, Slowikowski K, Fonseka CY, Liu Y, et al. Pathologically expanded peripheral T helper cell subset drives B cells in rheumatoid arthritis. Nature 2017;542:110–4.
20. Monney L, Sabatos CA, Gaglia JL, Ryu A, Waldner H, Chernova T, et al. Th1-specific cell surface protein TIM-3 regulates macrophage activation and severity of an autoimmune disease. Nature 2002;415:536–41.
21. Zhu C, Anderson AC, Schubart A, Xiong H, Imitola J, Khoury SJ, et al. The TIM-3 ligand galectin-9 negatively regulates T helper type 1 immunity. Nat Immunol 2005;6:1245–52.
22. Sabatos CA, Chakravarti S, Cha E, Schubart A, Sánchez-Fueyo A, Zheng XX, et al. Interaction of TIM-3 and TIM-3 ligand regulates T helper type 1 responses and induction of peripheral tolerance. Nat Immunol 2003;4:1102–10.
23. Gagliani N, Magnani CF, Huber S, Gianolini ME, Pala M, Licona-Limon P, et al. Coexpression of CD49b and LAG-3 identifies human and mouse T regulatory type 1 cells. Nat Med 2013;19:739–46.
24. Blackburn SD, Shin H, Haining WN, Zou T, Workman CJ, Polley A, et al. Coregulation of CD8+ T cell exhaustion by multiple inhibitory receptors during chronic viral infection. Nat Immunol 2009;10:29–37.

25. Romo-Tena J, Gómez-Martín D, Alcocer-Varela J. CTLA-4 and autoimmunity: new insights into the dual regulator of tolerance [review]. Autoimmun Rev 2013;12:1171–6.
26. Körmendy D, Hoff H, Hoff P, Bröker BM, Burmester GR, Brunner-Weinzierl MC. Impact of the CTLA-4/CD28 axis on the processes of joint inflammation in rheumatoid arthritis. Arthritis Rheum 2013; 65:81–7.
27. Tanaka A, Sakaguchi S. Regulatory T cells in cancer immunotherapy. Cell Res 2017;27:109–18.
28. Prevoo ML, van 't Hof MA, Kuper HH, van Leeuwen MA, van de Putte LB, van Riel PL. Modified disease activity scores that include twenty-eight–joint counts: development and validation in a prospective longitudinal study of patients with rheumatoid arthritis. Arthritis Rheum 1995;38:44–8.
29. Aletaha D, Nell VP, Stamm T, Uffmann M, Pflugbeil S, Machold K, et al. Acute phase reactants add little to composite disease activity indices for rheumatoid arthritis: validation of a clinical activity score. Arthritis Res Ther 2005;7:R796–806.
30. Pepper M, Jenkins MK. Origins of CD4(+) effector and central memory T cells. Nat Immunol 2011;12:467–71.
31. Takeshita M, Suzuki K, Kassai Y, Takiguchi M, Nakayama Y, Otomo Y, et al. Polarization diversity of human CD4+ stem cell memory T cells. Clin Immunol 2015;159:107–17.
32. Li S, Peng D, He Y, Zhang H, Sun H, Shan S, et al. Expression of TIM-3 on CD4+ and CD8+ T cells in the peripheral blood and synovial fluid of rheumatoid arthritis. APMIS 2014;122:899–904.
33. Liu MF, Yang CY, Li JS, Lai KA, Chao SC, Lei HY. Increased expression of down-regulatory CTLA-4 molecule on T lymphocytes from rheumatoid synovial compartment. Scand J Immunol 1999;50: 68–72.
34. Rangel-Moreno J, Hartson L, Navarro C, Gaxiola M, Selman M, Randall TD. Inducible bronchus-associated lymphoid tissue (iBALT) in patients with pulmonary complications of rheumatoid arthritis. J Clin Invest 2006;116:3183–94.
35. DeLong JH, Hall AO, Rausch M, Moodley D, Perry J, Park J, et al. IL-27 and TCR stimulation promote T cell expression of multiple inhibitory receptors. Immunohorizons 2019;3:13–25.
36. Linsley PS, Bradshaw J, Bradshaw J, Greene J, Peach R, Bennett KL, et al. Intracellular trafficking of CTLA-4 and focal localization towards sites of TCR engagement. Immunity 1996;4:535–43.
37. Keir ME, Butte MJ, Freeman GJ, Sharpe AH. PD-1 and its ligands in tolerance and immunity [review]. Annu Rev Immunol 2008;26: 677–704.
38. Jayaraman P, Sada-Ovalle I, Beladi S, Anderson AC, Dardalhon V, Hotta C, et al. TIM3 binding to galectin-9 stimulates antimicrobial immunity. J Exp Med 2010;207:2343–54.

Arthritis & Rheumatology
Vol. 73, No. 4, April 2021, pp 587–595
DOI 10.1002/art.41555

American College of Rheumatology
Empowering Rheumatology Professionals

Efficacy and Safety of E6011, an Anti-Fractalkine Monoclonal Antibody, in Patients With Active Rheumatoid Arthritis With Inadequate Response to Methotrexate: Results of a Randomized, Double-Blind, Placebo-Controlled Phase II Study

Yoshiya Tanaka,[1] Tsutomu Takeuchi,[2] Hisashi Yamanaka,[3] Toshihiro Nanki,[4] Hisanori Umehara,[5] Nobuyuki Yasuda,[6] Fumitoshi Tago,[7] Yasumi Kitahara,[7] Makoto Kawakubo,[7] Kentaro Torii,[7] Seiichiro Hojo,[7] Tetsu Kawano,[6] and Toshio Imai[6]

Objective. To evaluate the efficacy and safety of E6011, a humanized IgG2 monoclonal antibody against human fractalkine (FKN), in a phase II, double-blind, placebo-controlled study in rheumatoid arthritis (RA) patients.

Methods. Patients with moderate-to-severe RA who had an inadequate response to methotrexate were randomly assigned to a placebo group or to E6011 100-mg, 200-mg, or 400/200-mg groups at a 2:1:2:2 ratio. During the 24-week period, patients received the study drug subcutaneously at weeks 0, 1, and 2 and then once every 2 weeks. The primary end point was the American College of Rheumatology 20% improvement criteria (ACR20) response rate at week 12.

Results. Study drugs were administered to 190 patients (placebo, n = 54; E6011 100 mg, n = 28; E6011 200 mg, n = 54; E6011 400/200 mg, n = 54), and 169 patients completed treatment. A significant difference from placebo was not found in ACR20 response rates at week 12 (37.0% [placebo], 39.3% [100 mg], 48.1% [200 mg], and 46.3% [400/200 mg], using nonresponder imputation). As a secondary end point, ACR20 response rate in the 200-mg and 400/200-mg groups attained statistical significance at week 24 (35.2% [placebo], 39.3% [100 mg], 53.7% [200 mg], and 57.4% [400/200 mg]). Subsequent exploratory subgroup analysis revealed greater efficacy of E6011, particularly in patients with a higher baseline proportion of CD16+ monocytes; ACR20 response rates in this patient subgroup at week 24 were 30.0% (placebo), 46.7% (100 mg), 57.7% (200 mg), and 69.6% (400/200 mg). E6011 administered for 24 weeks was well tolerated.

Conclusion. This is the first evidence that E6011, a novel cell trafficking inhibitor targeting the FKN–CX_3CR1 interaction, is modestly effective with 24 weeks of treatment in RA patients, although the primary end point was not met.

Clinicaltrials.gov identifier: NCT02960438.
Supported by Eisai Company, Ltd.

[1]Yoshiya Tanaka, MD: University of Occupational and Environmental Health, Japan, Kitakyushu, Japan; [2]Tsutomu Takeuchi, MD: Keio University School of Medicine, Tokyo, Japan; [3]Hisashi Yamanaka, MD: Sanno Medical Center, Tokyo, Japan; [4]Toshihiro Nanki, MD: Toho University School of Medicine, Tokyo, Japan; [5]Hisanori Umehara, MD: Nagahama City Hospital, Shiga, Japan; [6]Nobuyuki Yasuda, PhD, Tetsu Kawano, MD, Toshio Imai, PhD: KAN Research Institute, Inc., Kobe, Japan; [7]Fumitoshi Tago, MS, Yasumi Kitahara, PhD, Makoto Kawakubo, MS, Kentaro Torii, MS, Seiichiro Hojo, MS: Eisai Company, Ltd., Tokyo, Japan.

Dr. Tanaka has received consulting fees, speaking fees, and/or honoraria from Pfizer, Sanofi, Asahi-kasei, GlaxoSmithKline, Mitsubishi-Tanabe, Gilead, and Janssen (less than $10,000 each) and from Daiichi-Sankyo, Eli Lilly, Novartis, YL Biologics, Bristol Myers Squibb, Eisai, Chugai, AbbVie, and Astellas (more than $10,000 each) and has received research grants from AbbVie, Mitsubishi-Tanabe, Chugai, Asahi-Kasei, Eisai, Takeda, and Daiichi-Sankyo. Dr. Takeuchi has received consulting fees, speaking fees and/or honoraria from Daiichi-Sankyo, Takeda, Ono Pharmaceutical, Gilead, Taiho Pharmaceutical, Taisho Pharmaceutical, A2 Healthcare Corporation, GlaxoSmithKline, Eli Lilly, Boehringer Ingelheim, Novartis, AYUMI, Pfizer, and Sanofi (less than $10,000 each) and from AbbVie, Asahi-Kasei, Astellas, Eisai, JCR, Mitsubishi-Tanabe, Chugai, Nippon Kayaku, UCB, and Bristol Myers Squibb (more than $10,000 each). Dr. Yamanaka has received consulting fees, speaking fees, and/or honoraria from AbbVie, Astellas, AYUMI, Bristol Myers Squibb, Chugai, Daiichi-Sankyo, Eisai, Kaken, Mitsubishi-Tanabe, Nippon Boehringer Ingelheim, Nippon Shinyaku, Novartis, Ono Pharmaceutical, Pfizer, Taisho Pharmaceutical, Takeda, Torii, and UCB (less than $10,000 each) and from Teijin Company and YL Biologics (more than $10,000 each). Dr. Nanki has received consulting fees, speaking fees, and/or honoraria from Daiichi Sankyo, Teijin, Takeda, Shionogi, UCB, Sanofi, Nippon Boehringer Ingelheim, Pfizer, Nihon Pharmaceutical, Yutoku Pharmaceutical, Janssen, Gilead, and Taiho Pharmaceutical (less than $10,000 each) and from Mitsubishi-Tanabe, Chugai, Eisai, Asahi-Kasei, Bristol Myers Squibb, Ono Pharmaceutical, AYUMI, Bayer Yakuhin, AbbVie, Eli Lilly, Novartis, Astellas, and Nippon Kayaku (more than $10,000 each). Dr. Umehara has received consulting fees from Eisai (less than $10,000). Drs. Yasuda, Kawano, and Imai own stock or stock options in KAN Research Institute, Inc. Mr. Tago, Dr. Kitahara, and Messers. Kawakubo, Torii, and Hojo own stock or stock options in Eisai.

Address correspondence to Yoshiya Tanaka, University of Occupational and Environmental Health, Japan, First Department of Internal Medicine, 1-1 Iseigaoka, Kitakyushu, Fukuoka 807-8555, Japan. Email: tanaka@med.uoeh-u.ac.jp.

Submitted for publication June 2, 2020; accepted in revised form October 6, 2020.

INTRODUCTION

Rheumatoid arthritis (RA) is an autoimmune disease characterized by persistent synovitis and systemic inflammation, ultimately resulting in joint damage, disability, decreased quality of life, and other comorbidities, when insufficiently treated. Disease-modifying antirheumatic drugs (DMARDs) are key therapeutic agents. They include conventional synthetic DMARDs, of which methotrexate (MTX) is the anchor drug, as well as biologic and targeted synthetic DMARDs targeting tumor necrosis factor (TNF), interleukin-6 (IL-6) receptor, T cell costimulation, B cells (CD20), and JAKs. Recent guidelines for the management of RA recommend rapid attainment of sustained remission or low disease activity in each patient (1–4). However, ~50–70% of patients fail to achieve remission or maintain low disease activity, even when they initially respond well to current therapies (5,6).

Fractalkine (FKN) is a membrane-bound CX_3C chemokine that possesses a chemokine/mucin hybrid structure and transmembrane domain (7,8). FKN is expressed on vascular endothelial cells (ECs), and its unique structure gives it 2 functional forms: an adhesion molecule when present in its membrane-bound form and a chemoattractant in its soluble form after shedding by metalloproteases (9). Expression of FKN is up-regulated on vascular ECs at inflamed lesions, such as RA synovia (10,11). Notably, both forms of FKN are recognized by its receptor, CX_3CR1, which is expressed on monocyte/macrophages and cytotoxic effector lymphocytes, including natural killer cells and cytotoxic T cells (7,12,13). Among monocytes, CX_3CR1 is highly expressed on CD16+ monocytes, which are known to be increased in RA (14,15). CD16+ monocytes adhere to vascular endothelium via FKN–CX_3CR1 interactions, where they produce large amounts of proinflammatory cytokines (e.g., TNF and IL-6) and chemokines that recruit other types of immune cells to areas where CD16+ monocytes are located (16,17). This results in augmented inflammatory reactions in affected synovia (18). CX_3CR1 is also expressed on terminally differentiated CD4+ and CD8+ T cells, which are increased in the peripheral blood of RA patients. These cells preferentially produce interferon-γ, TNF, granzyme A, and perforin (11), ultimately contributing to tissue damage, which is indicative of the role the FKN–CX_3CR1 axis plays in RA pathophysiology.

Previously, we investigated the safety and efficacy of E6011, a humanized IgG2 monoclonal antibody against human FKN, in a phase I/II, open-label, multiple-ascending-dose study in patients with active RA. E6011 was found to be safe and showed efficacy signals in these patients (19). We further evaluated E6011 in a phase II, double-blind, placebo-controlled study to confirm its efficacy, safety, and dose-response relationship in patients with moderately to severely active RA who had an inadequate response to MTX. Herein, we present the results of the 24-week treatment phase (double-blind portion) of this clinical trial. This is the first study to reveal the clinical benefit of blocking the FKN–CX_3CR1 axis for treatment of RA.

PATIENTS AND METHODS

Study design. This multicenter, randomized, double-blind, placebo-controlled, parallel-group comparison study was performed to evaluate the efficacy and safety of 3 dosages of E6011, compared with placebo, in RA patients in Japan (ClinicalTrials.gov identifier: NCT02960438). The following 4 treatment groups were selected for the study: E6011 100-mg group, E6011 200-mg group, E6011 400/200-mg group, and placebo group. The study consisted of screening, observation, treatment (double-blind), extension (open-label), and follow-up phases. Screening assessments were performed within 42 days prior to treatment initiation. The protocol was approved by the institutional review board of each study institution. This study was conducted in accordance with the standard operating procedures of the sponsor, which were designed to ensure adherence with the Declaration of Helsinki and Good Clinical Practice.

Patients. Japanese patients with active RA (ages 18–74 years) who were diagnosed according to the 1987 American College of Rheumatology (ACR) classification criteria (20) or the 2010 ACR/European League Against Rheumatism criteria (21) were screened for eligibility. Inclusion criteria included the following: tender joint count of ≥6 (of 68 joints), swollen joint count of ≥6 (of 66 joints), and C-reactive protein (CRP) level of ≥0.6 mg/dl, or erythrocyte sedimentation rate of ≥28 mm/hour after receiving MTX (6–16 mg/week) for ≥12 weeks before trial entry. Patients were excluded if they had previously been treated with biologics and discontinued treatment due to inadequate response or had a history of biologic treatment for RA within 12 weeks prior to the study. All participants provided written informed consent before participation.

Randomization and blinding. Patients who met the eligibility criteria during the screening and observation phase were randomly allocated to the placebo, 100-mg, 200-mg, and 400/200-mg groups at a 2:1:2:2 ratio. This dynamic allocation (minimization method) was performed using the following factors: CRP level at the screening phase, disease duration, and history of biologic treatment. Randomization was performed centrally using an interactive web response system (IWRS). The individual responsible for randomization generated the list of randomized drug numbers. At screening, the investigator or designee accessed the IWRS to register patient information. The independent enrollment center confirmed the eligibility of the patient, assigned each patient to a treatment group using a dynamic allocation algorithm, and provided the drug number to the investigator via email. Upon completing all planned assessments at the observation phase, the investigator prescribed the study drug for the eligible patient based on the drug number specified by the independent enrollment center. Therefore, in a double-blind manner, patients received either E6011 or placebo at weeks 0, 1, and 2, and then once every 2 weeks until week 22.

Procedures. During the treatment phase (24 weeks), patients were subcutaneously injected with either E6011 or placebo at weeks 0, 1, and 2, and then once every 2 weeks until week 22 in a double-blind manner. In the E6011 100-mg, E6011 200-mg, and placebo groups, patients received the study drug (100 mg, 200 mg, or placebo, respectively) at weeks 0, 1, and 2, and then once every 2 weeks. In the E6011 400/200-mg group, patients received 400 mg at weeks 0, 1, 2, 4, 6, 8, and 10 and then 200 mg once every 2 weeks. In our previous phase I/II study (19), 400 mg of E6011 sufficiently improved clinical symptoms. However, in the present study, administration of the 400-mg dose required subcutaneous injection at 4 sites with 100 mg/ml of study drug. Therefore, 400-mg administrations were limited to 10 weeks (for the primary end point) to reduce the burden on patients, and from week 12, patients received 200-mg subcutaneous administrations (injection at 2 sites).

Patients who completed evaluations at week 24 of the treatment phase entered the extension phase. The extension phase lasted until 104 weeks after the start of study treatment, and patients received open-label E6011 200 mg every 2 weeks until week 102. If patients completed or discontinued the study, a follow-up visit was conducted 28 days after completion or discontinuation of the study, and a follow-up visit or telephone interview was conducted 70 days after the last dosing. Here, we present the results of the 24-week treatment phase (double-blind portion) of this clinical trial.

Assessments. *Efficacy.* The primary end point was ACR 20% improvement criteria (ACR20) response rate at week 12. Major secondary end points were rates of ACR20 response at week 24, rates of ACR50 and ACR70 responses at weeks 12 and 24, and improvements in individual ACR components (number of tender joints, number of swollen joints, patient's and physician's global assessments, Health Assessment Questionnaire (22), and CRP level) over 24 weeks. Other secondary end points included change in Disease Activity Score in 28 joints using the CRP level (DAS28-CRP) (23) and the Clinical Disease Activity Index (CDAI) (24) over 24 weeks.

Biomarker. Peripheral blood samples were used to measure CD16+ monocytes at baseline and at weeks 2, 4, 8, 12, and 24. Whole blood was lysed with BD Pharm Lyse (BD Biosciences) and then incubated with Fc Receptor Blocking Reagent (Miltenyi Biotec). Blocked samples were incubated with Alexa Fluor 647–conjugated anti-human CD14 (BioLegend) and fluorescein isothiocyanate–conjugated anti-human CD16 (Abcam) for 30 minutes on ice and analyzed using a FACSCanto II apparatus (BD Biosciences). The percentage of CD16+ cells in total monocytes was calculated with a sequential gating strategy using FlowJo (BD Biosciences).

Safety. Safety was evaluated based on adverse events (AEs), clinical laboratory parameters, vital signs, standard 12-lead electrocardiogram (ECG) results, chest radiographs, neurologic findings, and CD4+ blood cell counts. AEs were coded using the Medical Dictionary for Regulatory Activities, version 20.1. Severity of AEs was graded on a 5-point scale according to the Common Terminology Criteria for Adverse Events (CTCAE; version 4.0).

Statistical analysis. The primary end point was analyzed using a logistic regression model with CRP level at baseline, RA disease duration, and history of treatment with biologics as covariates for comparison between the placebo group and either the E6011 200-mg or E6011 400/200-mg group. The overall significance level was defined as $\alpha = 0.025$ (1-sided). The Benjamini-Hochberg method was used to control the overall Type I error rate.

Sample size was conservatively calculated at a 1-sided significance level of $\alpha = 0.0125$ ($\alpha = 0.025/2$) considering multiplicity. The ACR20 response rate at week 12 was expected to be 30% in the placebo group and ≥60% in both the E6011 200-mg and 400/200-mg groups. Sample sizes of 50 for the 200-mg, 400/200-mg, and placebo groups had 91% power to detect a difference in response rate of 35% between the placebo group and each E6011 group and 79% power to detect a difference in response rate of 30% based on a chi-square test.

Multiplicity adjustment was not considered for secondary efficacy analyses. For ACR20 (excluding week 12), ACR50, and ACR70 response rates, analyses similar to those for the primary end point were conducted. Each component of the ACR response criteria, DAS28-CRP, and CDAI, and any changes from baseline, were summarized at each visit, according to treatment group. Changes from baseline were also analyzed using analysis of covariance with baseline value, CRP level at baseline, RA disease duration, and prior biologic treatment as covariates. The significance level for comparisons between the placebo group and each E6011 treatment group (100-mg, 200-mg, or 400/200-mg) was defined as $\alpha = 0.05$ (2-sided). The ACR20 and ACR50 response rates at week 24 were also analyzed in subgroups according to the baseline proportion of CD16+ monocytes.

The efficacy analysis set was the group of randomized patients who received the study drug and had ≥1 evaluable postdose primary efficacy data set available. The safety analysis set was the group of patients who received ≥1 dose of the study drug and had ≥1 evaluable postdose safety data set available. For efficacy analyses, the approach used to handle missing data for the ACR response criteria was the nonresponder imputation (NRI) method, and for continuous variables, the last observation carried forward method was used. For safety analysis, AEs that emerged during the 24-week treatment phase were evaluated.

RESULTS

Patient disposition and baseline characteristics. Between November 10, 2016 and September 7, 2017, 194 patients were randomly allocated to each treatment group. After randomization, 4 of 194 patients discontinued the study before

starting treatment with the study drug, because they failed to meet entry criteria. All treated patients (n = 190) were included in the efficacy and safety analyses. Of the 190 patients who received ≥1 dose of the study drug (placebo, n = 54; E6011 100 mg, n = 28; E6011 200 mg, n = 54; 400/200 mg, n = 54), 169 completed the planned treatment regimen, while 21 prematurely discontinued treatment within the 24-week double-blind period. All patients were included in each analysis. The number of patients who discontinued treatment was similar between the placebo and E6011 treatment groups (Figure 1).

Baseline demographic characteristics were similar among the 4 treatment groups (Table 1). Most patients (78.9%) were female, and the median age was 56.0 years. The mean ± disease duration was 7.1 ± 6.85 years. Approximately 23% of patients (43 of 190) had previously received biologic. The mean ± SD dose of MTX was 9.9 ± 2.84 mg/week, the mean ± SD baseline CRP level was 1.30 ± 1.49 mg/dl, and the mean ± SD baseline tender joint count (of 68 joints) and swollen joint count (of 66 joints) were 15.3 ± 7.90 and 12.6 ± 5.98, respectively. The proportion of oral glucocorticoid use in the E6011 400/200-mg treatment group was numerically higher, although the difference was not significant, compared with the other groups. Mean baseline scores for clinical measures were comparable across treatment groups.

ACR20 response rates at week 12 (using NRI) were 37.0% (placebo), 39.3% (100 mg), 48.1% (200 mg), and 46.3% (400/200 mg). Although the rates were higher in the 200-mg and 400/200-mg groups compared with the placebo group, statistical significance was not reached (P = 0.188 for the 200-mg and 400/200-mg groups, using the logistic regression model with the Benjamini-Hochberg method) (Figure 2A). Therefore, although this study did not meet the primary end point, it met multiple secondary end points. At week 24, ACR20 response rates were 35.2% (placebo), 39.3% (100 mg), 53.7% (200 mg), and 57.4% (400/200 mg), and the response rates in the E6011 200-mg and 400/200-mg groups were significantly higher than in the placebo group (P = 0.023 for the 200-mg group and P = 0.010 for the 400/200-mg group, using the logistic regression model with the Benjamini-Hochberg method) (Figure 2B). ACR50 response rates at weeks 12 and 24 (using NRI) were 14.8% and 16.7% (placebo), 10.7% and 17.9% (100 mg), 25.9% and 25.9% (200 mg), and 18.5% and 27.8% (400/200 mg), respectively. ACR70 response rates at weeks 12 and 24 (using NRI) were 3.7% and 5.6% (placebo), 3.6% and 14.3% (100 mg), 9.3% and 11.1% (200 mg), and 7.4% and 13.0% (400/200 mg), respectively (Figures 2A and B).

The DAS28-CRP and CDAI decreased sequentially from baseline after treatment with E6011. Decreases in the DAS28-CRP and CDAI were statistically significant between the placebo group and the 200-mg or 400/200-mg group as early as week 8 (for DAS28-CRP; Figure 2C) or week 4 (for CDAI; Figure 2D). In contrast, any apparent reduction in CRP level was not observed to be associated with E6011 treatment within the double-blind period (Figure 2E).

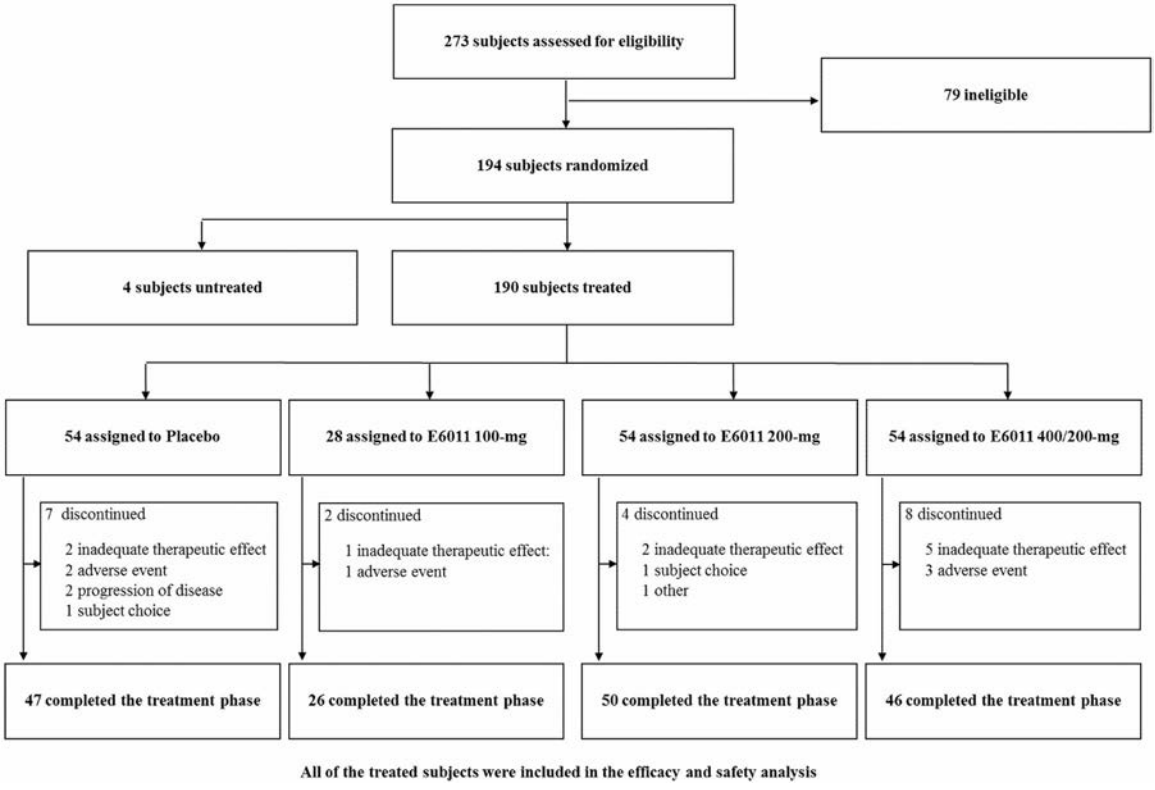

Figure 1. Patient disposition during the 24-week double-blind period.

Table 1. Patient baseline demographics and laboratory data*

	Placebo group (n = 54)	E6011 100-mg group (n = 28)	E6011 200-mg group (n = 54)	E6011 400/200-mg group (n = 54)
Age, years	57.6 ± 9.86	56.5 ± 10.4	56.5 ± 10.4	55.2 ± 9.13
Sex, no. (%)				
Male	9 (16.7)	6 (21.4)	10 (18.5)	15 (27.8)
Female	45 (83.3)	22 (78.6)	44 (81.5)	39 (72.2)
Weight, kg	54.7 ± 11.3	55.4 ± 11.0	57.9 ± 14.4	55.7 ± 11.2
RA duration, years	6.9 ± 7.35	6.4 ± 5.46	7.1 ± 6.58	7.6 ± 7.38
Prior biologic use, no. (%)	12 (22.2)	7 (25.0)	12 (22.2)	12 (22.2)
MTX dose, mg/week	9.6 ± 2.20	9.9 ± 3.22	10.1 ± 2.97	10.1 ± 3.10
Oral glucocorticoids				
Yes, no. (%)	23 (42.6)	11 (39.3)	24 (44.4)	31 (57.4)
Dose, mg/day†	3.65 ± 2.17	4.82 ± 2.33	4.15 ± 2.34	3.54 ± 2.13
RF-positive, no. (%)‡	45 (83.3)	23 (82.1)	46 (85.2)	44 (81.5)
Anti-CCP–positive, no. (%)§	51 (94.4)	26 (92.9)	46 (85.2)	45 (83.3)
TJC (of 68 joints)	13.7 ± 6.81	14.1 ± 7.24	16.3 ± 7.15	16.6 ± 9.61
SJC (of 66 joints)	12.7 ± 6.81	11.3 ± 5.27	12.4 ± 4.89	13.5 ± 6.41
CRP at screening, mg/dl	1.25 ± 1.04	1.38 ± 1.60	1.60 ± 3.33	1.34 ± 1.53
CRP at baseline, mg/dl	1.50 ± 1.63	1.44 ± 1.87	1.08 ± 0.84	1.24 ± 1.63
DAS28-CRP	5.04 ± 0.88	4.99 ± 1.01	5.08 ± 0.73	5.20 ± 0.93

* Except where indicated otherwise, values are the mean ± SD. RA = rheumatoid arthritis; MTX = methotrexate; RF = rheumatoid factor; anti-CCP = anti–cyclic citrullinated peptide; TJC = tender joint count; SJC = swollen joint count; DAS28-CRP = Disease Activity Score in 28 joints using C-reactive protein.
† Concomitant dose at baseline is shown in prednisolone equivalent.
‡ Positivity defined as >15 IU/ml.
§ Positivity defined as ≥4.5 units/ml.

Levels of CD16+ monocytes, which highly express CX_3CR1, in whole monocytes were sequentially measured. Baseline levels ranged broadly from 1.60% to 42.1%, and the median value derived from all patients was 10.35% (data not shown). Median values in each group at baseline were comparable (9.43% [placebo], 12.80% [100 mg], 11.15% [200 mg], and 10.80% [400/200 mg]). For further exploratory analyses, patients were divided into 2 groups by taking the baseline median yielded from all patients (10.35%) and applying it to CD16+ monocyte–low and CD16+ monocyte–high populations. In the population with

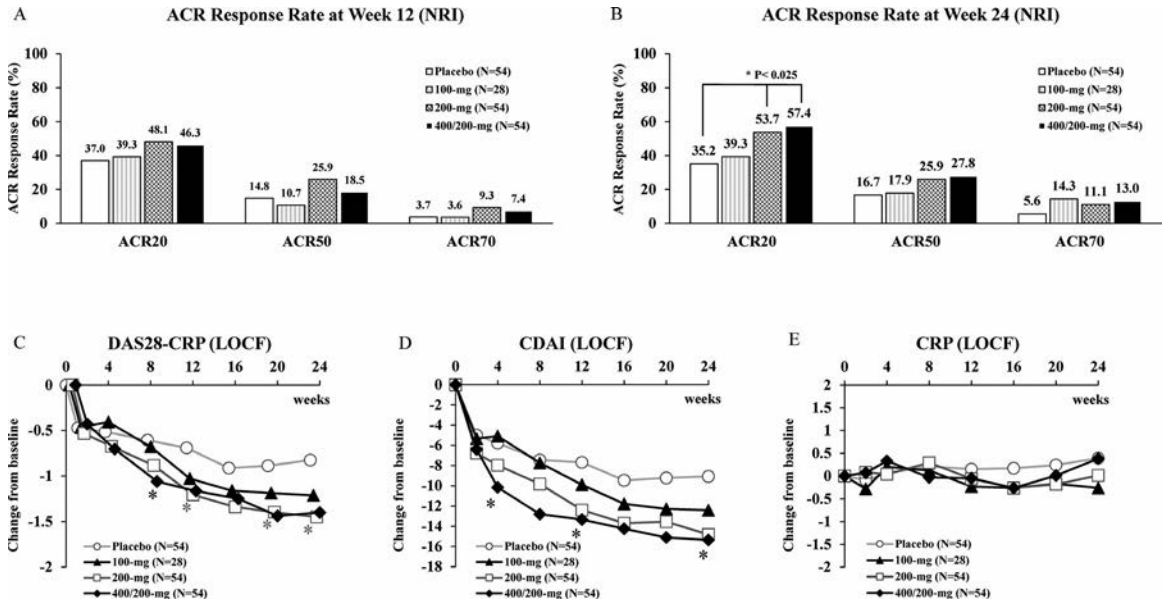

Figure 2. **A** and **B**, American College of Rheumatology 20% improvement criteria (ACR20), ACR50, and ACR70 response rate at weeks 12 (**A**) and 24 (**B**) (using nonresponder imputation [NRI]). **C–E**, Mean change from baseline in the Disease Activity Score in 28 joints using the C-reactive protein level (DAS28-CRP) (**C**), the Clinical Disease Activity Index (CDAI) (**D**), and the CRP level (**E**), according to E6011 dose (using the last observation carried forward [LOCF] approach). * = $P < 0.05$, versus placebo, in **C** and **D**.

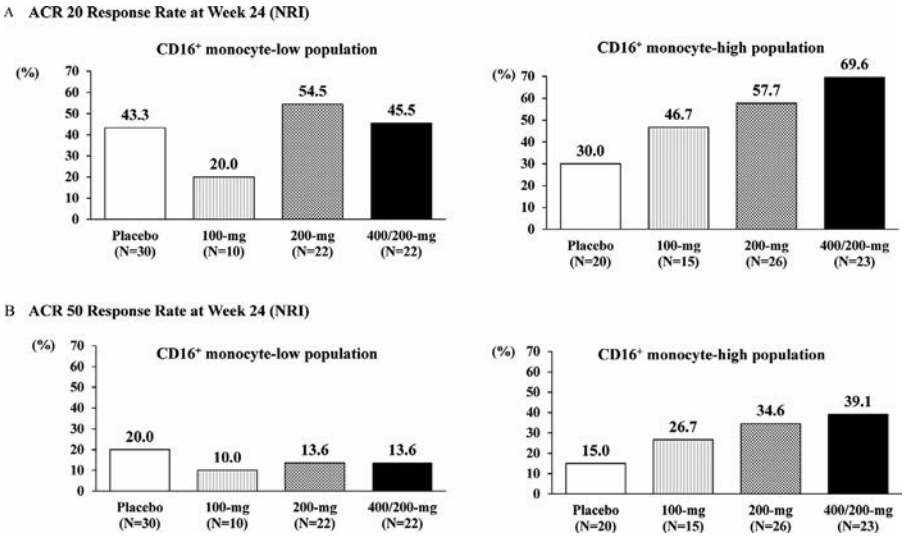

Figure 3. Subgroup analysis by baseline proportion of CD16+ monocytes. ACR20 response rates (**A**) and ACR50 response rates (**B**) at week 24 in populations with a low or high proportion of CD16+ monocytes are shown. See Figure 2 for definitions.

low CD16+ monocytes, there was no trend in terms of ACR20 response at week 24 (43.3% [placebo], 20.0% [100 mg], 54.5% [200 mg], and 45.5% [400/200 mg]) (Figure 3). The response in the CD16+ monocyte–high population showed a marked dose-dependent increase in ACR20 response rate (30.0% [placebo], 46.7% [100 mg], 57.7% [200 mg], and 69.6% [400/200 mg]). These results were also confirmed in the ACR50 responses at week 24 (20.0% [placebo], 10.0% [100 mg], 13.6% [200 mg], and 13.6% [400/200 mg] in the CD16 monocyte–low population, and 15.0% [placebo], 26.7% [100 mg], 34.6% [200 mg], and 39.1% [400/200 mg] in the CD16+ monocyte–high population) (Figure 3).

After initiation of treatment, CD16+ monocyte levels in total monocytes decreased significantly at week 2 in all E6011 groups, and reductions were sustained throughout the treatment period without dose dependency (Figure 4). AEs and treatment-related AEs occurred more frequently in the E6011 treatment groups than in the placebo group (AEs, 63.0% in the placebo group and 73.5% in the E6011 groups; treatment-related AEs, 22.2% in the placebo group and 39.7% in the E6011 groups) (Table 2). A dose response was found in the incidence of AEs (63.0% [placebo], 67.9% [100 mg], 70.4% [200 mg], and 79.6% [400/200 mg]), but not in the incidence of treatment-related AEs (22.2% [placebo], 46.4% [100 mg], 33.3% [200 mg], and 42.6% [400/200 mg]).

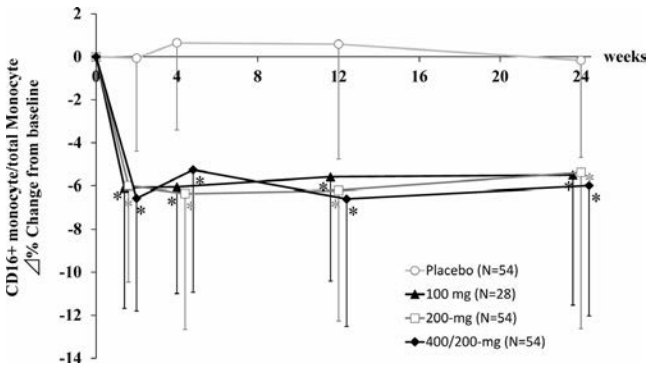

Figure 4. Changes in the proportion of CD16+ monocytes after E6011 treatment. Symbols and lines show the mean ± SD. * = $P <$ 0.001 versus placebo.

The incidence of grade 3 CTCAEs and grade 4 AEs and serious AEs that led to treatment discontinuation or dose interruptions was similar between the placebo group and E6011 treatment groups, and no apparent dose response was observed. AEs that occurred in ≥5% of patients in any E6011 treatment group included nasopharyngitis, upper respiratory tract infection, stomatitis, bronchitis, back pain, pharyngitis, and dental caries. Among the AEs that occurred in ≥5% of patients in any E6011 group, the following AEs occurred at a rate of ≥2-fold that observed in patients in the placebo group: stomatitis (1.9% in the placebo group versus 5.1% in E6011 groups), bronchitis (1.9% versus 4.4%), back pain (1.9% versus 4.4%), and dental caries (0% versus 2.2%). No clinically meaningful changes were observed in laboratory data or other safety assessments, such as standard 12-lead ECG results, chest radiographs, neurologic findings, or CD4+ blood cell counts.

DISCUSSION

E6011 is a novel investigational drug used to neutralize FKN, which is highly expressed in inflamed lesions and suppresses immune cell accumulation at affected lesions. This is the first multicenter, randomized, double-blind, placebo-controlled study to evaluate the efficacy and safety of E6011 for up to 24 weeks in patients with active RA who had an inadequate response to MTX.

With E6011, there was a trend toward increasing ACR20 response rate at week 12, the primary end point, although this

Table 2. AEs and laboratory data*

	Placebo group (n = 54)	E6011 100-mg group (n = 28)	E6011 200-mg group (n = 54)	E6011 400/200-mg group (n = 54)	E6011 total (n = 136)
All AEs	34 (63.0)	19 (67.9)	38 (70.4)	43 (79.6)	100 (73.5)
Treatment-related AEs	12 (22.2)	13 (46.4)	18 (33.3)	23 (42.6)	54 (39.7)
AE maximum grade					
Grade 1	7 (13.0)	4 (14.3)	10 (18.5)	9 (16.7)	23 (16.9)
Grade 2	25 (46.3)	13 (46.4)	25 (46.3)	32 (59.3)	70 (51.5)
Grade 3	2 (3.7)	1 (3.6)	3 (5.6)	0	4 (2.9)
Grade 4	0	1 (3.6)	0	2 (3.7)	3 (2.2)
Grade 5	0	0	0	0	0
Serious AEs	2 (3.7)	1 (3.6)	2 (3.7)	3 (5.6)	6 (4.4)
Death	0	0	0	0	0
AEs leading to withdrawal	2 (3.7)	1 (3.6)	0	2 (3.7)	3 (2.2)
AEs that occurred in ≥5% of patients in any group					
Nasopharyngitis	16 (29.6)	7 (25.0)	10 (18.5)	18 (33.3)	35 (25.7)
URI	2 (3.7)	2 (7.1)	4 (7.4)	2 (3.7)	8 (5.9)
Stomatitis	1 (1.9)	0	2 (3.7)	5 (9.3)	7 (5.1)
Bronchitis	1 (1.9)	2 (7.1)	1 (1.9)	3 (5.6)	6 (4.4)
Back pain	1 (1.9)	1 (3.6)	3 (5.6)	2 (3.7)	6 (4.4)
Pharyngitis	2 (3.7)	0	3 (5.6)	2 (3.7)	5 (3.7)
Dental caries	0	0	0	3 (5.6)	3 (2.2)
Headache	3 (5.6)	0	0	1 (1.9)	1 (0.7)
Laboratory data					
Hemoglobin, gm/liter	−2.0 ± 9.7	−1.6 ± 7.2	0.5 ± 10.3	−3.3 ± 10.4	−1.4 ± 9.9
Lymphocytes, 10^9/liter	−0.05 ± 0.61	0.08 ± 0.38	−0.01 ± 0.34	−0.06 ± 0.57	−0.01 ± 0.45
Neutrophils, 10^9/liter	−0.09 ± 2.02	−0.40 ± 1.42	−0.34 ± 1.49	−0.39 ± 2.22	−0.37 ± 1.79
ALT, units/liter	0.6 ± 12.0	3.9 ± 26.5	3.4 ± 12.8	0.3 ± 14.1	2.3 ± 16.9
Creatinine, μmoles/liter	0.7 ± 5.7	1.9 ± 6.1	0.7 ± 5.2	2.0 ± 21.3	1.4 ± 14.0
HDL cholesterol, mmoles/liter	−0.04 ± 0.28	0.05 ± 0.28	0.02 ± 0.24	0.05 ± 0.28	0.04 ± 0.26
LDL cholesterol, mmoles/liter	0.01 ± 0.44	−0.05 ± 0.40	−0.03 ± 0.55	0.03 ± 0.44	−0.01 ± 0.48
Creatine kinase, IU/liter	5.4 ± 25.3	7.2 ± 26.4	2.1 ± 34.8	18.4 ± 74.0	9.6 ± 53.1

* Adverse event (AE) values are the number (%) of patients. Laboratory data are the mean ± SD change from baseline at week 24 (using last observation carried forward). AEs emerged until week 24. However, for patients who discontinued the study drug during the treatment phase, AEs emerged until 70 days after the last intended dose. A patient with ≥2 AEs in the same preferred term was counted only once for that preferred term. MedDRA version 20.1 was used. URI = upper respiratory tract infection; ALT = alanine aminotransferase; HDL = high-density lipoprotein; LDL = low-density lipoprotein.

was not statistically significant (Figure 2A). Statistical significance was attained at week 24, which was the secondary end point, even though the response rate was lower than we expected and lower than that of existing marketed biologics for RA (Figure 2B). Regarding other secondary end points, ACR50 response rates were numerically higher in the E6011 groups than in the placebo group at week 24 (Figure 2B), although this was not statistically significant. CRP level was not reduced in correlation with symptomatic improvement during the 24 weeks (Figure 2E). The CDAI, which does not include CRP level, reached statistical significance earlier, at week 4, in the 400/200-mg group (Figure 2D). Such discrepancy in the clinical measures used may support the notion of a distinct mode of action of E6011, which suppresses cell migration from the circulation and accumulation in inflamed tissue but does not directly neutralize cytokines. The ACR response rate that is widely utilized as an end point in clinical studies may not accommodate evaluation of the cell trafficking inhibitor, E6011. Further studies are required to investigate the end point that sufficiently reflects the local effect of E6011.

For biomarker analysis, we focused on CD16+ monocytes because of their importance in RA pathophysiology and high expression of the FKN receptor, CX_3CR1. Although there was no relationship between background features of the disease and the proportion of CD16+ monocytes (data not shown), we conducted a subsequent exploratory analysis as to whether baseline levels of these cells were related to the response to E6011. As shown in Figure 3, CD16+ monocyte–high populations tended to respond better than CD16+ monocyte–low populations, while there were some variations in data on ACR20 response. While a more obvious dose-response tendency for ACR50 response was observed in CD16+ monocyte–high populations, these results should be interpreted carefully, as this subgroup analysis was ad hoc and exploratory and was immature for providing statistically convincing data because of its small sample size. Although this subsequent exploratory analysis had limitations, it provided some indication that E6011 may represent a potential treatment option for RA patients, especially with a precision medicine approach considering the baseline proportion of CD16+ monocytes.

After initiation of E6011 treatment, CD16+ monocyte levels were found to decrease quickly by week 2, without any dose response (Figure 4). No relationship was found between the magnitude of CD16+ monocyte level reduction and clinical response (data not shown). The FKN–CX_3CR1 interaction is known to elicit signals to promote the survival of human monocytes through activation of phosphoinositide 3-kinase (25). It is believed that E6011 may inhibit monocyte survival, although FKN–CX_3CR1 may not be a central or unique axis for monocyte survival or maintenance because of the lack of dose dependency observed. Decreased magnitude of CD16+ monocytes cannot pharmacodynamically reflect the dose of E6011 administered. Therefore, the importance of CD16+ monocytes in predicting response or as a pharmacodynamic biomarker for E6011 remains elusive and should be further explored.

Regarding the safety profile of E6011, the incidence of AEs showed modest dose dependency. Notably, nasopharyngitis, stomatitis, bronchitis, back pain, and dental caries occurred more frequently with higher doses of E6011, although these AEs were either mild or moderate (grade 1 or 2). Moreover, given that these AEs were the most common ones reported in other clinical trials, and that some of them represent potential adverse reactions to MTX, E6011 was found to generally be safe and well tolerated at any dose for 24 weeks. However, further accumulation of safety information is necessary through additional clinical studies.

Regarding laboratory data, an increased mean change in creatine kinase levels was observed in the 400/200-mg group (18.4 IU/liter). This was due to included data on 1 patient in the 400/200-mg group. Without this data point, the mean creatine kinase change from baseline in the 400/200-mg group (9.0%) was consistent with that in other groups. Additionally, this patient's high level of creatine kinase (240 IU/liter at 24 weeks) was subsequently improved to within normal range, despite continuation of the study drug.

Considering the mode of action of E6011, which primarily ameliorates local inflammation by regulating cell trafficking without direct suppression of the systemic inflammatory reaction (i.e., no change in CRP level), its safety profile may be preferable to that of other biologic agents. Anemic hemoglobin levels are generally expected to normalize with improvement in systemic inflammation, although E6011 did not confer an increase in hemoglobin level in this study. This may also suggest that E6011 exerts its biologic effect locally rather than systemically. In contrast, hemoglobin level increased slightly in responders to E6011, while it decreased in nonresponders (data not shown). However, such differences were not sufficient to affect the mean value in the cohort. It is therefore unlikely that E6011 reduced hemoglobin level in any of the patients. These results indicate that safety signals were similar among 100-mg, 200-mg, and 400-mg doses of E6011. However, a longer and more detailed evaluation is required to fully establish the safety profile of E6011.

In conclusion, although the primary end point in this study was not met, our data suggest that E6011 may have modest efficacy for patients with active RA who had an inadequate response to MTX, especially if they showed a higher proportion of CD16+ monocytes at baseline. The effect of E6011 may primarily emerge at locally inflamed lesions rather than systemically, which may be due to its mode of action, and conventional measures for clinical evaluation may not be appropriate for evaluating this treatment. The proportion of CD16+ monocytes in peripheral blood at baseline may indicate which patients will respond well to E6011. Although further evidence is necessary, this may help determine who should be treated with E6011. Because only preliminary evidence was obtained in this study, and our work cannot be translated to real-world clinical practice at present, further evaluation in future clinical trials is warranted to confirm the therapeutic benefit of E6011.

ACKNOWLEDGMENTS

The authors thank the study participants and all investigators. We thank Mark Abramovitz, PhD, and Richard Robins, PhD, from Edanz Group for editing a draft of the manuscript.

AUTHOR CONTRIBUTIONS

All authors were involved in drafting the article or revising it critically for important intellectual content, and all authors approved the final version to be published. Mr. Tago had full access to all of the data in the study and takes responsibility for the integrity of the data and the accuracy of the data analysis.

Study conception and design. Tanaka, Takeuchi, Yamanaka, Nanki, Umehara, Yasuda, Tago, Kitahara, Hojo, Kawano, Imai.

Acquisition of data. Kawakubo, Torii.

Analysis and interpretation of data. Tanaka, Takeuchi, Yamanaka, Nanki, Umehara, Yasuda, Tago, Kitahara, Kawakubo, Torii, Hojo, Kawano, Imai.

ROLE OF THE STUDY SPONSOR

This work was supported by funding from Eisai Company, Ltd. Eisai Company, Ltd. was involved in study design, data collection, analysis, and interpretation of data. The corresponding author had full access to all data and had responsibility for the decision to submit for publication. Publication of this article was not contingent upon approval by Eisai Company, Ltd.

REFERENCES

1. Smolen JS, Landewé R, Bijlsma J, Burmester G, Chatzidionysiou K, Dougados M, et al. EULAR recommendations for the management of rheumatoid arthritis with synthetic and biological disease-modifying antirheumatic drugs: 2016 update. Ann Rheum Dis 2017;76:960–77.
2. Smolen JS, Breedveld FC, Burmester GR, Bykerk V, Dougados M, Emery P, et al. Treating rheumatoid arthritis to target: 2014 update of the recommendations of an international task force. Ann Rheum Dis 2016;75:3–15.
3. Tanaka Y. Intensive treatment and treatment holiday of TNF-inhibitors in rheumatoid arthritis. Curr Opin Rheumatol 2012;24:319–26.
4. Tanaka Y. Current concepts in the management of rheumatoid arthritis. Korean J Intern Med 2016;31:210–8.
5. Iannone F, Sinigaglia L, Favalli EG, Sarzi-Puttini P, Atzeni F, Caporal R, et al. Drug survival of adalimumab in patients with rheumatoid arthritis over 10 years in the real-world settings: high rate

remission together with normal function ability. Clin Rheumatol 2016;35:2649–56.

6. Iannone F, Ferraccioli G, Sinigaglia L, Favalli EG, Sarzi-Puttini P, Atzeni F, et al. Real-world experience of tocilizumab in rheumatoid arthritis: sub-analysis of data from the Italian biologics' register GISEA. Clin Rheumatol 2018;37:315–21.
7. Imai T, Hieshima K, Haskell C, Baba M, Nagira M, Nishimura M, et al. Identification and molecular characterization of fractalkine receptor CX3CR1, which mediates both leukocyte migration and adhesion. Cell 1997;91:521–30.
8. Yoshie O, Imai T, Nomiyama H. Chemokines in immunity. Adv Immunol 2001;78:57–110.
9. Hundhausen C, Misztela D, Berkhout TA, Broadway N, Saftig P, Reiss K, et al. The disintegrin-like metalloproteinase ADAM10 is involved in constitutive cleavage of CX3CL1 (fractalkine) and regulates CX3CL1-mediated cell-cell adhesion. Blood 2003;102:1186–95.
10. Sawai H, Park YW, Roberson J, Imai T, Goronzy JJ, Weyand CM. T cell costimulation by fractalkine-expressing synoviocytes in rheumatoid arthritis. Arthritis Rheum 2005;52:1392–401.
11. Nanki T, Imai T, Nagasaka K, Urasaki Y, Nonomura Y, Taniguchi K, et al. Migration of CX3CR1-positive T cells producing type 1 cytokines and cytotoxic molecules into the synovium of patients with rheumatoid arthritis. Arthritis Rheum 2002;46:2878–83.
12. Nishimura M, Umehara H, Nakayama T, Yoneda O, Hieshima K, Kakizaki M, et al. Dual functions of fractalkine/CX3C ligand 1 in trafficking of perforin+/granzyme B+ cytotoxic effector lymphocytes that are defined by CX3CR1 expression. J Immunol 2002;168:6173–80.
13. Fong AM, Robinson LA, Steeber DA, Tedder TF, Yoshie O, Imai T, et al. Fractalkine and CX3CR1 mediate a novel mechanism of leukocyte capture, firm adhesion, and activation under physiologic flow. J Exp Med 1998;188:1413–9.
14. Tsukamoto M, Seta N, Yoshimoto K, Suzuki K, Yamaoka K, Takeuchi T. CD14^{bright}CD16+ intermediate monocytes are induced by interleukin-10 and positively correlate with disease activity in rheumatoid arthritis. Arthritis Res Ther 2017;19:1216.
15. Kawanaka N, Yamamura M, Aita T, Morita Y, Okamoto A, Kawashima M, et al. CD14+, CD16+ blood monocytes and joint inflammation in rheumatoid arthritis. Arthritis Rheum 2002;46:2578–86.
16. Cros J, Cagnard N, Woollard K, Patey N, Zhang SY, Senechal B, et al. Human CD14dim monocytes patrol and sense nucleic acids and viruses via TLR7 and TLR8 receptors. Immunity 2010;33:375–86.
17. Carlin LM, Stamatiades EG, Auffray C, Hanna RN, Glover L, Vizcay-Barrena G, et al. Nr4a1-dependent Ly6C(low) monocytes monitor endothelial cells and orchestrate their disposal. Cell 2013;153:362–75.
18. Yano R, Yamamura M, Sunahori K, Takasugi K, Yamana J, Kawashima M, et al. Recruitment of CD16+ monocytes into synovial tissues is mediated by fractalkine and CX3CR1 in rheumatoid arthritis patients. Acta Med Okayama 2007;61:89–98.
19. Tanaka Y, Takeuchi T, Umehara H, Nanki T, Yasuda N, Tago F, et al. Safety, pharmacokinetics, and efficacy of E6011, an anti-fractalkine monoclonal antibody, in a first-in-patient phase 1/2 study on rheumatoid arthritis. Mod Rheumatol 2018;28:58–65.
20. Arnett FC, Edworthy SM, Bloch DA, McShane DJ, Fries JF, Cooper NS, et al. The American Rheumatism Association 1987 revised criteria for the classification of rheumatoid arthritis. Arthritis Rheum 1988;31:315–24.
21. Aletaha D, Neogi T, Silman AJ, Funovits J, Felson DT, Bingham CO III, et al. Rheumatoid arthritis classification criteria: an American College of Rheumatology/European League Against Rheumatism collaborative initiative. Arthritis Rheum 2010;62:2569–81.
22. Fries JF, Spitz PW, Kraines RG, Holman HR. Measurement of patient outcome in arthritis. Arthritis Rheum 1980;23:137–45.
23. Prevoo ML, van't Hof MA, Kuper HH, van Leeuwen MA, van de Putte LB, van Riel PL. Modified disease activity scores that include twenty-eight–joint counts: development and validation in a prospective longitudinal study of patients with rheumatoid arthritis. Arthritis Rheum 1995;38:44–8.
24. Aletaha D, Nell VP, Stamm T, Uffmann M, Pflugbeil S, Machold K, et al. Acute phase reactants add little to composite disease activity indices for rheumatoid arthritis: validation of a clinical activity score. Arthritis Res Ther 2005;7:R796–806.
25. White GE, McNeill E, Channon KM, Greaves DR. Fractalkine promotes human monocyte survival via a reduction in oxidative stress. Arterioscler Thromb Vasc Biol 2014;34:2554–62.

American College of Rheumatology
Empowering Rheumatology Professionals

Arthritis & Rheumatology
Vol. 73, No. 4, April 2021, pp 596–603
DOI 10.1002/art.41601

In Utero and Early Life Exposure to the Great Chinese Famine and Risk of Rheumatoid Arthritis in Adulthood

Hannah VanEvery,[1] Wen-hao Yang,[2] Nancy Olsen,[3] Xinyuan Zhang,[1] Rong Shu,[2] Bing Lu,[4] Shouling Wu,[2] Liufu Cui,[2] and Xiang Gao[1]

Objective. To investigate whether early life exposure to the Great Chinese Famine of 1959–1961 is associated with the risk of RA development in adulthood.

Methods. This study included 101,510 participants who were enrolled in the Kailuan Study in 2006. RA cases were confirmed by medical record review. Logistic regression was used to calculate the odds ratio (OR) and 95% confidence interval (95% CI) for RA according to famine exposure status (exposed in utero or between ages 0 and 3 years, between ages 3 and 6 years, or at age 6 years or older), in comparison to participants born after 1961 who were not exposed to famine.

Results. During 12 years of follow-up (2006–2018), we identified 187 RA cases. Individuals exposed to famine in utero or between ages 0 and 3 years had a higher prevalence of RA relative to other groups (0.2–0.35% versus 0.08–0.20%). After adjustment for potential confounders, the OR for RA was 2.95 (95% CI 1.55–5.59) for individuals exposed in utero, 4.53 (95% CI 2.72–7.54) for those exposed between ages 0 and 3 years, 2.55 (95% CI 1.43–4.57) for those exposed between ages 3 and 6 years, and 2.72 (95% CI 1.70–4.36) for those exposed at age 6 years or older versus individuals born after 1961. Similar associations with the risk of RA were observed for men and women when subjects were stratified by sex (*P* for interaction = 0.89).

Conclusion. Individuals exposed to famine in utero or in early childhood (between ages 0 and 3 years) were more likely to develop RA in adulthood, highlighting the importance of early life as a vulnerable developmental period.

INTRODUCTION

Rheumatoid arthritis (RA) is a debilitating autoimmune disease that causes chronic synovial joint inflammation and increases an individual's risk for further chronic disease, such as cardiovascular disease (CVD) (1) and diabetes mellitus (2). Although several genetic and environmental risk factors have been identified, the etiology of RA remains uncertain (3–5).

In utero and early life adversity (e.g., exposure to famine, malnutrition, natural disaster, and war) have previously been associated with increased risk of CVD (6) and type 2 diabetes (7), both of which involve elevated systemic inflammation. These early life adversity events also have an acute impact on the immune system (8), but little is known about the long-term impact of these stressors on autoimmunity risk. Thus, we conducted this study to test the hypothesis that early life adversity events may be associated with the risk of RA in adulthood.

From 1959–1961, the devastating Great Chinese Famine resulted in millions of deaths (9). Among survivors, the famine caused widespread acute malnutrition and stress (10). The present study included ~100,000 participants, including those born before, during, and after the famine, from the ongoing Kailuan Study of Northern China to examine whether in utero or early life exposure to the Great Chinese Famine was associated with increased risk of RA development in adulthood.

PARTICIPANTS AND METHODS

Study population. The Kailuan Study is an ongoing prospective cohort study designed to investigate risk factors for CVD. After recruitment in 2006, 101,510 participants between ages 18

Supported by a start-up grant from Pennsylvania State University College of Health and Human Development and the Department of Nutritional Sciences.

[1]Hannah VanEvery, MS, Xinyuan Zhang, BS, Xiang Gao, MD, PhD: Pennsylvania State University, State College; [2]Wen-hao Yang, MD, Rong Shu, MD, Shouling Wu, MD, PhD, Liufu Cui, MD: Kailuan General Hospital, Tangshan, China; [3]Nancy Olsen, MD: Penn State Health Milton S. Hershey Medical Center, Hershey, Pennsylvania; [4]Bing Lu, DrPH, MD: Harvard Medical School, Boston, Massachusetts.

No potential conflicts of interest relevant to this article were reported.

Address correspondence to Xiang Gao, MD, PhD, Pennsylvania State University, Department of Nutritional Sciences, 109 Chandlee Lab, University Park, PA 16802 (email: xxg14@psu.edu); or to Liufu Cui, MD, Kailuan General Hospital, Department of Rheumatic Disease, 57 Xinhua East Road, Tangshan 063000, China (email: cuiliufu@hotmail.com).

Submitted for publication May 20, 2020; accepted in revised form November 24, 2020.

and 98 years (81,110 men and 20,400 women) were enrolled in the study. Each participant completed the baseline survey, referred to herein as the "2006 survey," between June 2006 and October 2007 (11–13). At baseline and every 2 years, each participant completed a questionnaire that included demographic information, lifestyle factors, medical conditions, and medication use. Participants also underwent laboratory tests and physical examinations biennially. Adverse events were documented annually. All 101,510 participants (mean age 51.9 years) enrolled in 2006 were included in the current analysis.

Standard protocol approvals and patient consents. This study protocol was approved by the Ethics Committee of the Kailuan Company, Kailuan General Hospital, and all participants provided their written informed consent.

Famine exposure and severity. Birth year was used to identify participants who were exposed to famine, as reported in previous studies of The Great Chinese Famine (7,9). Participants classified as in utero exposed were born between 1959 and 1961 (14). These participants were between ages 45 and 47 years at baseline in 2006. Participants born between 1956 and 1958 were classified as "exposed between ages 0 and 3 years," those born between 1953 and 1955 were classified as "exposed between ages 3 and 6 years," and those born before 1953 were classified as "exposed after age 6 years." Participants born after 1961 were not exposed to the famine and were thus classified as "not exposed"; this group was used as the reference group in our analyses.

While the Great Chinese Famine impacted the entire country of China, certain provinces were more severely affected (15). Provinces that had at least 50% excess mortality, which was calculated based on the highest mortality rate recorded during the famine for that province and the average mortality rate before the famine, were classified as "severely affected" by the famine, while the provinces with <50% excess mortality were classified as "less severely affected" (7,15). This method is consistent with previous studies of the Great Chinese Famine (7,13).

Assessment of RA diagnoses. The outcome of the present study was the diagnosis of RA. Possible RA cases were found by searching the Municipal Social Insurance Institution, which included all participants of the Kailuan Study. Upon identification, 3 rheumatologists (WY, RS, and LC) reviewed the medical records of potential cases to confirm the RA diagnosis, ensuring that each confirmed case met the American College of Rheumatology/European League Against Rheumatism RA classification criteria (16). Only rheumatologist-confirmed cases of RA were included in our analyses.

Assessment of covariates. At baseline, participants received a questionnaire that collected self-reported data on baseline age, sex, birthplace, smoking history, alcohol intake, and medical history (e.g., CVDs and current medications such as hypoglycemic, antihypertensive, and lipid-lowering agents). Trained nurses assessed each participant's blood pressure, height, and weight, as previously described (17). From the height and weight measurements, body mass index (BMI) was calculated by dividing weight (in kilograms) by height (in meters squared).

The same morning as the questionnaire was completed and after a fast of at least 12 hours, blood was collected in vacuum tubes containing EDTA. Using an autoanalyzer (Hitachi 747), plasma high-sensitivity C-reactive protein (hsCRP) levels, total cholesterol, triglycerides, high-density lipoprotein cholesterol (HDL cholesterol), low-density lipoprotein cholesterol (LDL cholesterol), and glucose were quantified in the central laboratory of Kailuan General Hospital.

Statistical analysis. We used logistic regression to investigate the association between in utero or early childhood exposure to famine and RA risk, after adjusting for potential cofounders, including sex, CRP level (<1 mg/liter,1–3 mg/liter, or >3 mg/liter), BMI (<23 kg/m^2, 23–27.5 kg/m^2, or >27.5 kg/m^2), HDL cholesterol (divided into quartiles), LDL cholesterol (divided into tertiles), and triglycerides (divided into tertiles), alcohol consumption (never or past, light to moderate [for women, 0–1.0 servings/day; for men, 0–2.0 servings/day], or heavy [for women, >1.0 serving/day; for men, >2 servings/day]), smoking history (never/past or occasional/daily), diabetes status (diabetic, prediabetic, or nondiabetic), and hypertension status (hypertension, prehypertension, or no hypertension). While we were aware that metabolic or cardiovascular disorders could be intermediate factors in the pathway of famine-related RA association (7), we decided to report results from the sex-adjusted model and multivariate-adjusted model, which could provide clues to whether the observed famine-associated RA risk could be beyond the pathways of these metabolic and CVD factors in middle life.

In all analyses using categorical variables, a missing indicator was used for missing data. Except for data on alcohol consumption, the percentage of missing data varied within a small range for all variables, from no missing data for sex to 3.17% of participants with missing data on smoking history. For alcohol consumption, data were missing for 14.1% of participants. Thus, we conducted an analysis using only participants with no missing data to determine its impact. The participants born after 1961 were used as the "not exposed" reference group in our analyses. In a secondary analysis, we further examined the potential impact of famine exposure on different subtypes of RA (seropositive RA versus seronegative RA).

RA presents most often in older adults (3), and because the reference group in our analysis included those born most recently (after the famine), the reference group contained the youngest participants. To explore whether the association between famine exposure and RA risk could be explained by the fact that the famine-exposed groups were older than the reference group, we performed 3 sensitivity analyses. We calculated the predicted

Table 1. Baseline characteristics in 2006 of the 101,510 Kailuan participants stratified by exposure to the Great Chinese Famine*

	Nonexposed (born after 1961) (n = 29,396)	In utero exposed (born between 1959 and 1961) (n = 6,245)	Exposed between ages 0 and 3 years (born between 1956 and 1958) (n = 10,928)	Exposed between ages 3 and 6 years (born between 1953 and 1955) (n = 11,889)	Exposed after age 6 years (born before 1953) (n = 43,052)
Women, %	26.1	26.4	20.8	16.4	15.9
Age, years	36.9 ± 6.5	46.8 ± 0.9	49.6 ± 0.9	52.4 ± 0.9	63.4 ± 7.7
Alcohol intake, grams/day	0.5 ± 1.5	0.6 ± 1.6	0.7 ± 1.7	0.7 ± 1.7	0.5 ± 1.4
Smoking status, no. (%)					
Never	17,577 (59.8)	3,671 (57.8)	6,163 (56.4)	6,509 (54.8)	24,734 (57.5)
Past	940 (3.2)	176 (2.82)	429 (3.9)	553 (4.7)	3,746 (8.7)
Current	10,695 (36.4)	2,338 (37.4)	4,183 (38.3)	4,430 (37.3)	12,144 (28.2)
Body mass index, kg/m^2, mean ± SEM	24.6 ± 0.02	24.9 ± 0.04	24.9 ± 0.03	25.0 ± 0.03	24.9 ± 0.02
Diabetes status, no. (%)					
Normoglycemic	22,572 (76.8)	4,303 (68.9)	7,379 (67.5)	7,748 (65.2)	28,394 (65.95)
Prediabetic	5,308 (18.1)	1,359 (21.8)	2,489 (22.8)	2,880 (24.2)	8,665 (20.1)
Diabetic	1,216 (4.1)	535 (8.6)	967 (8.9)	1,116 (9.4)	5,340 (12.4)
Hypertension status, no. (%)					
No hypertension	9,525 (32.4)	1,345 (21.5)	2,036 (18.6)	2,017 (17.0)	4,933 (11.5)
Prehypertension	14,870 (50.6)	3,215 (51.5)	5,520 (50.5)	5,738 (48.3)	19,504 (45.3)
Hypertension	4,784 (16.3)	1,637 (26.2)	3,290 (30.1)	3,999 (33.6)	17,946 (41.7)
hsCRP, mean ± SEM	0.58 ± 0.03	0.61 ± 0.08	0.70 ± 0.05	0.79 ± 0.07	1.10 ± 0.04
LDL cholesterol, mmoles/liter	2.36 ± 0.78	2.39 ± 0.80	2.36 ± 0.89	2.37 ± 0.91	2.32 ± 1.02
HDL cholesterol, mmoles/liter	1.50 ± 0.36	1.54 ± 0.37	1.54 ± 0.38	1.55 ± 0.40	1.58 ± 0.44
Total cholesterol, mmoles/liter	4.79 ± 1.11	5.03 ± 1.11	5.03 ± 1.11	5.03 ± 1.11	5.01 ± 1.19
Triglycerides, mmoles/liter, median (interquartile range)	1.21 (1.07)	1.27 (1.08)	1.30 (1.08)	1.30 (1.05)	1.30 (0.99)

* Except where indicated otherwise, values are the mean ± SD. hsCRP = high-sensitivity C-reactive protein; LDL = low-density lipoprotein; HDL = high-density lipoprotein.

prevalence of RA for each birth year based on age, sex, and other variables, which were included in the famine analysis as covariates (13). We then compared the predicted prevalence of RA to the actual prevalence of RA for each year from 1951 to 1967. We also repeated our analyses by excluding those age ≤40 years. To create a reference group with a similar mean age to the "exposed in utero" and "exposed between ages 0 and 3 years" famine groups, we repeated our analyses using both the old and young participants as the reference group (those born from 1953 to 1955 and those born after 1961). Participants born before 1953 were not included in the reference group because they greatly increased the age of the reference group above the mean age of the "exposed in utero" and "exposed between ages 0 and 3 years" famine groups.

In a secondary analysis, we assigned participants to the combined categories of in utero or early life exposure to famine and the severity of famine exposure (less severely affected versus severely affected). This allowed for further investigation of the age-independent effects of famine on the risk of RA. Each famine exposure group determined by birth year contained participants of roughly the same age. Thus, within a birth year group, the risk of future RA development in those exposed to severe famine versus less-severe famine cannot be due to differences in age between these severity groups.

To investigate whether sex, rheumatoid factor (RF) positivity, smoking status (never, past or current), or BMI (<18.5 kg/m^2, 18.5–23 kg/m^2, 23–27.5 kg/m^2, or >27.5 kg/m^2) impacted the association between in utero or early life exposure to famine and RA risk, we tested the multiplicative interaction between famine exposure and these variables using a likelihood ratio test, adjusting for the aforementioned covariates.

In these analyses, *P* values less than 0.05 (2-sided) were considered significant. All analyses were performed using SAS version 9.3.

RESULTS

Of the 101,510 participants, 6.2% (n = 6,245) were exposed to the Great Chinese Famine in utero, and 10.8% (n = 10,928) were exposed between ages 0 and 3 years. In comparison to the reference participants born after 1961, those exposed to famine in utero or before age 3 years were more likely to have a higher BMI, total cholesterol, systolic and diastolic blood pressure, fasting blood glucose level, and hsCRP levels, and were more likely to be smokers and not drink alcohol (Table 1).

We identified 187 RA cases. Interestingly, the group of participants born before 1953 (i.e., the oldest group) did not have the highest prevalence of RA (Figure 1). Participants born between 1956 and 1958 (age 0–3 years during famine) had the highest prevalence of RA, followed by the participants exposed in utero who were born between 1959 and 1960 (Figure 1). Upon adjustment for confounding factors, the odds ratio (OR) for RA was 4.53 (95% confidence interval [95% CI] 2.72–7.54) for participants exposed to the famine between ages 0 and 3 years and 2.95 (95% CI 1.55–5.59) for participants exposed to the famine in utero versus the reference nonexposed group (Table 2).

Sensitivity analysis yielded similar results. When participants age ≤40 years at baseline were excluded, the OR for RA was

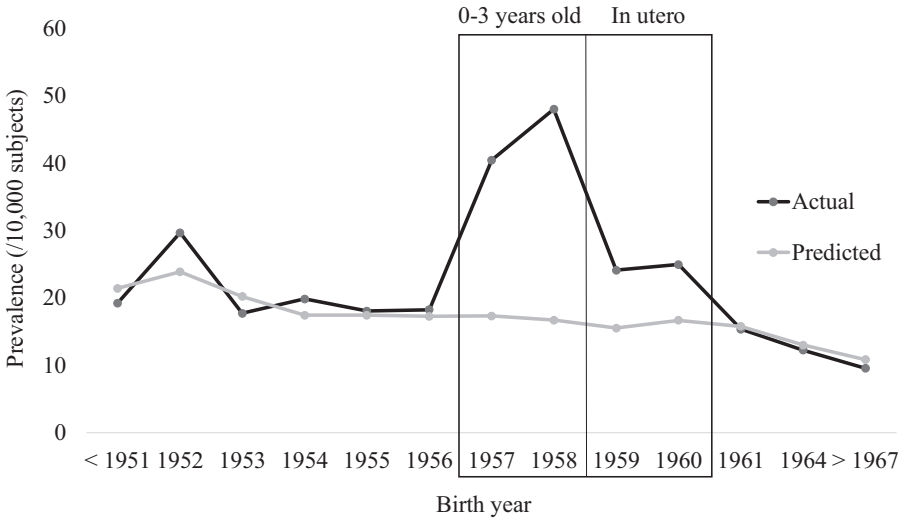

Figure 1. Actual and predicted prevalence of rheumatoid arthritis by birth year. Predicted prevalence was calculated based on birth year, sex, white blood cell counts (normal, <10 x 10^9/liter; elevated >10 x 10^9/liter), waist circumference (normal, <80 cm for women and <90 cm for men; elevated >80 cm for women and >90 cm for men), high-density lipoprotein cholesterol (divided into quartiles), low-density lipoprotein cholesterol (divided into tertiles), and triglycerides (divided into tertiles), alcohol consumption (never or past, light to moderate [for women, 0–1.0 servings/day; for men, 0–2.0 servings/day], or heavy [for women, >1.0 serving/day; for men, >2 servings/day]), smoking status (never/past or occasional/daily), and diabetes status (diabetic, prediabetic, or nondiabetic).

Table 2. Adjusted ORs for rheumatoid arthritis stratified by exposure to the Great Chinese Famine of 1959–1961*

	Nonexposed (born after 1961)	In utero exposed (born between 1959 and 1961)	Exposed between ages 0 and 3 years (born between 1956 and 1958)	Exposed between ages 3 and 6 years (born between 1953 and 1955)	Exposed after age 6 years (born before 1953)
No. of cases/no. of participants	26/29,396	15/6,245	38/10,928	22/11,889	86/43,052
Prevalence (per 10,000 participants)	8.8	24.0	34.8	18.5	20.0
Sex-adjusted OR (95% CI)	1.00 (referent)	2.71 (1.44–5.12)	4.28 (2.60–7.06)	2.45 (1.38–4.33)	2.67 (1.72–4.15)
Multivariate-adjusted OR (95% CI)†	1.00 (referent)	2.95 (1.55–5.59)	4.53 (2.72–7.54)	2.55 (1.43–4.57)	2.72 (1.70–4.36)
Excluding those age ≤40 years, OR (95% CI)†	1.00 (referent)	2.16 (1.05–4.43)	3.31 (1.81–6.05)	1.88 (0.97–3.64)	1.98 (1.12–3.50)
Excluding those with missing data, OR (95% CI)†	1.00 (referent)	2.72 (1.41–5.27)	3.97 (2.34–6.73)	2.07 (1.12–3.85)	2.19 (1.34–3.57)

* ORs = odds ratios; 95% CI = 95% confidence interval.
† Adjusted for sex, C-reactive protein level (<1 mg/liter,1–3 mg/liter, or >3 mg/liter), body mass index (<18.5 kg/m^2, 18.5–23 kg/m^2, 23–27.5 kg/m^2, or >27.5 kg/m^2), high-density lipoprotein cholesterol (divided into quartiles), low-density lipoprotein cholesterol (divided into tertiles), triglycerides (divided into tertiles), alcohol consumption (never or past, light to moderate [for women, 0–1.0 servings/day; for men, 0–2.0 servings/day], or heavy [for women, >1.0 serving/day; for men, >2 servings/day]), smoking status (never, past, or current), diabetes status (nondiabetic, prediabetic, or diabetic), and hypertension status (no hypertension, prehypertension, or hypertension).

3.31 (95% CI 1.81–6.05) for participants exposed to the famine between ages 0 and 3 years and the OR for RA was 2.16 (95% CI 1.05–4.43) for participants exposed to the famine in utero versus the reference nonexposed group (Table 2). Using both older and younger participants as the reference group (those born from 1953 to 1955 and those born after 1961), the OR for RA was 2.39 (95% CI 1.51–3.76) for participants exposed to the famine between ages 0 and 3 years and the OR for RA was 1.56 (95% CI 0.86–2.86) for participants exposed to the famine in utero versus the reference group (Supplementary Table 1, available on the *Arthritis & Rheumatology* website at http://onlinelibrary.wiley.com/doi/10.1002/art.41601/abstract). When only participants with no missing data were included, the OR for RA was 3.97 (95% CI 2.34–6.73) for participants exposed to the famine between ages 0 and 3 years, and the OR for RA was 2.72 (95% CI 1.41–5.27) for participants exposed to the famine in utero versus the reference group (Table 2).

The interaction between famine severity and famine exposure status (P = 0.10) is shown in Table 3. In the combined analysis, the OR for RA was 7.32 (95% CI 2.53–21.22) for participants exposed to severe famine between ages 0 and 3 years, and the OR for RA was 4.40 (95% CI 2.58–7.50) for participants exposed to less-severe famine between ages 0 and 3 years, in comparison to those born after 1961 (Table 3). Of note, due to the small

Table 3. Combined analysis of the impact of famine exposure and famine severity on the risk of rheumatoid arthritis*

Exposure status and severity of famine	No. of cases/no. of participants	Prevalence (per 10, 000 participants)	Odds ratio (95% confidence interval)†
Nonexposed (born after 1961)	26/29,396	8.8	1.00 (referent)
In utero exposed (born between 1959 and 1961)			
Less severe	15/5,339	28.1	3.47 (1.83–6.59)
Severe	0/454	–	–
Exposed between ages 0 and 3 years (born between 1956 and 1958)			
Less severe	31/9,312	33.2	4.40 (2.58–7.50)
Severe	4/655	61.1	7.32 (2.53–21.22)
Exposed between ages 3 and 6 years (born between 1953 and 1955)			
Less severe	21/9,931	21.1	2.90 (1.61–5.24)
Severe	0/705	–	–
Exposed after age 6 years (born before 1953)			
Less severe	67/31,668	21.2	2.76 (1.70–4.49)
Severe	3/2,009	14.9	1.82 (0.54–6.09)

* Participants without data on severity of famine (n = 12,041) were excluded. P for interaction of exposure status to famine and severity of famine with the risk of rheumatoid arthritis was 0.178.
† Adjusted for sex, C-reactive protein level (<1 mg/liter,1–3 mg/liter, or >3 mg/liter), body mass index (<18.5 kg/m^2, 18.5–23 kg/m^2, 23–27.5 kg/m^2, or >27.5 kg/m^2), high-density lipoprotein cholesterol (divided into quartiles), low-density lipoprotein cholesterol (divided into tertiles), triglycerides (divided into tertiles), alcohol consumption (never or past, light to moderate [for women, 0–1.0 servings/day; for men, 0–2.0 servings/day), or heavy [for women, >1.0 serving/day; for men, >2 servings/day]), smoking history (never, past, or current), diabetes status (nondiabetic, prediabetic, or diabetic), and hypertension status (no hypertension, prehypertension, or hypertension).

number of participants with RA, 2 combined categories had no RA cases, making it difficult to identify an overall pattern in the impact of famine severity on the risk of RA.

We did not observe a significant interaction between famine exposure and sex, smoking history, or BMI ($P_{interaction} > 0.2$ for all). The impact of famine exposure on the risk of future RA development was similar whether the RA diagnosis was seropositive or seronegative (Supplementary Table 2, available on the *Arthritis & Rheumatology* website at http://onlinelibrary.wiley.com/doi/10.1002/art.41601/abstract).

DISCUSSION

In this large-scale retrospective cohort study, in utero and early life exposure to the Great Chinese Famine was associated with a high risk of RA in adulthood irrespective of sex, smoking status, and other potential RA risk factors. The impact of famine on RA risk was the most prominent in participants who were exposed between ages 0 and 3 years.

These results are consistent with the developmental origins of disease hypothesis, and contribute to our understanding of the impact of early life adversity on RA risk (18). Globally, famine remains a consistent and serious public health problem. It is estimated that at least 1 billion people suffer from malnutrition, which continues to be an underlying cause of more than one-third of childhood deaths (19). As populations continue to grow and political instability continues to threaten societies across the globe, famine will remain a critical public health issue for the foreseeable future (20,21). Additionally, unexpected disasters and pandemics (e.g., coronavirus disease 2019) could accelerate preexisting food shortages and exacerbate food insecurity (22). Our results suggest that early life exposure to famine may increase the risk of RA in adulthood, possibly adding to the burden of countries and individuals already experiencing adversity. These results highlight early life as a critical period, during which adequate nutrition may have a long-term impact on health. This study also contributes to our understanding of the early life risk factors and etiology of RA.

We are not aware of any previously published studies that have explicitly explored the relationship between in utero or early life adversity and risk of RA in adulthood. However, 2 studies showed how exposure to the Great Chinese Famine in early childhood was associated with increased risk of arthritis, including all types (23,24). The findings of those 2 studies are consistent with our current analyses, yet depending on covariates included in the models, both studies identified an increased risk of RA (23-66%) when children were exposed to famine in early life (23,24). This increase in risk is considerably smaller than the increase in risk found in our analyses. This discrepancy may exist because the previous studies did not differentiate between types of arthritis (i.e., RA, osteoarthritis [OA], and spondyloarthritis) and collected the arthritis data via a self-report questionnaire, which could introduce misclassification and underestimate the potential association between famine and arthritis risk. It is likely that most of the cases of arthritis included in those studies were OA, as this is by far the most common type (25). While RA can be similar to other kinds of arthritis in symptomology, it is fundamentally different from OA, as RA involves an inflammatory autoimmune response directed at the synovium (3,25) while OA is not an autoimmune condition. The differing etiologies between RA and other types of arthritis may explain the difference in the magnitude of the effect of famine exposure.

There is evidence that other early life factors could affect RA risk in adulthood via multiple pathways. Sharing a bedroom in early childhood (a marker of hygiene) was associated with a significantly lower risk of RF positivity, an autoantibody that is strongly associated with RA (26), while hospitalization for infection before their first birthday tended to be associated with a higher risk of RA (OR 1.4 [95% CI 0.8–2.5]) (27). The in utero environment may also affect adult-onset RA risk. Higher birth weight has been associated with increased risk of RA (28,29), as has maternal smoking during pregnancy (30). These early life and in utero factors shed light on possible early metabolic and immunologic factors that may contribute to the pathogenesis of RA.

The precise mechanism by which early life famine exposure was associated with a high risk of RA in adulthood is unknown, but it is likely that several physiologic pathways are involved. Childhood undernutrition could have direct impacts on the immune system, via decreased leptin levels (31) or via thymic atrophy and loss of immature CD4+ and CD8+ lymphocytes (32) possibly disrupting T cell development, which plays a key role in the pathogenesis of RA (4). Undernutrition is also associated with increased susceptibility to infectious disease (33), which may be related to RA risk (27). Additionally, famine may affect the developing gut microbiome during breastfeeding (34). Early life dysbiosis has been associated with other inflammatory autoimmune conditions (i.e., inflammatory bowel disease) (35), and adults with RA display dysbiosis compared to healthy controls (36). Our data suggest that the age 0–3 years group is particularly vulnerable to the effects of famine, and that exposure during this time (as opposed to in utero or after age 3 years) was associated with a high risk of RA. This could be attributable to many factors, including the rapid expansion of T and B cells that occurs during the first 3 years (32) or the establishment of the microbiome (35). Future studies should be performed to investigate this possibility.

In addition to the nutritional components of famine exposure, the risk of RA in this population may also have been impacted by stress and environmental pollution due to the rapid industrialization that was occurring in China concomitantly with the Great Chinese Famine. Early life adversity is associated with persistent suppression of the hypothalamic–pituitary–adrenal (HPA) axis (37), and polymorphisms in the receptor for glucocorticoids, a key regulator of the HPA axis, have been associated with the risk of RA (38). Pollutant exposures of several types, including agricultural, occupational, and smoking-related, have been associated

with RA and may increase the risk of RA via changes in post-translational modification of proteins (e.g., acetylation and citrullination) (39). It is possible that the association observed in this study between early life exposure to famine and RA risk in adulthood is due to both nutritional and non-nutritional factors, which impact the modulation of several interrelated physiologic pathways (i.e., immunologic, metabolic, and neuroendocrine).

Our study has several strengths, including the large sample size of the Kailuan Study and rheumatologist-confirmed RA cases. Our study also had several limitations. Since this prospective cohort study began in 2006, it is possible that RA cases that occurred before 2006 were not recorded or captured in our search of the Municipal Social Insurance Institution, resulting in an underestimation of the prevalence of RA. However, the prevalence found in our study (0.18%) is consistent with current estimates of the prevalence of RA in China (0.18–0.20%) (40), indicating that missing RA cases are not likely a large source of error in our analyses. For those who were diagnosed as having RA prior to 2006, treatment for RA, or the disease itself, may have impacted the status of covariates (e.g., lipids, CRP level, blood glucose) that were evaluated by the study team in 2006. While the prevalence of seronegative RA cases was low (15.5%), inclusion of both seronegative RA and seropositive RA cases may be another source of error, as there is some etiologic difference between seropositive RA and seronegative RA. Selection bias may also have impacted our analyses, as the famine from 1959 to 1961 could have caused early mortality, and only individuals who were living in 2006 were included in this study. It is possible that medical conditions or treatments administered to participants before 2006 impacted their risk of RA in the present study. Covariates (e.g., anthropometric variables, blood lipid levels) were evaluated in 2006 and may have been influenced by famine exposure in early life. These variables could be considered mediators due to their collection timing, but in these analyses, they were treated as covariates, as anthropometric and metabolic data from birth were not available.

The results of this study may not be generalizable, because all participants were recruited from the Kailuan community and may not be representative of all races and ethnicities. As early life data (e.g., birth weight and diet) were not available, we cannot confirm the nutritional status of each participant at the time of birth. Thus, each participant's exposure to famine was inferred from the date of birth. Further, there were no exact beginning and end dates of the Great Chinese Famine. It is therefore possible that participants born at the beginning of 1959 may not have been exposed to famine in utero, and it is possible that those born just before 1959 were exposed to famine in utero. Also, a subset of in utero–exposed participants also experienced famine between ages 0 and 3 years. It is possible that this produced an additive effect on RA risk. Additionally, the impact of the Great Chinese Famine varied by socioeconomic status (10). It has been suggested that those with higher socioeconomic status experienced less starvation during the Great Chinese Famine due to their greater access to food compared to those with lower socioeconomic status (10). Because socioeconomic data from the time of birth were not available, we were not able to account for the variation in famine exposure due to socioeconomic variation. The analysis of the potential impact of famine severity on RA risk was also limited by the relatively small number of participants who experienced severe famine and the low prevalence of RA in this population.

Finally, the high RA risk observed among participants born from 1956 to 1960 could be due to cohort effect. For example, during the Great Chinese Famine, industrialization was rapidly spreading in China, and it is possible that the population in this study was exposed to pollution, including heavy metals, that could affect their future risk of RA independent of famine exposure (39). It is also possible that those born in the years just before and during the Great Chinese Famine experienced an increased risk of RA due to other, currently unknown factors.

In conclusion, the present study demonstrates that in utero and early life exposure to famine was associated with the high risk of RA in adulthood. The mechanisms underlying this association could be explored using animal models of RA and early life energy restriction. Future studies with large, diverse samples and detailed famine (or early life adversity events) data will help confirm the association identified in this study and improve our understanding of the impact of early life adversity on chronic disease risk.

AUTHOR CONTRIBUTIONS

All authors were involved in drafting the article or revising it critically for important intellectual content, and all authors approved the final version to be published. Dr. VanEvery had full access to all of the data in the study and takes responsibility for the integrity of the data and the accuracy of the data analysis.

Study conception and design. Wu, Gao.
Acquisition of data. Yang, Shu, Wu, Cui.
Analysis and interpretation of data. VanEvery, Olsen, Zhang, Lu, Gao.

REFERENCES

1. Willers J, Hahn A. Cardiovascular risk in patients with rheumatoid arthritis: assessment of several traditional risk parameters and a German risk score model. Rheumatol Int 2012;32:3741–9.
2. Jiang P, Li H, Li X. Diabetes mellitus risk factors in rheumatoid arthritis: a systematic review and meta-analysis. Clin Exp Rheumatol 2015;33:115–21.
3. Scott DL, Wolfe F, Huizinga TW. Rheumatoid arthritis. Lancet 2010; 376:1094–108.
4. Cooles FA, Isaacs JD. Pathophysiology of rheumatoid arthritis. Curr Opin Rheumatol 2011;23:233–40.
5. Van der Woude D, van der Helm-van Mil AH. Update on the epidemiology, risk factors, and disease outcomes of rheumatoid arthritis. Best Pract Res Clin Rheumatol 2018;32:174–87.
6. Plana-Ripoll O, Liu X, Momen NC, Parner E, Olsen J, Li J, et al. Prenatal exposure to maternal stress following bereavement and cardiovascular disease: a nationwide population-based and sibling-matched cohort study. Eur J Prev Cardiol 2016;23:1018–28.

7. Wang J, Li Y, Han X, Liu B, Hu H, Wang F, et al. Exposure to the Chinese Famine in childhood increases type 2 diabetes risk in adults. J Nutr 2016;146:2289–95.
8. Elwenspoek MM, Kuehn A, Muller CP, Turner JD. The effects of early life adversity on the immune system [review]. Psychoneuroendocrinology 2017;82:140–54.
9. Wang N, Chen Y, Ning Z, Li Q, Han B, Zhu C, et al. Exposure to famine in early life and nonalcoholic fatty liver disease in adulthood. J Clin Endocrinol Metab 2016;101:2218–25.
10. Lin JY, Yang DT. Food availability, entitlements and the Chinese famine of 1959–61. Econ J (London) 2000;110:136–58.
11. Wang L, Cui L, Wang Y, Vaidya A, Chen S, Zhang C, et al. Resting heart rate and the risk of developing impaired fasting glucose and diabetes: the Kailuan prospective study. Int J Epidemiol 2015;44:689–99.
12. Ma C, Gurol ME, Huang Z, Lichtenstein AH, Wang X, Wang Y, et al. Low-density lipoprotein cholesterol and risk of intracerebral hemorrhage: a prospective study. Neurology 2019;93:e445–57.
13. Li Y, Li Y, Gurol ME, Liu Y, Yang P, Shi J, et al. In utero exposure to the Great Chinese Famine and risk of intracerebral hemorrhage in midlife. Neurology 2020;94:e1996–2004.
14. St. Clair D, Xu M, Wang P, Yu Y, Fang Y, Zhang F, et al. Rates of adult schizophrenia following prenatal exposure to the Chinese Famine of 1959–1961. JAMA 2005;294:557–62.
15. Luo ZH, Mu R, Zhang XB. Famine and overweight in China. Rev Agricultural Econ 2006;28:296–304.
16. Aletaha D, Neogi T, Silman AJ, Funovits J, Felson DT, Bingham CO III, et al. 2010 rheumatoid arthritis classification criteria: an American College of Rheumatology/European League Against Rheumatism collaborative initiative. Arthritis Rheum 2010;62:2569–81.
17. Li W, Jin C, Vaidya A, Wu Y, Rexrode K, Zheng X, et al. Blood pressure trajectories and the risk of intracerebral hemorrhage and cerebral infarction: a prospective study. Hypertension 2017;70:508–14.
18. Gluckman PD, Hanson MA. Developmental origins of disease paradigm: a mechanistic and evolutionary perspective [review]. Pediatr Res 2004;56:311–7.
19. World Health Organization. Communicable diseases and severe food shortage: WHO technical note. October 2010. URL: https://www.who.int/malaria/publications/atoz/cds_severe_food_shortages/en/.
20. Proctor BD, Semega JL, Kollar MA. Income and poverty in the United States: 2015. URL: https://www.census.gov/library/publications/2016/demo/p60-256.html. US Census Bureau. September 2016.
21. Alexandratos N, Buinsma J. World agriculture towards 2030/2050: the 2012 revision. URL: http://www.fao.org/3/a-ap106e.pdf. Food and Agriculture Organization of the United Nations. 2012.
22. Cappelli A, Cini E. Will the COVID-19 pandemic make us reconsider the relevance of short food supply chains and local productions? Trends Food Sci Technol 2020;99:566–67.
23. Xu X, Liu L, Xie W, Zhang Y, Zeng H, Zhang F, et al. Increase in the prevalence of arthritis in adulthood among adults exposed to Chinese Famine of 1959 to 1961 during childhood: a cross-sectional survey. Medicine (Baltimore) 2017;96:e6496.
24. Wang Z, Zou Z, Dong B, Ma J, Arnold L. Association between the Great China Famine exposure in early life and risk of arthritis in adulthood. J Epidemiol Community Health 2018;72:790.
25. Glyn-Jones S, Palmer AJ, Agricola R, Price AJ, Vincent TL, Weinans H, et al. Osteoarthritis [review]. Lancet 2015;386:376–87.
26. Edwards CJ, Goswami R, Goswami P, Syddall H, Dennison EM, Arden NK, et al. Growth and infectious exposure during infancy and the risk of rheumatoid factor in adult life. Ann Rheum Dis 2006;65:401–4.
27. Carlens C, Jacobsson L, Brandt L, Cnattingius S, Stephansson O, Askling J. Perinatal characteristics, early life infections and later risk of rheumatoid arthritis and juvenile idiopathic arthritis. Ann Rheum Dis 2009;68:1159.
28. Mandl LA, Costenbader KH, Simard JF, Karlson EW. Is birthweight associated with risk of rheumatoid arthritis? Data from a large cohort study. Ann Rheum Dis 2009;68:514–8.
29. Jacobsson LT, Jacobsson ME, Askling J, Knowler WC. Perinatal characteristics and risk of rheumatoid arthritis. BMJ 2003;326:1068–9.
30. Jaakkola JJ, Gissler M. Maternal smoking in pregnancy as a determinant of rheumatoid arthritis and other inflammatory polyarthropathies during the first 7 years of life. Int J Epidemiol 2005;34:664–71.
31. Lord GM, Matarese G, Howard JK, Baker RJ, Bloom SR, Lechler RI. Leptin modulates the T-cell immune response and reverses starvation-induced immunosuppression. Nature 1998;394:897–901.
32. Savino W, Dardenne M, Velloso LA, Silva-Barbosa SD. The thymus is a common target in malnutrition and infection. Br J Nutr 2007;98:S11–6.
33. Wells JC, Sawaya AL, Wibaek R, Mwangome M, Poullas MS, Yajnik CS, et al. The double burden of malnutrition: aetiological pathways and consequences for health. Lancet 2020;395:75–88.
34. Subramanian S, Huq S, Yatsunenko T, Haque R, Mahfuz M, Alam MA, et al. Persistent gut microbiota immaturity in malnourished Bangladeshi children. Nature 2014;510:417–21.
35. Bernstein CN, Burchill C, Targownik LE, Singh H, Roos LL. Events within the first year of life, but not the neonatal period, affect risk for later development of inflammatory bowel diseases. Gastroenterology 2019;156:2190–7.
36. Zhang X, Zhang D, Jia H, Feng Q, Wang D, Liang D, et al. The oral and gut microbiomes are perturbed in rheumatoid arthritis and partly normalized after treatment. Nat Med 2015;21:895–905.
37. Schwaiger M, Grinberg M, Moser D, Zang JC, Heinrichs M, Hengstler JG, et al. Altered stress-induced regulation of genes in monocytes in adults with a history of childhood adversity. Neuropsychopharmacology 2016;41:2530–40.
38. Van Oosten MJ, Dolhain RJ, Koper JW, van Rossum EF, Emonts M, Han KH, et al. Polymorphisms in the glucocorticoid receptor gene that modulate glucocorticoid sensitivity are associated with rheumatoid arthritis. Arthritis Res Ther 2010;12:R159.
39. Joo SH, Lee J, Hutchinson D, Song YW. Prevalence of rheumatoid arthritis in relation to serum cadmium concentrations: cross-sectional study using Korean National Health and Nutrition Examination Survey (KNHANES) data. BMJ Open 2019;9:e023233.
40. Safiri S, Kolahi AA, Hoy D, Smith E, Bettampadi D, Mansournia MA, et al. Global, regional and national burden of rheumatoid arthritis 1990–2017: a systematic analysis of the global burden of disease study 2017. Ann Rheum Dis 2019;78:1463–71.

Arthritis & Rheumatology
Vol. 73, No. 4, April 2021, pp 604–616
DOI 10.1002/art.41553

American College of Rheumatology
Empowering Rheumatology Professionals

Efficacy and Safety of Guselkumab, an Interleukin-23p 19–Specific Monoclonal Antibody, Through One Year in Biologic-Naive Patients With Psoriatic Arthritis

Iain B. McInnes,[1] Proton Rahman,[2] Alice B. Gottlieb,[3] Elizabeth C. Hsia,[4] Alexa P. Kollmeier,[5] Soumya D. Chakravarty,[6] Xie L. Xu,[5] Ramanand A. Subramanian,[7] Prasheen Agarwal,[7] Shihong Sheng,[7] Yusang Jiang,[8] Bei Zhou,[7] Yanli Zhuang,[7] Désirée van der Heijde,[9] and Philip J. Mease[10]

Objective. Guselkumab, a human monoclonal antibody specific to interleukin-23p19, demonstrated efficacy and safety versus placebo through week 24 of the phase III DISCOVER-2 trial in biologic-naive patients with psoriatic arthritis (PsA). Here we report 1-year DISCOVER-2 findings.

Methods. Adults with active PsA (≥5 swollen and ≥5 tender joints; C-reactive protein level ≥0.6 mg/dl) despite standard nonbiologic treatment were randomized to receive subcutaneous injections of guselkumab 100 mg every 4 weeks, guselkumab 100 mg at week 0, week 4 and every 8 weeks thereafter, or placebo with crossover to guselkumab 100 mg every 4 weeks at week 24. We primarily evaluated clinical efficacy through week 52 by imputing missing data (nonresponse for categorical end points; no change/using multiple imputation for continuous end points). Observed radiographic scores and adverse events (AEs) were summarized.

Results. Of 739 randomized, treated patients, 93% completed week 52. The proportions of patients in whom a ≥20% improvement from baseline in American College of Rheumatology criteria (ACR20) was achieved were maintained after week 24, reaching 71% (173 of 245) and 75% (185 of 248) for patients randomized to receive treatment every 4 weeks or every 8 weeks, respectively, by week 52. The proportions of patients in whom ACR50/ACR70 and skin responses, minimal or very low disease activity, and dactylitis or enthesitis resolution were achieved at week 24 were also maintained through week 52. Further, low levels of radiographic progression, along with improvements in physical function and health-related quality of life, were sustained through week 52 with continued guselkumab treatment. Few patients experienced serious infections through week 52, with no evidence of a dosing regimen response or increase from weeks 0–24 (4 of 493 [0.8%]) to weeks 24–52 (3 of 493 [0.6%]) among guselkumab-randomized patients. No patient developed an opportunistic infection or died.

Conclusion. In biologic-naive PsA patients, guselkumab provided sustained improvements across diverse manifestations and maintained a favorable risk–benefit profile through week 52.

A video abstract of this article can be found at https://players.brightcove.net/656326989001/default_default/index.html?videoId=6207835525001.

ClinicalTrials.gov identifier: NCT03158285.

Supported by Janssen Research & Development, LLC.

[1]Iain B. McInnes, FRCP, PhD: University of Glasgow, Glasgow, UK; [2]Proton Rahman, MD: Memorial University of Newfoundland, St. Johns, Newfoundland, Canada; [3]Alice B. Gottlieb, MD, PhD: Icahn School of Medicine at Mount Sinai, New York, New York; [4]Elizabeth C. Hsia, MD: Janssen Research and Development, LLC, Spring House, Pennsylvania, and University of Pennsylvania Perelman School of Medicine, Philadelphia; [5]Alexa P. Kollmeier, MD, Xie L. Xu, PhD: Janssen Research and Development, LLC, San Diego, California; [6]Soumya D. Chakravarty, MD, PhD: Janssen Scientific Affairs, LLC, Horsham, Pennsylvania, and Drexel University College of Medicine, Philadelphia, Pennsylvania; [7]Ramanand A. Subramanian, PhD, Prasheen Agarwal, PhD, Shihong Sheng, PhD, Bei Zhou, PhD, Yanli Zhuang, PhD: Janssen Research & Development, LLC, Spring House, Pennsylvania; [8]Yusang Jiang, MA: Cytel, Inc., King of Prussia, Pennsylvania; [9]Désirée van der Heijde, MD, PhD: Leiden University Medical Center, Leiden, The Netherlands; [10]Philip J. Mease, MD: Swedish Medical Center/Providence St. Joseph Health and University of Washington, Seattle, Washington.

Dr. McInnes has received consulting fees, speaking fees, and/or honoraria from AbbVie, Boehringer Ingelheim, Bristol Myers Squibb, Celgene, Eli Lilly, Janssen, Novartis, Pfizer, and UCB (less than $10,000 each) and research grants from those companies. Dr. Rahman has received consulting fees from Abbott, AbbVie, Amgen, Bristol Myers Squibb, Celgene, Eli Lilly, Janssen, Novartis, and Pfizer (less than $10,000 each) and a research grant from Janssen. Dr. Gottlieb has received honoraria as an advisory board member and consultant for AnaptysBio, Avotres Therapeutics, Beiersdorf, Boehringer Ingelheim, Bristol-Myers-Squibb, Eli Lilly, Janssen, LEO Pharma, Novartis, Sun Pharmaceuticals UCB, and XBiotech (stock options only) (less than $10,000 each) and research/educational grants from Boehringer Ingelheim, Janssen, Novartis, Sun Pharmaceuticals, UCB, and XBiotech (all paid to Mt. Sinai School of Medicine). Drs. Hsia, Kollmeier, Chakravarty, Xu, Subramanian, Agarwal, Sheng, Zhou, and Zhuang own stock or stock options in Johnson & Johnson. Mr. Jiang has served as a consultant to Janssen Research & Development, LLC. Dr. van der Heijde

INTRODUCTION

Psoriatic arthritis (PsA), a heterogenous chronic inflammatory disorder, can encompass peripheral arthritis, psoriasis, enthesitis, dactylitis, and axial involvement. Current therapies vary in their ability to address the protean manifestations of PsA. Not all patients respond to each treatment, and some who experience an initial response lose the effect over time (1–3). In the Corrona registry, ~30% of tumor necrosis factor inhibitors (TNFi) started by PsA patients were discontinued within 1 year, and biologic-exposed patients demonstrated lower TNFi drug persistence than biologic-naive patients (4). The high proportion (80%) of these patients discontinuing the index TNFi because of inadequate efficacy (5) highlights the need to consider other modes of action to treat these PsA patients. Guselkumab (Janssen Biotech), a fully human monoclonal antibody specific to the p19 subunit of interleukin-23 (IL-23), was approved to treat adults with moderate-to-severe plaque psoriasis in 2017. More recently, guselkumab was the first selective IL-23 inhibitor approved in the US, as well as in Canada, Ecuador, and Brazil, to treat active PsA (6).

IL-23, comprising a p19 subunit and a p40 subunit shared with IL-12, is an upstream regulatory cytokine that modulates the expansion and survival of human CD4+ IL-17–producing Th17 cells, CD8+ IL-17–producing Tc17 cells, and innate immune cell subsets, all of which represent sources of downstream effector cytokines (e.g., IL-17A, IL-17F, TNF, and IL-22) known to drive inflammatory disease (7–10). Preclinical data suggested that the IL-23/Th17 pathway, and overexpression of IL-23 in particular, is a key driver of arthritis, psoriasiform lesions, enthesitis, and sacroiliitis, all features of PsA (11,12).

Guselkumab demonstrated robust benefit in patients with moderate-to-severe psoriasis (13–15). The high specificity and affinity of guselkumab for the IL-23p19 subunit (16) augured the ability of guselkumab to also treat PsA, and clinical data have borne that out (17–19). In recent reports of the 24-week placebo-controlled portions of 2 pivotal trials of guselkumab in PsA (DISCOVER-1 [ClinicalTrials.gov identifier: NCT03162796] and DISCOVER-2 [ClinicalTrials.gov identifier: NCT03158285]), guselkumab 100 mg every 4 weeks or every 8 weeks significantly improved signs and symptoms of joint and skin disease (18,19), and guselkumab 100 mg every 4 weeks significantly inhibited the progression of structural damage (19).

Herein we report the results of DISCOVER-2, the larger of these pivotal trials, through 52 weeks. Results include 1-year clinical and radiographic data for biologic-naive patients randomized to receive guselkumab, and the effects of guselkumab in patients randomized to receive placebo followed by guselkumab beginning at week 24.

PATIENTS AND METHODS

Patients. As previously reported, 739 adults with PsA were enrolled and treated in DISCOVER-2 (19). Participants had active PsA (≥5 tender and ≥5 swollen joints; C-reactive protein [CRP] ≥0.6 mg/dl) despite standard nonbiologic treatment (disease-modifying antirheumatic drugs [DMARDs], apremilast, or nonsteroidal antiinflammatory drugs [NSAIDs]) and were naive for biologic agents and JAK inhibitors. Patients provided written informed consent.

Study design. This phase III, randomized, double-blind, placebo-controlled, 3-arm study was conducted at 118 sites (in Bulgaria, the Czech Republic, Estonia, Latvia, Lithuania, Malaysia, Poland, Russia, Spain, Taiwan, Turkey, Ukraine, and the US). The trial design includes a 6-week screening period (beginning July 13, 2017), a 100-week treatment phase (placebo-controlled from week 0 to week 24 and active treatment from week 24 to week 100), and 12 weeks of safety follow-up. Data collected through week 52 (last visit September 10, 2019) are reported herein.

Participants were randomized 1:1:1 to receive subcutaneous injections of guselkumab 100 mg every 4 weeks; guselkumab 100 mg at week 0, week 4, and then every 8 weeks; or placebo every 4 weeks until starting guselkumab 100 mg every 4 weeks at week 24. Central randomization and blinding details were previously reported (19). Patients could continue baseline use of stable doses of selected nonbiologic DMARDs (limited to either methotrexate ≤25 mg/week, sulfasalazine ≤3 gm/day, hydroxychloroquine ≤400 mg/day, or leflunomide ≤20 mg/day), oral glucocorticoids ≤10 mg/day of prednisone or equivalent dose, and NSAIDs or other analgesics up to regionally approved doses.

DISCOVER-2 (ClinicalTrials.gov identifier: NCT03158285) is being conducted according to Declaration of Helsinki and Good Clinical Practice guidelines. The protocol was approved by governing ethics bodies.

has received consulting fees from AbbVie, Amgen, Astellas, AstraZeneca, Boehringer Ingelheim, Bristol Myers Squibb, Celgene, Cyxone, Daiichi, Eisai, Eli Lilly, Galápagos, Gilead, GlaxoSmithKline, Janssen, Merck, Novartis, Pfizer, Regeneron, Roche, Sanofi, Takeda, and UCB (less than $10,000 each) and serves as the director of Imaging and Rheumatology BV. Dr. Mease has received consulting fees, speaking fees, and/or honoraria from AbbVie, Amgen, Boehringer Ingelheim, Bristol Myers Squibb, Celgene, Eli Lilly, Galápagos, Genentech, Gilead, GlaxoSmithKline, Janssen, Novartis, Pfizer, Sun Pharmaceuticals, and UCB (less than $10,000 each) and research support from those companies.

The data sharing policy of Janssen Pharmaceutical Companies of Johnson & Johnson is available at https://www.janssen.com/clinical-trials/transparency. As noted on that site, requests for access to the study data can be submitted through Yale Open Data Access (YODA) Project site at http://yoda.yale.edu.

Address correspondence to Iain B. McInnes, FRCP, PhD, University of Glasgow, B4/13, Iii - Gbrc, University Place, Glasgow G12 8TA, UK. Email: iain.mcinnes@glasgow.ac.uk.

Submitted for publication June 15, 2020; accepted in revised form October 6, 2020.

Procedures. Study visits were scheduled for screening, baseline (week 0), week 2, and week 4, and then every 4 weeks. Independent assessors evaluated joints for tenderness (n = 68) and swelling (n = 66, excluding hips), enthesitis (Leeds Enthesitis Index [LEI]; total score 0–6 as summed for 6 nontender [score 0] or tender [score 1] anatomic sites) (20), and dactylitis (Dactylitis Severity Score; total score 0–60 as summed for each finger and toe, scored on a scale of 0–3, where 0 = no dactylitis, 1 = mild dactylitis, 2 = moderate dactylitis, and 3 = severe dactylitis) (21,22). Patients reported their pain level (on a 0–10-cm visual analog scale [VAS]), global impression of disease activity (0–10-cm VAS), and physical function (Health Assessment Questionnaire [HAQ] disability index [DI] [0–3 scale]) (23). Investigators completed the global assessment of disease activity (0–10-cm VAS), and serum CRP level (mg/dl) was determined.

Single radiographs of the hands (posteroanterior) and feet (anteroposterior), obtained at week 0 and week 24 (or at discontinuation if before week 24) for the first reading session and at week 0, week 24, and week 52 (or at discontinuation if between weeks 24 and 52) for the second reading session, were independently evaluated by 2 central primary readers, with a third reader for adjudication (assignment of readers to primary reader/adjudicator roles differed between reading sessions; see Supplementary Methods, available on the *Arthritis & Rheumatology* website at http://onlinelibrary.wiley.com/doi/10.1002/art.41553/abstract). Readers were blinded with regard to clinical data and radiograph ordering when scoring films using the modified Sharp/van der Heijde score (SHS) for PsA (24).

Investigators assessed the severity of skin disease using the Investigator's Global Assessment of psoriasis (IGA; total score 0–4 as averaged across induration, erythema, and scaling, graded on a scale of 0–4, where 0 = cleared, 1 = minimal, 2 = mild, 3 = moderate, and 4 = severe) (25). The Psoriasis Area and Severity Index (PASI; total score 0–72) (26) assessed the extent (percentage of body surface area [BSA] affected) and degree of associated redness, thickness, and scaling (each graded on a scale of 0–4, where 0 = none and 4 = maximum).

The Short Form 36 (SF-36) health survey (27) physical component summary (PCS) and mental component summary (MCS) scores were used to assess health-related quality of life (HRQoL). The presence of suicidal ideation/behavior or nonsuicidal self-injurious behavior was surveyed using electronic Columbia-Suicide Severity Rating Scale [eC-SSRS] questionnaires (28). Adverse events (AEs) and routine hematology and chemistry parameters were monitored. Details of guselkumab pharmacokinetic and immunogenicity assessments have been reported previously (19).

Outcome measures. Outcome measures assessed through week 52 included American College of Rheumatology criteria for 20% improvement (ACR20), ACR50, and ACR70 responses; change from baseline in the Disease Activity Score in 28 joints using the CRP; IGA skin response (score 0/1 and ≥2 grade improvement) and skin response assessed as ≥75%, ≥90%, or 100% improvement in the PASI (PASI75, PASI90, and PASI100, respectively), all among patients with ≥3% BSA with psoriasis and IGA ≥2 at baseline; changes from week 0 to week 2, week 24 to week 52, and week 0 to week 52 in total PsA-modified SHS score and component erosion and joint space narrowing subscores, derived from week 0, week 24, and week 52 images read in the second session; change from baseline in HAQ DI score and proportions of patients with a HAQ DI response (reduction ≥0.35 among patients with a baseline score ≥0.35) or HAQ DI score normalized to ≤0.5; resolution of enthesitis and changes from baseline in LEI scores in patients with enthesitis at baseline and resolution of dactylitis and changes from baseline in Dactylitis Severity Score in patients with dactylitis at baseline, both pooled across DISCOVER-1 and DISCOVER-2 (see Statistical analysis); changes from baseline in SF-36 PCS and MCS scores; and achievement of minimal disease activity (29) and very low disease activity (30).

Safety outcomes included AEs, serious AEs (SAEs), AEs resulting in discontinuation of study drug, infections, serious infections, injection-site reactions, malignancies, major adverse cardiovascular events (MACE; predefined as cardiovascular death, nonfatal myocardial infarction, or nonfatal stroke), suicidal ideation or behavior (based on eC-SSRS questionnaire or reported AEs), and clinical laboratory abnormalities classified by National Cancer Institute (NCI) Common Terminology Criteria for AEs (CTCAE) grade.

Statistical analysis. DISCOVER-2 sample size estimates were previously reported (19). All patients who continued treatment at week 24 received guselkumab; no formal hypothesis testing was planned.

As previously reported (19), treatment failure rules were applied to all clinical efficacy analyses through week 24, i.e., patients who discontinued study treatment, terminated study participation, initiated or increased doses of DMARDs or oral glucocorticoids, or initiated protocol-prohibited PsA treatment were considered nonresponders for binary end points, or as having no change from baseline for continuous end points. Missing data were imputed as nonresponders for binary end points, and using multiple imputation (MI; assumed to be missing-at-random) for continuous end points. Radiographic data through week 24 were imputed using MI with no treatment failure rules. The week 24 data have been reported previously (19) and are provided herein as context for evaluating week 52 data.

The statistical analysis plan prespecified summarizing observed efficacy data from week 24 to week 52 for patients continuing study treatment after week 24 (n = 712) (Figure 1). We also evaluated clinical (but not radiographic) efficacy data in all treated patients by randomized group (n = 739) with post hoc application of missing data imputation rules. Data missing due to treatment discontinuation were considered nonresponders for binary

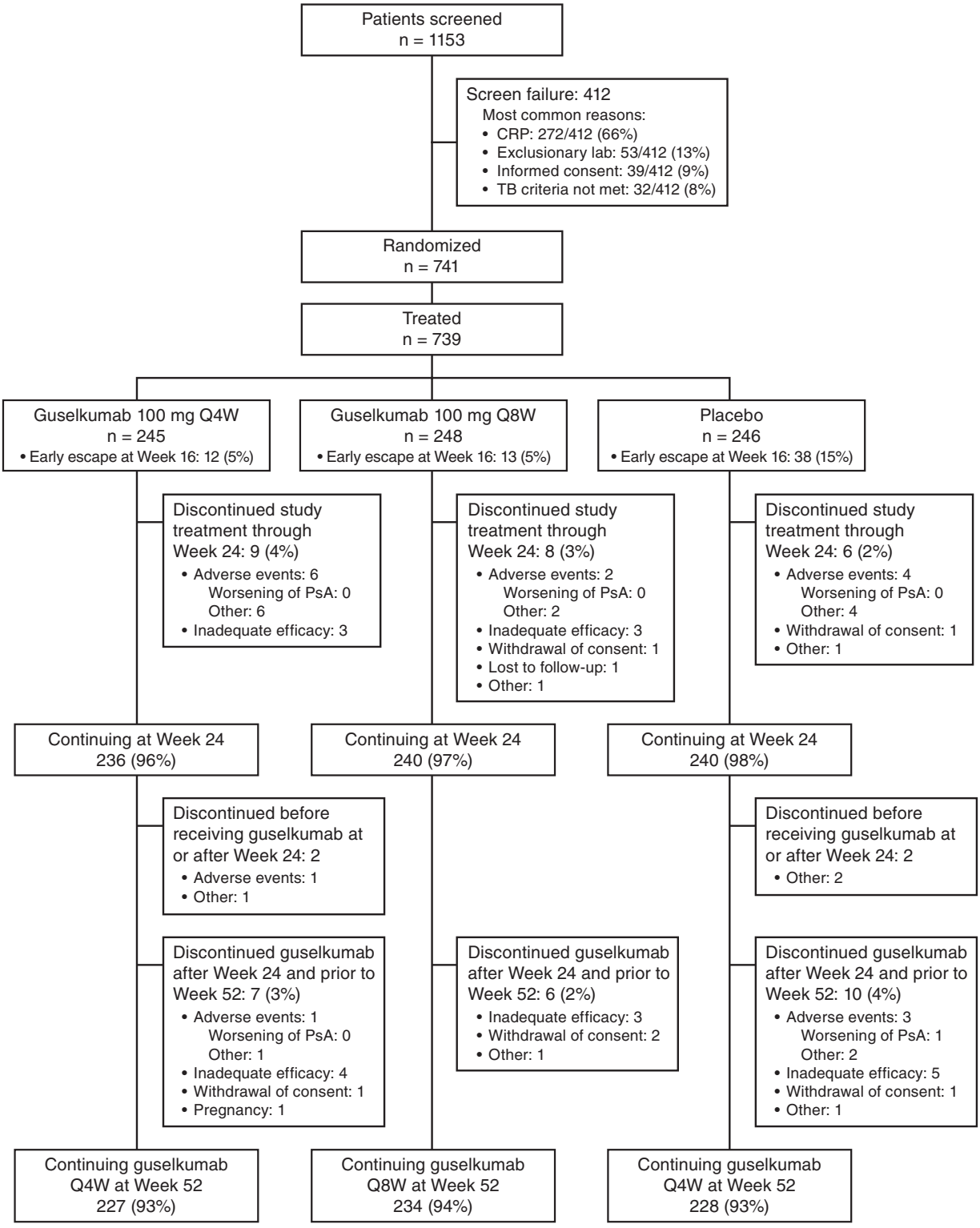

Figure 1. Disposition of the patients with psoriatic arthritis (PsA) through week 52 of the DISCOVER-2 trial. CRP = C-reactive protein; TB = tuberculosis; Q4W = every 4 weeks.

end points, or as having no change from baseline for continuous end points. Data missing for other reasons were imputed as nonresponders for binary end points, and using MI (assumed to be missing-at-random) for continuous end points. In this analysis, data provided for the 246 patients randomized to receive placebo followed by guselkumab every 4 weeks included 238 patients who crossed over to guselkumab treatment every 4 weeks and 8 patients who received only placebo prior to discontinuing

Table 1. Observed PsA-modified SHS from the second reading session of DISCOVER-2 (images obtained at week 0, week 24, and week 52)*

	Guselkumab every 4 weeks				Guselkumab every 8 weeks				Placebo (weeks 0–24) → guselkumab every 4 weeks (weeks 24–52)			
	Baseline (n = 232)	Weeks 0–24 (n = 232)	Weeks 24–52 (n = 229)	Weeks 0–52 (n = 229)	Baseline (n = 238)	Weeks 0–24 (n = 238)	Weeks 24–52 (n = 235)	Weeks 0–52 (n = 235)	Baseline (n = 231)	Weeks 0–24 (n = 231)	Weeks 24–52 (n = 230)	Weeks 0–52 (n = 230)
Baseline total PsA-modified SHS												
Mean ± SD	25.37 ± 40.24	–	–	–	22.39 ± 37.87	–	–	–	22.96 ± 39.45	–	–	–
Median	8.00	–	–	–	10.50	–	–	–	9.00	–	–	–
Range	(0.0–283.0)	–	–	–	(0.0–254.5)	–	–	–	(0.0–204.4)	–	–	–
IQR	(3.00–28.75)	–	–	–	(2.50–26.50)	–	–	–	(3.00–22.00)	–	–	–
Mean ± SD change in PsA-modified SHS												
Total†	–	0.46 ± 2.46	0.62 ± 2.53	1.07 ± 3.84	–	0.73 ± 2.50	0.23 ± 1.81	0.97 ± 3.62	–	1.00 ± 3.19	0.25 ± 1.64	1.25 ± 3.51
Erosion	–	0.31 ± 1.88	0.39 ± 1.72	0.70 ± 2.63	–	0.57 ± 2.04	0.10 ± 1.42	0.67 ± 2.71	–	0.75 ± 2.31	0.17 ± 1.28	0.92 ± 2.50
JSN	–	0.15 ± 0.97	0.23 ± 1.09	0.38 ± 1.63	–	0.16 ± 0.78	0.13 ± 0.70	0.29 ± 1.27	–	0.25 ± 1.14	0.07 ± 0.64	0.33 ± 1.36

* Intraclass correlation (ICC) estimates for the total psoriatic arthritis (PsA)–modified Sharp/van der Heijde score (SHS) at baseline, week 24, and week 52 were 0.92, 0.93, and 0.93, respectively. ICC estimates for changes in the total PsA-modified SHS during weeks 0–24, weeks 24–52, and weeks 0–52 were 0.69, 0.58, and 0.76, respectively. IQR = interquartile range; JSN = joint space narrowing.
† The smallest detectable change in the total PsA-modified SHS was 1.85 for weeks 0–24, 1.91 for weeks 24–52, and 2.39 for weeks 0–52.

treatment. Results based on these imputed data are the focus of this article; observed ACR responses are shown for reference.

Observed changes in SHS scores derived from the study's second reading session were summarized via descriptive statistics for patients who continued treatment at week 24 (see Supplementary Figure 1, available on the *Arthritis & Rheumatology* website at http://onlinelibrary.wiley.com/doi/10.1002/art.41553/abstract). Cumulative probability plots show the observed cumulative distribution of these scores, ranked from the lowest to highest (31), by study period (i.e., week 0 to week 24 and week 24 to week 52). Among patients with observed scores at baseline and ≥1 in-window postbaseline visit, a post hoc analysis was conducted to estimate annual radiographic progression by randomized treatment group. Further details of the analysis, which used linear extrapolation and MI of radiographic scores derived from both the first and second reading sessions, are provided in the Supplementary Methods.

To increase sample size and reliability, dactylitis and enthesitis data among patients with these conditions at baseline were prespecified to be summarized by pooling data across DISCOVER-1 (18) and DISCOVER-2 (19) at week 24. Pooled results are also reported at week 52 (reported in the main text); individual DISCOVER-1 and DISCOVER-2 data are summarized in the Supplementary Results, available on the *Arthritis & Rheumatology* website at http://onlinelibrary.wiley.com/doi/10.1002/art.41553/abstract.

AEs were summarized for treated patients who experienced at least 1 event. To account for the shorter period of placebo (24 weeks) compared to active treatment (52 weeks), incidences of AEs, SAEs, AEs leading to discontinuation of study agent, infections, and serious infections were also summarized as the number of patients or the number of events (Supplementary Methods) per 100 patient-years of follow-up, along with corresponding exact 95% confidence intervals (95% CIs). Deriving from the incidences of patients with these AEs in the combined guselkumab and placebo groups, the number needed to harm (NNH), i.e., patients needing to be treated for an additional AE, was calculated as: $R_0 = 1 - e^{(-\text{Placebo patients with events/Placebo patient-years})}$; $R_1 = 1 - e^{(-\text{Guselkumab patients with events/Guselkumab patient-years})}$; and $NNH = 1/(R_1 - R_0)$. Only positive NNH values are reported.

RESULTS

Patient disposition and baseline characteristics. The vast majority of randomized and treated patients (689 of 739 [93%]) completed the study through week 52; 7% of the patients discontinued study agent early, most commonly due to AEs or inadequate efficacy. The frequency of discontinuation was comparable across treatment groups (Figure 1). Of the patients who were randomized to receive placebo, 238 crossed over to guselkumab 100 mg every 4 weeks, and a total of 731 patients received guselkumab 100 mg for 608 patient-years (average follow-up 43.4 weeks, or 0.8 years).

Baseline characteristics of the 739 patients in the DISCOVER-2 study have been reported previously (19). Briefly, female (48%) and male (52%) participants had PsA for, on average, >5 years with no biologic treatment. At baseline, participants averaged 12–13 swollen and 20–22 tender joints, with median serum CRP levels of 1.2–1.3 mg/dl, across randomized groups. Nearly three-fourths (73%) of the patients had ≥3% BSA psoriasis involvement and an IGA score of ≥2 at week 0, while only 2% of the patients had clear skin (IGA 0) at enrollment. Approximately one-half had a psoriasis IGA score of 3–4 (46%) or dactylitis (45%), and two-thirds had enthesitis (68%). Patients started the study with impaired physical function and HRQoL, as evidenced by their mean HAQ DI scores (1.2–1.3; range 0–3), mean SF-36 PCS scores (32.4–33.3), and mean SF-36 MCS scores (47.2–48.4) (US general population norms 50.0). Baseline radiographic data showed an imbalance in total PsA-modified SHS scores between the guselkumab every 4 weeks group and the other 2 treatment groups (Table 1).

Pharmacokinetics and immunogenicity. See Supplementary Results for details on the pharmacokinetics and immunogenicity of guselkumab.

Efficacy. As previously reported, the DISCOVER-2 primary end point was met, i.e., an ACR20 response was achieved at week 24 in significantly greater proportions of patients treated with guselkumab every 4 weeks (64%) and patients treated with guselkumab every 8 weeks (64%) than patients treated with placebo (33%) (both $P < 0.0001$) (19). Numerical increases in the proportions of patients in whom an ACR20 response was achieved were observed after week 24. By week 52, 71% of the patients randomized to receive guselkumab every 4 weeks (173 of 245) and 75% of the patients randomized to receive guselkumab every 8 weeks (185 of 248) had ≥20% improvement from baseline in ACR components (Figure 2A). An ACR50 response was achieved at week 52 in nearly one-half, and an ACR70 response was achieved at week 52 in more than one-quarter of the patients randomized to receive guselkumab every 4 weeks or every 8 weeks (Figures 2C and E). Consistent patterns were evident for observed ACR responses (Figures 2B, D, and F).

For radiographs obtained at week 0, week 24, and week 52, intraclass correlation coefficients (ICCs) indicated good reader reliability for absolute scores (ICC 0.92–0.93) and moderate reader reliability for change scores (ICC 0.58–0.76) (Table 1). The smallest detectable changes in PsA-modified SHS total scores were 1.85 during weeks 0–24, 1.91 during weeks 24–52, and 2.39 during weeks 0–52 (Supplementary Figure 1). In the guselkumab every 4 weeks group, observed mean changes in total PsA-modified SHS scores were 0.46 and 0.62 during weeks 0–24 and weeks 24–52, respectively. Respective mean changes in the guselkumab every 8 weeks group were 0.73 and 0.23 (Table 1 and Supplementary Figure 1).

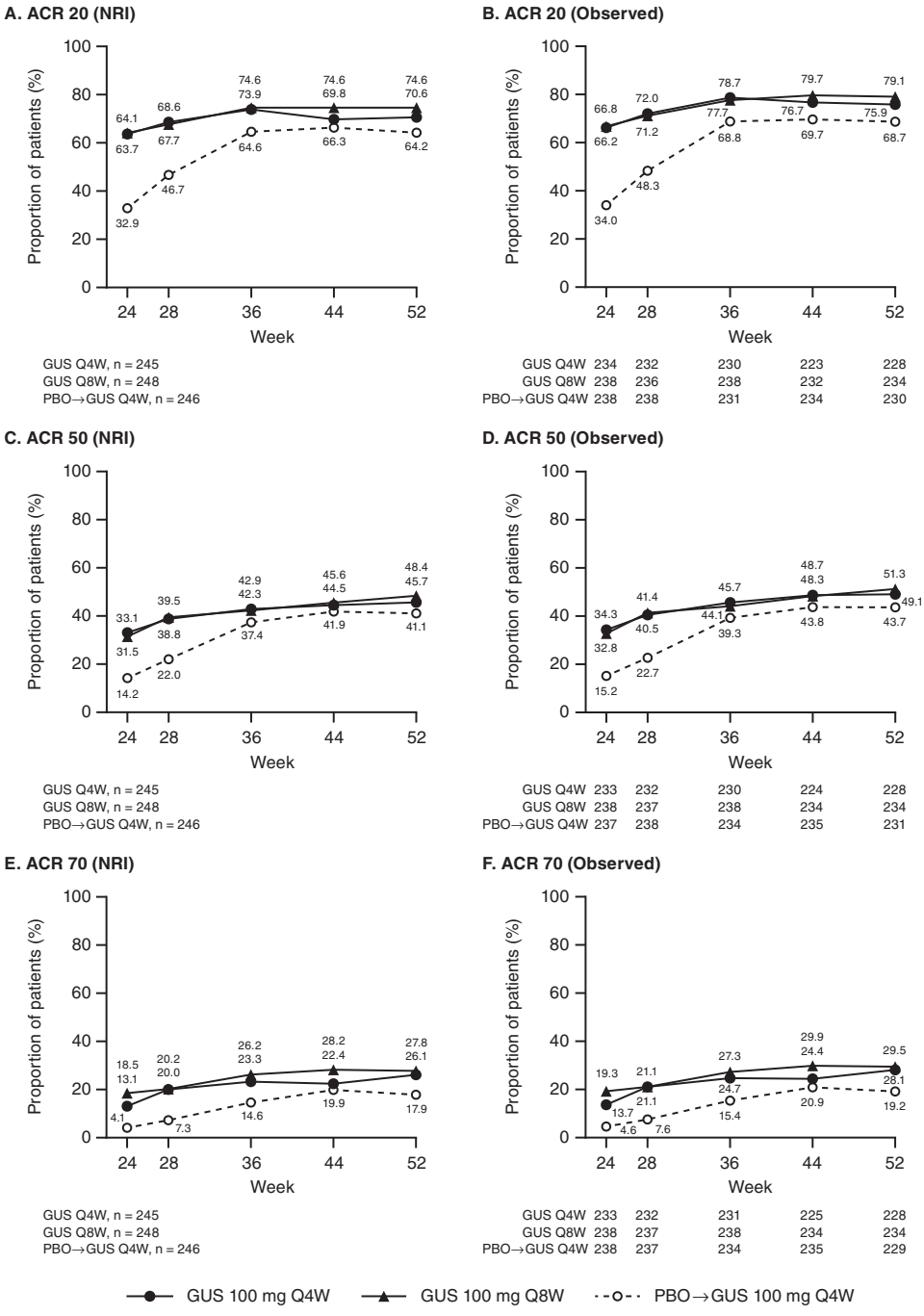

Figure 2. Proportions of patients with psoriatic arthritis who met the American College of Rheumatology criteria for 20% improvement (ACR20), ACR50, or ACR70 from week 24 through week 52. **A**, **C**, and **E**, Proportions of patients treated with guselkumab every 4 weeks (GUS Q4W), guselkumab every 8 weeks, or placebo (PBO) followed by guselkumab every 4 weeks who met the ACR20 (**A**), ACR50 (**C**), and ACR70 (**E**) criteria, with application of data handling rules using nonresponder imputation (NRI; see Patients and Methods). Week 24 data were reported previously (19) and are shown here for reference. Among 246 patients randomized to receive placebo, 238 crossed over to guselkumab treatment every 4 weeks (after week 24 response assessments), and 8 received placebo only before discontinuing treatment. **B**, **D**, and **F**, Observed data for the proportion of patients in each treatment group who met the ACR20 (**B**), ACR50 (**D**), and ACR70 (**F**) criteria. Observed data are shown for patients continuing study treatment at week 24, as prespecified in the statistical analysis plan.

Among patients with observed PsA-modified SHS scores at baseline and ≥1 in-window postbaseline visit, the least squares mean (LSM) change from baseline at week 52, based on a post hoc analysis employing linear extrapolation and MI of scores from both reading sessions (see Supplementary Methods), was estimated to be 2.16 for placebo (95% CI 1.56, 2.75). The estimated annual LSM changes for guselkumab every 4 weeks (1.10 [95% CI 0.48, 1.71]) and guselkumab every 8 weeks (1.13 [95% CI 0.52, 1.73])

yielded LSM differences from placebo of –1.06 (95% CI –1.89, –0.23) and –1.03 (95% CI –1.85, –0.20), respectively.

When pooling DISCOVER-1 and DISCOVER-2 patients with dactylitis or enthesitis at baseline, rates of resolution and improvements in dactylitis severity or LEI scores seen at week 24 were maintained at week 52, at which time 75% of the patients who were randomized to receive guselkumab every 4 weeks or every 8 weeks had resolution of dactylitis and 58% had resolution of enthesitis (Table 2). Response patterns within each trial were consistent (Supplementary Tables 1 and 2, available on the *Arthritis & Rheumatology* website at http://onlinelibrary.wiley.com/doi/10.1002/art.41553/abstract).

In patients with ≥3% of BSA with psoriasis involvement and an IGA score of ≥2 at baseline, the robust skin response rates at week 24 afforded by guselkumab every 4 weeks and every 8 weeks were maintained at week 52, at which time 79% and 74% of patients, respectively, had an IGA score of 0/1 and a ≥2-grade decrease from baseline, and 62% and 58%, respectively, achieved clear skin (IGA 0). Also at week 52, a PASI75 response was achieved in 86% of patients treated with guselkumab every 4 weeks and 86% of those treated with guselkumab every 8 weeks, a PASI90 response was achieved in 77% of patients treated with guselkumab every 4 weeks and 74% of patients treated with guselkumab every 8 weeks, and a PASI100 response was achieved in 58% of patients treated with guselkumab every 4 weeks and 53% of patients treated with guselkumab every 8 weeks (Table 3).

Improvements in physical function seen in the guselkumab every 4 weeks and every 8 weeks groups at week 24 were sustained through week 52 (LSM change in HAQ DI –0.49 and –0.45, respectively). Among patients with a baseline HAQ DI score ≥0.35 in the guselkumab every 4 weeks and every 8 weeks groups, nearly 60% had improvements in HAQ DI ≥0.35 at week 52. Also by week 52, 33% and 25% of the patients in the guselkumab every 4 weeks and every 8 weeks groups, respectively, with a HAQ DI ≥0.5 at baseline saw normalized physical function, i.e., HAQ DI <0.5. Consistently, guselkumab every 4 weeks or every 8 weeks continued to numerically improve physical aspects of HRQoL through week 52, at which time LSM changes in SF-36 PCS score were 8.6 and 9.0, respectively. The LSM improvements in mental components of HRQoL were maintained through week 52 (SF-36 MCS score 4.4 and 4.3, respectively) (Table 3).

Utilizing validated PsA composite indices, minimal disease activity was achieved in >30% of the patients in the guselkumab every 4 weeks and guselkumab every 8 weeks groups, and very low disease activity was achieved in 11% and 16% of the patients in the guselkumab every 4 weeks and every 8 weeks groups, respectively, at week 52 (Table 3).

In patients who received guselkumab every 4 weeks from week 24 to week 52 following treatment with placebo, clinical response rates at week 52 (e.g., ACR20 in 64%, IGA score of 0/1 in 79%, HAQ DI response in 48%, and minimal disease activity in 30%) were consistent with those observed in patients randomized to receive guselkumab (Tables 2 and 3 and Figure 2). Also in patients who crossed over from placebo to guselkumab every 4 weeks, mean changes in total PsA-modified SHS scores were 1.00 from week 0 to week 24 and 0.25 from week 24 to week 52 (Table 1 and Supplementary Figure 1).

Safety. Consistent with findings through week 24 of DISCOVER-2 (19), the most commonly reported AEs (>5% of patients in any guselkumab treatment group) through week 52 included upper respiratory tract infection (7% of patients randomized to treatment every 4 weeks, 7% of patients randomized to treatment every 8 weeks, and 10 per 100 patient-years for all guselkumab-treated patients), nasopharyngitis (7%, 8%, and 9 per 100 patient-years, respectively), bronchitis (6%, 2%, and 4 per 100

Table 2. Pooled DISCOVER-1 and DISCOVER-2 dactylitis and enthesitis data through week 52*

	Guselkumab every 4 weeks (n = 373)†		Guselkumab every 8 weeks (n = 375)†		Placebo (weeks 0–24) → guselkumab every 4 weeks (weeks 24–52) (n = 372)†§	
	Week 24‡	Week 52	Week 24‡	Week 52	Week 24‡	Week 52
No. with dactylitis at week 0	159	159	160	160	154¶	154
% with resolution	63.5	74.8	59.4	75.6	42.2	70.1
LSM change (95% CI)	−6.0 (−6.8, −5.1)	−6.5 (−7.1, −5.8)	−6.1 (−6.9, −5.3)	−7.1 (−7.8, −6.5)	−4.2 (−5.0, −3.4)	−6.6 (−7.3, −5.9)
No. with enthesitis at week 0	243	243	230	230	255#	255
% with resolution	44.9	57.6	49.6	57.8	29.4	61.6
LSM change (95% CI)	−1.6 (−1.8, −1.4)	−1.8 (−2.0, −1.6)	−1.5 (−1.7, −1.3)	−1.8 (−2.0, −1.6)	−1.0 (−1.2, −0.8)	−1.8 (−2.0, −1.7)

* Data are summarized by treatment group with application of missing data handling rules (see Patients and Methods). LSM = least squares mean; 95% CI = 95% confidence interval.
† Numbers of pooled randomized patients.
‡ Week 24 data were previously reported (19) and are shown here for reference.
§ Of these 372 patients, 352 crossed over to guselkumab treatment every 4 weeks (post–week 24 response assessments); 20 received placebo only before discontinuing treatment.
¶ Of these 154 patients, 142 crossed over to guselkumab treatment every 4 weeks (post–week 24 response assessments); 12 received placebo only before discontinuing treatment.
# Of these 255 patients, 243 crossed over to guselkumab treatment every 4 weeks (post–week 24 response assessments); 12 received placebo only before discontinuing treatment.

Table 3. Summary of skin, patient-reported, and composite end point outcomes through week 52 of the DISCOVER-2 trial*

	Guselkumab every 4 weeks		Guselkumab every 8 weeks		Placebo (weeks 0–24) → guselkumab every 4 weeks (weeks 24–52)	
	Week 24†	Week 52	Week 24†	Week 52	Week 24†	Week 52
No. with ≥3% BSA psoriasis and IGA ≥2 at week 0	184	184	176	176	183‡	183‡
IGA score of 0/1 and ≥2-grade decrease	68.5	79.3	70.5	74.4	19.1	79.2
IGA score of 0	50.5	62.5	50.0	58.0	7.7	62.8
PASI75	78.3	86.4	79.0	85.8	23.0	83.1
PASI90	60.9	76.6	68.8	74.4	9.8	72.1
PASI100	44.6	57.6	45.5	52.8	2.7	51.9
No. with HAQ DI available	245	245	248	248	246§	246§
LSM change (95% CI)	−0.40 (−0.46, −0.34)	−0.49 (−0.56, −0.42)	−0.37 (−0.43, −0.31)	−0.45 (−0.52, −0.38)	−0.13 (−0.19, −0.07)	−0.35 (−0.42, −0.29)
No. with HAQ DI ≥0.5 at week 0	225	225	221	221	227	227
HAQ DI <0.5	25.8	32.9	20.8	25.3	12.3	24.7
No. with HAQ DI ≥0.35 at week 0	228	228	228	228	236¶	236¶
≥0.35 improvement	56.1	58.8	50.0	57.5	31.4	47.5
No. with SF-36 scores available	245	245	248	248	246§	246§
PCS, LSM change (95% CI)	7.04 (6.14, 7.94)	8.64 (7.60, 9.68)	7.39 (6.50, 8.29)	8.97 (7.94, 10.00)	3.42 (2.53, 4.32)	7.53 (6.49, 8.56)
MCS, LSM change (95% CI)	4.22 (3.14, 5.29)	4.43 (3.37, 5.49)	4.17 (3.10, 5.23)	4.31 (3.26, 5.36)	2.14 (1.07, 3.22)	4.04 (2.99, 5.10)
No. with data on composite indices available	245	245	248	248	246§	246§
Minimal disease activity	18.8	34.3	25.0	31.0	6.1	29.7
Very low disease activity	4.9	11.4	4.4	16.1	1.2	6.5

* Data are summarized by treatment group with application of missing data handling rules (see Patients and Methods). Except where indicated otherwise, values are the percent of patients. BSA = body surface area; IGA = Investigator's Global Assessment of psoriasis; PASI75 = ≥75% improvement in the Psoriasis Area and Severity Index; HAQ DI = Health Assessment Questionnaire disability index; LSM = least squares mean; 95% CI = 95% confidence interval; SF-36 = Short Form 36; PCS = physical component summary; MCS = mental component summary.
† Week 24 data were previously reported (19) and are shown here for reference.
‡ Of these 183 patients, 176 crossed over to guselkumab treatment every 4 weeks (post–week 24 response assessments); 7 received placebo only before discontinuing treatment.
§ Of these 246 patients, 238 crossed over to guselkumab treatment every 4 weeks (post–week 24 response assessments); 8 received placebo only before discontinuing treatment.
¶ Of these 236 patients, 229 crossed over to guselkumab treatment every 4 weeks (post–week 24 response assessments); 7 received placebo only before discontinuing treatment.

patient-years, respectively), and investigator-reported laboratory investigations, including increased alanine aminotransferase (ALT) level (12%, 9%, and 13 per 100 patient-years, respectively) and increased aspartate aminotransferase (AST) level (7%, 7%, and 5 per 100 patient-years, respectively). When evaluating AEs with >5 events per 100 patient-years in any group, common AEs also included neutropenia and leukopenia (Supplementary Table 3, available on the *Arthritis & Rheumatology* website at http://onlinelibrary.wiley.com/doi/10.1002/art.41553/abstract). Across all AEs, time-adjusted incidences were 109 and 110 per 100 patient-years during weeks 0–52 for patients receiving guselkumab every 4 weeks or every 8 weeks, respectively (Table 4).

No deaths occurred through week 52. Overall, 4% of guselkumab-treated patients (31 of 731) had SAEs, with similar proportions observed in the guselkumab every 4 weeks and every 8 weeks groups (Table 4). Eighteen (58%) of 31 guselkumab-treated patients with SAEs were receiving methotrexate, 1 (3%) received leflunomide, and 12 (39%) did not receive any nonbiologic DMARDs. Lower limb fracture, goiter, pneumonia (1 identified as influenzal in origin), and pulmonary embolism each occurred in 2 guselkumab-treated patients. Other SAEs were singular events. One patient each with serious influenza/pneumonia, ischemic stroke, and acute hepatitis B in the guselkumab every 4 weeks group discontinued treatment. Most SAEs in guselkumab-treated patients resolved by week 52. Exceptions were extrapyramidal disorder, endometrial hyperplasia, and acute hepatitis B, each in 1 patient who received guselkumab every 4 weeks during weeks 0–52.

Guselkumab and placebo were each discontinued due to AEs by ~2% of patients. Nine guselkumab-treated patients (NNH 164) and 1 placebo-treated patient had serious infections through week 52. Serious infections were reported by similar proportions of patients receiving guselkumab every 4 weeks (1%) and those receiving guselkumab every 8 weeks (1%) during weeks 0–52, and by similar proportions of the 493 guselkumab-randomized patients during weeks 0–24 (4 patients [0.8%]) (19) and weeks 24–52 (3 patients [0.6%]) (Table 4). No patient had active tuberculosis (TB) or an opportunistic infection through week 52. Among

Table 4. Patients with AE categories of interest through week 52 of the DISCOVER-2 trial*

	Placebo → guselkumab 100 mg every 4 weeks		Guselkumab 100 mg (weeks 0–52)		
	Placebo (weeks 0–24)	Every 4 weeks (weeks 24–52)	Every 4 weeks	Every 8 weeks	All guselkumab
No. of treated patients	246	238†	245	248	731
Years of follow-up, mean	0.5	0.5	1.0	1.0	0.8
Overall patient-years, no.	115	127	239	243	608
All AEs					
Patient-years, no.	86	102	140	140	383
Number (%) of patients	100 (40.7)	87 (36.6)	152 (62.0)‡	155 (62.5)‡	394 (53.9)
Incidence per 100 patient-years (95% CI)	116.95 (95.16, 142.25)	84.94 (68.03, 104.77)	108.66 (92.07, 127.37)	110.40 (93.70, 129.21)	102.95 (93.03, 113.63)
SAEs					
Patient-years, no.	113	124	233	238	595
Number (%) of patients	7 (2.8)	10 (4.2)	11 (4.5)§	10 (4.0)§	31 (4.2)
Incidence per 100 patient-years (95% CI)	6.19 (2.49, 12.76)	8.04 (3.86, 14.79)	4.72 (2.36, 8.45)	4.20 (2.02, 7.73)	5.21 (3.54, 7.39)
AEs causing study agent discontinuation					
Patient-years, no.	114	127	236	242	605
Number (%) of patients	4 (1.6)	4 (1.7)	9 (3.7)¶	3 (1.2)¶	16 (2.2)
Incidence per 100 patient-years (95% CI)	3.51 (0.96, 8.99)	3.16 (0.86, 8.08)	3.81 (1.74, 7.23)	1.24 (0.26, 3.63)	2.65 (1.51, 4.30)
Infections					
Patient-years, no.	104	116	197	204	516
Number (%) of patients	45 (18.3)	41 (17.2)	67 (27.3)#	71 (28.6)#	179 (24.5)
Incidence per 100 patient-years (95% CI)	43.25 (31.55, 57.88)	35.47 (25.45, 48.11)	34.09 (26.42, 43.29)	34.89 (27.25, 44.01)	34.71 (29.81, 40.19)
Serious infections					
Patient-years, no.	115	126	237	241	605
Number (%) of patients	1 (0.4)**	3 (1.3)††	3 (1.2)‡‡	3 (1.2)§§	9 (1.2)
Incidence per 100 patient-years (95% CI)	0.87 (0.02, 4.85)	2.37 (0.49, 6.94)	1.26 (0.26, 3.69)	1.24 (0.26, 3.63)	1.49 (0.68, 2.82)

* 95% CI = 95% confidence interval; SAEs = serious adverse events.
† These 238 patients received placebo during weeks 0–24; only adverse events reported during weeks 24–52, after starting guselkumab, are summarized.
‡ One hundred thirteen (46.1%) of the patients receiving guselkumab 100 mg every 4 weeks and 114 (46.0%) of the patients receiving guselkumab 100 mg every 8 weeks reported AEs during weeks 0–24 (19).
§ Eight (3.3%) of the patients receiving guselkumab 100 mg every 4 weeks and 3 (1.2%) of the patients receiving guselkumab 100 mg every 8 weeks reported SAEs during weeks 0–24 (19).
¶ Seven (2.9%) of the patients receiving guselkumab 100 mg every 4 weeks and 2 (0.8%) of the patients receiving guselkumab 100 mg every 8 weeks discontinued study agent due to AEs during weeks 0–24 (19).
# Forty-nine (20.0%) of the patients receiving guselkumab 100 mg every 4 weeks and 40 (16.1%) of the patients receiving guselkumab 100 mg every 8 weeks reported infections during weeks 0–24 (19).
** Post-procedural fistula while receiving placebo prior to week 24 (19).
†† One patient each with influenza/tracheitis, pericarditis, and pneumonia while receiving guselkumab 100 mg every 4 weeks during weeks 24–52.
‡‡ One patient each with acute hepatitis B, oophoritis, and influenzal pneumonia prior to week 24 (19).
§§ One patient had pyrexia prior to week 24 (19) and urinary tract infection during weeks 24–52, and 1 patient each had cystitis and diverticulitis during weeks 24–52.

75 patients (10%) who were required to start treatment for latent TB prior to the first study agent administration, 2 (1 receiving placebo and 1 receiving guselkumab every 4 weeks [see below]) were reported to have isoniazid-induced liver injury. No AEs of inflammatory bowel disease were reported in guselkumab-treated patients.

No malignancies were reported during weeks 24–52, while 2 were reported during weeks 0–24 (melanoma in situ in the guselkumab every 8 weeks group and renal clear cell cancer in the placebo group) (19). No MACE occurred during weeks 24–52; 1 event (ischemic stroke in the guselkumab every 4 weeks group) was reported prior to week 24 (19).

One patient, who received guselkumab every 8 weeks, reported suicidal ideation during weeks 24–52; 2 patients (1 each in the placebo and guselkumab every 4 weeks groups) did so during weeks 0–24 (19). No events of self-injurious or suicidal behavior were reported through week 52. Injection-site reactions related to guselkumab injections occurred in 1.4% of guselkumab-treated patients (10 of 731) through week 52 (see Supplementary Results).

Through week 52, decreased neutrophil counts of NCI CTCAE grade 2 or higher ($<1.5 \times 10^9$/liter) were infrequent, occurring in 3.7% of patients (9 of 243) who received guselkumab every 4 weeks from week 0 and 3.6% of patients (9 of 247) who

received guselkumab every 8 weeks from week 0. Fewer than 1% of guselkumab-treated patients (5 of 731) had decreased neutrophil counts of grade 3 or higher, including 4 with grade 3 values (<1.0–0.5 × 10^9/liter) and 1 with grade 4 values (<0.5 × 10^9/liter). These findings were generally transient and reversible, resolved spontaneously without treatment, and did not require discontinuation of study agent. No associated infections were seen, except a case of mild nasopharyngitis temporally associated with grade 2 neutropenia. Decreased white blood cell counts of NCI CTCAE grade 2 (<3.0–2.0 × 10^9/liter) occurred in 2.1% of patients (5 of 243) who received guselkumab every 4 weeks from week 0 and 2.4% of patients (6 of 247) who received guselkumab every 8 weeks from week 0; no guselkumab-treated patient exhibited leukopenia of grade 3 or 4 (>2.0 × 10^9/liter) (Supplementary Table 4, available on the *Arthritis & Rheumatology* website at http://onlinelibrary.wiley.com/doi/10.1002/art.41553/abstract).

Through week 52, elevated ALT and/or AST concentrations of NCI CTCAE grade 2 or higher (>3 times the upper limit of normal [ULN]) occurred in 7.4% and 6.6%, respectively, of 243 patients receiving guselkumab every 4 weeks from week 0 and 2.0% and 3.2%, respectively, of 247 patients receiving guselkumab every 8 weeks from week 0. No additional grade 3 ALT or AST values (>5–20 times the ULN), which were uncommon during weeks 0–24 (1.4% and 1.2%, respectively, of 493 guselkumab-randomized patients) (19), occurred after week 24. No grade 4 ALT or AST values (>20 times the ULN) occurred through week 52 (Supplementary Table 4). No instance of elevated liver function test findings satisfied the criteria for Hy's Law (total bilirubin >2 times the ULN and ALT or AST ≥3 times the ULN) among guselkumab-treated patients. Most abnormal findings were transient, resolved, and did not require discontinuation of study agent. As exceptions and as reported previously, 2 patients randomized to receive guselkumab every 4 weeks discontinued guselkumab prior to week 24 (1 each with acute hepatitis B and isoniazid-induced liver injury) (19). Another patient, in the guselkumab every 4 weeks group, had an extended interruption of treatment before week 24 (owing to physician concerns surrounding alcohol use, hepatic steatosis, and chronic cholecystitis with persistently elevated transaminase levels [AST dominant]). One patient who switched from placebo to guselkumab every 4 weeks, with nonalcoholic fatty liver disease, had a grade 1 ALT elevation (>1–3 times the ULN) at week 52 and discontinued guselkumab after week 52. Increased ALT and AST concentrations occurred in 26% and 25%, respectively, of 436 guselkumab-treated patients receiving methotrexate, and in 24% and 20%, respectively, of 292 such patients not receiving methotrexate, at baseline.

Total bilirubin elevations in guselkumab-treated patients were either grade 1 (>1–1.5 times the ULN; 5% of all guselkumab-treated patients) or grade 2 (>1.5–3 times the ULN; 1% of all guselkumab-treated patients) (Supplementary Table 4). All such elevations were <2 times the ULN and not associated with direct bilirubin elevation.

DISCUSSION

Through week 52 of DISCOVER-2, a pivotal phase III guselkumab trial that enrolled biologic-naive PsA patients with extensive disease activity despite standard treatments, guselkumab 100 mg every 4 weeks and every 8 weeks provided clinically meaningful and sustained benefits to participants. The significant improvements in arthritis symptoms, psoriatic lesions, dactylitis and enthesitis, physical function, and physical components of HRQoL achieved at week 24 of DISCOVER-2 (19) were maintained at week 52. Further, numerical improvements seen through week 52 suggested that a further 6 months of guselkumab 100 mg every 4 weeks or every 8 weeks may provide added benefit across response measures. In placebo-treated patients who initiated guselkumab every 4 weeks at week 24, the onset and magnitude of the guselkumab effect confirmed initial observations in patients receiving guselkumab every 4 weeks from week 0 to week 24.

Structural joint damage, exhibited by nearly half of PsA patients within 2 years of symptom onset, often progresses to irreversible damage and disability (32). Understandably, inhibiting structural damage progression is a key PsA treatment goal (2,3). The guselkumab every 4 weeks regimen significantly inhibited structural damage progression, as measured by mean changes in total PsA-modified SHS scores, during weeks 0–24 (19). At the group level, limited radiographic progression was also observed during weeks 24–52 in patients who continued guselkumab every 4 weeks or every 8 weeks and in patients who initiated guselkumab every 4 weeks at week 24. Mean changes in PsA-modified SHS scores during weeks 0–52 were numerically similar for the guselkumab every 4 weeks and every 8 weeks regimens. It should be noted, however, that the average PsA-modified SHS score at baseline was numerically higher in the guselkumab every 4 weeks group, and a higher baseline radiographic score is a known risk factor for further radiographic progression (33). Overall, minimal radiographic progression was seen in the vast majority of patients, while only a few patients in each treatment group exhibited clinically meaningful progression of structural damage, through 1 year.

PsA is a complex, clinically diverse, chronic inflammatory disorder driven by excess IL-23/Th-17–mediated cytokines. The ability of selective IL-23 inhibition with guselkumab to sustain improvements in disparate areas of disease through up to 1 year is encouraging in a disorder that can recur after loss of initial response and that can be recalcitrant to biologics (1,34). Further, given the growing consensus surrounding the ultimate goal of PsA therapy and treatment-to-target, i.e., absence of symptoms for those with early disease or limited joint damage or low levels of disease activity for patients presenting with established disease and/or irreversible damage (35), minimal disease activity responses at week 52 suggest that treatment target was achieved in nearly one-third of these guselkumab-treated patients, who were biologic-naive and on average had PsA for >5 years at study outset. Thus, guselkumab

was shown to offer a novel mechanism, i.e., binding to the p19 subunit of IL-23 but not the p40 subunit it shares with IL-12, to target the key upstream regulatory cytokine implicated in PsA pathogenesis and elicit sustained clinical response.

Importantly, the favorable risk–benefit profile observed through week 24 (19) was supported by findings through week 52, representing a total of 608 patient-years of follow-up. Relative to previously reported data through week 24 of DISCOVER-2 (19), no increase in the incidence of serious infections occurred with continued guselkumab every 4 weeks or every 8 weeks. No patient had active TB or an opportunistic infection, and no deaths occurred, through week 52. No additional malignancies or MACE occurred after week 24, and inflammatory bowel disease was not reported in any patient while receiving guselkumab.

Interpretation of findings through 1 year of DISCOVER-2 is hampered by a shorter duration of placebo than active treatment. To address this, we estimated numbers of patients with AEs per 100 patient-years assuming a constant incidence over time, a customary approach to standardize AE data for comparative purposes. Further, because interpretation of observed efficacy data from clinical trial extensions can also be confounded by enriching the long-term data set with responders, we conservatively summarized clinical efficacy responses by imputing data missing due to discontinued treatment as nonresponse or no change from baseline. Joint counts were not adjusted for the presence of dactylitis in the same digit, as these disease domains were independently assessed. However, as ACR response rates were consistent in patients with or without dactylitis at baseline (data not shown), we do not anticipate any impact on study conclusions. One year is a limited period for assessing patient retention and safety, as well as the structural damage and disability that trail extended periods of untreated systemic inflammation in this chronic condition. Data obtained during the second year of DISCOVER-2 will augment current knowledge of the guselkumab risk–benefit profile and further our understanding of longer-term radiographic outcomes with both guselkumab dosing regimens.

In conclusion, guselkumab 100 mg every 4 weeks or every 8 weeks effectively treated the diverse manifestations of active PsA in biologic-naive patients. The overall treatment effect observed during the 24-week placebo-controlled period was well maintained, and the risk–benefit profile remained favorable for both guselkumab regimens, through week 52 of DISCOVER-2.

AUTHOR CONTRIBUTIONS

All authors were involved in drafting the article or revising it critically for important intellectual content, and all authors approved the final version to be published. Dr. McInnes had full access to all of the data in the study and takes responsibility for the integrity of the data and the accuracy of the data analysis.

Study conception and design. Hsia, Kollmeier, Xu, Subramanian
Acquisition of data. Hsia, Kollmeier, Xu, Subramanian
Analysis and interpretation of data. McInnes, Rahman, Gottlieb, Hsia, Kollmeier, Chakravarty, Xu, Subramanian, Agarwal, Sheng, Jiang, Zhou, Zhuang, van der Heijde, Mease.

ROLE OF THE STUDY SPONSOR

Janssen Research & Development facilitated the study design, provided writing assistance for the manuscript, and reviewed and approved the manuscript prior to submission. The authors independently collected the data, interpreted the results, and had the final decision to submit the manuscript for publication. Substantive manuscript review was provided by Diane D. Harrison, MD, MPH (consultant funded by Janssen), May Shawi, PhD (Janssen), and Chetan Karyekar, MD (Janssen). Programming support was provided by Michelle Pupuk, BS (Janssen). Manuscript preparation and submission assistance was provided by Michelle L. Perate, MS (consultant funded by Janssen). Janssen Research & Development also approved this manuscript prior to submission.

REFERENCES

1. Costa L, Perricone C, Chimenti MS, del Puente A, Caso P, Peluso R, et al. Switching between biological treatments in psoriatic arthritis: a review of the evidence. Drugs R D 2017;17:509–22.
2. Gossec L, Smolen JS, Ramiro S, de Wit M, Cutolo M, Dougados M, et al. European League Against Rheumatism (EULAR) recommendations for the management of psoriatic arthritis with pharmacological therapies: 2015 update. Ann Rheum Dis 2016;75:499–510.
3. Coates LC, Kavanaugh A, Mease PJ, Soriano ER, Acosta-Felquer ML, Armstrong AW, et al. Group for Research and Assessment of Psoriasis and Psoriatic Arthritis 2015 treatment recommendations for psoriatic arthritis. Arthritis Rheumatol 2016;68:1060–71.
4. Harrold LR, Stolshek BS, Rebello S, Collier DH, Mutebi A, Wade SW, et al. Impact of prior biologic use on persistence of treatment in patients with psoriatic arthritis enrolled in the US Corrona registry. Clin Rheumatol 2017;36:895–901.
5. Mease PJ, Accortt NA, Rebello S, Etzel CJ, Harrison RW, Aras GA, et al. Persistence of tumor necrosis factor inhibitor or conventional synthetic disease-modifying antirheumatic drug monotherapy or combination therapy in psoriatic arthritis in a real-world setting. Rheumatol Int 2019;39:1547–58.
6. TREMFYA® (guselkumab) injection, for subcutaneous use. Horsham (PA). Janssen Biotech, Inc.; 2020. URL: http://www.janssenlabels.com/package-insert/product-monograph/prescribing-information/TREMFYA-pi.pdf.
7. Ciric B, El-behi M, Cabrera R, Zhang GX, Rostami A. IL-23 drives pathogenic IL-17-producing $CD8^+$ T cells. J Immunol 2009;182:5296–305.
8. Ness-Schwickerath K, Jin C, Morita C. Cytokine requirements for the differentiation and expansion of IL-17A- and IL-22-producing human Vγ2Vδ2 T cells. J Immunol 2010;184:7268–80.
9. Teng M, Bowman E, McElwee J, Smyth MJ, Casanova JL, Cooper AM, et al. IL-12 and IL-23 cytokines: from discovery to targeted therapies for immune-mediated inflammatory diseases. Nat Med 2015;21:719–29.
10. Teunissen M, Munneke J, Bernink J, Spuls PI, Res PC, te Velde A, et al. Composition of innate lymphoid cell subsets in the human skin: enrichment of NCR^+ ILC3 in lesional skin and blood of psoriasis patients. J Invest Dermatol 2014;134:2351–60.
11. Suzuki E, Mellins ED, Gershwin ME, Nestle FO, Adamopoulos IE. The IL-23/IL-17 axis in psoriatic arthritis [review]. Autoimmun Rev 2014;13:496–502.
12. Girolomoni G, Strohal R, Puig L, Bachelez H, Barker J, Boehncke WH, et al. The role of IL-23 and the IL-23/TH 17 immune axis in the pathogenesis and treatment of psoriasis. J Eur Acad Dermatol Venereol 2017;31:1616–26.

13. Blauvelt A, Papp KA, Griffiths CE, Randazzo B, Wasfi Y, Shen YK, et al. Efficacy and safety of guselkumab, an anti-interleukin-23 monoclonal antibody, compared with adalimumab for the continuous treatment of patients with moderate to severe psoriasis: results from the phase III, double-blinded, placebo- and active comparator-controlled VOYAGE 1 trial. J Am Acad Dermatol 2017;76:405–17.
14. Reich K, Armstrong AW, Foley P, Song M, Wasfi Y, Randazzo B, et al. Efficacy and safety of guselkumab, an anti-interleukin-23 monoclonal antibody, compared with adalimumab for the treatment of patients with moderate to severe psoriasis with randomized withdrawal and retreatment: results from the phase III, double-blind, placebo- and active comparator-controlled VOYAGE 2 trial. J Am Acad Dermatol 2017;76:418–31.
15. Reich K, Armstrong AW, Langley RG, Flavin S, Randazzo B, Li S, et al. Guselkumab versus secukinumab for the treatment of moderate-to-severe psoriasis (ECLIPSE): results from a phase 3, randomised controlled trial. Lancet 2019;394:831–9.
16. Zhuang Y, Calderon C, Marciniak SJ Jr, Bouman-Thio E, Szapary P, Yang TY, et al. First-in-human study to assess guselkumab (anti-IL-23 mAb) pharmacokinetics/safety in healthy subjects and patients with moderate-to-severe psoriasis. Eur J Clin Pharmacol 2016;72:1303–10.
17. Deodhar A, Gottlieb AB, Boehncke WH, Dong B, Wang Y, Zhuang Y, et al, on behalf of the CNTO1959PSA2001 Study Group. Efficacy and safety of guselkumab in patients with active psoriatic arthritis: a randomised, double-blind, placebo-controlled, phase 2 study. Lancet 2018;391:2213–24.
18. Deodhar A, Helliwell PS, Boehncke WH, Kollmeier AP, Hsia EC, Subramanian RA, et al, on behalf of the DISCOVER-1 Study Group. Guselkumab in patients with active psoriatic arthritis who were biologic-naive or had previously received TNFα inhibitor treatment (DISCOVER-1): a double-blind, randomised, placebo-controlled phase 3 trial. Lancet 2020;395:1115–25.
19. Mease PJ, Rahman P, Gottlieb AB, Kollmeier AP, Hsia EC, Xu XL, et al, on behalf of the DISCOVER-2 Study Group. Guselkumab in biologic-naive patients with active psoriatic arthritis (DISCOVER-2): a double-blind, randomised, placebo-controlled phase 3 trial. Lancet 2020;395:1126–36.
20. Healy PJ, Helliwell PS. Measuring clinical enthesitis in psoriatic arthritis: assessment of existing measures and development of an instrument specific to psoriatic arthritis. Arthritis Rheum 2008;59:686–91.
21. Gladman DD, Inman RD, Cook RJ, Maksymowych WP, Braun J, Davis JC, et al. International spondyloarthritis interobserver reliability exercise—the INSPIRE study: II. Assessment of peripheral joints, enthesitis, and dactylitis. J Rheumatol 2007;34:1740–5.
22. Gladman DD, Ziouzina O, Thavaneswaran A, Chandran V. Dactylitis in psoriatic arthritis: prevalence and response to therapy in the biologic era. J Rheumatol 2013;40:1357–9.
23. Fries JF, Spitz P, Kraines RG, Holman HR. Measurement of patient outcome in arthritis. Arthritis Rheum 1980;23:137–45.
24. Van der Heijde D, Sharp J, Wassenberg S, Gladman DD. Psoriatic arthritis imaging: a review of scoring methods. Ann Rheum Dis 2005;64 Suppl 2:ii61–4.
25. Langley RG, Feldman SR, Nyirady J, van de Kerkhof P, Papavassilis C. The 5-point Investigator's Global Assessment (IGA) Scale: a modified tool for evaluating plaque psoriasis severity in clinical trials. J Dermatolog Treat 2015;26:23–31.
26. Fredriksson T, Pettersson U. Severe psoriasis—oral therapy with a new retinoid. Dermatologica 1978;157:238–44.
27. Ware JE Jr, Kosinski M, Keller SK. SF-36 physical and mental health summary scales: a user's manual. Boston: The Health Institute, New England Medical Center; 1994.
28. Mundt JC, Greist JH, Gelenberg AJ, Katzelnick DJ, Jefferson JW, Modell JG. Feasibility and validation of a computer-automated Columbia-Suicide Severity Rating Scale using interactive voice response technology. J Psychiatr Res 2010;44:1224–8.
29. Coates LC, Fransen J, Helliwell PS. Defining minimal disease activity in psoriatic arthritis: a proposed objective target for treatment. Ann Rheum Dis 2010;69:48–53.
30. Coates LC, Helliwell PS. Defining low disease activity states in psoriatic arthritis using novel composite disease instruments. J Rheumatol 2016;43:371–5.
31. Landewé R, van der Heijde D. Radiographic progression depicted by probability plots: presenting data with optimal use of individual values. Arthritis Rheum 2004;50:699–706.
32. Van der Heijde D, Gladman DD, Kavanaugh A, Mease PJ. Assessing structural damage progression in psoriatic arthritis and its role as an outcome in research. Arthritis Res Ther 2020;22:18.
33. Geijer M, Lindqvist U, Husmark T, Alenius GM, Larsson PT, Teleman A, et al. The Swedish Early Psoriatic Arthritis Registry 5-year followup: substantial radiographic progression mainly in men with high disease activity and development of dactylitis. J Rheumatol 2015;42:2110–7.
34. Fagerli KM, Lie E, van der Heijde D, Heiberg MS, Kalstad S, Rødevand E, et al. Switching between TNF inhibitors in psoriatic arthritis: data from the NOR-DMARD study. Ann Rheum Dis 2013;72:1840–4.
35. Mease PJ, Coates LC. Considerations for the definition of remission criteria in psoriatic arthritis. Semin Arthritis Rheum 2018;47:786–96.

Arthritis & Rheumatology
Vol. 73, No. 4, April 2021, pp 617–630
DOI 10.1002/art.41577

American College of Rheumatology
Empowering Rheumatology Professionals

Hospitalized Infections in Lupus: A Nationwide Study of Types of Infections, Time Trends, Health Care Utilization, and In-Hospital Mortality

Jasvinder A. Singh[1] and John D. Cleveland[2]

Objective. To examine the time trends in hospitalized infections in patients with systemic lupus erythematosus (SLE), and the factors associated with health care utilization and in-hospital mortality.

Methods. US National Inpatient Sample data from 1998–2016 were used to examine the epidemiology, time trends, and outcomes of 5 common hospitalized infections in patients with SLE, namely, pneumonia, sepsis/bacteremia, urinary tract infection (UTI), skin and soft tissue infections (SSTIs), and opportunistic infections (OIs). Time trends were compared using the Cochran-Armitage test. Multivariable-adjusted logistic regression models were used to examine the factors associated with health care utilization (hospital stay >3 days, hospital charges above the median, or discharge to a nonhome setting) and in-hospital mortality.

Results. Hospitalization rates per 100,000 claims among SLE patients in 1998–2000 versus in 2015–2016 were as follows: for OIs, 1.13 versus 1.61 (1.2-fold increase); for SSTIs, 4.78 versus 12.2 (2.5-fold increase); for UTI, 1.94 versus 6.12 (3.2-fold increase); for pneumonia, 15.09 versus 17.05 (1.1-fold increase); and for sepsis, 6.31 versus 39.64 (6.3-fold increase). In 2011–2012, sepsis surpassed pneumonia as the most common hospitalized infection in patients with SLE. In multivariable-adjusted models, a diagnosis of sepsis, older age, a Deyo-Charlson common comorbidities score of ≥2, having Medicare or Medicaid insurance, and urban hospital location were significantly associated with increased odds of in-hospital mortality and with all health care utilization outcomes. African American race was significantly associated with increased odds of health care utilization.

Conclusion. The results of this study indicate that the rates of hospitalized infections increased over time in patients with SLE, and that pneumonia was surpassed by sepsis as the most common hospitalized infection. In addition, associations of risk factors with poorer outcomes were identified. These findings may help inform patients, providers, and policy makers with regard to the burden of infection in SLE, and could lead to interventions/pathways to improve outcomes.

INTRODUCTION

Infections, in particular serious infections, are recognized as a major cause of morbidity and premature mortality in patients with systemic lupus erythematosus (SLE; hereafter referred to as lupus), contributing to up to one-third of all deaths and two-thirds of avoidable hospitalizations (1–7). Lupus disease activity and the use of immunosuppressive agents and glucocorticoids for treatment can increase the risk of infection, while hydroxychloroquine treatment lowers the infection risk in patients with lupus (3,4,8–11). Belimumab, a biologic drug, was approved for the treatment of lupus in 2011 in the US; this treatment has been shown to be associated with serious infections as a potential adverse event (12). The most common infection occurring in patients with lupus is pneumonia, accounting for 25–50% of all infections, followed by sepsis, skin infection, and pyelonephritis

The views presented in this article are solely the responsibility of the authors and do not necessarily represent the views of the Department of Veterans Affairs.

Supported by research funds from the Division of Rheumatology at the University of Alabama at Birmingham, and by the resources and facilities provided by the Birmingham VA Medical Center.

[1]Jasvinder A. Singh, MD, MBBS, MPH: University of Alabama at Birmingham and Birmingham VA Medical Center; [2]John D. Cleveland, MS: University of Alabama at Birmingham.

Dr. Singh has received consulting fees, speaking fees, and/or honoraria from Medisys, Fidia, UBM, Trio Health, Medscape, WebMD, Clinical Care Options, ClearView Healthcare Partners, Putnam Associates, Focus Forward, Navigant Consulting, Spherix, and Practice Point Communications (less than $10,000 each) and from Crealta/Horizon and Simply Speaking (more than $10,000 each) and owns stock or stock options in Vaxart and Charlotte's Web Holdings. No other disclosures relevant to this article were reported.

Address correspondence to Jasvinder A. Singh, MD, MBBS, MPH, University of Alabama at Birmingham, Faculty Office Tower 805B, 510 20th Street South, Birmingham, AL 35294. Email: Jasvinder.md@gmail.com.

Submitted for publication November 27, 2019; accepted in revised form October 29, 2020.

(2–5,7). The incidence of infections in lupus ranges from 4.4 per 100 person-years in a single-center study (13) to 10 per 100 person-years in a US Medicaid population (14).

A few studies have examined the incidence of infections in patients with lupus and have compared the rates to those in non-lupus cohorts (14–16). In an analysis of the US National Inpatient Sample (NIS) data from 1996–2011, compared to individuals without lupus, patients with lupus had 6 times higher rates of pneumonia and 10 times higher rates of urinary tract infection (UTI) in 1996, and by 2011 all relative risks of these infections were further increased (12 times) in patients with lupus (15). To our knowledge, representative national epidemiologic studies of hospitalized infections in lupus that examine associated health care utilization outcomes are needed. Since many hospitalized infections are avoidable (16), contemporary data on hospitalized infections in lupus are needed, since they can inform health care delivery and policy.

Therefore, our objective was to 1) examine the differences in rates of hospitalized infections by the presence of lupus versus absence of lupus (i.e., non-lupus), 2) assess the incidence and time trends of 5 common hospitalized infections and associated health care utilization outcomes during hospitalizations of lupus patients from 1998 to 2016, and 3) analyze the predictors of health care utilization and in-hospital mortality in patients with lupus hospitalized with infections. We hypothesized that health care utilization among subjects with hospitalized infections would be higher in lupus patients than in non-lupus patients, that all types of infections would increase in frequency over time, and that older age, male sex, higher numbers of comorbidities, and non-white race would be associated with poorer outcomes in lupus patients hospitalized with infections.

PATIENTS AND METHODS

Ethics/Institutional Review Board (IRB) approval and consent to participate. The IRB of the University of Alabama at Birmingham (UAB) approved the study, and all investigations were conducted in conformity with the UAB ethics principles of research (approval no. X120207004). The IRB waived the need for an informed consent for this database study.

Data source. Our study used the NIS data from 1998–2016. The US NIS is a de-identified, national all-payer inpatient health care database that represents a 20% stratified sample of all discharge records from all participating community hospitals from all participating states in the US (17). It is a component of the Agency for Healthcare Research and Quality Healthcare Cost and Utilization Project (www.ahrq.gov).

Cohort selection. We identified 5 types of hospitalized infections, as previously described (15,18), using the following International Classification of Diseases, Ninth Revision, Clinical Modification (ICD-9-CM) codes in the primary diagnosis position: 1) pneumonia (ICD-9-CM codes 003.22, 481.0, 513.0, 480.xx, 482.xx, 483.xx, 485.xx, and 486.xx); 2) sepsis/bacteremia (hereafter referred to as sepsis) (ICD-9-CM codes 038.xx and 790.7); 3) UTI (ICD-9-CM code 590.xx); 4) skin and soft tissue infections (SSTIs) (ICD-9-CM codes 040.0, 569.61, 681.xx, 682.xx, 785.4, 728.86, and 035.xx); and 5) opportunistic infections (OIs) (ICD-9-CM codes 010.xx –018.xx, 031.xx, 078.5, 075.xx, 053.xx, 112.4, 112.5, 112.81, 112.83, 130.xx, 136.3, 117.5, 027.0, 039.xx, 117.3, 114.xx, 115.xx, and 116.0). These diagnostic codes have been shown to be valid in administrative data sets, with positive predictive values of 70–100% in patients with rheumatoid arthritis (19–21). For the 2015–2016 data, we used the ICD-10-CM codes for infections, since the coding system changed from the ICD-9-CM to ICD-10-CM in 2015 in the US (see Supplementary Table 1, available on the *Arthritis & Rheumatology* website at http://onlinelibrary.wiley.com/doi/10.1002/art.41577/abstract). Composite infection was defined as any of the infection categories occurring as a primary diagnosis for hospitalization; this equates to the sum of all 5 infections for frequencies.

We identified patients with lupus by the presence of an ICD-9-CM code of 710.0 or ICD-10-CM code of M32.9 in the secondary (nonprimary) position for hospitalization, i.e., any position other than the primary. Our approach using an ICD-9-CM code for identifying patients with lupus using administrative data is a valid and reliable method (22) that has been used in previous epidemiologic and outcomes studies (15,16).

Statistical analysis. Descriptive statistics for demographic and clinical characteristics were compared between patients with lupus hospitalized with infections and subjects without lupus (non-lupus controls) hospitalized with infections. Characteristics were also compared according to each hospitalized infection in patients with lupus. We decided a priori to not calculate *P* values in unadjusted analyses of characteristics and outcomes, to avoid multiple comparisons.

Frequencies and rates of the 5 infections analyzed (per 100,000 claims) were each analyzed for trends over time using a Cochran-Armitage test, weighted by the number of hospitalizations in that year category. We compared health care utilization and in-hospital mortality for each of the 5 infection categories between 1998–2000 and 2015–2016.

Adjusted logistic regression models were used to examine the factors associated with a median hospital stay of >3 days, inflation-adjusted total hospital charges above the median (based on the median value for each year, with adjustment of the hospital charges to inflation-adjusted 2016 US dollars, using the Bureau of Labor Statistics Consumer Price Index All Urban Consumers US city average), discharge to nonhome setting (i.e., rehabilitation, nursing, or inpatient facility), and in-hospital mortality for composite infection. In sensitivity analyses, we adjusted the main models for each outcome for the year being examined, to assess whether a specific year was statistically significantly associated with these outcomes. Covariates were selected based on clinical

importance according to potential/known association with the risk of outcomes of serious/hospitalized infections. These covariates included demographics (age, sex, race/ethnicity, annual household income by quartile [23]), Deyo-Charlson index (a valid health measure consisting of 17 common medical comorbidities; score range 0–25, with higher scores indicating more comorbidity load [24]), insurance type (US Medicaid, US Medicare, private insurance, or self/other [25]), and hospital characteristics (bed size, location, and teaching status [rural, urban, or urban, teaching hospital]).

We calculated adjusted odds ratios (ORs) and 95% confidence intervals (95% CIs) for each correlation. A 95% CI excluding

Table 1. Demographic and clinical characteristics of the lupus patients with any hospitalization or infection hospitalization versus non-lupus control subjects with infection hospitalization*

	Any hospitalization in lupus patients (n = 2,685,623)	Infection hospitalization	
		Non-lupus controls (n = 49,637,826)	Lupus patients (n = 328,744)
Age, mean ± SEM; median years	51.7 ± 0.06; 51.2	59.9 ± 0.08; 65.1	52.5 ± 0.09; 51.9
Age category			
<50 years	1,221,769 (45.5)	13,940,265 (28.3)	142,406 (43.4)
50–64 years	806,720 (30.0)	9,896,435 (20.1)	99,576 (30.4)
65–79 years	509,107 (19.0)	13,222,914 (26.8)	65,071 (19.8)
≥80 years	147,661 (5.5)	12,204,911 (24.8)	20,724 (6.3)
Sex			
Male	294,157 (11.0)	23,419,036 (47.6)	40,155 (12.2)
Female	2,390,778 (89.0)	25,819,094 (52.4)	287,594 (87.7)
Race/ethnicity			
White	1,279,668 (47.6)	29,602,666 (60.1)	156,206 (47.7)
African American	639,196 (23.8)	5,267,591 (10.7)	75,487 (23.0)
Hispanic	258,933 (9.6)	4,185,067 (8.5)	36,809 (11.2)
Other/missing	507,619 (18.9)	10,226,912 (20.7)	59,282 (18.1)
Deyo-Charlson comorbidity score			
0	16 (0)	15,683,828 (31.8)	0 (0)
1	903,434 (33.6)	12,822,962 (26.0)	114,414 (34.9)
≥2	1,782,172 (66.4)	20,780,211 (42.2)	213,389 (65.1)
Income category			
0–25th percentile	744,212 (28.3)	12,883,940 (26.8)	95,737 (29.8)
25–50th percentile	670,221 (25.5)	13,221,834 (27.5)	83,474 (26.0)
50–75th percentile	618,437 (23.5)	11,543,240 (24.0)	74,328 (23.2)
75–100th percentile	593,719 (22.6)	10,467,811 (21.7)	67,294 (21.0)
Insurance			
Private	811,521 (30.3)	10,869,696 (22.1)	87,194 (26.6)
Medicare	1,260,555 (47.0)	27,313,205 (55.5)	162,373 (49.6)
Medicaid	448,849 (16.7)	7,029,793 (14.3)	57,650 (17.6)
Other	75,012 (2.8)	1,494,023 (3.0)	8,488 (2.6)
Self	85,087 (3.2)	2,474,225 (5.0)	11,591 (3.5)
Hospital location, type			
Rural	246,012 (9.2)	7,000,495 (15.0)	32,201 (10.1)
Urban	985,319 (36.8)	19,133,806 (40.9)	122,203 (38.4)
Urban, teaching	1,445,881 (54.0)	20,658,027 (44.1)	163,779 (51.5)
Length of hospital stay			
Days, mean ± SEM; median	5.5 ± 0.01; 3.2	5.9 ± 0.001; 3.7	6.7 ± 0.03; 4.1
>3 days	1,400,893 (52.2)	29,281,170 (59.4)	211,906 (64.6)
Total hospital charges			
≤ median†	795,508 (29.6)	21,043,862 (42.7)	111,460 (34.0)
> median†	1,890,115 (70.4)	28,243,139 (57.3)	216,343 (66.0)
US $, mean ± SEM; median	54,678 ± 566; 31,000	47,665 ± 338; 25,464	60,352 ± 889; 32,120
1998–2000	49,537 ± 927; 27,052	39,448 ± 524; 21,728	55,308 ± 1,470; 28,120
2015–2016	58,748 ± 709; 34,402	54,790 ± 436; 29,424	63,167 ± 1,118; 34,576
Discharge status			
Rehabilitation or nursing facility	389,886 (15.1)	11,613,783 (25.5)	53,774 (17.6)
Home	2,199,836 (84.9)	33,992,408 (74.5)	252,509 (82.4)
Died during hospitalization	57,191 (2.1)	3,062,394 (6.2)	16,675 (5.1)

* Except where indicated otherwise, values are the number (%) of subjects.
† Inflation-adjusted median total hospital charges by year for the US National Inpatient Sample: 1998, $16,650; 1999, $16,840; 2000, $17,711; 2001, $18,590; 2002, $19,647; 2003, $20,822; 2004, $20,067; 2005, $20,696; 2006, $21,617; 2007, $21,883; 2008, $21,965; 2009, $21,810; 2010, $21,051; 2011, $22,569; 2012, $23,676; 2013, $24,424; 2014, $24,385; 2015, $24,894; 2016, $25,261.

Table 2. Characteristics of the lupus patients according to each hospitalized infection*

	OI (n = 10,711; 3.3%)	SSTI (n = 62,585; 19%)	UTI (n = 20,917; 6.4%)	Pneumonia (n = 120,739; 36.8%)	Sepsis (n = 112,852; 34.4%)	Composite infection (n = 327,803; 100%)†
Age, mean ± SEM; median years	46.7 ± 0.42; 46.4	50.4 ± 0.16; 49.5	46.5 ± 0.27; 44.3	54.2 ± 0.13; 53.9	53.5 ± 0.13; 53.5	52.5 ± 0.09; 51.9
Age category						
<50 years	5,949 (55.6)	30,591 (48.9)	12,379 (59.2)	48,005 (39.8)	45,482 (40.3)	142,406 (43.4)
50–64 years	2,777 (25.9)	19,604 (31.3)	4,922 (23.5)	36,982 (30.6)	35,291 (31.3)	99,576 (30.4)
65–79 years	1,573 (14.7)	9,884 (15.8)	2,883 (13.8)	26,295 (21.8)	24,435 (21.7)	65,071 (19.9)
≥80 years	405 (3.8)	2,506 (4.0)	732 (3.5)	9,447 (7.8)	7,633 (6.8)	20,724 (6.3)
Sex						
Male	1,648 (15.4)	7,187 (11.5)	595 (2.8)	16,723 (13.9)	14,003 (12.4)	40,155 (12.3)
Female	9,056 (84.6)	55,383 (88.5)	20,313 (97.2)	104,003 (86.1)	98,839 (87.6)	287,594 (87.7)
Race						
White	3,888 (36.3)	33,032 (52.8)	9,806 (46.9)	56,563 (46.8)	52,916 (46.9)	156,206 (47.7)
African American	2,516 (23.5)	12,732 (20.3)	4,000 (19.1)	27,408 (22.7)	28,832 (25.6)	75,487 (23.0)
Hispanic	1,689 (15.8)	6,450 (10.3)	3,289 (15.7)	12,033 (10.0)	13,349 (11.8)	36,809 (11.2)
Other/missing	2,619 (24.4)	10,361 (16.6)	3,822 (18.3)	24,732 (20.5)	17,749 (15.7)	59,282 (18.1)
Deyo-Charlson comorbidity score						
0	0 (0)	0 (0)	0 (0)	0 (0)	0 (0)	0 (0)
1	4,833 (45.1)	27,454 (43.9)	10,710 (51.2)	38,924 (32.2)	32,493 (28.8)	114,414 (34.9)
≥2	5,879 (54.9)	35,131 (56.1)	10,206 (48.8)	81,815 (67.8)	80,359 (71.2)	213,389 (65.1)
Income category						
0–25th percentile	2,642 (25.1)	18,302 (29.9)	5,940 (29.0)	34,183 (29.0)	34,671 (31.3)	95,737 (29.8)
25–50th percentile	2,719 (25.8)	15,249 (24.9)	5,221 (25.5)	32,067 (27.2)	28,219 (25.5)	83,474 (26.0)
50–75th percentile	2,592 (24.6)	14,095 (23.0)	4,879 (23.8)	27,038 (22.9)	25,724 (23.3)	74,328 (23.2)
75–100th percentile	2,573 (24.4)	13,576 (22.2)	4,417 (21.6)	24,740 (21.0)	21,988 (19.9)	67,294 (21.0)
Insurance						
Private	3,530 (33.0)	17,126 (27.4)	6,992 (33.5)	32,592 (27.0)	26,955 (23.9)	87,194 (26.6)
Medicare	4,235 (39.6)	27,972 (44.8)	7,519 (36.0)	62,095 (51.5)	60,551 (53.7)	162,373 (49.6)
Medicaid	2,142 (20.0)	12,562 (20.1)	4,671 (22.4)	18,851 (15.6)	19,424 (17.2)	57,650 (17.6)
Other	409 (3.8)	1,911 (3.1)	711 (3.4)	2,965 (2.5)	2,492 (2.2)	8,488 (2.6)
Self	375 (3.5)	2,929 (4.7)	977 (4.7)	4,040 (3.4)	3,269 (2.9)	11,591 (3.5)
Hospital region						
Northeast	1,773 (16.5)	11,558 (18.4)	3,249 (15.5)	19,085 (15.7)	16,800 (14.9)	52,464 (16.0)
Midwest	2,130 (19.8)	12,529 (20.0)	3,816 (18.2)	25,476 (21.0)	22,334 (19.8)	66,284 (20.2)
South	4,360 (40.6)	26,779 (42.7)	9,025 (43.1)	55,222 (45.5)	48,623 (43.0)	144,010 (43.8)
West	2,467 (23.0)	11,817 (18.9)	4,847 (23.1)	21,567 (17.8)	25,287 (22.4)	65,985 (20.1)
Hospital location, type						
Rural	607 (5.8)	5,403 (8.9)	1,996 (9.9)	14,778 (12.8)	9,416 (8.5)	32,201 (10.1)
Urban	3,073 (29.5)	24,227 (39.9)	7,568 (37.5)	47,338 (40.9)	39,996 (36.0)	122,203 (38.4)
Urban, teaching	6,745 (64.7)	31,068 (51.2)	10,602 (52.6)	53,721 (46.4)	61,642 (55.5)	163,779 (51.5)
Hospital bed size						
Small	939 (8.8)	8,315 (13.3)	2,925 (14.0)	16,943 (14.0)	14,475 (12.8)	43,597 (13.3)
Medium	2,725 (25.5)	16,306 (26.1)	5,781 (27.7)	32,819 (27.1)	29,244 (25.9)	86,877 (26.5)
Large	7,019 (65.7)	37,862 (60.6)	12,162 (58.3)	71,195 (58.9)	68,998 (61.2)	197,237 (60.2)

(Continued)

Table 2. *(Cont'd)*

	OI (n = 10,711; 3.3%)	SSTI (n = 62,585; 19%)	UTI (n = 20,917; 6.4%)	Pneumonia (n = 120,739; 36.8%)	Sepsis (n = 112,852; 34.4%)	Composite infection (n = 327,803; 100%)†
Length of hospital stay						
>3 days	7,920 (73.9)	36,044 (57.6)	8,990 (43.0)	75,516 (62.5)	83,436 (73.9)	211,906 (64.6)
Days, mean ± SEM; median	10.0 ± 0.28; 5.6	5.3 ± 0.06; 3.5	4.0 ± 0.05; 2.7	6.0 ± 0.04; 3.9	8.5 ± 0.07; 5.3	6.7 ± 0.03; 4.1
Total hospital charges						
> median	7,734 (72.2)	33,615 (53.7)	10,196 (48.7)	77,534 (64.2)	87,265 (77.3)	216,343 (66.0)
US $, mean ± SEM; median	61,678 ± 2,315; 26,613	26.211 ± 374; 16,387	21,603 ± 432; 14,912	32,292 ± 385; 18,502	70,034 ± 844; 36,706	44,304 ± 395; 22,319
Discharge status						
Rehabilitation or nursing facility	1,401 (14.0)	6,766 (11.1)	1,613 (7.8)	16,038 (13.9)	27,955 (28.2)	53,774 (17.6)
Home	8,639 (86.0)	54,374 (88.9)	18,979 (92.2)	99,443 (86.1)	71,075 (71.8)	252,509 (82.4)
Died during hospitalization	541 (5.1)	360 (0.6)	53 (0.3)	3,611 (3.0)	12,110 (10.7)	16,675 (5.1)

* Except where indicated otherwise, values are the number (%) of patients. OI = opportunistic infection; SSTI = skin and soft tissue infection; UTI = urinary tract infection.
† Composite infection indicates any of the 5 infections as the primary diagnosis.

unity represented a statistically significant result, corresponding to a *P* value of less than 0.05.

We also examined the ranking of the frequencies of Clinical Classifications Software (CCS) categories in any position (primary or nonprimary) for all lupus hospitalizations (lupus as the secondary diagnosis) between 1998–1999 and 2013–2014, to understand the relative importance of infections versus other diseases as the admitting diagnosis in those with lupus. We chose these time periods because CCS data were not available for 2015–2016 and a change from ICD-9-CM to ICD-10-CM code occurred in 2015.

RESULTS

Demographic and clinical characteristics of lupus patients versus non-lupus controls hospitalized with infection. There were 49,637,826 hospitalizations with infections in non-lupus subjects and 328,744 in lupus patients. The mean age of patients with lupus with a primary diagnosis of 1 of the infections was 52.5 years, with a median age of 51.9 years (Table 1). Almost one-half of the patients with lupus who were admitted to the hospital with infection were age <50 years and were of nonwhite race/ethnicity. With regard to comorbidities, 65% of the patients with lupus hospitalized with infection had a Deyo-Charlson common comorbidity score of >2. Approximately 30% of patients with lupus and primary infection hospitalizations as well as ~30% of those with any hospitalization were in the lowest income quartile (Table 1).

Compared to non-lupus controls who were admitted with an infection, patients with lupus who were admitted with an infection diagnosis were younger (median age 65 years versus 52 years) and were more likely to be female (52% versus 88%), to be nonwhite (40% versus 52%), to be in the lowest income quartile (27% versus 30%), to have a Deyo-Charlson comorbidity score of at least 2 (42% versus 65%), and to have been admitted to an urban, teaching hospital (44% versus 52%). The frequencies of insurance payer types were similar between the non-lupus and lupus groups (Table 1).

Unadjusted health care utilization in lupus patients versus non-lupus controls hospitalized with infection. Compared to non-lupus controls hospitalized with infection, patients with lupus hospitalized with an infection diagnosis had higher inflation-adjusted hospital charges (median $47,665 versus $60,352), were more likely to have a hospital stay of >3 days (59% versus 64%), were more likely to have hospital charges above the median (57.3% versus 66%), and were more likely to be discharged home (74.5% versus 82.4%). Non-lupus controls hospitalized with an infection and patients with lupus hospitalized with an infection had similar rates of mortality (6.2% versus 5.1%) (Table 1). The median length of hospital stay was 3.7 days for non-lupus controls and 4.1 days for lupus patients (Table 1), which is higher than the overall NIS median hospital stay of 3 days. A longer hospital stay for patients with lupus compared to those without lupus was evident across each type of serious infection that resulted in hospitalization (see Supplementary Table 2, available on the *Arthritis & Rheumatology* website at http://onlinelibrary.wiley.com/doi/10.1002/art.41577/abstract).

Comparing the overall hospital charges for infection hospitalizations in patients with lupus between 2015–2016 and 1998–2000, we found an increase of 14% in the mean hospital charges and an increase of 23% in the median hospital charges (Table 1). Comparatively, when we examined the charges for infection hospitalizations in subjects without a lupus diagnosis, we noted an increase of 39% in the mean hospital charges and an increase of 35% in the median hospital charges over the same period.

Characteristics and outcomes for each hospitalized infection in patients with lupus. Over the study period, the most common hospitalized infections in lupus were sepsis (34%) and pneumonia (37%), followed by SSTIs (19%), UTI (6%), and OIs (3%) (Table 2). Lupus patients with pneumonia who were admitted for hospitalization were a decade older than those admitted with a UTI or OI, and were 5 years older than those admitted with an SSTI (Table 2).

The median length of hospital stay over the study period was the highest for those lupus patients with OI hospitalizations, whose median hospital stay was 5.6 days, and the lowest for those with UTI hospitalizations, at a median of 2.7 days (Table 2). OI, pneumonia, and sepsis infections led to above-median lengths of hospital stay in 64–77% of patients. Median hospital charges were highest for hospitalizations for sepsis in lupus patients, followed by OIs and pneumonia (Table 2).

Rates of infections and time trends in patients with lupus hospitalized with infections. We noted a significant increase in the frequency of all 5 hospitalized infection categories in people with lupus during the study period. In 2011–2012, sepsis surpassed pneumonia as the most common infection, and by 2015–2016, sepsis accounted for twice as many hospitalized infections as pneumonia in patients with lupus (Figures 1A and B) (see also Supplementary Table 3, available on the *Arthritis & Rheumatology* website at http://onlinelibrary.wiley.com/doi/10.1002/art.41577/abstract).

Over the study period, the hospitalization rate per 100,000 NIS claims increased significantly from 1998 to 2016 in patients with lupus for each infection and for composite infection (each $P < 0.001$). The hospitalization rates and increases in hospitalization rates were as follows: for OIs, 1.17 versus 1.71 (1.5-fold); for SSTIs, 4.66 versus 12.45 (2.7-fold); for UTI, 1.77 versus 7.99 (4.5-fold); for pneumonia, 13.65 versus 16.76 (1.2-fold); for sepsis, 6.56 versus 39.55 (6.0-fold); and for composite infection, 27.82 versus 78.46 (2.8-fold). When considering a different denominator, the hospitalization rate per 100,000 lupus claims, as compared to 1998–2000, the increases in rates in 2015–2016 were

Figure 1. Time trends in the rates of various infections in patients with systemic lupus erythematosus. Infection rates are expressed per 100,000 National Inpatient Sample (NIS) claims (**A**) and per 100,000 lupus claims (**B**). The y-axis scales are different for the 2 panels. The x-axis shows study time periods from 1998 to 2016. OI = opportunistic infection; SSTI = skin and soft tissue infection; UTI = urinary tract infection.

as follows: for OIs, 0.8-fold; for SSTIs, 1.5-fold; for UTI, 2.5-fold; for pneumonia, 0.7-fold; for sepsis, 3.4-fold; and for composite infection, 1.6-fold (Table 3).

Hospitalization for any of these 5 infections (composite) increased from 10.7% of all lupus hospitalizations in 1998–2000 to 15.6% in 2015–2016 (10,748 versus 15,645 per 100,000 lupus hospitalization claims) (see Supplementary Table 4, available on the *Arthritis & Rheumatology* website at http://onlinelibrary.wiley.com/doi/10.1002/art.41577/abstract). The corresponding rate of composite infection in the general NIS population increased from 5.8% in 1998–2000 to 10.2% in 2015–2016 (5,836 versus 10,171 per 100,000 NIS hospitalization claims) (see Supplementary Table 5, available on the *Arthritis & Rheumatology* website at http://onlinelibrary.wiley.com/doi/10.1002/art.41577/abstract). Similarly, the lupus/non-lupus diagnosis rate increased in each of the 5 hospitalized infection claims; a positive slope indicated that lupus claims were increasing faster than non-lupus claims among those with primary hospitalized infection (see Supplementary Tables 6 and 7, available on the *Arthritis & Rheumatology* website at http://onlinelibrary.wiley.com/doi/10.1002/art.41577/abstract).

Time trends in health care utilization and mortality, overall and for each hospitalized infection, among patients with lupus hospitalized with infection. We found that, in lupus patients, the median hospital stay for composite infection decreased from 4.5 days in 1998–2000 to 3.9 days in 2015–2016, and also decreased for each infection (Table 4). The reduction in median hospital stay was greatest for OIs, decreasing from 6.9 to 4.9 days, and for sepsis, decreasing from 6 to 4.8 days.

The frequency of in-hospital mortality for composite infection also decreased in lupus patients, from 6.4% in 1998–2000 to 4.8% in 2015–2016. The largest reductions

Table 3. Rates of hospitalized infections in patients with lupus over time, using 2 different denominators*

	OI	SSTI	UTI	Pneumonia	Sepsis	Composite infection†	Total claims
Rate per 100,000 NIS claims							
1998	1.17	4.66	1.77	13.65	6.56	27.82	33,923,632
1999	1.29	4.41	1.87	16.27	6.72	30.55	34,440,994
2000	1.53	5.26	2.17	15.31	5.66	29.93	35,300,425
2001	1.19	6.08	2.20	15.42	6.02	30.91	36,093,550
2002	1.26	6.20	2.38	16.48	5.91	32.23	36,523,831
2003	1.55	7.17	2.51	16.92	7.21	35.36	37,074,605
2004	1.40	7.62	2.74	17.08	8.53	37.37	37,496,978
2005	1.71	8.76	2.80	18.11	9.71	41.10	37,843,039
2006	1.59	9.11	2.83	17.25	11.72	42.49	38,076,556
2007	1.59	9.02	2.84	17.98	12.41	43.85	38,155,908
2008	1.70	9.01	2.37	16.43	10.46	39.97	38,210,889
2009	1.50	9.78	2.71	18.01	13.62	45.62	37,734,584
2010	1.75	11.72	2.92	18.14	16.89	51.42	37,352,013
2011	1.69	11.68	3.10	19.50	22.40	58.36	36,962,415
2012	1.82	10.95	3.08	20.05	23.89	59.79	36,484,846
2013	1.73	12.16	3.33	19.58	28.75	65.55	35,597,792
2014	1.57	12.90	3.45	19.88	34.63	72.43	35,358,818
2015‡	1.51	11.95	4.26	17.35	39.73	74.80	35,769,942
2016‡	1.71	12.45	7.9	16.76	39.55	78.46	35,675,421
P§	<0.001	<0.001	<0.001	<0.001	<0.001	<0.001	–
Rate per 100,000 lupus claims							
1998	445.57	1,769.59	673.93	5,187.82	2,491.99	10,569.41	89,286
1999	466.16	1,597.83	676.75	5,896.59	2,437.79	11,075.32	95,004
2000	541.30	1,863.59	766.65	5,420.26	2,004.01	10,595.79	99,700
2001	402.91	2,056.78	744.34	5,211.25	2,034.30	10,449.66	106,769
2002	394.21	1,938.96	744.04	5,150.30	1,845.69	10,072.13	116,867
2003	462.37	2,141.47	749.20	5,052.87	2,152.75	10,559.17	124,167
2004	406.03	2,212.61	795.58	4,956.12	2,474.19	10,844.03	129,214
2005	478.04	2,442.04	781.10	5,051.36	2,707.32	11,460.80	135,706
2006	427.82	2,444.37	759.33	4,630.70	3,145.18	11,406.84	141,836
2007	418.62	2,370.18	746.45	4,724.52	3,260.55	11,520.37	145,221
2008	450.07	2,377.89	624.68	4,339.08	2,762.81	10,554.36	144,708
2009	372.81	2,436.61	674.01	4,487.03	3,393.16	11,363.80	151,481
2010	407.81	2,737.09	681.46	4,235.67	3,944.33	12,006.80	159,951
2011	359.03	2,480.99	657.61	4,142.26	4,760.21	12,400.34	173,963
2012	389.06	2,337.28	658.18	4,279.65	5,098.73	12,762.91	170,925
2013	358.35	2,523.02	690.48	4,061.30	5,963.76	13,596.90	171,620
2014	309.58	2,543.58	680.52	3,921.35	6,830.29	14,285.32	179,275
2015‡	295.94	2,342.85	835.75	3,400.56	7,787.58	14,662.68	182,470
2016‡	364.27	2,651.38	1,701.90	3,571.00	8,425.89	16,714.44	167,460
P§	<0.001	<0.001	<0.001	<0.001	<0.001	<0.001	–

* The first time period assessed is 3 years in duration and the subsequent time periods assessed are 2 years in duration. OI = opportunistic infection; SSTI = skin and soft tissue infection; UTI = urinary tract infection; NIS = National Inpatient Sample.
† Composite infection indicates any of the 5 infections as the primary diagnosis.
‡ Estimates in this period reflect the only study period in which International Classification of Diseases, Clinical Modification (ICD-CM) codes transitioned from the Ninth Revision (ICD-9-CM) to the Tenth Revision (ICD-10-CM), and therefore the estimates may be a little unstable.
§ *P* value is from Cochran-Armitage 2-sided test for trend.

in in-hospital mortality rates between these time periods occurred in patients with sepsis, decreasing from 14.4% to 8.1%, in those with OIs, decreasing from 9.6% to 3.5%, and in those with pneumonia, decreasing from 5.2% to 1.9% (Table 4).

There was a small increase in the overall inflation-adjusted median hospital charges for composite infection and for each hospitalized infection in lupus patients from 1998–2000 to 2015–2016 (Table 4).

Predictors of health care utilization and mortality in patients with lupus hospitalized with infection. Multivariable-adjusted analyses showed that compared to sepsis, other infections were associated with lower health care

Table 4. Time trends in health care utilization for each infection hospitalization in lupus patients*

	OI	SSTI	UTI	Pneumonia	Sepsis	Composite infection
Length of stay >3 days						
1998–2000	1,130 (81.8)	2,875 (58.0)	910 (45.3)	10,828 (69.2)	5,227 (79.9)	20,970 (68.7)
2015–2016	745 (64.8)	4,620 (53.0)	1,845 (42.2)	6,895 (56.6)	19,965 (70.5)	34,070 (62.2)
Length of stay, mean ± SEM; median days						
1998–2000	11.3 ± 0.80; 6.9	5.6 ± 0.18; 3.6	4.1 ± 0.18; 2.8	7.0 ± 0.1; 4.5	9.3 ± 0.28; 6.0	7.2 ± 0.11; 4.5
2015–2016	9.4 ± 1.23; 4.9	4.7 ± 0.10; 3.2	3.9 ± 0.11; 2.6	5.3 ± 0.10; 3.4	7.9 ± 0.12; 4.8	6.5 ± 0.08; 3.9
Total hospital charges > median						
1998–2000	1,132 (82.0)	2,869 (57.9)	989 (49.2)	10,955 (70.1)	5,261 (80.5)	21,206 (69.5)
2015–2016	725 (63.0)	4,115 (47.2)	1,920 (43.9)	6,805 (55.8)	20,775 (73.4)	34,340 (62.7)
Total hospital charges, mean ± SEM; median US $						
1998–2000	94,472 ± 8,751; 46,091	33,741 ± 1,590; 20,519	24,995 ± 1,471; 18,007	51,279 ± 1,718; 27,511	82,285 ± 4,240; 41,825	55,308 ± 1,470; 28,120
2015–2016	78,193 ± 7,317; 36,338	34,682 ± 964; 24,115	30,406 ± 1,238; 22,102	44,741 ± 1,280; 28,954	84,519 ± 1,875; 45,074	63,167 ± 1,117; 34,576
Died during hospitalization						
1998–2000	133 (9.6)	73 (1.5)	4 (0.2)	810 (5.2)	942 (14.4)	1,962 (6.4)
2015–2016	40 (3.5)	40 (0.5)	10 (0.2)	235 (1.9)	2,285 (8.1)	2,610 (4.8)

* Time trends are based on comparing the first and the last study periods, 1998–2000 versus 2015–2016. Except where indicated otherwise, values are the number (%) of patients. OI = opportunistic infection; SSTI = skin and soft tissue infection; UTI = urinary tract infection.

utilization and mortality (Table 5). Compared to rural hospitals, urban hospitals had 2.2–2.6 times higher odds of having hospital charges above the median. In addition, hospitals in the Northeast had significantly higher odds of having above-median hospital charges compared to hospitals in the Midwest and the South (Table 5).

We found that compared to other infections, sepsis was associated with 2–4-fold higher odds of discharge to an inpatient facility (Table 5). Compared to patients with lupus who were younger than age 50 years, those in the age groups 50–64 years, 65–79 years, and >80 years had 2-fold, 3-fold, and 6-fold increased odds of discharge to an inpatient facility, respectively.

Length of hospital stay showed the same pattern as the other models in lupus patients. Compared to sepsis, hospitalizations for all other types of infections, except OIs, were associated with significantly lower odds of a length of hospital stay above the NIS median of 3 days (Table 5). Sepsis was associated with worse health care utilization and mortality outcomes compared to other infections, and older age was a risk factor (Table 5).

African American race was significantly associated with increased odds of poorer health care utilization outcomes, higher odds of hospital charges above the median, higher odds of discharge to an inpatient facility, and higher odds of a length of hospital stay above the median (Table 5).

Compared to sepsis, pneumonia and OIs were associated with a reduced risk of in-hospital mortality (74% and 50% lower risk, respectively). SSTIs and UTI were associated with even lower in-hospital mortality risk (Table 5). Older age was associated with a 3-fold increase in the odds of in-hospital mortality, and having a Deyo-Charlson comorbidity score of >2 was associated with 1.4-fold increased odds of in-hospital mortality (Table 5). Other factors associated with various outcomes are shown in Table 5.

In sensitivity analyses, calendar year was statistically significantly associated with each outcome: OR 0.97 for hospital charges above the median, OR 1.02 for discharge to an inpatient facility, OR 0.98 for hospital stay of >3 days, and OR 0.97 for in-hospital mortality. All ORs were close to 1.0 (see Supplementary Table 8, available on the *Arthritis & Rheumatology* website at http://onlinelibrary.wiley.com/doi/10.1002/art.41577/abstract).

Time trends in infection diagnoses in the top 25 CCS categories in lupus patients. Pneumonia was one of the top 10 CCS categories (ranked 9th) and infection/parasitic diseases and bacterial infections were in the top 25 (ranked 18th and 24th, respectively) in 1998–1999 among patients hospitalized with lupus as the nonprimary diagnosis (see Supplementary Table 9, available on the *Arthritis & Rheumatology* website at http://onlinelibrary.wiley.com/doi/10.1002/art.41577/abstract). In total, there were 5 infection CCS categories that accounted for a total of 23.9% of lupus hospitalizations in 1998–1999. In 2013–2014, there was an increase in CCS categories that included infections: septicemia, bacterial infections, and infection/parasitic diseases were in the top 10 CCS categories (ranked 9th, 6th, and 8th, respectively) (Supplementary Table 9). Pneumonia fell out of the top 10 by this time period, but it was still present in the list of the top 25 (ranked 18th and 22nd for the respective separate CCS categories of Pneumonia, except that caused by tuberculosis or sexually transmitted disease, and Pneumonia, organism unspecified). In

Table 5. Multivariable-adjusted correlates of healthcare utilization and mortality in lupus patients with hospitalized infections*

	Total hospital charges > median	Discharge to rehabilitation or nursing facility	Length of hospital stay > median	In-hospital mortality
Age category				
<50 years	Referent	Referent	Referent	Referent
50–64 years	1.09 (1.05–1.14)†	1.77 (1.67–1.88)†	1.27 (1.22–1.32)†	1.47 (1.33–1.61)†
65–79 years	0.98 (0.92–1.03)	2.88 (2.68–3.09)†	1.35 (1.28–1.42)†	2.13 (1.91–2.39)†
≥80 years	0.92 (0.85–1.00)	6.21 (5.67–6.81)†	1.60 (1.47–1.73)†	2.90 (2.51–3.34)†
Sex				
Male	Referent	Referent	Referent	Referent
Female	1.00 (0.95–1.06)	1.06 (0.99–1.14)	1.04 (0.99–1.10)	0.79 (0.72–0.88)†
Race/ethnicity				
White	Referent	Referent	Referent	Referent
African American	1.16 (1.10–1.21)†	1.17 (1.10–1.24)†	1.12 (1.07–1.17)†	1.06 (0.96–1.17)
Hispanic	1.30 (1.22–1.38)†	0.76 (0.69–0.83)†	1.03 (0.97–1.09)	0.95 (0.84–1.08)
Other/missing	1.13 (1.08–1.19)†	1.00 (0.94–1.07)	1.09 (1.04–1.14)†	1.26 (1.14–1.40)†
Deyo-Charlson comorbidity score				
0	Not estimable‡	Not estimable‡	Not estimable‡	Not estimable‡
1	Referent	Referent	Referent	Referent
≥2	1.34 (1.29–1.39)†	1.47 (1.39–1.55)†	1.38 (1.33–1.43)†	1.40 (1.28–1.53)†
Income category				
0–25th percentile	0.96 (0.91–1.02)	0.96 (0.89–1.03)	0.97 (0.92–1.02)	0.94 (0.85–1.05)
25–50th percentile	1.00 (0.95–1.06)	0.95 (0.89–1.02)	1.05 (1.00–1.11)	1.01 (0.91–1.12)
50–75th percentile	0.96 (0.91–1.01)	1.01 (0.94–1.08)	0.98 (0.93–1.03)	0.95 (0.85–1.06)
75–100th percentile	Referent	Referent	Referent	Referent
Primary infection diagnosis				
Sepsis	Referent	Referent	Referent	Referent
OI	0.75 (0.68–0.83)†	0.52 (0.45–0.59)†	1.08 (0.97–1.20)	0.50 (0.41–0.61)†
SSTI	0.35 (0.33–0.37)†	0.34 (0.32–0.36)†	0.51 (0.48–0.53)†	0.05 (0.04–0.07)†
UTI	0.30 (0.28–0.33)†	0.27 (0.24–0.30)†	0.30 (0.28–0.32)†	0.03 (0.02–0.05)†
Pneumonia	0.57 (0.54–0.59)	0.35 (0.33–0.37)†	0.59 (0.57–0.62)†	0.26 (0.24–0.28)†
Insurance payer				
Medicare	1.19 (1.14–1.25)†	1.67 (1.56–1.78)†	1.14 (1.09–1.19)†	1.13 (1.01–1.25)†
Medicaid	1.11 (1.05–1.17)†	1.41 (1.30–1.53)†	1.09 (1.03–1.15)†	1.14 (1.00–1.29)†
Other	1.08 (0.97–1.21)	1.08 (0.90–1.29)	1.01 (0.91–1.12)	1.24 (0.97–1.60)
Private	Referent	Referent	Referent	Referent
Self	1.04 (0.94–1.14)	0.68 (0.56–0.83)†	0.96 (0.87–1.05)	1.12 (0.88–1.42)
Hospital region				
Northeast	Referent	Referent	Referent	Referent
Midwest	0.69 (0.65–0.73)†	1.02 (0.95–1.10)	0.80 (0.76–0.85)†	0.73 (0.64–0.83)†
South	0.85 (0.80–0.89)†	0.83 (0.78–0.89)†	0.98 (0.93–1.03)	1.00 (0.90–1.12)
West	1.11 (1.04–1.18)†	0.83 (0.77–0.90)†	0.72 (0.68–0.77)	0.91 (0.80–1.03)
Hospital location, type				
Rural	Referent	Referent	Referent	Referent
Urban	2.63 (2.47–2.80)†	0.86 (0.79–0.93)†	1.42 (1.34–1.51)†	1.29 (1.11–1.49)†
Urban, teaching	2.25 (2.12–2.39)†	0.73 (0.67–0.79)†	1.36 (1.28–1.44)†	1.43 (1.24–1.65)†
Hospital bed size				
Small	Referent	Referent	Referent	Referent
Medium	1.26 (1.19–1.34)†	0.89 (0.83–0.96)†	1.14 (1.07–1.20)†	1.41 (1.23–1.62)†
Large	1.72 (1.64–1.82)†	0.83 (0.77–0.89)†	1.30 (1.23–1.37)†	1.56 (1.37–1.77)†

* Values are the adjusted odds ratio (95% confidence interval). OI = opportunistic infection; SSTI = skin and soft tissue infection; UTI = urinary tract infection.

† $P < 0.05$.

‡ Not estimable because there were no patients in this category. When the model is built based on the entire sample, the beta and design matrix are set. In a domain analysis, it does not throw away columns (like a BY statement would), it only modifies the weights. This means that the parameters are still in the model because there are columns for them in the design matrix. Since estimates in a logistic model are based on a nonlinear operation of the design matrix, it is still possible to get parameters where they did not appear in the domain. Therefore, depending on the parameterization coding, it is possible for the parameter estimates to come back for a particular level as non-zero, even if there is no observation falling into that level in a particular domain. This is different from linear regression, in which a zero weight for a particular domain always results in a complete zero estimate for that level in that domain.

2013–2014, there were 7 infection CCS categories in the top 25 that accounted for 37.4% of lupus hospitalizations.

DISCUSSION

In this study, we found that compared to non-lupus patients, patients with lupus who were hospitalized with 1 of the 5 infections were younger in age (median age lower by 13 years) and were more likely to be female, to be nonwhite, to have a Deyo-Charlson index score of ≥2, and to be in the lowest income quartile. In unadjusted comparisons, patients with lupus were more likely to be discharged home and had a slightly lower in-hospital mortality (5% versus 6% of non-lupus controls), as would be expected for a younger cohort of female subjects (26). However, patients with lupus had a slightly longer hospital stay.

Among patients with lupus, sepsis surpassed pneumonia as the most common hospitalized infection in 2011–2012, as hinted in a previous study of the US national data from 2011 (15). Sepsis hospitalizations in patients with lupus were 2.3-fold more common than the pneumonia hospitalizations in 2015–2016, which is the reverse of the finding that there were 2.3-fold more pneumonia hospitalizations than sepsis hospitalizations in 1998–2000. We noted significant increases in the rates of sepsis hospitalizations (as well as UTI and SSTI hospitalizations) in patients with lupus over time, and stable/declining rates of pneumonia and OI hospitalizations (depending on the denominator used). This may be attributable to increasing rates of immunization for pneumonia in patients with lupus over time (27,28) or to a lower threshold for outpatient treatment of pneumonia that avoids pneumonia hospitalizations. Systematic up-coding of pneumonia to sepsis and some misclassification error with sepsis diagnostic codes has been noted (29,30), which may explain the increased rate of sepsis diagnosis over time versus pneumonia, at least partially. We also noted a continuing decline in the rates of pneumonia among all lupus claims (Figure 1B), but not as much decline in the total claims of pneumonia (Figure 1A). This could be attributable to an increasing recognition of lupus pneumonitis over time.

We also noted that infection diagnoses in CCS categories increased more rapidly over time than did noninfection diagnoses for hospitalizations in patients with lupus (primary or secondary diagnosis). This is an interesting novel finding that might signal the evolving epidemiology of hospitalizations in lupus. Patients with lupus being treated with existing immunosuppressive drugs and new biologic drugs need to be aware of early signs of serious infections and seek help immediately to avoid infection hospitalizations and their consequences.

The crude rate of composite infection hospitalizations per 100,000 NIS claims in patients with lupus increased 2.8-fold over 2 decades (Table 3), compared to the corresponding 1.6-fold increase in the general population without lupus (Supplementary Table 4 [http://onlinelibrary.wiley.com/doi/10.1002/art.41577/abstract]). A positive slope for lupus/non-lupus diagnosis among primary hospitalized infections indicated that lupus claims were increasing faster than non-lupus claims (Supplementary Tables 6 and 7] http://onlinelibrary.wiley.com/doi/10.1002/art.41577/abstract]). Potential interventions to reduce serious infection risk in patients with lupus include increasing the uptake of factors protective against infection, i.e., hydroxychloroquine use, adult vaccinations) and decreasing the dose and duration of glucocorticoid use, a strong risk factor for infection (31–34), as well as screening for tuberculosis and viral hepatitis at the first clinical encounter (35).

In this study of primary infection hospitalizations in lupus patients, we found a reduction in the mean hospital stay from 4.5 days to 3.9 days, respectively. The in-hospital mortality for hospitalized infections in patients with lupus decreased from 6.4% in 1998–2000 to 4.8% in 2015–2016, extending the observation of reduced mortality following hospitalized infection in patients with lupus from 2002–2010 (15). This 25% reduction in in-hospital mortality is clinically meaningful. It might be related to any of the following reasons: an earlier diagnosis and treatment of infections, since early infection diagnosis prevents complications and renal failure (36); the availability of more effective antibiotics and antifungal medications over time (37–39); and/or higher rates of the use of hydroxychloroquine treatment in patients with lupus over time, which reduces the risk of serious infections and mortality (40,41).

Overall, in patients with lupus, OI hospitalizations had the highest median hospital stay, at 5.6 days, and UTI hospitalizations had the lowest median hospital stay, at 2.7 days. SSTI, pneumonia, and sepsis had median hospital stays of 3.5 days, 3.9 days, and 5.3 days, respectively. OIs have been commonly reported in lupus and are associated with significant morbidity and mortality (42,43). Glucocorticoid exposure and dose are associated with increased risk of OIs in lupus (44). The use of immunosuppressive drugs and glucocorticoids for the treatment of lupus increases the risk of serious infections (45). Studies found that higher prednisone dose, treatment with pulse methylprednisolone, higher lupus disease activity, or more severe lupus damage were each independently associated with a higher risk of serious infection, and the use of hydroxychloroquine was associated with a lower risk (3,4,9–11). While use of immunosuppressive drugs increases the risk of serious infections in patients with lupus, a study of a US Medicaid population found no differences in the risk of serious infections between those receiving mycophenolate mofetil, azathioprine, or cyclophosphamide (8). The NIS data do not include medication use or disease severity measures, and therefore we are unable to evaluate these important factors as contributors to infection hospitalizations in lupus, or to assess time trends. Future studies should evaluate the contribution of lupus disease activity versus the contribution of medications (glucocorticoids, immunosuppressive drugs, biologics) to serious infection risk, to help develop interventions/programs to reduce morbidity and mortality risk.

We found several factors associated with in-hospital mortality in patients with lupus hospitalized with infections. In multivariable-adjusted analyses, compared to sepsis, the odds of in-hospital mortality were lower for each of the other hospitalized infections, at 0.03 to 0.50, which extends the previous finding of higher in-hospital mortality with sepsis or OIs (15).

Older age was associated with a 190% increase in the odds of in-hospital mortality, and a Deyo-Charlson score of >2 was associated with 40% increased odds of in-hospital mortality. In multivariable-adjusted analyses, older age, a higher Deyo-Charlson score, African American race, or having a Medicare or Medicaid insurance payer were associated with higher health care utilization in patients with lupus with hospitalized infections. Our findings identify these characteristics as risk factors for higher in-hospital mortality and higher health care utilization associated with hospitalized infections in lupus, and thus add to the current knowledge.

The association of African American race with poorer health care utilization outcomes adds to the growing evidence of racial and ethnic disparities in lupus, in which those of nonwhite race/ethnicity tend to experience a higher incidence of lupus and have more severe disease and worse outcomes (46–48). Our noted association of having Medicaid as an insurance payer with higher mortality and greater health care utilization in lupus patients with hospitalized infections extends prior observations of an association of poor socioeconomic status and having a Medicaid payer with worse lupus outcomes (49,50).

Our study findings must be interpreted cautiously, considering the limitations and strengths of the study. Our study is at risk of misclassification bias, since we used the ICD-9-CM codes to identify patients with lupus, some of which may have been erroneous. While no validation of these codes can be done in the NIS, the infection (15,18–21) and lupus (22) diagnostic codes were valid in administrative data sets, with high positive predictive values. The NIS counts hospitalizations, not people, and therefore the unit of analysis is hospitalizations. The NIS does not provide longitudinal data after hospital discharge, which limits the ability to examine the postdischarge outcomes, and/or readmission risk.

The NIS also does not have data on disease severity measures, laboratory test findings, and medications, and therefore these important disease variables cannot be examined with regard to their impact on the outcomes. Our study objective was not to examine people admitted with lupus as the primary diagnosis who developed infection during the index hospitalization, i.e., a secondary infection, and therefore this would be an important question for a future study. A large sample size, as in our study, can make small differences appear statistically significant; the interpretation of our study findings must take into account whether these differences are also clinically relevant/meaningful.

Our study strengths include the use of US national inpatient data, inclusion of several potential confounders, and the identification of sufficient numbers of hospitalized infections in patients with lupus.

In conclusion, we found an increasing rate of hospitalized infections in patients with lupus, outpacing the increase in rate in the general US population. We also found that sepsis surpassed pneumonia as the most common hospitalized infection in patients with lupus in 2011–2012. By 2015–2016, sepsis accounted for twice as many hospitalized infections as pneumonia in patients with lupus. In adjusted analyses, sepsis was associated with the highest health care utilization, worse outcomes, and highest in-hospital mortality rates. We identified novel factors associated with higher health care utilization and higher risk of mortality for serious infection hospitalizations. Findings from our study can be used to design hospital- and systems-level interventions to improve outcomes in patients with lupus who have been admitted with infections, and may potentially reduce the associated high rates of health care utilization and mortality.

ACKNOWLEDGMENT

We thank several lupus patients in our rheumatology clinic who raised important questions about the risk of infections, which led us to perform the present study.

AUTHOR CONTRIBUTIONS

Both authors were involved in drafting the article or revising it critically for important intellectual content, and both approved the final version to be published. Drs. Singh and Cleveland had full access to all of the data in the study and take responsibility for the integrity of the data and the accuracy of the data analysis.

Study conception and design. Singh.
Acquisition of data. Singh, Cleveland.
Analysis and interpretation of data. Singh, Cleveland.

REFERENCES

1. Cervera R, Khamashta MA, Font J, Sebastiani GD, Gil A, Lavilla P, et al. Morbidity and mortality in systemic lupus erythematosus during a 10-year period: a comparison of early and late manifestations in a cohort of 1,000 patients. Medicine (Baltimore) 2003;82:299–308.
2. Edwards CJ, Lian TY, Badsha H, Teh CL, Arden N, Chng HH. Hospitalization of individuals with systemic lupus erythematosus: characteristics and predictors of outcome. Lupus 2003;12:672–6.
3. Gladman DD, Hussain F, Ibanez D, Urowitz MB. The nature and outcome of infection in systemic lupus erythematosus. Lupus 2002;11:234–9.
4. Goldblatt F, Chambers S, Rahman A, Isenberg DA. Serious infections in British patients with systemic lupus erythematosus: hospitalisations and mortality. Lupus 2009;18:682–9.
5. Petri M, Genovese M. Incidence of and risk factors for hospitalizations in systemic lupus erythematosus: a prospective study of the Hopkins Lupus Cohort. J Rheumatol 1992;19:1559–65.
6. Urowitz MB, Bookman AA, Koehler BE, Gordon DA, Smythe HA, Ogryzlo MA. The bimodal mortality pattern of systemic lupus erythematosus. Am J Med 1976;60:221–5.

7. Lee J, Dhillon N, Pope J. All-cause hospitalizations in systemic lupus erythematosus from a large Canadian referral centre. Rheumatology (Oxford) 2013;52:905–9.
8. Feldman CH, Marty FM, Winkelmayer WC, Guan H, Franklin JM, Solomon DH, et al. Comparative rates of serious infections among patients with systemic lupus erythematosus receiving immunosuppressive medications. Arthritis Rheumatol 2017;69:387–97.
9. Pimentel-Quiroz VR, Ugarte-Gil MF, Harvey GB, Wojdyla D, Pons-Estel GJ, Quintana R, et al. Factors predictive of serious infections over time in systemic lupus erythematosus patients: data from a multi-ethnic, multi-national, Latin American lupus cohort. Lupus 2019;28:1101–10.
10. Jung JY, Yoon D, Choi Y, Kim HA, Suh CH. Associated clinical factors for serious infections in patients with systemic lupus erythematosus. Sci Rep 2019;9:9704.
11. Staples PJ, Gerding DN, Decker JL, Gordon RS Jr. Incidence of infection in systemic lupus erythematosus. Arthritis Rheum 1974;17:1–10.
12. BENLYSTA (belimumab) prescribing information. Rockville, MD: GlaxoSmithKline; 2011. URL: https://www.accessdata.fda.gov/drugsatfda_docs/label/2017/761043lbl.pdf.
13. Jeong SJ, Choi H, Lee HS, Han SH, Chin BS, Baek JH, et al. Incidence and risk factors of infection in a single cohort of 110 adults with systemic lupus erythematosus. Scand J Infect Dis 2009;41:268–74.
14. Feldman CH, Hiraki LT, Winkelmayer WC, Marty FM, Franklin JM, Kim SC, et al. Serious infections among adult Medicaid beneficiaries with systemic lupus erythematosus and lupus nephritis. Arthritis Rheumatol 2015;67:1577–85.
15. Tektonidou MG, Wang Z, Dasgupta A, Ward MM. Burden of serious infections in adults with systemic lupus erythematosus: a national population-based study, 1996–2011. Arthritis Care Res (Hoboken) 2015;67:1078–85.
16. Ward MM. Avoidable hospitalizations in patients with systemic lupus erythematosus. Arthritis Rheum 2008;59:162–8.
17. Overview of the Nationwide Inpatient Sample (NIS). Healthcare Cost and Utilization Project (HCUP): 2012–2018. Agency for Healthcare Research and Quality. URL: https://www.hcup-us.ahrq.gov/nisoverview.jsp.
18. Jinno S, Lu N, Jafarzadeh SR, Dubreuil M. Trends in hospitalizations for serious infections in patients with rheumatoid arthritis in the US between 1993 and 2013. Arthritis Care Res (Hoboken) 2018;70:652–8.
19. Schneeweiss S, Robicsek A, Scranton R, Zuckerman D, Solomon DH. Veteran's affairs hospital discharge databases coded serious bacterial infections accurately. J Clin Epidemiol 2007;60:397–409.
20. Grijalva CG, Chung CP, Stein CM, Gideon PS, Dyer SM, Mitchel EF Jr, et al. Computerized definitions showed high positive predictive values for identifying hospitalizations for congestive heart failure and selected infections in Medicaid enrollees with rheumatoid arthritis. Pharmacoepidemiol Drug Saf 2008;17:890–5.
21. Patkar NM, Curtis JR, Teng GG, Allison JJ, Saag M, Martin C, et al. Administrative codes combined with medical records based criteria accurately identified bacterial infections among rheumatoid arthritis patients. J Clin Epidemiol 2009;62:321–7.
22. Bernatsky S, Linehan T, Hanly JG. The accuracy of administrative data diagnoses of systemic autoimmune rheumatic diseases. J Rheumatol 2011;38:1612–6.
23. ZIPINC_QRTL: Median household income for patient's ZIP code (based on current year). Healthcare Cost and Utilization Project (HCUP): 1997–2019. Agency for Healthcare Research and Quality. URL: http://www.hcup-us.ahrq.gov/db/vars/zipinc_qrtl/nisnote.jsp.
24. Deyo RA, Cherkin DC, Ciol MA. Adapting a clinical comorbidity index for use with ICD-9-CM administrative databases. J Clin Epidemiol 1992;45:613–9.
25. eHealth Medicare. Medicare eligibility: who qualifies for medicare? 2017. URL: https://www.ehealthmedicare.com/about-medicare/eligibility/.
26. Doria A, Iaccarino L, Ghirardello A, Zampieri S, Arienti S, Sarzi-Puttini P, et al. Long-term prognosis and causes of death in systemic lupus erythematosus. Am J Med 2006;119:700–6.
27. Murdaca G, Orsi A, Spano F, Puppo F, Durando P, Icardi G, et al. Influenza and pneumococcal vaccinations of patients with systemic lupus erythematosus: current views upon safety and immunogenicity [review]. Autoimmun Rev 2014;13:75–84.
28. Garg S, Tsagaris K, Cozmuta R, Lipson A. Improving the combination pneumococcal vaccination rate in systemic lupus erythematosus patients at an adult rheumatology practice. J Rheumatol 2018;45:1656–62.
29. Lindenauer PK, Lagu T, Shieh MS, Pekow PS, Rothberg MB. Association of diagnostic coding with trends in hospitalizations and mortality of patients with pneumonia, 2003–2009. JAMA 2012;307:1405–13.
30. Rhee C, Dantes R, Epstein L, Murphy DJ, Seymour CW, Iwashyna TJ, et al. Incidence and trends of sepsis in US hospitals using clinical vs claims data, 2009–2014. JAMA 2017;318:1241–9.
31. Sciascia S, Ceberio L, Garcia-Fernandez C, Roccatello D, Karim Y, Cuadrado MJ. Systemic lupus erythematosus and infections: clinical importance of conventional and upcoming biomarkers [review]. Autoimmun Rev 2012;12:157–63.
32. Bosch X, Guilabert A, Pallares L, Cerveral R, Ramos-Casals M, Bove A, et al. Infections in systemic lupus erythematosus: a prospective and controlled study of 110 patients. Lupus 2006;15:584–9.
33. Ruiz-Irastorza G, Olivares N, Ruiz-Arruza I, Martinez-Berriotxoa A, Egurbide MV, Aguirre C. Predictors of major infections in systemic lupus erythematosus. Arthritis Res Ther 2009;11:R109.
34. Noel V, Lortholary O, Casassus P, Cohen P, Genereau T, Andre MH, et al. Risk factors and prognostic influence of infection in a single cohort of 87 adults with systemic lupus erythematosus. Ann Rheum Dis 2001;60:1141–4.
35. Barber C, Gold WL, Fortin PR. Infections in the lupus patient: perspectives on prevention. Curr Opin Rheumatol 2011;23:358–65.
36. Fiehn C, Hajjar Y, Mueller K, Waldherr R, Ho AD, Andrassy K. Improved clinical outcome of lupus nephritis during the past decade: importance of early diagnosis and treatment. Ann Rheum Dis 2003;62:435–9.
37. Raymond DP, Pelletier SJ, Crabtree TD, Gleason TG, Hamm LL, Pruett TL, et al. Impact of a rotating empiric antibiotic schedule on infectious mortality in an intensive care unit. Crit Care Med 2001;29:1101–8.
38. Gafter-Gvili A, Fraser A, Paul M, Leibovici L. Meta-analysis: antibiotic prophylaxis reduces mortality in neutropenic patients. Ann Intern Med 2005;142:979–95.
39. Marr KA, Boeckh M, Carter RA, Kim HW, Corey L. Combination antifungal therapy for invasive aspergillosis. Clin Infect Dis 2004;39:797–802.
40. Kamen DL. How can we reduce the risk of serious infection for patients with systemic lupus erythematosus? [editorial]. Arthritis Res Ther 2009;11:129.
41. Alarcon GS, McGwin G, Bertoli AM, Fessler BJ, Calvo-Alen J, Bastian HM, et al. Effect of hydroxychloroquine on the survival of patients with systemic lupus erythematosus: data from LUMINA, a multiethnic US cohort (LUMINA L). Ann Rheum Dis 2007;66:1168–72.
42. Banerjee S, Biehl A, Ghaderi-Yeganeh M, Manna Z, Hasni S. Low incidence of opportunistic infections in lupus patients treated with

cyclophosphamide and steroids in a tertiary care setting. Med Res Arch 2017;5:10.18103.
43. Paton NI. Infections in systemic lupus erythematosus patients. Ann Acad Med Singapore 1997;26:694–700.
44. Yang SC, Lai YY, Huang MC, Tsai CS, Wang JL. Corticosteroid dose and the risk of opportunistic infection in a national systemic lupus erythematosus cohort. Lupus 2018;27:1819–27.
45. Singh JA, Hossain A, Kotb A, Wells G. Risk of serious infections with immunosuppressive drugs and glucocorticoids for lupus nephritis: a systematic review and network meta-analysis. BMC Med 2016;14:137.
46. Odutola J, Ward MM. Ethnic and socioeconomic disparities in health among patients with rheumatic disease. Current Opin Rheumatol 2005;17:147–52.
47. Alarcon GS, Friedman AW, Straaton KV, Moulds JM, Lisse J, Bastian HM, et al. Systemic lupus erythematosus in three ethnic groups. Part III. A comparison of characteristics early in the natural history of the LUMINA cohort. Lupus 1999;8:197–209.
48. Krishnan E. Hospitalization and mortality of patients with systemic lupus erythematosus. J Rheumatol 2006;33:1770–4.
49. Sutcliffe N, Clarke AE, Gordon C, Farewell V, Isenberg DA. The association of socio-economic status, race, psychosocial factors and outcome in patients with systemic lupus erythematosus. Rheumatology (Oxford) 1999;38:1130–7.
50. Ward MM. Medical insurance, socioeconomic status, and age of onset of endstage renal disease in patients with lupus nephritis. J Rheumatol 2007;34:2024–7.

DOI 10.1002/art.41629

Clinical Images: Wong-type dermatomyositis in an African American patient

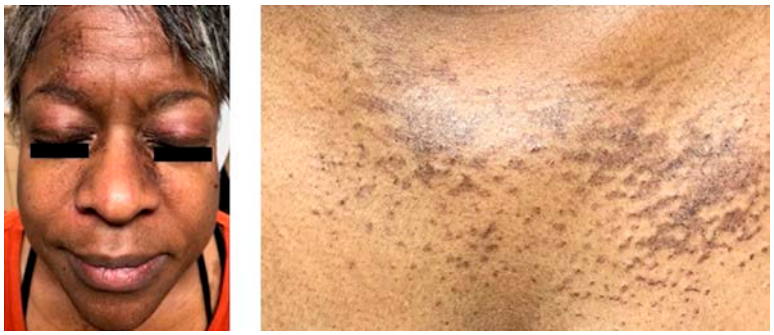

The patient, a 57-year-old African American woman, presented to the dermatology department with a 2-year history of a pruritic rash initially involving the face, which had progressed to her forearms, back, ears, dorsal hands, and abdomen. Physical examination revealed erythematous papules overlying the metacarpal and interphalangeal joints, periungual telangiectasias, periorbital edema, and violaceous erythema of the upper eyelids, as well as areas of dyspigmentation (left). There were 1–2-mm skin-colored hyperkeratotic follicular papules on the extensor arms, upper back, and abdomen, and hyperpigmented follicular plugging on the chest (right). Biopsy of a papule on the forearm demonstrated superficial lymphocytic perivascular and interface dermatitis with basal vacuolar change and dyskeratosis, as well as increased mucin deposition. A myositis panel was positive for anti–transcription intermediary factor 1γ antibodies and antinuclear antibodies (1:640; speckled pattern), with normal aldolase, creatinine kinase, and complement C3 and C4 levels. Findings of a comprehensive evaluation for malignancy were negative. A review of systems did not reveal muscle/joint symptoms or other pertinent findings. The patient was diagnosed as having Wong-type dermatomyositis (DM), a rare variant of DM characterized by hyperkeratotic follicular papules (1). The atypical presence of follicular papules, combined with the rarity of this disease variant, with only 29 cases having been reported to date, often delays diagnosis (2). Patients are frequently misdiagnosed as having pityriasis rubra pilaris or lupus erythematosus. While Wong-type DM has been reported in Asian patients (3), to our knowledge, no cases in patients of African American descent have been reported. In particular, subtle, active erythema interspersed with dyspigmentation due to resolved erythema is a notable clinical feature that should not be overlooked in this population. It is therefore particularly important for clinicians to be aware of this rare entity and its presentation in skin of color to avoid further delays in diagnosis, given that evaluation for malignancy and interstitial lung disease is recommended after diagnosis of DM.

Supported by the US Department of Veterans Affairs (Veterans Health Administration Office of Research and Development and Biomedical Laboratory Research and Development) and the NIH (grant R01-AR-076766 to Dr. Werth).

1. Wong KO. Dermatomyositis: a clinical investigation of twenty-three cases in Hong Kong. Br J Dermatol 1969;81:544–7.
2. Mutasim DF, Egesi A, Spicknall KE. Wong-type dermatomyositis: a mimic of many dermatoses. J Cutan Pathol 2016;43:781–6.
3. Ishikawa M, Yamamoto T. Wong-type dermatomyositis: a first report from Japan. J Dermatol 2017;44:e336–7.

Christina E. Bax, BA
Madison Grinnell, BA
Josef Symon S. Concha, MD
Victoria P. Werth, MD
Corporal Michael J. Crescenz VA Medical Center and University of Pennsylvania Perelman School of Medicine
Philadelphia, PA

Arthritis & Rheumatology
Vol. 73, No. 4, April 2021, pp 631–640
DOI 10.1002/art.41558

American College of Rheumatology
Empowering Rheumatology Professionals

Interleukin-7/Interferon Axis Drives T Cell and Salivary Gland Epithelial Cell Interactions in Sjögren's Syndrome

Elodie Rivière,[1] Juliette Pascaud,[2] Alexandre Virone,[2] Anastasia Dupré,[2] Bineta Ly,[2] Audrey Paoletti,[2] Raphaèle Seror,[2] Nicolas Tchitchek,[2] Michael Mingueneau,[3] Nikaïa Smith,[4] Darragh Duffy,[4] Lydie Cassard,[5] Nathalie Chaput,[5] Sabrina Pengam,[6] Vanessa Gauttier,[6] Nicolas Poirier,[6] Xavier Mariette,[2] and Gaetane Nocturne[2]

Objective. Primary Sjögren's syndrome (SS) is characterized by a lymphocytic infiltration of salivary glands (SGs) and the presence of an interferon (IFN) signature. SG epithelial cells (SGECs) play an active role in primary SS pathophysiology. We undertook this study to examine the interactions between SGECs and T cells in primary SS and the role of the interleukin-7 (IL-7)/IFN axis.

Methods. Primary cultured SGECs from control subjects and patients with primary SS were stimulated with poly(I-C), IFNα, or IFNγ. T cells were sorted from blood and stimulated with IL-7. CD25 expression was assessed by flow cytometry. SG explants were cultured for 4 days with anti–IL-7 receptor (IL-7R) antagonist antibody (OSE-127), and transcriptomic analysis was performed using the NanoString platform.

Results. Serum IL-7 level was increased in patients with primary SS compared to controls and was associated with B cell biomarkers. *IL7R* expression was decreased in T cells from patients with primary SS compared to controls. SGECs stimulated with poly(I-C), IFNα, or IFNγ secreted IL-7. IL-7 stimulation increased the activation of T cells, as well as IFNγ secretion. Transcriptomic analysis of SG explants showed a correlation between *IL7* and *IFN* expression. Finally, explants cultured with anti–IL-7R antibody showed decreased IFN-stimulated gene expression.

Conclusion. These results suggest the presence of an IL-7/IFNγ amplification loop involving SGECs and T cells in primary SS. IL-7 was secreted by SGECs stimulated with type I or type II IFN and, in turn, activated T cells that secrete type II IFN. An anti–IL-7R antibody decreased the IFN signature in T cells in primary SS and could be of therapeutic interest.

INTRODUCTION

Primary Sjögren's syndrome (SS) is a chronic autoimmune disease characterized by a lymphocytic infiltration of salivary glands (SGs). The major components of the SG infiltrate are T and B lymphocytes. SG epithelial cells (SGECs) can be a driver and also a passive target of disease pathophysiology. Autoreactive effector T cells could play a pathogenic role in primary SS in

Supported by the Laboratory of Excellence in Research on Medication and Therapeutic Innovation (LERMIT) (grant ANR10), the Fondation pour la Recherche Médicale (grant DEQ20150934719), an unrestricted grant from Biogen to Université Paris-Sud (grant UPSud/SAIC N 97731), and the Innovative Medicines Initiative 2 Joint Undertaking (IMI 2 JU) (NECESSITY grant 806975). The Joint Undertaking received support from the European Union's Horizon 2020 Research and Innovation Program and from the European Federation of Pharmaceutical Industries and Associations. The Laboratoire d'Immunomonitoring en Oncologie is supported by SIRIC SOCRATE 2.0 (INCa-DGOS-INSERM_12551). Dr. Rivière is recipient of a PhD fellowship from Arthritis Fondation Courtin and Arthritis Recherche et Développement (grant CIFRE 2016/1406).

[1]Elodie Rivière, MD, PhD: Université Paris-Saclay, INSERM, CEA, Centre de Recherche en Immunologie des Infections Virales et des Maladies Auto-Immunes, Hôpital Bicêtre, AP-HP, Arthritis Recherche et Développement, Fondation Courtin, Paris, France; [2]Juliette Pascaud, BSc, Alexandre Virone, MD, Anastasia Dupré, MD, Bineta Ly, BSc, Audrey Paoletti, PhD, Raphaèle Seror, MD, PhD, Nicolas Tchitchek, PhD, Xavier Mariette, MD, PhD, Gaetane Nocturne, MD, PhD: Université Paris-Saclay, INSERM, CEA, Centre de Recherche en Immunologie des Infections Virales et des Maladies Auto-Immunes, Hôpital Bicêtre, AP-HP, Paris, France; [3]Michael Mingueneau, PhD: Biogen, Cambridge, Massachusetts; [4]Nikaïa Smith, PhD, Darragh Duffy, PhD: Laboratoire d'Immunobiologie des Cellules Dendritiques, INSERM U1223, Institut Pasteur, Paris, France; [5]Lydie Cassard, BSc, Nathalie Chaput, PhD: Université Paris-Saclay, Institut Gustave Roussy, Analyse moléculaire, modélisation et imagerie de la maladie cancéreuse, Laboratoire d'Immunomonitoring en Oncologie, INSERM, CNRS, Paris, France; [6]Sabrina Pengam, BSc, Vanessa Gauttier, PhD, Nicolas Poirier, PhD: OSE Immunotherapeutics, Nantes, France.

Drs. Rivière and Pascaud contributed equally to this work. Drs. Mariette and Nocturne contributed equally to this work.

Dr. Mariette has received an honorarium from Servier (less than $10,000) and research grants from OSE Immunotherapeutics and Servier. No other disclosures relevant to this article were reported.

Address correspondence to Gaetane Nocturne, MD, PhD, Université Paris-Sud, AP-HP, Hôpitaux Universitaires Paris-Sud, INSERM U1184, 78 Rue du Général Leclerc, 94275 Le Kremlin Bicêtre, France. Email: gaetane.nocturne@aphp.fr.

Submitted for publication April 17, 2020; accepted in revised form October 8, 2020.

different ways, including providing help for promoting B cell hyperactivity (1). One characteristic of primary SS is the presence of an interferon (IFN) gene signature in circulating leukocytes and in the SGs of patients with primary SS (2–5). However, the initial trigger responsible for this IFN signature still has not been identified, nor has the predominant involvement of type I or type II IFNs.

Interleukin-7 (IL-7) is a pleiotropic cytokine produced by nonhematopoietic cells, such as stromal and epithelial cells, that plays a central role in T lymphocyte homeostasis. Several observations have highlighted the potential role of the IL-7/IL-7 receptor α (IL-7Rα) axis in primary SS pathophysiology. Levels of IL-7 and IL-7Rα, also known as CD127, were found to be elevated in the SGs of patients with primary SS (6). Using immunohistochemistry, Bikker et al demonstrated an association between the presence of IL-7Rα–positive T cells in the SGs of patients with primary SS and the severity of sialadenitis and IL-7 expression (7). IL-7 activity might be modulated by the soluble form of its receptor (sIL-7R). Of note, Lundström et al showed a diminished consumption of IL-7 in the presence of sIL-7Rα (8). Interestingly, Hillen et al showed an increased serum sIL-7R level and SG supernatant in patients with primary SS who had increased inflammation and decreased salivary output (9). Moreover, the IL-7/IL-7Rα axis has been found to be involved in the formation of ectopic lymphoid structures in SGs (10). Interestingly, Jin et al showed that exogenous IL-7 administration accelerated primary SS onset in a mouse model, whereas blockade of endogenous IL-7Rα signals prevented its development (11). Finally, IL-7 stimulation of T cells in vitro enhanced IL-2, IL-10, and IFNγ production, which may also play a role in primary SS (12,13).

Considering these findings, we aimed to study the interactions between SGECs and T cells in primary SS and the impact of IL-7 in this process, using a fully antagonist anti–IL-7R monoclonal antibody (14).

PATIENTS AND METHODS

Patients. Serum levels of cytokines and chemokines were assessed in patients from the French multicenter 5-year prospective Assessment of Systemic Signs and Evolution of SS (ASSESS) cohort. In total, 395 patients were included in this cohort. All patients fulfilled the American–European Consensus Group criteria for primary SS (15). Baseline characteristics of the patients have previously been described (16). Chemokine levels were also measured in 73 age- and sex-matched control subjects who had symptoms of dry eyes and mouth and in whom no autoantibodies or lymphocytic infiltrates were detected on minor SG (MSG) biopsy.

MSG biopsy specimens were obtained from consecutive patients referred for suspected primary SS to the rheumatology department of Bicêtre Hospital, a tertiary reference center for systemic autoimmune diseases. Primary SS was defined according to the 2016 American College of Rheumatology/European League Against Rheumatism (EULAR) criteria (17) or the American–European Consensus Group criteria for primary SS (15). The EULAR SS Disease Activity Index (ESSDAI) was used to assess primary SS activity. Controls presented sicca symptoms without anti-Ro/SSA and anti-La/SSB antibodies detected and with normal or subnormal MSG findings (i.e., focus score <1).

T lymphocytes used for in vitro experiments were sorted from the blood of patients with primary SS and controls. The experimental design of the study can be found in Supplementary Figure 1 (available on the *Arthritis & Rheumatology* website at http://onlinelibrary.wiley.com/doi/10.1002/art.41558/abstract).

Biologic sample assessment. Serum samples were obtained at enrollment. All biologic samples were immediately frozen, stored (–80°C), and shipped to the Centre de Ressources Biologiques of Bichat Hospital, Paris, which has obtained the certification of the French Association for Quality Assurance (certification no. 2009/34457) according to the norm 96900. Serum markers were assessed centrally and with blinding with regard to any clinical or other biologic data. Rheumatoid factor (RF) was assessed by enzyme-linked immunosorbent assay, and C3 and C4 levels were assessed by nephelometry (decreased C3 and C4 levels were defined as <0.8 gm/liter and 0.15 gm/liter, respectively). Beta$_2$-microglobulin, total Ig levels, and κ and λ free light chains of Ig were assessed by nephelometry using a Freelite kit (Binding Site). Anti-Ro/SSA and anti-La/SSB antibodies were detected by addressable laser bead immunoassay flow cytometry with a Bioplex 2200 (Bio-Rad). Detection was confirmed by immunodot assay Ana 3b from Euroimmun. CD4 and CD8 T cell counts were determined by flow cytometry. CD4+ T lymphocytopenia was defined by an absolute CD4 count of <300 cells/ml.

Assessment of IL-7, CXCL13, CCL19, CXCL10, and IFN levels. Methods used to assess levels of IL-7, CXCL13, CCL19, CXCL10, and IFN are described in Supplementary Methods (http://onlinelibrary.wiley.com/doi/10.1002/art.41558/abstract).

RNA sequencing (RNA-Seq) of CD4 and CD8 T cells sorted from SG biopsy specimens and blood, and polymerase chain reaction (PCR) validation of genes that were differentially expressed by RNA-Seq. IFNα, IFNγ, and IFNλ gene expression was evaluated by RNA-Seq in CD4 and CD8 T cells sorted form SG biopsy samples and peripheral blood mononuclear cells. Methods used for sample collection, cell isolation, RNA-Seq, and PCR validation are described in Supplementary Methods (http://onlinelibrary.wiley.com/doi/10.1002/art.41558/abstract).

Assessment of CD127, inducible costimulator (ICOS), and programmed death 1 (PD-1) in CD4 and CD8 T cells. Fresh whole blood (100 μl) was incubated with fluorochrome-conjugated antibodies for 15 minutes at room temperature in the dark, followed by 20 minutes of lysis (VersaLyse; Beckman Coulter) and washed twice with phosphate buffered saline for

surface staining. For Ki-67 and FoxP3 staining, cells were fixed and permeabilized after cell surface staining using a PerFix-nc kit, according to the instructions of the manufacturer (Beckman Coulter). Stained cells were acquired using a Gallios flow cytometer (Beckman Coulter). Data were analyzed with Kaluza software (Beckman Coulter). The antibodies used in the experiments are described in Supplementary Table 1 (http://onlinelibrary.wiley.com/doi/10.1002/art.41558/abstract). The gating strategy is described in Supplementary Figure 2 (http://onlinelibrary.wiley.com/doi/10.1002/art.41558/ abstract).

Isolation of T lymphocytes and IL-7 stimulation. Peripheral blood mononuclear cells were isolated from residual apheresis blood from patients with primary SS and healthy controls (French blood donors) by Ficoll gradient separation. T lymphocytes were isolated by magnetic bead negative selection according to the manufacturer's instructions (Pan T cells negative isolation kit; Miltenyi Biotec) in order to achieve a purity of >70% as assessed by fluorescence-activated cell sorting (FACS) analysis (percentage of CD3+ cells in live cells). T cells were seeded at 1 million/ml in RPMI 1640 supplemented with 10% heat-inactivated fetal bovine serum (FBS) and penicillin/streptomycin (1×) and stimulated with IL-7 0.1 ng/ml or 2 ng/ml (PeproTech). T cells were harvested on day 1 or 3 for flow cytometry. Stimulated T lymphocytes were stained with CD3, CD4, CD8, CD127, CD25, or Fixable Viability Dye eFluor 780. The antibodies used in these experiments are listed in Supplementary Table 1 (http://onlinelibrary.wiley.com/doi/10.1002/art.41558/abstract). Samples were analyzed using a BD FACS Canto Flow Cytometer and BD FACS Diva Software (BD Biosciences). Results were analyzed with FlowJo software, version 10.

Primary cultures of SGECs and stimulation. Primary cultures of SGECs were established from MSGs as previously described (18). After 2–3 weeks of culture, cells at 70–80% confluence were dissociated with 0.125% trypsin–EDTA. Cell suspension was suspended in basal epithelial medium and added at 80,000 cells/cm^2 to a 6-well type I collagen plate (Institut de Biotechnologies) coated and incubated at 37°C and with 5% CO_2 in a humidified atmosphere. The basal epithelial medium was changed on day 1 to remove nonadherent epithelial cells. The epithelial origin of cultured cells was confirmed by staining with monoclonal antibodies against CD326 (Miltenyi Biotec), an epithelium-specific marker. The following stimuli were added to the medium: poly (I-C) 30 μg/ml (Invivogen), IFNα 600 IU/ml (Roferon-A; Roche), IFNγ 5 ng/ml (Sigma-Aldrich), or IFNλ (IL-28) 25 ng/ml (PeproTech). Supernatants and SGECs were harvested after 72 hours and frozen (–80°C).

Quantitative PCR. Total RNA from SGECs that had been left unstimulated or stimulated for 24 hours was extracted using an RNeasy Mini kit, according to the specifications of the manufacturer (Qiagen). Contaminating DNA was removed using an RNase-free DNase set, according to instructions of the manufacturer (Qiagen). One microgram of RNA was used to produce complementary DNA with a First-Strand Synthesis Kit (Sigma-Aldrich). The quantification of messenger RNA (mRNA) expression was determined by real-time PCR according to the instructions of the manufacturer (TaqMan; Life Technologies) using a TaqMan Gene Expression Master Mix (Life Technologies) and CFX96 (Bio-Rad). The level of *IL7* was normalized to that of the endogenous *GAPDH*. Calculation of mRNA expression levels was performed using the comparative C_t ($\Delta\Delta C_t$) method. Data analyses were performed using CFX Manager software (Bio-Rad).

Culture of SG explants. Each MSG was cut into 2 parts and cultured for 4 days in 200 μl RPMI 1640 supplemented with 10% heat-inactivated FBS and penicillin/streptomycin (1×), with OSE-127 humanized anti-human CD127 monoclonal antibody (anti–IL-7R) (OSE Immunotherapeutics) (14) or control isotype (Ultra-LEAF Purified Human IgG4 Isotype Control Recombinant; BioLegend). After 4 days, supernatant was separated from the explants. Supernatant was centrifugated in order to isolate cells that escaped from the explant (pellet cells) and the explant itself (explant cells). Pellet cells and explant cells were collected in the RLT buffer from an RNeasy Mini kit supplemented with β-mercaptoethanol at 1% and frozen (–80°C) before RNA extraction.

NanoString gene expression. RNA from SG biopsy samples (cells or explants) was extracted using the FastPrep system. Gene expression was quantified using the NanoString nCounter platform with 15–50 ng total RNA, according to the type of sample, in the nCounter Human Immunology Panel_V2 (NanoString Technologies). The code set was hybridized with RNA overnight at 65°C. RNA transcripts were immobilized and counted using the NanoString nCounter Sprint. Normalized expression data were analyzed with nSolver software. The statistical analysis of data did not involve multiple hypothesis testing.

Statistical analysis of serum IL-7 level and correlations. Categorical variables are reported as the number (percentage) and were compared using the chi-square test or, when appropriate, Fisher's exact test. Quantitative variables are reported as the median (interquartile range [IQR]) or the mean ± SD and were compared using the Mann-Whitney test. For correlation analyses between 2 quantitative variables, Spearman's correlation coefficients were calculated. In univariate analyses, the correlation/association between disease activity, serum chemokine levels, serum B cell biomarkers, and serum IL-7 level was assessed using Spearman's correlation coefficient (for continuous data) and Mann-Whitney U test (for categorical data). Variables with *P* values <0.05 in univariate analysis or with R values ≥0.20 were entered into a multivariate model to identify the factors independently associated with serum IL-7 level. Variables were selected using

Table 1. Characteristics of the patients with primary Sjögren's syndrome*

	Experimental condition					
	CD127 and PD-1 assessment of T cells (n = 15)	RNA-Seq of biopsy specimen–sorted cells (n = 9)	RNA-Seq of blood-sorted cells (n = 16)	T cells stimulated with IL-7 (n = 12)	Primary cultured SGECs for IL-7 dosage (n = 5)	SG explants for NanoString (n = 9)
Age, median (range) years	59 (40–59)	51 (47–71)	55 (47–68)	65 (38–88)	50 (40–64)	41 (38–52)
Female sex	13 (86)	8 (89)	15 (94)	12 (100)	4 (80)	9 (100)
Focus score ≥1	4 (100)†	4 (44)	3 (50)‡	NA	4 (80)	5 (55)
SSA antibodies	10 (71)	7 (78)	13 (81)	9 (75)	4 (80)	8 (88)
ESSDAI, median (range)	5 (2–8)	2 (0–4.5)	1 (0–2.75)	3 (0–15)	3 (2–12)	2 (1–4)

* Except where indicated otherwise, values are the number (%) of patients. PD-1 = programmed death 1; IL-7 = interleukin-7; SGECs = salivary gland epithelial cells; NA = not applicable; ESSDAI = European League Against Rheumatism Sjögren's Syndrome Disease Activity Index.
† Data were available for 4 patients.
‡ Data were available for 6 patients.

backward selection. Statistical analyses were performed using SAS 9.3 statistical software.

Statistical analysis of RNA-Seq profiles of sorted cells. Reads were first quality control–filtered and trimmed by Trimmomatic (19). Paired reads were aligned to the Ensembl human reference genome (version 38.79) (20) using STAR software (version 2.5.0c) (21). Statistical analyses involved the DESeq2 package (22). A cutoff *P* value of less than 0.05 was used to define differentially expressed genes. The Interferome version 2.01 database (23) was used to identify and characterize IFN-induced genes. Functional enrichment analysis of differentially expressed genes was performed for genes with absolute fold change value of ≥1.5 using ingenuity pathway analysis software (Qiagen). Statistical analyses of data did not use multiple hypothesis testing.

Study approval. This study was approved by the local ethics committee, and informed consent was obtained from all patients and controls.

RESULTS

Patient characteristics. The characteristics of patients included in the ASSESS cohort for serum cytokine evaluation have previously been described (16). The characteristics of patients

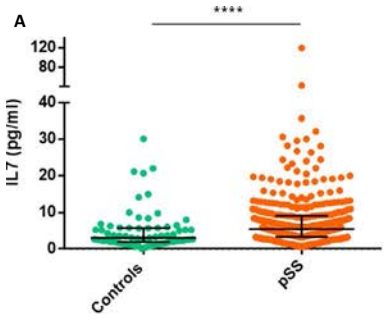

B

Parameter	Spearman correlation coefficient	p-value
CXCL13	r=0.35	<0.0001
CCL19 (MIP-3b)	r=0.20	<0.0001
CXCL10 (IP-10)	r=0.23	0.0002
Gammaglobulins	r=0.27	<0.0001
Total IgG	r=0.28	<0.0001
Kappa Light Chain	r=0.30	<0.0001
Lambda Light Chain	r=0.28	<0.0001
β2-microglobulins	r=0.27	<0.0001
Rheumatoid Factor	r=0.32	<0.0001
Level of lymphocytes	r= -0.28	<0.0001
C4 level	r= -0.22	<0.0001

C

Parameter	p-value
UNIVARIATE ANALYSIS	
Anti-SSA	p<0.0001
Anti-SSB	p<0.0001
RF	p<0.0001
Lymphopenia	p=0.0002
Low C4	p<0.0001
Lymphoma	p=0.005
MULTIVARIATE ANALYSIS	
Anti-SSA	p=0.019
CXCL13	p=0.043
Rheumatoid Factor	p=0.003
Kappa Light Chain	p=0.024
Low C4	p=0.024

Figure 1. Serum interluekin-7 (IL-7) levels in patients with primary Sjögren's syndrome (pSS) and controls. **A**, Assessment of serum IL-7 level in 372 patients with primary SS (Assessment of Systemic Signs and Evolution of SS cohort) and 73 controls, by enzyme-linked immunosorbent assay. Each symbol represents an individual subject; bars show the median and interquartile range. **** = $P < 0.0001$ by Mann-Whitney test. **B**, Correlation between serum IL-7 level and B cell activation markers, interferon (IFN)–induced chemokines, and disease activity markers in patients with primary SS. **C**, Association between clinicobiologic parameters and serum IL-7 level, by univariate and multivariate analysis, in patients with primary SS. MIP-3β = macrophage inflammatory protein 3β; IP-10 = IFNγ-inducible 10-kd protein; RF = rheumatoid factor.

and controls included in the present study are described in Table 1, and the experimental design is described in Supplementary Figure 1 (http://onlinelibrary.wiley.com/doi/10.1002/art.41558/abstract).

Increased serum IL-7 level and decreased IL-7R expression on CD4 and CD8 T cells in primary SS. Patients with primary SS showed higher serum IL-7 levels than controls (median 5.47 ng/ml [IQR 3.33–9.08] versus median 3.03 ng/ml [IQR 1.90–5.76]; $P < 0.0001$) (Figure 1A). Serum IL-7 levels were positively correlated with B cell activation markers, IFN-induced chemokines, and disease activity markers (Figure 1B). A univariate analysis of clinicobiologic parameters associated with serum IL-7 levels identified an association with anti-SSA and anti-SSB antibodies, RF positivity, lymphopenia, low C4 levels, and past or current lymphoma (Figure 1C). In the multivariate analysis, serum IL-7 level was found to be associated with anti-SSA antibody positivity, serum level of CXCL13, RF positivity, high κ light chain, and low C4 level (Figure 1C).

Consistent with this increase in serum IL-7 level, we observed a decrease in IL-7R (CD127) expression on CD4 and CD8 T cells from patients with primary SS compared to controls ($P < 0.05$ and $P < 0.01$, respectively) (Figure 2A), a finding that potentially demonstrates IL-7R internalization after IL-7 binding (24). Of note, IL-7R expression was decreased on CD4 and CD8 T cells from patients with primary SS and controls that were cultured after IL-7 stimulation (Supplementary Figure 3, http://onlinelibrary.wiley.com/doi/10.1002/art.41558/abstract). IL-7R mean fluorescence intensity on CD4 and CD8 T cells did not differ between patients with primary SS and controls (data not shown), nor did *IL7R* gene expression differ between the 2 groups at the transcriptomic level (Supplementary Figure 4, http://onlinelibrary.wiley.com/doi/10.1002/art.41558/abstract).

The comparison of PD-1 expression on CD8 and CD4 T cells between CD127+ and CD127– T cells showed increased expression of PD-1 on CD127– CD8 and CD127– CD4 T cells from patients with primary SS ($P < 0.05$ and $P < 0.0001$, respectively) (Figure 2B). Additionally, ICOS expression was increased on CD127– CD4 T cells compared to CD127+ CD4 T cells from patients with primary SS ($P < 0.001$) (Figure 2C).

SGECs as a source of IL-7. We previously showed that SGECs sorted from primary SS and control SGs expressed *IL7* RNA and that this expression was higher in SGECs from patients with primary SS than from controls (25). Given this finding, we hypothesized that SGECs could be a source of IL-7 in primary SS. Primary cultured SGECs from patients with primary SS and controls stimulated with poly(I-C), IFNα, IFNγ, and IFNλ secreted IL-7 (Figure 3A). *IL7* mRNA expression

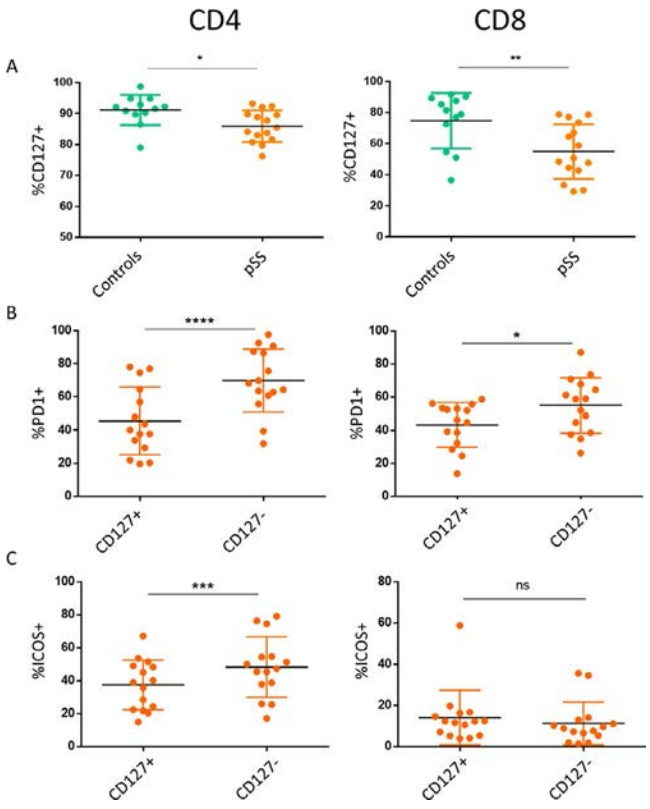

Figure 2. Percentage of CD127+ CD4 and CD8 T cells is decreased in patients with primary SS compared to controls, and levels of programmed death 1 (PD-1) and inducible costimulator (ICOS) are higher in CD127– CD4 T cells than in CD127+ CD4 T cells. Expression of CD127 (IL-7 receptor) in CD4 and CD8 T cells sorted from blood from patients with primary SS (n = 15) and controls (n = 12) (**A**), expression of PD-1 in CD127+ and CD127– CD4 and CD8 T cells in patients with primary SS (n = 15) (**B**), and expression of ICOS in CD127+ and CD127– CD4 and CD8 T cells in patients with primary SS (n = 15) (**C**) are shown. Each symbol represents an individual subject; bars show the mean ± SD. * = $P < 0.05$; ** = $P < 0.01$; *** = $P < 0.001$; **** = $P < 0.0001$, by Mann-Whitney test for unpaired data and Wilcoxon's test for paired data. NS = not significant (see Figure 1 for other definitions).

was confirmed by quantitative reverse transcriptase–PCR (Figure 3C). The protein levels of IL-7 after stimulation with IFNα, IFNλ, and poly(I-C) were higher in SGECs from patients with primary SS compared to controls (Figures 3B).

Relationship between IL-7 and type I and type II IFNs in blood and SGs. Stimulation with IL-7 (2 ng/ml) of blood T cells increased CD25 expression in CD4 and CD8 T lymphocytes, compared to the unstimulated condition in both CD4 and CD8 T cells from patients with primary SS and controls (Supplementary Figures 5A and B, http://onlinelibrary.wiley.com/doi/10.1002/art.41558/abstract). Moreover, CD25 expression was higher in CD4 T cells from patients with primary SS on day 1 and higher in CD8 T cells on day 3 after stimulation with IL-7 (0.1 ng/ml), compared to controls ($P = 0.03$; Supplementary Figures 5C and

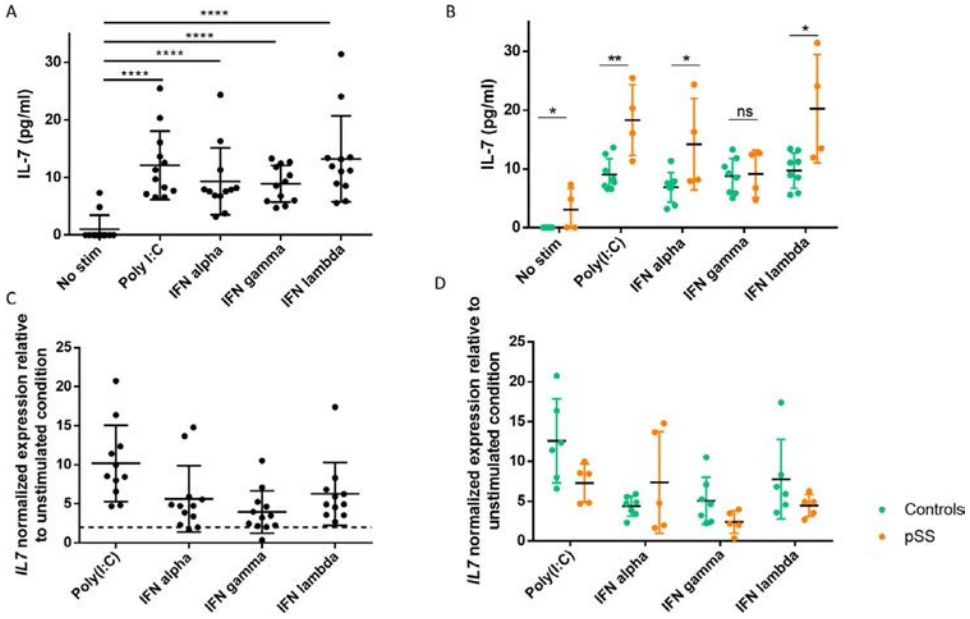

Figure 3. Secretion of IL-7 by salivary gland epithelial cells (SGECs) and *IL7* expression. **A** and **B**, Assessment, by enzyme-linked immunosorbent assay (ELISA), of IL-7 secretion by SGECs, under different stimulation conditions (no stimulation [no stim], poly[I-C] 30 μg/ml, IFNα 5 ng/ml, IFNγ 600 IU/ml, or IFNλ 25 ng/ml) after 3 days, in patients with primary SS and controls combined (**A**) and separately (**B**). **C** and **D**, Quantitative polymerase chain reaction analysis of mRNA levels of *IL7* in SGECs under different conditions of stimulation relative to unstimulated conditions, in patients with primary SS and controls combined (**C**) and separately (**D**). In **C**, the broken line shows the lower detection threshold of the IL-7 ELISA kit. Each symbol represents an individual subject; bars show the mean ± SD. * = $P < 0.05$; ** = $P < 0.01$; **** = $P < 0.0001$, by Mann-Whitney test for unpaired data and Wilcoxon's test for paired data. NS = not significant (see Figure 1 for other definitions).

D, http://onlinelibrary.wiley.com/doi/10.1002/art.41558/abstract). IFNγ was detected in supernatants from T cells stimulated with IL-7 (2 ng/ml). There was a significant increase in IFNγ secretion by IL-7–stimulated T cells from patients with primary SS, but not from controls (Figure 4A). As expected, IL-7 did not stimulate IFNα production in T cells (Figure 4B). Of note, in the whole SG tissue, IL-7 expression was correlated with IFN expression; NanoString transcriptomic analysis of SG explants from patients with primary SS showed a positive correlation between *IL7* mRNA expression and IFNα1, FNα2, IFNβ, and IFNγ gene expression (R^2 = 0.4, 0.5, 0.6, and 0.5, respectively) (Figure 4C).

Up-regulation of IFN signaling pathway and *IFNG* expression in primary SS T cells. The comparison of gene expression in sorted CD4 T cells from the blood of patients with primary SS and controls showed 474 differentially expressed genes: 312 up-regulated and 162 down-regulated. Functional enrichment pathway analysis highlighted an overrepresentation of the eukaryotic initiation factor 2 (eIF2) and the IFN signaling pathways, as well as Th1 and Th2 pathways (Supplementary Table 2, http://onlinelibrary.wiley.com/doi/10.1002/art.41558/abstract). IFN-induced genes such as *IFI27*, *IFIT1*, and *IFI44L* were among the most significantly up-regulated genes in patients with primary SS compared to controls (log_2 fold change = 3.295, 3.029, and 2.552, respectively). Among the 312 up-regulated genes in blood CD4 T cells from patients with primary SS, 198 were IFN-regulated genes (type I = 25, type II = 46, types I and II = 105, and types I, II, and III = 22). Of note, an up-regulation of *PDCD1* gene expression (log_2 fold change = 2.667) was observed in patients with primary SS versus controls.

When comparing gene expression in sorted CD8 T cells from the blood of patients with primary SS and controls, 532 differentially expressed genes were detected: 325 up-regulated and 207 down-regulated. As in CD4 T cells, functional enrichment pathway analysis highlighted an overrepresentation of eIF2 signaling and IFN signaling pathways in CD8 T cells (Supplementary Table 2, http://onlinelibrary.wiley.com/doi/10.1002/art.41558/abstract). IFN-induced genes such as *IFI44L*, *IFI44, OAS1*, *IFIT3*, and *MX1* were up-regulated in patients with primary SS compared to controls (log_2 fold change = 4.073, 1.944, 1.735, 1.7, and 1.542, respectively). Among the 325 up-regulated genes in blood CD8 T cells from patients with primary SS, 42 were IFN-regulated genes (type I = 1, types I and II = 20, and types I, II, and III = 21).

CD8 T cells sorted from SGs and blood expressed *IFNG* and *IFNL* (Supplementary Figure 6, http://onlinelibrary.wiley.com/doi/10.1002/art.41558/abstract). Interestingly, *IFNG* expression was up-regulated in blood CD8 T cells from patients with primary SS compared to controls (log_2 fold change = 1.809) (Supplementary Figure 6). *IFNG* expression was also detected in CD4 T cells

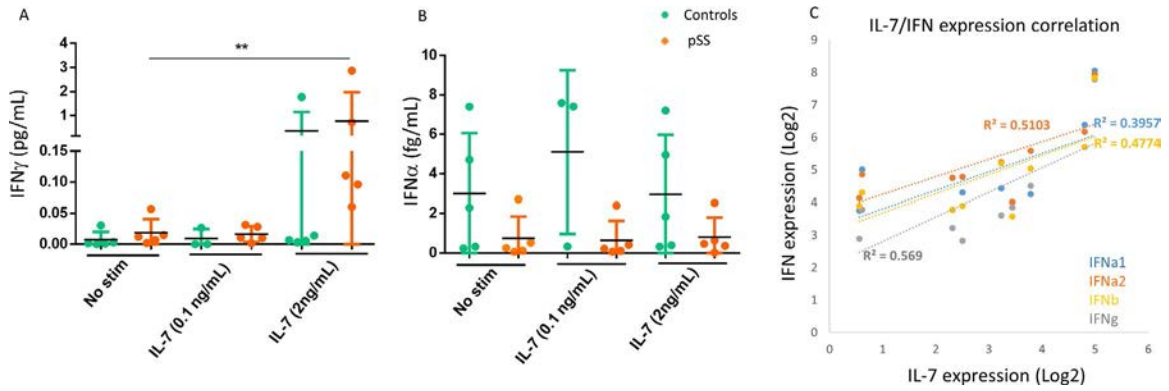

Figure 4. Association between IL-7 and IFN in blood and salivary glands (SGs). **A** and **B**, Detection of IFNγ protein (**A**) and IFNα protein (**B**) in supernatants from T cells stimulated with IL-7 (0.1 ng/ml and 2 ng/ml) for 3 days or left unstimulated (no stim), sorted from blood from patients with primary SS and controls. Each symbol represents an individual subject; bars show the mean ± SD. ** = $P < 0.01$ by Wilcoxon's test. **C**, Correlation between *IL7* gene expression and *IFNA1*, *IFNA2*, *IFNB*, and *IFNG* expression in SG explant cells from patients with primary SS (n = 9). Spearman's correlation coefficient was used. See Figure 1 for other definitions.

from biopsy samples and blood. As expected, type I IFN expression (*IFNA1*, *IFNA2*, *IFNA17*, and *IFNB*) was not detected in CD4 and CD8 T cells from biopsy samples and blood (data not shown).

In sorted CD4 T cells from biopsy specimens from patients with primary SS and controls, 539 differentially expressed genes were detected: 305 up-regulated and 234 down-regulated. Enrichment analysis identified only 3 overrepresented pathways: 14-3-3–mediated signaling, insulin-like growth factor 1 signaling, and natural killer cell signaling (Supplementary Table 2, http://onlinelibrary.wiley.com/doi/10.1002/art.41558/abstract).

In sorted CD8 T cells from biopsy specimens from patients with primary SS and controls, 373 differentially expressed genes were detected: 207 up-regulated and 166 down-regulated. Enrichment analysis did not identify significant pathways (Supplementary Table 2, http://onlinelibrary.wiley.com/doi/10.1002/art.41558/abstract).

Four patients with primary SS had data available at the same time for T cells sorted from biopsy samples and blood. *IFNG* expression was up-regulated in CD4 and CD8 T cells ($\log_2$ fold change = 3.36 [$P = 0.02$] and $\log_2$ fold change = 3.64 [$P = 0.02$], respectively). *IFNL1* was up-regulated in CD4 T cells sorted from biopsy samples versus from blood ($\log_2$ fold change = 6.51 [$P = 0.011$]).

Decreased IFN signature in SGs due to IL-7R inhibition. We analyzed the transcriptomic modifications induced by adding an anti–IL-7R antibody (OSE-127) to the culture of MSG explants from patients with primary SS. The pellet cells corresponded to the cells that escaped from the explant during the culture, and explant cells corresponded to the explant itself (Figure 5A). Analysis of the mRNA signature revealed that inhibition of IL-7 signaling by OSE-127 decreased the IFN gene signature as assessed by decreased expression of *IFITM1* and *MX1*, both in explant and pellet cells (Figure 5B). Looking at the different IFN subtypes, we observed that OSE-127 decreased the expression of *IFNG* specifically in pellet cells (Figure 5C).

DISCUSSION

In this study, we found that IL-7 levels were increased in patients with primary SS, compared to controls, with higher IL-7 levels in serum from patients and decreased IL-7R expression level in circulating T cells. Also, serum IL-7 level was associated with B cell biomarkers and IFN-related biomarkers in primary SS, such as anti-SSA antibody and CXCL13. In addition, SGECs were producers of IL-7 upon type I and type II IFN activation, and T cells stimulated with IL-7 secreted IFNγ. T cells from patients with primary SS were more prone to secrete IFNγ after IL-7 stimulation than T cells from controls. Finally, blocking the IL-7 pathway with an anti–IL-7R monoclonal antibody was associated with a decrease in IFN-related gene expression in SG explants. Given these findings, we hypothesized that there exists an IFN/IL-7 axis in primary SS. SGECs stimulated with both types of IFN might produce IL-7, which activates T lymphocytes able to secrete IFNγ (Figure 5D). This vicious circle could be potentially inhibited by an anti–IL-7R antibody.

IL-7 is a key cytokine involved in T lymphocyte homeostasis. The presence of lymphopenia, affecting mainly T cells, is one of the hallmarks of some systemic autoimmune diseases, such as systemic lupus and primary SS. In primary SS, lymphopenia is included in the biologic criteria used to assess activity in the ESSDAI score, and the presence of lymphopenia is associated with risk of lymphoma (26). Circulating levels of IL-7 are increased in response to lymphopenia. An interesting question in primary SS is whether the increased IL-7 level is a reaction to lymphopenia or whether lymphopoiesis is nonresponsive to IL-7 stimulation.

IL-7 is produced by stromal cells but also by epithelial cells, such as small intestinal epithelial cells (27) or enterocytes (28). We demonstrated that SGECs could produce IL-7 after stimulation with all types of IFNs or a Toll-like receptor 3 agonist. The IFN/IL-7 pathway that we describe could be involved in the organization

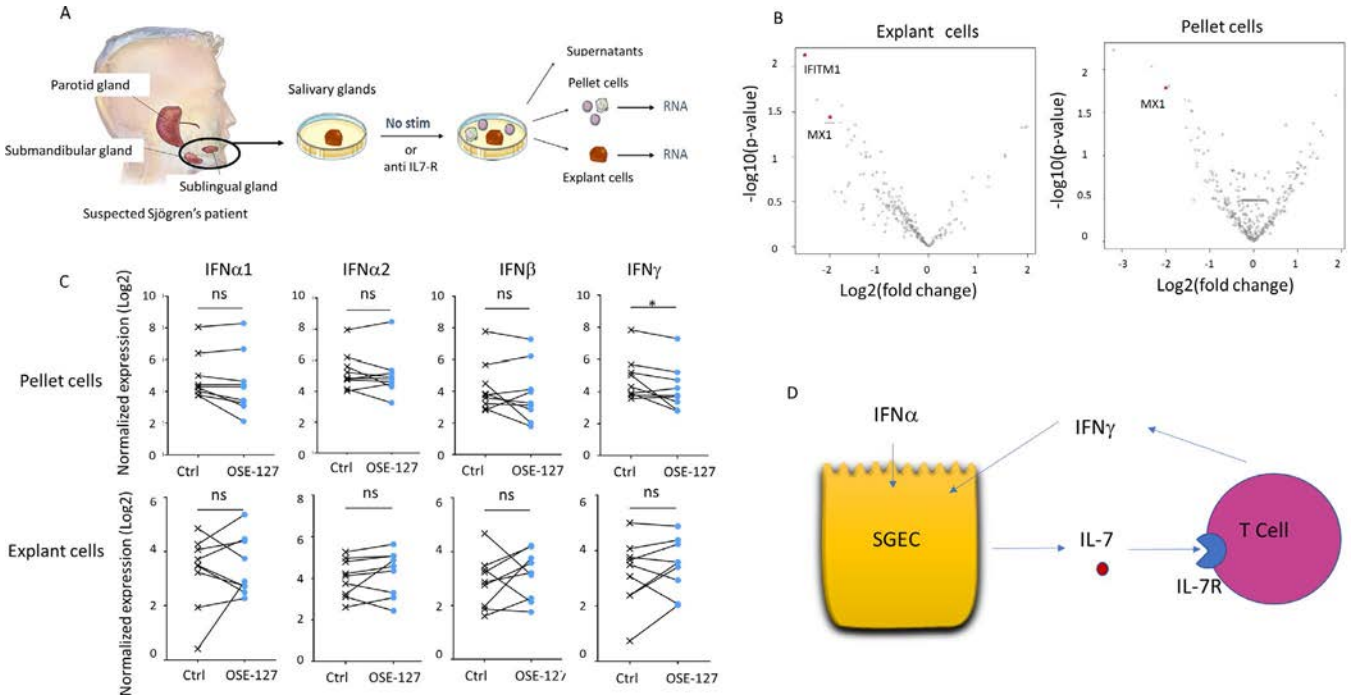

Figure 5. **A**, Schematic representation of the protocol used for NanoString experiments. **B**, Volcano plot representation of differentially expressed genes after treatment with anti–IL-7 receptor (anti–IL-7R) monoclonal antibody (OSE-127) compared to control isotype in explant and pellet cells. **C**, Effect of anti–IL-7R monoclonal antibody (OSE-127) on *IFN* mRNA expression in pellet cells and in explant cells compared to control (ctrl) isotype. * = $P < 0.05$. **D**, Simplified schematic representation of the relationship between salivary gland epithelial cells (SGECs) and T cells via the IL-7/IFN axis. No stim = not stimulated; NS = not significant (see Figure 1 for other definitions).

of ectopic lymphoid structures found in primary SS SGs. Seo et al demonstrated that IL-7 plays a pivotal role in follicular helper T (Tfh) cell generation and germinal center formation in vivo, because treatment with an anti–IL-7 neutralizing antibody markedly impaired the development of Tfh cells and IgG responses (29). Interestingly, we found more CD127– T cells in patients with primary SS than in controls, probably because of the internalization of CD127, or IL-7R, after IL-7 binding (24). Moreover, we showed that CD127– CD4 and CD8 T cells from patients with primary SS showed increased expression of PD-1, and expression of ICOS was higher in CD127– CD4 T cells from patients with primary SS than in CD127+ T cells. These findings suggest that IL-7 could be involved in CD4 T cell differentiation to Tfh cells, which are positive for PD-1 and ICOS.

Tfh cells are specialized providers of T cell help to B cells and are essential for germinal center formation, affinity maturation, and the development of high-affinity antibodies and memory B cells. The link between high IL-7 level and increased B cell biomarkers is intriguing. Since we did not find any expression of IL-7R mRNA on RNA-Seq of blood or SG B cells (Supplementary Figure 4A, http://onlinelibrary.wiley.com/doi/10.1002/art.41558/abstract), this interaction is indirect. IL-7 plays a pivotal role in Tfh cell generation and germinal center formation in vivo (29), which might explain the correlation between serum IL-7 level and B cell biomarkers. Alternatively, since IL-7 levels are increased in patients with active primary SS, and type I IFN and BAFF levels are also increased in the same subgroup of patients, the correlation between IL-7 and B cell biomarkers may reflect a parallel augmentation in patients with the most active disease. Conversely, the impact of IL-7 stimulation on CD8 T cells might drive IFNγ production. The differences between CD4 and CD8 T cell involvement require better characterization. Of note, RNA-Seq analysis showed higher *IFNG* expression in CD8 but not in CD4 T cells from patients with primary SS versus controls. Moreover, in 4 patients with both blood and biopsy samples available, the mRNA expression of *IFNG* and *IFNL1* was up-regulated in T cells sorted from biopsy specimens but not blood. These findings support the role of the SG tissue microenvironment, especially the interactions between T cells and SGECs.

One limitation of this study is that we hypothesized that the action of IL-7 was mainly due to its effect on T cells resulting in IFNγ secretion. However, IL-7 contributes to arthritis in recombination-activating gene–deficient mice, which lack T cells and B cells. Thus, cells other than T and B cells might express IL-7R and be sensitive to IL-7 signaling. For example, the presence of IL-7R+ macrophages was associated with joint inflammation and IL-7 enhanced inflammation and osteoclastogenesis, independently of T cells and B cells in that mouse model (30). Moreover, innate lymphoid cells (ILCs) express IL-7R and are also involved in IL-7–mediated inflammation (31). Notably, group 3 ILCs play a role in IL-7–mediated lymphoid

structure formation. In addition to ILCs, some tissue-resident cells with innate-like properties, such as IL-7R+ mucosal–associated invariant T cells and IL-7R+CCR9+ T cells could contribute to IFNγ secretion. Interestingly, these cells have been found to be increased in target tissues in several autoimmune diseases, notably in the SGs of patients with primary SS (32).

Finally, inhibiting this IL-7 stimulation showed interesting results in terms of *IFN* expression. Confirmation of the transcriptomic results at the protein level would have been interesting, but IFN dosages in supernatants of explants containing a few cells were not contributive, even when using sensitive techniques such as Simoa. It was recently demonstrated that the administration of a blocking antibody against the IL-7Rα chain to female NOD mice ameliorated primary SS characteristics, including hyposalivation and leukocyte infiltration of submandibular glands. Moreover, the authors observed a decrease in IFNγ-producing CD4 and CD8 T cells in the submandibular glands (33). The use of OSE-127, an anti–IL-7Rα monoclonal antibody, showed interesting results in nonhuman primates for controlling skin inflammation despite repeated antigen challenges (34). Additionally, IFNγ level was significantly decreased in humanized mouse models of colitis and ex vivo colon explant cultures from ulcerative colitis (35). Of note, no modification in T cell numbers, phenotype, function, or metabolism was observed in peripheral blood in that study.

In conclusion, IL-7 secreted by SGECs under the influence of both types of IFN may activate T cells, which in turn secrete IFNγ, thus amplifying this vicious circle. Based on these findings and those already described in the "Sjögren-like" NOD mouse model, targeting the IL-7 pathway in primary SS could represent an interesting therapeutic option.

ACKNOWLEDGMENTS

We thank C. Le Pajolec (AP-HP, Hôpitaux Universitaires Paris-Sud, Le Kremlin-Bicêtre, France) and E. Berge (Rheumatology, Université Paris Sud, Le Kremlin Bicêtre, France), who participated in the recruitment of patients. We thank Vincent Bondet (Immunobiology of Dendritic Cells Laboratory, INSERM U1223/Institut Pasteur, Paris, France), who participated in Simoa experiments.

AUTHOR CONTRIBUTIONS

All authors were involved in drafting the article or revising it critically for important intellectual content, and all authors approved the final version to be published. Dr. Rivière had full access to all of the data in the study and takes responsibility for the integrity of the data and the accuracy of the data analysis.

Study conception and design. Rivière, Pascaud, Virone, Dupré, Ly, Paoletti, Mingueneau, Duffy, Chaput, Gauttier, Poirier, Mariette, Nocturne.
Acquisition of data. Rivière, Pascaud, Virone, Dupré, Mingueneau, Smith, Duffy, Cassard, Chaput, Pengam, Gauttier, Nocturne.
Analysis and interpretation of data. Rivière, Pascaud, Virone, Dupré, Ly, Paoletti, Seror, Tchitchek, Mingueneau, Gauttier, Poirier, Mariette, Nocturne.

ADDITIONAL DISCLOSURES

Author Mingueneau is an employee of Biogen. Authors Pengam, Gauttier, and Poirier are employees of OSE Immunotherapeutics.

REFERENCES

1. Singh N, Cohen PL. The T cell in Sjogren's syndrome: force majeure, not spectateur. J Autoimmun 2012;39:229–33.
2. Nezos A, Gravani F, Tassidou A, Kapsogeorgou EK, Voulgarelis M, Koutsilieris M, et al. Type I and II interferon signatures in Sjogren's syndrome pathogenesis: contributions in distinct clinical phenotypes and Sjogren's related lymphomagenesis. J Autoimmun 2015;63:47–58.
3. Gottenberg JE, Cagnard N, Lucchesi C, Letourneur F, Mistou S, Lazure T, et al. Activation of IFN pathways and plasmacytoid dendritic cell recruitment in target organs of primary Sjögren's syndrome. Proc Natl Acad Sci U S A 2006;103:2770–5.
4. Khuder SA, Al-Hashimi I, Mutgi AB, Altorok N. Identification of potential genomic biomarkers for Sjögren's syndrome using data pooling of gene expression microarrays. Rheumatol Int 2015;35:829–36.
5. Hall JC, Baer AN, Shah AA, Criswell LA, Shiboski CH, Rosen A, et al. Molecular subsetting of interferon pathways in Sjögren's syndrome. Arthritis Rheumatol 2015;67:2437–46.
6. Bikker A, van Woerkom JM, Kruize AA, Wenting-van Wijk M, de Jager W, Bijlsma JW, et al. Increased expression of interleukin-7 in labial SGs of patients with primary Sjögren's syndrome correlates with increased inflammation. Arthritis Rheum 2010;62:969–77.
7. Bikker A, Kruize AA, Wenting M, Versnel MA, Bijlsma JW, Lafeber FP, et al. Increased interleukin (IL)-7Rα expression in SGs of patients with primary Sjogren's syndrome is restricted to T cells and correlates with IL-7 expression, lymphocyte numbers and activity. Ann Rheum Dis 2012;71:1027–33.
8. Lundström W, Highfill S, Walsh ST, Beq S, Morse E, Kockum I, et al. Soluble IL7Rα potentiates IL-7 bioactivity and promotes autoimmunity. Proc Natl Acad Sci U S A 2013;110:E1761–70.
9. Hillen MR, Blokland SL, Risselada AP, Bikker A, Lauwerys BR, Kruize AA, et al. High soluble IL-7 receptor expression in Sjögren's syndrome identifies patients with increased immunopathology and dryness [letter]. Ann Rheum Dis 2016;75:1735–6.
10. Timmer TC, Baltus B, Vondenhoff M, Huizinga TW, Tak PP, Verweij CL, et al. Inflammation and ectopic lymphoid structures in rheumatoid arthritis synovial tissues dissected by genomics technology: identification of the interleukin-7 signaling pathway in tissues with lymphoid neogenesis. Arthritis Rheum 2007;56:2492–502.
11. Jin JO, Kawai T, Cha S, Yu Q. Interleukin-7 enhances the Th1 response to promote the development of Sjögren's syndrome–like autoimmune exocrinopathy in mice. Arthritis Rheum 2013;65:2132–42.
12. Shmarov VA, Malashchenko VV, Meniailo ME, Gazatova ND, Todosenko NM, Melashchenko OB, et al. Direct effects of interleukin-7 on the function of human T cells in vitro. Eur Cytokine Netw 2016;27:102–7.
13. Van Roon JA, Glaudemans K, Bijlsma J, Lafeber F. Interleukin 7 stimulates tumour necrosis factor α and Th1 cytokine production in joints of patients with rheumatoid arthritis. Ann Rheum Dis 2003;62:113–9.
14. Belarif L, Mary C, Jacquemont L, Mai HL, Danger R, Hervouet J, et al. IL-7 receptor blockade blunts antigen-specific memory T cell responses and chronic inflammation in primates. Nat Commun 2018;9:4483.
15. Vitali C, Bombardieri S, Jonsson R, Moutsopoulos HM, Alexander EL, Carsons SE, et al. Classification criteria for Sjögren's syndrome: a revised version of the European criteria proposed by the American-European Consensus Group. Ann Rheum Dis 2002;61:554–8.
16. Gottenberg JE, Seror R, Miceli-Richard C, Benessiano J, Devauchelle-Pensec V, Dieude P, et al. Serum levels of β2-microglobulin and free light chains of immunoglobulins are associated with systemic disease activity in primary Sjögren's syndrome: data at enrollment in the prospective ASSESS cohort. PLoS One 2013;8:e59868.

17. Shiboski CH, Shiboski SC, Seror R, Criswell LA, Labetoulle M, Lietman TM, et al. 2016 American College of Rheumatology/European League Against Rheumatism classification criteria for primary Sjögren's syndrome: a consensus and data-driven methodology involving three international patient cohorts. Arthritis Rheumatol 2017;69:35–45.
18. Dimitriou ID, Kapsogeorgou EK, Abu-Helu RF, Moutsopoulos HM, Manoussakis MN. Establishment of a convenient system for the long-term culture and study of non-neoplastic human SG epithelial cells. Eur J Oral Sci 2002;110:21–30.
19. Bolger AM, Lohse M, Usadel B. Trimmomatic: a flexible trimmer for Illumina sequence data. Bioinforma Oxf Engl 2014;30:2114–20.
20. Cunningham F, Achuthan P, Akanni W, Allen J, Amode M, Armean I, et al. Ensembl 2019. Nucleic Acids Res 2019;47:D745–51.
21. Dobin A, Davis C, Schlesinger F, Drenkow J, Zaleski C, Jha S, et al. STAR: ultrafast universal RNA-seq aligner. Bioinforma Oxf Engl 2013;29:15–21.
22. Love MI, Huber W, Anders S. Moderated estimation of fold change and dispersion for RNA-seq data with DESeq2. Genome Biol 2014;15:550.
23. Rusinova I, Forster S, Yu S, Kannan A, Masse M, Cumming H, et al. Interferome v2.0: an updated database of annotated interferon-regulated genes. Nucleic Acids Res 2013;41:D1040–6.
24. Henriques CM, Rino J, Nibbs RJ, Graham GJ, Barata JT. IL-7 induces rapid clathrin-mediated internalization and JAK3-dependent degradation of IL-7Rα in T cells. Blood 2010;115:3269–77.
25. Rivière E, Pascaud J, Tchitchek N, Boudaoud S, Paoletti A, Ly B, et al. SG epithelial cells from patients with Sjögren's syndrome induce B-lymphocyte survival and activation. Ann Rheum Dis 2020;79:1468–77.
26. Nocturne G, Virone A, Ng WF, Le Guern V, Hachulla E, Cornec D, et al. Rheumatoid factor and disease activity are independent predictors of lymphoma in primary Sjögren's syndrome. Arthritis Rheumatol 2016;68:977–85.
27. Madrigal-Estebas L, McManus R, Byrne B, Lynch S, Doherty DG, Kelleher D, et al. Human small intestinal epithelial cells secrete interleukin-7 and differentially express two different interleukin-7 mRNA transcripts: implications for extrathymic T-cell differentiation. Hum Immunol 1997;58:83–90.
28. Laky K, Lefrançois L, Lingenheld EG, Ishikawa H, Lewis JM, Olson S, et al. Enterocyte expression of interleukin 7 induces development of γΔ T cells and Peyer's patches. J Exp Med 2000;191:1569–80.
29. Seo YB, Im SJ, Namkoong H, Kim SW, Choi YW, Kang MC, et al. Crucial roles of interleukin-7 in the development of T follicular helper cells and in the induction of humoral immunity. J Virol 2014;88:8998–9009.
30. Kim SJ, Chang HJ, Volin MV, Umar S, van Raemdonck K, Chevalier A, et al. Macrophages are the primary effector cells in IL-7-induced arthritis. Cell Mol Immunol 2020;17:728–40.
31. Hinrichs AC, van Roon JA. Do IL-7 R+ innate cells orchestrate autoimmune pathology? [review]. Nat Rev Rheumatol 2019;15:640–2.
32. Blokland SL, Hillen MR, Kruize AA, Meller S, Homey B, Smithson GM, et al. Increased CCL25 and T helper cells expressing CCR9 in the SGs of patients with primary Sjögren's syndrome: potential new axis in lymphoid neogenesis. Arthritis Rheumatol 2017;69:2038–51.
33. Zhou J, Yu Q. Anti-IL-7 receptor-α treatment ameliorates newly established Sjögren's-like exocrinopathy in non-obese diabetic mice. Biochim Biophys Acta Mol Basis Dis 2018;1864:2438–47.
34. Belarif L, Mary C, Jacquemont L, Mai HL, Danger R, Hervouet J, et al. IL-7 receptor blockade blunts antigen-specific memory T cell responses and chronic inflammation in primates. Nat Commun 2018;9:4483.
35. Belarif L, Danger R, Kermarrec L, Nerrière-Daguin V, Pengam S, Durand T, et al. IL-7 receptor influences anti-TNF responsiveness and T cell gut homing in inflammatory bowel disease. J Clin Invest 2019;129:1910–25.

Arthritis & Rheumatology
Vol. 73, No. 4, April 2021, pp 641–650
DOI 10.1002/art.41551

American College of Rheumatology
Empowering Rheumatology Professionals

Sustained Remission of Granulomatosis With Polyangiitis After Discontinuation of Glucocorticoids and Immunosuppressant Therapy: Data From the French Vasculitis Study Group Registry

Xavier Puéchal,[1] Michele Iudici,[1] Christian Pagnoux,[1] Alexandre Karras,[2] Pascal Cohen,[1] François Maurier,[3] Thomas Quéméneur,[4] François Lifermann,[5] Mohamed Hamidou,[6] Luc Mouthon,[1] Benjamin Terrier,[1] and Loïc Guillevin,[1] for the French Vasculitis Study Group

Objective. Data on sustained remission of granulomatosis with polyangiitis (GPA) after discontinuation of therapy (referred to as GPA with sustained remission off-therapy [SROT]) are scarce. In the present study, SROT among GPA patients from the French Vasculitis Study Group Registry was evaluated to identify factors associated with its occurrence and durability.

Methods. For inclusion of patients in the study, the diagnosis of GPA had to meet the GPA classification criteria defined by the American College of Rheumatology and/or the revised Chapel Hill Consensus Conference nomenclature for vasculitis. SROT was defined as achievement of remission (a Birmingham Vasculitis Activity Score of 0) that was sustained for ≥6 consecutive months after having discontinued glucocorticoid (GC) and immunosuppressant treatments. The characteristics of the patients at baseline and treatments received were compared at 3, 5, and 10 years postdiagnosis according to whether or not SROT had been reached and maintained.

Results. Among 795 patients with GPA, 92 GPA patients with SROT at 3 years postdiagnosis were compared to 342 control subjects who had experienced disease relapse and/or were still receiving GCs or immunosuppressants. No baseline differences were found, but patients with SROT at 3 years postdiagnosis had more frequently received intravenous cyclophosphamide as induction therapy compared to control subjects ($P = 0.01$), with a higher median number of infusions ($P = 0.05$). At 5 years postdiagnosis, no baseline differences were observed between groups, but patients with SROT at 5 years postdiagnosis had received more cyclophosphamide infusions compared to control subjects ($P = 0.03$). More patients with SROT had received rituximab as maintenance therapy than control subjects at 3 years and 5 years postdiagnosis ($P = 0.09$ and $P < 0.001$, respectively). Of the 74 patients enrolled in the GPA Registry with 10-year follow-up data after having received conventional maintenance therapy, 15 (20%) had reached SROT at 3 years, and 5 (7%) maintained SROT at 10 years postdiagnosis.

Conclusion. After conventional therapies, 7% of GPA patients had reached SROT at 10 years postdiagnosis. No baseline vasculitis characteristics distinguished patients who achieved/maintained SROT from those who experienced disease relapse and/or those who continued to receive GCs or immunosuppressant therapy, but patients with SROT had received more intensive induction therapy and rituximab as maintenance therapy more frequently.

INTRODUCTION

Granulomatosis with polyangiitis (GPA) is characterized by necrotizing granulomatous inflammation commonly involving the upper and lower respiratory tract, necrotizing vasculitis predominantly affecting small-to-medium–sized vessels, and frequent anti–proteinase 3 (anti-PR3) antineutrophil cytoplasmic antibodies (ANCAs) (1). The current standard of care is based on a 2-staged

Several authors of this publication are members of the European Reference Network for Rare Immunodeficiency, Autoinflammatory, and Autoimmune Diseases, Project ID No. 739543.

[1]Xavier Puéchal, MD, PhD, Michele Iudici, MD, PhD (current address: Geneva University Hospitals, Geneva, Switzerland), Christian Pagnoux, MD, MSc, MPH (current address: Vasculitis Clinic, Mount Sinai Hospital, Toronto, Ontario, Canada), Pascal Cohen, MD, Luc Mouthon, MD, PhD, Benjamin Terrier, MD, PhD, Loïc Guillevin, MD: National Referral Center for Rare Systemic Autoimmune Diseases, Université de Paris, Hôpital Cochin, AP-HP, Paris, France; [2]Alexandre Karras, MD, PhD: Hôpital Européen Georges

therapeutic approach, with the use of glucocorticoids (GCs) combined with cyclophosphamide (CYC) or rituximab (RTX) to induce remission, followed by a remission-maintenance therapy to prevent relapses of disease (2). However, despite these regimens, the risk for GPA relapse has remained substantial, leading to cumulative organ damage (3–6).

One-quarter of GPA patients experience relapse of disease within 2 years of diagnosis, and over half of these patients experience a relapse of GPA within 5 years (3). Because most relapses occur after stopping treatment (6–8), prolonged treatment with immunosuppressants and GCs is typically administered to patients. Therefore, clinical outcomes are assessed in trials and most observational cohorts while maintenance therapy is ongoing.

Long-term prognosis in GPA is now a central issue to consider when discussing treatment strategies with patients (9). Patients continue to be burdened with complications from uncontrolled disease and collateral GC- and immunosuppressant-associated adverse events. Moreover, in clinical practice, after stopping prolonged treatment, patients with GPA often wonder whether or not they are "cured". No simple answer exists, as late relapses have been described (7), and data on discontinuation of therapy after achievement of sustained remission of GPA (referred to as GPA with sustained remission off-therapy [SROT]) are limited. SROT is a new concept, mainly emerging as RTX use became widespread, and is only reported in a few GPA studies (8,10). GPA and microscopic polyangiitis (MPA) have often been studied together (4,6,11–13), with less frequent relapses of MPA reported (8), but specific GPA outcomes have not been reported (4,11–13). Furthermore, it remains unknown whether achievement of SROT in patients with GPA might be affected by specific characteristics of the vasculitic disease and/or the patient's treatment regimen. This study aimed to analyze SROT in GPA patients and identify factors associated with its achievement and durability during follow-up.

PATIENTS AND METHODS

Study participants. This retrospective, multicenter analysis included patients with newly diagnosed GPA enrolled in the French Vasculitis Study Group (FVSG) Registry from 1983 to 2018 (see Appendix A for a list of the FVSG investigators). This database includes information from vasculitis patients referred to FVSG members, specifically patients who were participants in trials conducted within our French network and for whom follow-up data were available. For study inclusion, diagnoses of GPA had to meet the 1990 American College of Rheumatology classification criteria and/or revised Chapel Hill Consensus Nomenclature (1,14). This study was conducted in accordance with the Declaration of Helsinki and approved by the Cochin University Hospital Ethics Committee (no. AAA-2019-08018).

Definition of remission. In accordance with the European League Against Rheumatism recommendations for conducting clinical studies and/or clinical trials in systemic vasculitis (15), the following definitions were applied in the present study: for remission, the absence of signs of "new/worsening" disease activity, which was defined as having a score of 0 on version 3 of the Birmingham Vasculitis Activity Score (BVAS) (16), and for relapse, the recurrence or new appearance of disease activity attributable to active vasculitis.

SROT was defined as achievement of sustained remission (BVAS of 0) for ≥6 months (i.e., 2 consecutive visits) after having stopped treatment with GCs and immunosuppressants. Only the first SROT recorded postdiagnosis was considered, with the off-therapy time period ending at the time of reinitiation of GC or immunosuppressant treatment. SROT and its duration were extracted from the database. SROT at 3 years postdiagnosis was defined as achievement of SROT after 3 years of follow-up since the diagnosis of GPA (mean ± SD 36 ± 6 months postdiagnosis, according to the available visit date closest to 3 years). SROT at 5 years postdiagnosis was defined as achievement of SROT at 3 years along with an additional 2 years of follow-up without relapse of disease. Control subjects were GPA patients enrolled in the FVSG Registry with available data at 3 or 5 years postdiagnosis who had not reached SROT (i.e., a relapse of disease and/or GC and/or immunosuppressant use had been recorded at 3 or 5 years postdiagnosis).

Demographic, clinical, and biologic information was collected on electronic case report forms at diagnosis (baseline) and at each follow-up visit. Organ involvement was assessed separately for granulomatous components (sinusitis, orbital masses, subglottic or bronchus stenosis, pulmonary masses, and pachymeningitis) (17) or vasculitic components (alveolar hemorrhage,

Pompidou, AP-HP, Paris, France; [3]François Maurier, MD: Hôpitaux Privés de Metz, Metz, France; [4]Thomas Quéméneur, MD: Centre Hospitalier de Valenciennes, Valenciennes, France; [5]François Lifermann, MD: Centre Hospitalier Côte d'Argent, Dax, France; [6]Mohamed Hamidou, MD, PhD: Centre Hospitalier Universitaire Hôtel-Dieu, Nantes, France.

Drs. Puéchal and Iudici contributed equally to this work.

Dr. Puéchal has received consulting fees, speaking fees, and/or honoraria from Boehringer Ingelheim and Sanofi (less than $10,000 each) and research support from Roche. Dr. Pagnoux has received consulting fees, speaking fees, and/or honoraria from Hoffmann–La Roche, Sanofi, ChemoCentryx, InflaRx, and GlaxoSmithKline (less than $10,000 each) and research support from Roche. Dr. Quéméneur has received consulting fees, speaking fees, and/or honoraria from MSD, Sanofi-Genzyme, and LFB (less than $10,000 each). Dr. Mouthon has received consulting fees, speaking fees, and/or honoraria from Roche (less than $10,000) and research support from Roche. Dr. Terrier has received consulting fees, speaking fees, and/or honoraria from Roche, Grifols, LFB, and AstraZeneca (less than $10,000 each) and research support from Roche. Drs. Iudici, Karras, Cohen, Maurier, Lifermann, Hamidou, and Guillevin have received research support from Roche.

Address correspondence to Xavier Puéchal, MD, PhD, National Referral Center for Rare Systemic Autoimmune Diseases, Hôpital Cochin, 27 Rue du Faubourg St. Jacques, 75679 Paris Cedex 14, France. Email: xavier.puechal@aphp.fr.

Submitted for publication June 23, 2020; accepted in revised form October 1, 2020.

glomerulonephritis, and peripheral neuropathy). Patients were then categorized as having pure granulomatous disease characteristics, pure vasculitic disease characteristics, or mixed disease characteristics.

Assessment of baseline characteristics and therapeutic regimens in the study population. Baseline characteristics of the patients were analyzed to evaluate possible associations with the occurrence and sustainability of SROT, with particular attention to granulomatosis or vasculitic manifestations, renal involvement, ANCA type, and therapeutic regimens. We first identified and described all of the first SROT episodes in GPA patients from the FVSG Registry. We then evaluated only GPA patients enrolled in the FVSG Registry who had follow-up data of ≥3 years and compared the baseline characteristics and therapeutic regimens of patients with SROT versus control subjects at 3 years and 5 years postdiagnosis, as well as the baseline characteristics and therapeutic regimens of patients with SROT at 5 years postdiagnosis versus patients with SROT at 3 years postdiagnosis who experienced a relapse of disease between 3 and 5 years postdiagnosis. Finally, we analyzed relapse-free–survival rate in patients with SROT at 3 years who had ≥7 years of additional follow-up and the factors associated with it.

Statistical analysis. Quantitative variables are reported as the median (interquartile range [IQR]) and qualitative variables as the number (percentage). For patients with GPA who had reached SROT, Kaplan-Meier curves illustrated the estimated probability of not experiencing a relapse of disease. Statistical analyses were computed with SAS version 9.4 (SAS Institute Inc) and R software version 3.2.2 (R Core Team). *P* values less than 0.05 were considered significant.

RESULTS

Overall description of patients from the FVSG Registry with GPA in SROT. The FVSG Registry database included 795 patients who were diagnosed as having new-onset GPA

Table 1. Clinical and biologic characteristics at baseline of patients who reached SROT at 3 years postdiagnosis compared to control subjects who did not reach SROT*

Characteristic	Patients with SROT at 3 years (n = 92)	Control subjects without SROT (n = 342)
Female sex	43 (47)	139 (41)
Age, median (IQR) years	55 (41–65)	53 (43–62)
BVAS, median (IQR)	16.5 (12–24)	15 (10.5–22)
Organ involvement		
General†	72 (78)	265 (77)
Skin	37 (40)	105 (31)
Eyes	30 (33)	92 (27)
ENT	74 (80)	278 (81)
Lung	56 (61)	230 (67)
Cardiovascular	11 (21)	49 (14)
Abdominal	10 (11)	25 (7)
Nervous system	25 (27)	105 (31)
Kidney	52 (57)	170 (50)
Laboratory		
Serum creatinine, median (IQR) μmoles/liter	100 (77–231)	90 (70–140)
Pure granulomatous	18 (20)	78 (23)
Pure vasculitic	30 (32)¶	77 (22)
Mixed (granulomatous and vasculitic)	44 (48)	187 (55)
cANCA positivity‡	61 (67)	221 (65)
pANCA positivity‡	15 (16)	37 (11)
Anti-PR3 ANCA positivity§	67 (74)	260 (79)
Anti-MPO ANCA positivity§	17 (19)	43 (13)

* Except where indicated otherwise, values are the number (%) of patients. Except where indicated, *P* values for all other comparisons were not significant. IQR = interquartile range; ENT = ear, nose and throat; cANCA = antineutrophil cytoplasmic antibodies with cytoplasmic immunofluorescence labeling pattern; pANCA = ANCAs with perinuclear immunofluorescence labeling pattern; PR3 = proteinase 3; MPO = myeloperoxidase.
† Includes myalgias, arthralgias/arthritis, fever of ≥38°C, and weight loss of ≥2 kg attributable to active vasculitis according to the Birmingham Vasculitis Activity Score (BVAS).
‡ Data available for 91 patients (99%) with sustained remission of granulomatosis with polyangiitis (GPA) after discontinuation of therapy (referred to as GPA with sustained remission off-therapy [SROT]) at 3 years postdiagnosis and all patients who did not reach SROT.
§ Data available for 90 patients (98%) who reached SROT at 3 years postdiagnosis and 328 patients (96%) who did not reach SROT.
¶ *P* = 0.05 versus controls.

from May 1983 to April 2018. Clinical characteristics of these patients have been described previously (18) (Table 1). Of these patients, 80% received conventional induction therapy (GCs and CYC), and 71% received azathioprine (AZA) or methotrexate (MTX) maintenance therapy (Table 2). Only 3.5% and 19.1% of the patients received RTX induction therapy and maintenance therapy, respectively. Median follow-up was 3.5 years (range 1.7–6.5 years).

SROT was reached at least 1 time at some point during the disease course in 259 patients (33%), after a median of 36 months (range 28–63 months) of follow-up postdiagnosis. For the 202 patients with a follow-up visit after achieving SROT (Figure 1), the median SROT duration was 14 months (range 18–32 months). Among these 202 patients, 129 (64%) experienced a disease flare during a median of 11 months (range 7–18 months) of follow-up, whereas SROT was maintained by 73 patients (36%) during a median of 34 months (range 13–45 months) of follow-up.

Table 2. Induction and maintenance treatments received by patients who achieved SROT 3 years postdiagnosis versus control subjects who did not reach SROT*

Treatment	Patients with SROT at 3 years (n = 92)	Control subjects without SROT (n = 342)
Induction		
Cyclophosphamide†		
Oral	4 (4)	16 (5)
IV	82 (89)‡	264 (77)
Number of infusions, median (IQR)	7.5 (6–10)§¶	6 (6–9.75)#
Rituximab	4 (4)††	11 (3)
Methotrexate	2 (2)	23 (7)
Glucocorticoids	88 (96)	332 (97)
Dose, median (IQR), mg/day	60 (50–70)‡‡	60 (50–70)§§
Methylprednisolone bolus	24 (26)	88 (26)
Plasma exchanges	8 (9)	20 (6)
Maintenance		
GC cumulative dose, median (IQR) mg	10,872 (7,256–14,250)	10,121 (6,901–15,310)
GC duration, median (IQR) months	29 (23–34)	30 (24–35)
Azathioprine	46 (50)	180 (53)
Methotrexate	14 (15)	68 (20)
Rituximab	25 (27)	58 (17)

* Except where indicated otherwise, values are the number (%) of patients. Except where indicated, *P* values for all other comparisons were not significant. IQR = interquartile range; GC = glucocorticoid.
† Three of the patients with sustained remission of granulomatosis with polyangiitis (GPA) after discontinuation of therapy (referred to as GPA with sustained remission off-therapy [SROT]) at 3 years postdiagnosis and 7 of the controls subjects without SROT received mixed oral/intravenous (IV) cyclophosphamide therapy.
‡ *P* = 0.01 versus controls.
§ Data available for 66 patients (72%).
¶ *P* = 0.05 versus controls.
# Data available for 207 patients (61%).
†† Two patients received a combination of cyclophosphamide and rituximab as induction therapy.
‡‡ Data available for 64 patients (70%).
§§ Data available for 228 patients (67%).

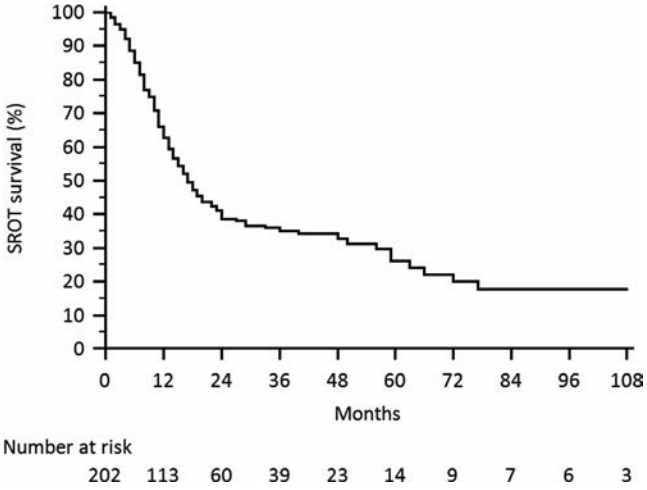

Figure 1. Survival rates of 202 patients from the French Vasculitis Study Group (FVSG) Registry with sustained remission of granulomatosis with polyangiitis (GPA) after discontinuation of therapy (referred to as GPA with sustained remission off-therapy [SROT]). Time 0 is the date SROT was achieved, i.e., a median of 3 years postdiagnosis. Of the 202 patients, 129 (64%) experienced a disease flare after a median follow-up of 11 months (range 7–18 months), and 73 (36%) maintained SROT for a median follow-up of 34 months (range 13–45 months).

Comparison of patients who reached SROT at 3 years postdiagnosis versus controls who did not reach SROT at 3 years. Of the patients with GPA in the FVSG Registry, 434 were followed up for ≥3 years postdiagnosis, with the last diagnosis recorded in January 2015 (Figure 2). Overall, 92 patients (21%) reached SROT at 3 years postdiagnosis, with a stable rate over time (4 [17%] of 23, 37 [23%] of 160, and 51 [20%] of 251 patients diagnosed between 1983 and 1995, 1996 and 2005, and 2006 and 2015, respectively; *P* = 0.71). At 3 years postdiagnosis, 92 patients who had reached SROT were compared to 342 control subjects who had experienced a disease relapse and/or were still receiving GCs and/or immunosuppressants at that time point (Table 1). At baseline, clinical characteristics (ear, nose, and throat [ENT], pulmonary, cardiovascular, and renal involvement) for those groups were comparable, as were ANCA positivity and labeling patterns. A higher percentage of patients with pure vasculitic manifestations tended to achieve SROT at 3 years postdiagnosis.

Among patients who reached SROT compared to control subjects, induction therapy was significantly more intensive, with a higher percentage having received intravenous (IV) CYC and a higher median number of infusions, leading to a higher cumulative CYC dose (Table 2). Results from sensitivity analyses performed after the exclusion of 40 patients (5 who reached SROT at 3 years postdiagnosis and 35 in the control group) who did not receive any non-GC immunosuppressants as induction therapy were in line with results from analyses performed on the whole sample of patients and also a higher percentage of individuals who received

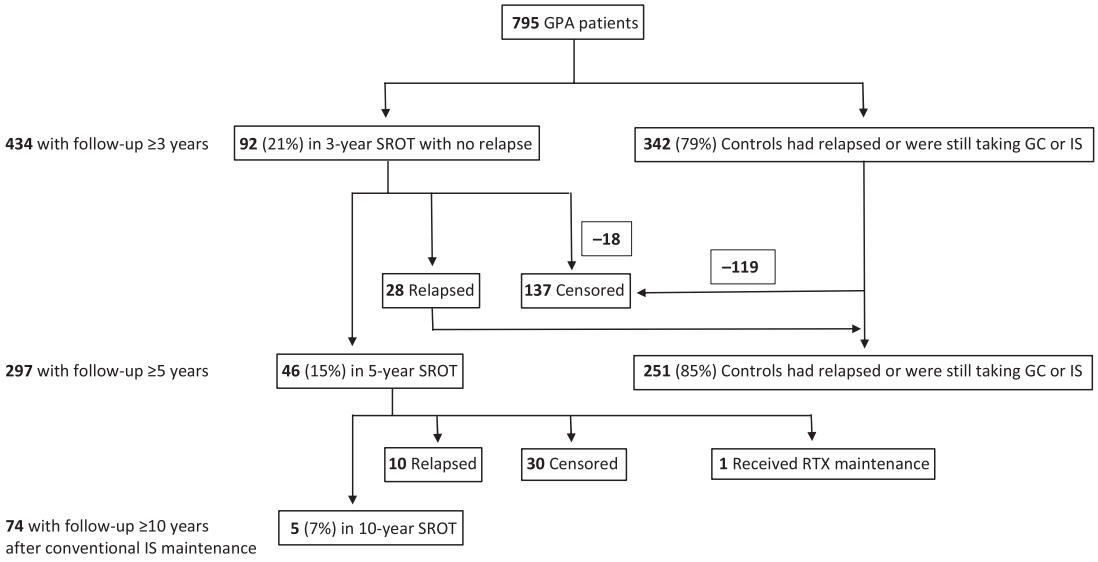

Figure 2. Flow chart of the 795 GPA patients from the FVSG Registry according to follow-up duration. GC = glucocorticoids; IS = immunosuppressants; RTX = rituximab (see Figure 1 for other definitions).

IV CYC therapy in the SROT group ($P = 0.03$). Only 82 (23.7%) of 346 patients who were treated with IV CYC therapy versus 4 (26.7%) of 15 patients who received RTX for induction reached SROT at 3 years postdiagnosis ($P = 0.76$). No between-group differences in the frequency of SROT at 3 years were found for the patients who had received RTX (3.5%) or MTX (5.3%) as induction therapy or as a function of their GC intake during induction or maintenance. The median duration of RTX versus conventional MTX or AZA maintenance therapy was comparable (21 months [range 17–26 months] versus 22 months [range 15–29 months]). In comparing the frequency of SROT according to maintenance therapy, there was a trend toward a higher number of patients achieving SROT after RTX therapy (30.1%) than after treatment with conventional immunosuppressants (19.5%) ($P = 0.05$). However, none of the differences between maintenance therapy groups were significant (frequency of SROT at 3 years, 30.1% in the RTX group versus 20.3% in the AZA group and 17.0% in the MTX group; $P = 0.09$ for RTX versus AZA, $P = 0.07$ for RTX versus MTX, and $P = 0.63$ for AZA versus MTX).

Analyses of patients who reached SROT at 3 years postdiagnosis for whom follow-up data were available. Of the 89 patients who had reached SROT at 3 years postdiagnosis and who had at least 1 follow-up visit, 46 (52%) experienced a disease flare after a median of 18.5 months (range 7.8–36.2 months) after achieving SROT at 3 years postdiagnosis, and 43 (48%) maintained SROT for a median of 40 months (range 21–57 months). Among the 74 patients who reached SROT at 3 years who were monitored for at least 2 additional years, 46 (62%) reached SROT at 5 years postdiagnosis (2 [50%] of 4, 17 [63%] of 27, and 27 [63%] of 43 patients diagnosed between 1983 and 1995, 1996 and 2005, and 2006 and 2012, respectively; $P = 0.26$). The remaining 28 patients (38%) experienced a disease flare. Relapse-free survival rates in patients who reached SROT at 3 years are shown in Figure 3.

Comparison of patients who reached SROT versus control subjects who did not achieve SROT at 5 years postdiagnosis. Among the 297 FVSG Registry patients monitored for at least 5 years, 46 (15%) attained SROT at 5 years postdiagnosis (Figure 2). Their clinical and biologic characteristics were also similar to those of control subjects who did not achieve SROT at 5 years postdiagnosis (Supplementary Table 1, available on the *Arthritis & Rheumatology* website at http://onlinelibrary.wiley.com/doi/10.1002/art.41551/abstract). However, these 46 patients had received a significantly higher median number of CYC infusions, leading to a higher cumulative CYC dose (Table 3). Significantly more patients who reached SROT at 5 years postdiagnosis had also received RTX maintenance therapy compared to control subjects.

Comparison of patients who maintained SROT at 3 years and 5 years postdiagnosis versus patients who reached SROT at 3 years postdiagnosis and experienced a relapse of disease between 3 and 5 years postdiagnosis. The baseline clinical characteristics (ENT, pulmonary, cardiovascular or renal involvement, and biologic characteristics) of patients who reached SROT at 3 years postdiagnosis who also maintained SROT at 5 years postdiagnosis were comparable to those who experienced a relapse of disease between year 3 and year 5 (Supplementary Table 2, available on the *Arthritis & Rheumatology* website at http://onlinelibrary.wiley.com/doi/10.1002/art.41551/abstract). There was a trend toward a greater number of those who experienced relapse being PR3-ANCA positive at baseline

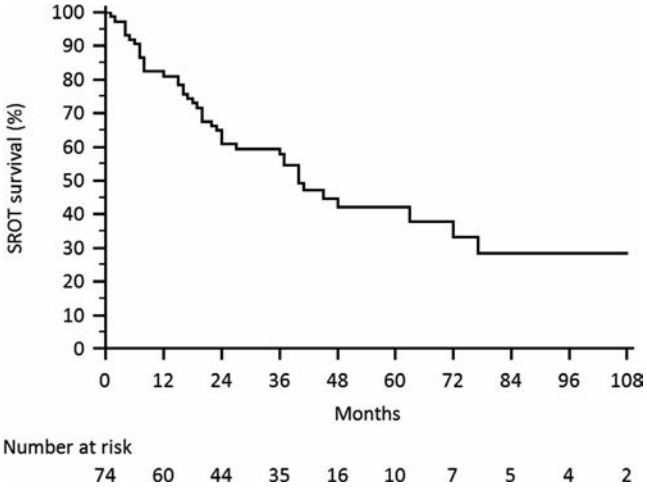

Figure 3. Survival rates of 74 GPA patients from the FVSG Registry who had reached SROT at 3 years postdiagnosis and had ≥2 years of follow-up data available. Time 0 is the date SROT at 3 years postdiagnosis was reached, i.e., a median of 32 months postdiagnosis. Of the 74 GPA patients, 28 (38%) who reached SROT at 3 years postdiagnosis experienced a disease flare between 3 years and 5 years postdiagnosis, and 46 (62%) reached SROT at 5 years postdiagnosis. See Figure 1 for definitions.

and at 3 years compared to those who maintained SROT for 5 years (P = 0.08 for each). Both groups had received comparable induction and maintenance therapies (Supplementary Table 3, available on the *Arthritis & Rheumatology* website at http://onlinelibrary.wiley.com/doi/10.1002/art.41551/abstract).

Analysis of patients who reached SROT at 3 years postdiagnosis who had ≥7 years of follow-up data available. Sixteen GPA patients who reached SROT at 3 years postdiagnosis had a follow-up visit ≥7 years later, with 10 (62.5%) of 16 experiencing a flare before 7 years postdiagnosis and 6 (38%) of 16 reaching SROT at 10 years postdiagnosis (Figure 2). Among the 74 FVSG Registry patients with GPA who had 10-year follow-up data available after receiving conventional maintenance therapy, 15 reached SROT at 3 years postdiagnosis, which was maintained by 5 patients (7%) at 10 years postdiagnosis.

DISCUSSION

The results of the present study elucidate the long-term prognosis of GPA, notably that only 7% of GPA patients reached SROT at 10 years postdiagnosis after receiving conventional maintenance therapies. No vasculitis characteristics at baseline helped distinguish patients who achieved/maintained SROT and those who experienced a relapse of disease. However, patients reaching SROT at 3 or 5 years postdiagnosis had received more intensive induction and RTX maintenance therapy more frequently than those who experienced a disease relapse or who were still receiving GCs or immunosuppressants. SROT is an ultimate goal for GPA patients and might be a new indicator of a potential "cure" or its first surrogate marker. We think SROT should be added to clinical outcome measures in future studies evaluating and comparing new strategies, given the recent major breakthroughs in GPA management (e.g., RTX maintenance therapy).

Extended follow-up of GPA populations is very important, and data on long-term prognosis of GPA are scarce. Our study is rare among similar investigations in that it includes detailed monitoring for over more than 10 years, which enabled the analyses of SROT. Late-onset relapses have been described in GPA patients who were included in observational cohorts and long-term follow-up

Table 3. Primary characteristics and treatments received by patients at baseline who reached SROT at 5 years postdiagnosis versus control subjects who did not reach SROT*

	Patients with SROT at 5 years (n = 46)	Control subjects without SROT (n = 251)
Characteristic		
Pure granulomatous	9 (20)	57 (23)
Pure vasculitic	13 (28)	55 (22)
Mixed (granulomatous and vasculitic)	24 (52)	139 (55)
cANCA positivity†	29 (63)	168 (67)
pANCA positivity†	7 (15)	25 (10)
Anti-PR3 ANCA positivity‡	32 (80)	198 (82)
Anti-MPO ANCA positivity‡	7 (18)	32 (13)
Induction treatment		
Cyclophosphamide		
Oral	1 (2)	15 (6)
IV	42 (91)	202 (80)
Number of infusions, median (IQR)	9 (6–12)§	6 (6–9)
Rituximab	1 (2)	4 (2)
Methotrexate	1 (2)	13 (5)
Glucocorticoids	45 (98)	241 (96)
Dose, median (IQR) mg/day	60 (60–80)¶	60 (60–70)#
Methylprednisolone bolus	15 (33)	64 (25)
Plasma exchanges	5 (11)	13 (5)
Maintenance treatment		
Azathioprine	20 (43)	140 (56)
Methotrexate	9 (20)	43 (17)
Mycophenolate mofetil	0 (0)	11 (4.3)
Rituximab	16 (35)**	35 (14)

* Except where indicated otherwise, values are the number (%) of patients. Except where indicated, P values for all other comparisons were not significant. cANCA = antineutrophil cytoplasmic antibodies with cytoplasmic immunofluorescence labeling pattern; pANCA = ANCAs with perinuclear immunofluorescence labeling pattern; PR3 = proteinase 3; MPO = myeloperoxidase; IV = intravenous; IQR = interquartile range.
† Data available for all patients with sustained remission of granulomatosis with polyangiitis (GPA) after discontinuation of therapy (referred to as GPA with sustained remission off-therapy [SROT]) at 5 years postdiagnosis and 249 control subjects (99%) without SROT.
‡ Data available for 40 patients (87%) with SROT at 5 years postdiagnosis and 240 control subjects (96%) without SROT.
§ $P < 0.05$ versus controls.
¶ Data available for 30 patients (65%).
# Data available for 175 patients (70%).
** P = 0.001 versus controls.

of clinical trials. Hoffman et al reported that relapses occurred 3 months to 16 years after achieving remission (7). Ten (18.5%) of 54 GPA patients with over 10 years of follow-up data available had periods of remission lasting at least 10 consecutive years, though 2 (20%) subsequently experienced a relapse of disease. Similarly, long-term outcomes in 97 GPA patients in the Wegener's Granulomatosis-Entretien (WEGENT) trial showed 5- and 10-year relapse-free survival rates of only 37.6% and 23.3%, respectively (6).

In the Rituximab for ANCA-Associated Vasculitis (RAVE) trial, which included GPA and MPA patients, most patients who were monitored for sufficiently long periods of time eventually experienced a relapse of disease (12,13,19). Durable complete remissions at 12 and 18 months without any maintenance treatment or GC use were obtained by 48% and 39% of the patients in the RTX groups who fulfilled our criteria for SROT (13). The Glomerular Disease Collaborative Network (GDCN) inception cohort enrolled patients with all forms of ANCA-associated vasculitis (AAV), including 123 individuals with GPA, for more than 35 years (20). Among their 63 patients with AAV who maintained SROT for a minimum of 5 years, only 35 (56%) remained in remission at the median follow-up of 94 months. The possibility of late-term relapses of GPA after stopping therapy illustrates that prolonged remission that continues long after any treatment is not synonymous with "cure" and that further research is needed to define characteristics associated with SROT occurrence and continuation.

We found that 21% and 15% of patients with GPA reached SROT at 3 years and 5 years, respectively, in line with findings from the GDCN cohort. It was noted in the GDCN that 23% of AAV patients had stopped treatment for periods of ≥5 years (20), fulfilling our definition of SROT. However, only 59% of GPA patients in that cohort discontinued treatment. Intriguingly, women as well as patients who received pulse methylprednisolone in the GDCN cohort were more likely to stop treatment, though we cannot confirm that observation in the present study. Our results were consistent with patients first stopping therapy at a median of 20 months as well as patients not receiving treatment for a median of 36 months in the GDCN cohort.

In our study, no vasculitis characteristic at baseline was associated with obtaining SROT or its persistence, including ENT and cardiovascular involvements that have been associated with increased risk of GPA relapses (21,22). Conversely, renal involvement, which is associated with a lower GPA relapse rate (23), does not seem to impact reaching or maintaining SROT. In line with data from the GDCN cohort (20), our analyses did not reveal any demographic characteristics or current clinical phenotypes that were helpful in determining which patients can stop therapy.

Patients in the RAVE trial who had a diagnosis of GPA, were positive for PR3-ANCA at baseline, and had relapsing disease had the highest risk of experiencing a relapse (13). Seventy-five percent of our study population consisted of GPA patients with PR3-ANCA positivity, all of whom at baseline had the highest risk for relapse of disease. However, even though we analyzed 60 GPA patients in the FVSG Registry with antimyeloperoxidase (anti-MPO) antibodies and 3 years of available follow-up data, we could not confirm that patients with PR3-ANCA positivity were less prone to reaching SROT. These results might be explained by PR3-ANCA positivity having been associated with an increased risk of relapse in most but not all studies (24) that included a limited number of GPA patients with MPO-ANCA positivity (24–26) or both GPA patients and MPA patients (13,27,28). In addition, it is likely that treating physicians may have decided to treat PR3-ANCA positive patients for longer periods, minimizing the impact of PR3-ANCA positivity on SROT.

Although our study design cannot definitely demonstrate a causal link between any therapy and SROT achievement/persistence, our results strengthen the already observed benefit of CYC-based induction therapy (4,29–32) and the impact of its intensity. Although it has long been thought that high cumulative CYC doses could be associated with better quality remissions than lower doses (21,30), analyses highlighted the associated toxicity, with no short-term benefit of its initial intensification by oral intake (31,33). Nevertheless, long-term trial data suggested that oral CYC induction obtained a lower rate of disease relapse (20.8%) than IV CYC (39.5%) (28). Furthermore, it has already been shown that patients receiving MTX therapy had higher rates of relapse at 18 months, most of which occurred after therapy was tapered off (29). Our results indicated that a higher cumulative CYC dose, according to definitive guidelines (34,35), was associated with better long-term disease control. Enough long-term data on RTX induction has not yet been accumulated in our FVSG Registry for analysis in order to determine its effect on GPA SROT occurrence and maintenance.

In the present study, RTX maintenance therapy was more effective in maintaining remission compared to other maintenance therapies, demonstrating a significantly higher percentage of patients who attained SROT at 5 years postdiagnosis as well as a trend toward attaining SROT at 3 years postdiagnosis. It was also found in the GDCN cohort that RTX had been administered more frequently to patients who stopped therapy (24%) than those who did not stop therapy (14%) (20). Those observations are in line with results from the Maintenance of Remission Using Rituximab in Systemic ANCA-Associated Vasculitis (MAINRITSAN) trial demonstrating that more patients who received low-dose, preemptive, RTX maintenance treatment reached sustained remission compared to patients who received AZA therapy (36).

Early therapy discontinuation is known to be associated with a higher risk of disease relapse (8,29), but no consensus exists with regard to the optimal duration of maintenance therapy for GPA (35). The design of our observational study prevents the ability to evaluate the ideal duration of such therapy, which could potentially be flawed by time-dependent biases (37). Results from 2 trials on conventional immunosuppressant maintenance therapy showed

that extended AZA use led to lower rates of disease (38,39). In the trial that compared the effects of standard AZA therapy and extended AZA therapy in AAV patients who persistently exhibited positivity for PR3–classic ANCA at remission onset, 11 patients (46%) experienced a relapse of disease after receiving standard AZA therapy compared to 5 patients (24%) who experienced a relapse after receiving extended AZA therapy, though statistical significance was not reached due to slow recruitment and early termination (38). The other trial confirmed that prolonging AZA and GC remission maintenance therapy beyond 24 months postdiagnosis was associated with a significant 3-fold lower relapse rate until 48 months postdiagnosis (39). However, RTX maintenance is now replacing conventional maintenance therapies as second-line treatment, and extended low-dose RTX maintenance therapy has also been shown to lower relapse rates (40).

Our study has several strengths. Certainly, the importance of the FVSG Registry database with its detailed and thorough information from diagnosis onward cannot be underestimated. It provided data on 795 patients with GPA exclusively, with long-term follow-up available for most participants, thereby enabling the analysis of what remission after treatment has been stopped looks like in GPA. Patients were recruited from 35 French vasculitis centers, across several specialties (e.g., rheumatology, respiratory diseases, nephrology, dermatology). Thus, we believe that our data are likely to be representative of the entire GPA spectrum and that our findings should be applicable to other GPA populations. Moreover, our work and that of the GDCN might provide fundamental clues to achieving favorable long-term GPA outcomes and contribute to defining new outcome measures that are now making more sense with more effective treatments (e.g., RTX, especially as maintenance therapy), allowing SROT to become a more frequent reality.

Some study limitations must also be acknowledged. The design of the present study is retrospective. There were some missing data, and information on some relapses and/or treatments may have been missed. No predefined guidelines specified when to stop GC or immunosuppressant use. Cumulative drug doses were not always available. The AAV therapeutic strategy has evolved markedly over the 35 years of patient enrollment in the FVSG registry. Furthermore, the 7% of patients achieving SROT at 10 years postdiagnosis after conventional maintenance therapy must be interpreted with caution, given that there could possibly be overrepresentation of FVSG Registry patients with favorable outcomes. Only 74 GPA patients had 10-year follow-up visits at 3 years postdiagnosis after conventional maintenance regimens. Nevertheless, 795 GPA patients were included, with median follow-up exceeding 3 years, making the present study one of the largest studies to date on this rare disease and documenting that SROT at 10 years postdiagnosis is attainable in a small percentage of patients.

In conclusion, SROT in GPA has rarely been achieved with conventional therapies. SROT was found to be associated with induction therapy intensity and low-dose, preemptive, RTX maintenance therapy, but not vasculitis characteristics at baseline. Henceforth, SROT should be systematically documented and analyzed in future studies.

ACKNOWLEDGMENT

The authors thank Janet Jacobson for editorial assistance.

AUTHOR CONTRIBUTIONS

All authors were involved in drafting the article or revising it critically for important intellectual content, and all authors approved the final version to be published. Dr. Puéchal had full access to all the study data and takes responsibility for the integrity of the data and the accuracy of the data analysis.

Study conception and design. Puéchal, Iudici, Guillevin.

Acquisition of data. Puéchal, Iudici, Pagnoux, Karras, Cohen, Maurier, Quéméneur, Lifermann, Hamidou, Mouthon, Terrier, Guillevin.

Analysis and/or interpretation of data. Puéchal, Iudici, Pagnoux, Guillevin.

REFERENCES

1. Jennette JC, Falk RJ, Bacon PA, Basu N, Cid MC, Ferrario F, et al. 2012 revised International Chapel Hill Consensus Conference Nomenclature of Vasculitides. Arthritis Rheum 2013;65:1–11.
2. Jayne D, Rasmussen N, Andrassy K, Bacon P, Tervaert JW, Dadoniené J, et al. A randomized trial of maintenance therapy for vasculitis associated with antineutrophil cytoplasmic autoantibodies. N Engl J Med 2003;349:36–44.
3. Mukhtyar C, Flossmann O, Hellmich B, Bacon P, Cid M, Cohen-Tervaert JW, et al. Outcomes from studies of antineutrophil cytoplasm antibody associated vasculitis: a systematic review by the European League Against Rheumatism Systemic Vasculitis Task Force. Ann Rheum Dis 2008;67:1004–10.
4. Faurschou M, Westman K, Rasmussen N, de Groot K, Flossmann O, Höglund P, et al. Long-term outcome of a randomized clinical trial comparing methotrexate to cyclophosphamide for remission induction in early systemic antineutrophil cytoplasmic antibody–associated vasculitis. Arthritis Rheum 2012;64:3472–7.
5. Robson J, Doll H, Suppiah R, Flossmann O, Harper L, Höglund P, et al. Glucocorticoid treatment and damage in the anti-neutrophil cytoplasm antibody-associated vasculitides: long-term data from the European Vasculitis Study Group trials. Rheumatology (Oxford) 2015;54:471–81.
6. Puéchal X, Pagnoux C, Perrodeau É, Hamidou M, Boffa JJ, Kyndt X, et al. Long-term outcomes among participants in the WEGENT trial of remission-maintenance therapy for granulomatosis with polyangiitis (Wegener's) or microscopic polyangiitis. Arthritis Rheumatol 2016;68:690–701.
7. Hoffman GS, Kerr GS, Leavitt RY, Hallahan CW, Lebovics RS, Travis WD, et al. Wegener granulomatosis: an analysis of 158 patients. Ann Intern Med 1992;116:488–98.
8. Springer J, Nutter B, Langford CA, Hoffman GS, Villa-Forte A. Granulomatosis with polyangiitis (Wegener's): impact of maintenance therapy duration. Medicine (Baltimore) 2014;93:82–90.
9. Cornec D, Cornec-Le Gall E, Fervenza FC, Specks U. ANCA-associated vasculitis—clinical utility of using ANCA specificity to classify patients [review]. Nat Rev Rheumatol 2016;12:570–9.
10. Fauci AS, Haynes BF, Katz P, Wolff SM. Wegener's granulomatosis: prospective clinical and therapeutic experience with 85 patients for 21 years. Ann Intern Med 1983;98:76–85.
11. Hogan SL, Falk RJ, Chin H, Cai J, Jennette CE, Jennette JC, et al. Predictors of relapse and treatment resistance in antineutrophil

cytoplasmic antibody-associated small-vessel vasculitis. Ann Intern Med 2005;143:621–31.

12. Stone JH, Merkel PA, Spiera R, Seo P, Langford CA, Hoffman GS, et al. Rituximab versus cyclophosphamide for ANCA-associated vasculitis. N Engl J Med 2010;363:221–32.
13. Specks U, Merkel PA, Seo P, Spiera R, Langford CA, Hoffman GS, et al. Efficacy of remission-induction regimens for ANCA-associated vasculitis. N Engl J Med 2013;369:417–27.
14. Leavitt RY, Fauci AS, Bloch DA, Michel BA, Hunder GG, Arend WP, et al. The American College of Rheumatology 1990 criteria for the classification of Wegener's granulomatosis. Arthritis Rheum 1990;33:1101–7.
15. Hellmich B, Flossmann O, Gross WL, Bacon P, Cohen-Tervaert JW, Guillevin L, et al. EULAR recommendations for conducting clinical studies and/or clinical trials in systemic vasculitis: focus on anti-neutrophil cytoplasm antibody-associated vasculitis. Ann Rheum Dis 2007;66:605–17.
16. Mukhtyar C, Lee R, Brown D, Carruthers D, Dasgupta B, Dubey S, et al. Modification and validation of the Birmingham Vasculitis Activity Score (version 3). Ann Rheum Dis 2009;68:1827–32.
17. Holle JU, Dubrau C, Herlyn K, Heller M, Ambrosch P, Noelle B, et al. Rituximab for refractory granulomatosis with polyangiitis (Wegener's granulomatosis): comparison of efficacy in granulomatous versus vasculitic manifestations. Ann Rheum Dis 2012;71:327–33.
18. Iudici M, Pagnoux C, Courvoisier D, Cohen P, Hamidou M, Aouba A, et al. Granulomatosis with polyangiitis: data from the French Vasculitis Study Group Registry [abstract]. Arthritis Rheumatol 2019;71 Suppl 10. URL: https://acrabstracts.org/abstract/granulomatosis-with-polyangiitis-data-from-the-french-vasculitis-study-group-registry/.
19. Miloslavsky EM, Specks U, Merkel PA, Seo P, Spiera R, Langford CA, et al. Clinical outcomes of remission induction therapy for severe antineutrophil cytoplasmic antibody–associated vasculitis. Arthritis Rheum 2013;65:2441–9.
20. Hogan SL, Nachman PH, Poulton CJ, Hu Y, Blazek LN, Free ME, et al. Understanding long-term remission off therapy in antineutrophil cytoplasmic antibody-associated vasculitis. Kidney Int Rep 2019;4:551–60.
21. Koldingsnes W, Nossent JC. Baseline features and initial treatment as predictors of remission and relapse in Wegener's granulomatosis. J Rheumatol 2003;30:80–8.
22. Puéchal X, Iudici M, Calich AL, Vivot A, Terrier B, Régent A, et al. Rituximab for induction and maintenance therapy of granulomatosis with polyangiitis: a single-centre cohort study on 114 patients. Rheumatology (Oxford) 2019;58:401–9.
23. Stegeman CA, Tervaert JW, Sluiter WJ, Manson WL, de Jong PE, Kallenberg CG. Association of chronic nasal carriage of Staphylococcus aureus and higher relapse rates in Wegener granulomatosis. Ann Intern Med 1994;120:12–7.
24. Miloslavsky EM, Lu N, Unizony S, Choi HK, Merkel PA, Seo P, et al. Myeloperoxidase–antineutrophil cytoplasmic antibody (ANCA)–positive and ANCA-negative patients with granulomatosis with polyangiitis (Wegener's): distinct patient subsets. Arthritis Rheumatol 2016;68:2945–52.
25. Lionaki S, Blyth ER, Hogan SL, Hu Y, Senior BA, Jennette CE, et al. Classification of antineutrophil cytoplasmic autoantibody vasculitides: the role of antineutrophil cytoplasmic autoantibody specificity for myeloperoxidase or proteinase 3 in disease recognition and prognosis. Arthritis Rheum 2012;64:3452–62.
26. Trivioli G, Vaglio A. Long-term disease control in granulomatosis with polyangiitis: is low-dose rituximab the cure? [editorial]. Rheumatology (Oxford) 2019;58:380–1.
27. Schirmer JH, Wright MN, Herrmann K, Laudien M, Nölle B, Reinhold-Keller E, et al. Myeloperoxidase–antineutrophil cytoplasmic antibody (ANCA)–positive granulomatosis with polyangiitis (Wegener's) is a clinically distinct subset of ANCA-associated vasculitis: a retrospective analysis of 315 patients from a German vasculitis referral center. Arthritis Rheumatol 2016;68:2953–63.
28. Harper L, Morgan MD, Walsh M, Hoglund P, Westman K, Flossmann O, et al, for the EUVAS investigators. Pulse versus daily oral cyclophosphamide for induction of remission in ANCA-associated vasculitis: long-term follow-up. Ann Rheum Dis 2012;71:955–60.
29. De Groot K, Rasmussen N, Bacon PA, Tervaert JW, Feighery C, Gregorini G, et al. Randomized trial of cyclophosphamide versus methotrexate for induction of remission in early systemic antineutrophil cytoplasmic antibody–associated vasculitis. Arthritis Rheum 2005;52:2461–9.
30. Hoffman GS. Treatment of Wegener's granulomatosis: time to change the standard of care? [editorial]. Arthritis Rheum 1997;40:2099–104.
31. Guillevin L, Cordier JF, Lhote F, Cohen P, Jarrousse B, Royer I, et al. A prospective, multicenter, randomized trial comparing steroids and pulse cyclophosphamide versus steroids and oral cyclophosphamide in the treatment of generalized Wegener's granulomatosis. Arthritis Rheum 1997;40:2187–98.
32. Haubitz M, Schellong S, Gobel U, Schurek HJ, Schaumann D, Koch KM, et al. Intravenous pulse administration of cyclophosphamide versus daily oral treatment in patients with antineutrophil cytoplasmic antibody–associated vasculitis and renal involvement: a prospective, randomized study. Arthritis Rheum 1998;41:1835–44.
33. De Groot K, Adu D, Savage CO, for the EUVAS (European Vasculitis Study Group). The value of pulse cyclophosphamide in ANCA associated vasculitis: meta-analysis and critical review. Nephrol Dial Transplant 2001;16:2018–27.
34. Terrier B, Darbon R, Durel CA, Hachulla E, Karras A, Maillard H, et al. French recommendations for the management of systemic necrotizing vasculitides (polyarteritis nodosa and ANCA-associated vasculitides). Orphanet J Rare Dis 2020;15:351.
35. Yates M, Watts RA, Bajema IM, Cid MC, Crestani B, Hauser T, et al. EULAR/ERA-EDTA recommendations for the management of ANCA-associated vasculitis [published erratum appears in Ann Rheum Dis 2017;76:1480]. Ann Rheum Dis 2016;75:1583–94.
36. Guillevin L, Pagnoux C, Karras A, Khouatra C, Aumaitre O, Cohen P, et al, for the French Vasculitis Study Group. Rituximab versus azathioprine for maintenance in ANCA-associated vasculitis. N Engl J Med 2014;371:1771–80.
37. Iudici M, Porcher R, Riveros C, Ravaud P. Time-dependent biases in observational studies of comparative effectiveness research in rheumatology: a methodological review. Ann Rheum Dis 2019;78:562–9.
38. Sanders JS, de Joode AA, DeSevaux RG, Broekroelofs J, Voskuyl AE, van Paassen P, et al. Extended versus standard azathioprine maintenance therapy in newly diagnosed proteinase-3 anti-neutrophil cytoplasmic antibody-associated vasculitis patients who remain cytoplasmic anti-neutrophil cytoplasmic antibody-positive after induction of remission: a randomized clinical trial. Nephrol Dial Transplant 2016;31:1453–9.
39. Karras A, Pagnoux C, Haubitz M, Groot K, Puéchal X, Tervaert JW, et al. Randomised controlled trial of prolonged treatment in the remission phase of ANCA-associated vasculitis. Ann Rheum Dis 2017;76:1662–8.
40. Charles P, Perrodeau É, Samson M, Bonnotte B, Néel A, Agard C, et al. Long-term rituximab use to maintain remission of ANCA-associated vasculitis: a randomized trial. Ann Intern Med 2020;173:179–87.

APPENDIX A: THE FVSG INVESTIGATORS

The FVSG investigators and their affiliated institutions (all in France) are as follows: B. Ayach (Néphrologie, Centre Hospitalier [CH] Charleville-Mézières), B. Imbert (Médecine Interne, CH Universitaire [CHU] Grenoble), B. Graffin (Médecine Interne, Polyclinique Mutualiste, Ollioules), B. Legallicier (Néphrologie, CHU Rouen), C. Achard-Hottelart (Néphrologie, CHU Limoges), C. Hanrotel-Saliou (Néphrologie, CHU Brest), C. Khouatra (Pneumologie, CHU Lyon), C. Leské (Rhumatologie, CH Cholet), C. Charasse (Néphrologie, CH Saint-Brieuc), C. Le Hello (Médecine Vasculaire, CHU Caen), D. Merrien (Médecine Interne, CH Compiègne), E. Pasqualoni (Médecine Interne, CH Saint-Denis), E. Diot (Médecine Interne, CHU Tours), F. Grassin (Pneumologie, Hôpital d'Instruction des Armées, Brest), G. Jebrak (Pneumologie, CHU Bichat, Paris), G. Gondran (Médecine Interne, CHU Limoges), H. Desmurs-Clavel (Médecine Interne, CHU Lyon), H. Bezanahary (Médecine Interne, CHU Limoges), I. de Lacroix-Szmania (CH Intercommunal, Créteil), J.-J. Dion (Néphrologie, CH Charleville-Mézières), N. Limal (Médecine Interne, CHU Créteil), P. Godmer (Médecine Interne, CH Vannes), S. Vinzio (Médecine Interne, Groupe Hospitalier Mutualiste, Grenoble), S. Lanot (Rhumatologie, CH Alençon), T. Colin (Rhumatologie, CH Cherbourg), X. Delbrel (Médecine Polyvalente, CH Pau), Y. Ollivier (Médecine Interne, CHU Caen), Y. Crabol (Médecine Interne, Hôpital Cochin, Paris), J.-J. Boffa (Néphrologie, Hôpital Tenon, Paris), A. Lequellec (Médecine Interne, CHU Montpellier), A. Mahr (Médecine Interne, CHU Saint-Louis, Paris), B. Godeau (Médecine Interne, CHU Henri-Mondor, Créteil), B. Bienvenu (Médecine Interne, CHU Caen), C. Le Jeunne (Médecine Interne, Hôpital Cochin, Paris), É. Thervet (Néphrologie, HEGP, Paris), I. Marie (Médecine Interne, CHU Lyon), J. Rossert (Néphrologie, Hôpital Tenon, Paris), M. Michel (Médecine Interne, CHU Henri-Mondor, Créteil), and V. Loustaud-Ratti (Médecine Interne, CHU Limoges).

Arthritis & Rheumatology
Vol. 73, No. 4, April 2021, pp 651–659
DOI 10.1002/art.41557

American College of Rheumatology
Empowering Rheumatology Professionals

Multimorbidity in Antineutrophil Cytoplasmic Antibody–Associated Vasculitis: Results From a Longitudinal, Multicenter Data Linkage Study

Shifa H. Sarica,[1] Peter J. Gallacher,[2] Neeraj Dhaun,[2] Jan Sznajd,[3] John Harvie,[3] John McLaren,[4] Lucy McGeoch,[5] Vinod Kumar,[6] Nicole Amft,[7] Lars Erwig,[8] Angharad Marks,[9] Laura Bruno,[10] York Zöllner,[10] Corri Black,[1] and Neil Basu[11]

Objective. Antineutrophil cytoplasmic antibody–associated vasculitis (AAV) is considered a chronic, relapsing condition. To date, no studies have investigated multimorbidity in AAV nationally. This study was undertaken to characterize temporal trends in multimorbidity and report excess health care expenditures associated with multimorbidities in a national AAV cohort from Scotland.

Methods. Eligible patients with AAV were diagnosed between 1997 and 2017. Each patient was matched with up to 5 general population controls. Linked morbidity and health care expenditure data were retrieved from a Scottish national hospitalization repository and from published national cost data. Multimorbidity was defined as the development of ≥2 disorders. Prespecified morbidities, individually and together, were analyzed for risks and associations over time using modified Poisson regression, discrete interval analysis, and chi-square test for trend. The relationship between multimorbidities and health care expenditure was investigated using multivariate linear regression.

Results. In total, 543 patients with AAV (median age 58.7 years [range 48.9–68.0 years]; 53.6% male) and 2,672 general population controls (median age 58.7 years [range 48.9–68.0 years]; 53.7% male) were matched and followed up for a median of 5.1 years. AAV patients were more likely to develop individual morbidities at all time points, but especially <2 years after diagnosis. The highest proportional risk observed was for osteoporosis (adjusted incidence rate ratio 8.0, 95% confidence interval [95% CI] 4.5–14.2). After 1 year, 23.0% of AAV patients and 9.3% of controls had developed multimorbidity ($P < 0.0001$). After 10 years, 37.0% of AAV patients and 17.3% of controls were reported to have multimorbidity ($P < 0.0001$). Multimorbidity was associated with disproportionate increases in health care expenditures in AAV patients. Health care expenditure was highest for AAV patients with ≥3 morbidities (3.89-fold increase in costs, 95% CI 2.83–5.31; $P < 0.001$ versus no morbidities).

Conclusion. These findings emphasize the importance of holistic care in patients with AAV, and may identify a potentially critical opportunity to consider early screening.

This work was supported by the Aberdeen Development Trust and the Farr Institute of Health Informatics Research. The Farr Institute was supported by a 10-funder consortium: Arthritis Research UK, the British Heart Foundation, Cancer Research UK, the Economic and Social Research Council, the Engineering and Physical Sciences Research Council, the MRC, the NIHR, the National Institute for Social Care and Health Research, the Scottish Government Health Directorates Chief Scientist Office, and the Wellcome Trust (Scotland MR/K007017/1). Dr. Gallacher's work is supported by the Mason Medical Research Foundation, Lorna Smith Charitable Trust, and a Research Excellence award from the British Heart Foundation (grant RE/18/5/34216).

[1]Shifa H. Sarica, PhD, MPH, Corri Black, MBChB, BMedSci (Hons), MSc, MRCP, MFPH: University of Aberdeen, Aberdeen, UK; [2]Peter J. Gallacher, MBChB, MPH, Neeraj Dhaun, MBChB, PhD: University of Edinburgh British Heart Foundation Center of Research Excellence, University of Edinburgh, Edinburgh, UK; [3]Jan Sznajd, MBChB, John Harvie, MBChB, FRCP: Raigmore Hospital, Inverness, UK; [4]John McLaren, MBChB, FRCP: Whyteman's Brae Hospital, Kirkcaldy, UK; [5]Lucy McGeoch, MBChB, MRCP: Glasgow Royal Infirmary, Glasgow, UK; [6]Vinod Kumar, MBChB, MRCP: Ninewells Hospital, Dundee, UK; [7]Nicole Amft, MD, PhD: University Hospitals Birmingham NHS Foundation Trust, Birmingham, UK; [8]Lars Erwig, MD, PhD: GlaxoSmithKline, Stevenage, UK; [9]Angharad Marks, MBBCh, MSc, PhD: Abertawe Bro Morgannwg University Health Board, Swansea, UK; [10]Laura Bruno, MSc, York Zöllner, PhD: Hamburg University of Applied Sciences, Hamburg, Germany; [11]Neil Basu, MD, PhD: University of Glasgow, Glasgow, UK.

Drs. Sarica and Gallacher contributed equally to this work. Prof. Black and Dr. Basu are joint senior authors.

Dr. Erwig owns stock or stock options in Janssen. No other disclosures relevant to this article were reported.

Address correspondence to Neil Basu, MD, PhD, Institute of Infection, Immunity & Inflammation, University of Glasgow, Sir Graeme Davies Building, 120 University Place, Glasgow G12 8TA, UK. Email: neil.basu@glasgow.ac.uk.

Submitted for publication August 7, 2020; accepted in revised form October 8, 2020.

INTRODUCTION

The antineutrophil cytoplasmic antibody (ANCA)–associated vasculitides (AAVs) are a set of systemic autoimmune diseases comprising granulomatosis with polyangiitis (GPA), microscopic polyangiitis (MPA), and eosinophilic granulomatosis with polyangiitis (EGPA) (1). With modern immunosuppressive therapy, these previously fatal diseases have become chronic, relapsing conditions in which the mean 5-year survival rate is ~70% (2).

With improved survival, AAV patients are now at an increased risk of multimorbidity, defined as the presence of ≥2 concurrent long-term disorders (3). Multimorbidity is increasingly common in the general population (4) and has also been described in other chronic inflammatory conditions, including rheumatoid arthritis (5,6). It complicates chronic disease management and is associated with reduced functional status, decreased quality of life, and increased mortality (7,8). Multimorbidity also has important implications for the organization and delivery of health care, which is traditionally structured to optimize the management of individual diseases (9).

Previous studies have demonstrated an increased risk of several individual morbidities in AAV, including cardiovascular disease, diabetes mellitus, and venous thromboembolic disease (10–13). These associations are thought to be a consequence of chronic inflammation or the increasingly potent and toxic medications used to treat AAV (14). However, to our knowledge, no studies have yet investigated the frequency or burden of multimorbidity in AAV patients. In this Scottish national, multicenter data linkage study, we compare temporal trends in the incidence of a wide range of individual morbidities and multimorbidity between AAV patients and matched general population controls, and report the cost of excess resource consumption attributable to multimorbidity in AAV patients.

PATIENTS AND METHODS

Ethical considerations. This study was conducted in compliance with the Declaration of Helsinki. Approval was received from the Scotland Research Ethics Committee A (reference no. 15-SS-0152). Individual patient consent was not required as the research was approved by the Public Benefit and Privacy Panel for Health and Social Care, which oversees studies accessing anonymized health care data held by the NHS Scotland. Information governance, confidentiality, and data protection were undertaken according to the Data Protection Act of 1998. All study data were analyzed and held within a unique, secure national safe-haven environment (15) administered by the Electronic Data and Innovation Service, NHS Scotland.

Study design and data linkage. We performed a retrospective, matched-cohort, population-based data linkage study using routine health care data from multiple national registries in Scotland (see the flow diagram in Supplementary Figure 1, available on the *Arthritis & Rheumatology* website at http://onlinelibrary.wiley.com/doi/10.1002/art.41557/abstract). Record linkage was conducted by investigators at NHS Scotland, using a robust methodology that has previously been shown to produce highly accurate and complete data (16,17).

Study population. AAV patients were identified by clinicians using the European Medicines Agency criteria (18) in 7 secondary and tertiary care hospitals across Scotland. Patients were eligible for inclusion if they were diagnosed as having AAV after January 1, 1995 and were age ≥16 years at the time of data linkage. The date of AAV diagnosis was assigned as the index date. Each patient was matched with at least 1, but up to 5, general population controls based on age (±2 years), sex, and postal code of residence. General population controls were assigned the same index date as their matched AAV patient.

Study follow-up. Patients were followed up from the index date until their date of death or February 28, 2017, whichever came first. Information regarding cause of death was obtained via data linkage from the National Records of Scotland death registry, which records all deaths in Scotland (19).

Definition and identification of individual morbidities and multimorbidity. Morbidities were defined as clinically distinct diseases co-occurring with AAV, but which were not a direct complication of AAV itself (e.g., chronic kidney disease, neuropathy, arthritis, and sino-nasal disease). Our analysis focused a priori on a set of 12 individual morbidities of public health concern in elderly populations (as shown in Supplementary Figure 1 [http://onlinelibrary.wiley.com/doi/10.1002/art.41557/abstract]), which were identified following discussions between senior coauthors and an extensive review of the relevant literature describing multimorbidity in AAV (20,21). The majority of these morbidities have previously been shown to be identifiable from administrative data sets with moderate-to-high validity (21). Multimorbidity was defined as the presence of ≥2 disorders and was determined by summing each patient's individual morbidities at specific time points (years 1, 2, 5, and 10). Information regarding each patient's morbidities was obtained via data linkage with a Scottish national, population-based hospitalization repository. This registry holds information on the discharge codes of all hospitalizations in Scotland since the 1980s and details up to 6 diagnoses per admission (22). The first diagnosis corresponds to the primary reason for hospitalization, while the remaining diagnoses capture information regarding the patient's morbidities. All diagnostic codes recorded for each hospitalization were included in this analysis.

Morbidities were identified using previously validated International Classification of Diseases, Ninth Revision (ICD-9) codes (ICD-9 pre-1996; ICD-10 post-1996) (as listed in Supplementary Table 1, available on the *Arthritis & Rheumatology* website at http://onlinelibrary.wiley.com/doi/10.1002/art.41557/abstract)

(21,23,24). The first date that a relevant diagnostic code appeared in a patient's record was assigned as the incident date for that specific morbidity. Individual morbidities identified during the 5 years prior to the patient's enrollment in the study (i.e., prior to the index date) were classified as preexisting morbidities and were thus excluded from the analysis. This duration of "look-back" period has previously been shown to allow incident morbidities to be distinguished from prevalent morbidities with accuracy and reliability (25).

Determination of health care expenditure. Count data regarding the number of outpatient encounters, number of inpatient hospitalizations, and overall length of inpatient stay (on both general medical wards and intensive care units) were obtained via data linkage with the Scottish outpatients and hospitalizations registries for each study year (see Supplementary Figure 1 [http://onlinelibrary.wiley.com/doi/10.1002/art.41557/abstract]). The NHS Scottish Health Service Costs Book was used to obtain annual tariffs for resource consumption (26). Tariffs were inflated to 2016 values using the Hospital and Community Health Service Index. Inaccessible data regarding tariffs from pre-2002 were estimated using the 2002 tariff as the reference for deflation.

Statistical analysis. Baseline characteristics of the AAV patients and matched general population controls were summarized. Incident morbidities were summed for each participant and used to derive an ordinal variable representing patients with 0, 1, 2, or ≥3 morbidities. Differences in the proportions of AAV patients and general population controls in each of these categories were compared using a chi-square test for trend.

The overall risk of individual morbidities in AAV patients and matched controls was compared using modified Poisson regression models, adjusted for age, sex, and local health board (27,28). Discrete-time analysis was conducted with follow-up at 1, 2, 5, and 10 years using Lexis expansions (29). These time points were selected a priori based on current treatment guidelines on the duration of induction and remission therapy in AAV (30), in order to provide sufficient granularity to observe potential temporal changes in the occurrence of morbidities. The incidence rates for individual morbidities at each interval were calculated by dividing the number of morbidities observed in each interval by person-years of follow-up included in each interval. Data are expressed as the adjusted incidence rate ratio (IRR) with 95% confidence interval (95% CI), computed using the Poisson assumption (31).

A multivariate linear regression model, adjusted for age, sex, and socioeconomic deprivation status (for further clarification, see Supplementary Methods, available on the *Arthritis & Rheumatology* website at http://onlinelibrary.wiley.com/doi/10.1002/art.41557/abstract), was created to determine the relationship between number of individual morbidities and health care expenditure. As the residuals were not normally distributed, the continuous dependent variable "health care expenditure" was log-transformed using the natural logarithm. Homoscedasticity was evaluated using the Breusch-Pagan test. All analyses were performed in Stata (version 14) (32) and R (version 3.6.1) (33).

RESULTS

Patient characteristics. In total, 543 patients with AAV (median age at index date 58.7 years [range 48.9–68.0 years]; 53.6% male) were matched with 2,672 general population controls (median age at index date 58.7 years [range 48.9–68.0 years]; 53.7% male) and followed up for a median of 5.1 years (range 2.5–9.4 years) (Table 1). Of the patients with AAV, 316 (58.2%) had GPA, 157 (28.9%) had MPA, and 68 (12.5%) had EGPA. ANCAs with the proteinase 3 specificity were present in 52.7% of patients (286 of 543) and ANCAs with the myeloperoxidase specificity were present in 34.6% of patients (188 of 543). A total of 12.0% of patients with AAV (65 of 543) were classified as ANCA negative.

Risk of developing individual morbidities in AAV. The risk of developing most individual morbidities was higher in AAV patients than in general population controls (Figure 1). The morbidity most frequently observed in AAV patients during study follow-up was hypertension (19.7% of AAV patients [92 of 466] versus 9.4% of general population controls [234 of 2,482]; $P < 0.0001$) (Table 2). However, the highest proportional risk difference between AAV patients and general population controls was observed for osteoporosis (adjusted IRR 8.0, 95% CI 4.5–14.2) (Figure 1).

Table 1. Baseline characteristics of the AAV patients and general population controls*

	AAV patients	General population controls
No. of participants	543	2,672
Male sex, no. (%)	291 (53.6)	1,434 (53.7)
Age at index, median (IQR) years	58.7 (48.9–68.0)	58.7 (48.9–68.0)
Follow-up, median (IQR) years	5.1 (2.5–9.4)	5.2 (2.5–9.5)
AAV type, no. (%)		NA
GPA	316 (58.2)	
MPA	157 (28.9)	
EGPA	68 (12.5)	
Missing	2 (0.4)	
ANCA seropositivity, no. (%)		NA
PR3-ANCA	286 (52.7)	
MPO-ANCA	188 (34.6)	
ANCA negative	65 (12.0)	
Missing	4 (0.7)	

* AAV = antineutrophil cytoplasmic antibody (ANCA)–associated vasculitis; GPA = granulomatosis with polyangiitis; MPA = microscopic polyangiitis; EGPA = eosinophilic granulomatosis with polyangiitis; PR3 = proteinase 3; MPO = myeloperoxidase; NA = not applicable.

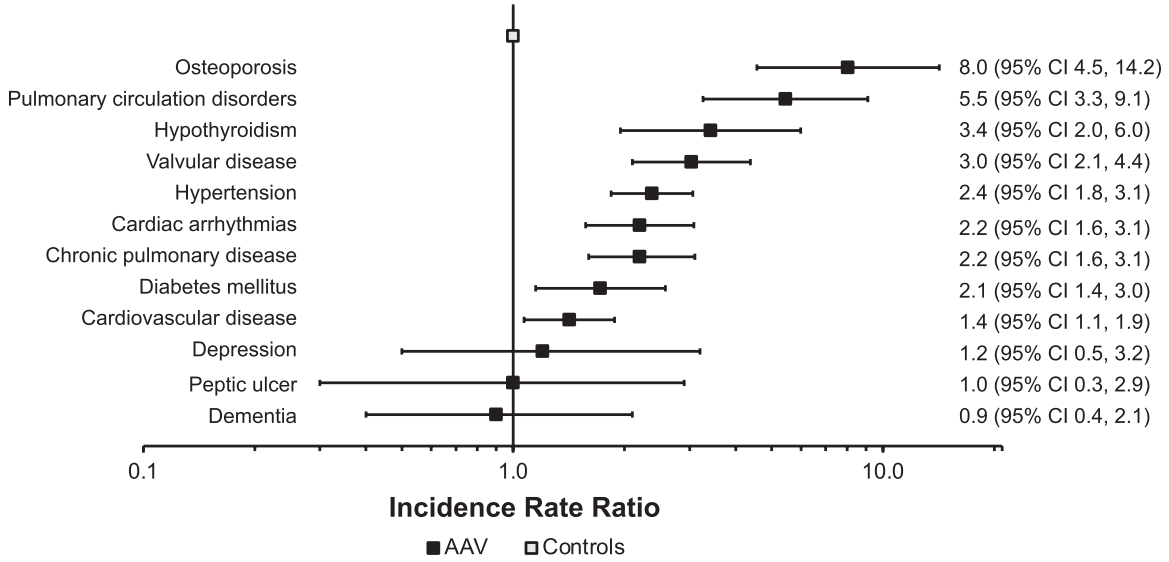

Figure 1. Comparison of the incidence of individual morbidities between patients with antineutrophil cytoplasmic antibody–associated vasculitis (AAV) and general population controls. Results are incidence rate ratios with 95% confidence intervals (95% CIs), adjusted for age, sex, and local health board. The rate of incident morbidity in the general population controls was set as the referent.

A sensitivity analysis exploring the proportional risk of hospital admissions due to hip fractures was performed to validate this finding. The risk of hip fractures in AAV patients was found to be twice that in general population controls (adjusted IRR 2.0, 95% CI 1.1–3.7).

To explore the influence of surveillance bias, a further sensitivity analysis was performed to evaluate the proportional risk of hypothyroidism and stroke in only those patients and controls with a record of at least 1 hospitalization during study follow-up (see Supplementary Results, available on the *Arthritis & Rheumatology* website at http://onlinelibrary.wiley.com/doi/10.1002/art.41557/abstract).

Table 2. Comparison of incident morbidities between AAV patients and general population controls during follow-up*

	AAV patients	General population controls	*P*
Cardiac arrhythmias	49 (9.6)	119 (5.0)	<0.0001
Cardiovascular disease	61 (12.6)	236 (9.5)	0.042
Chronic pulmonary disease	46 (9.7)	120 (4.7)	<0.0001
Depression	<5 (<0.9)	21 (0.8)	0.749
Diabetes mellitus	37 (7.2)	94 (3.6)	<0.0001
Dementia	6 (1.1)	32 (1.2)	0.846
Hypertension	92 (19.7)	234 (9.4)	<0.0001
Hypothyroidism	21 (4.0)	34 (1.3)	<0.0001
Osteoporosis	29 (5.4)	22 (0.8)	<0.0001
Peptic ulcer disease	<5 (<0.9)	21 (0.8)	0.918
Pulmonary circulation disorders†	31 (5.8)	30 (1.1)	<0.0001
Valvular disease	46 (8.7)	80 (3.0)	<0.0001

* Values are the number (%) of subjects. AAV = antineutrophil cytoplasmic antibody–associated vasculitis.
† A full list of conditions encompassed by this term is provided in the Supplementary materials.

Temporal trends in individual morbidities and multimorbidity in AAV. Figure 2 illustrates trends in the incidence of individual morbidities over time following the diagnosis of AAV. In general, the highest incidence for most morbidities was observed during the first 2 years of follow-up. This was especially marked for hypertension and hypothyroidism. However, a further increase in the incidence of several morbidities, including cardiovascular disease, diabetes mellitus, and chronic pulmonary disease, was also noted at 5–10 years after AAV diagnosis.

The proportion of study participants developing at least 1 incident morbidity increased over time in both AAV patients and general population controls (Figure 3). However, at every time point, AAV patients developed a significantly higher number of individual morbidities compared to general population controls ($P < 0.0001$ for all time points) (Figure 3).

Multimorbidity (defined as the presence of ≥2 disorders) was also more common in AAV patients than in general population controls at all time points. For example, after 1 year of follow-up, 23.0% of AAV patients (125 of 543) could be considered to have developed multimorbidity versus 9.3% of general population controls (248 of 2,672) ($P < 0.0001$). Ten years after diagnosis, a further 37.0% of AAV patients (101 of 273) had developed multimorbidity, compared with 17.3% of general population controls (235 of 1,362) ($P < 0.0001$).

Health care expenditure attributable to multimorbidity in AAV patients. Figure 4 illustrates the relationship between the number of individual incident morbidities and the total cost (in British pound sterling) of excess resource

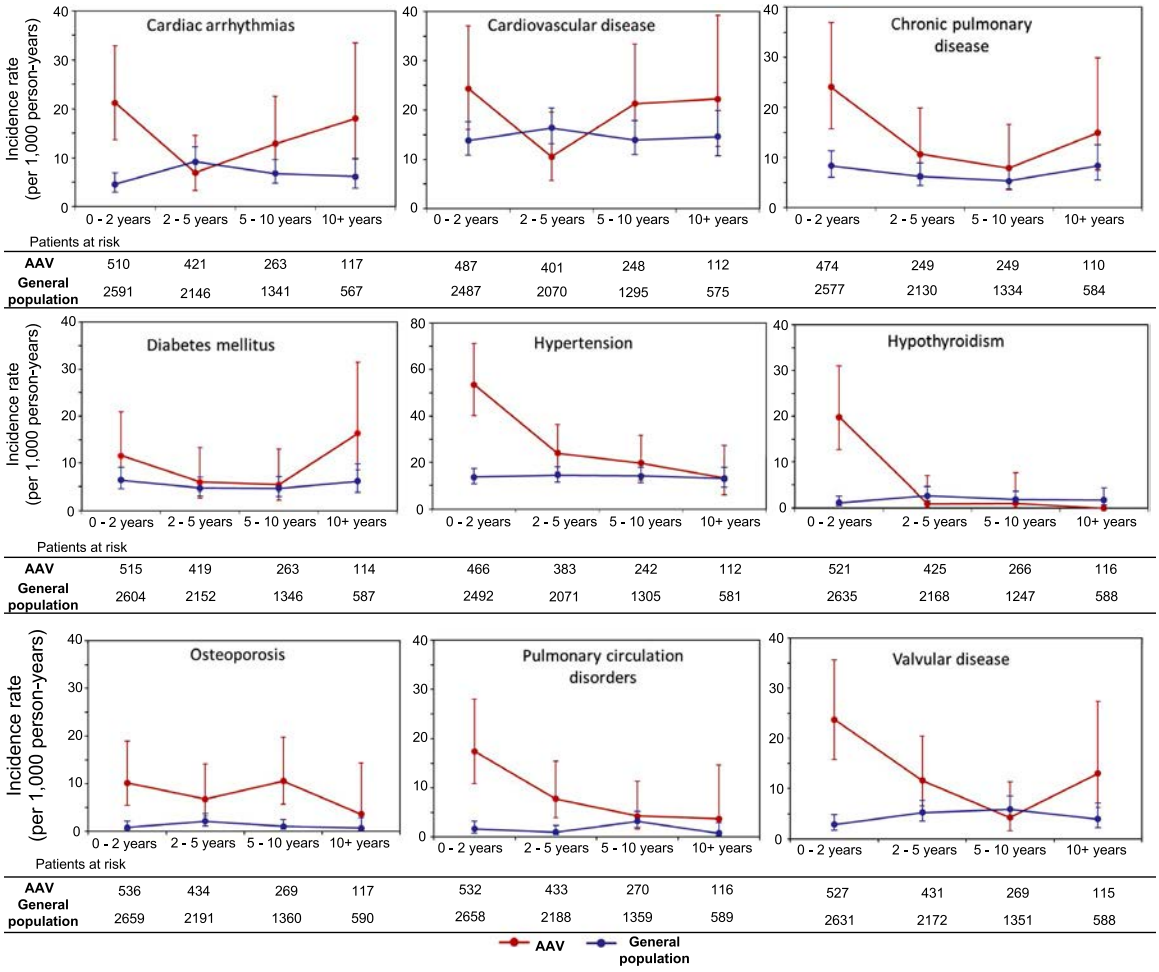

Figure 2. Temporal trends in the incidence of individual morbidities in patients with antineutrophil cytoplasmic antibody–associated vasculitis (AAV) and general population controls. Scale of the y-axis is different for hypertension. Numbers of subjects at each time point are shown below the graphs.

consumption due to outpatient encounters and inpatient hospitalizations (on both general medical wards and intensive care units) in 502 AAV patients during study follow-up. Multivariate linear regression modeling confirmed that the development of multimorbidity was associated with a proportionally higher cost of excess resource consumption in AAV patients (results shown in Supplementary Table 2, available on the *Arthritis & Rheumatology* website at http://onlinelibrary.wiley.com/doi/10.1002/art.41557/abstract). Compared to the development of no morbidities during study follow-up, the development of 2 morbidities was associated with a 2.78-fold increase (95% CI 2.09–3.71) ($P < 0.0001$) in health care expenditure in AAV patients, while the development of ≥3 morbidities was associated with a 3.89-fold increase (95% CI 2.83–5.31; $P < 0.001$) in health care expenditure in AAV patients. The increases in total health care expenditure observed with the development of multimorbidity were predominantly related to increases in inpatient, rather than outpatient, health care expenditure (see Supplementary Results and Supplementary Tables 3 and 4, available on the *Arthritis & Rheumatology* website at http://onlinelibrary.wiley.com/doi/10.1002/art.41557/abstract).

DISCUSSION

This is the first study to describe longitudinal trends in the incidence of multimorbidity and report the health care expenditure attributable to multimorbidity in a large national cohort of AAV patients from Scotland. We report a number of important observations.

First, AAV patients are at a significant risk of developing individual morbidities throughout their disease course, but especially in the first 2 years following diagnosis. Second, multimorbidity (the presence of ≥2 disorders) is common in AAV patients and significantly increases in frequency over time. Indeed, it affected almost one-quarter of the AAV patients in their first year after diagnosis, and affected more than one-third of patients by year 10 of follow-up. Third, multimorbidity is associated with an ~3-fold increase in excess health care expenditure in AAV patients.

Figure 3. Prevalence of morbidities at baseline and cumulative incidence of morbidities and multimorbidity at 1, 2, 5, and 10 years in patients with antineutrophil cytoplasmic antibody–associated vasculitis (AAV) and general population controls. $P < 0.0001$ by chi-square test for trend for all time points. Numbers of subjects at risk at each time point are shown below the graph.

Uniquely, our study demonstrates that AAV patients are at an increased risk of developing multimorbidity compared to general population controls. While the impact of multimorbidity has not been studied previously in AAV, we also found that multimorbidity is associated with a disproportionate increase in the cost of overall excess resource consumption. In comparison to AAV patients with no morbidities, the development of multimorbidity in AAV patients is associated with a 2–4-fold increase in total health care expenditure, but a 3–5-fold increase in inpatient health care expenditure. Relevant studies in other chronic disease populations, for example in patients with cardiovascular disease (34) or chronic kidney disease (35), have also demonstrated that multimorbidity is becoming the rule rather than the exception (9,36). The implications of this are significant, given the striking association of multimorbidity with polypharmacy, greater resource consumption, reduced quality of life, and poorer outcomes (7–9,37).

Our findings are also consistent with previous assessments of individual morbidities in AAV. In relation to the risk of cardiovascular disease, we demonstrate an increased risk in both early and late stages of AAV (10,11,38). Uniquely, our study extends these findings to other cardiovascular disorders, including valvular disease and arrhythmias, both of which demonstrate a similar bimodal risk pattern over time. Although primary cardiovascular disease is relatively uncommon in AAV, the observed risk may be due to a combination of chronic inflammation and glucocorticoid toxicity (39,40). It is possible that these findings are partly explained by surveillance bias. For example, valvular heart disease may have been diagnosed during routine echocardiography, an investigation that AAV patients are more likely to undergo than general population controls.

As general population controls were not selected from the time point of a new diagnosis, the increased risk observed for several morbidities early in the AAV disease course may also be explained by surveillance bias, due to the additional investigations performed in AAV patients following their index diagnosis. For example, AAV patients are commonly tested for hypothyroidism as part of their diagnostic evaluation. Nevertheless, an increased risk of hypothyroidism has previously been demonstrated in AAV patients prior to diagnosis, which aligns with accumulating evidence supporting shared mechanisms across the autoimmune disease spectrum (41). Similarly, the increased risk of osteoporosis in AAV patients observed in the present study may be related to current guideline recommendations for dual energy x-ray absorptiometry scans when patients commence treatment with glucocorticoids (30). Hip fractures are a reliable surrogate end point unlikely to be affected by surveillance bias and, as a result, we performed a sensitivity analysis to evaluate the risk of hip fractures during follow-up. Interestingly, we observed that the risk of hip fractures in AAV patients was twice that of general population controls—verifying our finding that osteoporosis risk is indeed increased in AAV patients.

Our findings have important implications for clinical practice. Specifically, the results of our temporal analysis highlight the importance of early screening for many common conditions in AAV patients, while also highlighting the significance of late-onset cardiovascular disease and diabetes mellitus. Our observation that peptic ulcer disease is no more likely in AAV patients than in general population controls, despite the frequent administration of high-dose glucocorticoids to patients with AAV, also appears to reflect the relative success of prophylactic therapies aimed at

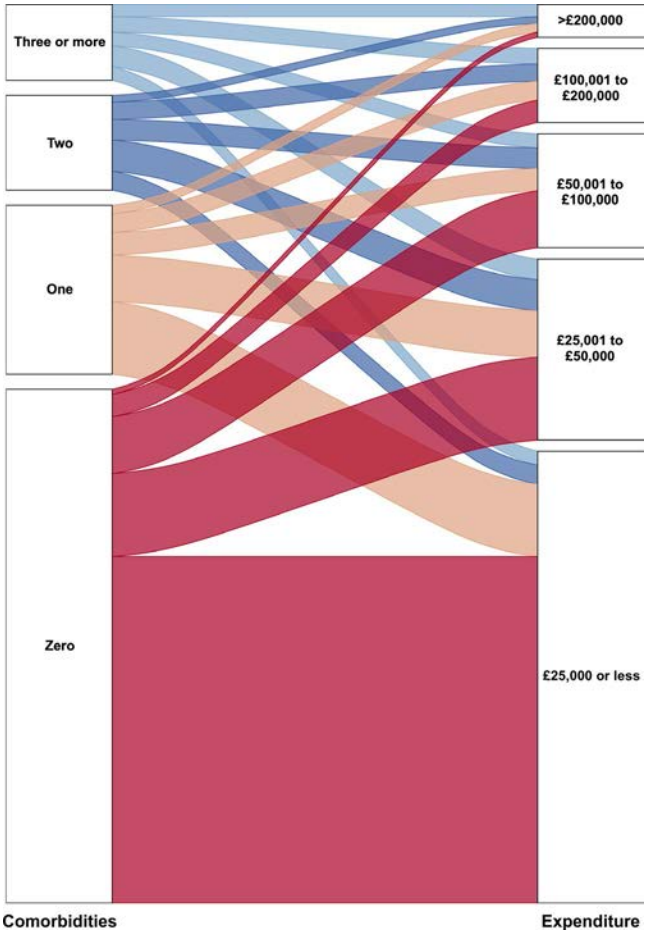

Figure 4. Alluvial plot illustrating the relationship between number of incident morbidities and total excess health care expenditure during the study follow-up in patients with antineutrophil cytoplasmic antibody–associated vasculitis (n = 502). Color figure can be viewed in the online issue, which is available at http://onlinelibrary.wiley.com/doi/10.1002/art.41557/abstract.

suppressing gastric acid secretion. Therefore, our data encourage similar preventative strategies for other morbidities.

Further research is required to understand what exact mechanisms underlie the increased risk of multimorbidity observed in AAV patients in the present study. Given the relationship between multimorbidity and adverse pharmacologic effects, such work could ultimately incentivize a shift toward a reduction in the use of pharmacologic therapies associated with numerous adverse effects, such as glucocorticoids. Indeed, with the transformation of AAV into a chronic disease, it is timely to prioritize a more holistic approach toward the management of AAV. This is analogous to the concept of "cancer survivorship," which has been established in oncology in response to improvements in cancer-related mortality. The overarching aim of cancer survivorship is to address the physical, psychological, and social health burden that arises as a consequence of cancer patients living longer (42). Clinicians must therefore consider how best to organize and deliver health care to AAV patients, in order to fully address both their multimorbidity and their primary disease. Greater collaboration with primary care providers is likely be critical to the potential success of any such move toward a more holistic approach to patient care in AAV.

Our study has several important strengths. Utilizing one of the largest cohorts of AAV patients, we adopted a comprehensive approach for improving our understanding of the burden associated with multimorbidity in AAV patients. Indeed, our method for identifying AAV patients suitable for inclusion in our cohort was also robust. In addition, we assessed prevalent morbidity burden using a validated length of "look-back" period (25) and previously verified ICD9/ICD-10 discharge coding (21,23,24), which has a reported accuracy of ~96% for common diagnoses recorded in the SMR01 data set (43).

However, a number of limitations must be considered. First, our study identified morbidities from secondary care records, which mostly capture major disorders. Despite including all available diagnostic codes, relatively minor disorders may have been overlooked by secondary care coders, and therefore our incidence estimates are likely to be conservative. However, this will have affected AAV patients and general population controls equally.

Second, given the higher hospitalization rate observed among AAV patients (98% versus 79% of general population controls), the IRRs for conditions managed in primary care are likely to be overestimates. To address this limitation, we performed a sensitivity analysis including only those patients and controls with a hospitalization record, and found that the degree of overestimation was small for hypothyroidism, stroke, and myocardial infarction (see Supplementary Results [http://onlinelibrary.wiley.com/doi/10.1002/art.41557/abstract]).

Third, patients not hospitalized in the 5 years prior to their index date were classified as having no preexisting morbidities. It is therefore difficult to be certain exactly when these patients developed "incident" morbidities. To limit the impact of this, we utilized a validated, fixed 5-year look-back period (25) to standardize the identification of baseline morbidities across all patients.

Fourth, study follow-up was limited to a median period of 5 years, which may partly explain why we failed to demonstrate an increased risk of depression or dementia in AAV patients. Although sufficient for identifying relatively acute-onset conditions, longer follow-up is required to reliably establish the occurrence of more gradual-onset disorders, such as depression and dementia.

Fifth, despite being one of the largest studies of its kind, we were unable to undertake stratified analysis by AAV type, due to a lack of statistical power.

In conclusion, this novel study is the most comprehensive and detailed analysis of multimorbidity in AAV patients to date. AAV patients are at a high risk of developing individual morbidities, especially early in their disease course. Multimorbidity is also common in AAV patients and is associated with disproportionate increases in health care expenditure. Our findings emphasize the importance of holistic care in AAV patients and the need to consider early screening for other conditions.

ACKNOWLEDGMENTS

The authors wish to thank electronic Data Research and Innovation Service Scotland for assisting with study approvals and data access in the National Safe Haven, as well as the University of Aberdeen Health Economics Research Unit for their support with the health care utilization analysis.

AUTHOR CONTRIBUTIONS

All authors were involved in drafting the article or revising it critically for important intellectual content, and all authors approved the final version to be published. Dr. Basu had full access to all of the data in the study and takes responsibility for the integrity of the data and the accuracy of the data analysis.

Study conception and design. Sarica, Marks, Black, Basu.
Acquisition of data. Sarica, Gallacher, Dhaun, Sznajd, Harvie, McLaren, McGeoch, Kumar, Amft, Erwig, Marks, Bruno, Zöllner, Black, Basu.
Analysis and interpretation of data. Sarica, Gallacher, Amft, Black, Basu.

ADDITIONAL DISCLOSURE

Author Erwig is an employee of GlaxoSmithKline.

REFERENCES

1. Watts RA, Lane SE, Bentham G, Scott DG. Epidemiology of systemic vasculitis: a ten-year study in the United Kingdom. Arthritis Rheum 2000;43:414–9.
2. Rhee RL, Hogan SL, Poulton CJ, McGregor JA, Landis JR, Falk RJ, et al. Trends in long-term outcomes among patients with antineutrophil cytoplasmic antibody–associated vasculitis with renal disease. Arthritis Rheumatol 2016;68:1711–20.
3. Diederichs C, Berger K, Bartels DB. The measurement of multiple chronic diseases—a systematic review on existing multimorbidity indices. J Gerontol A Biol Sci 2011;66:301–11.
4. Cassell A, Edwards D, Harshfield A, Rhodes K, Brimicombe J, Payne R, et al. The epidemiology of multimorbidity in primary care: a retrospective cohort study. Brit J Gen Pract 2018;68:e245–51.
5. Radner H, Yoshida K, Smolen JS, Solomon DH. Multimorbidity and rheumatic conditions—enhancing the concept of comorbidity [review]. Nat Rev Rheumatol 2014;10:252–6.
6. Daïen CI, Tubery A, Beurai-Weber M, du Cailar G, Picot MC, Jaussent A, et al. Relevance and feasibility of a systematic screening of multimorbidities in patients with chronic inflammatory rheumatic diseases. Joint Bone Spine 2019;86:49–54.
7. Gijsen R, Hoeymans N, Schellevis FG, Ruwaard D, Satariano WA, van den Bos GA. Causes and consequences of comorbidity: a review. J Clin Epidemiol 2001;54:661–74.
8. Fortin M, Lapointe L, Hudon C, Vanasse A, Ntetu AL, Maltais D. Multimorbidity and quality of life in primary care: a systematic review. Health Qual Life Outcomes 2004;2:51.
9. Barnett K, Mercer SW, Norbury M, Watt G, Wyke S, Guthrie B. Epidemiology of multimorbidity and implications for health care, research, and medical education: a cross-sectional study. Lancet 2012;380:37–43.
10. Houben E, Penne EL, Voskuyl AE, van der Heijden JW, Otten RH, Boers M, et al. Cardiovascular events in anti-neutrophil cytoplasmic antibody-associated vasculitis: a meta-analysis of observational studies. Rheumatology (Oxford) 2018;57:555–62.
11. Morgan MD, Turnbull J, Selamet U, Kaur-Hayer M, Nightingale P, Ferro CJ, et al. Increased incidence of cardiovascular events in patients with antineutrophil cytoplasmic antibody–associated vasculitides: a matched-pair cohort study. Arthritis Rheum 2009;60:3493–500.
12. Englund M, Merkel PA, Tomasson G, Segelmark M, Mohammad AJ. Comorbidities in patients with antineutrophil cytoplasmic antibody-associated vasculitis versus the general population. J Rheumatol 2016;43:1553–8.
13. Li L, Neogi T, Jick S. A cohort study of comorbidity in patients with granulomatosis with polyangiitis. Rheumatology (Oxford) 2018;57:291–9.
14. King C, Harper L, Little M. The complications of vasculitis and its treatment. Best Pract Res Clin Rheumatol 2018;32:125–36.
15. Pavis S, Morris AD. Unleashing the power of administrative health data: the Scottish model. Public Health Res Pract 2015;25:e2541541.
16. Evans JM, MacDonald TM. Record-linkage for pharmacovigilance in Scotland. Br J Clin Pharmacol 1998;47:105–10.
17. ScotPHO: Public Health Information for Scotland. ISD linked database. October 2016. URL: http://www.scotpho.org.uk/publications/overview-of-key-data-sources/scottish-national-data-schemes/isd-linked-database.
18. Watts R, Lane S, Hanslik T, Hauser T, Hellmich B, Koldingsnes W, et al. Development and validation of a consensus methodology for the classification of the ANCA-associated vasculitides and polyarteritis nodosa for epidemiological studies. Ann Rheum Dis 2007;66:222–7.
19. National Records of Scotland (NRS). Deaths: background information. URL: https://www.nrscotland.gov.uk/statistics-and-data/statistics/statistics-by-theme/vital-events/deaths/deaths-background-information.
20. Boyd CM, Darer J, Boult C, Fried LP, Boult L, Wu AW. Clinical practice guidelines and quality of care for older patients with multiple comorbid diseases: implications for pay for performance. JAMA 2005;294:716–24.
21. Tonelli M, Wiebe N, Fortin M, Guthrie B, Hemmelgarn BR, James MT, et al. Methods for identifying 30 chronic conditions: application to administrative data. BMC Med Inform Decis Mak 2015;15:1–11.
22. NHS Scotland Information Services Division (ISD). SMR datasets. SMR01: general/acute inpatient and day case dataset. URL: https://www.ndc.scot.nhs.uk/Data-Dictionary/SMR-Datasets/SMR01-General-Acute-Inpatient-and-Day-Case/.
23. Quan H, Sundararajan V, Halfon P, Fong A, Burnand B, Luthi JC, et al. Coding algorithms for defining comorbidities in ICD-9-CM and ICD-10 administrative data. Med Care 2005;43:1130–9.
24. O'Donnell S, for the Canadian Chronic Disease Surveillance System (CCDSS) Osteoporosis Working Group. Use of administrative data for national surveillance of osteoporosis and related fractures in Canada: results from a feasibility study. Arch Osteoporos 2013;8:143.
25. Preen DB, Holman CD, Spilsbury K, Semmens JB, Brameld KJ. Length of comorbidity lookback period affected regression model performance of administrative health data. J Clin Epidemiol 2006;59:940–6.
26. Public Health Scotland. NHS Scotland Information Services Division (ISD) costs book. 2019. URL: https://www.isdscotland.org/Health-topics/Finance/Costs/Detailed-tables/.
27. Zou GY. A modified Poisson regression approach to prospective studies with binary data. Am J Epidemiol 2004;159:702–6.
28. Zou GY, Donner A. Extension of the modified Poisson regression model to prospective studies with correlated binary data. Stat Methods Med Res 2013;22:661–70.
29. Stsplit: split and join time-span records. College Station (TX): StataCorp; 2013.
30. Yates M, Watts RA, Bajema IM, Cid MC, Crestani B, Hauser T, et al. EULAR/ERA-EDTA recommendations for the management of ANCA-associated vasculitis. Ann Rheum Dis 2016;75:1583–94.
31. Kirkwood BR, Sterne JAC. Essential medical statistics. 2nd ed. Oxford: Wiley-Blackwell; 2003.

32. Stata statistical software: release 14.0. College Station (TX): StataCorp; 2015.
33. The R project for statistical computing. URL: https://www.R-project.org/.
34. Glynn LG, Buckley B, Reddan D, Newell J, Hinde J, Dinneen SF, et al. Multimorbidity and risk among patients with established cardiovascular disease: a cohort study. Br J Gen Pract 2008;58:488–94.
35. Fraser SD, Taal MW. Multimorbidity in people with chronic kidney disease: implications for outcomes and treatment. Curr Opin Nephrol Hypertens 2016;25:465–72.
36. Violan C, Foguet-Boreu Q, Flores-Mateo G, Salisbury C, Blom J, Freitag M, et al. Prevalence, determinants and patterns of multimorbidity in primary care: a systematic review of observational studies. PLoS One 2014;9:e102149.
37. Gallacher KI, Batty GD, McLean G, Mercer SW, Guthrie B, May CR, et al. Stroke, multimorbidity and polypharmacy in a nationally representative sample of 1,424,378 patients in Scotland: implications for treatment burden. BMC Med 2014;12:1–9.
38. Aviña-Zubieta JA, Mai A, Amiri N, Dehghan N, Tan JA, Sayre EC, et al. Risk of myocardial infarction and stroke in patients with granulomatosis with polyangiitis (Wegener's): a population-based study. Arthritis Rheumatol 2016;68:2752–9.
39. Christiansen CF, Christensen S, Mehnert F, Cummings SR, Chapurlat RD, Sørensen HT. Glucocorticoid use and risk of atrial fibrillation or flutter: a population-based, case-control study. Arch Intern Med 2009;169:1677–83.
40. Booth AD, Almond MK, Burns A, Ellis P, Gaskin G, Neild GH, et al. Outcome of ANCA-associated renal vasculitis: a 5-year retrospective study. Am J Kidney Dis 2003;41:776–84.
41. Prendecki M, Martin L, Tanna A, Antonelou M, Pusey CD. Increased prevalence of thyroid disease in patients with antineutrophil cytoplasmic antibodies-associated vasculitis. J Rheumatol 2018;45:686–9.
42. Lagergren P, Schandl A, Aaronson NK, Adami HO, de Lorenzo F, Denis L, et al. Cancer survivorship: an integral part of Europe's research agenda [review]. Mol Oncol 2019;13:624–35.
43. Public Health Scotland. Data quality assurance; products and services. URL: http://www.isdscotland.org/Products-and-Services/Data-Quality/Assessments/index.asp?Co=Y.

American College of Rheumatology
Empowering Rheumatology Professionals

Arthritis & Rheumatology
Vol. 73, No. 4, April 2021, pp 660–670
DOI 10.1002/art.41570

Large-Scale Characterization of Systemic Sclerosis Serum Protein Profile: Comparison to Peripheral Blood Cell Transcriptome and Correlations With Skin/Lung Fibrosis

Chiara Bellocchi,[1] Jun Ying,[2] Ellen A. Goldmuntz,[3] Lynette Keyes-Elstein,[4] John Varga,[5] Monique E. Hinchcliff,[6] Marka A. Lyons,[2] Peter McSweeney,[7] Daniel E. Furst,[8] Richard Nash,[7] Leslie J. Crofford,[9] Beverly Welch,[3] Jonathan G. Goldin,[10] Ashley Pinckney,[4] Maureen D. Mayes,[2] Keith M. Sullivan,[11] and Shervin Assassi[2]

Objective. To provide a large-scale assessment of serum protein dysregulation in diffuse cutaneous systemic sclerosis (dcSSc) and to investigate serum protein correlates of SSc fibrotic features.

Methods. We investigated serum protein profiles of 66 participants with dcSSc at baseline who were enrolled in the Scleroderma: Cyclophosphamide or Transplant Trial and 66 age- and sex-matched healthy control subjects. A panel of 230 proteins, including several cytokines and chemokines, was investigated. Whole blood gene expression profiling in concomitantly collected samples was performed.

Results. Among the participants with dcSSc, the mean disease duration was 2.3 years. All had interstitial lung disease (ILD), and none were being treated with immunosuppressive agents at baseline. Ninety proteins were differentially expressed in participants with dcSSc compared to healthy control subjects. Similar to previous global skin transcript results, hepatic fibrosis, granulocyte and agranulocyte adhesion, and diapedesis were the top overrepresented pathways. Eighteen proteins correlated with the modified Rodnan skin thickness score (MRSS). Soluble epidermal growth factor receptor was significantly down-regulated in dcSSc and showed the strongest negative correlation with the MRSS, being predictive of the score's course over time, whereas α_1-antichymotrypsin was significantly up-regulated in dcSSc and showed the strongest positive correlation with the MRSS. Furthermore, higher levels of cancer antigen 15-3 correlated with more severe ILD, based on findings of reduced forced vital capacity and higher scores of disease activity on high-resolution computed tomography. Only 14 genes showed significant differential expression in the same direction in serum protein and whole blood RNA gene expression analyses.

Conclusion. Diffuse cutaneous SSc has a distinct serum protein profile with prominent dysregulation of proteins related to fibrosis and immune cell adhesion/diapedesis. The differential expression for most serum proteins in SSc is likely to originate outside the peripheral blood cells.

INTRODUCTION

Systemic sclerosis (SSc; scleroderma) is a complex autoimmune disorder in which vascular involvement, immune dysregulation with autoantibody production, and fibrosis are the main pathologic processes (1). As is evident from a standardized mortality ratio of 3.5 (2), SSc is associated with a substantial mortality and disease burden. Development of effective

Supported by the Karen Brown Scleroderma Foundation, the NIH (grants R01-AR-073284 and UL1-TR-000371 and National Institute of Arthritis and Musculoskeletal and Skin Diseases grant P30-AR-061271), and the Department of Defense (grant W81XWH-16-1-0296). The Scleroderma: Cyclophosphamide or Transplantation (SCOT) study was supported by awards from the National Institute of Allergy and Infectious Diseases, NIH, to the study contract holder Duke University (grants N01-AI-05419 and HHSN 272201100025C).

[1]Chiara Bellocchi, MD: The University of Texas Health Science Center at Houston and McGovern Medical School, Houston, and Fondazione IRCCS Ca' Granda Ospedale Maggiore Policlinico di Milano, Milan, Italy; [2]Jun Ying, MS, Marka A. Lyons, MA, Maureen D. Mayes, MD, MPH, Shervin Assassi, MD, MS: The University of Texas Health Science Center at Houston and McGovern Medical School, Houston; [3]Ellen A. Goldmuntz, MD, PhD, Beverly Welch, RN, MSN: National Institute of Allergy and Infectious Diseases, NIH, Rockville, Maryland; [4]Lynette Keyes-Elstein, DrPH, Ashley Pinckney, MS: Rho Federal Systems Division, Inc., Durham, North Carolina; [5]John Varga, MD: Northwestern University, Chicago, Illinois; [6]Monique E. Hinchcliff, MD: Yale University School of Medicine, New Haven, Connecticut; [7]Peter McSweeney, MD, Richard Nash, MD: Colorado Blood Cancer Institute, Denver; [8]Daniel E. Furst, MD: University of California Los Angeles, University of Washington, Seattle, and University of Florence, Florence, Italy; [9]Leslie J. Crofford, MD: Vanderbilt University Medical Center, Nashville, Tennessee; [10]Jonathan G. Goldin, MD, PhD: University of California Los Angeles; [11]Keith M. Sullivan, MD: Duke University, Durham, North Carolina.

No potential conflicts of interest relevant to this article were reported.

Address correspondence to Shervin Assassi, MD, MS, 6431 Fannin, MSB 5.266, Houston, TX 77030. Email: shervin.assassi@uth.tmc.edu.

Submitted for publication February 19, 2020; accepted in revised form October 27, 2020.

treatment strategies for SSc has been hampered by an incomplete understanding of disease pathogenesis and the underlying molecular heterogeneity. Genome-wide association studies (3,4) and whole genome microarray studies (5,6) have provided new insights into disease pathogenesis at the DNA and RNA levels. An interferon (IFN) signature is the most prominent gene expression signature in SSc peripheral blood cells (5), and IFN-inducible chemokines correlate with disease severity (7).

Although changes in serum protein profiles, as opposed to findings at the DNA or RNA level, may be more closely associated with disease pathogenesis, data on large-scale examination of serum proteins in SSc are still scarce. Investigations performed on small panels of proteins showed that chemokines, vascular growth factors, and adhesion molecules such as interleukin-8 (IL-8), vascular endothelial growth factor (VEGF), angiopoietin 2 (Ang-1), platelet endothelial cellular adhesion molecule 1 (PECAM-1) are markers of early disease and reflect endothelial dysregulation in SSc (8–10). IL-6 is related to lung fibrosis and might be predictive of disease progression in early SSc interstitial lung disease (ILD) (11). Moreover, levels of adipokines, such as leptin and adiponectin, have a negative correlation with changes in SSc skin fibrosis (12–14).

Recently, a study performed with the use of SOMAscan aptamer technology in 34 patients with diffuse cutaneous SSc (dcSSc) and 15 control subjects identified tumor necrosis factor (TNF), IFNγ, transforming growth factor β (TGFβ), and IL-13 as potential upstream regulators in SSc (15). Few other studies have recently explored larger panels of serum proteins in SSc (16,17).

In the present study, we investigated an extended panel of 230 serum proteins in serum samples obtained at baseline from individuals with dcSSc (18) who were enrolled in the Scleroderma: Cyclophosphamide or Transplantation (SCOT) Trial and compared these findings at a 1:1 ratio to serum proteins from matched healthy control subjects in order to provide a hypothesis-generating assessment of serum protein dysregulation and its clinical correlates in SSc (19). Moreover, availability of concomitantly collected whole blood RNA samples enabled direct comparison between SSc serum protein and whole blood gene expression profiles, showing that the differential expression for most serum proteins in SSc is likely to originate outside the peripheral blood cells.

PATIENTS AND METHODS

Selection of study population. Of the 75 participants with dsSSc who were included in the SCOT trial, 66 had a serum sample obtained at baseline available for analysis. Samples obtained at baseline were examined in the present study. None of the participants were receiving immunosuppressive agents except for ≤10 mg per day of prednisone or its equivalent during blood sample collection at baseline. However, 27 participants had received immunosuppressive agents in the 2 months prior to baseline sample collection.

Briefly, the inclusion criteria included diffuse cutaneous involvement, lung or kidney involvement, and a disease duration of <5 years (calculated from the onset of the first non–Raynaud's symptom). Exclusion criteria included significant prior treatment with cyclophosphamide (CYC; either oral or intravenous), presence of clinically significant rheumatic diseases other than SSc, any active uncontrolled infection, or HIV, hepatitis C virus, and hepatitis B virus infections. All SCOT participants provided informed consent, and the SCOT protocol was approved by the Institutional Review Board of all participating institutions. Detailed information on the selection of participants and study design have been published previously (19). Additionally, serum from healthy controls that were matched at a 1:1 ratio based on age (±10 years) and sex was also investigated in the present study.

Severity of lung involvement was evaluated by forced vital capacity percent predicted (FVC%) (19). As another surrogate for ILD severity, standardized volumetric high-resolution computed tomography (HRCT) scanning was performed, and quantitative interstitial lung disease (QILD) score was measured using an established algorithm. The QILD score (expressed as a percentage) represents the sum of quantitative lung fibrosis, quantitative ground glass, and quantitative honeycombing for all lung lobes (20,21). The MRSS was used to assess severity of skin involvement (22). Antibody profiles were determined using commercial laboratories at each site.

Serum protein determination. Serum protein assays were performed by Myriad Rules-Based Medicine using Human Discovery Multi-Analyte Profiling (MAP) (https://myriadrbm.com/scientific-media/multiplex-assay-development-white-paper/) multiplexed immune assay version 2, which was the most comprehensive panel of proteins available with this technology at the time of study. This panel includes an extensive list of cytokines, chemokines, metabolic markers, hormones, growth factors, tissue remodeling proteins, angiogenesis markers, acute-phase reactants, and cancer markers that can reliably and reproducibly be measured with this technology. Levels of 228 serum proteins were determined with this assay.

All samples were stored at a temperature lower than –70°C and had not been previously thawed. An aliquot of each sample was added to individual microsphere multiplexes of the selected MAP and blocker. After incubation, multiplexed cocktails of biotinylated reporter antibodies were added. Multiplexes were labeled using an excess of streptavidin–phycoerythrin solution. The resulting data were interpreted using proprietary software developed by Myriad Rules-Based Medicine. In addition, 2 cytokines considered to be pertinent to SSc pathogenesis, IL-10 and IL-6, were determined by ultrasensitive Simoa Assays (Quanterix) (23).

For each assay, the lower limit of quantification (LLOQ) and upper limit of quantification (ULOQ) were determined by Myriad Rules-Based Medicine, representing the concentration at the lower and upper limit of the linear range of the standard curve,

respectively (i.e., the lowest and highest amount of protein that can be detected accurately).

Analysis of gene expression and its relationship to serum proteins. Global gene expression studies on whole blood RNA samples obtained at baseline (stored in Tempus tubes) from SCOT participants and from matched controls were examined using Illumina Human HT-12 bead arrays. All microarray experiments were performed in a single batch (24). Data were normalized according to the quantile method. A corresponding transcript was present on the microarray platform for the majority of investigated proteins. We focused on the transcripts that corresponded to the investigated proteins. Specifically, 282 transcripts corresponding to 172 examined proteins were identified. Only 10 (5.5%) of 182 serum proteins did not have a matching probe on the microarray platform. For the transcript analysis, the data set was filtered by the list of corresponding 282 transcripts. Differentially expressed transcripts identified at a false discovery rate (FDR) of <0.1 in SSc participants compared to controls were analyzed by 2-sample *t*-test. We used a less stringent FDR cutoff for the analysis of differentially expressed transcripts than was used for the protein analysis (FDR of <0.1 versus FDR of <0.05) as the effect size (i.e., fold change) tends to be lower at the RNA level than at the protein level. For example, fold changes in transcript levels in SSc participants compared to controls among the 282 transcripts investigated ranged from 0.61 to 1.41 whereas the fold change in the corresponding proteins ranged from 0.4 to 3.68. Subsequently, the list of differentially expressed transcripts was intersected with the list of differentially expressed proteins. Microarray analysis was performed with BRB ArrayTools (National Cancer Institute, National Institutes of Health) (25).

Interferome database search. We examined whether the differentially expressed serum proteins in SSc participants versus control subjects were IFN-inducible using the Interferome version 2.01 database (http://interferome.its.monash.edu.au/interferome/) (26). For the Interferome database, *Homo sapiens* was chosen as species and lung, skin, and blood were selected as organs. A list of type I IFN–inducible proteins was generated.

Statistical analysis. Proteins with levels below the LLOQ in >50% of SSc samples collected at baseline were excluded from the analysis. A total of 182 proteins (79.1%) had a detectable level in >50% of SSc samples. Of these 182 proteins, 128 proteins (70.2%) had measurements above the LLOQ in all samples. For the remainder of proteins, levels below the LLOQ were replaced by the LLOQ. Moreover, protein measurements above the ULOQ were replaced by the ULOQ. As shown in Supplementary Figure 1 (http://onlinelibrary.wiley.com/doi/10.1002/art.41570/abstract), raw values of the majority of the serum proteins showed a right-skewed distribution, and protein expression data were natural log–transformed to approximately conform to normality. Principal components analysis (PCA) was performed to identify outliers. *T*-tests were used to estimate differential expression for each protein between SSc participants and control subjects. *P* values were adjusted for multiple testing using the Benjamini-Hochberg method (27).

Proteins with an FDR of <0.05 were considered to be differentially expressed in the comparison of SSc participants to control subjects. Subsequently, differentially expressed proteins were modeled using Ingenuity Pathway Analysis software (Qiagen [https://digitalinsights.qiagen.com/products-overview/discovery-insights-portfolio/analysis-and-visualization/qiagen-ipa/]) to identify the overrepresented canonical pathways and to predict activated upstream cytokines/growth factors. The goal of Upstream Regulator Analysis is to identify upstream regulators of a molecular profile and predict whether they are activated or inhibited. This analysis is based on expected causal effects between upstream cytokines/growth factors and targets; the expected causal effects are derived from the literature compiled in Ingenuity Knowledge Base (28). A Z score algorithm is used to make predictions. The

Table 1. Demographic and clinical characteristics of the SCOT participants and control subjects*

Features	Participants with dcSSc (n = 66)	Control subjects (n = 66)
Age, mean ± SD years	45.3 ± 10.3	46.3 ± 9.5
Female sex	40 (60.6)	40 (60.6)
Race		
African American	6 (9.1)	9 (13.6)
Asian	3 (4.5)	0 (0)
Other	6 (9.1)	0 (0)
White	51 (77.3)	57 (86.4)
Disease duration, mean ± SD years	2.31 ± 1.25	NA
MRSS score, mean ± SD	29.22 ± 9.35	NA
FVC%, mean ± SD	74.62 ± 15.61	NA
QILD score, mean ± SD	22.92 ± 11.63	NA
QILD score of >0	66 (100)	NA
Autoantibodies		
Positive		
ANAs	57 (86.4)	NA
ACAs	4 (6.1)	NA
ATAs	26 (39.4)	NA
RNPs	10 (15.2)	NA
Negative		
ANAs	7 (10.6)	NA
ACAs	56 (84.8)	NA
ATAs	39 (59.1)	NA
RNPs	55 (83.3)	NA
Testing not performed		
ANAs	2 (3)	NA
ACAs	6 (9.1)	NA
ATAs	1 (1.5)	NA
RNPs	1 (1.5)	NA

* Except where indicated, values are the number (%). SCOT = Scleroderma: Cyclophosphamide or Transplantation; dcSSc = diffuse cutaneous systemic sclerosis; ANAs = antinuclear antibodies; ACAs = anticentromere antibodies; ATAs = anti–topoisomerase I antibodies; MRSS = modified Rodnan skin thickness score; FVC% = forced vital capacity percent predicted; QILD = quantitative interstitial lung disease score; NA = not applicable.

primary purpose of the activation Z score is to infer the activation states of predicted expression regulators. Given the observed differential regulation of a molecule ("up" or "down") in the data set, the activation state of an upstream regulator is determined by the regulation direction associated with the relationship from the regulator to the molecule. In practice, Z scores >2 or <–2 can be considered significant.

For correlation with clinical variables (i.e., the MRSS, FVC%, HRCT–QILD score), Pearson's correlation was calculated, and proteins that reached the nominal significance level ($P < 0.05$) in the univariable analysis and a Pearson's correlation coefficient of ≥0.3 or ≤–0.3 were considered as significantly correlated. For this, we did not account for multiple comparisons as this was a hypothesis-generating analysis. Multivariable analyses with adjustment for age and sex were also performed. Partial correlation coefficients after adjustment for these demographic factors were also provided.

In an exploratory analysis, the predictive significance of serum proteins found to correlate with MRSS scores and FVC% was examined for the serial measurement of MRSS scores and FVC% obtained 3–14 months after randomization in the CYC arm (representing the active treatment period) and transplantation arm, separately. For this analysis, mixed-effects linear regression modeling was used after controlling for disease severity at baseline (i.e., the MRSS or FVC% at baseline) and time variable. Fixed effects were serum protein levels and the MRSS or FVC% at baseline as well as time point (all as continuous), and random effects were the intercept and time point. An unstructured correlation matrix was used. Analyses were performed using R Studio version 0.99.489 (RStudio Consortium) and SAS version 9.4 (SAS Institute Inc.).

RESULTS

Demographic and clinical characteristics. Demographic and clinical characteristics of study patients at baseline are presented in Table 1. As expected in diffuse disease, anti–topoisomerase I (Scl-70) was the most common disease-specific autoantibody observed (39.4%), followed by anti-RNP antibodies (15.2%). All SCOT participants had signs of alveolitis on HRCT as evidenced by visual confirmation of ground glass opacity, and mean disease duration was 2.3 years.

Serum protein levels. Ninety of 182 proteins were differentially expressed in SSc participants compared to control subjects, with an FDR of <0.05. A heatmap shows 90 differentially expressed proteins in samples from SCOT participants at baseline compared to healthy controls (Supplementary Figure 2, http://onlinelibrary.wiley.com/doi/10.1002/art.41570/abstract). The 10 most up-regulated and down-regulated proteins based

Table 2. Top up-regulated and down-regulated serum proteins in the SCOT participants compared to control subjects*

Protein name	Gene name	Fold change	P_{raw}	P_{FDR}	Direction of difference
Growth hormone	GH1†	3.69	<0.001	<0.001	Up-regulated
Ferritin	FTH1	3.04	<0.001	<0.001	Up-regulated
C-reactive protein	CRP	2.98	<0.001	<0.001	Up-regulated
Chromogranin A	CHGA	2.77	<0.001	<0.001	Up-regulated
MIP-3β	CCL19†	2.48	<0.001	<0.001	Up-regulated
MCP-1	CCL2†	2.48	<0.001	<0.001	Up-regulated
Myoglobin	MB	2.38	<0.001	<0.001	Up-regulated
MIG	CXCL9†	2.30	<0.001	<0.001	Up-regulated
BLC	CXCL13†	2.19	<0.001	<0.001	Up-regulated
Prolactin	PRL	2.08	<0.001	<0.001	Up-regulated
Lactoylglutathione lyase	GLO1†	0.49	<0.001	<0.001	Down-regulated
Neuron-specific enolase	ENO2†	0.56	0.002	0.007	Down-regulated
Vitamin K–dependent protein S	PROS1†	0.56	0.005	0.013	Down-regulated
SOD1	SOD1	0.65	<0.001	<0.001	Down-regulated
Protein S100A6	S100A6†	0.69	0.002	0.006	Down-regulated
MIF	MIF	0.71	0.023	0.046	Down-regulated
Adiponectin	ADIPOQ	0.72	<0.001	<0.001	Down-regulated
Kallikrein 7	KLK7†	0.73	<0.001	<0.001	Down-regulated
IGFBP6	IGFBP6	0.73	<0.001	<0.001	Down-regulated
Tetranectin	CLEC3B†	0.75	<0.001	<0.001	Down-regulated

* Values of >1 refer to up-regulated expression of proteins, and values of <1 refer to down-regulated expression of proteins in Scleroderma: Cyclophosphamide or Transplantation (SCOT) study participants compared to values measured in control subjects. For example, a fold change of 2.30 is equivalent to an increase of 130% from the reference value, and a fold change of 0.65 is equivalent to a decrease of 35% from the reference value. FDR = false discovery rate; MIP-3β = macrophage inflammatory protein 3β; MCP-1 = monocyte chemotactic protein 1; MIG = monokine induced by interferon-γ; BLC = B lymphocyte chemoattractant; SOD1 = superoxide dismutase 1; MIF = macrophage migration inhibitory factor; IGFBP6 = insulin-like growth factor binding protein 6.
† Interferon-inducible proteins.

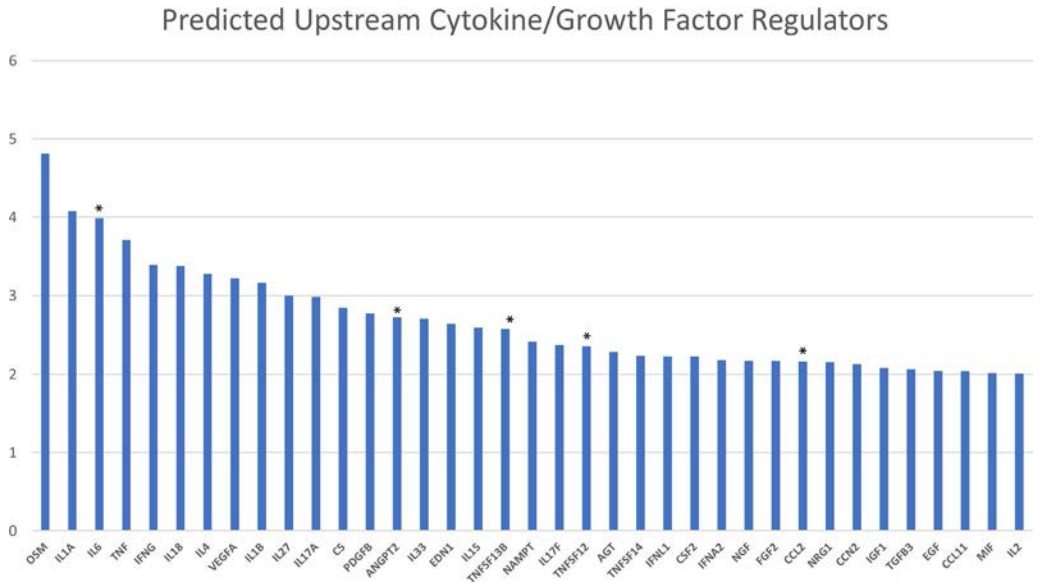

Figure 1. Top predicted upstream cytokine and growth factor regulators based on the Ingenuity Knowledge Base. Y axis shows the activation Z score calculated based on the Ingenuity Pathway Analysis for identifying upstream regulators (see Patients and Methods for further details). Proteins that were differentially expressed in participants with diffuse cutaneous systemic sclerosis compared to control subjects are shown (asterisks). Color figure can be viewed in the online issue, which is available at http://onlinelibrary.wiley.com/doi/10.1002/art.41570/abstract.

on the fold change are presented in Table 2. The complete list of 90 differentially expressed proteins in SSc is available in Supplementary Table 1 (http://onlinelibrary.wiley.com/doi/10.1002/art.41570/abstract). Complete analysis results for all examined 182 serum proteins are available in an additional data file on the Scleroderma Program at McGovern Medical School website

Table 3. Significant correlations between serum protein expression and the modified Rodnan skin thickness score at baseline*

		Correlation			
		Univariable†		Multivariable‡	
Protein name	Gene name	r	*P*	Partial correlation	*P*
α_1-antichymotrypsin§	SERPINA3	0.42	0.001	0.42	0.001
NT-proBNP§	NPPB	0.38	0.002	0.38	0.002
Endostatin§	COL18A1	0.37	0.002	0.38	0.002
Osteopontin§	SPP1	0.34	0.006	0.38	0.002
Ang-2§	ANGPT2	0.33	0.005	0.33	0.007
SAP component	APCS	0.32	0.008	0.32	0.010
Tenascin-C§	TNC	0.31	0.011	0.32	0.010
α_1-microglobulin	AMBP	0.31	0.011	0.32	0.012
IGFBP4§	IGFBP4	0.30	0.018	0.34	0.009
IL-22	IL22	−0.30	0.016	−0.29	0.020
HGF receptor	MET	−0.30	0.016	−0.31	0.012
Tetranectin¶	CLEC3B	−0.31	0.011	−0.34	0.007
Kallikrein 5¶	KLK5	−0.33	0.007	−0.33	0.007
uPA	PLAU	−0.34	0.005	−0.35	0.005
TARC	CCL17	−0.35	0.003	−0.36	0.003
Tamm-Horsfall urinary glycoprotein	UMOD	−0.40	0.001	−0.42	0.001
MDC¶	CCL22	−0.43	<0.001	−0.44	<0.001
EGFR¶	EGFR	−0.43	<0.001	−0.43	0.001

* Correlations were determined using Pearson's correlation coefficients. NT-proBNP = N-terminal pro–brain natriuretic peptide; Ang-2 = angiopoietin 2; SAP = serum amyloid P; IGFBP4 = insulin-like growth factor binding protein 4; IL-22 = interleukin-22; HGF = hepatocyte growth factor; uPA = urokinase plasminogen activator; TARC = thymus and activation–regulated chemokine; MDC = macrophage-derived chemokine; EGFR = epidermal growth factor receptor.
† Calculated using a univariable model.
‡ Calculated using a multivariable model after adjustment for age and sex.
§ Proteins differentially expressed and up-regulated in participants with diffuse cutaneous systemic sclerosis (dcSSc) compared to control subjects.
¶ Proteins differentially expressed and down-regulated in participants with dcSSc compared to control subjects.

(https://www.uth.tmc.edu/scleroderma/), and individual level protein data are available at ImmPort (https://www.immport.org).

As shown in the Supplementary Figure 3 (http://onlinelibrary.wiley.com/doi/10.1002/art.41570/abstract), PCA identified only 1 outlier. PCA showed that the majority of SCOT participants had a different serum protein profile compared to control subjects. Furthermore, the 27 individuals who received immunosuppressive therapy 2 months prior to sample collection did not group separately from other SCOT participants. Supplementary Tables 2 and 3 (http://onlinelibrary.wiley.com/doi/10.1002/art.41570/abstract) show the demographic/clinical characteristics, as well as the list and duration of prior immunosuppressive treatment in SCOT participants dichotomized based on whether they were treated with immunosuppressive agents 2 months prior to sample collection.

Prominent role of profibrotic and granulocyte/agranulocyte extravasation pathways in SSc serum profile. An Ingenuity Canonical Pathway Analysis of differentially expressed serum proteins in SSc participants compared to control subjects revealed hepatic fibrosis, granulocyte adhesion and diapedesis, and agranulocyte adhesion and diapedesis as the top 3 overrepresented pathways. Of note, the same 3 pathways were found to be the top dysregulated pathways in our previously published global gene expression study on SSc skin (29). Interestingly, the top overrepresented canonical pathways in the concomitantly collected whole blood RNA samples were antigen presentation, IFN, and natural killer cell pathways. The complete list of overrepresented canonical pathways in both data sets is shown in the additional data file on the Scleroderma Program at McGovern Medical School website (https://www.uth.tmc.edu/scleroderma/).

As shown in Figure 1, the top predicted activated upstream cytokines/growth factors (based on an activation Z score of >2) for the observed SSc serum protein profile included prominent profibrotic proteins such as oncostatin M (OSM), IL-6, IL-18, IL-4, IL-33, B–cell activating factor (TNFSF13B), and monocyte chemotactic protein 1 (MCP-1; CCL2).

Correlation of serum protein expression with MRSS scores. In SSc participants compared to controls, levels of α_1-antichymotrypsin, N-terminal pro–brain natriuretic peptide (NT-proBNP), endostatin, osteopontin, tenascin, and insulin-like growth factor binding protein 4 (IGFBP-4) were up-regulated ($P < 0.05$) (Supplementary Table 1, http://onlinelibrary.wiley.com/doi/10.1002/art.41570/abstract) and showed a positive correlation with the MRSS (Table 3). Epidermal growth factor receptor (EGFR), macrophage-derived chemokine, kallikrein 5, and tetranectin were down-regulated in SSc participants compared to control subjects ($P < 0.05$) (Supplementary Table 1) and were negatively correlated with the MRSS. All serum proteins that correlated with MRSS scores are shown in Table 3. Furthermore, complete analysis results for all proteins can be found at https://www.uth.tmc.edu/scleroderma/.

In an exploratory analysis, the predictive significance of serum proteins listed in Table 3 for the course of MRSS scores from 3–14 months after randomization in the CYC arm (representing active treatment period; n = 32) and transplantation arm (n = 30) was investigated. As shown in Supplementary Table 4 (http://onlinelibrary.wiley.com/doi/10.1002/art.41570/abstract), NT-proBNP and Ang-2 serum levels at baseline predicted higher subsequent MRSS scores ($P = 0.013$ and $P = 0.038$, respectively), whereas EGFR and kallikrein 5 serum levels at baseline predicted lower subsequent MRSS scores ($P = 0.034$ and $P = 0.003$, respectively) in the CYC arm after adjustment for MRSS scores at baseline. Similarly, EGFR and kallikrein 5 predicted lower subsequent MRSS scores in the transplantation arm ($P = 0.019$ and $P = 0.004$, respectively).

Correlation of serum protein levels with ILD severity. Serum protein correlates of FVC and HRCT–QILD score are shown in Supplementary Tables 5 and 6 (http://onlinelibrary.wiley.com/doi/10.1002/art.41570/abstract). Notably, cancer antigen 15-3 (CA 15-3) and growth-regulated α protein were associated with more severe involvement (i.e., lower FVC and higher HRCT–QILD scores) in both analyses (Figure 2). As shown in Supplementary Table 7 (http://onlinelibrary.wiley.com/doi/10.1002/art.41570/abstract), no proteins that correlated with FVC at the

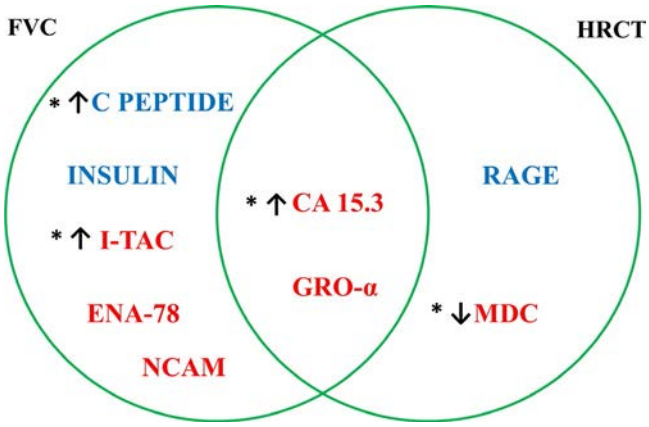

Figure 2. Venn diagram showing serum proteins that correlate with forced vital capacity (FVC) and high-resolution computed tomography quantitative interstitial lung disease (HRCT–QILD) score in participants with diffuse cutaneous systemic sclerosis (dcSSc). Associations with a better FVC and HRCT–QILD score (blue font) and associations with a worse FVC and HRCT–QILD score (red font) are shown. **Asterisks** indicate proteins that were differentially expressed and up-regulated (**up arrows**) or down-regulated (**down arrows**) in participants with dcSSc compared to control subjects. I-TAC = interferon-inducible T cell α chemoattractant; CA 15.3 = cancer antigen 15-3; RAGE = receptor for advanced glycosylation end products; ENA-78 = epithelial-derived neutrophil activating protein 78; GRO-α = growth-regulated α protein; MDC = macrophage-derived chemokine; NCAM = neuronal cell adhesion molecule.

baseline visit predicted the course of FVC 3–14 months after randomization in both treatment arms (n = 32 each for CYC and transplantation arms).

Whole blood gene expression versus serum proteins. After filtering the whole blood gene expression data set by 282 transcripts corresponding to 172 examined proteins, we compared transcript profiles between SSc participants and control subjects. A total of 52 transcripts were differentially expressed (FDR of <0.1) in dcSSc participants versus controls. Among this list, 24 transcripts had a corresponding differentially expressed protein, of which only 17 transcripts (belonging to 14 genes) showed a differential expression in the concordant direction in its corresponding protein (Table 4). Of note, 7 transcripts were differentially expressed in the opposite direction, indicating that the observed differential expression in the serum proteins does not stem from peripheral blood cells. Among concordantly expressed transcript–serum protein pairs, IL-1β was the only one with a decreased number at both whole blood gene expression and serum protein levels whereas the remainder were up-regulated in SSc at both levels. Moreover, endostatin was up-regulated both at RNA transcript and protein levels and positively correlated with the MRSS (Table 3). CA 15-3 was up-regulated both at transcript and serum protein levels and was positively correlated with the presence of lung fibrosis (Supplementary Tables 5 and 6, http://onlinelibrary.wiley.com/doi/10.1002/art.41570/abstract).

Type I IFN–inducible proteins. Among the 90 differentially expressed proteins in SSc participants, 40 up-regulated molecules are known to be type I IFN–inducible (44.4%) whereas 10 down-regulated proteins were type I IFN–inducible (11.1%), according to the Interferome database search (Supplementary Table 1, http://onlinelibrary.wiley.com/doi/10.1002/art.41570/abstract). MCP-1, monokine induced by IFNγ (MIG), IFNγ-induced protein 10 (IP-10), IFN-inducible T cell α chemoattractant (I-TAC), as well as CA 15-3 are among these up-regulated type I IFN–inducible proteins (Supplementary Table 8, http://onlinelibrary.wiley.com/doi/10.1002/art.41570/abstract).

DISCUSSION

The present study represents a large-scale analysis of serum proteins in participants with dcSSc compared at a 1:1 ratio to matched healthy control subjects. Ninety differentially expressed proteins were identified among the 230 assayed by the utilized platform (Supplementary Table 1, http://onlinelibrary.wiley.com/doi/10.1002/art.41570/abstract). Candidate proteins emerged from correlation analysis with the MRSS, FVC, and QILD score. Ingenuity Pathway Analysis revealed fibrosis and extravasation-related pathways as the top overrepresented biologic processes. Lastly, transcripts and proteins showing differential expression at whole blood RNA and serum protein levels were identified, showing that only a small portion of differentially expressed serum proteins were also differentially expressed in a concordant direction in the whole blood RNA samples.

Table 4. Whole blood gene expression versus serum protein expression at baseline*

			Whole blood gene expression			Serum proteins		
Analyte name	Gene name	Direction†	Fold change	P_{raw}	P_{FDR}	Fold change	P_{raw}	P_{FDR}
IL-1β	IL1B	Down-regulated	0.71	<0.001	<0.001	0.89	0.015	0.032
α_1-antitrypsin	SERPINA1	Up-regulated	1.04	0.018	0.092	1.22	<0.001	0.001
MIG	CXCL9	Up-regulated	1.05	0.001	0.010	2.30	<0.001	<0.001
IL-2Rα	IL2RA	Up-regulated	1.05	0.017	0.091	1.97	<0.001	<0.001
Cancer antigen 15-3	MUC1‡	Up-regulated	1.06	<0.001	0.006	1.67	0.001	0.004
Cancer antigen 15-3	MUC1‡	Up-regulated	1.11	<0.001	<0.001	1.67	0.001	0.004
TNF ligand superfamily member 13	TNFSF13‡	Up-regulated	1.08	0.001	0.008	1.23	0.017	0.037
TNF ligand superfamily member 13	TNFSF13‡	Up-regulated	1.1	<0.001	0.005	1.23	0.017	0.037
MCP-1	CCL2	Up-regulated	1.12	<0.001	0.001	2.48	<0.001	<0.001
IL-16	IL16	Up-regulated	1.15	<0.001	0.005	1.08	0.019	0.040
LOX-1	OLR1	Up-regulated	1.15	0.006	0.040	1.38	<0.001	<0.001
Endostatin	COL18A1	Up-regulated	1.16	<0.001	0.001	1.28	<0.001	<0.001
BAFF	TNFSF13B‡	Up-regulated	1.17	0.015	0.081	1.83	<0.001	<0.001
BAFF	TNFSF13B‡	Up-regulated	1.23	0.001	0.009	1.83	<0.001	<0.001
IP-10	CXCL10	Up-regulated	1.26	<0.001	0.001	2.03	<0.001	<0.001
Haptoglobin	HP	Up-regulated	1.29	0.001	0.008	1.71	<0.001	<0.001
MPO	MPO	Up-regulated	1.41	<0.001	0.006	1.84	<0.001	<0.001

* FDR = false discovery rate; IL-1β = interleukin-1β; MIG = monokine induced by interferon-γ; IL-2Rα = IL-2 receptor α; TNF = tumor necrosis factor; MCP-1 = monocyte chemotactic protein 1; LOX-1 = lectin-like oxidized low-density lipoprotein receptor 1; IP-10 = interferon-γ–inducible 10-kd protein; MPO = myeloperoxidase.
† Concordant direction of whole blood RNA expression versus serum protein expression.
‡ Two transcript variants of this gene were differentially expressed.

In the present proteomics analysis, the majority of samples obtained from participants with early-stage dcSSc had a distinct serum protein profile compared to samples obtained from control subjects, confirming the presence of a prominent IFN signature in SSc (5,7,30). Among the 65 serum proteins that were up-regulated, 40 were type I IFN–inducible proteins, with 10 of those being chemokines (MCP-1, macrophage inflammatory protein 1β [MIP-1β], MCP-2, MCP-4, MIP-3β, myeloid progenitor inhibitory factor 1, MIG, IP-10, I-TAC, and B lymphocyte chemoattractant) as well as 30 other proteins, including osteopontin (SPP-1) and β_2-microglobulin. Additionally, several type I IFN–inducible molecules were commonly dysregulated at both the RNA and protein level (*CXCL9*/MIG, *CCL2*/MCP-1, *MUC1*/CA 15-3, *IL16*/IL-16, *CXCL10*/IP-10, *SERPINA1*/α_1-antitrypsin, *TNFSF13*/TNF ligand superfamily, *OLR1*/lectin-like oxidized low-density lipoprotein receptor 1, and *TNFSF13B*/B cell–activating factor). Of note, plasma IP-10 and I-TAC were previously found to be up-regulated in 266 individuals with early-stage SSc enrolled in the GENISOS cohort, and these levels correlated with a peripheral blood cell IFN gene expression score (7). Moreover, in a phase I open-label clinical trial of anifrolumab (an anti–IFNα receptor 1 monoclonal antibody) conducted in 34 patients with SSc, levels of SPP-1 correlated with IFN activity (whole blood type I IFN gene signature score) whereas β_2-microglobulin, IP-10, and MCP-4 were suppressed after treatment with anifrolumab, supporting the notion that these proteins are regulated by type I IFN (16).

In our correlation analysis, serum soluble EGFR showed the strongest negative correlation with the MRSS and was significantly down-regulated in participants with SSc compared to controls. Soluble EGFR can inhibit the activation of its transmembrane receptor by binding EGF or by directly binding the transmembrane receptor itself, which can disrupt EGF/EGFR cell signaling (31). Decreased soluble EGFR in SSc might lead to an activation of EGF pathways, as already described for some subtypes of lung cancers (32). Indeed, a recent multicohort analysis of SSc skin transcriptome data across 7 data sets from 6 centers comprising 515 samples identified 6 signaling proteins which positively correlated with the SSc signature, 4 of which were EGFR ligands (33). Our data provide further support for EGFR signaling as a potential driver of fibrosis in SSc skin. Of note, a correlation between serum soluble EGFR and lung FVC or QILD score was not observed.

In our study, α_1-antichymotrypsin showed the strongest positive correlation with the MRSS. This protein is an acute-phase reactant produced by the liver (34). Its biologic function is to inhibit several serine proteases, mainly cathepsin G, which is contained in the neutrophil granules and released at the site of inflammation. Notably, an excess of cathepsin G function is linked to tissue damage (35). Moreover, 2 proteins mainly associated with SSc vascular manifestation, endostatin and NT-proBNP, also showed a moderately positive correlation with the MRSS. Endostatin is a peptide derived from the C-terminus of type XVIII collagen produced by fibroblasts with antiangiogenic properties. Previous studies have shown that endostatin is up-regulated in SSc serum (36,37). Its antiangiogenic role suggests a feedback loop between endostatin and features of vascular impairment such as digital ulcers, pulmonary arterial hypertension (PAH), and scleroderma renal crisis (38–40). Vascular involvement and extensive skin involvement are not mutually exclusive. In fact, 2 previous studies have shown an association between serum levels of endostatin and more extensive skin involvement (39,41). Of note, endostatin-derived peptides have exhibited antifibrotic properties and were able to prevent and reverse dermal TGFβ–induced fibrosis in both ex vivo human skin and in vivo mouse models (42). Similarly, NT-proBNP has a more established link with vascular abnormalities in SSc, particularly with PAH, cardiac damage, and mortality (43), but previous studies have also shown a positive correlation of NT-proBNP with MRSS scores (44–46).

In our correlative analyses with SSc–ILD features, the availability of both FVC and QILD scores at the baseline visit in all SCOT participants enabled us to identify serum proteins that correlate with functional lung volume, as well as scleroderma-related radiographic findings. Significant correlations were observed in CA 15-3 and growth-regulated α protein (GROα) with both FVC and QILD scores in a clinically concordant direction, but only CA 15-3 also showed significant up-regulation in SSc participants compared to controls. CA 15-3 significantly correlated with lower FVC and higher QILD scores on HRCT. CA 15-3 is a mucin encoded by the gene *MUC1*, which also encodes Krebs von den Lungen 6 protein. CA 15-3 is produced by epithelial cells, including type 2 pneumocytes, and is commonly used as a tumor marker in clinical practice for breast and ovarian cancer (47,48). In a previous retrospective study of 221 individuals with SSc, CA 15-3 was a useful marker in identifying individuals with significant ILD and also correlated with decreased FVC and higher lung fibrosis scores (49). Of note, CA 15-3 did not show a significant positive correlation with the MRSS, underscoring its value as a lung-specific marker. GROα is a neutrophil chemoattractant, and consistent with our results, a previous study indicated that this protein was up-regulated in SSc sera and was associated with lung impairment in SSc, correlating with decreased diffusing capacity for carbon monoxide and FVC (50).

Building on the availability of concomitantly collected serum and whole blood RNA samples, we performed a direct comparison between these 2 sample types, showing that the differential expression for most proteins in SSc serum is most likely to originate outside peripheral blood cells. Our studies focused on serum and peripheral blood RNA, which can be readily obtained and are practical sources of biomarker development during routine clinical care. The 3 overrepresented pathways in SSc serum were exactly the same 3 overrepresented pathways previously identified in our global SSc skin gene expression study (hepatic fibrosis, granulocyte adhesion and diapedesis, and agranulocyte adhesion and diapedesis) (29). To further investigate this

finding, we compared the list of 90 differentially expressed serum proteins with the differentially expressed transcripts in concomitantly collected peripheral blood cell RNA samples. This analysis yielded only 14 molecules that were differentially expressed in both sample types in the concordant direction. There were even 7 molecules that were differentially expressed in the opposite direction. These results support the notion that the source for the majority of differentially expressed serum proteins is likely to be outside of peripheral blood cells.

In line with our findings, a recently published SOMAscan proteome analysis in 2 cohorts of 14 and 20 patients with SSc showed that most of the differentially expressed serum proteins overlapped with serum proteins from 2 previously published SSc skin messenger RNA expression data sets (15). Prominently affected end organs in SSc such as the skin and lungs are potential sources for the SSc serum protein signature, although it is possible that other organs such as the liver are also contributing to the SSc protein profile.

The present study has some weaknesses. It is mainly hypothesis-generating and does not include mechanistic experiments. Moreover, although we used the most comprehensive proteomics MAP panel provided by the Myriad Rules-Based Medicine at the time of study, we cannot provide a comprehensive view of protein dysregulation, in contrast to the findings in genome-wide association and genome-wide gene expression studies, due to the technical limitations of the available proteomics assays. It is likely that a more comprehensive proteomics platform will lead to identification of additional candidate biomarkers. Furthermore, though we had access to concomitantly collected whole blood RNA samples, samples from affected end organs (skin or lung) were not available in the SCOT trial. Moreover, an independent validation cohort was not included in the present study. Future studies are needed to confirm the association of identified serum proteins with SSc fibrotic features.

The present study also has several strengths. To our knowledge, this investigation represents the largest serum protein study in SSc with validated and robust multiplex protein assays. We analyzed a well-characterized subset of dcSSc participants with early progressive fibrotic disease. SCOT participants were matched at a 1:1 ratio for age and sex with control subjects in order to avoid the potential confounding effect of differences in demographic characteristics and to generate sufficient power for identification of differentially expressed proteins. Moreover, the availability of FVC as well as QILD scores on HRCT enabled us to identify serum proteins that correlate with lung function as well as the extent of radiographic involvement. Lastly, to our knowledge, the present study is the first to directly compare a large-scale SSc serum protein profile to the concurrently obtained whole blood transcriptome.

In conclusion, 4 important observations emerged from the present study. Namely, SSc serum samples from SSc participants showed a distinct proteomics profile compared to samples from control subjects, which includes an activation of prominent profibrotic cytokines. Moreover, up-regulation of several type I IFN–inducible proteins was also observed, confirming previous genetic and gene expression studies and demonstrating a prominent IFN signature in SSc. Furthermore, a direct comparison between the serum protein expression profile and peripheral blood gene expression profile indicated that the primary source for the SSc serum proteomics profile lies outside peripheral blood cells. Lastly, we were able to identify serum protein correlates of the MRSS and ILD severity, suggesting that EGFR, α_1-antichymotrypsin, and CA 15-3 are candidate proteins for future mechanistic studies in SSc.

AUTHOR CONTRIBUTIONS

All authors were involved in drafting the article or revising it critically for important intellectual content, and all authors approved the final version to be published. Dr. Bellocchi had full access to all the study data and takes responsibility for the integrity of the data and the accuracy of the data analysis.

Study conception and design. Bellocchi, Goldmuntz, Keyes-Elstein, McSweeney, Furst, Crofford, Mayes, Sullivan, Assassi.

Acquisition of data. Bellocchi, Goldmuntz, Keyes-Elstein, Varga, Hinchcliff, McSweeney, Furst, Nash, Crofford, Welch, Goldin, Pinckney, Mayes, Sullivan, Assassi.

ADDITIONAL DISCLOSURES

Author Pinckney is an employee of Rho Federal Systems Division.

REFERENCES

1. Varga J, Trojanowska M, Kuwana M. Pathogenesis of systemic sclerosis: recent insights of molecular and cellular mechanisms and therapeutic opportunities. J Scleroderma Relat Disord 2017;2:137–52.
2. Elhai M, Meune C. Trends in mortality in patients with systemic sclerosis over 40 years: a systematic review and meta-analysis of cohort studies. Rheumatology (Oxford) 2012;51:1017–26.
3. Radstake TR, Gorlova O, Rueda B, Martin JE, Alizadeh BZ, Palomino-Morales R, et al. Genome-wide association study of systemic sclerosis identifies CD247 as a new susceptibility locus. Nat Genet 2010;42:426–9.
4. Allanore Y, Saad M, Dieudè P, Avouac J, Distler JH, Amouyel P, et al. Genome-wide scan identifies TNIP1, PSORS1C1, and RHOB as novel risk loci for systemic sclerosis. PLoS Genet 2011;7:e1002091.
5. Assassi S, Mayes MD, Arnett FC, Gourh P, Agarwal SK, Mcnearney TA, et al. Systemic sclerosis and lupus: points in an interferon-mediated continuum. Arthritis Rheum 2010;62:589–98.
6. Whitfield ML, Finlay DR, Murray JI, Troyanskaya OG, Chi JT, Pergamenschikov A, et al. Systemic and cell type-specific gene expression patterns in scleroderma skin. Proc Natl Acad Sci U S A 2003;100:12319–24.
7. Liu X, Mayes MD, Tan FK, Wu M, Reveille JD, Harper BE, et al. Correlation of interferon-inducible chemokine plasma levels with disease severity in systemic sclerosis. Arthritis Rheum 2013;65:226–35.
8. Bandinelli F, del Rosso A, Gabrielli A, Giacomelli R, Bartoli F, Guiducci S, et al. CCL2, CCL3 and CCL5 chemokines in systemic sclerosis: the correlation with SSc clinical features and the effect of prostaglandin E1 treatment. Clin Exp Rheumatol 2012;30:S44–9.

9. Cossu M, Andracco R, Santaniello A, Marchini M, Severino A, Caronni M, et al. Serum levels of vascular dysfunction markers reflect disease severity and stage in systemic sclerosis patients. Rheumatology (Oxford) 2016;55:1112–6.
10. Riccieri V, Stefanantoni K, Vasile M, Macrì V, Sciarra I, Iannace N, et al. Abnormal plasma levels of different angiogenic molecules are associated with different clinical manifestations in patients with systemic sclerosis. Clin Exp Rheumatol 2011;29:S46–52.
11. De Lauretis A, Sestini P, Pantelidis P, Hoyles R, David M, Goh NS, et al. Serum interleukin 6 is predictive of early functional decline and mortality in interstitial lung disease associated with systemic sclerosis. J Rheumatol 2013;40:435–46.
12. Masui Y, Asano Y, Shibata S, Noda S, Aozasa N, Akamata K, et al. Serum adiponectin levels inversely correlate with the activity of progressive skin sclerosis in patients with diffuse cutaneous systemic sclerosis. J Eur Acad Dermatol Venereol 2012;26:354–60.
13. Fantuzzi G. Adiponectin and inflammation: consensus and controversy. J Allergy Clin Immunol 2008;121:326–30.
14. Lakota K, Wei J, Carns M, Hinchcliff M, Lee J, Whitfield ML, et al. Levels of adiponectin, a marker for PPAR-γ activity, correlate with skin fibrosis in systemic sclerosis: potential utility as biomarker? Arthritis Res Ther 2012;14:R102.
15. Rice LM, Mantero JC, Stifano G, Ziemek J, Simms RW, Gordon J, et al. A proteome-derived longitudinal pharmacodynamic biomarker for diffuse systemic sclerosis skin. J Invest Dermatol 2017;137:62–70.
16. Guo X, Higgs BW, Bay-Jensen AC, Karsdal MA, Yao Y, Roskos LK, et al. Suppression of T cell activation and collagen accumulation by an anti-IFNAR1 mAb, anifrolumab, in adult patients with systemic sclerosis. J Invest Dermatol 2015;135:2402–9.
17. Beirne P, Pantelidis P, Charles P, Wells AU, Abraham DJ, Denton CP, et al. Multiplex immune serum biomarker profiling in sarcoidosis and systemic sclerosis. Eur Respir J 2009;34:1376–82.
18. LeRoy EC, Black C, Fleischmajer R, Jablonska S, Krieg T, Medsger TA, et al. Scleroderma (systemic sclerosis): classification, subsets and pathogenesis. J Rheumatol 1988;15:202–5.
19. Sullivan KM, Goldmuntz EA, Keyes-Elstein L, McSweeney PA, Pinckney A, Welch B, et al. Myeloablative autologous stem-cell transplantation for severe scleroderma. N Engl J Med 2018; 378:35–47.
20. Kim HJ, Li G, Gjertson D, Elashoff R, Shah SK, Ochs R, et al. Classification of parenchymal abnormality in scleroderma lung using a novel approach to denoise images collected via a multicenter study. Acad Radiol 2008;15:1004–16.
21. Khanna D, Nagaraja V, Tseng C, Abtin F, Suh R, Kim G, et al. Predictors of lung function decline in scleroderma-related interstitial lung disease based on high-resolution computed tomography: implications for cohort enrichment in systemic sclerosis–associated interstitial lung disease trials. Arthritis Res Ther 2015;17:372.
22. Clements P, Lachenbruch P, Siebold J, White B, Weiner S, Martin R, et al. Inter and intraobserver variability of total skin thickness score (modified Rodnan TSS) in systemic sclerosis. J Rheumatol 1995;22:1281–5.
23. Rivnak AJ, Rissin DM, Kan CW, Song L, Fishburn MW, Piech T, et al. A fully-automated, six-plex single molecule immunoassay for measuring cytokines in blood. J Immunol Methods 2015;424:20–7.
24. Assassi S, Wang X, Chen G, Goldmuntz E, Keyes-Elstein L, Ying J, et al. Myeloablation followed by autologous stem cell transplantation normalises systemic sclerosis molecular signatures. Ann Rheum Dis 2019;78:1371–8.
25. Simon R, Lam A, Li MC, Ngan M, Menenzes S, Zhao Y. Analysis of gene expression data using BRB-ArrayTools. Cancer Inform 2007;3:11–7.
26. Rusinova I, Forster S, Yu S, Kannan A, Masse M, Cumming H, et al. Interferome v2.0: an updated database of annotated interferon-regulated genes. Nucleic Acids Res 2013;41:1040–6.
27. Benjamini Y, Hochberg Y. Controlling the false discovery rate: a practical and powerful approach to multiple testing. J R Stat Soc Series B Stat Methodol 1995;57:289–300.
28. Krämer A, Green J, Pollard J, Tugendreich S. Causal analysis approaches in ingenuity pathway analysis. Bioinformatics 2014;30: 523–30.
29. Assassi S, Swindell WR, Wu M, Tan FD, Khanna D, Furst DE, et al. Dissecting the heterogeneity of skin gene expression patterns in systemic sclerosis. Arthritis Rheumatol 2015;67:3016–26.
30. López-Isac E, Martín JE, Assassi S, Simeón CP, Carreira P, Ortego-Centeno N, et al. IRF4 newly identified as a common susceptibility locus for systemic sclerosis and rheumatoid arthritis in a cross-disease meta-analysis of genome-wide association studies. Arthritis Rheumatol 2016;68:2338–44.
31. Basu A, Raghunath M, Bishayee S, Das M. Inhibition of tyrosine kinase activity of the epidermal growth factor (EGF) receptor by a truncated receptor form that binds to EGF: role for interreceptor interaction in kinase regulation. Mol Cell Biol 1989;9:671–7.
32. Lococo F, Paci M, Rapicetta C, Rossi T, Sancisi V, Braglia L, et al. Preliminary evidence on the diagnostic and molecular role of circulating soluble EGFR in non-small cell lung cancer. Int J Mol Sci 2015;16:19612–30.
33. Lofgren S, Hinchcliff M, Carns M, Wood T, Aren K, Arroyo E, et al. Integrated, multicohort analysis of systemic sclerosis identifies robust transcriptional signature of disease severity. JCI Insight 2016;1:e89073.
34. Bode JG, Albrecht U, Häussinger D, Heinrich PC, Schaper F. Hepatic acute phase proteins–regulation by IL-6- and IL-1-type cytokines involving STAT3 and its crosstalk with NF-κB-dependent signaling [review]. Eur J Cell Biol 2012;91:496–505.
35. Baker C, Belbin O, Kalsheker N, Morgan K. SERPINA3 (aka α-1-antichymotrypsin). Front Biosci 2007;12:2821–35.
36. Sedie AD, Riente L, Maggiorini L, Pratesi F, Tavoni A, Migliorini P, et al. Potential biomarkers in patients with systemic sclerosis. Int J Rheum Dis 2018;21:261–5.
37. Distler O, del Rosso A, Giacomelli R, Cipriani P, Conforti ML, Guiducci S, et al. Angiogenic and angiostatic factors in systemic sclerosis: increased levels of vascular endothelial growth factor are a feature of the earliest disease stages and are associated with the absence of fingertip ulcers. Arthritis Res 2002;4:R11.
38. Reiseter S, Molberg Ø, Gunnarsson R, Lund MB, Aalokken TM, Aukrust P, et al. Associations between circulating endostatin levels and vascular organ damage in systemic sclerosis and mixed connective tissue disease: an observational study. Arthritis Res Ther 2015;17:231.
39. Hebbar M, Peyrat JP, Hornez L, Hatron PY, Hachulla E, Devulder B. Increased concentrations of the circulating angiogenesis inhibitor endostatin in patients with systemic sclerosis. Arthritis Rheum 2000;43:889–93.
40. Mecoli CA, Shah AA, Boin F, Wigley FM, Hummers LK. The utility of plasma vascular biomarkers in systemic sclerosis: a prospective longitudinal analysis. Arthritis Rheumatol 2020;72:1341–9.
41. Farouk HM, Hamza SH, El Bakry SA, Youssef SS, Aly IM, Moustafa AA, et al. Dysregulation of angiogenic homeostasis in systemic sclerosis. Int J Rheum Dis 2013;16:448–54.
42. Yamaguchi Y, Takihara T, Chambers RA, Veraldi KL, Larregina AT, Feghali-Bostwick CA. A peptide derived from endostatin ameliorates organ fibrosis. Sci Transl Med 2012;4:136ra71.
43. Allanore Y, Komocsi A, Vettori S, Hachulla E, Hunzelmann N, Distler J, et al. N-terminal pro-brain natriuretic peptide is a strong predictor of mortality in systemic sclerosis. Int J Cardiol 2016;223:385–9.
44. Carlo-Stella N, Belloli L, Biondi ML, Marasini B. Serum N-terminal pro-brain natriuretic peptide, a marker of skin thickness in systemic sclerosis? [letter]. Clin Rheumatol 2009;28:241–2.
45. Choi HJ, Shin YK, Lee HJ, Kee JY, Shin DW, Lee EY, et al. The clinical significance of serum N-terminal pro-brain natriuretic peptide in systemic sclerosis patients. Clin Rheumatol 2008;27:437–42.

46. Elshamy HA, Ibrahim SE, Farouk HM, Moustafa AA, Aly IM, Osman WM. N-terminal pro-brain natriuretic peptide in systemic sclerosis: new insights. Eur J Dermatol 2011;21:686–90.
47. Apostolopoulos V, Stojanovska L, Gargosky SE. MUC1 (CD227): a multi-tasked molecule. Cell Mol Life Sci 2015;72:4475–500.
48. Lakshmanan I, Ponnusamy MP, Macha MA, Haridas D, Majhi PD, Kaur S, et al. Mucins in lung cancer: diagnostic, prognostic, and therapeutic implications. J Thorac Oncol 2015;10:19–27.
49. Celeste S, Santaniello A, Caronni M, Franchi J, Severino A, Scorza R, et al. Carbohydrate antigen 15.3 as a serum biomarker of interstitial lung disease in systemic sclerosis patients. Eur J Intern Med 2013;24:671–6.
50. Furuse S, Fujii H, Kaburagi Y, Fujimoto M, Hasegawa M, Takehara K, et al. Serum concentrations of the CXC chemokines interleukin 8 and growth-regulated oncogene-α are elevated in patients with systemic sclerosis. J Rheumatol 2003;30:1524–8.

Arthritis & Rheumatology
Vol. 73, No. 4, April 2021, pp 671–676
DOI 10.1002/art.41576

American College of Rheumatology
Empowering Rheumatology Professionals

Effect of Nintedanib on Lung Function in Patients With Systemic Sclerosis–Associated Interstitial Lung Disease: Further Analyses of a Randomized, Double-Blind, Placebo-Controlled Trial

Toby M. Maher,[1] Maureen D. Mayes,[2] Michael Kreuter,[3] Elizabeth R. Volkmann,[4] Martin Aringer,[5] Ivan Castellvi,[6] Maurizio Cutolo,[7] Christian Stock,[8] Nils Schoof,[9] Margarida Alves,[9] and Ganesh Raghu,[10] on behalf of the SENSCIS Trial Investigators

Objective. In the SENSCIS trial in subjects with systemic sclerosis–associated interstitial lung disease (SSc-ILD), nintedanib reduced the rate of decline in forced vital capacity (FVC) over 52 weeks by 44% versus placebo. This study was undertaken to investigate the effects of nintedanib on categorical changes in FVC and other measures of ILD progression.

Methods. In post hoc analyses, we assessed the proportions of subjects with categorical changes in FVC % predicted at week 52 and the time to absolute decline in FVC of ≥5% predicted or death and absolute decline in FVC of ≥10% predicted or death.

Results. A total of 288 subjects received nintedanib and 288 subjects received placebo. At week 52, in subjects treated with nintedanib and placebo, respectively, 55.7% and 66.3% had any decline in FVC % predicted, 13.6% and 20.1% had a decline in FVC of >5% to ≤10% predicted, and 3.5% and 5.2% had a decline in FVC of >10% to ≤15% predicted; 34.5% and 43.8% had a decrease in FVC of ≥3.3% predicted (proposed minimal clinically important difference [MCID] for worsening of FVC), while 23.0% and 14.9% had an increase in FVC of ≥3.0% predicted (proposed MCID for improvement in FVC). Over 52 weeks, the hazard ratio (HR) for an absolute decline in FVC of ≥5% predicted or death with nintedanib versus placebo was 0.83 (95% confidence interval [95% CI] 0.66–1.06) (P = 0.14), and the HR for an absolute decline in FVC of ≥10% predicted was 0.64 (95% CI 0.43–0.95) (P = 0.029).

Conclusion. These results suggest that nintedanib has a clinically relevant benefit on the progression of SSc-ILD.

INTRODUCTION

Systemic sclerosis (SSc) is a rare and heterogeneous autoimmune disease characterized by microvascular damage and progressive fibrosis of the skin and internal organs (1). Interstitial lung disease (ILD) is a common manifestation of SSc and the leading cause of death in subjects with SSc (2). The course of SSc-associated ILD (SSc-ILD) is unpredictable, but a decline in forced

ClinicalTrials.gov identifier: NCT02597933.
Supported by Boehringer Ingelheim.

[1]Toby M. Maher, MD: National Heart and Lung Institute, Imperial College London and NIHR Clinical Research Facility, Royal Brompton Hospital, London, UK, and Keck School of Medicine, University of Southern California, Los Angeles; [2]Maureen D. Mayes, MD: University of Texas McGovern Medical School, Houston; [3]Michael Kreuter, MD: Thoraxklinik University of Heidelberg, and the German Center for Lung Research, Heidelberg, Germany; [4]Elizabeth R. Volkmann, MD: University of California, David Geffen School of Medicine, Los Angeles; [5]Martin Aringer, MD: University Medical Center and Faculty of Medicine Carl Gustav Carus, TU Dresden, Dresden, Germany; [6]Ivan Castellvi, MD: Hospital de la Santa Creu i Sant Pau, Barcelona, Spain; [7]Maurizio Cutolo, MD: University of Genova, IRCCS San Martino Polyclinic Hospital, Genova, Italy; [8]Christian Stock, PhD: Boehringer Ingelheim Pharma GmbH & Co. KG, Ingelheim am Rhein, Germany; [9]Nils Schoof, PhD, Margarida Alves, MD: Boehringer Ingelheim International GmbH, Ingelheim am Rhein, Germany; [10]Ganesh Raghu, MD: University of Washington, Seattle.

Dr. Maher has received consulting fees, speaking fees, and/or honoraria from AstraZeneca, Blade Therapeutics, Boehringer Ingelheim, Bristol Myers Squibb, Galápagos, GlaxoSmithKline, Indalo, Pliant, Respivant, Roche, and Theravance (less than $10,000 each). Dr. Mayes has received consulting fees, speaking fees, and/or honoraria from Boehringer Ingelheim, Corbus, Eicos Sciences, Galápagos, and Mitsubishi Tanabe (less than $10,000 each). Dr. Kreuter has received consulting fees, speaking fees, and/or honoraria from Boehringer Ingelheim and Roche (less than $10,000 each). Dr. Volkmann has received consulting fees, speaking fees, and/or honoraria from Boehringer Ingelheim (more than $10,000). Dr. Aringer has received consulting fees, speaking fees, and/or honoraria from Boehringer Ingelheim (less than $10,000). Dr. Castellvi has received consulting fees, speaking fees, and/or honoraria from Boehringer Ingelheim, Bristol Myers Squibb, Janssen-Cilag, Roche, and Sanofi (less than $10,000 each). Dr. Cutolo has received consulting fees, speaking fees, and/or honoraria from Bristol Myers Squibb (less than $10,000). Drs. Stock, Schoof, and Alves are employees of Boehringer Ingelheim. Dr. Raghu has received consulting fees, speaking fees, and/or honoraria from Roche-Genentech (less than $10,000) and from Boehringer Ingelheim (more than $10,000).

Address correspondence to Toby M. Maher, Keck School of Medicine, University of Southern California, Los Angeles, CA 90033. Email: toby.maher@med.usc.edu.

Submitted for publication March 17, 2020; accepted in revised form October 29, 2020.

vital capacity (FVC) in subjects with SSc-ILD is an indicator of ILD progression and is associated with mortality (3–7). While there is no established definition for progression of ILD, in 2015, the Outcome Measures in Rheumatology (OMERACT) connective tissue disease–associated ILD (CTD-ILD) Working Group agreed that a relative decline in FVC % predicted of ≥10%, or a relative decline in FVC % predicted of ≥5% to <10% with a relative decline in diffusing capacity for carbon monoxide (DL_{CO}) % predicted ≥15%, represents clinically meaningful progression of SSc-ILD (8).

Nintedanib, an intracellular inhibitor of tyrosine kinases (9), has been approved in many countries for the treatment of idiopathic pulmonary fibrosis (IPF) and SSc-ILD. Clinical trials in subjects with IPF (INPULSIS) (10), with SSc-ILD (SENSCIS) (11), and with various forms of progressive fibrosing ILDs (INBUILD) (12), including progressive autoimmune disease-related ILDs (13), have shown that nintedanib reduces the rate of decline in FVC (milliliters/year). The objective of the current analyses was to investigate the effects of nintedanib on categorical changes in FVC and other measures of ILD progression in subjects with SSc-ILD in the SENSCIS trial.

PATIENTS AND METHODS

Trial design. The design of the SENSCIS trial (ClinicalTrials.gov identifier: NCT02597933) has been published previously, together with the trial protocol (11). Briefly, eligible subjects had SSc with onset of first non–Raynaud's phenomenon symptom <7 years before screening, extent of fibrotic ILD ≥10% on a high-resolution computed tomography (HRCT) scan (based on assessment of the whole lung), FVC ≥40% predicted, and DL_{CO} of the lung (corrected for hemoglobin) 30–89% predicted. Subjects receiving prednisone ≤10 mg/day or equivalent and/or stable therapy with mycophenolate or methotrexate for ≥6 months prior to randomization were allowed to participate. Spirometers were provided to the sites and the results were confirmed centrally. Spirometry was performed in accordance with guidelines issued by the American Thoracic Society and European Respiratory Society (14), including daily calibration of the spirometer. Percent predicted values for FVC were calculated using the Global Lung Initiative equations based on the subject's age, sex, race, and height (15). The method used to measure DL_{CO} and the equation used to calculate percent predicted values for DL_{CO} were chosen by the site.

Subjects were randomized 1:1 to receive nintedanib 150 mg twice a day or placebo, stratified by the presence of anti–topoisomerase I (anti–topo I) antibodies. Subjects could continue to receive treatment in a blinded manner until the last subject had reached week 52, but for ≤100 weeks. Subjects who discontinued treatment prematurely were asked to remain in the trial and attend visits as originally planned. The trial was conducted in accordance with the trial protocol, the principles of the Declaration of Helsinki, and the International Council for Harmonisation Guidelines for Good Clinical Practice, and was approved by local authorities. All subjects provided written informed consent.

End points. The following were assessed in the nintedanib and placebo groups based on data at week 52: the proportion of subjects with categorical absolute declines or increases in FVC % predicted or categorical relative declines or increases in FVC (milliliters) (as listed in the Results section); the proportion of subjects who met proposed thresholds for minimal clinically important differences (MCID) for improvement in FVC (absolute increase of ≥3.0% predicted), stable FVC (absolute increase of <3.0% predicted or decrease of <3.3% predicted), and worsening of FVC (absolute decrease of ≥3.3% predicted) based on data from Scleroderma Lung Studies I and II, anchored to the health transition question from the Medical Outcomes Study Short Form-36 (16); and time to 1) an absolute decline in FVC of ≥5% predicted or death; 2) an absolute decline in FVC of ≥10% predicted or death; and 3) an absolute decline in FVC of ≥10% predicted or absolute decline in FVC of ≥5% to <10% predicted with an absolute decline in DL_{CO} of ≥15% predicted, or death. The proportions of subjects who met proposed thresholds for improvement in FVC, stable FVC, and worsening of FVC at week 52 were also assessed in subgroups defined by the following baseline characteristics: FVC of <80% versus ≥80% predicted, extent of fibrotic ILD on HRCT of <20% versus ≥20%, time since onset of first non–Raynaud's phenomenon symptom ≤3 versus >3 years, and glucocorticoid use.

Statistical analysis. Analyses were conducted post hoc in subjects who received ≥1 dose of trial medication (intention-to-treat). The proportions of subjects with categorical declines or increases in FVC % predicted and FVC measured in milliliters at week 52, and the proportions of subjects who met proposed thresholds for improvement in FVC, stable FVC, and worsening of FVC at week 52 were compared between treatment groups using a Cochran-Mantel-Haenszel test, stratified by anti–topo I antibody status. In the subgroup analyses, the proportions of subjects who met proposed thresholds for improvement in FVC, stable FVC, and worsening of FVC at week 52 were compared between treatment groups using a logistic regression model, including trial medication (nintedanib/placebo), anti–topo I antibody status, subgroup, and treatment-by-subgroup interaction as terms. Missing values were imputed using a worst value carried forward approach. Exploratory interaction *P* values were calculated to assess potential heterogeneity in the treatment effect of nintedanib versus placebo across the subgroups. Time-to-event end points were analyzed based on data from 52 weeks (± 7 days) using a Cox regression model with a term for treatment and stratified by anti–topo I antibody status. Analyses were not adjusted for multiplicity. Hazard ratios (HRs) or odds ratios and 95% confidence intervals (95% CIs) were calculated.

RESULTS

Characteristics of the study subjects. A total of 576 subjects received ≥1 dose of trial medication (288 received nintedanib and 288 received placebo). The baseline

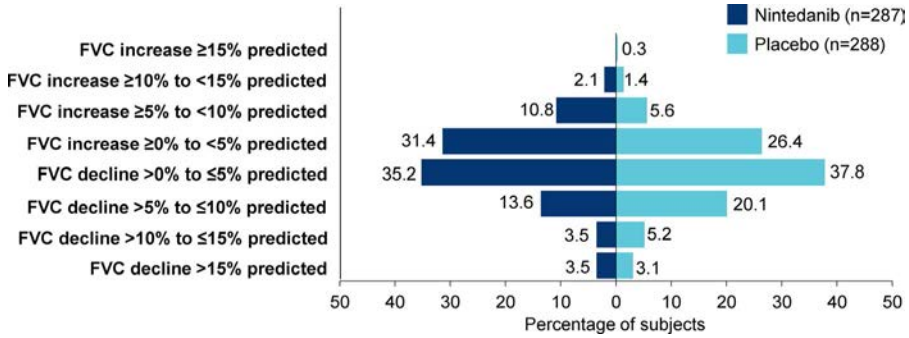

Figure 1. Proportions of subjects with systemic sclerosis–associated interstitial lung disease (SSc-ILD) treated with nintedanib or placebo in the SENSCIS trial who had the indicated absolute increases and declines in forced vital capacity (FVC) % predicted at week 52. A post-baseline FVC measurement was not available for 1 patient.

characteristics of subjects in the SENSCIS trial have been described previously (11). The mean ± SD age was 54.0 ± 12.2 years, 75.2% of subjects were female, and 67.2% were White. The mean ± SD FVC was 2,500 ± 777 milliliters and 72.5 ± 16.7 % predicted, and the mean ± SD DL_{CO} was 53.0 ± 15.1 % predicted. Baseline characteristics were similar between the treatment groups (11).

Categorical changes in FVC % predicted. In total, 46 subjects (16.0%) in the nintedanib group and 31 subjects (10.8%) in the placebo group had missing FVC data at week 52. At week 52, 55.7% of subjects in the nintedanib group and 66.3% of subjects in the placebo group had a decline in FVC % predicted. At week 52 the proportions of subjects in the nintedanib group with an absolute decline in FVC of >5% to ≤10% predicted and an absolute decline in FVC of >10% to ≤15% predicted were 13.6% and 3.5%, respectively, while the proportions of subjects in the placebo group with an absolute decline in FVC of >5% to ≤10% predicted and an absolute decline in FVC of >10% to ≤15% predicted were 20.1% and 5.2%, respectively (Figure 1). The proportions of subjects who met thresholds for relative declines or increases in FVC (in milliliters) are shown in Supplementary Figure 1 (available on the *Arthritis & Rheumatology* website at http://onlinelibrary.wiley.com/doi/10.1002/art.41576/abstract). In the nintedanib and placebo groups, respectively, 34.5% versus 43.8% of subjects had an absolute decrease in FVC of ≥3.3% predicted at week 52 (the proposed MCID for worsening of FVC), while 23.0% versus 14.9% had an absolute increase in FVC of ≥3.0% predicted at week 52 (the proposed MCID for improvement in FVC) (Figure 2). Exploratory interaction *P* values did not indicate heterogeneity in the effect of nintedanib versus placebo between subgroups classified by FVC % predicted, extent of fibrotic ILD on HRCT, time since onset of first non–Raynaud's phenomenon symptom at baseline, or glucocorticoid

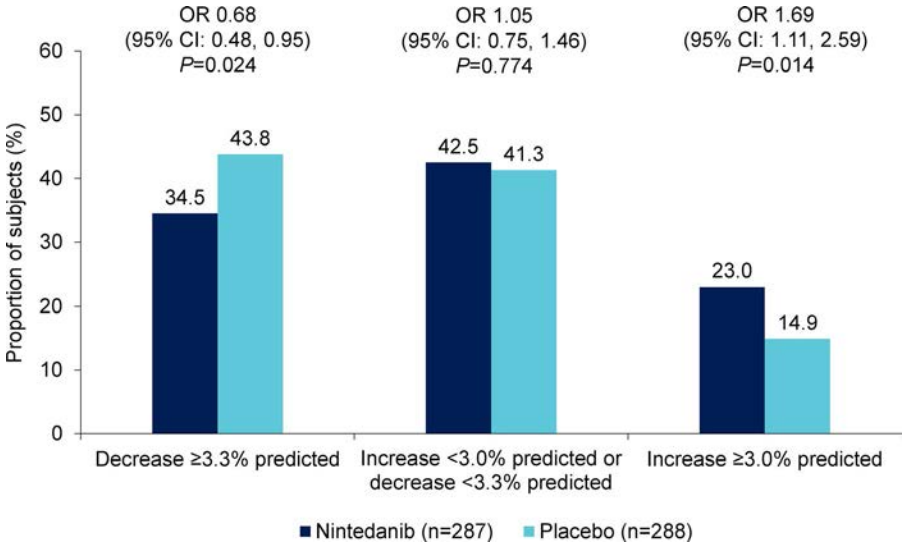

Figure 2. Proportions of subjects with SSc-ILD treated with nintedanib or placebo in the SENSCIS trial who met the proposed threshold for worsening of FVC (decrease of ≥3.3% predicted), stable FVC (increase of <3.0% predicted or decrease of <3.3% predicted), or improvement in FVC (increase of ≥3.0% predicted) at week 52. A post-baseline FVC measurement was not available for 1 patient. OR = odds ratio; 95% CI = 95% confidence interval (see Figure 1 for other definitions).

Table 1. Proportions of subjects with absolute declines in FVC % predicted or death over 52 weeks in the SENSCIS trial*

	Nintedanib (n = 288)	Placebo (n = 288)
Absolute decline in FVC ≥5% predicted or death		
Subjects with event, no. (%)	124 (43.1)	145 (50.3)
Hazard ratio (95% confidence interval)	0.83 (0.66–1.06)	
P	0.14	
Absolute decline in FVC ≥10% predicted or death		
Subjects with event, no. (%)	40 (13.9)	62 (21.5)
Hazard ratio (95% confidence interval)	0.64 (0.43–0.95)	
P	0.03	
Absolute decline in FVC ≥10% predicted or absolute decline in FVC ≥5% to <10% predicted with absolute decline in DLco ≥15% predicted, or death		
Subjects with event, no. (%)	39 (13.5)	69 (22.9)
Hazard ratio (95% confidence interval)	0.58 (0.39–0.87)	
P	0.008	

* FVC = forced vital capacity; DLco = diffusing capacity for carbon monoxide.

use (*P* > 0.05 for treatment-by-subgroup interactions) (Supplementary Figure 2, available on the *Arthritis & Rheumatology* website at http://onlinelibrary.wiley.com/doi/10.1002/art.41576/abstract).

Time to lung function decline or death. Over 52 weeks, an absolute decline in FVC of ≥5% predicted or death occurred in 43.1% of the subjects in the nintedanib group and 50.3% of the subjects in the placebo group (HR 0.83 [95% CI 0.66–1.06]; *P* = 0.14), and an absolute decline in FVC of ≥10% predicted or death occurred in 13.9% of the subjects in the nintedanib group and 21.5% of the subjects in the placebo group (HR 0.64 [95% CI 0.43–0.95]; *P* = 0.029) (Table 1 and Figure 3). Over 52 weeks, an absolute decline in FVC of ≥10% predicted, absolute decline in FVC of ≥5% to <10% predicted with an absolute decline in DLco of ≥15% predicted, or death occurred in 13.5% and 22.9% of subjects in the nintedanib and placebo groups, respectively (HR 0.58 [95% CI 0.39–0.87]; *P* = 0.008) (Table 1).

DISCUSSION

These findings from the SENSCIS trial provide further evidence that nintedanib has a clinically relevant effect on the progression of SSc-ILD. Although there is no established definition for the progression of ILD, declines in FVC of >10% predicted have been used to assess the proportion of subjects with clinically relevant ILD progression in previous studies of SSc-ILD (6,7) and other ILDs (17–20), based on the association between decline in FVC and mortality. In addition, thresholds for improvement and worsening of FVC, derived based on anchoring to the health transition question from the Medical Outcomes Study Short Form-36 in the Scleroderma Lung Studies I and II, have been proposed as MCIDs at a population level (16). In a recent European Delphi consensus study, physicians experienced in the management of SSc-ILD agreed that the progression of SSc-ILD can be assessed using changes in % predicted values for FVC and DLco and that measurement of lung function is an effective tool in long-term follow-up of ILD progression in patients with SSc-ILD (21).

Several studies have shown that a decline in FVC is associated with mortality in patients with SSc-ILD. A study of 171 patients at a single center showed that patients who died within 4 years of SSc-ILD diagnosis had a higher annual rate of decline in FVC than those who died between 4 and 8 years after their SSc-ILD diagnosis or who survived for >8 years (22). Data from Scleroderma Lung Study I (n = 158) showed that absolute declines in FVC of ≥10%

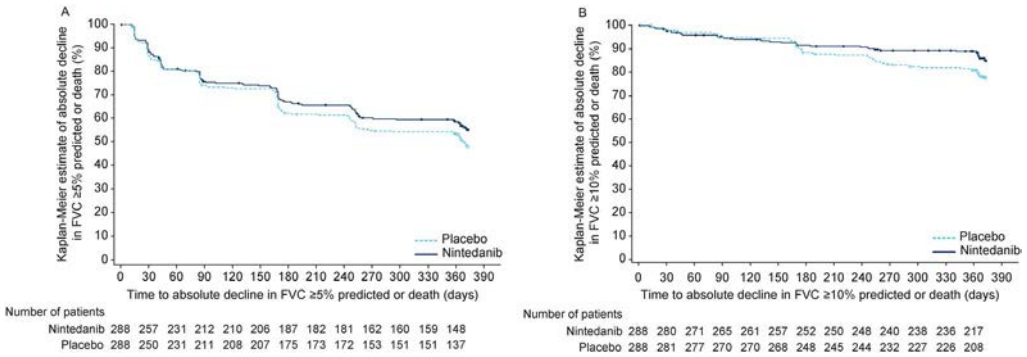

Figure 3. Time to **A**, absolute decline in FVC of ≥5% predicted or death and **B**, absolute decline in FVC of ≥10% predicted or death, over 52 weeks in patients with SSc-ILD treated with nintedanib or placebo in the SENSCIS trial. See Figure 1 for definitions.

predicted or DLco of ≥15% predicted over 2 years were associated with mortality over a median follow-up period of 8 years, while data from Scleroderma Lung Study II (n = 142) showed that an absolute decline in FVC of ≥10% predicted at 1 year was associated with mortality over a median follow-up period of 4 years (7). In a large cohort of subjects in the European Scleroderma Trials and Research (EUSTAR) database (n = 857), an absolute decline in FVC of ≥10% predicted, or an absolute decline in FVC of ≥5% predicted with a decline in DLco of ≥15% predicted, over 12 months was predictive of mortality over a maximum follow-up period of 5 years (5). Recent data from a well-characterized Norwegian cohort (n = 391) showed that ILD progression defined as severe (absolute decline in FVC of >10% predicted or decline in FVC of 5–10% predicted with decline in DLco of ≥15% predicted) or moderate (absolute decline in FVC of 5–10% predicted with decline in DLco of <15% predicted) over a mean follow-up period of almost 4 years was associated with lower survival compared with stable FVC (change <5% predicted), with 10-year survival rates of 59% versus 78% (6). In a long-term UK study of 162 patients, a relative decline in FVC (in milliliters) of ≥10%, or a relative decline in FVC (in milliliters) of 5–9% with a relative decline in DLco of >15% at 1 year was strongly associated with mortality over 15 years (4).

Subgroup analyses of the data from the SENSCIS trial suggest that the proportions of subjects who met proposed thresholds for worsening and improvement in FVC were consistent across subgroups based on FVC % predicted, time since onset of first non–Raynaud's phenomenon symptom, extent of fibrotic ILD on HRCT, and glucocorticoid use at baseline. Previous analyses have shown that the proportions of subjects who met these thresholds were similar across subgroups by anti–topo I antibody status (23), SSc subtype (limited versus diffuse cutaneous SSc) (24), and mycophenolate use at baseline (25). Taken together, these data support a benefit of nintedanib in reducing the proportion of patients with clinically relevant progression of ILD, and increasing the proportion of patients with stable or increased FVC, across a broad population of subjects with SSc-ILD, consistent with the effects of nintedanib previously demonstrated in patients with IPF (26–28).

Strengths of our study include the participation of a large number of well-characterized subjects with SSc-ILD and the highly standardized procedure used for measurement of FVC. Limitations of our analyses include that they were conducted post hoc and, as such, should be considered exploratory. The present study did not assess whether the categorical changes in FVC translated into meaningful improvements/declines in patient-reported outcomes. Our analyses were not adjusted for multiple testing or for confounding factors such as use of mycophenolate. The number of deaths was too small to enable associations between FVC decline and mortality to be studied.

In conclusion, these further analyses of FVC decline in the SENSCIS trial support a clinically meaningful effect of nintedanib on slowing the progression of SSc-ILD.

ACKNOWLEDGMENTS

We would like to thank the subjects who participated in this trial.

AUTHOR CONTRIBUTIONS

All authors were involved in drafting the article or revising it critically for important intellectual content, and all authors approved the final version to be published. Dr. Maher had full access to all of the data in the study and takes responsibility for the integrity of the data and the accuracy of the data analysis.

Study conception and design. Maher, Mayes, Stock, Schoof, Alves, Raghu.
Acquisition of data. Maher, Mayes, Kreuter, Aringer, Castellvi, Cutolo.
Analysis and interpretation of data. Maher, Mayes, Kreuter, Volkmann, Aringer, Castellvi, Cutolo, Stock, Schoof, Alves, Raghu.

ROLE OF THE STUDY SPONSOR

Boehringer Ingelheim was involved in the design of the study, the interpretation of the data, and the writing of the manuscript. The authors had the final decision to submit the manuscript for publication. Writing assistance was provided by Julie Fleming and Wendy Morris (FleishmanHillard Fishburn, London, UK; supported financially by Boehringer Ingelheim).

REFERENCES

1. Van den Hoogen F, Khanna D, Fransen J, Johnson SR, Baron M, Tyndall A, et al. 2013 classification criteria for systemic sclerosis: an American College of Rheumatology/European League against Rheumatism collaborative initiative. Arthritis Rheum 2013;65:2737–47.
2. Elhai M, Meune C, Boubaya M, Avouac J, Hachulla E, Balbir-Gurman A, et al. Mapping and predicting mortality from systemic sclerosis. Ann Rheum Dis 2017;76:1897–905.
3. Goh NS, Desai SR, Veeraraghavan S, Hansell DM, Copley SJ, Maher TM, et al. Interstitial lung disease in systemic sclerosis: a simple staging system. Am J Respir Crit Care Med 2008;177:1248–54.
4. Goh NS, Hoyles RK, Denton CP, Hansell DM, Renzoni EA, Maher TM, et al. Short-term pulmonary function trends are predictive of mortality in interstitial lung disease associated with systemic sclerosis. Arthritis Rheumatol 2017;69:1670–8.
5. Sobanski V, de Vries-Bouwstra J, Hoffmann-Vold A, Huscher D, Alves M, Matucci-Cerinic M, et al. Association of short-term longitudinal changes in clinical and physiologic variables with overall survival in patients with systemic sclerosis-associated interstitial lung disease [abstract]. Arthritis Rheumatol 2018;70 Suppl 10. URL: https://acrabstracts.org/abstract/association-of-short-term-longitudinal-changes-in-clinical-and-physiologic-variables-with-overall-survival-in-patients-with-systemic-sclerosis-associated-interstitial-lung-disease-ssc-ild/.
6. Hoffmann-Vold AM, Fretheim H, Halse AK, Seip M, Bitter H, Wallenius M, et al. Tracking impact of interstitial lung disease in systemic sclerosis in a complete nationwide cohort. Am J Respir Crit Care Med 2019;200:1258–66.
7. Volkmann ER, Tashkin DP, Sim M, Li N, Goldmuntz E, Keyes-Elstein L, et al. Short-term progression of interstitial lung disease in systemic sclerosis predicts long-term survival in two independent clinical trial cohorts. Ann Rheum Dis 2019;78:122–30.
8. Khanna D, Mittoo S, Aggarwal R, Proudman SM, Dalbeth N, Matteson EL, et al. Connective Tissue Disease-associated Interstitial

Lung Diseases (CTD-ILD): report from OMERACT CTD-ILD Working Group. J Rheumatol 2015;42:2168–71.

9. Wollin L, Distler JH, Redente EF, Riches DW, Stowasser S, Schlenker-Herceg R, et al. Potential of nintedanib in treatment of progressive fibrosing interstitial lung diseases. Eur Respir J 2019; 54:1900161.
10. Richeldi L, du Bois RM, Raghu G, Azuma A, Brown KK, Costabel U, et al. Efficacy and safety of nintedanib in idiopathic pulmonary fibrosis. N Engl J Med 2014;370:2071–82.
11. Distler O, Highland KB, Gahlemann M, Azuma A, Fischer A, Mayes MD, et al. Nintedanib for systemic sclerosis-associated interstitial lung disease. N Engl J Med 2019;380:2518–28.
12. Flaherty KR, Wells AU, Cottin V, Devaraj A, Walsh SL, Inoue Y, et al. Nintedanib in progressive fibrosing interstitial lung diseases. N Engl J Med 2019;381:1718–27.
13. Wells AU, Flaherty KR, Brown KK, Inoue Y, Devaraj A, Richeldi L, et al. Nintedanib in patients with progressive fibrosing interstitial lung diseases: subgroup analyses by interstitial lung disease diagnosis in the randomised, placebo-controlled INBUILD trial. Lancet Respir Med 2020;8:453–60.
14. Miller MR, Hankinson J, Brusasco V, Burgos F, Casaburi R, Coates A, et al. Standardisation of spirometry. Eur Respir J 2005;26:319–38.
15. Quanjer PH, Stanojevic S, Cole TJ, Baur X, Hall GL, Culver BH, et al. Multi-ethnic reference values for spirometry for the 3–95-yr age range: the global lung function 2012 equations. Eur Respir J 2012;40:1324–43.
16. Kafaja S, Clements PJ, Wilhalme H, Tseng CH, Furst DE, Kim GH, et al. Reliability and minimal clinically important differences of forced vital capacity: results from the Scleroderma Lung Studies (SLS-I and SLS-II). Am J Respir Crit Care Med 2018;197:644–52.
17. Zappala CJ, Latsi PI, Nicholson AG, Colby TV, Cramer D, Renzoni EA, et al. Marginal decline in forced vital capacity is associated with a poor outcome in idiopathic pulmonary fibrosis. Eur Respir J 2010;35:830–6.
18. Solomon JJ, Chung JH, Cosgrove GP, Demoruelle MK, Fernandez-Perez ER, Fischer A, et al. Predictors of mortality in rheumatoid arthritis-associated interstitial lung disease. Eur Respir J 2016;47:588–96.
19. Gimenez A, Storrer K, Kuranishi L, Soares MR, Ferreira RG, Pereira CA. Change in FVC and survival in chronic fibrotic hypersensitivity pneumonitis [letter]. Thorax 2017;73:391–2.
20. Paterniti MO, Bi Y, Rekić D, Wang Y, Karimi-Shah BA, Chowdhury BA. Acute exacerbation and decline in forced vital capacity are associated with increased mortality in idiopathic pulmonary fibrosis. Ann Am Thorac Soc 2017;14:1395–402.
21. Hoffmann-Vold A, Maher TM, Philpot EE, Ashrafzadeh A, Barake R, Barsotti S, et al. The identification and management of interstitial lung disease in systemic sclerosis: evidence-based European consensus statements. Lancet Rheumatol 2020;2:E71–83.
22. Guler SA, Winstone TA, Murphy D, Hague C, Soon J, Sulaiman N, et al. Does systemic sclerosis-associated interstitial lung disease burn out? Specific phenotypes of disease progression. Ann Am Thorac Soc 2018;15:1427–33.
23. Mayes MD, Highland KB, Gahlemann M, Fischer A, Raghu G, Girard M, et al. Effect of anti-topoisomerase I antibody status on decline in lung function in patients with systemic sclerosis-associated interstitial lung disease (SSc-ILD): data from the SENSCIS trial [poster]. American College of Rheumatology: Poster presented at the 2019 Annual Meeting, Atlanta, Georgia. November 8–13, 2019. URL: http://ILDPosters2019.com/pdf/ACR_SENSCISATAsubgroups_Mayes.pdf.
24. Kuwana M, Highland KB, Gahlemann M, Denton CP, Fischer A, Mayes MD, et al. Effects of nintedanib in patients with diffuse and limited cutaneous systemic sclerosis and interstitial lung disease: subgroup analysis of the SENSCIS trial. American College of Rheumatology: Poster presented at the 2019 Annual Meeting, Atlanta, Georgia. November 8–13, 2019. URL: http://ILDPosters2019.com/pdf/ACR_SENSCISlcSScvsdcSSc_Kuwana.pdf.
25. Highland KB, Distler O, Kuwana M, Allanore Y, Assassi S, Azuma A, et al. Efficacy and safety of nintedanib in patients with systemic sclerosis-associated interstitial lung disease treated with mycophenolate: subgroup analysis of the SENSCIS trial. Lancet Respir Med 2021;9:96–106.
26. Costabel U, Inoue Y, Richeldi L, Collard HR, Tschoepe I, Stowasser S, et al. Efficacy of nintedanib in idiopathic pulmonary fibrosis across prespecified subgroups in INPULSIS. Am J Respir Crit Care Med 2016;193:178–85.
27. Brown KK, Flaherty KR, Cottin V, Raghu G, Inoue Y, Azuma A, et al. Lung function outcomes in the INPULSIS trials of nintedanib in idiopathic pulmonary fibrosis. Respir Med 2019;146:42–8.
28. Richeldi L, Crestani B, Azuma A, Kolb M, Selman M, Stansen W, et al. Outcomes following decline in forced vital capacity in patients with idiopathic pulmonary fibrosis: results from the INPULSIS and INPULSIS-ON trials of nintedanib. Respir Med 2019;156:20–5.

Arthritis & Rheumatology
Vol. 73, No. 4, April 2021, pp 677–686
DOI 10.1002/art.41566

American College of Rheumatology
Empowering Rheumatology Professionals

Risk Prediction Modeling Based on a Combination of Initial Serum Biomarker Levels in Polymyositis/Dermatomyositis–Associated Interstitial Lung Disease

Takahisa Gono,[1] Kenichi Masui,[2] Naoshi Nishina,[3] Yasushi Kawaguchi,[4] Atsushi Kawakami,[5] Kei Ikeda,[6] Yohei Kirino,[7] Yumiko Sugiyama,[8] Yoshinori Tanino,[9] Takahiro Nunokawa,[10] Yuko Kaneko,[3] Shinji Sato,[11] Katsuaki Asakawa,[12] Taro Ukichi,[13] Shinjiro Kaieda,[14] Taio Naniwa,[15] Yutaka Okano,[16] Masataka Kuwana,[1] and the Multicenter Retrospective Cohort of Japanese Patients with Myositis-Associated ILD (JAMI) Investigators

Objective. To establish predictive models for mortality in patients with polymyositis/dermatomyositis–associated interstitial lung disease (PM/DM-ILD) using a combination of initial serum biomarker levels.

Methods. The Multicenter Retrospective Cohort of Japanese Patients with Myositis-Associated ILD (JAMI) database of 497 incident cases of PM/DM-ILD was used as a derivation cohort, and 111 cases were additionally collected as a validation cohort. Risk factors predictive of all-cause mortality were identified by univariate and multivariable Cox regression analyses using candidate serum biomarkers as explanatory variables. The predictive models for mortality were generated in patients with and those without anti–melanoma differentiation–associated gene 5 (MDA-5) antibody, using a combination of risk factors. Cumulative survival rates were assessed using Kaplan-Meier analysis, and were compared between subgroups using the Breslow test.

Results. In the derivation cohort, C-reactive protein (CRP) and Krebs von den Lungen 6 (KL-6) levels were identified as independent risk factors for mortality in both anti–MDA-5–positive and anti–MDA-5–negative patients. We then developed a prediction model based on anti–MDA-5 antibody status, CRP level, and KL-6 level, termed the "MCK model," to identify patients at low (<15%), moderate (15–50%), or high (≥50%) risk of mortality, based on the number of risk factors. The MCK model successfully differentiated cumulative survival rates in anti–MDA-5–positive patients ($P < 0.01$ for low versus moderate risk and $P = 0.03$ for moderate versus high risk) and in anti–MDA-5–negative patients ($P < 0.001$ for low versus moderate risk). The utility of the MCK model was replicated in the validation cohort.

Conclusion. Our findings indicate that an evidence-based risk prediction model using CRP and KL-6 levels combined with anti–MDA-5 antibody status might be useful for predicting prognosis in patients with PM/DM-ILD.

Supported in part by a research grant from the Japanese Ministry of Health, Labor, and Welfare and a research grant from Astellas Pharma.

[1]Takahisa Gono, MD, PhD, Masataka Kuwana, MD, PhD: Nippon Medical School Graduate School of Medicine, Tokyo, Japan; [2]Kenichi Masui, MD: National Defense Medical College School of Medicine, Saitama, Japan, and Show University Hospital, Tokyo, Japan; [3]Naoshi Nishina, MD, PhD, Yuko Kaneko, MD: Keio University School of Medicine, Tokyo, Japan; [4]Yasushi Kawaguchi, MD, PhD: Tokyo Women's Medical University, Tokyo, Japan; [5]Atsushi Kawakami, MD, PhD: Nagasaki University Graduate School of Biomedical Sciences, Nagasaki, Japan; [6]Kei Ikeda, MD, PhD: Chiba University Hospital, Chiba, Japan; [7]Yohei Kirino, MD, PhD: Yokohama City University Graduate School of Medicine, Yokohama, Japan; [8]Yumiko Sugiyama, MD, PhD: Yokohama City University Medical Center, Yokohama, Japan; [9]Yoshinori Tanino, MD, PhD: Fukushima Medical University School of Medicine, Fukushima, Japan; [10]Takahiro Nunokawa, MD: Tokyo Metropolitan Tama Medical Center, Tokyo, Japan; [11]Shinji Sato, MD: Tokai University School of Medicine, Kanagawa, Japan; [12]Katsuaki Asakawa, MD: Niigata University Medical and Dental Hospital, Niigata, Japan; [13]Taro Ukichi, MD, PhD: The Jikei University School of Medicine, Tokyo, Japan; [14]Shinjiro Kaieda, MD: Kurume University School of Medicine, Fukuoka, Japan; [15]Taio Naniwa, MD, PhD: Nagoya City University School of Medicine, Aichi, Japan; [16]Yutaka Okano, MD: Kawasaki Municipal Hospital, Kawasaki, Japan.

Drs. Gono and Masui contributed equally to this work.

Dr. Kawakami has received consulting fees, speaking fees, and/or honoraria from AbbVie, Actelion, Asahi Kasei, Astellas, AstraZeneca, Alexion, Boehringer Ingelheim, Bristol Myers Squibb, Chugai, Cosmic, Daiichi Sankyo, Eisai, Eli Lilly, Kissei, Janssen, Kowa, Kyowa Kirin, Mitsubishi Tanabe, Mochida, MSD, Nihon Medi-Physics, Nippon Kayaku, Novartis, Pfizer, Ono, Otsuka, Sanofi, Sumitomo Dainippon, Taisho Toyama, Takeda, Teijin, UCB, and YI Biologics (less than $10,000 each) and research grants from those companies. Drs. Sato and Kuwana hold the patent for the anti–MDA-5 antibody measurement kit that was used in this study. Dr. Kuwana has received consulting fees, speaking fees, and/or honoraria from AbbVie, Actelion, Asahi Kasei, Astellas, Boehringer Ingelheim, Bayer, Chugai, Eisai, Corbus, CSL Behring, Janssen, MBL, Mitsubishi Tanabe, Mochida, Nippon Shinyaku, Novartis, Pfizer, Ono, Reata, Takeda, Teijin, and UCB (less than $10,000 each) and research grants from those companies. No other disclosures relevant to this article were reported.

Address correspondence to Masataka Kuwana, MD, PhD, Department of Allergy and Rheumatology, Nippon Medical School Graduate School of Medicine, 1-1-5 Sendagi, Bunkyo-ku, Tokyo 113-8603, Japan. Email: kuwanam@nms.ac.jp.

Submitted for publication September 21, 2019; accepted in revised form October 22, 2020.

INTRODUCTION

Polymyositis/dermatomyositis (PM/DM) is characterized by the inflammation of skeletal muscles and skin. Patients with PM/DM often develop extramuscular manifestations, such as arthritis, cardiomyopathy, and interstitial lung disease (ILD) (1). Of these, ILD is one of the leading causes of mortality (2). The clinical course, response to treatment, and prognosis of PM/DM-ILD are highly variable among patients. For example, rapidly progressive ILD can occur over the course of days or weeks and is often refractory to immunosuppressive treatment, leading to death early in the disease course, while subacute ILD progresses over the course of weeks or months and often responds favorably to immunosuppressive treatment (3,4). Therefore, in the clinical setting, it is critical to predict the ILD course to pursue proper management.

A number of potential risk factors associated with poor ILD outcomes have been reported in PM/DM patients, and include demographic characteristics, physical findings, imaging features, and biomarkers (5–15). Of these, measurement of circulating biomarkers has the advantages of convenience and minimal invasiveness. Furthermore, biomarkers are not only correlated with clinical features, such as disease activity and severity, but are also closely involved in the pathophysiology of the disease (16).

In PM/DM patients, myositis-specific autoantibodies are the most reliable biomarker, i.e., patients with anti–melanoma differentiation–associated gene 5 (anti–MDA-5) antibody are more likely to develop rapidly progressive ILD with high mortality (4,6,8,13,17–19), while anti–aminoacyl transfer RNA synthetase (anti-ARS) antibodies are associated with subacute ILD, which frequently recurs after a reduction in treatment intensity (4). However, more than half of anti–MDA-5–positive patients with ILD survive (20,21), and rapidly progressive ILD can occur in patients with anti-ARS antibody (22). These findings clearly indicate that the presence or absence of myositis-specific autoantibodies alone is not sufficient to predict treatment response and mortality accurately. Nevertheless, higher anti–MDA-5 antibody levels measured by enzyme-linked immunosorbent assay (ELISA) were shown to correlate with poor outcomes (23).

Other circulating biomarkers reported to be associated with poor survival include C-reactive protein (CRP), ferritin, Krebs von den Lungen 6 (KL-6), surfactant protein D (SP-D), interferon-α (IFNα), tumor necrosis factor, interleukin-6 (IL-6), IL-8, IL-18, CXCL9, and CXCL10 levels (5,7,9–11,14,15,24–28). In this study, we aimed to establish a convenient risk stratification model based on a combination of initial serum biomarker levels using the large-scale Multicenter Retrospective Cohort of Japanese Patients with Myositis-Associated ILD (JAMI) (21).

PATIENTS AND METHODS

JAMI database. This study used clinical information on 497 adult patients with PM, classic DM, or clinically amyopathic DM (CADM) who were enrolled in the JAMI database as a derivation cohort. Patients with ILD alone without any muscle involvement or hallmark cutaneous manifestation of DM were not included. JAMI is a multicenter, retrospective cohort of incident cases with PM/DM-ILD who visited participating centers between October 2011 and October 2015 (21). See Appendix A for a list of the JAMI investigators. The study protocol has been described in detail elsewhere (21). Briefly, all patients fulfilled the Bohan and Peter criteria for definite or probable PM/DM (29) or the Sontheimer criteria for CADM (30), except that patients were not required to meet the condition of no clinical evidence of myositis for at least 6 months. Demographic characteristics and clinical, laboratory, and imaging data at diagnosis prior to the initiation of immunosuppressive treatment as well as information on initial treatment regimens were collected anonymously in a dedicated electronic database. Information on survival and causes of death, if death occurred, was collected retrospectively and prospectively.

As a validation cohort, we additionally collected 111 adult incident cases with PM/DM-ILD who visited JAMI participating centers after enrollment into the original JAMI cohort had closed, using the same Bohan and Peter criteria (29) or Sontheimer criteria (30) for enrollment. The study protocol was approved by the Ethics Committee of the coordinating center (Nippon Medical School; 26-03-434) and by individual participating centers. The JAMI cohort was registered in the University Hospitals Medical Information Network Clinical Trial Registry (UMIN000018663).

Serum biomarkers. Anti–MDA-5 antibody, anti-ARS antibody, and CRP, ferritin, KL-6, and SP-D levels were chosen as candidate serum biomarkers for the prediction model for mortality, for the following reasons: 1) utility in predicting outcomes in PM/DM-ILD has been reported in the literature (9–12,15,20), and 2) assay systems have been established and validated for clinical use. Anti–MDA-5 antibody was measured using an in-house ELISA (17). Results are shown in units, and a cutoff level for positivity was set at 8 units. Anti-ARS antibody was identified using RNA immunoprecipitation assay (31). CRP, ferritin, KL-6, and SP-D levels were measured in the clinical laboratories of individual participating centers at the time of diagnosis.

Statistical analysis. All statistical analyses were performed by an independent medical statistician (KM) using SPSS Statistics version 23 (IBM), Prism 8.4.2 (GraphPad Software), JMP Pro 14.0.0 (SAS Institute), and R 3.4.3 (The R Foundation for Statistical Computing). Continuous values are shown as the median (2.5–97.5 percentile). Two patients who had both anti–MDA-5 and anti-ARS antibodies were included in both the

Table 1. Baseline characteristics and initial treatment of patients with PM/DM-ILD in the derivation and validation cohorts*

	Derivation cohort (n = 497)	Validation cohort (n = 111)	*P*
Demographic characteristics			
Age at onset, years	57 (29–80)	55 (25–85)	0.86
Male sex, no. (%)	167 (34)	31 (28)	0.25
Disease duration at diagnosis, months	3 (1–62)†	3 (1–51)	0.006
Diagnosis, no. (%)			0.04
PM	76 (15)	10 (9)	
Classic DM	158 (32)	48 (43)	
CADM	263 (53)	53 (48)	
Laboratory parameters			
CK, IU/liter	202 (32–4,267)‡	191 (26–8,212)	0.96
CRP, mg/dl	0.7 (0.02–13.4)‡	0.81 (0.03–16.3)	0.26
Ferritin, ng/ml	357 (22–3,846)§	386 (12–2,011)	0.84
KL-6, units/ml	801 (208–4,431)¶	609 (183–2,828)	0.0003
SP-D, ng/ml	91 (16–615)#	NA	–
Myositis-specific autoantibodies			
Anti–MDA-5 antibody, no. (%)	209 (42)**	60 (54)	0.03
Anti–MDA-5 antibody level, units	106 (11–1,075)	NA	–
Anti-ARS antibody, no. (%)	165 (33)††	46 (41)	0.08
Drugs used for initial treatment, no. (%)			
High-dose glucocorticoids	289 (58)	85 (77)	0.0003
Calcineurin inhibitors	238 (48)	98 (89)	<0.0001
Cyclophosphamide	223 (45)	51 (46)	0.84
IVIG	86 (17)	19 (17)	0.96

* Except where indicated otherwise, values are the median (2.5–97.5 percentile). PM/DM-ILD = polymyositis/dermatomyositis–associated interstitial lung disease; CADM = clinically amyopathic dermatomyositis; CK = creatine kinase; CRP = C-reactive protein; KL-6 = Krebs von den Lungen 6; SP-D = surfactant protein D; NA = not available; anti–MDA-5 = anti–melanoma differentiation–associated gene 5; anti-ARS = anti–aminoacyl transfer RNA synthetase; IVIG = intravenous immunoglobulin.
† Data were available for 495 patients (99.6%).
‡ Data were available for 486 patients (98%).
§ Data were available for 361 patients (73%).
¶ Data were available for 476 patients (96%).
# Data were available for 380 patients (76%).
** Data were available for 493 patients (99%).
†† Data were available for 489 patients (98%).

anti–MDA-5–positive and anti-ARS–positive groups. Multivariable analysis was conducted separately for the anti–MDA-5–positive and anti–MDA-5–negative groups. The cutoff values for the candidate biomarkers for all-cause mortality were determined using receiver operating characteristic (ROC) analysis with multivariable analysis. After assessing multicollinearity, dichotomous variables of biomarkers were applied to the Cox proportional hazards model to identify optimal models for predicting all-cause mortality. No continuous variable was applied to the multivariate analyses. The biomarkers selected by the Breslow test were used to determine the final Cox proportional hazards model. Stepwise backward deletion ($P \geq 0.10$) was performed using the Wald test to select the predictor variables in the model. To examine the impact of treatment on the prediction model, initial treatment agents, including high-dose glucocorticoids (prednisolone equivalent ≥50 mg daily), calcineurin inhibitors (cyclosporine or tacrolimus), cyclophosphamide, and intravenous immunoglobulin, were forcibly included in the final multivariable model as potential confounders.

To verify the original Cox proportional hazards models, a multiple imputation method was applied using 1,000 imputed data sets for all of the missing values of dichotomous variables. For multiple imputation, we used all dichotomous or categorical variables that were significant in a previous study (21). The results are presented as the hazard ratio (HR) and 95% confidence interval (95% CI). We then developed a prediction model for mortality using significant variables derived from the Cox proportional hazards model. Additionally, mortality rates were determined for each score from the original data set, and 95% CIs were calculated using bootstrap analysis with 1,000 resampling data sets. *P* values for multiple comparisons were adjusted using the Benjamini-Hochberg method. Cumulative survival rates were assessed using Kaplan-Meier analysis and were compared between subgroups by the Breslow test. *P* values less than 0.05 were considered significant.

RESULTS

Baseline patient characteristics and outcomes. Selected baseline characteristics and initial treatment of patients in the derivation and validation cohorts are shown in Table 1. The median disease duration at diagnosis was 3 months in

Table 2. Cutoff values for initial serum biomarkers for predicting all-cause mortality in patients with PM/DM-ILD, stratified by the presence or absence of anti–MDA-5 antibody*

Biomarker	Cutoff value†	Sensitivity/specificity,%	AUC	*P*‡	No. of patients with data available
Anti–MDA-5–positive patients					
CRP, mg/dl	0.8	75/59	0.734	<0.001	206
Ferritin, ng/ml	1,000	43/79	0.681	0.001	168
KL-6, units/ml	1,000	78/44	0.717	0.009	204
SP-D, ng/ml	40	68/42	0.544	0.306	167
Anti–MDA-5 antibody level, units	180	45/70	0.624	0.027	209
Anti–MDA-5–negative patients					
CRP, mg/dl	1.1	68/65	0.682	0.002	276
Ferritin, ng/ml	300	44/67	0.694	0.274	191
KL-6, units/ml	1,000	79/62	0.689	0.003	268
SP-D, ng/ml	130	81/44	0.696	0.060	209

* AUC = area under the curve (see Table 1 for other definitions).
† Cutoff values were determined by the multivariable receiver operating characteristic curve.
‡ By Kaplan-Meier analysis with the Breslow test (for details, see Supplementary Figure 1, available on the *Arthritis & Rheumatology* website at http://onlinelibrary.wiley.com/doi/10.1002/art.41566/abstract).

both cohorts, indicating that most patients were diagnosed and treated at an early stage. Our cohort consisted mainly of patients with classic DM or CADM. In the derivation cohort, 91% of the patients fulfilled the 2017 European League against Rheumatism/American College of Rheumatology classification criteria for adult and juvenile idiopathic inflammatory myopathies (32). Anti–MDA-5 and anti-ARS antibodies were detected in 42% and 33%, respectively, of the patients in the derivation cohort.

Ninety-three patients (19%) died during a median observation period of 20 months (range 1–50 months). The causes of death included respiratory insufficiency directly related to ILD in 76 patients (82%), infection in 5 patients (5%), malignancy in 5 patients (5%), and other causes, such as renal insufficiency, cardiomyopathy, and suicide, in 7 patients (8%), indicating that most of the patients in the JAMI cohort died directly of ILD. Of the 93 patients who died, 73 (78%) were positive for anti–MDA-5 antibody, clearly indicating that anti–MDA-5 antibody was the strongest predictor of mortality in the JAMI cohort. The major cause of mortality in anti–MDA-5–positive patients was respiratory insufficiency directly related to ILD (92%; n = 67).

Identification of initial serum biomarkers useful for predicting mortality. In the JAMI cohort, most of the patients who died were anti–MDA-5–positive (21). In fact, patients with anti–MDA-5 antibody had worse survival rates, and those with anti-ARS antibody had better survival rates, than patients without the antibodies ($P < 0.001$ for both comparisons) (Supplementary Figure 1, available on the *Arthritis & Rheumatology* website at http://onlinelibrary.wiley.com/doi/10.1002/art.41566/abstract). In particular, the survival rate decreased dramatically to 70% within 3 months after diagnosis for patients with anti–MDA-5 antibody. Therefore, we decided to develop prediction models for all-cause mortality in anti–MDA-5–positive and anti–MDA-5–negative patients independently.

As candidate serum biomarkers for predictors, CRP, ferritin, KL-6, SP-D, and anti–MDA-5 antibody levels were chosen for anti–MDA-5–positive patients, while CRP, ferritin, KL-6, SP-D levels, and anti-ARS antibody were chosen for anti–MDA-5–negative patients. The maximum variance inflation factors for serum biomarkers were 1.20 and 1.39 in anti–MDA-5–positive patients and anti–MDA-5–negative patients, respectively, indicating a lack of multicollinearity. We then conducted multivariable ROC analysis to determine optimal cutoff values for continuous variables, such as CRP, ferritin, KL-6, SP-D, and anti–MDA-5 antibody levels, for predicting all-cause mortality. The individual cutoff values were selected based on the highest area under the curve (AUC) and were rounded off (Table 2). Interestingly, optimal cutoff levels for serum biomarkers, except KL-6, differed between anti–MDA-5–positive and anti–MDA-5–negative patients, justifying the development of independent prediction models in patient subgroups stratified by the presence or absence of anti–MDA-5 antibody.

Kaplan-Meier curves were determined for patients with PM/DM-ILD stratified by the cutoff values for CRP, ferritin, KL-6, SP-D, and anti–MDA-5 antibody level (for anti–MDA-5–positive patients only), or the presence or absence of anti-ARS antibody (for anti–MDA-5–negative patients only) (Supplementary Figure 2, available on the *Arthritis & Rheumatology* website at http://onlinelibrary.wiley.com/doi/10.1002/art.41566/abstract). The cumulative survival rates were significantly different between the groups divided according to cutoff levels for CRP and KL-6 for both the anti–MDA-5–positive and anti–MDA-5–negative groups, while ferritin and anti–MDA-5 antibody levels were useful for the prediction of survival only in patients with anti–MDA-5 antibody.

To select serum biomarkers for the prediction models, all candidate biomarkers, i.e., CRP, ferritin, KL-6, and anti–MDA-5

Table 3. Initial serum biomarkers for predicting all-cause mortality in patients with PM/DM-ILD, stratified by the presence or absence of anti–MDA-5 antibody*

	Crude		Adjusted for treatment		Multiple imputation		Multiple imputation and adjusted for treatment	
Serum biomarker	HR (95% CI)	*P*	HR (95% CI)	*P*	HR (95% CI)	*P*	HR (95% CI)	*P*
Anti–MDA-5–positive patients†								
CRP ≥0.8 mg/dl	3.1 (1.8–5.3)	<0.001	2.5 (1.4–4.3)	0.001	3.2 (1.9–5.5)	<0.001	2.6 (1.5–4.6)	0.001
KL-6 ≥1,000 units/ml	1.7 (1.0–2.7)	0.033	1.8 (1.1–2.9)	0.012	1.7 (1.0–2.7)	0.031	1.8 (1.1–2.9)	0.011
Anti–MDA-5–negative patients‡								
CRP ≥1.1 mg/dl	3.7 (1.3–10.1)	0.011	4.9 (1.8–13.5)	0.002	3.8 (1.4–10.0)	0.007	4.9 (1.8–13.5)	0.002
KL-6 ≥1,000 units/ml	3.6 (1.2–11.3)	0.017	6.1 (1.9–19.8)	0.003	5.7 (1.9–17.2)	0.002	6.0 (1.8–19.8)	0.003

* Hazard ratios (HRs), 95% confidence intervals (95% CIs), and *P* values were obtained by Cox proportional hazards model using CRP level and KL-6 as explanatory variables. See Table 1 for other definitions.
† n = 203; n = 209 for multiple imputation.
‡ n = 267; n = 284 for multiple imputation.

antibody levels for anti–MDA-5–positive patients, and CRP and KL-6 levels for anti–MDA-5–negative patients, were subjected to Cox regression analysis as potential explanatory variables. Through stepwise backward deletion, we finally selected CRP and KL-6 levels as significant independent risk factors for all-cause mortality in both anti–MDA-5–positive and anti–MDA-5–negative patients. Sensitivity analysis showed that statistical significance was consistent among different models adjusted for initial treatment regimens and/or complementation of the missing data by multiple imputation (Table 3).

Predictive modeling for mortality based on a combination of serum biomarkers. We then generated a predictive model for all-cause mortality based on the levels at diagnosis of a combination of independent serum biomarkers, in anti–MDA-5–positive and anti–MDA-5–negative patients separately (CRP ≥0.8 mg/dl and KL-6 ≥1,000 units/ml for anti–MDA-5–positive patients, and CRP ≥1.1 mg/dl and KL-6 ≥1,000 units/ml for anti–MDA-5–negative patients) (Table 4). When the risk score was defined as the number of risk factors, the mortality rates for patients with risk scores of 0, 1, and 2 were 13.6%, 39.2%, and 57.5%, respectively, in anti–MDA-5–positive patients. In this 3-group model, the 95% CIs of the mortality rates estimated by the bootstrap method were separated with minimum overlap among the subgroups. However, in anti–MDA-5–negative patients, observed mortality rates for patients with risk scores of 0, 1, and 2 were 2.0%, 4.7%, and 27.5%, respectively. The 95% CIs of the mortality rates estimated by the bootstrap method had an apparent overlap between patients with a score of 0 and those with a score of 1. Therefore, we combined the patients with a risk score of 0 and those with a risk score of 1 to create a 2-group model, resulting in good separation of the 95% CIs between the 2 groups. Given these results, we built a prognostic matrix model, based

Table 4. All-cause mortality rates by the risk score observed in the cohort and estimated by the bootstrap method, stratified by the presence or absence of anti–MDA-5 antibody*

Risk score†	Observed mortality rate, %	Mortality rate estimated by the bootstrap method, median % (95% CI)
Anti–MDA-5–positive patients (3-group model)		
0 (n = 66)	13.6	13.4 (6.0–22.2)
1 (n = 97)	39.2	39.9 (30.0–50.0)
2 (n = 40)	57.5	57.5 (43.1–73.0)
Anti–MDA-5–negative patients (3-group model)		
0 (n = 100)	2.0	1.9 (0.0–5.3)
1 (n = 127)	4.7	4.5 (1.5–8.5)
2 (n = 40)	27.5	27.1 (13.9–41.7)
Anti–MDA-5–negative patients (2-group model)		
0 or 1 (n = 227)	3.5	3.1 (0.0–7.8)
2 (n = 40)	27.5	27.1 (13.9–41.7)

* 95% CI = 95% confidence interval (see Table 1 for other definitions).
† Number of individual risk factors (CRP level ≥0.8 mg/dl and KL-6 ≥1,000 units/ml for anti–MDA-5–positive patients, and CRP level ≥1.1 mg/dl and KL-6 ≥1,000 units/ml for anti–MDA-5–negative patients).

on anti–MDA-5 antibody, CRP level, and KL-6 level, termed "MCK model," identifying patients with PM/DM-ILD at low (<15%), moderate (15–50%), or high (≥50%) risk of mortality during the follow-up period (Figure 1A).

Kaplan-Meier analysis with the Breslow test revealed that the survival curves were significantly differentiated between anti–MDA-5–positive patients stratified by risk score, confirming the validity of this 3-group model (Figure 1C). In anti–MDA-5–negative patients, there was no difference in the cumulative survival rates between patients with a score of 0 and those with a score of 1 in the 3-group model, but differentiation of survival curves in the 2-group model was excellent (Figure 1E). When we divided anti–MDA-5–positive patients into 2 groups based on antibody level (≥180 units and <180 units), survival curves differed according to the MCK model score in both groups, but the MCK model performed better in patients with anti–MDA-5 antibody level <180 units (Supplementary Figure 3, available on the *Arthritis & Rheumatology* website at http://onlinelibrary.wiley.com/doi/10.1002/art.41566/abstract). Concordant results were obtained when these models were tested for mortality due to respiratory insufficiency directly related to ILD instead of all-cause mortality (Supplementary Figure 4, available on the *Arthritis & Rheumatology* website at http://onlinelibrary.wiley.com/doi/10.1002/art.41566/abstract).

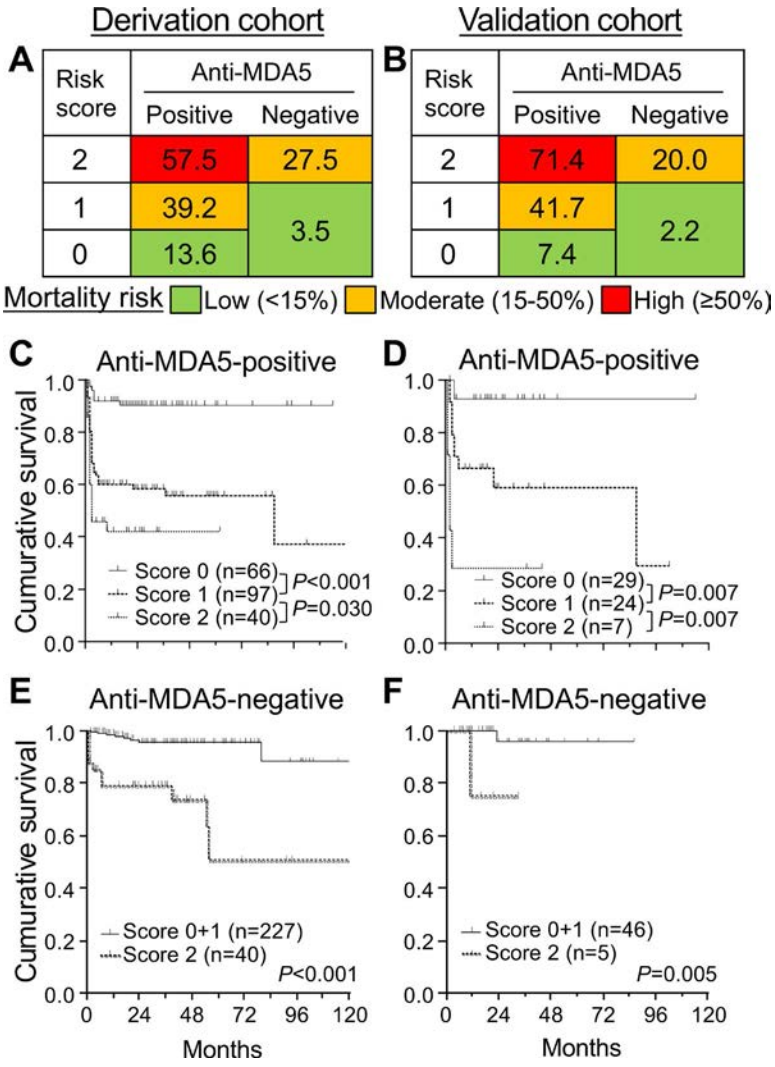

Figure 1. A model of mortality risk in patients with polymyositis/dermatomyositis–associated interstitial lung disease (PM/DM-ILD) based on anti–melanoma differentiation–associated gene 5 (anti–MDA-5) antibody status, C-reactive protein (CRP) level, and Krebs von den Lungen 6 (KL-6) (the MCK matrix model), and cumulative survival rates in patients with PM/DM-ILD classified by risk score. The risk score was defined as the number of risk factors (CRP ≥0.8 mg/dl and KL-6 ≥1,000 units/ml for anti–MDA-5–positive patients, and CRP ≥1.1 mg/dl and KL-6 ≥ 1,000 units/ml for anti–MDA-5–negative patients). **A** and **B**, The MCK matrix model of mortality risk (low, moderate, or high) based on the risk score and anti–MDA-5 antibody status in the derivation cohort (**A**) and validation cohort (**B**). Values in the matrices are the rates of all-cause mortality. **C** and **D**, Survival curves using the 3-group model for anti–MDA-5–positive patients in the derivation cohort (**C**) and validation cohort (**D**). **E** and **F**, Survival curves using the 2-group model for anti–MDA-5–negative patients in the derivation cohort (**E**) and validation cohort (**F**). Survival curves were determined by Kaplan-Meier analysis with the Breslow test.

Table 5. Performance of the MCK model compared with anti–MDA-5 antibody testing alone in predicting mortality in patients with PM/DM-ILD*

	Sensitivity	Specificity	PPV	NPV	Accuracy
All-cause mortality (n = 470)					
Anti–MDA-5 antibody testing alone	79	65	35	93	68
MCK model					
Low risk	81	73	41	94	74
High risk	26	96	58	84	82
Mortality due to ILD (n = 470)					
Anti–MDA-5 antibody testing alone	88	66	32	97	69
MCK model					
Low risk	87	72	37	97	74
High risk	29	95	55	88	85

* Risk stratification in the MDA-5, CRP, and KL-6 (MCK) model was determined based on the prognostic matrix model shown in Figure 1. Values are the percent. PPV = positive predictive value; NPV = negative predictive value (see Table 1 for other definitions).

The performance of the MCK model for predicting mortality in patients with PM/DM-ILD was compared with anti–MDA-5 antibody testing alone (Table 5). Anti–MDA-5 antibody testing was a binary variable and had a sensitivity of 79%, specificity of 65%, positive predictive value (PPV) of 35%, negative predictive value of 93%, and accuracy of 68% for all-cause mortality. In contrast, the MCK model enabled us to divide the patients into 3 risk groups: high risk, moderate risk, and low risk. Identification of patients with low risk resulted in increased sensitivity and specificity (81% and 73%, respectively) without decreases in other indices. When patients with high risk were selected, specificity was increased to 96% with a PPV of 58% and accuracy of 82%. Almost concordant findings were observed when we evaluated the risk of mortality due to ILD. These findings suggest improvement of risk stratification in patients with PM/DM-ILD using the MCK model.

Validation of the MCK model in a validation cohort. An independent validation cohort consisting of 111 adult incident cases of PM/DM-ILD was used to assess the reproducibility of the MCK model for the prediction of mortality risk. In the validation cohort, 19 patients (17%) died during a median of 21 months. The baseline characteristics were similar between the cohorts, while anti–MDA-5 antibody was more prevalent and the patients were treated more intensively in the validation cohort than in the derivation cohort (Table 1). The prognostic MCK matrix model developed in the derivation cohort was principally replicated in the validation cohort (Figure 1B). In addition, cumulative survival rates stratified by the MCK model were principally similar to those in the derivation cohort (Figures 1D and F).

Simplified MCK model. In the MCK model, different cutoff levels for CRP were applied for anti–MDA-5–positive and anti–MDA-5–negative patients (0.8 and 1.1 mg/dl, respectively). To make the modeling more convenient, the optimal cutoff level for CRP for the entire cohort was investigated using ROC analysis, and found to be 1.0 mg/dl (AUC 0.704). The simplified MCK model using CRP ≥1.0 mg/dl and KL-6 ≥1,000 units/ml for all patients with PM/DM-ILD showed acceptable performance in terms of discrimination of cumulative survival rates in both anti–MDA-5–positive and anti–MDA-5–negative patients (Supplementary Figure 5, available on the *Arthritis & Rheumatology* website at http://onlinelibrary.wiley.com/doi/10.1002/art.41566/abstract).

DISCUSSION

We successfully developed an evidence-based MCK risk stratification model for mortality in patients with PM/DM-ILD, based on a combination of serum biomarkers measured at diagnosis. Anti–MDA-5 antibody was the strongest predictor of poor survival in patients with PM/DM-ILD in the JAMI cohort (21), but we showed that the additional measurement of CRP and KL-6 levels enhanced the accuracy for predicting outcomes. Interestingly, the same predictors, CRP and KL-6 levels, were identified in both anti–MDA-5–positive and anti–MDA-5–negative patients, resulting in the development of the simplified, convenient modeling. The MCK model has several advantages over anti–MDA-5 antibody testing alone: it provides more detailed risk stratification by dividing patients into 3 risk groups, and it enables us to subdivide mortality risk by anti–MDA-5 antibody status. A strength of our study is the consistency of the utility of the MCK model across independent derivation and validation cohorts, which were selected in different treatment eras. However, the MCK model still needs to be validated in prospective studies involving various patient populations.

The MCK model is potentially useful in clinical practice for predicting prognosis and deciding on treatment regimens for patients newly diagnosed as having PM/DM-ILD. Since the predictors used for the MCK model remained significant even after adjustment for treatment, therapeutic regimens had little impact on the prediction of mortality risk. Up-front aggressive immunosuppression consisting of high-dose glucocorticoids and a combination of immunosuppressants was used for the treatment of DM-ILD based solely

on anti–MDA-5 antibody positivity (33), but severe infection while receiving excessive immunosuppression is reported to be a critical prognostic factor in this patient population (34). Since the MCK model was able to identify patients with a low risk of mortality, it might provide information useful to avoid unnecessary excessive immunosuppression in such patients. The MCK model identified patients with a high mortality risk with a specificity of 96%. These patients should be treated with aggressive immunosuppression, and might be eligible for clinical trials of potential novel treatments, such as tofacitinib (35) and plasma exchange (36). Taken together, these findings indicate that the MCK model could contribute to personalized medicine in patients with PM/DM-ILD (37).

Our prediction model was able to identify patients with moderate mortality risk in the anti–MDA-5–negative patient subset, although its proportion was relatively small (15% and 10% in the derivation and validation cohorts, respectively). In the JAMI cohort, anti-ARS antibody had less prognostic value in anti–MDA-5–negative patients. Rapidly progressive ILD can occur in patients with antisynthetase syndrome, but there is no reliable predictor of poor prognosis (22,38), indicating the value of the MCK model in anti–MDA-5–negative patients with PM/DM-ILD.

The independent risk factors for mortality identified in this study are not only biomarkers, but also may reflect the ongoing pathogenic process of PM/DM-ILD. MDA-5 is a sensor for double-stranded RNA viruses such as picornavirus, and is involved in the synthesis of type I IFN and the activation of NF-κB (39). The pathogenic contribution of the anti–MDA-5 antibody itself is not well documented, but a recent study suggested that anti–MDA-5 antibodies induce epithelial cell injury and a resultant release of inflammatory cytokines by promoting the formation of neutrophil extracellular traps (40). A high titer of anti–MDA-5 antibody was shown to correlate with poor treatment outcomes in patients with PM/DM-ILD (22,41,42), but our study failed to show that anti–MDA-5 antibody level was an independent predictor of mortality.

The level of CRP produced, which is under the control of IL-6 signaling (43), has been shown to be associated with disease activity and poor prognosis in patients with PM/DM-ILD (44–46). KL-6 is a mucin-like, high molecular weight glycoprotein expressed mainly on the surface membrane of type 2 alveolar pneumocytes, and an elevated level of circulating KL-6 is thought to result from the injury of alveolar cells and the destruction of vasculature in the lungs (47,48). Interestingly, CRP and KL-6 were identified as risk factors for mortality independent of anti–MDA-5 antibody status. Therefore, the biomarkers identified may reflect ongoing pathogenic processes of PM/DM-ILD, including injury of alveolar epithelium and vasculature, and the activation of inflammatory cytokine pathways.

There were several limitations to this study. First, the participating centers of the JAMI cohort consist mainly of tertiary referral hospitals, which were likely to enroll patients with more severe disease. In fact, patients with anti–MDA-5 antibodies dominated the JAMI cohort, but a series of analyses indicated that CRP and KL-6 levels were predictors of mortality independent of anti–MDA-5 antibody positivity. Second, JAMI did not enroll patients with anti-ARS antibody without any muscle or skin symptoms. This is simply because JAMI protocol was established in 2011 when measurement of anti-ARS and anti–MDA-5 antibodies was not routinely feasible in clinical practice and thus was not part of the inclusion criteria. Expansion of the disease spectrum of PM/DM-ILD and inclusion of antisynthetase syndrome should be an interesting future research agenda. Third, candidate serum biomarkers were selected based on availability in the JAMI database, and were not chosen from a large panel of potential biomarkers. Finally, measurement of KL-6 level is currently available in clinical practice only in some countries. Nevertheless, there is accumulating evidence showing the utility of KL-6 as a biomarker for diagnosis, and for the prediction of disease progression, prognosis, and treatment response in patients with various types of ILD, especially those with a progressive phenotype and poor outcomes, such as idiopathic pulmonary fibrosis and ILD associated with systemic sclerosis, rheumatoid arthritis, and PM/DM (49,50), supporting widespread use of KL-6 measurement in routine clinical practice.

In conclusion, we successfully established the MCK risk stratification model using serum biomarkers in patients with PM/DM-ILD using data from a large cohort. The MCK model might help physicians decide how to manage patients with newly diagnosed PM/DM-ILD, and could be also useful for cohort enrichment in future clinical trials.

AUTHOR CONTRIBUTIONS

All authors were involved in drafting the article or revising it critically for important intellectual content, and all authors approved the final version to be published. Dr. Kuwana had full access to all of the data in the study and takes responsibility for the integrity of the data and the accuracy of the data analysis.

Study conception and design. Gono, Masui, Nishina, Sato, Kuwana.
Acquisition of data. Gono, Masui, Nishina, Kawaguchi, Kawakami, Ikeda, Kirino, Sugiyama, Tanino, Nunokawa, Kaneko, Sato, Asakawa, Ukichi, Kaieda, Naniwa, Okano, Kuwana.
Analysis and interpretation of data. Masui.

REFERENCES

1. Lundberg IE, de Visser M, Werth VP. Classification of myositis [review]. Nat Rev Rheumatol 2018;14:269–78.
2. Marie I. Morbidity and mortality in adult polymyositis and dermatomyositis. Curr Rheumatol Rep 2012;14:275–85.
3. Kawasumi H, Gono T, Kawaguchi Y, Yamanaka H. Recent treatment of interstitial lung disease with idiopathic inflammatory myopathies. Clin Med Insights Circ Respir Pulm Med 2015;9 Suppl:9–17.
4. Gono T, Kuwana M. Inflammatory myopathies: choosing the right biomarkers to predict ILD in myositis [review]. Nat Rev Rheumatol 2016;12:504–6.
5. Takada T, Suzuki E, Nakano M, Kagamu H, Tsukada H, Hasegawa T, et al. Clinical features of polymyositis/dermatomyositis with steroid-resistant interstitial lung disease. Intern Med 1998;37:669–73.
6. Selva-O'Callaghan A, Labrador-Horrillo M, Muñoz-Gall X, Martínez-Gomez X, Majó-Masferrer J, Solans-Laque R, et al. Polymyositis/

dermatomyositis-associated lung disease: analysis of a series of 81 patients. Lupus 2005;14:534–42.
7. Cao H, Xia Q, Pan M, Zhao X, Li X, Shi R, et al. Gottron papules and Gottron sign with ulceration: a distinctive cutaneous feature in a subset of patients with classic dermatomyositis and clinically amyopathic dermatomyositis. J Rheumatol 2016;43:1735–42.
8. Sato S, Hirakata M, Kuwana M, Suwa A, Inada S, Mimori T, et al. Autoantibodies to a 140-kd polypeptide, CADM-140, in Japanese patients with clinically amyopathic dermatomyositis. Arthritis Rheum 2005;52:1571–6.
9. Gono T, Kawaguchi Y, Satoh T, Kuwana M, Katsumata Y, Takagi K, et al. Clinical manifestation and prognostic factor in anti-melanoma differentiation-associated gene 5 antibody-associated interstitial lung disease as a complication of dermatomyositis. Rheumatology (Oxford) 2010;49:1713–9.
10. Xu Y, Yang CS, Li YJ, Liu XD, Wang JN, Zhao Q, et al. Predictive factors of rapidly progressive-interstitial lung disease in patients with clinically amyopathic dermatomyositis. Clin Rheumatol 2016; 35:113–6.
11. Arai S, Kurasawa K, Maezawa R, Owada T, Okada H, Fukuda T. Marked increase in serum KL-6 and surfactant protein D levels during the first 4 weeks after treatment predicts poor prognosis in patients with active interstitial pneumonia associated with polymyositis/dermatomyositis. Mod Rheumatol 2013;23:872–83.
12. Hozumi H, Fujisawa T, Nakashima R, Johkoh T, Sumikawa H, Murakami A, et al. Comprehensive assessment of myositis-specific autoantibodies in polymyositis/dermatomyositis-associated interstitial lung disease. Respir Med 2016;121:91–9.
13. Koga T, Fujikawa K, Horai Y, Okada A, Kawashiri SY, Iwamoto N, et al. The diagnostic utility of anti-melanoma differentiation-associated gene 5 antibody testing for predicting the prognosis of Japanese patients with DM. Rheumatology (Oxford) 2012;51:1278–84.
14. Tanizawa K, Handa T, Nakashima R, Kubo T, Hosono Y, Aihara K, et al. The prognostic value of HRCT in myositis-associated interstitial lung disease. Respir Med 2013;107:745–52.
15. Fujiki Y, Kotani T, Isoda K, Ishida T, Shoda T, Yoshida S, et al. Evaluation of clinical prognostic factors for interstitial pneumonia in anti-MDA5 antibody-positive dermatomyositis patients. Mod Rheumatol 2018;28:133–40.
16. Jog NR, James JA. Biomarkers in connective tissue diseases. J Allergy Clin Immunol 2017;140:1473–83.
17. Sato S, Hoshino K, Satoh T, Fujita T, Kawakami Y, Kuwana M. RNA helicase encoded by melanoma differentiation–associated gene 5 is a major autoantigen in patients with clinically amyopathic dermatomyositis: association with rapidly progressive interstitial lung disease. Arthritis Rheum 2009;60:2193–200.
18. Moghadam-Kia S, Oddis CV, Sato S, Kuwana M, Aggarwal R. Anti–melanoma differentiation–associated gene 5 is associated with rapidly progressive lung disease and poor survival in US patients with amyopathic and myopathic dermatomyositis. Arthritis Care Res (Hoboken) 2016;68:689–94.
19. Moghadam-Kia S, Oddis CV, Sato S, Kuwana M, Aggarwal R. Antimelanoma differentiation-associated gene 5 antibody: expanding the clinical spectrum in North American patients with dermatomyositis. J Rheumatol 2017;44:319–25.
20. Gono T, Sato S, Kawaguchi Y, Kuwana M, Hanaoka M, Katsumata Y, et al. Anti-MDA5 antibody, ferritin and IL-18 are useful for the evaluation of response to treatment in interstitial lung disease with anti-MDA5 antibody-positive dermatomyositis. Rheumatology (Oxford) 2012;51:1563–70.
21. Sato S, Masui K, Nishina N, Kawaguchi Y, Kawakami A, Tamura M, et al. Initial predictors of poor survival in myositis-associated interstitial lung disease: a multicentre cohort of 497 patients. Rheumatology (Oxford) 2018;57:1212–21.
22. Huang K, Aggarwal R. Antisynthetase syndrome: a distinct disease spectrum. J Scleroderma Relet Disord 2020;5:178–91.
23. Sato S, Kuwana M, Fujita T, Suzuki Y. Anti-CADM-140/MDA5 autoantibody titer correlates with disease activity and predicts disease outcome in patients with dermatomyositis and rapidly progressive interstitial lung disease. Mod Rheumatol 2013;23: 496–502.
24. Zhang L, Wu G, Gao D, Liu G, Pan L, Ni L, et al. Factors associated with interstitial lung disease in patients with polymyositis and dermatomyositis: a systematic review and meta-analysis. PLoS One 2016;11:e0155381.
25. Horai Y, Koga T, Fujikawa K, Takatani A, Nishino A, Nakashima Y, et al. Serum interferon-α is a useful biomarker in patients with anti-melanoma differentiation-associated gene 5 (MDA5) antibody-positive dermatomyositis. Mod Rheumatol 2015;25:85–9.
26. Kawasumi H, Gono T, Kawaguchi Y, Kaneko H, Katsumata Y, Hanaoka M, et al. IL-6, IL-8, and IL-10 are associated with hyperferritinemia in rapidly progressive interstitial lung disease with polymyositis/dermatomyositis. Biomed Res Int 2014;2014:815245.
27. Richards TJ, Eggebeen A, Gibson K, Yousem S, Fuhrman C, Gochuico BR, et al. Characterization and peripheral blood biomarker assessment of anti–Jo-1 antibody–positive interstitial lung disease. Arthritis Rheum 2009;60:2183–92.
28. Zou J, Chen J, Yan Q, Guo Q, Bao C. Serum IL8 and mRNA level of CD11b in circulating neutrophils are increased in clinically amyopathic dermatomyositis with active interstitial lung disease. Clin Rheumatol 2016;35:117–25.
29. Bohan A, Peter JB. Polymyositis and dermatomyositis (first of two parts). N Engl J Med 1975;292:344–7.
30. Sontheimer RD. Would a new name hasten the acceptance of amyopathic dermatomyositis (dermatomyositis siné myositis) as a distinctive subset within the idiopathic inflammatory dermatomyopathies spectrum of clinical illness? J Am Acad Dermatol 2002;46:626–36.
31. Forman MS, Nakamura M, Mimori T, Gelpi C, Hardin JA. Detection of antibodies to small nuclear ribonucleoproteins and small cytoplasmic ribonucleoproteins using unlabeled cell extracts. Arthritis Rheum 1985;28:1356–61.
32. Lundberg IE, Tjärnlund A, Bottai M, Werth VP, Pilkington C, de Visser M, et al. 2017 European League Against Rheumatism/American College of Rheumatology classification criteria for adult and juvenile idiopathic inflammatory myopathies and their major subgroups. Arthritis Rheumatol 2017;69:2271–82.
33. Tsuji H, Nakashima R, Hosono Y, Imura Y, Yagita M, Yoshifuji H, et al. Multicenter prospective study of the efficacy and safety of combined immunosuppressive therapy with high-dose glucocorticoid, tacrolimus, and cyclophosphamide in interstitial lung diseases accompanied by anti–melanoma differentiation–associated gene 5–positive dermatomyositis. Arthritis Rheumatol 2020;72:488–98.
34. Sugiyama Y, Yoshimi R, Tamura M, Takeno M, Kunishita Y, Kishimoto D, et al. The predictive prognostic factors for polymyositis/dermatomyositis-associated interstitial lung disease. Arthritis Res Ther 2018;20:7.
35. Chen Z, Wang X, Ye S. Tofacitinib in amyopathic dermatomyositis-associated interstitial lung disease. N Engl J Med 2019;381: 291–93.
36. Shirakashi M, Nakashima R, Tsuji H, Tanizawa K, Handa T, Hosono Y, et al. Efficacy of plasma exchange in anti-MDA5-positive dermatomyositis with interstitial lung disease under combined immunosuppressive treatment. Rheumatology (Oxford) 2020;59:3284–92.

37. Romero-Bueno F, del Campo PD, Trallero-Araguás E, Ruiz-Rodríguez JC, Castellvi I, Rodriguez-Nieto MJ, et al. Recommendations for the treatment of anti-melanoma differentiation-associated gene 5-positive dermatomyositis-associated rapidly progressive interstitial lung disease. Semin Arthritis Rheum 2020;50:776–90.
38. Vuillard C, de Chambrun MP, de Prost N, Guérin C, Schmidt M, Dargent A, et al. Clinical features and outcome of patients with acute respiratory failure revealing anti-synthetase or anti-MDA-5 dermato-pulmonary syndrome: a French multicenter retrospective study. Ann Intensive Care 2018;8:87.
39. Takeuchi O, Akira S. MDA5/RIG-I and virus recognition. Curr Opin Immunol 2008;20:17–22.
40. Peng Y, Zhang S, Zhao Y, Liu Y, Yan B. Neutrophil extracellular traps may contribute to interstitial lung disease associated with anti-MDA5 autoantibody positive dermatomyositis. Clin Rheumatol 2018;37:107–15.
41. Sato S, Kuwana M, Fujita T, Suzuki Y. Amyopathic dermatomyositis developing rapidly progressive interstitial lung disease with elevation of anti-CADM-140/MDA5 autoantibodies. Mod Rheumatol 2012;22:625–9.
42. Sato S, Murakami A, Kuwajima A, Takehara K, Mimori T, Kawakami A, et al. Clinical utility of an enzyme-linked immunosorbent assay for detecting anti-melanoma differentiation-associated gene 5 autoantibodies. PLoS One 2016;11:e0154285.
43. Deichmann M, Benner A, Waldmann V, Bock M, Jäckel A, Näher H. Interleukin-6 and its surrogate C-reactive protein are useful serum markers for monitoring metastasized malignant melanoma. J Exp Clin Cancer Res 2000;19:301–7.
44. Gono T, Kawaguchi Y, Hara M, Masuda I, Katsumata Y, Shinozaki M, et al. Increased ferritin predicts development and severity of acute interstitial lung disease as a complication of dermatomyositis. Rheumatology (Oxford) 2010;49:1354–60.
45. Gono T, Kawaguchi Y, Ozeki E, Ota Y, Satoh T, Kuwana M, et al. Serum ferritin correlates with activity of anti-MDA5 antibody-associated acute interstitial lung disease as a complication of dermatomyositis. Mod Rheumatol 2011;21:223–7.
46. Isoda K, Takeuchi T, Kotani T, Hata K, Shoda T, Ishida T, et al. Pretreatment ferritin level and alveolar-arterial oxygen gradient can predict mortality rate due to acute/subacute interstitial pneumonia in dermatomyositis treated by cyclosporine a/glucocorticosteroid combination therapy: a case control study. PLoS One 2014;9:e89610.
47. Kohno N, Kyoizumi S, Awaya Y, Fukuhara H, Yamakido M, Akiyama M. New serum indicator of interstitial pneumonitis activity. Sialylated carbohydrate antigen KL-6. Chest 1989;96:68–73.
48. Ishikawa N, Hattori N, Yokoyama A, Kohno N. Utility of KL-6/MUC1 in the clinical management of interstitial lung diseases. Respir Investig 2012;50:3–13.
49. Chiba H, Otsuka M, Takahashi H. Significance of molecular biomarkers in idiopathic pulmonary fibrosis: a mini review. Respir Investig 2018;56:384–91.
50. Inoue Y, Kaner RJ, Guiot J, Maher TM, Tomassetti S, Moiseev S, et al. Diagnostic and prognostic biomarkers for chronic fibrosing interstitial lung diseases with a progressive phenotype. Chest 2020;158:646–59.

APPENDIX A: THE JAMI INVESTIGATORS

The JAMI Investigators are as follows: Yukie Yamaguchi (Yokohama City University Graduate School of Medicine), Yoshinori Taniguchi (Kochi Medical School, Kochi University), Jun Kikuchi (Saitama Medical Center, Saitama Medical University), Makoto Kubo (Yamaguchi University Graduate School of Medicine), Masaki Watanabe (Graduate School of Medical and Dental Sciences, Kagoshima University), Tatsuhiko Harada (Nagasaki University School of Medicine), Taisuke Kazuyori (The Jikei University School of Medicine Katsushika Medical Center), Hideto Kameda (Toho University Ohashi Medical Center), Makoto Kaburaki (Toho University School of Medicine), Yasuo Matsuzawa (Toho University Medical Center, Sakura Hospital), Shunji Yoshida (Fujita Health University School of Medicine), Yasuko Yoshioka (Juntendo University Urayasu Hospital), Takuya Hirai (Juntendo University Urayasu Hospital), Yoko Wada (Niigata University Graduate School of Medical and Dental Sciences), Koji Ishii (Faculty of Medicine, Oita University), Sakuhei Fujiwara (Faculty of Medicine, Oita University), Takeshi Saraya (Kyorin University), Kozo Morimoto (Fukujuji Hospital, Japan Anti-Tuberculosis Association), Tetsu Hara (Hiratsuka Kyosai Hospital), Hiroki Suzuki (Saiseikai Yamagata Saisei Hospital), Hideki Shibuya (Tokyo Teishin Hospital), Yoshinao Muro (Nagoya University Graduate School of Medicine), Ryoichi Aki (Kitasato University School of Medicine), Takuo Shibayama (National Hospital Organization Okayama Medical Center), Shiro Ohshima (National Hospital Organization Osaka Minami Medical Center), Yuko Yasuda (Saiseikai Kumamoto Hospital), Masaki Terada (Saiseikai Niigata Daini Hospital), and Yoshie Kawahara (Keiyu Hospital).

Arthritis & Rheumatology
Vol. 73, No. 4, April 2021, pp 687–692
DOI 10.1002/art.41569

American College of Rheumatology
Empowering Rheumatology Professionals

BRIEF REPORT

Can Dual-Energy Computed Tomography Be Used to Identify Early Calcium Crystal Deposition in the Knees of Patients With Calcium Pyrophosphate Deposition?

Jean-François Budzik,[1] Claire Marzin,[2] Julie Legrand,[2] Laurène Norberciak,[2] Fabio Becce,[3] and Tristan Pascart[1]

Objective. To assess the ability of dual-energy computed tomography (DECT) in identifying early calcium crystal deposition in menisci and articular cartilage of the knee, depending on the presence/absence of chondrocalcinosis seen on conventional CT.

Methods. One hundred thirty-two knee DECT scans from patients with suspected crystal-associated arthropathy were reviewed and assigned to a calcium pyrophosphate deposition (CPPD) group (n = 50) or a control group (n = 82). Five DECT attenuation parameters were measured in preset regions of interest (ROIs) in menisci and articular cartilage and compared between groups using linear mixed models with adjustment for confounders. Subgroup analysis, excluding ROIs with chondrocalcinosis seen on conventional CT, was performed.

Results. In both menisci and articular cartilage, and for all 5 DECT attenuation parameters, calcified ROIs in CPPD patients showed significantly higher values than ROIs in controls ($P \leq 0.036$). Conversely, noncalcified ROIs in CPPD patients were comparable with those in controls ($P \geq 0.09$). While specific DECT parameters yielded good accuracy (area under the curve [AUC] 0.87–0.88) in differentiating calcified ROIs in CPPD patients from ROIs in controls, DECT failed to distinguish between noncalcified ROIs in CPPD patients and controls (AUC 0.58–0.59).

Conclusion. While DECT has the potential to characterize knee intraarticular mineralization, this technique cannot yet accurately identify early calcium crystal deposition that is not visible as chondrocalcinosis on conventional CT.

INTRODUCTION

The prevalence of calcium pyrophosphate deposition (CPPD)—currently underestimated at ~0.4% of the general population when defined by radiographic chondrocalcinosis—is increasing with the aging population (1). While definite diagnosis of CPPD is currently made by polarized light microscopic identification of characteristic CPP crystals in synovial fluid (2), the accuracy and reliability of polarized light microscopy for identifying CPP crystals is moderate compared with its ability to identify monosodium urate (MSU) in gout (3). Furthermore, this technique does not enable quantification or mapping of articular crystal deposition.

Because clinical features of CPPD disease are nonspecific, ranging from acute ("pseudogout") to chronic CPP crystal inflammatory arthritis with or without osteoarthritis (OA), the diagnosis still often relies on identification of chondrocalcinosis by imaging (2). Although both ultrasound (4) and conventional computed tomography (CT) (5) have higher sensitivity for chondrocalcinosis than plain radiography, none of these techniques can yet be used to accurately characterize calcium crystal deposition in and around joints.

Dual-energy CT (DECT), owing to its material decomposition capabilities, has the potential to noninvasively characterize tissues by determining their x-ray attenuation biochemical signatures (6). Briefly, DECT relies on the principle that x-ray tissue attenuation—represented by CT numbers in Hounsfield units (HU)—depends

[1]Jean-François Budzik, MD, PhD, Tristan Pascart, MD, PhD: Lille Catholic University Hospital Group, MABLab ULR 4490, University of Lille, Lille, France; [2]Claire Marzin, MD, Julie Legrand, MD, Laurène Norberciak, BSc: Lille Catholic University Hospital Group, University of Lille, Lille, France; [3]Fabio Becce, MD: Lausanne University Hospital and University of Lausanne, Lausanne, Switzerland.

Drs. Budzik and Marzin contributed equally to this work. Drs. Becce and Pascart contributed equally to this work.

Dr. Becce has a research agreement with Siemens Healthineers related to dual-energy computed tomography. No other disclosures relevant to this article were reported.

Address correspondence to Jean-François Budzik, MD, PhD, Hôpital Saint Vincent de Paul, Service d'Imagerie Diagnostique et Interventionnelle, Boulevard de Belfort, Lille 59020, France. Email: budzik.jean-francois@ghicl.net.

Submitted for publication April 23, 2020; accepted in revised form October 27, 2020.

on 1) tissue density (in kg/m^3), 2) its chemical composition, characterized by its HU effective atomic number (Z_{eff}), and 3) the effective energy of the polychromatic x-ray photon beam (in keV). Given that the x-ray beam characteristics are specific to the DECT system and protocol used—mainly tube potential (in kV)—and thus known, tissues are characterized by their density and Z_{eff}, which can be summarized by their dual-energy index (DEI), i.e., (CT number at low kV – CT number at high kV)/(CT number at low kV – CT number at high kV + 2,000). At the energy levels used in clinical CT imaging, tissue attenuation is primarily due to Compton scattering and photoelectric absorption. While Compton scattering mainly depends on the electron density (rho), which is correlated with the volumetric mass density, it does not depend on the x-ray energy and is therefore the main determinant of soft tissue (containing low-Z elements, such as MSU) attenuation. In contrast, photoelectric absorption depends heavily on the Z_{eff} and the x-ray energy (~Z^3/E^3). Calcium crystal deposits, such as CPP and basic calcium phosphate (BCP) (both made of intermediate-Z elements) are characterized by both their density and their Z_{eff}. While CT numbers and DEI can be measured/calculated directly from the PACS workstation, obtaining rho and Z_{eff} values requires a commercially available proprietary postprocessing software and more complex computations.

In a recent pilot clinical study we showed that DECT was able to differentiate meniscal CPP deposition from calcium hydroxyapatite in subchondral and trabecular bone in the knee (7). However, the question remains: does early deposition of ~1–20-μm CPP crystals alter DECT attenuation characteristics of menisci and articular cartilage prior to detection of larger crystal aggregates by conventional CT with its ~250-μm minimum spatial resolution? In other words, would DECT lower the detection limit for early calcium crystal deposition ("nonradiographic/non–computed tomographic chondrocalcinosis")? Therefore, in the present study we aimed to assess the ability of DECT to identify early calcium crystal deposition in menisci and articular cartilage of the knee, depending on the presence/absence of chondrocalcinosis seen on conventional CT.

PATIENTS AND METHODS

Ethical considerations. This single-center cross-sectional study with phantom validation was in compliance with the Declaration of Helsinki. It was approved by the institutional ethics committee of Lille Catholic University Hospitals (protocol 2016-04-16), and all patients provided written informed consent.

Patients. From April 2016 to November 2018, we prospectively enrolled 157 patients to undergo DECT scans of both knees for suspected acute or chronic crystal-associated arthropathy (gout and/or CPPD according to the 2015 American College of Rheumatology/European League Against Rheumatism [EULAR] gout classification criteria [8] and 2011 EULAR CPPD diagnosis recommendations [2], respectively). Additional details on the study design have been published previously (7). Twenty-five patients with metal artifacts were excluded. The remaining 132 patients were retrospectively assigned to the CPPD group (n = 50) or control group (n = 82) by the same senior rheumatologist (TP), according to the aforementioned criteria.

Phantom study. As validation of clinical DECT data, CT calibration phantoms of synthetic CPP crystals at 3 known concentrations (0, 50, and 200 mg/cm^3) were manufactured using a lipid resin with no photoelectric absorption (Computerized Imaging Reference Systems).

DECT protocol. DECT scanning was performed using a single-source CT system (Somatom Definition Edge; Siemens Healthineers). Both knees were scanned simultaneously using a previously described clinical DECT protocol (7), whose main features are as follows: tube potentials 80 and 140 kV, tube current-time products 125–216 and 30–55 mAs, respectively, beam collimation 128 × 0.6 mm, pitch 0.7. Images were reconstructed at a section thickness/overlap of 0.75/0.25 mm.

Image analysis. DECT data sets were postprocessed and analyzed using a commercially available proprietary software (syngo.CT DE Rho/Z; Siemens Healthineers). A radiologist (CM), who was blinded with regard to the patient's study group assigned by the rheumatologist, placed regions of interest (ROIs) on the medial and lateral menisci and the medial and lateral tibiofemoral articular cartilage on preset coronal-oblique DECT images of both knees (each passing through the intercondylar eminence) (Supplementary Figure 1, on the *Arthritis & Rheumatology* website at http://onlinelibrary.wiley.com/doi/10.1002/art.41569/abstract). ROIs were further placed on 5 consecutive DECT sections in CPP crystal calibration phantoms. Particular attention was given to avoiding any partial volume effect. When menisci and/or articular cartilage were not clearly identified because of advanced degeneration/OA, ROIs were not drawn. The same observer also noted whether at least 1 calcification was present/absent within ROIs placed on the preset DECT and corresponding conventional CT images, to define ROIs as positive or negative for calcium crystal deposition. When visible, the area of the largest calcification was measured using polygonal ROIs. For each ROI, we recorded 5 DECT attenuation parameters: CT numbers (in HU) at 80 kV (low) and 140 kV (high), with the corresponding DEI and the derived rho and Z_{eff}. Fifteen randomly selected cases were independently analyzed by a senior musculoskeletal radiologist (J-FB) to assess interobserver reliability.

Statistical analysis. Data were analyzed using R (R Foundation for Statistical Computing). The significance of differences in patient characteristics between the CPPD and control groups, and of phantom DECT data, was assessed by Student's *t*-test or the Wilcoxon-Mann-Whitney test, and chi-square or Fisher's exact test where appropriate. Given repeated measurements on

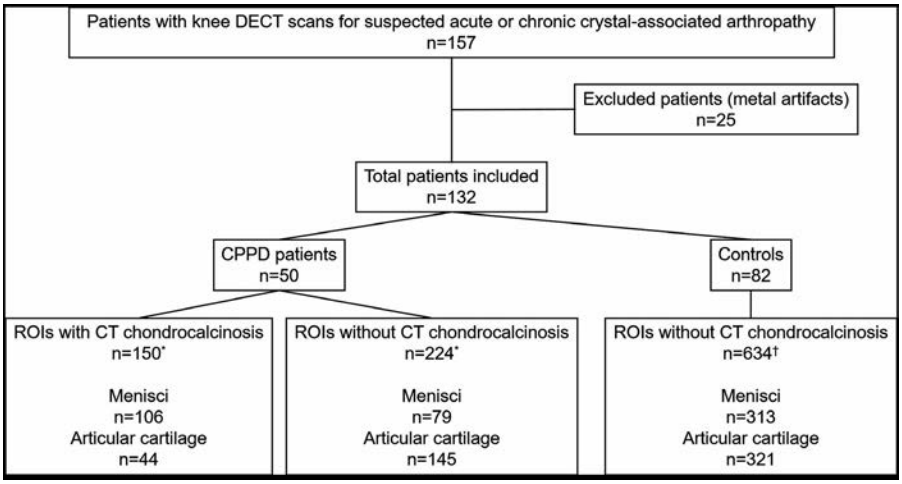

Figure 1. Patient flow diagram including the detailed count of regions of interest (ROIs) measured in menisci and tibiofemoral articular cartilage of patients with calcium pyrophosphate dihydrate (CPPD) deposition and controls. * Fifteen menisci and 11 articular cartilage ROIs were not clearly identified and were excluded. † No control patient had chondrocalcinosis within ROIs on conventional computed tomography (CT); 15 menisci and 7 articular cartilage ROIs were not clearly identified and were excluded. DECT = dual-energy CT.

each subject, the different knee structures/ROIs were compared using linear mixed models, considering the knee (side) as random effect, and age, knee OA status, and gout status as fixed effects when adjusting for confounders. *P* values were adjusted for each parameter within zone categories/knee structures (menisci, articular cartilage) using Holm's technique to avoid α risk inflation due to repeated comparisons of the same parameters and groups within zones. Additional details on the statistical methods have been published previously (7). The correlation between the calcification area within ROIs and DEI, rho, and Z_{eff} was evaluated using Spearman's correlation coefficient including 95% confidence intervals (95% CIs). Receiver operating characteristic (ROC) curves were plotted to assess the diagnostic performance and determine the best accuracy thresholds for DEI, rho, and Z_{eff} in menisci and articular cartilage in differentiating between CPPD patients with/without chondrocalcinosis in measured ROIs and controls. Interobserver reliability of DECT attenuation parameter measurements was assessed by calculating intraclass correlation coefficients (ICCs) with 95% CIs on a random sample of 60 ROIs.

RESULTS

Patient characteristics. A patient flow diagram including measured ROIs is detailed in Figure 1. The CPPD patient group (37 men and 13 women; mean ± SD age 73 ± 11 years) and control patient group (70 men and 12 women; mean ± SD age 60 ± 15 years) differed significantly in age ($P < 0.0001$), presence of knee OA ($P = 0.011$), and presence of coexisting gout ($P = 0.002$) (Supplementary Table 1, on the *Arthritis & Rheumatology* website at http://onlinelibrary.wiley.com/doi/10.1002/art.41569/abstract). The presence of crystals in synovial fluid had been confirmed in 9 CPPD patients (18%), and 18 (36%) had prior flares of acute CPP crystal arthritis. The mean ± SD duration of CPPD disease (since first symptoms) was 0.8 ± 1.1 years.

In vivo DECT attenuation characteristics of menisci and articular cartilage in patients with CPPD and controls. In both menisci and tibiofemoral articular cartilage, and for all 5 DECT attenuation parameters, values in calcified ROIs in CPPD patients were significantly increased compared with ROIs in controls (all $P \leq 0.036$) (Figure 2 and Supplementary Figure 2, http://onlinelibrary.wiley.com/doi/10.1002/art.41569/abstract). Conversely, in noncalcified ROIs, values in CPPD patients were comparable with those in controls (all $P \geq 0.09$). However, a statistical trend toward higher DEI in noncalcified ROIs in CPPD patients was noted ($P = 0.09$). Spearman's correlation coefficients between DEI or Z_{eff} and the calcification size (area) within ROIs were weak (0.28 [95% CI 0.12–0.43] and 0.32 [95% CI 0.19–0.45], respectively).

Diagnostic performance of DECT attenuation parameters in differentiating CPPD patients with and without chondrocalcinosis from controls. With areas under the ROC curve (AUC) of 0.87 (best threshold value 0.0044, sensitivity 70.8% [95% CI 62.2–78.3], specificity 89.8% [95% CI 86.3–93.0]) and 0.88 (best threshold value 7.74, sensitivity 76.4% [95% CI 67.9, 84.0%], specificity 85.0% [95% CI 80.8–88.8%]), respectively, DEI and Z_{eff} both yielded good accuracy in differentiating calcified meniscal ROIs in CPPD patients from ROIs in controls (Figure 3). However, DEI (AUC 0.59) and Z_{eff} (AUC 0.58) both failed to distinguish between noncalcified meniscal ROIs in CPPD patients and those in controls (Supplementary Figure 3, http://onlinelibrary.wiley.com/doi/10.1002/art.41569/abstract). Similar results were found for ROIs in the tibiofemoral articular cartilage.

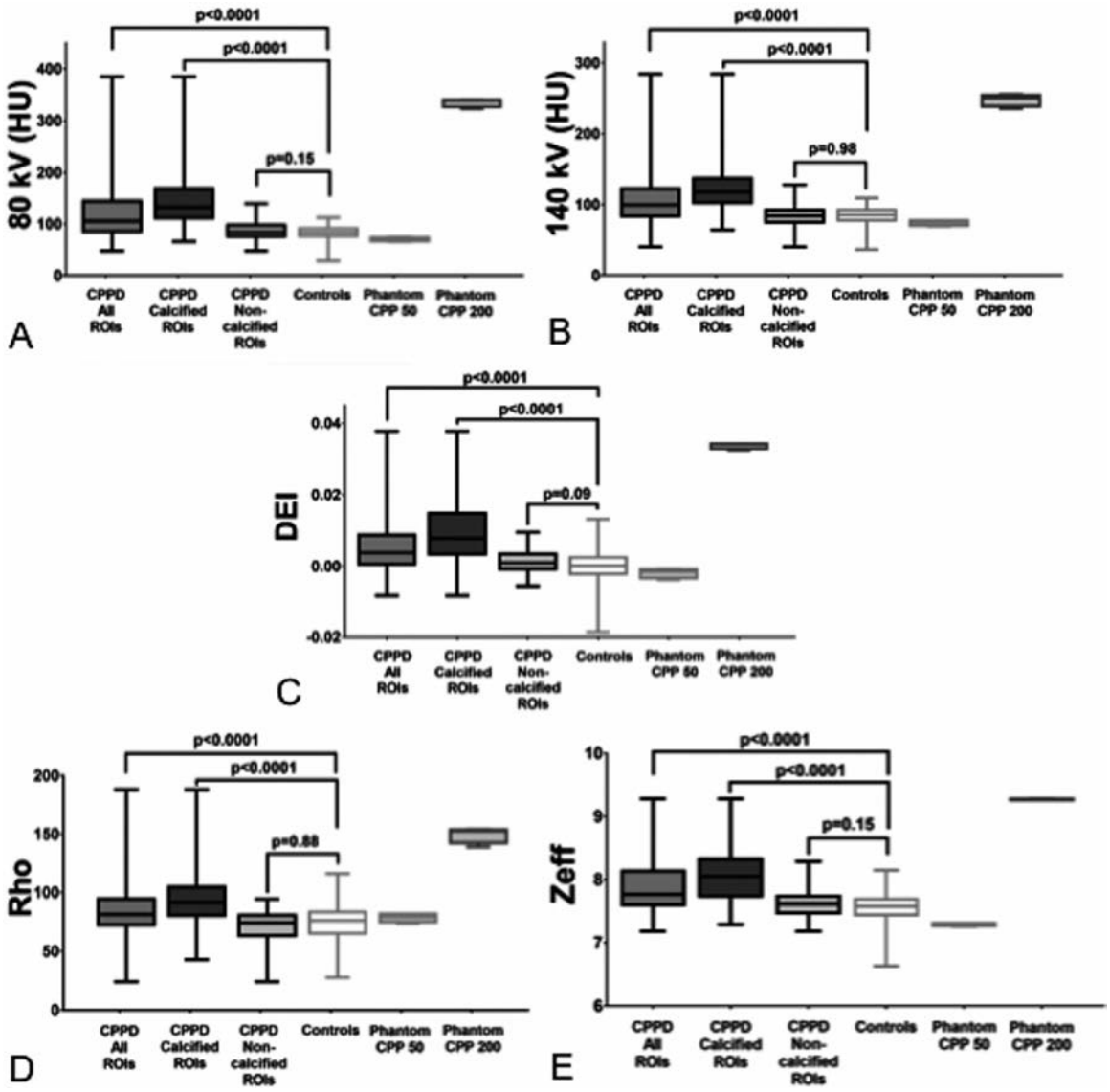

Figure 2. Knee meniscus dual-energy computed tomography (DECT) attenuation characteristics (CT numbers at 80 kV [**A**] and 140 kV [**B**], with the corresponding dual-energy index [DEI] [**C**], electron density [rho] [**D**], and effective atomic number [Z_{eff}] [**E**]), in patients with calcium pyrophosphate dihydrate (CPPD) deposition and controls, as well as synthetic CPP crystal calibration phantoms. For all 5 DECT parameters, calcified meniscal regions of interest (ROIs) in CPPD patients showed significantly higher values than those in controls, while values in noncalcified meniscal ROIs in CPPD patients were comparable with those in controls. Data are shown as box plots. Each box represents the 25th to 75th percentile. Lines inside the boxes represent the median. Lines outside the boxes represent the 10th and 90th percentiles. HU = Hounsfield units.

Phantom DECT validation. Synthetic CPP phantoms at 2 known concentrations differed significantly between concentrations for all 5 DECT attenuation parameters (all $P \leq 0.03$) (Figure 2). However, numerical differences in DEI and Z_{eff} were small (though statistically significant) (between 0 and 50 mg/cm^3 compared to 200 mg/cm^3), suggesting that the signal was weak at low crystal concentrations.

Reliability of DECT measurements. Overall, interobserver reliability of DECT attenuation parameter measurements ranged from moderate for rho in the articular cartilage (ICC 0.58 [95% CI 0.39–0.73]) to very good for Z_{eff} in menisci (ICC 0.90 [95% CI 0.84–0.94]) (Supplementary Table 2, http://onlinelibrary.wiley.com/doi/10.1002/art.41569/abstract).

DISCUSSION

The present study addressed one of the issues recently raised by the first clinical use of DECT in CPPD (7,9–11): does early calcium crystal deposition alter DECT attenuation characteristics in menisci and articular cartilage prior to the appearance of detectable chondrocalcinosis by conventional CT? In this study, with a large enough sample size to detect clinically relevant changes in DECT attenuation characteristics, we found that with

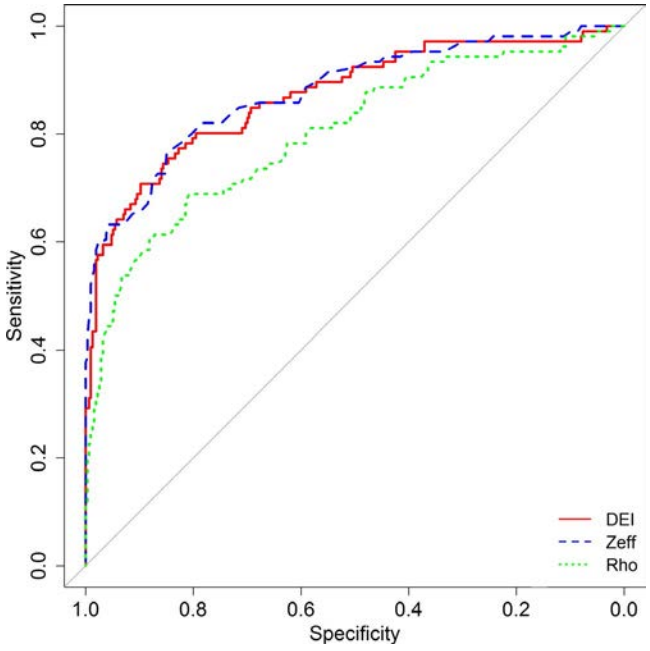

Figure 3. Receiver operating characteristic curves showing the diagnostic accuracy of DEI, Z_{eff}, and rho in differentiating calcified meniscal ROIs in patients with CPPD from ROIs in controls. DEI and Z_{eff} both outperformed rho and exhibited comparable diagnostic performances. See Figure 2 for definitions.

currently available DECT technology (7), the answer was no. While DECT parameters—particularly DEI and Z_{eff}—were accurate in differentiating calcified menisci and tibiofemoral articular cartilage of CPPD patients from controls, DECT failed to distinguish between noncalcified structures in CPPD patients and controls. Differences in CT numbers were expected, as they are the digital representation of grayscale variations on conventional CT images. In contrast, DEI, rho, and Z_{eff} are specific DECT parameters depicting the genuine interaction of x-rays with chemical compounds.

In addition, our study emphasizes the main potential clinical utility of DECT in calcium crystal–associated rheumatic and musculoskeletal diseases: characterizing larger ("macro")/higher-concentration crystal aggregates, rather than lowering the detection limit for early ("micro")/lower-concentration calcium crystal deposition not visible with conventional CT (7,10,11). This was supported by our phantom validation study, which showed that for all 5 DECT attenuation parameters, in particular DEI, CPP detectability improved with increasing synthetic CPP crystal concentration. However, when translated in vivo, no significant differences in DECT parameters were found between noncalcified menisci and articular cartilage of CPPD patients and controls, even though a statistical trend was noted for DEI. This suggests that a minimum crystal concentration threshold is needed to generate clinically detectable and relevant differences in DECT attenuation. Furthermore, DEI and Z_{eff} values were both weakly correlated with the size of visible calcifications, implying that as long as calcifications are visible on conventional CT, DECT parameters are sufficiently altered to allow discrimination of CPPD patients from controls, regardless of their size. This suggests that DECT is neither more nor less sensitive than conventional CT in assessing chondrocalcinosis.

Based on its technical characteristics, the primary role of DECT in crystal-associated arthropathies should be to characterize and quantify articular and periarticular crystal deposits rather than to detect them (6,12), considering that DECT has a slightly lower spatial resolution than conventional CT performed in high-resolution mode. In an initial ex vivo study to investigate the sensitivity of DECT for knee CPPD (9), Tanikawa et al obtained menisci from 26 patients undergoing knee replacement surgery and compared the diagnostic performance of postoperative DECT versus preoperative conventional radiography for identification of meniscal chondrocalcinosis, using polarized light microscopy of synovial fluid aspirates as the reference standard. They reported that DECT showed higher sensitivity (77.8% versus 44.4%) but lower specificity (93.8% versus 100%) compared with radiography (9). However, they did not compare DECT with high-resolution conventional CT or characterize intraarticular mineralization by distinguishing between CPP and BCP crystal aggregates. In a subsequent study (7), we aimed to determine the DECT attenuation characteristics of meniscal calcifications in CPPD patients in vivo, thereby proving the concept of calcium crystal discrimination using DECT, but in that investigation we did not assess its diagnostic performance against any reference standard. Tedeschi and colleagues recently conducted a pilot study of 10 patients with acute CPP crystal arthritis, assessing DECT sensitivity compared with ultrasound, plain radiography, and conventional CT (10). Meniscal and articular cartilage CPP deposits were characterized by DECT using a custom postprocessing algorithm relying on DEI values. Diagnostic performance was comparable between DECT and conventional CT, with DECT appearing to be slightly more accurate in assessment of the hands owing to color-coding of tiny structures.

Taken together, our present results and the study findings described above indicate that the main strength of DECT is not higher sensitivity (lower detection limit) but rather higher capacity for tissue characterization by decomposition of the x-ray photoelectric absorption (represented by DEI and Z_{eff} values) and Compton scattering (reflected by the rho value). These features are the basis for the development of DECT quantification tools used for assessment of MSU crystal deposition in gout for more than a decade (6,12,13).

The main limitations of this study include the retrospective analysis of knee DECT scans, originally obtained for the purpose of studying gout, from a prospective patient cohort with crystal-associated arthropathies. Gout patients from the control group might indeed have had small amounts of coexisting calcium crystals in their knees, not visible with clinical imaging techniques due to spatial resolution limitations. The same applies for OA, which was prevalent in both CPPD patients and controls and is associated with articular calcium crystal deposition (14–16). However, our results were adjusted for these 2 confounders, and major

changes due to gout were not expected because MSU shares very similar DECT attenuation characteristics with meniscal fibrocartilage and hyaline articular cartilage (no photoelectric absorption, and therefore no alteration in DEI or Z_{eff}) (6,7). Further studies are needed to evaluate the impact of early OA or MSU deposition on DECT attenuation characteristics in articular cartilage. Second, we only compared calcified with noncalcified knee structures, without the ability to differentiate CPP from BCP crystals (no ex vivo validation with advanced diagnostic methods), the latter of which are known to coexist in osteoarthritic knee joints (7,14–16). Finally, although special care was taken to avoid partial volume effect, ROIs were small and close to subchondral bone, which may have impacted our results. However, we did not consider joint spaces with advanced OA, and our clinical DECT measurements proved to be reliable and supported by phantom validation with synthetic CPP crystals.

In conclusion, while DECT has the potential to characterize large/denser calcium crystal aggregates in the knee, currently available DECT technology does not yet allow identification of early calcium crystal deposition that is not visible as chondrocalcinosis on conventional CT. It should therefore be considered as a clinically available imaging technique to distinguish between various crystal deposits, but not to lower their detection limit. Further advances in DECT and emerging multi-energy photon-counting CT techniques—with improvements in both spatial and contrast resolution (17,18)—are awaited to enable noninvasive identification and characterization of early calcium crystal deposition and to provide new insights into the role of intraarticular mineralization in crystal-associated arthropathies and osteoarthritis.

AUTHOR CONTRIBUTIONS

All authors were involved in drafting the article or revising it critically for important intellectual content, and all authors approved the final version to be published. Dr. Budzik had full access to all of the data in the study and takes responsibility for the integrity of the data and the accuracy of the data analysis.

Study conception and design. Budzik, Pascart.
Acquisition of data. Budzik, Marzin, Legrand, Pascart.
Analysis and interpretation of data. Budzik, Marzin, Legrand, Norberciak, Becce, Pascart.

REFERENCES

1. Abhishek A. Calcium pyrophosphate deposition disease: a review of epidemiologic findings. Curr Opin Rheumatol 2016;28:133–9.
2. Zhang W, Doherty M, Pascual E, Barskova V, Guerne PA, Jansen TL, et al. EULAR recommendations for calcium pyrophosphate deposition. Part II. Management. Ann Rheum Dis 2011;70:571–5.
3. Andrés M, Vela P, Jovaní V, Pascual E. Most needle-shaped calcium pyrophosphate crystals lack birefringence. Rheumatology (Oxford) 2019;58:1095–8.
4. Filippou G, Adinolfi A, Iagnocco A, Filippucci E, Cimmino MA, Bertoldi I, et al. Ultrasound in the diagnosis of calcium pyrophosphate dihydrate deposition disease: a systematic literature review and a meta-analysis. Osteoarthritis Cartilage 2016;24:973–81.
5. Misra D, Guermazi A, Sieren JP, Lynch J, Torner J, Neogi T, et al. CT imaging for evaluation of calcium crystal deposition in the knee: initial experience from the Multicenter Osteoarthritis (MOST) study. Osteoarthritis Cartilage 2015;23:244–8.
6. Omoumi P, Becce F, Racine D, Ott JG, Andreisek G, Verdun FR. Dual-energy CT: basic principles, technical approaches, and applications in musculoskeletal imaging (Part 1). Semin Musculoskelet Radiol 2015;19:431–7.
7. Pascart T, Norberciak L, Legrand J, Becce F, Budzik JF. Dual-energy computed tomography in calcium pyrophosphate deposition: initial clinical experience. Osteoarthritis Cartilage 2019;27:1309–14.
8. Neogi T, Jansen TL, Dalbeth N, Fransen J, Schumacher HR, Berendsen D, et al. 2015 gout classification criteria: an American College of Rheumatology/European League Against Rheumatism collaborative initiative. Arthritis Rheumatol 2015;67:2557–68.
9. Tanikawa H, Ogawa R, Okuma K, Harato K, Niki Y, Kobayashi S, et al. Detection of calcium pyrophosphate dihydrate crystals in knee meniscus by dual-energy computed tomography. J Orthop Surg 2018;13:73.
10. Tedeschi SK, Solomon DH, Yoshida K, Vanni K, Suh DH, Smith SE. A prospective study of dual-energy CT scanning, US and X-ray in acute calcium pyrophosphate crystal arthritis. Rheumatology (Oxford) 2020;59:900–3.
11. Pascart T, Falgayrac G, Norberciak L, Lalanne C, Legrand J, Houvenagel E, et al. Dual-energy computed-tomography-based discrimination between basic calcium phosphate and calcium pyrophosphate crystal deposition in vivo. Ther Adv Musculoskelet Dis 2020;12:1759720X20936060.
12. Becce F, Viry A, Stamp LK, Pascart T, Budzik JF, Raja A, et al, on behalf of the MARS Collaboration. Winds of change in imaging of calcium crystal deposition diseases [editorial]. Joint Bone Spine 2019;86:665–8.
13. Choi HK, Al-Arfaj AM, Eftekhari A, Munk PL, Shojania K, Reid G, et al. Dual energy computed tomography in tophaceous gout. Ann Rheum Dis 2009;68:1609–12.
14. Nguyen C, Bazin D, Daudon M, Chatron-Colliet A, Hannouche D, Bianchi A, et al. Revisiting spatial distribution and biochemical composition of calcium-containing crystals in human osteoarthritic articular cartilage. Arthritis Res Ther 2013;15:R103.
15. Ryu K, Iriuchishima T, Oshida M, Kato Y, Saito A, Imada M, et al. The prevalence of and factors related to calcium pyrophosphate dihydrate crystal deposition in the knee joint. Osteoarthritis Cartilage 2014;22:975–9.
16. Fuerst M, Bertrand J, Lammers L, Dreier R, Echtermeyer F, Nitschke Y, et al. Calcification of articular cartilage in human osteoarthritis. Arthritis Rheum 2009;60:2694–703.
17. Kirkbride TE, Raja AY, Müller K, Bateman CJ, Becce F, Anderson NG. Discrimination between calcium hydroxyapatite and calcium oxalate using multienergy spectral photon-counting CT. AJR Am J Roentgenol 2017;209:1088–92.
18. Stamp LK, Anderson NG, Becce F, Rajeswari M, Polson M, Guyen O, et al. Clinical utility of multi-energy spectral photon-counting computed tomography in crystal arthritis. Arthritis Rheumatol 2019; 71:1158–62.

Arthritis & Rheumatology
Vol. 73, No. 4, April 2021, pp 693–701
DOI 10.1002/art.41561

American College of Rheumatology
Empowering Rheumatology Professionals

Platelet Glycoprotein Ib α-Chain as a Putative Therapeutic Target for Juvenile Idiopathic Arthritis: A Mendelian Randomization Study

Shan Luo,[1] Sarah L. N. Clarke,[2] Athimalaipet V. Ramanan,[2] Susan D. Thompson,[3] Carl D. Langefeld,[4] Miranda C. Marion,[4] Alexei A. Grom,[5] C. Mary Schooling,[6] Tom R. Gaunt,[7] Shiu Lun Au Yeung,[8] and Jie Zheng[9]

Objective. To ascertain the role of platelet glycoprotein Ib α-chain (GPIbα) plasma protein levels in cardiovascular, autoimmune, and autoinflammatory diseases and whether its effects are mediated by platelet count.

Methods. We performed a two-sample Mendelian randomization (MR) study, using both a *cis*-acting protein quantitative trait locus (*cis*-pQTL) and *trans*-pQTL near the *GP1BA* and *BRAP* genes as instruments. To assess if platelet count mediated the effect, we then performed a two-step MR study. Putative associations (GPIbα/platelet count/disease) detected by MR analyses were subsequently assessed using multiple-trait colocalization analyses.

Results. After correction for multiple testing (Bonferroni-corrected threshold $P \leq 2 \times 10^{-3}$), GPIbα, instrumented by either *cis*-pQTL or *trans*-pQTL, was causally implicated with an increased risk of oligoarticular and rheumatoid factor (RF)–negative polyarticular juvenile idiopathic arthritis (JIA). These effects of GPIbα appeared to be mediated by platelet count and were supported by strong evidence of colocalization (probability of all 3 traits sharing a common causal variant ≥0.80). GPIbα instrumented by *cis*-pQTL did not appear to affect cardiovascular risk, although the GPIbα *trans*-pQTL was associated with an increased risk of cardiovascular diseases and autoimmune diseases but a decreased risk of autoinflammatory diseases, suggesting that this *trans*-acting instrument operates through other pathways.

Conclusion. The role of platelets in thrombosis is well-established; however, our findings provide some novel genetic evidence that platelets may be causally implicated in the development of oligoarticular and RF-negative polyarticular JIA, and indicate that GPIbα may serve as a putative therapeutic target for these JIA subtypes.

INTRODUCTION

Platelet glycoprotein Ib α-chain (GPIbα) is a platelet surface membrane protein (1). It functions as a receptor for von Willebrand factor (vWF) and is implicated in atherothrombosis (2). Genetic evidence supports the assertion that GPIbα influences atherothrombosis via increased platelet counts (3). Given the potential of GPIbα as an antithrombotic target, its

The views expressed herein are those of the authors and not necessarily those of the NHS, the National Institute for Health Research, the Department of Health, or any other funder.

Supported by the NIHR Biomedical Research Centre at University Hospitals Bristol NHS Foundation Trust and the University of Bristol. Dr. Luo's work was supported by the Bau Tsu Zung Bau Kwan Yeun Hing Research and Clinical Fellowship from the University of Hong Kong. Dr. Clarke's work was supported by the Wellcome Trust GW4 Clinical Academic Training Programme (grant 211030/Z/18/Z0). Dr. Zheng's work was supported by a Vice-Chancellor Fellowship from the University of Bristol. Drs. Clarke, Gaunt, and Zheng's work was supported by the MRC and the University of Bristol (grant MC_UU_00011/4). Drs. Gaunt and Zheng's work was supported by a British Heart Foundation Accelerator award (grant AA/18/7/34219).

[1]Shan Luo, PhD: The University of Hong Kong, Hong Kong, China, and University of Bristol, Bristol, UK; [2]Sarah Clarke, MBChB, Athimalaipet Ramanan, PhD: University of Bristol and University Hospitals Bristol NHS Foundation Trust, Bristol, UK; [3]Susan D. Thompson, PhD: University of Cincinnati College of Medicine and Cincinnati Children's Hospital Medical Center, Cincinnati, Ohio; [4]Carl D. Langefeld, PhD, Miranda C. Marion, MS: Wake Forest School of Medicine, Winston-Salem, North Carolina; [5]Alexei A. Grom, MD: Cincinnati Children's Hospital Medical Center, Cincinnati, Ohio; [6]C. Mary Schooling, PhD: The University of Hong Kong, Hong Kong, China, and The City University of New York; [7]Tom R. Gaunt, PhD: University of Bristol and NIHR Bristol Biomedical Research Centre, Bristol, UK; [8]Shiu Lun Au Yeung, PhD: The University of Hong Kong, Hong Kong, China; [9]Jie Zheng, PhD: University of Bristol, Bristol, UK.

Drs. Schooling, Gaunt, Au Yeung, and Zheng contributed equally to this work.

Dr. Gaunt has received research support from GlaxoSmithKline and Biogen for previous work. No other disclosures relevant to this article were reported.

Address correspondence to Jie Zheng, PhD, 2/F Oakfield House, Oakfield Grove, Bristol BS8 2BN, UK (email: jie.zheng@bristol.ac.uk); or to Shan Luo, PhD, 1/F Patrick Manson Building, North Wing, 7 Sassoon Road, Pokfulam, Hong Kong (email: luoshan@connect.hku.hk).

Submitted for publication June 2, 2020; accepted in revised form October 15, 2020.

efficacy for the treatment of thrombotic thrombocytopenic purpura is currently being investigated in a phase II trial (3). Recent studies have also indicated a role for platelets in inflammation and immunity (4,5), which may imply potential for repurposing GPIbα as a target for prevention/treatment of immune-related disease. However, these putative associations have not been systematically evaluated.

Mendelian randomization (MR) studies utilize genetic variants, randomly allocated during conception, as instruments to infer causality and are less prone to confounding and reverse causation than observational studies (6). They are increasingly used to ascertain the health effects of potential therapeutic targets. Colocalization can further help to distinguish causal effects from confounding via linkage disequilibrium (LD) (7). Collectively, applying MR and colocalization to -omics data can provide a distinct strand of genetic validation for putative causal gene targets and thus improve the success rate of drug trials (8,9).

To understand the effects of GPIbα on cardiovascular, autoimmune, and autoinflammatory diseases, and whether these are mediated by platelet count, we conducted a two-step, two-sample MR study. We subsequently performed multiple-trait colocalization analyses (i.e., on GPIbα, platelet count, and a disease) to complement the evidence for causal associations detected in our MR study.

MATERIALS AND METHODS

Study design. MR relies on 3 core assumptions. First, the genetic variant is robustly associated with the exposure. Second, the genetic variant is independent of confounders of the exposure–outcome association. Third, the genetic variant is independent of the outcome except via the exposure (10).

In this study, we first performed a two-sample MR study to assess the association of GPIbα with cardiovascular, autoimmune, and autoinflammatory disease risk (Figure 1A). To further assess whether platelets mediate the effects of GPIbα on disease, we subsequently performed a two-step, two-sample MR study. First, we assessed the association of GPIbα with platelet count. Second, we assessed the effect of platelet count on the disease outcome (Figure 1B).

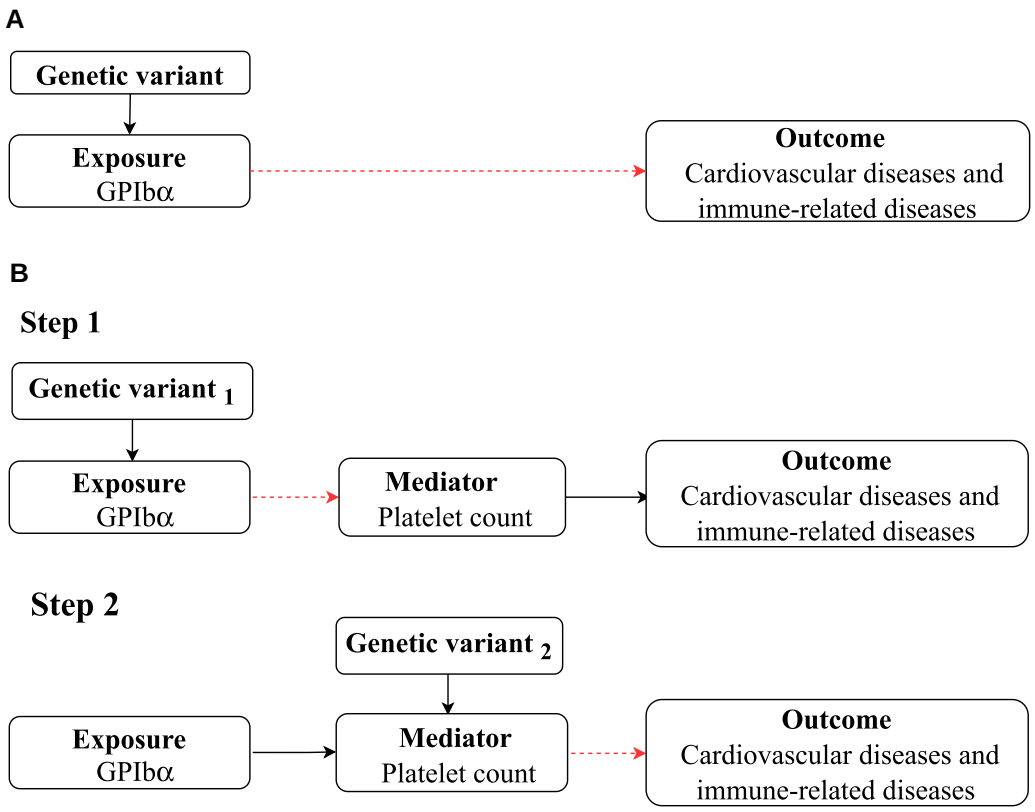

Figure 1. Schematic diagram of **A**, standard Mendelian randomization (MR) analysis of glycoprotein Ib α-chain (GPIbα) and **B**, two-step MR analysis of mediation by platelet count. Two-step MR tests the association between a genetic variant and the exposure (GPIbα) postulated to influence the outcome (cardiovascular and immune-related diseases) via an altered mediator (platelet count). **Broken arrows** indicate the causal pathway to be assessed. Color figure can be viewed in the online issue, which is available at http://onlinelibrary.wiley.com/doi/10.1002/art.41561/abstract.

Genetic instruments of GPIbα. A proteome genome-wide association study (GWAS) was conducted in 3,301 healthy blood donors of European ancestry (3) randomly selected from the INTERVAL study (50% male) (11). The plasma protein concentrations were quantified by aptamer-based multiplex protein assay (SOMAscan) (3). Genotyping was performed on an Affymetrix Axiom array and was imputed using a combined 1000 Genomes Phase 3-UK10K reference panel (3). Genetic variants were excluded if they had a call rate of <99%, had a minor allele count of <8, deviated from Hardy-Weinberg equilibrium ($P < 5 \times 10^{-6}$), or had an info score of <0.7 (3). The genetic associations were obtained in an additive genetic model adjusted for age, sex, duration between blood draw and processing, and the first 3 principal components of ancestry (3). Conditionally uncorrelated variants (with the lowest *P* value having LD $r^2 < 0.001$) associated with GPIbα ($P < 5 \times 10^{-8}$) were selected as instruments.

Genetic instruments of platelet count. At the time of analyses, the largest hematologic GWAS that had been conducted included 173,480 participants of European ancestry (12). Participants were from the UK Biobank (n = 132,959; 48% male) and the INTERVAL studies (n = 40,521; 50% male) (11). Complete blood cell count was performed using a combination of fluorescence and impedance flow cytometry within 36 hours (12). Genotyping was undertaken using Affymetrix UK BiLEVE and UK Biobank Axiom arrays, and imputation was to a reference set combining the UK10K and Haplotype Reference Consortium reference panels (12). Genetic associations were obtained from a linear mixed model adjusted for the top 10 principal components of ancestry and recruitment center (12). Conditionally uncorrelated variants (with the lowest *P* value having LD $r^2 < 0.001$) associated with platelet count ($P < 8.31 \times 10^{-9}$, a threshold for common, low frequency, and rare variants) (13) were selected as instruments. Since the genetic instruments for GPIbα were also strongly associated with platelet count, we undertook a sensitivity analysis which estimated the instrument-specific effect of platelet count on the diseases of interest.

Genetic associations of selected outcomes. Outcomes included platelet count (per nl), 10 major cardiovascular diseases (coronary heart disease [CHD], myocardial infarction [MI], arterial embolism and thrombosis, deep venous thrombosis [DVT], phlebitis and thrombophlebitis, any stroke, any ischemic stroke, cardioembolic stroke, large artery stroke, and small vessel stroke), and 12 immune-related diseases. Immune-related diseases were classified (14) as autoimmune diseases (type 1 diabetes mellitus [type 1 DM], juvenile idiopathic arthritis [JIA; oligoarticular and rheumatoid factor [RF]–negative polyarticular subtypes], rheumatoid arthritis [RA], systemic lupus erythematosus, psoriasis, multiple sclerosis, primary sclerosing cholangitis, and primary biliary cirrhosis), autoinflammatory diseases (inflammatory bowel disease [IBD], Crohn's disease [CD], and ulcerative colitis [UC]), or atopic disease (eczema) (15). We obtained summary genetic associations (including estimates of regression coefficient, the corresponding standard error and *P* value, effect allele, other allele, and effect allele frequency) for each outcome from the largest publicly available GWAS at the time of analyses (16–27) (Supplementary Table 1, available on the *Arthritis & Rheumatology* website at http://onlinelibrary.wiley.com/doi/10.1002/art.41561/abstract).

MR analysis. To estimate the effect of exposure on outcome (β_{XY}), we used the Wald estimate, i.e., the ratio of the genetic association with outcome (β_{GY}) to the genetic association with exposure (β_{GX}) (28) (Supplementary Figure 1, available on the *Arthritis & Rheumatology* website at http://onlinelibrary.wiley.com/doi/10.1002/art.41561/abstract). Wald estimates for multiple variants for the same exposure were combined using inverse variance–weighted (IVW) MR with multiplicative random effects (28), weighted median (29), and MR-Egger (30) because these methods rely on different assumptions for valid causal inference. The MR-Egger intercept with $P < 0.05$ indicates the presence of horizontal pleiotropy (30). Directionally consistent results from different methods increase confidence in the results of MR analyses. To orientate the direction of the effects of instruments, we applied Steiger filtering (31). Steiger filtering examines whether the variance explained between each variant–exposure (R^2_{GX}) is larger than the variance explained between each variant–outcome effect (R^2_{GY}), and therefore whether the instrument primarily influences the outcome through the exposure (and not vice versa) (31). Two-sided *P* values are reported throughout, with a Bonferroni correction for multiple testing threshold ($P \leq 2 \times 10^{-3}$, given 22 disease traits were considered). Several of the traits examined in this study are likely to share clinical and underlying immunopathogenic features despite their distinct phenotypes; therefore, using this stringent correction provides a balance between reducing false positives and providing rigorous results.

Instrument strength. F statistics were calculated for each instrument of GPIbα as $\frac{R^2/K}{(1-R^2)(N-K-1)}$, where R^2 indicates the proportion of exposure variability explained by the instrument, K indicates the number of instruments, and N indicates the sample size. R^2 was calculated as $2EAF(1 - EAF)\beta^2$, where EAF is the effect allele frequency and β is the effect size of the effect allele. Higher F statistic values reflect a lower risk of weak instrument bias (32).

Multiple-trait colocalization analysis. To differentiate whether any putative causal association detected by two-step MR is driven by a common causal variant across multiple traits (i.e., GPIbα/platelet count/disease) or just confounded by LD, we subsequently performed multiple-trait colocalization analyses at each locus (7). Under the assumption of a single causal variant within each region, the Bayesian statistical framework quantifies the posterior probability of association (PPA) for each of the possible hypotheses of colocalization (variant sharing)

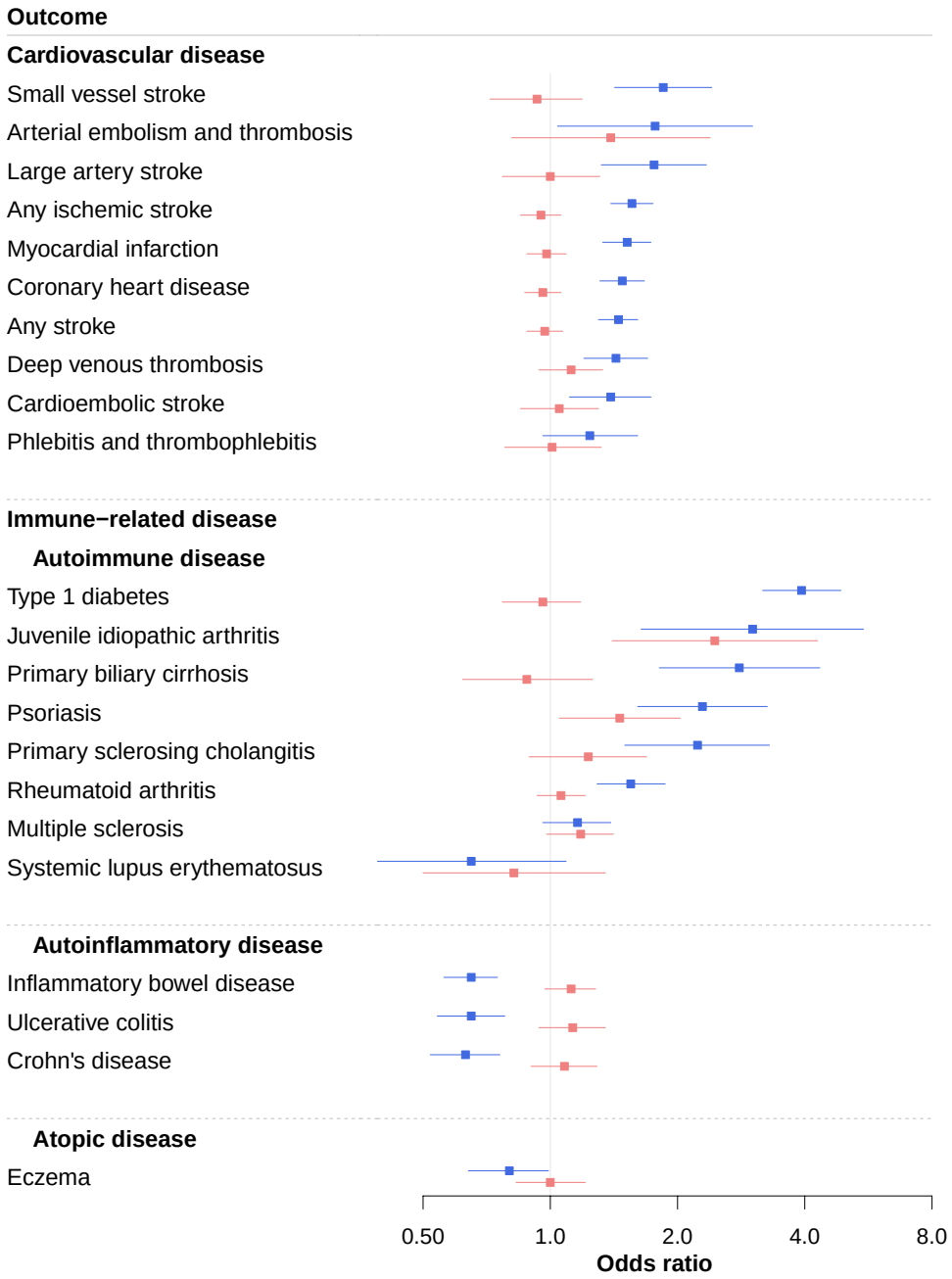

Figure 2. Mendelian randomization estimates for effect of glycoprotein Ib α-chain on cardiovascular and immune-related diseases. Values are the odds ratio (point estimate of effect) and 95% confidence interval. Red represents GPIbα instrumented by the *cis*-acting protein quantitative trait locus (*cis*-pQTL) within the *GP1BA* gene, and blue represents GPIbα instrumented by the *trans*-pQTL near the *BRAP* gene.

among the 3 traits (all hypotheses are listed in Supplementary Table 2, available on the *Arthritis & Rheumatology* website at http://onlinelibrary.wiley.com/doi/10.1002/art.41561/abstract). A lead variant-centric approach was applied, where we extracted effect estimates and allele information for all variants within 1 megabase upstream and downstream of the *cis*-acting protein quantitative trait locus (*cis*-pQTL) and *trans*-acting pQTL for each trait (GPIbα/platelet count/disease), respectively. To provide reliable evidence of colocalization, at least 50 variants (with minor allele frequency >1%), including the causal variant of interest, within the test region for all 3 traits were assessed (7). We assigned prior probabilities that a variant is equally associated with 1 trait ($p1 = 1 \times 10^{-4}$), 2 traits ($p2 = 1 \times 10^{-6}$), and 3 traits ($p3 = 1 \times 10^{-7}$), as recommended (7). The PPA for all 3 traits was ≥0.80, which was considered strong evidence of colocalization (7).

MR analyses were performed using the *TwoSampleMR* package, and multiple-trait colocalization analyses were conducted

using the *moloc* package. Results were visualized using the *forestplot* package in the R software platform (version 3.5.1; R Development Core Team).

RESULTS

Genetic instruments for GPIbα and instrument strength. Two conditionally uncorrelated (LD $r^2 < 0.001$) pQTLs associated with GPIbα were used as instruments: *cis*-pQTL (rs72835078 within the *GP1BA* gene) and *trans*-pQTL (rs11065979 near the *BRAP* gene). The F statistic for *cis*-pQTL was 48, with 1.4% of the variance in GPIbα explained by *cis*-pQTL, and the F statistic for *trans*-pQTL was 50, with 1.5% of the variance in GPIbα explained by *trans*-pQTL (Supplementary Table 3, available on the *Arthritis & Rheumatology* website at http://onlinelibrary.wiley.com/doi/10.1002/art.41561/abstract).

Association of GPIbα with JIA. Using a Bonferroni-corrected threshold of $P \leq 2 \times 10^{-3}$ (equivalent to $P \leq 0.05$ for a single test), the two-sample MR analysis (Figure 1A) suggested that increased GPIbα level was positively associated with an increased risk of JIA. Higher GPIbα level instrumented by *cis*-pQTL was associated with a higher risk of JIA, with an odds ratio (OR) of 2.45 (95% confidence interval [95% CI] 1.40–4.29) ($P = 1.71 \times 10^{-3}$) (Figure 2 and Supplementary Table 4, available on the *Arthritis & Rheumatology* website at http://onlinelibrary.wiley.com/doi/10.1002/art.41561/abstract). Higher GPIbα level instrumented by *trans*-pQTL was also associated with a higher risk of JIA (OR 3.01 [95% CI 1.64–5.51], $P = 3.66 \times 10^{-4}$) (Figure 2 and Supplementary Table 5, available on the *Arthritis & Rheumatology* website at http://onlinelibrary.wiley.com/doi/10.1002/art.41561/abstract). When combining the estimates instrumented by both *cis*-pQTL and *trans*-pQTL, per unit increase in GPIbα level was associated with a 169% higher risk of JIA (OR 2.69 [95% CI 1.79–4.06], $P = 2.33 \times 10^{-6}$).

There was little evidence of an association of GPIbα level instrumented by *cis*-pQTL with cardiovascular diseases (Figure 2 and Supplementary Table 4). However, the GPIbα *trans*-pQTL was associated with an increased risk of cardiovascular diseases (small vessel stroke, large artery stroke, any ischemic stroke, MI, CHD, any stroke, and DVT) and autoimmune diseases (type 1 DM, JIA, primary biliary cirrhosis, psoriasis, primary sclerosing cholangitis, and RA) but decreased risk of autoinflammatory diseases (IBD, UC, and CD) (Figure 2 and Supplementary Table 5). The Steiger filtering tests suggested that the instruments primarily influenced the outcome through the exposure (GPIbα).

The association of GPIbα with JIA is mediated by platelet count. Figure 1B demonstrates how two-step MR estimates whether the effect of GPIbα on JIA is mediated by platelet count. In the first step, increased GPIbα level was associated with higher platelet count (β = 0.37 [95% CI 0.03–0.70]; $P = 0.03$), among which the effect instrumented by *trans*-pQTL (β = 0.54 [95% CI 0.49–0.58]; $P = 1.37 \times 10^{-143}$) was larger than that instrumented by *cis*-pQTL (β = 0.19 [95% CI 0.15–0.23]; $P = 2.54 \times 10^{-19}$) (Figure 3). In the second step, there were 135 conditionally uncorrelated variants (LD $r^2 < 0.001$) associated with platelet count ($P < 8.31 \times 10^{-9}$) (Supplementary Table 6, available on the *Arthritis & Rheumatology* website at http://onlinelibrary.wiley.com/doi/10.1002/art.41561/abstract). Using the IVW method, genome-wide genetically predicted platelet count was positively associated with the risk of JIA (OR 1.88 [95% CI 1.12–3.16], $P = 0.02$) (Figure 4). The weighted median and MR-Egger methods provided consistent findings, with no evidence of horizontal pleiotropy (Supplementary Table 7, available on the *Arthritis & Rheumatology* website at http://onlinelibrary.wiley.com/doi/10.1002/art.41561/abstract). Sensitivity analyses restricted to each specific instrument for GPIbα also showed that platelet count increased the risk of JIA (Supplementary Table 7).

Multiple-trait colocalization analysis supports the causal association of GPIbα mediated by platelet count with JIA. The two-step MR analyses suggested that GPIbα mediated by platelet count has an impact on JIA ($P \leq 2 \times 10^{-3}$); this association was assessed using multiple-trait colocalization analysis. The association (GPIbα instrumented by *trans*-pQTL/platelet count/JIA) was supported by strong evidence of colocalization (PPA ≥ 0.80), indicating that the same causal variant affects 3 traits. The association of GPIbα instrumented by *cis*-pQTL meditated by

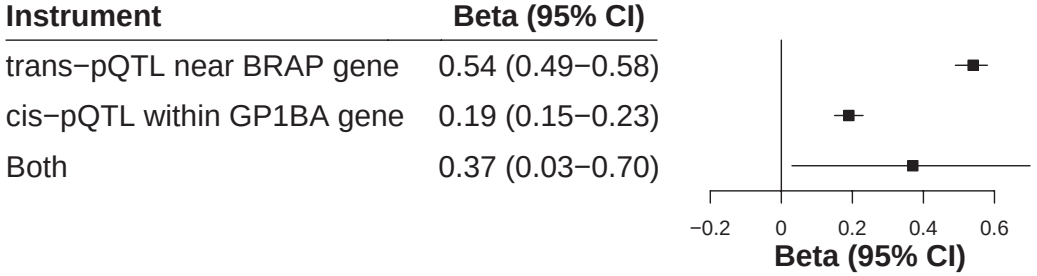

Figure 3. Mendelian randomization estimates for the effect of glycoprotein Ib α-chain (GPIbα) on platelet count. Values are the beta (point estimate of effect) and 95% confidence interval (95% CI). pQTL = protein quantitative trait locus.

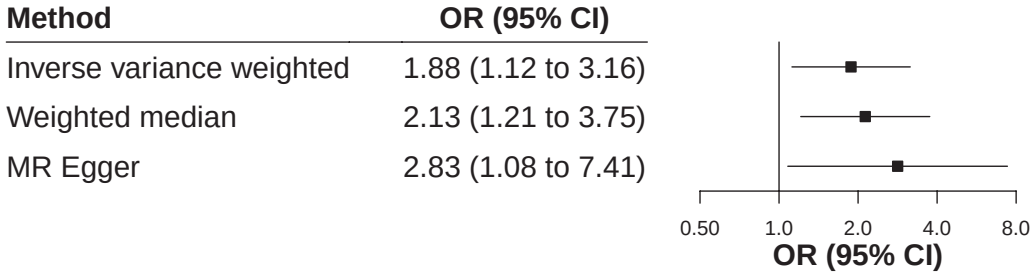

Figure 4. Mendelian randomization (MR) estimates for effect of platelet count on juvenile idiopathic arthritis. Values are the odds ratio (OR; point estimates of effect) and 95% confidence interval (95% CI).

platelet count with JIA could not be assessed because the causal variant of interest was not available for the outcome (Supplementary Table 8, available on the *Arthritis & Rheumatology* website at http://onlinelibrary.wiley.com/doi/10.1002/art.41561/abstract).

DISCUSSION

In this MR study, we observed that GPIbα instrumented by *cis*-pQTL and GPIbα instrumented by *trans*-pQTL both increased the risk of oligoarticular and RF-negative polyarticular JIA. We found no evidence of an association of GPIbα instrumented by *cis*-pQTL with cardiovascular diseases. However, GPIbα instrumented by *trans*-pQTL increased the risk of cardiovascular and autoimmune diseases but decreased the risk of autoinflammatory diseases, suggesting potential pleiotropic effects of this *trans*-pQTL on multiple disease outcomes. Two-step, two-sample MR analysis showed that the effect of GPIbα on the increased risk of oligoarticular and RF-negative polyarticular JIA was mediated by platelet count, which was supported by strong evidence of colocalization. Apart from the well-established role of platelets in thrombosis (4), our findings provide novel evidence that platelets are causally implicated in oligoarticular and RF-negative polyarticular JIA.

The GPIb–IX–V complex is a well-characterized adhesion receptor for vWF and collagen, of which the subunit GPIbα is associated with an increased risk of ischemic cerebrovascular disease in genetic studies (33,34). Murine data show that absence of GPIbα significantly reduces platelet count and down-regulates atherosclerosis and inflammation (35), consistent with our findings. Our results also align with a large GWAS of 1 million participants of European ancestry which found that the lead variant at the *BRAP* gene (rs11065979) was positively associated with cardiometabolic and autoimmune diseases in overall and sex-specific analyses (36). Activated platelets secrete a wide range of cytokines (e.g., interleukin-6 [IL-6] and IL-1), neutrophil chemoattractant (e.g., IL-8), growth factors, and potent vasoconstrictors (e.g., thromboxane) (4), which play an important role in amplifying inflammatory and thrombotic cascades in these conditions (37,38). Consistent with our findings, in vivo, platelet-derived cellular microparticles have been observed in synovial fluid from patients with inflammatory polyarthropathies (e.g., RA, JIA, and psoriatic arthritis) but not from patients with noninflammatory arthritis (osteoarthritis) (37). Furthermore, platelet indices were associated with increased disease activity and severity of JIA (oligoarticular, RF-negative polyarticular, and systemic subtypes) and were highly labile, particularly in the acute phase (39).

Our findings are consistent with those of a growing number of studies that illustrate the close relationship between atherosclerotic and immune-mediated disorders (40), leading to the exploration of the role of antiatherosclerotic agents in the autoimmune arena. The antiplatelet agent ticagrelor is under investigation in RA (Clinicaltrials.gov identifier: NCT02874092), and abciximab (a glycoprotein IIb/IIIa inhibitor) is used in children with Kawasaki disease (an inflammatory vasculitis that particularly affects the heart) (41). With regard to the role of platelets in JIA, JIA patients have been shown to have impaired vascular function and thus potentially increased cardiovascular risk (42). Existing therapies for JIA include nonselective nonsteroidal antiinflammatory drugs, which have been shown to antagonize platelet function, and escalation to biologic therapies including anti–tumor necrosis factor (e.g., infliximab, adalimumab, and golimumab), anti–IL-6 (tocilizumab), and anti–IL-1 (canakinumab and anakinra) (43). IL-1 blockade with anakinra has limited efficacy in RA (44), and it has been postulated that this is, in part, due to difficulty in antagonizing platelet microparticle–derived IL-1 (37). Conversely, IL-1 blockade is highly effective in the treatment of systemic JIA (45), where very high platelet counts are common.

In our study, GPIbα was associated with an increased risk of both oligoarticular and RF-negative polyarticular JIA, and this association was shown to be mediated by platelet count. Our findings imply a novel role for platelets in oligoarticular and RF-negative polyarticular JIA, extending the pathogenic role of platelets in JIA to include disease causation. Therefore, GPIbα represents a potential new therapeutic strategy or a drug repurposing opportunity for these JIA subtypes, which is supported within the current literature. However, given multiple physiologic drivers and functions of platelets (46), such approaches need to be carefully explored to ensure therapeutic benefit. In addition, JIA consists of 7 subtypes (of which oligoarticular and polyarticular subtypes account for up to 90%) (47), and it is increasingly recognized that these comprise discrete clinical entities (48). Further work will be required to ascertain whether these

findings are applicable to other JIA subtypes, in particular systemic JIA.

The limitations of this study include, first, that ~8% of the participants from the INTERVAL study (3,300 of 40,521) overlapped between the proteome GWAS and the hematologic GWAS. Nonetheless, bias due to sample overlap is likely to be negligible in this study due to the presence of strong instruments (49). Second, exposures instrumented by a single variant precluded the use of pleiotropy-robust MR methods, such as weighted median and MR-Egger (29,30), which require a large number of instruments. Therefore, to improve the reliability of causal inference, we used multiple-trait colocalization to complement the MR findings, as recommended (50). Third, it is important to note that although multiple-trait colocalization analysis provided strong evidence that GPIbα impacts disease via its effects on platelet count, other potential interpretations such as horizontal pleiotropy should be considered. Fourth, *BRAP* also associates with 3 other proteins (vascular cell adhesion molecule 1, β_2-microglobulin, and CXCL16), which may also play a role (3). Nevertheless, these proteins are also on the same biologic pathway as GPIbα (9). Fifth, we used platelet count as the mediator; however, platelet count alone may not represent a major or sole determinant of thrombosis and inflammation, and other platelet indices may also be important. Sixth, genetic contributions to complex traits are partitioned into effects from *cis*-genes and *trans*-genes (51). However, authoritative analysis conclusively assessing gene regulatory networks on complex traits is beyond the scope of this study. Seventh, summary statistics are subject to the quality control and covariable adjustments conducted by the original researchers of the GWAS based on the specific optimization requirements of their data sets; the use of summary statistics precluded re-adjustment of data. Finally, this investigation was conducted using summary statistics obtained from participants of European ancestry, and therefore might not be generalizable to other ethnic populations (52). Replication of our findings in other ethnic populations will be helpful to improve the generalizability, and evaluate whether there are underlying ethnic differences in the pathogenesis of disease (53), once data become available.

Using two-step MR and multiple-trait colocalization approaches, we provide reliable genetic evidence that the genetic variants that regulate GPIbα proteomic pathways, with well-characterized biology function on platelet count, have a causal etiologic role in oligoarticular and RF-negative polyarticular JIA. Our findings highlight the active role of platelets in these JIA subtypes, and GPIbα as a putative therapeutic target for these JIA subtypes.

ACKNOWLEDGMENTS

This work would not have been possible without access to publicly available summary data. Summary data on coronary artery disease and myocardial infarction were contributed by CARDIoGRAMplusC4D investigators and downloaded from www.cardiogramplusc4d.org. Summary data on stroke and stroke subtypes were contributed by the MEGASTROKE investigators and downloaded from http://www.megastroke.org/. The MEGASTROKE project received funding from sources specified at http://megastroke.org/acknowledgements.html. Summary data on deep venous thrombosis were downloaded from the Neale Lab (http://www.nealelab.is/). Summary data on arterial embolism, and thrombosis and phlebitis and thrombophlebitis were downloaded from the Lee Lab (https://www.leelabsg.org/resources). Summary data on multiple sclerosis were contributed by the International Multiple Sclerosis Consortium and downloaded from http://imsgc.net/. Summary data on primary sclerosing cholangitis were contributed by the International Primary Sclerosing Cholangitis Study Group Consortium and downloaded from https://www.ipscsg.org/. Summary data on eczema were contributed by the EArly Genetics and Lifecourse Epidemiology Consortium and downloaded from http://copsac.com/. Summary data on inflammatory bowel disease, Crohn's disease, and ulcerative colitis were contributed by investigators (26) and summary data on platelet count were contributed by investigators (12) and downloaded from the GWAS Catalog. Summary data on systemic lupus erythematosus (21), rheumatoid arthritis (20), juvenile idiopathic arthritis (19), type 1 diabetes mellitus (18), psoriasis (22), and primary biliary cirrhosis (25) were obtained from MR-Base (http://www.mrbase.org/) and the IEU GWAS database (http://gwas.mrcieu.ac.uk).

AUTHOR CONTRIBUTIONS

All authors were involved in drafting the article or revising it critically for important intellectual content, and all authors approved the final version to be published. Dr. Luo had full access to all of the data in the study and takes responsibility for the integrity of the data and the accuracy of the data analysis.

Study conception and design. Luo, Clarke, Ramanan, Schooling, Gaunt, Au Yeung, Zheng.

Acquisition of data. Luo, Thompson, Langefeld, Marion, Grom, Gaunt, Zheng.

Analysis and interpretation of data. Luo, Clarke, Ramanan, Schooling, Gaunt, Au Yeung, Zheng.

REFERENCES

1. Luo SZ, Mo X, Afshar-Kharghan V, Srinivasan S, Lopez JA, Li R. Glycoprotein Ibα forms disulfide bonds with 2 glycoprotein Ibβ subunits in the resting platelet. Blood 2007;109:603–9.
2. Bergmeier W, Piffath CL, Goerge T, Cifuni SM, Ruggeri ZM, Ware J, et al. The role of platelet adhesion receptor GPIbα far exceeds that of its main ligand, von Willebrand factor, in arterial thrombosis. Proc Natl Acad Sci U S A 2006;103:16900–5.
3. Sun BB, Maranville JC, Peters JE, Stacey D, Staley JR, Blackshaw J, et al. Genomic atlas of the human plasma proteome. Nature 2018;558:73–9.
4. Van der Meijden PE, Heemskerk JW. Platelet biology and functions: new concepts and clinical perspectives [review]. Nat Rev Cardiol 2019;16:166–79.
5. Koupenova M, Clancy L, Corkrey HA, Freedman JE. Circulating platelets as mediators of immunity, inflammation, and thrombosis. Circ Res 2018;122:337–51.
6. Relton CL, Davey Smith G. Two-step epigenetic Mendelian randomization: a strategy for establishing the causal role of epigenetic processes in pathways to disease. Int J Epidemiol 2012;41:161–76.
7. Giambartolomei C, Liu JA, Zhang W, Hauberg M, Shi H, Boocock J, et al. A Bayesian framework for multiple trait colocalization from summary association statistics. Bioinformatics 2018;34:2538–45.
8. Nelson MR, Tipney H, Painter JL, Shen J, Nicoletti P, Shen Y, et al. The support of human genetic evidence for approved drug indications. Nat Genet 2015;47:856–60.
9. Zheng J, Haberland V, Baird D, Walker V, Haycock PC, Hurle MR, et al. Phenome-wide Mendelian randomization mapping the influence of the plasma proteome on complex diseases. Nat Genet 2020;52:1122–31.

10. Lawlor DA, Harbord RM, Sterne JA, Timpson N, Smith GD. Mendelian randomization: using genes as instruments for making causal inferences in epidemiology. Stat Med 2008;27:1133–63.
11. Di Angelantonio E, Thompson SG, Kaptoge S, Moore C, Walker M, Armitage J, et al. Efficiency and safety of varying the frequency of whole blood donation (INTERVAL): a randomised trial of 45 000 donors. Lancet 2017;390:2360–71.
12. Astle WJ, Elding H, Jiang T, Allen D, Ruklisa D, Mann AL, et al. The allelic landscape of human blood cell trait variation and links to common complex disease. Cell 2016;167:1415–29.
13. UK10K Consortium, Walter K, Min JL, Huang J, Crooks L, Memari Y, et al. The UK10K project identifies rare variants in health and disease. Nature 2015;526:82–90.
14. McGonagle D, McDermott MF. A proposed classification of the immunological diseases. PLoS Med 2006;3:e297.
15. Doria A, Zen M, Bettio S, Gatto M, Bassi N, Nalotto L, et al. Autoinflammation and autoimmunity: bridging the divide [review]. Autoimmun Rev 2012;12:22–30.
16. Nikpay M, Goel A, Won HH, Hall LM, Willenborg C, Kanoni S, et al. A comprehensive 1,000 genomes-based genome-wide association meta-analysis of coronary artery disease. Nat Genet 2015;47:1121–30.
17. Malik R, Chauhan G, Traylor M, Sargurupremraj M, Okada Y, Mishra A, et al. Multiancestry genome-wide association study of 520,000 subjects identifies 32 loci associated with stroke and stroke subtypes. Nat Genet 2018;50:524–37.
18. Onengut-Gumuscu S, Chen WM, Burren O, Cooper NJ, Quinlan AR, Mychaleckyj JC, et al. Fine mapping of type 1 diabetes susceptibility loci and evidence for colocalization of causal variants with lymphoid gene enhancers. Nat Genet 2015;47:381–6.
19. Hinks A, Cobb J, Marion MC, Prahalad S, Sudman M, Bowes J, et al. Dense genotyping of immune-related disease regions identifies 14 new susceptibility loci for juvenile idiopathic arthritis. Nat Genet 2013;45:664–9.
20. Okada Y, Wu D, Trynka G, Raj T, Terao C, Ikari K, et al. Genetics of rheumatoid arthritis contributes to biology and drug discovery. Nature 2014;506:376–81.
21. Hom G, Graham RR, Modrek B, Taylor KE, Ortmann W, Garnier S, et al. Association of systemic lupus erythematosus with C8orf13-BLK and ITGAM-ITGAX. N Engl J Med 2008;358:900–9.
22. Tsoi LC, Spain SL, Knight J, Ellinghaus E, Stuart PE, Capon F, et al. Identification of 15 new psoriasis susceptibility loci highlights the role of innate immunity. Nat Genet 2012;44:1341–8.
23. International Multiple Sclerosis Genetics Consortium, Beecham AH, Patsopoulos NA, Xifara DK, Davis MF, Kemppinen A, et al. Analysis of immune-related loci identifies 48 new susceptibility variants for multiple sclerosis. Nat Genet 2013;45:1353–60.
24. Ji SG, Juran BD, Mucha S, Folseraas T, Jostins L, Melum E, et al. Genome-wide association study of primary sclerosing cholangitis identifies new risk loci and quantifies the genetic relationship with inflammatory bowel disease. Nat Genet 2017;49:269–73.
25. Cordell HJ, Han Y, Mells GF, Li Y, Hirschfield GM, Greene CS, et al. International genome-wide meta-analysis identifies new primary biliary cirrhosis risk loci and targetable pathogenic pathways. Nat Commun 2015;6:8019.
26. De Lange KM, Moutsianas L, Lee JC, Lamb CA, Luo Y, Kennedy NA, et al. Genome-wide association study implicates immune activation of multiple integrin genes in inflammatory bowel disease. Nat Genet 2017;49:256–61.
27. Paternoster L, Standl M, Waage J, Baurecht H, Hotze M, Strachan DP, et al. Multi-ancestry genome-wide association study of 21,000 cases and 95,000 controls identifies new risk loci for atopic dermatitis. Nat Genet 2015;47:1449–56.
28. Burgess S, Dudbridge F, Thompson SG. Combining information on multiple instrumental variables in Mendelian randomization: comparison of allele score and summarized data methods. Stat Med 2016;35:1880–906.
29. Bowden J, Smith GD, Haycock PC, Burgess S. Consistent estimation in Mendelian randomization with some invalid instruments using a weighted median estimator. Genet Epidemiol 2016;40:304–14.
30. Bowden J, del Greco MF, Minelli C, Smith GD, Sheehan NA, Thompson JR. Assessing the suitability of summary data for two-sample Mendelian randomization analyses using MR-Egger regression: the role of the I2 statistic. Int J Epidemiol 2016;45:1961–74.
31. Hemani G, Tilling K, Smith GD. Orienting the causal relationship between imprecisely measured traits using GWAS summary data. PLoS Genet 2017;13:e1007081.
32. Burgess S. Sample size and power calculations in Mendelian randomization with a single instrumental variable and a binary outcome. Int J Epidemiol 2014;43:922–9.
33. Baker RI, Eikelboom J, Lofthouse E, Staples N, Afshar-Kharghan V, Lopez JA, et al. Platelet glycoprotein Ibα Kozak polymorphism is associated with an increased risk of ischemic stroke. Blood 2001;98:36–40.
34. Sonoda A, Murata M, Ito D, Tanahashi N, Ohta A, Tada Y, et al. Association between platelet glycoprotein Ibα genotype and ischemic cerebrovascular disease. Stroke 2000;31:493–7.
35. Koltsova EK, Sundd P, Zarpellon A, Ouyang H, Mikulski Z, Zampolli A, et al. Genetic deletion of platelet glycoprotein Ibα but not its extracellular domain protects from atherosclerosis. Thromb Haemost 2014;112:1252–63.
36. Timmers PR, Mounier N, Lall K, Fischer K, Ning Z, Feng X, et al. Genomics of 1 million parent lifespans implicates novel pathways and common diseases and distinguishes survival chances. Elife 2019;8:e39856.
37. Boilard E, Nigrovic PA, Larabee K, Watts GF, Coblyn JS, Weinblatt ME, et al. Platelets amplify inflammation in arthritis via collagen-dependent microparticle production. Science 2010;327:580–3.
38. Corken A, Russell S, Dent J, Post SR, Ware J. Platelet glycoprotein Ib-IX as a regulator of systemic inflammation. Arterioscler Thromb Vasc Biol 2014;34:996–1001.
39. Vakili M, Ziaee V, Moradinejad MH, Raeeskarami SR, Kompani F, Rahamooz T. Changes of platelet indices in juvenile idiopathic arthritis in acute phase and after two months treatment. Iran J Pediatr 2016;26:e5006.
40. Sanjadi M, Sichanie ZR, Totonchi H, Karami J, Rezaei R, Aslani S. Atherosclerosis and autoimmunity: a growing relationship. Int J Rheum Dis 2018;21:908–21.
41. Bachlava E, Loukopoulou S, Karanasios E, Chrousos G, Michos A. Management of coronary artery aneurysms using abciximab in children with Kawasaki disease. Int J Cardiol 2016;220:65–9.
42. Vlahos AP, Theocharis P, Bechlioulis A, Naka KK, Vakalis K, Papamichael ND, et al. Changes in vascular function and structure in juvenile idiopathic arthritis. Arthritis Care Res (Hoboken) 2011;63:1736–44.
43. Giancane G, Consolaro A, Lanni S, Davi S, Schiappapietra B, Ravelli A. Juvenile idiopathic arthritis: diagnosis and treatment. Rheumatol Ther 2016;3:187–207.
44. Mertens M, Singh JA. Anakinra for rheumatoid arthritis. Cochrane Database Syst Rev 2009:CD005121.
45. Ruperto N, Brunner HI, Quartier P, Constantin T, Wulffraat N, Horneff G, et al. Two randomized trials of canakinumab in systemic juvenile idiopathic arthritis. N Engl J Med 2012;367:2396–406.
46. Gremmel T, Frelinger AL III, Michelson AD. Platelet physiology. Semin Thromb Hemost 2016;42:191–204.
47. Ravelli A, Martini A. Juvenile idiopathic arthritis. Lancet 2007;369:767–78.
48. Petty RE, Southwood TR, Manners P, Baum J, Glass DN, Goldenberg J, et al. International League of Associations for

Rheumatology classification of juvenile idiopathic arthritis: second revision, Edmonton, 2001. J Rheumatol 2004;31:390–2.
49. Burgess S, Davies NM, Thompson SG. Bias due to participant overlap in two-sample Mendelian randomization. Genet Epidemiol 2016;40:597–608.
50. Wainberg M, Sinnott-Armstrong N, Mancuso N, Barbeira AN, Knowles DA, Golan D, et al. Opportunities and challenges for transcriptome-wide association studies. Nat Genet 2019;51:592–9.
51. Liu X, Li YI, Pritchard JK. Trans effects on gene expression can drive omnigenic inheritance. Cell 2019;177:1022–34.
52. Carlson CS, Matise TC, North KE, Haiman CA, Fesinmeyer MD, Buyske S, et al. Generalization and dilution of association results from European GWAS in populations of non-European ancestry: the PAGE study. PLoS Biol 2013;11:e1001661.
53. Wojcik GL, Graff M, Nishimura KK, Tao R, Haessler J, Gignoux CR, et al. Genetic analyses of diverse populations improves discovery for complex traits. Nature 2019;570:514–8.

Corrigendum

DOI 10.1002/art.41680

In the article by Ciccia et al in the December 2018 issue of *Arthritis & Rheumatology* (Proinflammatory CX_3CR1+CD59+ Tumor Necrosis Factor–Like Molecule 1A+Interleukin-23+ Monocytes Are Expanded in Patients With Ankylosing Spondylitis and Modulate Innate Lymphoid Cell 3 Immune Functions [pages 2003–2013]), errors in the plots shown in Figure 6B were inadvertently introduced in the preparation of the figure. The corrected figure is shown below.

The authors regret the errors.

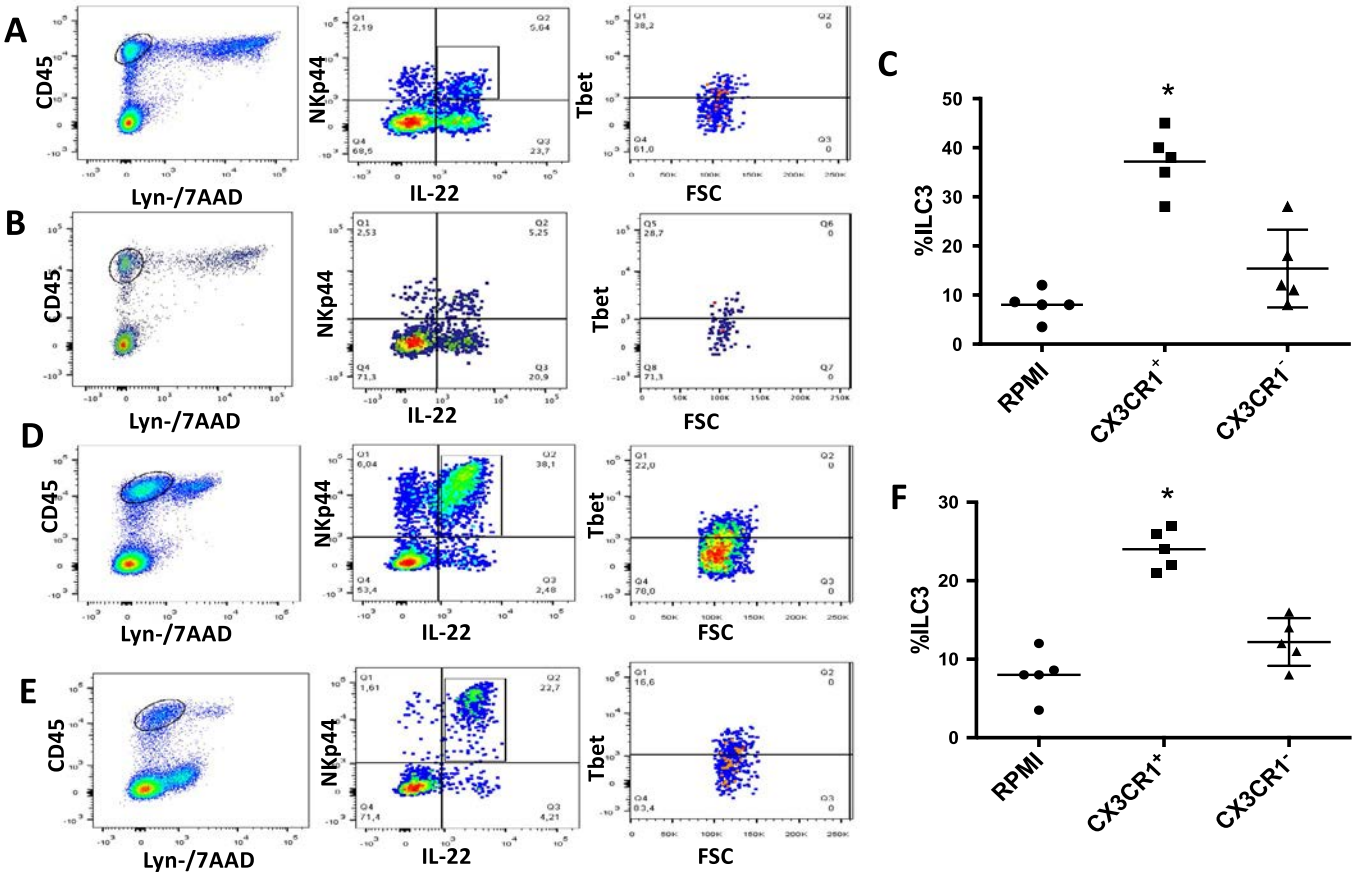

Figure 6. CX_3CR1+ mononuclear phagocytes (MNPs) drive innate lymphoid cell 3 (ILC-3) expansion. **A** and **B**, CX_3CR1+ (**A**) and CX_3CR1– (**B**) cells were isolated from the gut of patients with ankylosing spondylitis (AS) and cocultured with isolated peripheral Lyn–T-bet+NKp44+ ILC3. **C**, Percentages of ILC3 cells after coculture with intestinal CX_3CR1+ and CX_3CR1– cells. There was significant expansion of interleukin-22 (IL-22)+T-bet+ ILC3 with coculture with CX_3CR1+ cells compared to CX_3CR1– cells and no coculture (RPMI). **D** and **E**, CX_3CR1+ (**D**) and CX_3CR1– (**E**) cells were isolated from the peripheral blood of patients with AS and cocultured with isolated peripheral Lyn–T-bet+NKp44+ ILC3. **F**, Percentages of ILC3 cells after coculture with peripheral CX_3CR1+ and CX_3CR1– cells. There was significant expansion of IL22+T-bet+ ILC3 with coculture with CX_3CR1+ cells, but not with CX_3CR1– cells, compared to no coculture. In **C** and **F**, symbols represent individual patients; horizontal lines show the mean. * = $P < 0.05$ versus RPMI. 7-AAD = 7-aminoactinomycin D.

American College of Rheumatology
Empowering Rheumatology Professionals

Arthritis & Rheumatology
Vol. 73, No. 4, April 2021, pp 702–714
DOI 10.1002/art.41571

Prevalence, Deaths, and Disability-Adjusted Life Years Due to Musculoskeletal Disorders for 195 Countries and Territories 1990–2017

Saeid Safiri,[1] Ali-Asghar Kolahi,[2] Marita Cross,[3] Catherine Hill,[4] Emma Smith,[5] Kristin Carson-Chahhoud,[6] Mohammad Ali Mansournia,[7] Amir Almasi-Hashiani,[8] Ahad Ashrafi-Asgarabad,[9] Jay Kaufman,[10] Mahdi Sepidarkish,[11] Seyed Kazem Shakouri,[12] Damian Hoy,[13] Anthony D. Woolf,[14] Lyn March,[3] Gary Collins,[15] and Rachelle Buchbinder[16]

Objective. To report the levels and trends of prevalence, deaths, and disability-adjusted life years (DALYs) due to musculoskeletal disorders, categorized as low back pain, neck pain, osteoarthritis (OA), rheumatoid arthritis (RA), gout, and other musculoskeletal disorders, across 195 countries and territories from 1990 to 2017 according to age, sex, and Sociodemographic Index (SDI; a composite of sociodemographic factors).

Methods. Data were obtained from the Global Burden of Disease (GBD) Study 2017. The fatal and nonfatal burdens of musculoskeletal disorders were estimated using the Cause of Death Ensemble model and Bayesian meta-regression tool, respectively. Estimates were provided for all musculoskeletal disorders and the corresponding 6 categories at global, regional, and national levels from 1990 to 2017. Counts and age-standardized rates per 100,000 population along with 95% uncertainty intervals (95% UIs) were reported for prevalence, deaths, and DALYs.

Results. Globally, there were ~1.3 billion prevalent cases (95% UI 1.2 billion, 1.4 billion), 121.3 thousand deaths (95% UI 105.6 thousand, 126.2 thousand), and 138.7 million DALYs (95% UI 101.9 million, 182.6 million) due to musculoskeletal disorders in 2017. Age-standardized prevalence, death, and DALY rates per 100,000 population were 16,276.2 (95% UI 15,495.5, 17,145.8), 1.6 (95% UI 1.4, 1.6), and 1,720 (95% UI 1,264.4, 2,259.2), respectively. Age-standardized prevalence (–1.6% [95% UI –2.4, –0.8]) and DALY rates (–3.5% [95% UI –4.7, –2.3]) decreased slightly from 1990. The global point prevalence rate of musculoskeletal disorders in 2017 was higher in women than in men and increased with age up to the oldest age group. Globally, the proportion of prevalent cases according to category of musculoskeletal disorders in 2017 was greatest for low back pain (36.8%), followed by other musculoskeletal disorders (21.5%), OA (19.3%), neck pain (18.4%), gout (2.6%), and RA (1.3%). These proportions did not change appreciably compared with 1990. The burden due to musculoskeletal conditions was higher in developed countries. The countries with the highest age-standardized prevalence rates of musculoskeletal disorders in 2017 were Switzerland (23,346.0 [95% UI 22,392.6, 24,329.8]), Chile (23,007.9 [95% UI 21,746.5, 24,165.8]), and Denmark (22,166.1 [95% UI 20,817.2, 23,542.1]). The greatest increases from 1990 were found in Chile (10.8% [95% UI 6.6, 15.4]), Benin (8.8% [95% UI 6.7, 11.1]), and El Salvador (8.5% [95% UI 5.5, 11.9]).

Conclusion. There is a large burden of musculoskeletal disorders globally, with some notable inter-country variation. Some countries have twice the burden of other countries. Increasing population awareness regarding risk factors, consequences, and evidence-informed treatment strategies for musculoskeletal disorders with a focus on the older female population in developed countries is needed, particularly for low back and neck pain and OA, which contribute a large burden among this cohort.

This study is based on publicly available data and solely reflects the opinions of the authors and not those of the Institute for Health Metrics and Evaluation.

Supported by Shahid Beheshti University of Medical Sciences (grant 21740-4-7). The Global Burden of Disease Study was supported by the Bill and Melinda Gates Foundation. Dr. Cross's work was supported by the Institute of Bone and Joint Research and the Global Alliance for Musculoskeletal Health. Dr. Buchbinder's work was supported by an Australian National Health and Medical Research Council (NHMRC) Senior Principal Research Fellowship.

[1]Saeid Safiri, PhD: Aging Research Institute, School of Medicine, Tabriz University of Medical Sciences, Tabriz, Iran; [2]Ali-Asghar Kolahi, MD: Social Determinants of Health Research Center, Shahid Beheshti University of Medical Sciences, Tehran, Iran; [3]Marita Cross, MD, Lyn March, MD: Institute

INTRODUCTION

As populations around the world are rapidly aging, most of us aspire to live a long and healthy life (1). Good musculoskeletal health is needed for people to have economic, social, and functional independence throughout their life course (2). Yet the importance of musculoskeletal disorders is often underappreciated since they are rarely fatal and are assumed to be irreversible and associated with age (3). The burden from musculoskeletal disorders is greatest among aging populations, with resultant enormous costs to the economy and the health care system (2,4,5). In common with many other chronic diseases, modifiable risk factors for some musculoskeletal disorders include excess body weight, poor nutrition, smoking, and a sedentary lifestyle (6).

Although the global burden of specific musculoskeletal disorders has been reported in previous studies (7–15), and included in multiple *Lancet* articles (16,17), no study to date has provided an overview of the burden of all musculoskeletal disorders combined in a single article. One 2003 review reported the burden of major musculoskeletal disorders (18), although new data are available that supersede the results of that study. Another more recent report described the burden of musculoskeletal disorders in 2015 using the World Health Organization Global Health Estimates Database (19). However, prevalence and deaths due to musculoskeletal disorders were not reported, and there was no information regarding age- and sex-based patterns of musculoskeletal disorders. Hence, the aim of the present study was to report the global, regional, and national burden of musculoskeletal disorders, including rheumatoid arthritis (RA), osteoarthritis (OA), low back pain, neck pain, gout, and other musculoskeletal disorders, in terms of counts and age-standardized rates from 1990 to 2017 across 195 countries and territories according to age, sex, and Sociodemographic Index (SDI; a composite of sociodemographic factors). Importantly, this study provides a single, updated report across all musculoskeletal conditions, including additional analyses not presented in earlier Global Burden of Disease (GBD) reports.

METHODS

Overview. The GBD study, conducted by the Institute for Health Metrics and Evaluation (IHME) and its many global collaborators, is the most comprehensive study measuring the burden of diseases, injuries, and risk factors frequently. In the last round, GBD 2017, the burden of 359 diseases and injuries, 282 causes of death, and 84 risk factors was studied across 21 regions and 195 countries and territories from 1990 to 2017 (16,17,20). Publicly available estimates can be found at https://vizhub.healthdata.org/gbd-compare/ and http://ghdx.healthdata.org/gbd-results-tool (21,22). A detailed description of the methods for estimating the fatal and nonfatal burdens of diseases and injuries has been provided previously (16,17,20). An abbreviated summary of methods pertinent to estimating the burden of musculoskeletal disorders is provided below. This study was approved by the ethics committee of Shahid Beheshti University of Medical Sciences, Tehran, Iran (IR.SBMU.RETECH.REC.1399.311).

Case definition and data sources. In GBD 2017, musculoskeletal disorders were categorized into 6 groups: RA, OA, low back pain, neck pain, gout, and an "other" musculoskeletal disorders category that included all other musculoskeletal disorders (for example, systemic lupus erythematosus, axial spondyloarthritides, and other inflammatory arthritis, etc) (16). The definitions of each category are provided in Supplementary Table 1, available on the *Arthritis & Rheumatology* website at http://onlinelibrary.wiley.com/doi/10.1002/art.41571/abstract.

Data used to estimate the fatal and nonfatal burdens of musculoskeletal disorders were obtained from vital registration systems, sample vital registration, verbal autopsies, record data of surveys in the Global Health Data Exchange, the GBD repository of population health data, including the World Health surveys and national health surveys, and published population-based studies (16,17).

Disease model. Fatal burden was only considered for RA and other musculoskeletal disorders. Within other musculoskeletal disorders, conditions such as vasculitis, systemic lupus erythematosus, and systemic sclerosis were considered to have increased

of Bone and Joint Research, The University of Sydney, Sydney, New South Wales, Australia; [4]Catherine Hill, MD: The Queen Elizabeth Hospital and the Royal Adelaide Hospitals, Adelaide, South Australia, Australia; [5]Emma Smith, MD: Institute of Bone and Joint Research and Pain Management Research Institute, The University of Sydney, Sydney, New South Wales, Australia; [6]Kristin Carson-Chahhoud, PhD: School of Health Sciences, University of South Australia, Adelaide, Australia; [7]Mohammad Ali Mansournia, MD, PhD: School of Public Health, Tehran University of Medical Sciences, Tehran, Iran; [8]Amir Almasi-Hashiani, PhD: School of Health, Arak University of Medical Sciences, Arak, Iran; [9]Ahad Ashrafi-Asgarabad, MSc: School of Health, Bam University of Medical Sciences, Bam, Iran; [10]Jay Kaufman, PhD: Faculty of Medicine, McGill University, Montreal, Quebec, Canada; [11]Mahdi Sepidarkish, PhD: School of Public Health, Babol University of Medical Sciences, Babol, Iran; [12]Seyed Kazem Shakouri, MD: Physical Medicine and Rehabilitation Research Center, Tabriz University of Medical Sciences, Tabriz, Iran; [13]Damian Hoy, PhD: Institute of Bone and Joint Research, The University of Sydney, Sydney, New South Wales, Australia, and Global Alliance for Musculoskeletal Health, Royal Cornwall Hospital, Truro, UK; [14]Anthony D. Woolf, MD: Royal Cornwall Hospital and University of Exeter Medical School, Truro, UK; [15]Gary Collins, PhD: Botnar Research Centre, University of Oxford, NIHR Oxford Biomedical Research Centre, Oxford University Hospitals NHS Foundation Trust, Oxford, UK; [16]Rachelle Buchbinder, MD: Cabrini Institute and School of Public Health and Preventive Medicine, Monash University, Melbourne, Victoria, Australia.

No potential conflicts of interest relevant to this article were reported.

Address correspondence to Rachelle Buchbinder, MD, Cabrini Institute, Monash Department of Clinical Epidemiology, 4 Drysdale Street, Malvern, Victoria 3144, Australia. Email: rachelle.buchbinder@monash.edu.

Submitted for publication May 20, 2020; accepted in revised form October 27, 2020.

Table 1. Prevalent cases, deaths, and DALYs for musculoskeletal disorders in 2017 for both sexes and percentage change in age-standardized rates by GBD region*

	Prevalence (95% UI)			Deaths (95% UI)			DALYs (95% UI)		
	Counts (2017)	Age-standardized rates (2017)	Percentage change in age-standardized rates between 1990 and 2017	Counts (2017)	Age-standardized rates (2017)	Percentage change in age-standardized rates between 1990 and 2017	Counts (2017)	Age-standardized rates (2017)	Percentage change in age-standardized rates between 1990 and 2017
Global	1,312,131,317 (1,248,058,740, 1,383,422,599)	16,276.2 (15,495.5, 17,145.8)	−1.6 (−2.4, −0.8)	121,269 (105,635, 126,226)	1.6 (1.4, 1.6)	−5.7 (−13, 0.1)	138,723,945 (101,940,849, 182,552,790)	1,720.5 (1,264.4, 2,259.2)	−3.5 (−4.7, −2.3)
High-income Asia Pacific	54,492,405 (51,490,666, 57,486,629)	19,375.4 (18,222.9, 20,637)	2.5 (1.5, 3.5)	4,559 (4,337, 4,804)	1 (0.9, 1)	−43.3 (−46.2, −39.9)	5,786,261 (4,197,002, 7,762,401)	2,136.6 (1,554.9, 2,879.1)	2.3 (1, 3.6)
High-income North America	101,055,824 (98,034,649, 104,024,525)	21,155.5 (20,480.6, 21,821)	3.5 (0.8, 6.4)	10,856 (10,482, 11,206)	1.8 (1.7, 1.9)	−3.2 (−7.1, 1.2)	10,787,684 (7,966,000, 14,072,299)	2,283.3 (1,679.8, 2,980.7)	0.8 (−2.8, 4.4)
Western Europe	122,014,221 (116,142,913, 128,376,742)	20,228.5 (19,141.1, 21,373.9)	0.7 (−0.2, 1.6)	13,286 (12,760, 13,848)	1.3 (1.2, 1.3)	−26.2 (−29.5, −23)	13,556,409 (9,951,227, 18,021,592)	2,296.8 (1,677.4, 3,073.6)	−0.1 (−1.3, 1)
Australasia	7,351,047 (6,943,120, 7,759,044)	19,871.9 (18,680.9, 21,116.4)	0.4 (−2.1, 2.7)	957 (872, 1,047)	1.8 (1.6, 2)	−13.1 (−21.6, −4.8)	787,545 (578,079, 1,046,905)	2,165.1 (1,585.8, 2,871.3)	−1.2 (−4.4, 2)
Andean Latin America	8,476,196 (7,995,576, 8,990,684)	14,584.5 (13,775.8, 15,468.1)	5.3 (3.8, 6.7)	604 (546, 728)	1.1 (1, 1.3)	−26.1 (−36, −1.2)	903,172 (662,810, 1,199,310)	1,544.9 (1,132.8, 2,051)	5 (3, 7.1)
Tropical Latin America	42,028,605 (39,526,964, 44,810,902)	17,635.4 (16,596.2, 18,792.9)	1.2 (0, 2.2)	3,314 (3,196, 3,430)	1.4 (1.4, 1.5)	7.5 (3.1, 13)	4,707,550 (3,471,660, 6,259,228)	1,972 (1,455.1, 2,617.1)	0.2 (−1.3, 1.7)
Central Latin America	32,327,154 (30,558,575, 34,214,301)	12,890.5 (12,191.9, 13,628)	3.2 (2.1, 4.4)	5,206 (5,001, 5,462)	2.2 (2.1, 2.3)	−9.5 (−13.5, −4.5)	3,399,420 (2,521,425, 4,486,060)	1,345.8 (998.5, 1,767.7)	2.1 (0.6, 3.7)
Southern Latin America	15,497,872 (14,698,291, 16,372,699)	20,952.4 (19,843.1, 22,168.6)	5.8 (3.8, 7.9)	1,069 (975, 1,170)	1.3 (1.2, 1.5)	−51.6 (−56.3, −46.5)	1,726,002 (1,267,078, 2,304,403)	2,349 (1,721.2, 3,126)	5.6 (2.9, 8.3)
Caribbean	6,787,966 (6,418,690, 7,167,496)	13,619.1 (12,879.6, 14,370.1)	−1.2 (−3, 0.2)	790 (685, 913)	1.6 (1.4, 1.8)	−7.4 (−18.4, 5.6)	701,729 (514,394, 924,395)	1,411.9 (1,032.4, 1,856.6)	−2.3 (−4.4, −0.2)
Central Europe	26,315,295 (24,880,070, 27,846,010)	15,936.5 (15,015, 16,947.1)	0.6 (−0.8, 2.3)	1,385 (1,316, 1,449)	0.7 (0.6, 0.7)	−24.7 (−29.4, −20.4)	2,912,792 (2,109,579, 3,885,266)	1,789.9 (1,293.5, 2,419.1)	0.2 (−1.7, 2.4)
Eastern Europe	42,913,492 (40,207,107, 45,756,154)	14,786.5 (13,849, 15,808.2)	−3.1 (−4.5, −1.6)	2,405 (2,291, 2,511)	0.8 (0.7, 0.8)	10.7 (6.2, 16.2)	4,574,173 (3,332,255, 6,120,504)	1,599.3 (1,164.8, 2,151.4)	−5.5 (−7.4, −3.5)
Central Asia	11,462,038 (10,697,541, 12,308,715)	13,390.5 (12,558.3, 14,304.9)	0.6 (−0.3, 1.6)	458 (421, 498)	0.6 (0.6, 0.7)	13.1 (2.8, 26.5)	1,255,526 (912,094, 1,705,965)	1,452.1 (1,058.5, 1,951.1)	−0.2 (−1.4, 1.2)

(Continued)

Table 1. (*Cont'd*)

	Prevalence (95% UI)			Deaths (95% UI)			DALYs (95% UI)		
	Counts (2017)	Age-standardized rates (2017)	Percentage change in age-standardized rates between 1990 and 2017	Counts (2017)	Age-standardized rates (2017)	Percentage change in age-standardized rates between 1990 and 2017	Counts (2017)	Age-standardized rates (2017)	Percentage change in age-standardized rates between 1990 and 2017
North Africa and Middle East	102,981,818 (97,116,242, 109,306,805)	19,252.4 (18,275.7, 20,378.8)	1.7 (0.8, 2.6)	2,903 (2,420, 3,175)	0.7 (0.5, 0.7)	−5.6 (−25.6, 11.7)	11,239,371 (8,256,016, 15,084,270)	2,075.5 (1,530.2, 2,766.2)	1.2 (−0.2, 2.4)
South Asia	269,289,816 (253,686,298, 285,011,163)	16,916.9 (15,997.7, 17,853)	−2.1 (−3, −1.2)	40,750 (30,481, 44,610)	3.8 (2.9, 4.2)	13.3 (−3.2, 29.6)	28,019,491 (20,686,020, 36,815,004)	1,754.6 (1,301.4, 2,298.1)	−3.2 (−4.6, −1.8)
Southeast Asia	108,073,478 (102,477,726, 113,929,789)	16,203.1 (15,416.2, 17,049.1)	1.6 (0.6, 2.5)	6,550 (5,925, 7,497)	1.1 (1, 1.3)	−25.5 (−33.4, −10.5)	11,518,008 (8,441,556, 15,176,334)	1,715.5 (1,259.7, 2,251.1)	1.1 (−0.2, 2.4)
East Asia	270,556,523 (254,016,737, 287,188,169)	13,909.8 (13,115.7, 14,733.5)	−4 (−5.7, −2.1)	18,592 (15,433, 20,332)	1 (0.8, 1.1)	−3.9 (−30, 9.6)	26,910,389 (19,656,401, 35,707,263)	1,392.7 (1,021, 1,849)	−6.9 (−9.5, −4.4)
Oceania	1,618,895 (1,521,851, 1,721,771)	16,740.9 (15,871.9, 17,711.8)	2 (0.2, 3.9)	175 (115, 278)	1.8 (1.2, 2.7)	9.8 (−12.4, 32.2)	175,015 (130,057, 229,675)	1,750.5 (1,306, 2,293.6)	2.3 (−0.2, 5)
Western sub-Saharan Africa	40,548,309 (37,878,521, 43,373,813)	14,830.7 (14,010.4, 15,767.3)	4.1 (2.7, 5.6)	2,218 (1,677, 2,762)	1 (0.8, 1.3)	1.3 (−17.4, 23.6)	4,484,009 (3,264,474, 5,925,285)	1,602.3 (1,181.4, 2,123.8)	4.9 (3, 6.8)
Eastern sub-Saharan Africa	28,925,321 (26,950,602, 31,082,863)	12,633.8 (11,842.5, 13,473.9)	2.2 (1.4, 3.1)	3,351 (2,748, 4,185)	2.4 (1.9, 2.9)	−17.9 (−31.5, −1.2)	3,194,436 (2,335,703, 4,299,439)	1,369.4 (1,003.9, 1,826.5)	1.9 (0, 3.4)
Central sub-Saharan Africa	10,579,290 (9,830,321, 11,415,424)	13,885.5 (13,020.4, 14,877.1)	0.2 (−1.5, 1.9)	886 (567, 1,193)	1.6 (1.1, 2.3)	−19.4 (−32.3, 0.7)	1,168,143 (858,095, 1,555,699)	1,495.8 (1,099.8, 2,009.2)	0.3 (−2.3, 2.6)
Southern sub-Saharan Africa	8,835,752 (8,329,367, 9,374,007)	13,332.6 (12,621.4, 14,107.9)	−0.8 (−1.9, 0.3)	957 (848, 1,124)	1.7 (1.5, 2)	−18.3 (−26.3, 1.6)	916,819 (676,955, 1,210,882)	1,362 (1,012.4, 1,786.1)	−4.8 (−6.4, −3.2)

* Generated from data available from http://ghdx.healthdata.org/gbd-results-tool. DALYs = disability-adjusted life years; GBD = Global Burden of Disease; 95% UI = 95% uncertainty interval.

cause-specific mortality. Deaths, in addition to years of life lost (YLLs) due to premature death, were therefore only assigned to these groups. Deaths were estimated using the GBD standard Cause of Death Ensemble model (CODEm), which is a framework that models most cause-specific death rates in the GBD study (17). Based on all available data, various plausible models are developed to capture well-documented associations in the estimates. After examining the out-of-sample predictive validity for all individual models, these are then ranked for use in the ensemble modeling stage, and different combinations of individual models are then assessed to select the ensemble model with the highest out-of-sample predictive validity (23). Covariates used in the CODEm for RA and other musculoskeletal disorders are listed in Supplementary Table 2, available on the *Arthritis & Rheumatology* website at http://onlinelibrary.wiley.com/doi/10.1002/art.41571/abstract (11,17).

To estimate nonfatal burden, the prevalence, incidence, and mortality data were imported into the IHME Bayesian meta-regression tool DisMod-MR 2.1. This tool provides consistent estimates by pooling and adjusting methodologically different studies. It uses meta-regression to estimate a weighted average, adjusting for sources of variability between studies (24). It is able to combine epidemiologic data from multiple sources, reconcile data that are inconsistent, and extrapolate data for locations with no or sparse data using data from like locations.

Severity and years lived with disability. The International Classification of Diseases versions 9 and 10 were used in the GBD 2017 study. Supplementary Table 3 (available on the *Arthritis & Rheumatology* website at http://onlinelibrary.wiley.com/doi/10.1002/art.41571/abstract) shows the different sequelae along with sequelae-specific disability weights that were used for each musculoskeletal disorder. The disability weights were derived from the GBD 2013 European Disability Weights Measurement Study and GBD 2010 Disability Weights Measurement Study (16,25). Initially, sequelae-specific years lived with disability (YLDs) were calculated by multiplying the prevalence of each sequelae by sequelae-specific disability weights. Total YLDs for each disorder were then computed by summing the sequelae-specific YLDs for each disorder.

Estimates for burden including YLDs attributable to musculoskeletal disorders, similar to all conditions included in GBD 2017, were adjusted for comorbidity using a microsimulation process (16). In brief, co-occurrence of different diseases is estimated by simulating 40,000 individuals in each location/age/sex/year combination as exposed to the independent probability of having any of the sequelae included in GBD 2017 based on disease prevalence. Age was the main predictor of comorbidity, such that age-specific microsimulations accommodated most of the required comorbidity correction. Total YLDs attributable to musculoskeletal disorders were estimated by summing the YLDs across the 6 categories of musculoskeletal disorders (16).

Compilation of results. YLLs were calculated by multiplying the number of deaths in an age group by the remaining life expectancy in that age group, taken from the GBD standard life table. Disability-adjusted life years (DALYs) were then calculated by summing the YLDs and YLLs (20). Where there is no mortality for a condition, YLDs are equal to DALYs. DALYs are one of the most important metrics allowing comparison between fatal and nonfatal diseases and injuries across regions and over time. One DALY equals 1 lost year of healthy life (20). IHME reports all of the estimates along with their uncertainty interval (UI). Using a bootstrap method, uncertainty arising from multiple sources, such as input data, corrections of measurement error, and estimates of residual non-sampling error, is incorporated by sampling 1,000 draws with the 2.5th and 97.5th percentile of values defined as the lower and upper limits, respectively, of UIs.

Smoothing splines models were applied by our team to examine the shape of associations between the burden of musculoskeletal disorders and SDI for 21 regions and 195 countries and territories (26). Generally, the R^2 of smoothing splines is higher than their corresponding linear models, but our main goal was to focus on the shape of association, not model fit. SDI is composed of 3 indicators, including lag-distributed income per capita (i.e., gross domestic product per capita that has been smoothed over the preceding 10 years), mean education for those ages 15 years and older, and total fertility rate for those younger than 25 years. The SDI ranges from 0 (less developed) to 1 (most developed). R software version 3.5.2 was used to generate the map for prevalence, deaths, and DALY estimates from data available at http://ghdx.healthdata.org/gbd-results-tool.

RESULTS

Global level. Globally, the number of prevalent cases of musculoskeletal disorders was 1.3 billion in 2017 (95% UI 1.2 billion, 1.4 billion), with an age-standardized point prevalence of 16,276.2 per 100,000 population (95% UI 15,495.5, 17,145.8), a 1.6% decrease between 1990 and 2017 (95% UI 0.8, 2.4). RA and other musculoskeletal disorders were responsible for 121.3 thousand deaths globally (95% UI 105.6 thousand, 126.2 thousand), with an age-standardized death rate of 1.6 per 100,000 population (95% UI 1.4, 1.6), which declined from 1990 to 2017 (–5.7% [95% UI –13.0, 0.1]) (Table 1). The number of DALYs due to musculoskeletal disorders in 2017 was 138.7 million (95% UI 101.9 million, 182.6 million), with an age-standardized rate of 1,720 DALYs per 100,000 population (95% UI 1,264.4, 2,259.2), a decrease of 3.5% compared with 1990 (95% UI 2.3, 4.7) (Table 1).

Regional level. The age-standardized point prevalence of musculoskeletal disorders observed in 2017 was highest in high-income North America (21,155.5 [95% UI 20,480.6, 21,821]), followed by southern Latin America (20,952.4 [95%

UI 19,843.1, 22,168.6]) and Western Europe (20,228.5 [95% UI 19,141.1, 21,373.9]). In contrast, eastern sub-Saharan Africa (12,633.8 [95% UI 11,842.5, 13,473.9]), central Latin America (12,890.5 [95% UI 12,191.9, 13,628]), and southern sub-Saharan Africa (13,332.6 [95% UI 12,621.4, 14,107.9]) showed the lowest age-standardized estimates (Table 1).

South Asia (3.8 [95% UI 2.9, 4.2]), eastern sub-Saharan Africa (2.4 [95% UI 1.9, 2.9]), and central Latin America (2.2 [95% UI 2.1, 2.3]) had the highest age-standardized death rates from RA and other musculoskeletal disorders. These rates were lowest for central Asia (0.6 [95% UI 0.6, 0.7]), North Africa and the Middle East (0.7 [95% UI 0.5, 0.7]), and central Europe (0.7 [95% UI 0.6, 0.7]) (Table 1).

Southern Latin America (2,349 [95% UI 1,721.2, 3,126]), Western Europe (2,296.8 [95% UI 1,677.4, 3,073.6]), and high-income North America (2,283.3 [95% UI 1,679.8, 2,980.7]) had the highest age-standardized DALY rates in 2017. In contrast, central Latin America (1,345.8 [95% UI 998.5, 1,767.7]), southern sub-Saharan Africa (1,362 [95% UI 1,012.4, 1,786.1]), and eastern sub-Saharan Africa (1,369.4 [95% UI 1,003.9, 1,826.5]) had the lowest age-standardized DALY rates (Table 1). The age-standardized point prevalence, deaths, and DALY rates of musculoskeletal disorders for all GBD regions in 2017 are presented for men and women in Supplementary Figures 1–3, respectively (available on the *Arthritis & Rheumatology* website at http://onlinelibrary.wiley.com/doi/10.1002/art.41571/abstract).

Percentage change in age-standardized prevalence estimates between 1990 and 2017 varied between regions. Southern Latin America (5.8% [95% UI 3.8, 7.9]), Andean Latin America (5.3% [95% UI 3.8, 6.7]), and western sub-Saharan Africa (4.1% [95% UI 2.7, 5.6]) had the greatest increasing trend in the age-standardized point prevalence of musculoskeletal disorders between 1990 and 2017. In contrast, the greatest decreasing trends were observed for East Asia (–4% [95% UI –5.7, –2.1]), Eastern Europe (–3.1% [95% UI –4.5, –1.6]), and South Asia (–2.1% [95% UI –3, –1.2]) (Table 1).

The greatest increasing trends in age-standardized death rates for RA and other musculoskeletal disorders between 1990 and 2017 were observed for Central Asia (13.1% [95% UI 2.8, 26.5]), Eastern Europe (10.7% [95% UI 6.2, 16.2]), and tropical Latin America (7.5% [95% UI 3.1, 13]), while southern Latin America (–51.6% [95% UI –56.3, –46.5]), high-income Asia Pacific (–43.3% [95% UI –46.2, –39.9]), and Western Europe (–26.2% [95% UI –29.5, –23]) showed the greatest decreasing trends (Table 1).

The largest increases in age-standardized DALY rates during 1990–2017 were observed in southern Latin America (5.6% [95% UI 2.9, 8.3]), Andean Latin America (5% [95% UI 3, 7.1]), and western sub-Saharan Africa (4.9% [95% UI 3, 6.8]). In contrast, East Asia (–6.9% [95% UI –9.5, –4.4]), Eastern Europe (–5.5% [95% UI –7.4, –3.5]), and southern sub-Saharan Africa (–4.8% [95% UI –6.4, –3.2]) showed the greatest decreasing trends during the measurement period (Table 1). Sex-specific percentage changes in age-standardized point prevalence, deaths, and DALY rates of musculoskeletal disorders between 1990 and 2017 are presented in Supplementary Figures 4–6, respectively (available on the *Arthritis & Rheumatology* website at http://onlinelibrary.wiley.com/doi/10.1002/art.41571/abstract).

The number of prevalent cases of musculoskeletal disorders increased from 770.8 million in 1990 (95% UI 728.8 million, 816.5 million) to 1.3 billion in 2017 (95% UI 1.2 billion, 1.4 billion). East Asia (270.6 million [95% UI 254.0 million, 287.2 million]), South Asia (269.3 million [95% UI 253.7 million, 285.0 million]), and Western Europe (122.0 million [95% UI 116.1 million, 128.4 million]) had the highest numbers of prevalent cases in 2017 (Table 1 and Supplementary Figure 7, available on the *Arthritis & Rheumatology* website at http://onlinelibrary.wiley.com/doi/10.1002/art.41571/abstract). Likewise, the number of deaths due to RA and other musculoskeletal disorders increased from 64.7 thousand in 1990 (95% UI 59.9 thousand, 70.0 thousand) to 121.3 thousand in 2017 (95% UI 105.6 thousand, 126.2 thousand), and South Asia (40.8 thousand [95% UI 30.5 thousand, 44.6 thousand]), East Asia (18.6 thousand [95% UI 15.4 thousand, 20.3 thousand]), and Western Europe (13.3 thousand [95% UI 12.8 thousand, 13.8 thousand]) had the highest numbers of deaths due to these disorders in 2017 (Table 1 and Supplementary Figure 8, available on the *Arthritis & Rheumatology* website at http://onlinelibrary.wiley.com/doi/10.1002/art.41571/abstract).

National level. National age-standardized point prevalence estimates of musculoskeletal disorders in 2017 ranged from 10,799.8 to 23,346.0 cases per 100,000 population. Switzerland (23,346.0 [95% UI 22,392.6, 24,329.8]), Chile (23,007.9 [95% UI 21,746.5, 24,165.8]), and Denmark (22,166.1 [95% UI 20,817.2, 23,542.1]) had the 3 highest age-standardized point prevalence estimates in 2017, while Eritrea (10,799.8 [95% UI 10,013.6, 11,630.5]), Rwanda (11,642.4 [95% UI 10,830.6, 12,542.0]), and Burundi (11,796.3 [95% UI 10,933.8, 12,704.4]) showed the lowest rates (Figure 1 and Supplementary Table 4, available on the *Arthritis & Rheumatology* website at http://onlinelibrary.wiley.com/doi/10.1002/art.41571/abstract).

The national age-standardized death rates due to RA and other musculoskeletal disorders in 2017 varied from 0.23 to 4.1 cases per 100,000 population. India (4.1 [95% UI 3.0, 4.6]), Pakistan (3.6 [95% UI 2.5, 5.2]), and Barbados (3.3 [95% UI 2.9, 3.6]) had the highest age-standardized death rates in 2017, while Azerbaijan (0.2 [95% UI 0.2, 0.3]) and Kazakhstan (0.2 [95% UI 0.2, 0.3]) had the lowest rates (Supplementary Figure 9 and Supplementary Table 5, available on the *Arthritis & Rheumatology* website at http://onlinelibrary.wiley.com/doi/10.1002/art.41571/abstract).

The national age-standardized DALY rate of musculoskeletal disorders in 2017 ranged from 1,169.3 to 2,769.8 cases per 100,000 population. The highest rates were observed in Switzerland (2,769.8 [95% UI 2,001.0, 3,644.1]), Chile (2,650.1 [95%

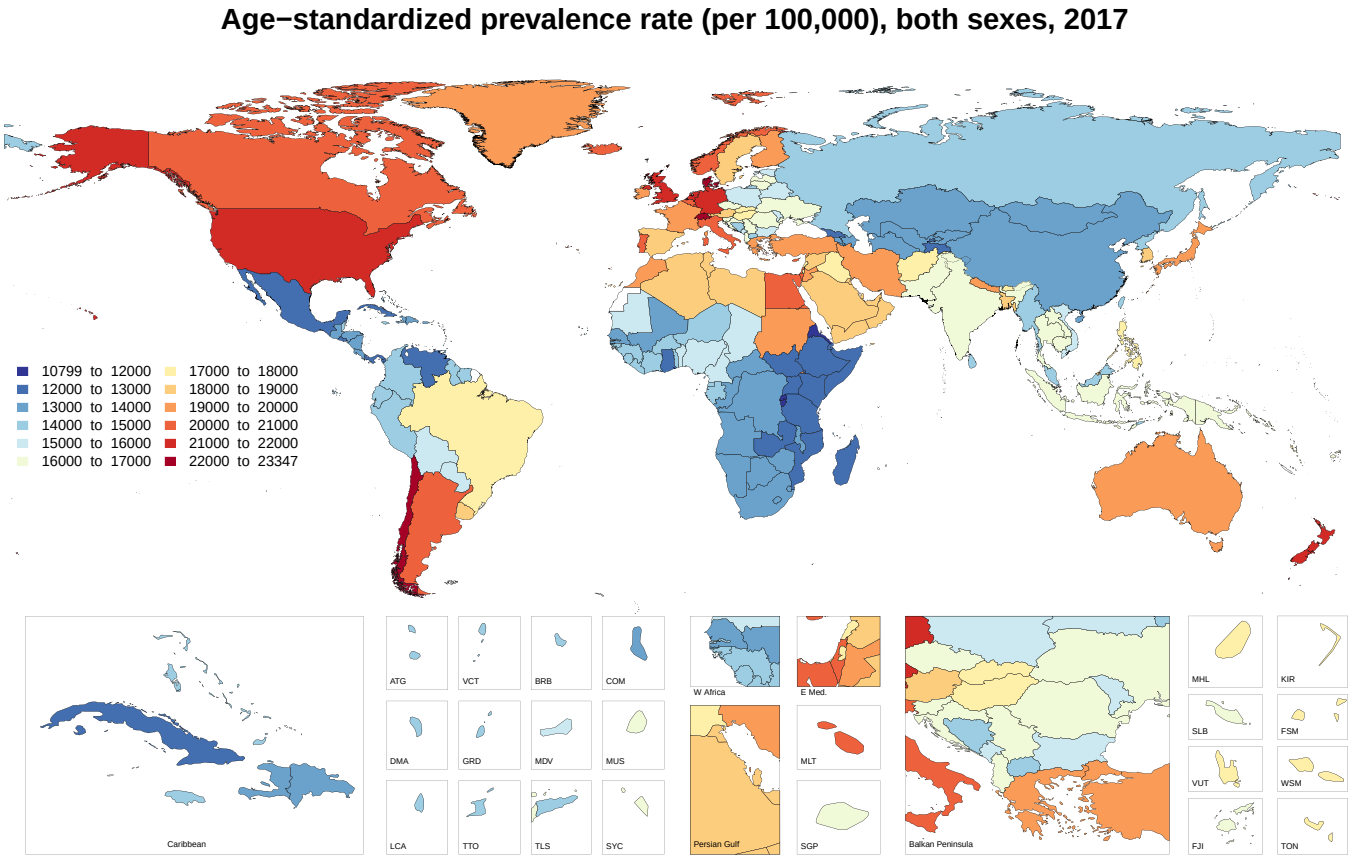

Figure 1. Age-standardized prevalence estimates of musculoskeletal disorders per 100,000 population in 2017, by country (generated from data available from http://ghdx.healthdata.org/gbd-results-tool). ATG = Antigua and Barbuda; VCT = Saint Vincent and the Grenadines; BRB = Barbados; COM = Comoros; DMA = Dominica; GRD = Grenada; MDV = Maldives; MUS = Mauritius; LCA = Saint Lucia; TTO = Trinidad and Tobago; TLS = Timor-Leste; SYC = Seychelles; E. Med = Eastern Mediterranean; MLT = Malta; SGP = Singapore; MHL = Marshall Islands; KIR = Kiribati; SLB = Solomon Islands; FSM = Federated States of Micronesia; VUT = Vanuatu; WSM = Samoa; FJI = Fiji; TON = Tonga.

UI 1,929.3, 3,501.1]), and Denmark (2,602.2 [95% UI 1,890, 3,449.4]), with the lowest found in Eritrea (1,169.3 [95% UI 862.6, 1,560.4]), Mexico (1,263.2 [95% UI 940.6, 1,662.8]), and Rwanda (1,265 [95% UI 921, 1,706.7]) (Supplementary Figure 10 and Supplementary Table 6, available on the *Arthritis & Rheumatology* website at http://onlinelibrary.wiley.com/doi/10.1002/art.41571/abstract).

The percentage change in age-standardized point prevalence estimates of musculoskeletal disorders between 1990 and 2017 differed substantially between countries. Chile (10.8% [95% UI 6.6, 15.4]), Benin (8.8% [95% UI 6.7, 11.1]), and El Salvador (8.5% [95% UI 5.5, 11.9]) showed the greatest increases during the measurement period. In contrast, Haiti (–7.0% [95% UI –11.5, –3.3]), Rwanda (–6.5% [95% UI –9.5, –3.2]), and Finland (–5.2% [95% UI –7.5, –2.7]) showed the largest decreases in age-standardized point prevalence of musculoskeletal disorders from 1990 (Supplementary Table 4). Ukraine (173.2% [95% UI 127.6, 233.4]), Armenia (133.6% [95% UI 73.4, 238]), and Guatemala (126.7% [95% UI 90.6, 177.2]) had the largest increases in age-standardized death rates from RA and other musculoskeletal disorders, while Spain (–75.4% [95% UI –77.6, –73.3]), Uruguay (–66.5% [95% UI –71.3, –60.9]), and Singapore (–66.2% [95% UI –70.5, –61.1]) had the largest decreases (Supplementary Table 5).

The percentage change in age-standardized DALY rates of musculoskeletal disorders also varied substantially between countries from 1990 to 2017. Chile (12.1% [95% UI 6.4, 18.6]), Paraguay (11.8% [95% UI 8.2, 15.3]), and Benin (10.5% [95% UI 7.5, 13.6]) showed the largest increases during the measurement period. In contrast, Finland (–9.1% [95% UI –12.2, –5.9]), the Russian Federation (–8.4% [95% UI –10.9, –5.7]), and Thailand (–8.2% [95% UI –11.6, –4.9]) showed the largest decreases (Supplementary Table 6).

Age- and sex-based patterns. The global point prevalence of musculoskeletal disorders in 2017 was higher among women than men and increased with age up to the oldest age group (95 years and older). Similarly, the number of prevalent cases increased with age and peaked at age 50–54 years for both men and women, followed by decreasing trends with increasing age (Figure 2). In 2017, the global death rate from RA and other musculoskeletal disorders was also reported to be higher in women and increased with age, particularly after

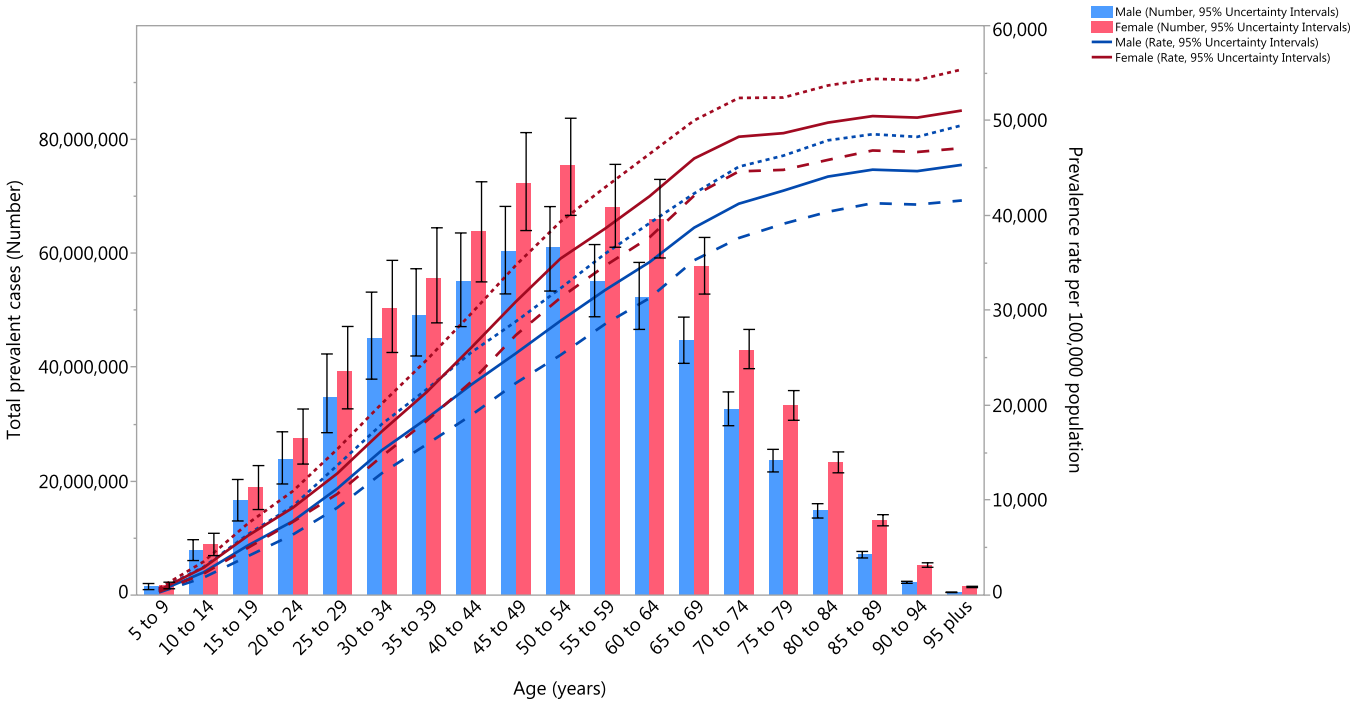

Figure 2. Global number of prevalent cases and prevalence estimates of musculoskeletal disorders per 100,000 population by age and sex, 2017 (generated from data available from http://ghdx.healthdata.org/gbd-results-tool). Dotted and broken lines indicate the upper and lower 95% uncertainty intervals, respectively. Color figure can be viewed in the online issue, which is available at http://onlinelibrary.wiley.com/doi/10.1002/art.41571/abstract.

the age of 60 years (Supplementary Figure 11, available on the *Arthritis & Rheumatology* website at http://onlinelibrary.wiley.com/doi/10.1002/art.41571/abstract). This corresponded to an increased number of deaths among women, reaching the highest level at 80–84 years of age and 75–79 years of age for women and men, respectively.

The global age-standardized DALY rate of musculoskeletal disorders in 2017 was also higher in women and peaked at 70–74 years of age and 80–84 years of age for women and men, respectively. In addition, the number of DALYs increased with age up to the 50–54 years and 45–49 years categories for women and men, respectively, and then decreased (Supplementary Figure 12, available on the *Arthritis & Rheumatology* website at http://onlinelibrary.wiley.com/doi/10.1002/art.41571/abstract).

Categories of musculoskeletal disorders. Globally, the proportion of prevalent cases due to categories of musculoskeletal disorders in 2017 was greatest for low back pain (36.8%), followed by other musculoskeletal disorders (21.5%), OA (19.3%), neck pain (18.4%), gout (2.6%), and RA (1.3%). These proportions did not change appreciably from 1990 (Figure 3).

Contributions of musculoskeletal disorder prevalent cases by region changed from 1990 to 2017. In 2017 the lowest and highest proportions of prevalent cases were as follows: for low back pain, lowest in East Asia (21.6%) and highest in Central Europe (59.7%); for other musculoskeletal disorders, lowest in Central Europe (0.5%) and highest in South Asia (35.8%); for OA, lowest in western sub-Saharan Africa (11.2%) and highest in high-income Asia Pacific (26.6%); for neck pain, lowest in Australasia (10.7%) and highest in East Asia (29.1%); for gout, lowest in tropical Latin America (1.5%) and highest in Australasia (5.8%); and for RA, lowest in Southeast Asia (0.5%) and highest in the Caribbean (2.2%) (Figure 3).

The prevalence of musculoskeletal disorders globally increased with age for both sexes in 2017. Specific musculoskeletal conditions peaked at different age groups in 2017 among both sexes: low back pain peaked in the age 85–89 years group, other musculoskeletal disorders in the age 65–69 years group, OA in the age 95 years and older group, neck pain in the age 70–74 years group, gout in the age 85–89 years group, and RA in the age 70–74 years group (Figure 4). The number of prevalent cases of musculoskeletal disorders in 2017 was highest in the age 50–54 years group, and low back pain, neck pain, and other musculoskeletal disorders had the 3 highest numbers of prevalent cases in that age group (Figure 4).

The death rate from RA and other musculoskeletal disorders generally increased with age and peaked in the oldest age group for both causes in 2017. The death rate from other musculoskeletal disorders was higher than that for RA in most of the age groups. The number of deaths was highest in the age 80–84 years group, with other musculoskeletal disorders having a slightly higher contribution (Supplementary Figure 13, available on the

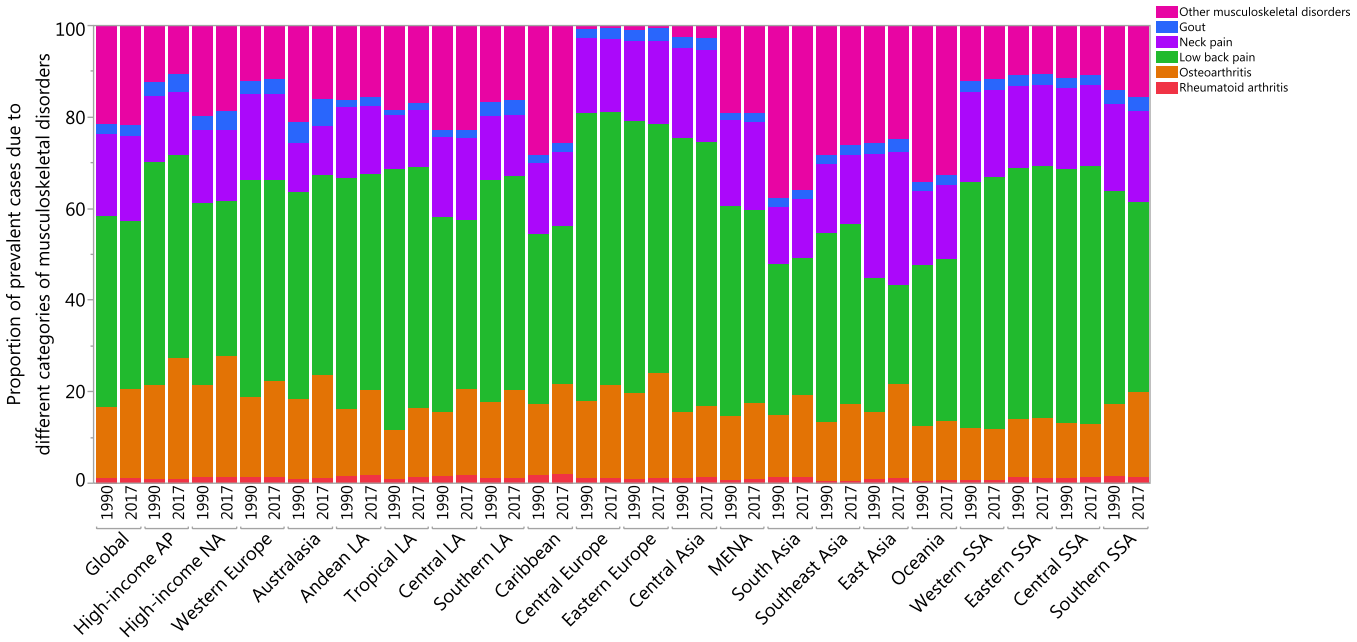

Figure 3. Proportion of prevalent cases according to category of musculoskeletal disorder for both sexes in 1990 and 2017 for 21 Global Burden of Disease regions (generated from data available from http://ghdx.healthdata.org/gbd-results-tool). AP = Asia Pacific; NA = North America; LA = Latin America; MENA = Middle East and North Africa; SSA = sub-Saharan Africa. Color figure can be viewed in the online issue, which is available at http://onlinelibrary.wiley.com/doi/10.1002/art.41571/abstract.

Arthritis & Rheumatology website at http://onlinelibrary.wiley.com/doi/10.1002/art.41571/abstract).

The DALY rate for different categories of musculoskeletal disorders generally increased with age for both sexes but peaked in different age groups in 2017. The DALY rate for low back pain was much higher than that for other causes and peaked in the age 80–84 years group. The DALY rate for neck pain and other musculoskeletal disorders peaked at age 70–74 years and age 65–69

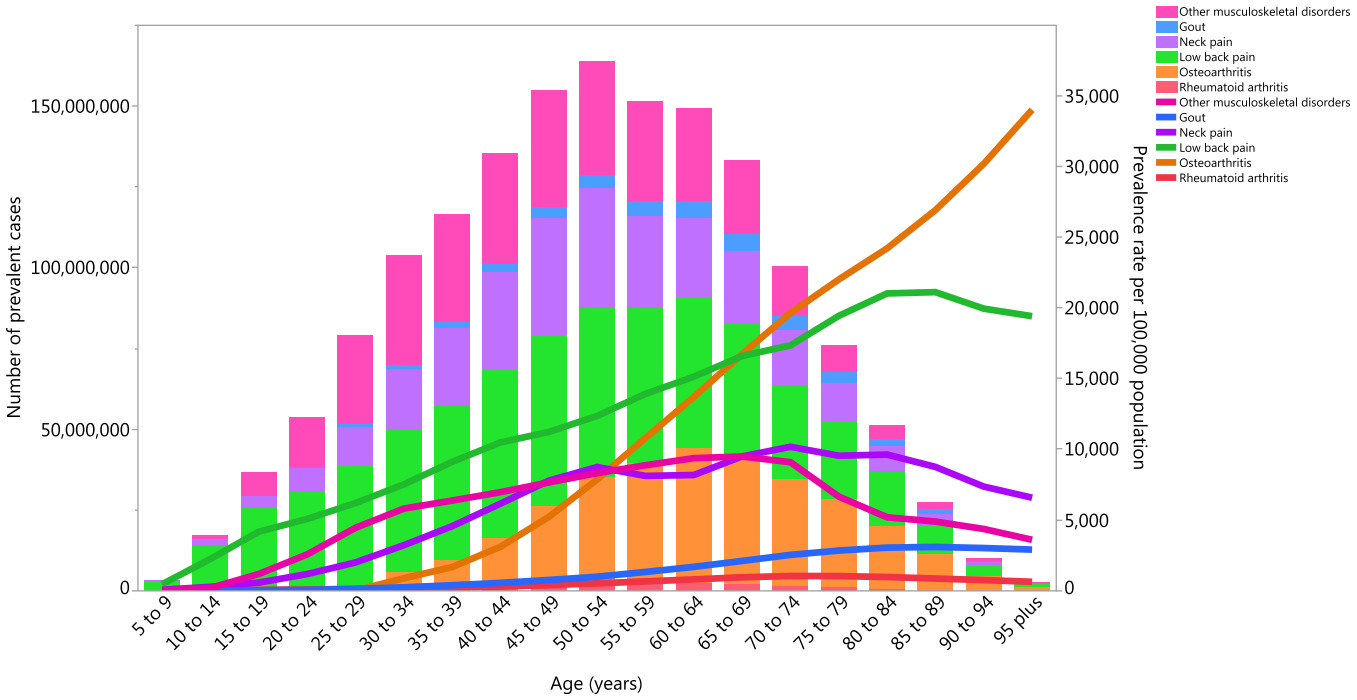

Figure 4. Global number of prevalent cases and prevalence estimates of categories of musculoskeletal disorders per 100,000 population by age, 2017 (generated from data available from http://ghdx.healthdata.org/gbd-results-tool). Color figure can be viewed in the online issue, which is available at http://onlinelibrary.wiley.com/doi/10.1002/art.41571/abstract.

years, respectively, followed by a decreasing trend. OA had an increasing trend, peaking in the oldest group such that it was the second leading cause of DALY across all 3 of the older age categories (85–89 years, 90–94 years, and 95 years and older). Although RA and gout did not contribute substantially compared to other causes, they were found to peak in the age 75–79 years and age 80–84 years groups, respectively (Supplementary Figure 14, available on the *Arthritis & Rheumatology* website at http://onlinelibrary.wiley.com/doi/10.1002/art.41571/abstract).

Age-standardized DALY rates were higher in women for all musculoskeletal disorder categories globally except for gout. The few exceptions where higher rates were reported for men included southern Latin America (gout and other musculoskeletal disorders), Eastern Europe (gout and OA), western sub-Saharan Africa (gout and low back pain), eastern sub-Saharan Africa (gout, low back pain, and other musculoskeletal disorders), central sub-Saharan Africa (gout and low back pain), and southern sub-Saharan Africa (gout, low back pain, and OA) (Supplementary Figure 15, available on the *Arthritis & Rheumatology* website at http://onlinelibrary.wiley.com/doi/10.1002/art.41571/abstract).

Burden of musculoskeletal disorders according to SDI. A positive association was observed between age-standardized DALY rate of musculoskeletal disorders and SDI at the global and regional levels from 1990 and 2017, such that the burden of musculoskeletal disorders increased with SDI (Figure 5). Although the observed global burden of musculoskeletal disorders is decreasing and reached a lower than expected burden based on SDI, some regions were found to have much higher than expected burdens (above the black solid line in Figure 5) over 28 years of observation. These regions included southern Latin America, North Africa and the Middle East, and tropical Latin America. In contrast, regions such as central Latin America, southern sub-Saharan Africa, and East Asia had a much lower than expected burden (below the solid black line in Figure 5) of musculoskeletal disorders between 1990 and 2017.

At the national level, a generally positive association was found between age-standardized DALY rates of musculoskeletal disorders and SDI for 195 countries in 2017 (Supplementary Figure 16, available on the *Arthritis & Rheumatology* website at http://onlinelibrary.wiley.com/doi/10.1002/art.41571/abstract). Countries such as Switzerland, Chile, Argentina, Iran, and Nepal had a higher than expected burden of musculoskeletal disorders based on the SDI in 2017. In contrast, Singapore, Puerto Rico, Mexico, and Eritrea had a lower than expected burden (Supplementary Figure 16).

DISCUSSION

This study provides up-to-date musculoskeletal disorder prevalence, death, and DALY counts between 1990 and 2017, in addition to age-standardized rates across regional and

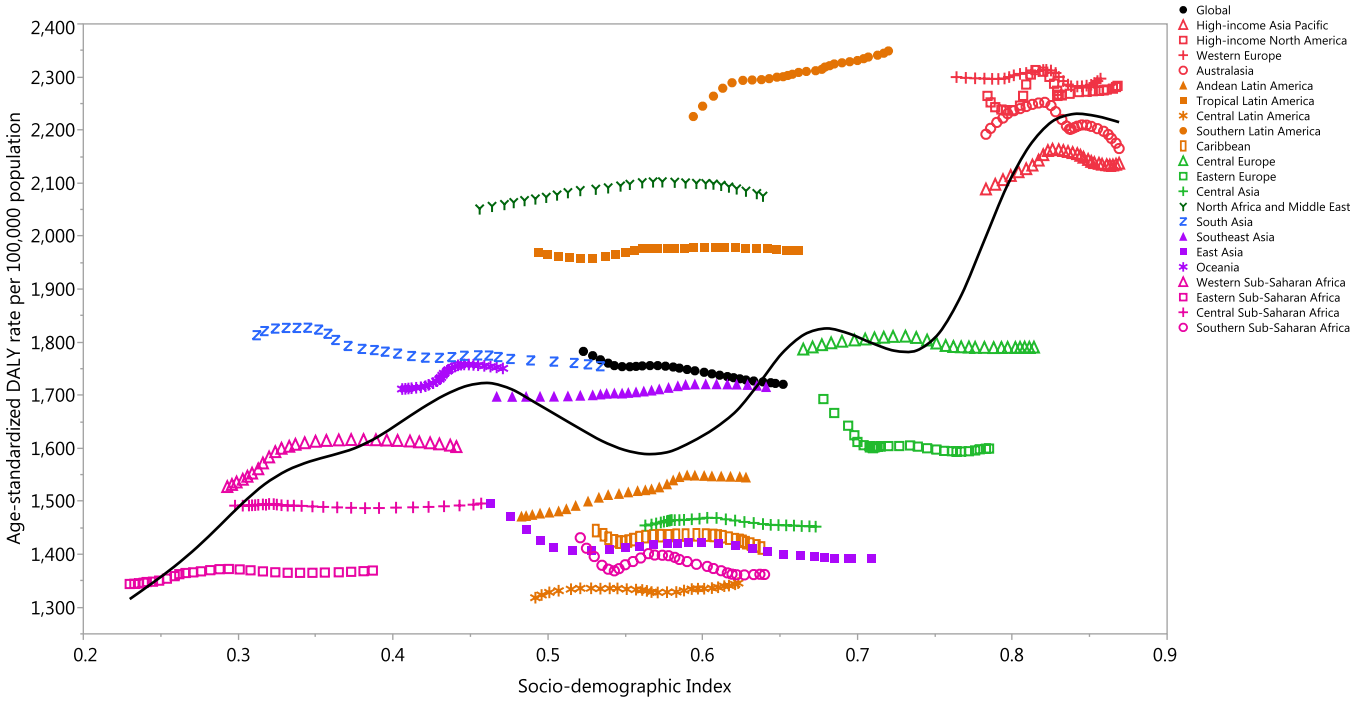

Figure 5. Age-standardized disability-adjusted life year (DALY) rates for musculoskeletal disorders for 21 Global Burden of Disease (GBD) regions according to Sociodemographic Index (SDI), 1990–2017 (generated from data available from http://ghdx.healthdata.org/gbd-results-tool). Black line indicates expected values in all locations based on SDI and disease rates. Twenty-eight points are plotted for each GBD region and show observed age-standardized DALY rates from 1990 to 2017 for that region. Color figure can be viewed in the online issue, which is available at http://onlinelibrary.wiley.com/doi/10.1002/art.41571/abstract.

national levels according to age, sex, SDI, and categories of musculoskeletal disorders as defined by the GBD project. These data were derived from publicly available GBD 2017 data (https://vizhub.healthdata.org/gbd-compare/ and http://ghdx.healthdata.org/gbd-results-tool) (21,22). In 2017, musculoskeletal disorders accounted for 1.3 billion prevalent cases, 121.3 thousand deaths (only attributable to RA and other musculoskeletal disorders), and 138.7 million DALYs.

Comparison with the GBD 2010 study is not possible as that study did not provide overall global or regional estimates of musculoskeletal disorders. Burden estimates in the present study also cannot be directly compared with other studies that have estimated the global burden of musculoskeletal disorders, due to differences in data sources and methodologies used, although some overall comparisons are possible. For example, a recent study of the worldwide burden of musculoskeletal disorders from 2000 to 2015 based on data extracted for 183 countries from the World Health Organization Global Health Estimates Database estimated that the number of DALYs attributable to musculoskeletal disorders increased from 80.2 million in 2000 to 107.9 million in 2015 (19). This rising trajectory is consistent with our finding of 138.7 million DALYs based on 2017 data.

Although the number of DALYs in our study was found to increase during the measurement period, a slightly decreasing trend in age-standardized DALY rate was observed during this period. Globally, our data indicate that the age-standardized prevalence and DALYs due to musculoskeletal disorders decreased by 1.6% and 3.5%, respectively, from 1990 to 2017. While this might appear to be at odds with the increase in overall DALYs, the number of DALYs is affected by population growth and an aging population and typically correlates with an increasing trend in disease burden; therefore, these results should be interpreted with caution.

Our data should also be considered in relation to the change in burden from other diseases. Based on the age-standardized DALY rate for both sexes, in 2017 musculoskeletal disorders ranked 5th highest compared to a ranking of 10th in 1990. This indicates that they continue to impose a considerable global burden, after cardiovascular diseases, maternal and neonatal disorders, cancer, and tuberculosis and respiratory infections and are now ranked higher compared to mental disorders, neurologic disorders, and chronic respiratory diseases (27). Another study also found an increasing trend in crude DALY rates of musculoskeletal disorders between 1990 and 2013 for the eastern Mediterranean region using GBD 2013 study data (28). However, these metrics may be misleading, since DALY rates are affected by population age structure, and percentage change in age-standardized rates were not used in that study (28).

The present study shows that the burden of musculoskeletal disorders in 2017 generally increased with age for both sexes and was more prevalent among women, which is consistent with previous studies (18,28). Although age- and sex-based patterns typically increased with age across all musculoskeletal categories, they peaked at different age groups. With the exception of gout, all remaining categories of musculoskeletal disorders were higher among women globally. These findings are also consistent with previous articles based on GBD 2010 data (7–10).

Positive associations between the burden of musculoskeletal disorders and development level were observed at both regional and national levels in our study, which is consistent with the findings of a previous study (19). Using the SDI, we reported the expected burden of disease across regions and countries that can be compared with corresponding observed values. This allows for a better judgment of health care system performance within regions and countries. For example, although Austria and Algeria have similar observed age-standardized DALY rates, the burden in Austria is lower than expected values, while this rate was higher than expected for Algeria, consistent with likely better health care system performance in Austria.

While musculoskeletal disorder experts have continued to highlight the high burden of musculoskeletal disorders (10,29,30), the lack of any significant observable decline in musculoskeletal burden suggests that there has been little concerted effort to address the problem. The present study shows that musculoskeletal disorders continue to impose a remarkable burden of disease on the world's population, with low back pain, neck pain, and OA contributing the largest burden. These conditions are very costly. For example, a recent study investigating US health care spending by payor and health condition found that among 154 conditions studied, low back pain and neck pain had the highest amount of health care spending (US$134.5 billion in 2016), while other musculoskeletal disorders accounted for the second highest amount (US$129.8 billion in 2016) (31).

Increasing population awareness about risk factors, consequences, and best evidence-informed care for these conditions needs to be better addressed in public and health policy. For some conditions such as low back pain, the rising burden is partly iatrogenic, with non–evidence-based care wasting valuable health care resources and contributing to harm (32). A call to action published in *The Lancet* in 2018 highlighted the need to address the rising global burden of low back pain and outlined a series of actions that are required to meet this challenge (33). As there are many shared commonalities between low back pain, neck pain, and OA, particularly with regard to biopsychosocial risk factors for disability, taking these actions is likely to reduce burden from these conditions as well.

There is an urgent need to identify strategies that have the greatest potential to decrease the societal burden of musculoskeletal disorders, and these are likely to vary by setting. Importantly, many of the most prevalent musculoskeletal disorders, such as low back pain, disproportionately affect those with lower socioeconomic status and education, widening social inequality (6). This is likely to be magnified in developing countries due to limitations in access to high-quality care, more informal employment,

nonexistent or poorly monitored occupational musculoskeletal health policies, and lack of social support systems.

Integrated strategies for addressing the burden of noncommunicable diseases including musculoskeletal disorders are now needed. In most countries these now far outweigh the burden due to communicable diseases, and maternal, neonatal, and nutritional disorders (16,27). Unfortunately, even among Organisation for Economic Co-operation and Development member states only half mention musculoskeletal health when describing integrated strategies for the prevention and management of noncommunicable diseases (34).

Promising solutions to address the burden of musculoskeletal disorders include a focus on implementation of best evidence-informed practice. This has been promoted by initiatives such as Choosing Wisely, which is clinician led and aims to reduce low-value practices by specialty area of practice, and Clinical Care Standards that outline the care that patients should expect to receive, but these approaches need more evaluation (35). In addition to public health and prevention strategies, other promising solutions that need to be properly evaluated include redesigning clinical pathways, integrating health and occupational care, and altering payment systems and legislation so that the right care is rewarded. Much also needs to be done to counter vested interests that are contributing to the burden by promoting the use of medicines and procedures such as opioids and unnecessary surgery that do more harm than good (36,37).

To our knowledge, this study is the most up-to-date reporting on the global burden of musculoskeletal disorders across different categories from 1990 to 2017. However, this study has some limitations. First, while the most prevalent musculoskeletal disorders are included as separate categories in GBD, some burdensome disorders such as shoulder pain, systemic lupus erythematosus, and scleroderma are not reported separately but are included in the other musculoskeletal disorders group together with less prevalent conditions such as osteomyelitis. To date, only OA of the hip and knee are included in the estimates for OA and as such are likely to be an underestimate of the true burden of OA. However, other sites of OA, such as hand OA, are likely to be included in future GBD studies. In addition, some musculoskeletal conditions such as fractures are not included at all, while low bone mineral density, a risk factor for fractures, is also not an attributable risk factor within the GBD musculoskeletal disorders category.

It is also likely that overall deaths attributable to musculoskeletal disorders have been underestimated, since only deaths due to RA and other musculoskeletal disorders were included in the GBD 2017 study modeling process. For example, deaths are known to occur from untreated gout due to renal failure and from opioid use and surgical complications arising from treatment of chronic back pain and OA. Data sparsity, especially in developing countries, is of particular concern in the GBD study overall, and this was also observed as a problem in the estimation of the burden from musculoskeletal disorders. Estimates in these countries are mainly produced by modeled data in DISMOD-MR 2.1 and are reported with wide UIs. Therefore, these data need to be interpreted with caution.

The global burden of musculoskeletal disorders is significant, and there is notable inter-country variation, with some countries having twice the burden of other countries. Increasing population awareness regarding risk factors, consequences, and evidence-informed treatment strategies for musculoskeletal disorders, particularly for low back and neck pain and OA, is needed, with a focus on older, and especially female, populations. In addition, provision of safe workplaces would also likely contribute to a substantial decline in the impact of these musculoskeletal disorders. It will be important to monitor trends over time to more accurately inform required changes to policy and practice. Standardizing methods for collecting data on the prevalence and impact of musculoskeletal disorders across the world as well as collecting data where none currently exist will be crucial to these efforts and would enable better measurement and benchmarking of our progress.

ACKNOWLEDGMENTS

We would like to thank the staff of the Institute for Health Metrics and Evaluation and its collaborators who prepared these publicly available data. Also, we would like to thank the Social Determinants of Health Research Center of Shahid Beheshti University of Medical Sciences for their support.

AUTHOR CONTRIBUTIONS

All authors were involved in drafting the article or revising it critically for important intellectual content, and all authors approved the final version to be published. Dr. Buchbinder had full access to all of the data in the study and takes responsibility for the integrity of the data and the accuracy of the data analysis.

Study conception and design. Safiri, Kolahi, March, Buchbinder.

Acquisition of data. Safiri, Kolahi, Almasi-Hashiani, Ashrafi-Asgarabad, Sepidarkish.

Analysis and interpretation of data. Safiri, Cross, Hill, Smith, Carson-Chahhoud, Mansournia, Kaufman, Shakouri, Hoy, Woolf, March, Collins, Buchbinder.

REFERENCES

1. Beard JR, Bloom DE. Towards a comprehensive public health response to population ageing. Lancet 2015;385:658–61.
2. Briggs AM, Cross MJ, Hoy DG, Sanchez-Riera L, Blyth FM, Woolf AD, et al. Musculoskeletal health conditions represent a global threat to healthy aging: a report for the 2015 World Health Organization world report on ageing and health. Gerontologist 2016;56 Suppl:S243–55.
3. Woolf AD, Åkesson K. Understanding the burden of musculoskeletal conditions [editorial]. BMJ 2001;322:7294.
4. Fatoye F. The economic impact of musculoskeletal pain [editorial]. Pain Rehabilitation 2018;2018:3–4.
5. Lewis R, Álvarez CB, Rayman M, Lanham-New S, Woolf A, Mobasheri A. Strategies for optimising musculoskeletal health in the 21st century [review]. BMC Musculoskelet Disord 2019;20:164.
6. Hartvigsen J, Hancock MJ, Kongsted A, Louw Q, Ferreira ML, Genevay S, et al. What low back pain is and why we need to pay attention. Lancet 2018;391:2356–67.

7. Cross M, Smith E, Hoy D, Nolte S, Ackerman I, Fransen M, et al. The global burden of hip and knee osteoarthritis: estimates from the global burden of disease 2010 study. Ann Rheum Dis 2014;73:1323–30.
8. Smith E, Hoy D, Cross M, Merriman TR, Vos T, Buchbinder R, et al. The global burden of gout: estimates from the Global Burden of Disease 2010 study. Ann Rheum Dis 2014;73:1470–6.
9. Hoy D, March L, Woolf A, Blyth F, Brooks P, Smith E, et al. The global burden of neck pain: estimates from the global burden of disease 2010 study. Ann Rheum Dis 2014;73:1309–15.
10. Hoy D, March L, Brooks P, Blyth F, Woolf A, Bain C, et al. The global burden of low back pain: estimates from the Global Burden of Disease 2010 study. Ann Rheum Dis 2014;73:968–74.
11. Safiri S, Kolahi AA, Hoy D, Smith E, Bettampadi D, Mansournia MA, et al. Global, regional and national burden of rheumatoid arthritis 1990–2017: a systematic analysis of the Global Burden of Disease study 2017. Ann Rheum Dis 2019;78:1463–71.
12. Safiri S, Kolahi AA, Hoy D, Smith E, Bettampadi D, Mansournia MA, et al. Global, regional and national burden of osteoarthritis 1990–2017: a systematic analysis of the Global Burden of Disease Study 2017. Ann Rheum Dis 2020;79:819–28.
13. Safiri S, Kolahi AA, Hoy D, Buchbinder R, Mansournia MA, Bettampadi D, et al. Global, regional, and national burden of neck pain in the general population, 1990–2017: systematic analysis of the Global Burden of Disease Study 2017. BMJ 2020;368:m791.
14. Safiri S, Kolahi AA, Cross M, Carson-Chahhoud K, Hoy D, Almasi-Hashiani A, et al. Prevalence, incidence and years lived with disability due to gout and its attributable risk factors for 195 countries and territories 1990–2017: a systematic analysis of the Global Burden of Disease Study 2017. Arthritis Rheumatol 2020;72:1916–27.
15. Safiri S, Kolahi AA, Cross M, Carson-Chahhoud K, Almasi-Hashiani A, Kaufman J, et al. Global, regional, and national burden of other musculoskeletal disorders 1990–2017: results from the Global Burden of Disease Study 2017. Rheumatology (Oxford) 2021;60:855–65.
16. James SL, Abate D, Abate KH, Abay SM, Abbafati C, Abbasi N, et al. Global, regional, and national incidence, prevalence, and years lived with disability for 354 diseases and injuries for 195 countries and territories, 1990–2017: a systematic analysis for the Global Burden of Disease Study 2017. Lancet 2018;392:1789–858.
17. Roth GA, Abate D, Abate KH, Abay SM, Abbafati C, Abbasi N, et al. Global, regional, and national age-sex-specific mortality for 282 causes of death in 195 countries and territories, 1980–2017: a systematic analysis for the Global Burden of Disease Study 2017. Lancet 2018;392:1736–88.
18. Woolf AD, Pfleger B. Burden of major musculoskeletal conditions. Bull World Health Organ 2003;81:646–56.
19. Sebbag E, Felten R, Sagez F, Sibilia J, Devilliers H, Arnaud L. The world-wide burden of musculoskeletal diseases: a systematic analysis of the World Health Organization Burden of Diseases Database. Ann Rheum Dis 2019;78:844–8.
20. Stanaway JD, Afshin A, Gakidou E, Lim SS, Abate D, Abate KH, et al. Global, regional, and national comparative risk assessment of 84 behavioural, environmental and occupational, and metabolic risks or clusters of risks for 195 countries and territories, 1990–2017: a systematic analysis for the Global Burden of Disease Study 2017. Lancet 2018;392:1923–94.
21. GBD Compare Viz Hub. Institute for Health Metrics and Evaluation. URL: https://vizhub.healthdata.org/gbd-compare/.
22. Institute for Health Metrics and Evaluation. GBD results tool. URL: http://ghdx.healthdata.org/gbd-results-tool.
23. Foreman KJ, Lozano R, Lopez AD, Murray CJ. Modeling causes of death: an integrated approach using CODEm. Popul Health Metr 2012;10:1.
24. Thompson SG, Higgins JP. How should meta-regression analyses be undertaken and interpreted? Stat Med 2002;21:1559–73.
25. Salomon JA, Haagsma JA, Davis A, de Noordhout CM, Polinder S, Havelaar AH, et al. Disability weights for the Global Burden of Disease 2013 study. Lancet Glob Health 2015;3:e712–23.
26. Wang Y. Smoothing splines: methods and applications. New York: Chapman and Hall/CRC; 2011.
27. Kyu HH, Abate D, Abate KH, Abay SM, Abbafati C, Abbasi N, et al. Global, regional, and national disability-adjusted life-years (DALYs) for 359 diseases and injuries and healthy life expectancy (HALE) for 195 countries and territories, 1990–2017: a systematic analysis for the Global Burden of Disease Study 2017. Lancet 2018;392:1859–922.
28. Moradi-Lakeh M, Forouzanfar MH, Vollset SE, El Bcheraoui C, Daoud F, Afshin A, et al. Burden of musculoskeletal disorders in the Eastern Mediterranean Region, 1990–2013: findings from the Global Burden of Disease Study 2013. Ann Rheum Dis 2017;76:1365–73.
29. Woolf AD, Erwin J, March L. The need to address the burden of musculoskeletal conditions. Best Pract Res Clin Rheumatol 2012;26:183–224.
30. Mody GM, Brooks PM. Improving musculoskeletal health: global issues. Best Pract Res Clin Rheumatol 2012;26:237–49.
31. Dieleman JL, Cao J, Chapin A, Chen C, Li Z, Liu A, et al. US health care spending by payer and health condition, 1996–2016. JAMA 2020;323:863–84.
32. Foster NE, Anema JR, Cherkin D, Chou R, Cohen SP, Gross DP, et al. Prevention and treatment of low back pain: evidence, challenges, and promising directions. Lancet 2018;391:2368–83.
33. Buchbinder R, van Tulder M, Öberg B, Costa LM, Woolf A, Schoene M, et al. Low back pain: a call for action. Lancet 2018;391:2384–8.
34. Briggs AM, Persaud JG, Deverell ML, Bunzli S, Tampin B, Sumi Y, et al. Integrated prevention and management of non-communicable diseases, including musculoskeletal health: a systematic policy analysis among OECD countries. BMJ Glob Health 2019;4:e001806.
35. Levinson W, Kallewaard M, Bhatia RS, Wolfson D, Shortt S, Kerr EA. 'Choosing Wisely': a growing international campaign. BMJ Qual Saf 2015;24:167–74.
36. Ashaye T, Hounsome N, Carnes D, Taylor SJ, Homer K, Eldridge S, et al. Opioid prescribing for chronic musculoskeletal pain in UK primary care: results from a cohort analysis of the COPERS trial. BMJ Open 2018;8:e019491.
37. Maher CG, O'Keeffe M, Buchbinder R, Harris IA. Musculoskeletal healthcare: have we over-egged the pudding? [editorial]. Int J Rheum Dis 2019;22:1957–60.

Arthritis & Rheumatology
Vol. 73, No. 4, April 2021, pp 715–720

American College of Rheumatology
Empowering Rheumatology Professionals

LETTERS

DOI 10.1002/art.41588

Different control populations may lead to different understanding of hydroxychloroquine blood levels as a risk factor for retinopathy: comment on the article by Petri et al

To the Editor:

We read with great interest the article by Petri et al on their study of the association between hydroxychloroquine (HCQ) blood levels and HCQ retinopathy in systemic lupus erythematosus (SLE) (1). Retinopathy occurred in 4.3% of 537 patients with SLE. Both mean and maximum HCQ blood levels predicted HCQ retinopathy ($P = 0.0124$ and $P = 0.034$, respectively). In contrast, in a recent case–control study (2) that included 23 SLE patients with HCQ retinopathy and 547 controls, we found no association between HCQ blood levels and HCQ retinopathy, with a median HCQ blood level of 944 ng/ml in the retinopathy group versus 849 ng/ml in the control group ($P = 0.46$).

Understanding the differences between these studies is important, as the contrasting outcomes may be attributable to treatment adherence and the chosen control groups. By definition, patients with confirmed HCQ retinopathy have taken their HCQ and, in our experience, are usually among those with higher treatment adherence. Their HCQ levels are bound to be higher than those in a cohort of patients with variable adherence, especially if the cohort includes patients with a high degree of nonadherence (3,4).

In our study, control patients were from the PLUS study, which excluded patients who reported having been nonadherent with their HCQ regimen. Their HCQ blood levels would thus inevitably be higher than those in unselected patients (such as those in the study by Petri et al), and closer than those in patients with retinopathy.

Comparing median HCQ levels between studies is difficult because of factors influencing HCQ blood levels, such as HCQ dose or kidney insufficiency. However, since the most nonadherent patients are at risk of flare (4)—but probably protected against long-term side effects—it would be interesting to know if Petri and colleagues' conclusions would be similar if such patients are excluded.

These differences aside, we fully agree that measurements of HCQ levels are an important tool in the management of SLE, as a marker and predictor of flares (5), and are helpful for monitoring and improving medication adherence (4). Higher levels (e.g., >1,500 ng/ml) most likely indicate that patients are particularly adherent and at risk of retinopathy. Because lower levels (~1,000 ng/ml) have been proven effective (5), we also suggest reducing the dose of HCQ.

Tiphaine Lenfant, MD
Centre de Référence des Maladies Auto-Immunes et Systémiques Rares d'Ile de France
Cochin Hospital AP-HP
Gaëlle Leroux, MD
Centre de Référence des Maladies Auto-Immunes et Systémiques Rares d'Ile-de-France
Pitié-Salpetrière University Hospital AP-HP
Nathalie Costedoat-Chalumeau, MD, PhD
Centre de Référence des Maladies Auto-Immunes et Systémiques Rares d'Ile de France
Cochin Hospital AP-HP
Université de Paris
and INSERM Unité 1153 Center for Epidemiology and Statistics
Paris, France

1. Petri M, Elkhalifa M, Li J, Magder LS, Goldman DW. Hydroxychloroquine blood levels predict hydroxychloroquine retinopathy. Arthritis Rheumatol 2020;72:448–53.
2. Lenfant T, Salah S, Leroux G, Bousquet E, Le Guern V, Chasset F, et al. Risk factors for hydroxychloroquine retinopathy in systemic lupus erythematosus: a case-control study with hydroxychloroquine blood-level analysis. Rheumatology (Oxford) 2020;59:3807–16.
3. Feldman CH, Collins J, Zhang Z, Subramanian SV, Solomon DH, Kawachi I, et al. Dynamic patterns and predictors of hydroxychloroquine nonadherence among Medicaid beneficiaries with systemic lupus erythematosus. Semin Arthritis Rheum 2018;48:205–13.
4. Costedoat-Chalumeau N, Amoura Z, Hulot JS, Aymard G, Leroux G, Marra D, et al. Very low blood hydroxychloroquine concentration as an objective marker of poor adherence to treatment of systemic lupus erythematosus. Ann Rheum Dis 2007;66:821–4.
5. Costedoat-Chalumeau N, Amoura Z, Hulot JS, Hammoud HA, Aymard G, Cacoub P, et al. Low blood concentration of hydroxychloroquine is a marker for and predictor of disease exacerbations in patients with systemic lupus erythematosus. Arthritis Rheum 2006;54:3284–90.

DOI 10.1002/art.41578

Lenabasum for systemic sclerosis—are cannabinoids the missing link? Comment on the article by Spiera et al

To the Editor:

We read with great interest the article by Spiera et al on their trial of lenabasum in systemic sclerosis (SSc) (1). After many recent studies that failed to show promising results, we are excited to come across a positive drug trial in SSc.

However, the systemic manifestations in the subjects i.e., pulmonary manifestations such as pulmonary hypertension

and interstitial lung disease, deserve a more detailed analysis, including their response to treatment. Second, efficacy in the group with disease duration >3 years needs to be described separately, because lenabasum may not be as effective once fibrosis has already developed. Moreover, although 2 different dose regimens were used in the study, comparison between the 2 is not reported. As the gut is the most commonly involved organ system in SSc, clinical trials of these agents should include analysis of the effects on gastrointestinal (GI) system manifestations and GI toxicity. While the Combined Response Index in diffuse cutaneous Systemic Sclerosis (CRISS) score has demonstrated validity as a composite outcome measure in SSc, it may not adequately reflect changes in individual organ systems.

The fact that there were no major adverse events (AEs) with lenabasum makes this drug discovery even more exciting. However, among subjects in the lenabasum group, there were 10 nervous system disorder AEs and 3 psychiatric disorder AEs. It would be important to know the details of these. Also, there was 1 neoplasm AE in the lenabasum group, the details of which were not provided. Long-term follow-up will be needed to evaluate the safety of lenabasum.

Mood-altering effects of cannabinoids are well known. The improvements in patient-reported outcomes and Health Assessment Questionnaire disability index scores may well be due to the effect on mood and feeling of general well-being, rather than the effect of the drug on disease pathology.

Most patients in the study were receiving concurrent immunosuppressant treatment, with 63% of subjects in the lenabasum group receiving mycophenolic acid. The efficacy of lenabasum should be assessed independent of concomitant treatment.

Recently presented results of the open-label extension indicate a remarkable improvement in CRISS scores, with mild-to-moderate adverse effects in 97% of lenabasum-treated subjects (2). We eagerly await the details of these results and the phase III trial. Future studies should also include patients with limited SSc. Investigations of lenabasum in other autoimmune and fibrosing diseases will also be of interest.

Sakshi Mittal, MD
Shefali Sharma, MD
Post Graduate Institute of Medical Education and Research
Chandigarh, India

1. Spiera R, Hummers L, Chung L, Frech TM, Domsic R, Hsu V, et al. Safety and efficacy of lenabasum in a phase II, randomized, placebo-controlled trial in adults with systemic sclerosis. Arthritis Rheumatol 2020;72:1350–60.
2. Spiera R, Hummers L, Chung L, Frech T, Domsic R, Hsu V, et al. Safety and efficacy of lenabasum in an open-label extension of a phase 2 study in diffuse cutaneous systemic sclerosis subjects (DCSSC) [abstract]. Ann Rheum Dis 2019;78 Suppl 2:245.

DOI 10.1002/art.41579

Reply

To the Editor:

We appreciate Drs. Mittal and Sharma's interest in the results of our phase II study of lenabasum for the treatment of diffuse cutaneous SSc (dcSSc). The small sample size and specified set of efficacy analyses done in this study preclude separate subset analyses of the course of interstitial lung disease (ILD), pulmonary hypertension (PH), GI involvement, or all efficacy analyses by disease duration or background immunosuppressant use, beyond 16 weeks.

The initial 4 weeks of dosing were used to explore dose-dependency of AEs (no dose-dependency was observed in the range tested) and measure plasma concentrations of lenabasum at 5-mg and 20-mg doses (levels were as expected from phase II data in healthy volunteers). There was no intent to separately assess efficacy in the 3 groups of subjects (n = 9 each) who received lenabasum doses of 5 mg once daily, 20 mg once daily, or 20 mg twice daily because these groups were quite small and exposure to different doses of lenabasum was limited to the first 4 weeks of the study. Thereafter, all subjects who received lenabasum in the first 4 weeks received the same lenabasum dose of 20 mg twice daily for the next 8 weeks, and efficacy results in the combined group of all subjects who received lenabasum are compared with those in subjects who received placebo throughout. Use of background immunosuppressants (yes/no) was tested as a fixed effect in the mixed-effects model repeated-measures statistical analysis of the primary efficacy outcome and did not make a significant contribution to the model.

GI disorder AEs occurred in 20% of subjects in the placebo arm and 22% of subjects in the lenabasum arm. Only nausea occurred in >2 subjects (2 placebo-treated subjects and 1 lenabasum-treated subject). Psychiatric disorder AEs occurred in 13% of subjects in the placebo arm and 11% of subjects (n = 3) in the lenabasum arm. Only insomnia occurred in >1 subject (1 lenabasum-treated and 1 placebo-treated subject). Of subjects who received lenabasum and had psychiatric AEs, 1 with a history of anxiety experienced worsening anxiety and paranoia, 1 with a history of anxiety and depression experienced dysphoria and insomnia, and 1 with a history of anxiety and depression felt "sluggish." Nervous system disorder AEs occurred in 10 subjects (37%) in the lenabasum arm and 4 subjects (27%) in the placebo arm. Of the 10 lenabasum-treated subjects, 6 had dizziness/lightheadedness and 3 of the 6 had additional nervous system AEs (difficulty focusing in 1 and headache in 2). One subject each had headache, tingling, numbness in the arm, and "mental fog," the latter occurring in a subject with depression at

baseline. One subject had a benign thyroid nodule. It is important to note that there were no serious or severe AEs, infections, or laboratory test abnormalities that were attributed to lenabasum treatment.

No data from this study suggest that improvements in patient-reported outcomes reflected direct effects of lenabasum on mood. In lenabasum-treated subjects, there was a complete absence of psychiatric AEs of euphoria or similar terms and no significant change or differences from placebo-treated subjects in patient-reported outcomes on a drug effects questionnaire (Addiction Research Center Inventory-Marijuana questionnaire) that assesses somatic experiences associated with marijuana use.

Testing for overall improvement in SSc, such as this phase II study, would become especially difficult if both subjects with dcSSc and subjects with limited cutaneous SSc were included in the same study because inclusion of both groups would increase subject heterogeneity. Inclusion of both groups may be more appropriate in studies of a specific disease manifestation, such as digital ulcers, PH, or ILD.

Robert Spiera, MD
Weill Cornell Medicine
New York, NY
Lorinda Chung, MD
Stanford University School of Medicine
Stanford, CA
and Palo Alto VA Health Care System
Palo Alto, CA
Tracy Frech, MD
University of Utah
and Salt Lake City VA Health Care System
Salt Lake City, UT
Robyn Domsic, MD
University of Pittsburgh School of Medicine
Pittsburgh, PA
Vivien Hsu, MD
Rutgers Robert Wood Johnson Medical School
New Brunswick, NJ
Daniel E. Furst, MD
University of California, Los Angeles
Robert Simms, MD
Boston University School of Medicine
Boston, MA
Maureen Mayes, MD
University of Texas Health Science Center
at Houston
Viktor Martyanov, PhD
Michael L. Whitfield, PhD
Geisel School of Medicine at Dartmouth
Hanover, NH
Nancy Dgetluck, MS
Quinn Dinh, MD
Barbara White, MD
Corbus Pharmaceuticals
Norwood, MA

DOI 10.1002/art.41582

Should the biopsychosocial model be considered in systemic autoimmune diseases? Comment on the article by Posada et al

To the Editor:

We read with interest the article by Posada et al (1) on their study evaluating the therapeutic effects of RSLV-132 (a new RNase compound) in patients with primary Sjögren's syndrome (SS). At first glance, one may be surprised by their enthusiastic conclusion despite their observing a biologic effect opposite of what was expected, namely, increased expression of interferon (IFN)–stimulated genes (ISG), while primary SS is considered an acquired interferonopathy. However, therapeutic trials also present a unique opportunity to learn about the pathogenesis of such complex conditions. Indeed, this study showed a significant improvement of fatigue (measured by various validated scales) in treated patients, which, surprisingly, correlated with the increased expression of ISG.

We wish to put this puzzling observation into perspective by considering results from other studies assessing fatigue or related quality of life (QoL) parameters, IFN biology (cytokines and/or ISG expression), or disease activity in primary SS or systemic lupus erythematosus (SLE). In primary SS, previous studies have shown that higher levels of proinflammatory cytokines were associated with lower patient-reported fatigue (2). Analysis of ISG expression through a modular framework, as used by Posada and colleagues (1), did not identify any correlation between the IFN modular score and fatigue in a primary SS data set (3). Finally, in another study, patients with primary SS who exhibited an IFN signature reported a better QoL than those who did not (4). Importantly, in the latter study, patients treated with hydroxychloroquine displayed a decreased IFN signature with no benefit on fatigue (4).

The same paradoxical picture was observed in SLE patients, who also display a strong IFN signature. Studies have demonstrated that type I IFN is not correlated with fatigue in SLE patients, at the cytokine and gene expression levels (5,6). In a recent study, our group observed that some components of the Short Form 36 health survey (7) (social functioning and mental health) were even positively correlated with the IFN modular score (3). Recent clinical studies confirmed that both QoL (8) and severe fatigue (9) were correlated not with disease activity but rather with anxiety and depression (9). Finally, in a therapeutic trial, hydroxychloroquine blood levels were not correlated with QoL (10).

In the study by Posada et al (1), while the small number of treated patients and short follow-up (1) preclude any conclusions on the safety of RSLV-132, and while this drug would probably not have been proposed for primary SS if the increase in ISG expression had been anticipated, the paradoxical improvement of fatigue

in treated patients with increased ISG expression warrants attention. Historically, the induction of inflammation to relieve psychological symptoms has been used before, by Julius Wagner-Jauregg and his "fever therapy," which earned him the Nobel Prize (11). Collectively, these data provide evidence for considering the biopsychosocial model, which assumes a balance between somatic (i.e., immunologically driven) and psychic (i.e., psychic fatigue) symptoms, in patients with complex systemic autoimmune diseases. If confirmed, this "psychosomatic balance" should be considered in the design and end points of clinical trials and in the daily therapeutic objectives set with patients with primary SS and SLE.

Laurent Chiche, MD, PhD
Hôpital Européen
Noémie Jourde-Chiche, MD, PhD
Centre de Nephrologie et Transplantation Renale
Hôpital de la Conception
AP-HM
Marseillle, France
Divi Cornec, MD, PhD
CHU de Brest
Brest, France

1. Posada J, Valadkhan S, Burge D, Davies K, Tarn J, Casement J, et al. Improvement of severe fatigue following nuclease therapy in patients with primary Sjögren's syndrome: a randomized clinical trial. Arthritis Rheumatol 2021;73:143–50.
2. Howard Tripp N, Tarn J, Natasari A, Gillespie C, Mitchell S, Hackett KL, et al. Fatigue in primary Sjögren's syndrome is associated with lower levels of proinflammatory cytokines. RMD Open 2016;2:e000282.
3. Seguier J, Jouve E, Bobot M, Whalen E, Dussol B, Gentile S, et al. Paradoxical association between blood modular interferon signatures and quality of life in patients with systemic lupus erythematosus. Rheumatology (Oxford) 2020;59:1975–83.
4. Bodewes IL, Gottenberg JE, van Helden-Meeuwsen CG, Mariette X, Versnel MA. Hydroxychloroquine treatment downregulates systemic interferon activation in primary Sjögren's syndrome in the JOQUER randomized trial. Rheumatology (Oxford) 2020;59:107–11.
5. Omdal R, Mellgren SI, Koldingsnes W, Jacobsen EA, Husby G. Fatigue in patients with systemic lupus erythematosus: lack of associations to serum cytokines, antiphospholipid antibodies, or other disease characteristics. J Rheumatol 2002;29:482–6.
6. Kellner ES, Lee PY, Li Y, Switanek J, Zhuang H, Segal MS, et al. Endogenous type-I interferon activity is not associated with depression or fatigue in systemic lupus erythematosus. J Neuroimmunol 2010;223:13–9.
7. Ware JE Jr, Sherbourne CD. The MOS 36-item Short-Form health survey (SF-36). I. Conceptual framework and item selection. Med Care 1992;30:473–83.
8. Gu M, Cheng Q, Wang X, Yuan F, Sam NB, Pan H, et al. The impact of SLE on health-related quality of life assessed with SF-36: a systemic review and meta-analysis. Lupus 2019;28:371–82.
9. Arnaud L, Gavand PE, Voll R, Schwarting A, Maurier F, Blaison G, et al. Predictors of fatigue and severe fatigue in a large international cohort of patients with systemic lupus erythematosus and a systematic review of the literature. Rheumatology (Oxford) 2019;58:987–96.
10. Jolly M, Galicier L, Aumaître O, Francès C, Le Guern V, Lioté F, et al. Quality of life in systemic lupus erythematosus: description in a cohort of French patients and association with blood hydroxychloroquine levels. Lupus 2016;25:735–40.
11. Wagner-Jauregg J. Fever therapy: its rationale in diseases of the nervous system. Edinb Med J 1936;43:1–12.

DOI 10.1002/art.41581

Reply

To the Editor:

We thank Dr. Chiche et al for their interest in our article. SS patients consistently report profound, debilitating fatigue as the single symptom that most severely decreases their QoL. Although this information should inform drug development efforts, the voice of the patient has not been well represented in SS clinical trials. The primary end points in many of the clinical studies conducted over the past decade have relied on the European League Against Rheumatism Sjögren's Syndrome Disease Activity Index, which does not measure fatigue or ocular and/or oral dryness, the chief symptoms of concern to these patients. How the patient is feeling in response to an experimental medicine should be a central focus of drug development efforts in SS. At the 2016 International Symposium on Sjögren's Syndrome, a senior US Food and Drug Administration representative discussed the agency's commitment to patient-focused drug development as mandated under the Prescription Drug User Fee Act, and encouraged sponsors to consider patient input during the drug development process. Although sponsors have historically viewed the use of patient questionnaires in drug development with skepticism, a gradual but encouraging movement toward the use of patient-reported outcome measures is underway, with several current SS clinical trials utilizing patient-reported outcome instruments as the primary end point. For example, Tarn et al recently reported using patient-reported outcome measures to stratify SS patients into 4 distinct pathobiologic subtypes (1), further underscoring the value of patient-reported outcome instruments in the assessment of SS patients.

Our clinical trial demonstrated the ability of RSLV-132, a catalytically active RNase enzyme, to induce a significant improvement in profound fatigue in our cohort of SS patients using 3 different, independent, validated patient-reported outcome instruments, which was further corroborated by the finding of associated improvement in neurocognitive performance. Interestingly, the impact of the drug on the IFN pathway was in stark contrast to our original hypothesis that digesting RNA complexed with anti-Ro autoantibodies would decrease Toll-like receptor 7 activation and the production of IFN (as measured using surrogate IFN-inducible genes). Instead, an increase in selected well-characterized IFN-inducible genes was observed to correlate with an improvement in fatigue, challenging the presumed role of IFN in mediating fatigue in SS, as Chiche and colleagues suggest. To our knowledge, our trial is the first interventional study in SS that demonstrates the ability of a therapeutic agent to induce a significant improvement in fatigue coupled with an increase in selected IFN-inducible genes, raising the possibility that IFN activation may be beneficial in combating SS symptoms rather than causing them. Although these findings are very intriguing and may shed new light on the role of IFN in SS, the small size of our patient population requires

replication in larger clinical studies. We will examine the pharmacodynamic mechanism of RSLV-132 as it relates to the IFN pathway in upcoming larger SS clinical trials.

Supported by Resolve Therapeutics, LLC. Dr. Posada owns stock or stock options in Resolve Therapeutics. Dr. Fisher has received consulting fees from Novartis, Roche, Bristol Myers Squibb, and Servier (less than $10,000 each), and from Galapagos (more than $10,000). Dr. Ng has received consulting fees from GlaxoSmithKline, Novartis, AbbVie, MedImmune, Bristol Myers Squibb, Sanofi, and UCB (less than $10,000 each).

James Posada, PhD
Resolve Therapeutics
St. Petersburg, FL
Benjamin A. Fisher, MD
NIHR Birmingham Biomedical Research Centre
University Hospitals Birmingham NHS Foundation Trust and University of Birmingham
Birmingham, UK
Wan-Fai Ng, PhD
Newcastle University
and NIHR Newcastle Biomedical Research Centre
Newcastle upon Tyne, UK

1. Tarn JR, Howard-Tripp N, Lendrem DW, Mariette X, Saraux A, Devauchelle-Pensec V, et al. Symptom-based stratification of patients with primary Sjögren's syndrome: multi-dimensional characterisation of international observational cohorts and reanalyses of randomised clinical trials. Lancet Rheumatol 2019;1:E85–94.

DOI 10.1002/art.41590

Recognition of rare, atypical manifestations is important for diagnosis and management of antineutrophil cytoplasmic antibody–associated vasculitis: comment on the article by Delaval et al

To the Editor:

I read with great interest the article by Delaval et al reporting on their study of the largest case series of temporal arteritis (TA) in antineutrophil cytoplasmic antibody (ANCA)–associated vasculitides (AAVs), including clinical, serologic, and histologic manifestations (1). Recent progress in the understanding of AAV has revealed that it can present rare, atypical manifestations, such as isolated dacryosialadenitis, isolated retroperitoneal fibrosis, and isolated hypertrophic pachymeningitis (2–4). Therefore, in such cases, it is important to recognize AAV as one of the differential diagnoses and to conduct histologic examination and ANCA testing for appropriate disease management. I would like to ask some questions for further clarification.

First, how many patients had "isolated" TA without any other AAV-associated organ manifestations at initial diagnosis and during follow-up? Among those, how many patients were diagnosed as having AAV on the basis of histologic findings and/or ANCA testing? It is important for physicians to recognize the possibility of "isolated" TA in patients with AAV and to know how diagnoses could be made.

Second, Delaval and colleagues noted that small branch vasculitis was a characteristic finding on temporal artery biopsy (TAB) in TA-AAV but not in giant cell arteritis (GCA). They reported that 23% of patients with TA-AAV were positive for small branch vasculitis, compared with 0% of patients with GCA. This result is difficult to interpret because in several previous studies, it was reported that small branch vasculitis and vasa vasorum vasculitis were histologic findings in TA-GCA (5).

Third, Delaval et al assessed only mononuclear cell infiltrates on TAB, not polymorphonuclear cell infiltrates. However, neutrophils are one of the pathogenic drivers of AAV, and the neutrophil infiltrates are frequently observed in the affected lesions in AAV (6). On the other hand, neutrophils are generally rare in temporal artery lesions in GCA (7). In this regard, it would be helpful to know whether neutrophilic inflammation was observed in temporal artery lesions from patients with AAV.

Mitsuhiro Akiyama, MD, PhD
Keio University School of Medicine
Tokyo, Japan

1. Delaval L, Samson M, Schein F, Agard C, Tréfond L, Deroux A, et al. Temporal arteritis revealing antineutrophil cytoplasmic antibody–associated vasculitides: case–control study. Arthritis Rheumatol 2021; 73:286–94.
2. Akiyama M, Kaneko Y, Takeuchi T. Eosinophilic granulomatosis with polyangiitis can manifest lacrimal and salivary glands swelling by granulomatous inflammation: a potential mimicker of IgG4-related disease [letter]. Ann Rheum Dis 2020. E-pub ahead of print.
3. Akiyama M, Kaneko Y, Takeuchi T. Characteristics and prognosis of ANCA-positive retroperitoneal fibrosis: a systematic literature review. Autoimmun Rev 2020;19:102642.
4. Matsumoto K, Akiyama M, Kajio N, Otomo K, Suzuki K, Nishina N, et al. Adolescent PR3-ANCA-positive hypertrophic pachymeningitis: a case report and review of the literature. Medicine (Baltimore) 2018;97:e0521.
5. Restuccia G, Cavazza A, Boiardi L, Pipitone N, Macchioni P, Bajocchi G, et al. Small-vessel vasculitis surrounding an uninflamed temporal artery and isolated vasa vasorum vasculitis of the temporal artery: two subsets of giant cell arteritis. Arthritis Rheum 2012;64: 549–56.
6. Akiyama M, Zeisbrich M, Ibrahim N, Ohtsuki S, Berry GJ, Hwang PH, et al. Neutrophil extracellular traps induce tissue-invasive monocytes in granulomatosis with polyangiitis. Front Immunol 2019;10:2617.
7. Weyand CM, Watanabe R, Zhang H, Akiyama M, Berry GJ, Goronzy JJ. Cytokines, growth factors and proteases in medium and large vessel vasculitis [review]. Clin Immunol 2019;206:33–41.

DOI 10.1002/art.41592

Reply

To the Editor:

We thank Dr. Akiyama for his interest in our study of TA revealing AAV (TA-AAV) and the importance of recognizing AAV as one of the differential diagnoses in certain situations. We appreciate the opportunity to address some questions that Dr. Akiyama raises.

First, 17 patients had "isolated" TA without any other feature suggestive of AAV-associated organ manifestations. Among them, all but 1 patient were positive for ANCAs, 7 had atypical histologic findings for GCA on TAB, and 5 had histologic evidence on tissue biopsy other than TAB.

Second, Dr. Akiyama suggests that small branch vasculitis and vasa vasorum vasculitis are consistent with the diagnosis of GCA (1). However, these data remain controversial in many different studies (2,3). In our opinion, these findings remain atypical for classic GCA.

Third, regarding characterization of inflammatory infiltrates in GCA versus TA-AAV (i.e., mononuclear cells versus neutrophils), unfortunately we were not able to perform a centralized review to address this question. However, we agree that it would be an interesting question for future study.

Laure Delaval, MD
Benjamin Terrier, MD, PhD
Hôpital Cochin
National Referral Center for Systemic and Autoimmune Diseases
Université de Paris
Paris, France

1. Restuccia G, Cavazza A, Boiardi L, Pipitone N, Macchioni P, Bajocchi G, et al. Small-vessel vasculitis surrounding an uninflamed temporal artery and isolated vasa vasorum vasculitis of the temporal artery: two subsets of giant cell arteritis. Arthritis Rheum 2012;64:549–56.
2. Corcoran GM, Prayson RA, Herzog KM. The significance of perivascular inflammation in the absence of arteritis in temporal artery biopsy specimens. Am J Clin Pathol 2001;115:342–7.
3. Chakrabarty A, Franks AJ. Temporal artery biopsy: is there any value in examining biopsies at multiple levels? J Clin Pathol 2000;53:131–6.

Erratum

DOI 10.1002/art.41681

In the article by Bernstein et al in the November 2020 issue of *Arthritis & Rheumatology* (Performance Characteristics of Pulmonary Function Tests for the Detection of Interstitial Lung Disease in Adults With Early Diffuse Cutaneous Systemic Sclerosis [pages 1892–1896]), the fourth author, Flavia V. Castelino, MD, was inadvertently not listed in the byline or elsewhere. Dr. Castelino is affiliated with Massachusetts General Hospital in Boston. She has received consulting fees from Boehringer Ingelheim (<$10,000). She made substantial contributions to the acquisition of data for the study, was involved in drafting the article and/or revising it critically for important intellectual content, and provided final approval of the version of the article to be published.

We regret the error.

Arthritis & Rheumatology
Vol. 73, No. 4, April 2021, pp e13–e29
DOI 10.1002/art.41616

American College of Rheumatology
Empowering Rheumatology Professionals

American College of Rheumatology Clinical Guidance for Multisystem Inflammatory Syndrome in Children Associated With SARS–CoV-2 and Hyperinflammation in Pediatric COVID-19: Version 2

Lauren A. Henderson,[1] Scott W. Canna,[2] Kevin G. Friedman,[1] Mark Gorelik,[3] Sivia K. Lapidus,[4] Hamid Bassiri,[5] Edward M. Behrens,[5] Anne Ferris,[6] Kate F. Kernan,[7] Grant S. Schulert,[8] Philip Seo,[9] Mary Beth F. Son,[1] Adriana H. Tremoulet,[10] Rae S. M. Yeung,[11] Amy S. Mudano,[12] Amy S. Turner,[13] David R. Karp,[14] and Jay J. Mehta[5]

Due to the rapidly expanding information and evolving evidence related to COVID-19, which may lead to modification of some guidance statements over time, it is anticipated that updated versions of this article will be published, with the version number included in the title. Readers should ensure that they are consulting the most current version.

Guidance developed and/or endorsed by the American College of Rheumatology (ACR) is intended to inform particular patterns of practice and not to dictate the care of a particular patient. The ACR considers adherence to this guidance to be voluntary, with the ultimate determination regarding its application to be made by the physician in light of each patient's individual circumstances. Guidance statements are intended to promote beneficial or desirable outcomes but cannot guarantee any specific outcome. Guidance developed or endorsed by the ACR is subject to periodic revision as warranted by the evolution of medical knowledge, technology, and practice.

The American College of Rheumatology is an independent, professional medical and scientific society which does not guarantee, warrant, or endorse any commercial product or service.

Objective. To provide guidance on the management of Multisystem Inflammatory Syndrome in Children (MIS-C), a condition characterized by fever, inflammation, and multiorgan dysfunction that manifests late in the course of severe acute respiratory syndrome coronavirus 2 (SARS–CoV-2) infection. Recommendations are also provided for children with hyperinflammation during coronavirus disease 2019 (COVID-19), the acute, infectious phase of SARS–CoV-2 infection.

Methods. The Task Force was composed of 9 pediatric rheumatologists and 2 adult rheumatologists, 2 pediatric cardiologists, 2 pediatric infectious disease specialists, and 1 pediatric critical care physician. Preliminary statements addressing clinical questions related to MIS-C and hyperinflammation in COVID-19 were developed based on evidence reports. Consensus was built through a modified Delphi process that involved anonymous voting and webinar discussion. A 9-point scale was used to determine the appropriateness of each statement (median scores of 1–3 for inappropriate, 4–6 for uncertain, and 7–9 for appropriate). Consensus was rated as low, moderate, or high based on dispersion of the votes. Approved guidance statements were those that were classified as appropriate with moderate or high levels of consensus, which were prespecified before voting.

Results. The first version of the guidance was approved in June 2020, and consisted of 40 final guidance statements accompanied by a flow diagram depicting the diagnostic pathway for MIS-C. The document was revised in November 2020, and a new flow diagram with recommendations for initial immunomodulatory treatment of MIS-C was added.

Conclusion. Our understanding of SARS–CoV-2–related syndromes in the pediatric population continues to evolve. This guidance document reflects currently available evidence coupled with expert opinion, and will be revised as further evidence becomes available.

INTRODUCTION

Since its initial description in December 2019 in Wuhan China, coronavirus disease 2019 (COVID-19), caused by infection with severe acute respiratory syndrome coronavirus 2 (SARS–CoV-2), has rapidly evolved into a worldwide pandemic affecting millions of lives (1). Unlike adults, the vast majority of children with COVID-19 have mild symptoms. However, there are children who have significant respiratory disease, and some children may develop a hyperinflammatory response similar to what has been observed in adults with COVID-19. Furthermore, in late April 2020, reports emerged of children with a different clinical syndrome resembling Kawasaki Disease (KD) and toxic shock syndrome; these patients frequently had evidence of prior exposure to SARS–CoV-2 (2,3). Subsequent to these initial reports from Italy and the United Kingdom, multiple case series from Europe and the United States have surfaced describing a similar phenomenon (4–10). While this constellation of symptoms has been given many names, for the purposes of this discussion we refer to it as multisystem inflammatory syndrome in children (MIS-C).

For a number of reasons, there is an urgent need to provide guidance to healthcare providers evaluating patients in whom MIS-C is a diagnostic consideration. These reasons include the fact that 1) there are variable case definitions for MIS-C, 2) the clinical description of MIS-C is limited to case series, 3) clinical features of MIS-C may also be seen in other types of infections and malignant entities and in other rheumatic diseases in childhood, 4) suggested treatment strategies have relied on extrapolation from other inflammatory or rheumatic conditions with similar clinical presentations, and 5) myocardial dysfunction may present insidiously but is a major source of morbidity and mortality in MIS-C. In addition, pediatric rheumatologists are often asked to recommend immunomodulatory therapy for patients developing hyperinflammation as a result of acute SARS–CoV-2 infection.

Therefore, the American College of Rheumatology (ACR) convened the MIS-C and COVID-19–Related Hyperinflammation Task Force on May 22, 2020, which was charged by ACR leadership to provide guidance to clinicians in the evaluation and management of MIS-C and COVID-19–related hyperinflammatory syndromes in children. Clinical guidance generated from this effort is intended to aid in the care of individual patients, but it is not meant to supplant clinical decision-making. Modifications to treatment plans, particularly in patients with complex conditions, are highly disease-, patient-, geography-, and time-specific, and therefore must be individualized as part of a shared decision-making process.

METHODS

Task force. Panelists were selected by the Task Force leadership (LAH and JJM) based on their clinical expertise in rheumatology, infectious diseases, cardiology, cytokine storm–related syndromes, and KD, as well as their experience in managing MIS-C and hyperinflammation in acute SARS–CoV-2 infection. The multidisciplinary Task Force was composed of clinicians from the United States and Canada and included 9 pediatric rheumatologists, 2 adult rheumatologists, 2 pediatric cardiologists, 2 pediatric infectious disease specialists, and 1 pediatric critical care physician. All individuals who were approached to develop this guidance agreed to participate.

Initial guidance. Prior to the first meeting, Task Force members were subdivided into 4 work groups to address the following clinical topics related to MIS-C and hyperinflammation in COVID-19: 1) diagnostic evaluation of MIS-C (led by SKL); 2) cardiac management of MIS-C (led by KGF); 3) treatment of MIS-C (led by MG); and 4) management of hyperinflammation in COVID-19 (led by SWC). During the first webinar on May 22, 2020, participants agreed with the importance of addressing these 4 overarching topics and the structure of the work groups. The first webinar was used to confirm the target audience for the guidance, which focuses on clinicians in North America managing

Supported by the American College of Rheumatology.

[1]Lauren A. Henderson, MD, MMSc, Kevin G. Friedman, MD, Mary Beth F. Son, MD: Boston Children's Hospital and Harvard Medical School, Boston, Massachusetts; [2]Scott W. Canna, MD: UPMC Children's Hospital of Pittsburgh and University of Pittsburgh, Pittsburgh, Pennsylvania; [3]Mark Gorelik, MD: Morgan Stanley Children's Hospital and Columbia University, New York, New York; [4]Sivia K. Lapidus, MD: Joseph M. Sanzari Children's Hospital at Hackensack University Medical Center and Hackensack Meridian School of Medicine, Hackensack, New Jersey; [5]Hamid Bassiri, MD, PhD, Edward M. Behrens, MD, Jay J. Mehta, MD: Children's Hospital of Philadelphia and University of Pennsylvania Perelman School of Medicine; [6]Anne Ferris, MBBS: Columbia University Irving Medical Center, New York, New York; [7]Kate F. Kernan, MD: University of Pittsburgh School of Medicine, Pittsburgh, Pennsylvania; [8]Grant S. Schulert, MD: Cincinnati Children's Hospital Medical Center and University of Cincinnati College of Medicine, Cincinnati, Ohio; [9]Philip Seo, MD, MHS: Johns Hopkins University School of Medicine, Baltimore, Maryland; [10]Adriana H. Tremoulet, MD, MAS: University of California San Diego and Rady Children's Hospital, San Diego, California; [11]Rae S. M. Yeung, MD, PhD: The Hospital for Sick Children and University of Toronto, Toronto, Ontario, Canada; [12]Amy S. Mudano, MPH: University of Alabama at Birmingham; [13]Amy S. Turner: American College of Rheumatology, Atlanta, Georgia; [14]David R. Karp, MD, PhD: University of Texas Southwestern Medical Center, Dallas.

Dr. Henderson has received consulting fees from Sobi (less than $10,000) and research support from the Childhood Arthritis and Rheumatology Research Alliance. Dr. Canna has received research support from AB2 Bio and IMMvention Therapeutix. Dr. Bassiri owns stock or stock options in CSL Behring. Dr. Schulert has received consulting fees from Novartis and Sobi (less than $10,000 each). Drs. Son and Mehta have received salary support from the Childhood Arthritis and Rheumatology Research Alliance. Dr. Yeung has received consulting fees from Novartis and Eli Lilly (less than $10,000 each). No other disclosures relevant to this article were reported.

Address correspondence to Lauren A. Henderson, MD, MMSc, Karp Family Research Building, 10th Floor, 1 Blackfan Circle, Boston, MA 02115. Email: Lauren.Henderson@childrens.harvard.edu.

Submitted for publication November 23, 2020; accepted in revised form December 3, 2020.

inflammatory syndromes in children related to recent or concurrent infections with SARS–CoV-2. Notably, the Task Force deliberately did not attempt to create a new case definition for MIS-C, as several already exist (8–10) (Table 1). Instead, the Task Force elected to leverage consensus building to identify the most appropriate diagnostic and therapeutic steps that providers should consider at the present time. All panelists agreed to develop consensus through a modified Delphi process, which involved 2 rounds of asynchronous, anonymous voting and 2 webinars to discuss voting results.

Evidence review. From May 22 to May 29, 2020, the work groups developed preliminary recommendation statements within their assigned topic, based on expert opinion and evidence reviewed from publications listed in PubMed, scientific briefings from the World Health Organization, health alerts from the Centers of Disease Control and Prevention, and guidance provided by the Royal College of Paediatrics and Child Health. Each work group generated an evidence report supporting the recommendations, which was shared with the entire Task Force.

Voting. *Round 1.* The Task Force voted virtually and anonymously using the RAND/University of California at Los Angeles (UCLA) Appropriateness Method (11). A 9-point scale was used by panelists to rate the appropriateness of each of the statements. A score of 9 was considered to be the highest level of appropriateness, while a score of 1 indicated that the statement was entirely inappropriate. Prior to voting, median scores of 1–3 were defined as inappropriate, 4–6 as uncertain, and 7–9 as appropriate. Consensus was prespecified as high if all 16 votes coalesced within the same tertile, while low consensus was recognized when voting was dispersed widely along the 9-point scale (with ≥5 votes in the 1–3 score range and ≥5 votes in the 7–9 score range). Moderate consensus

Table 1. Case definitions of MIS-C*

Criteria	RCPCH†	CDC	WHO‡
Age	All children (age not defined)	<21 years	0–19 years
Fever	Persistent fever (≥38.5°C)	Temperature ≥38.0°C for ≥24 hours *or* subjective fever for ≥24 hours	Fever for ≥3 days
Clinical symptoms	Both of the following: 1. single or multiorgan dysfunction; *and* 2. additional features	Both of the following: 1. severe illness (hospitalized); *and* 2. ≥2 organ systems involved	At least 2 of the following: 1. rash, conjunctivitis, and mucocutaneous inflammation; 2. hypotension or shock; 3. cardiac involvement; 4. coagulopathy; 5. acute GI symptoms
Inflammation	All 3 of the following: 1. neutrophilia; *and* 2. increased CRP; *and* 3. lymphopenia	Laboratory evidence of inflammation including, but not limited to, 1 or more of the following: 1. ↑CRP; 2. ↑ESR; 3. ↑fibrinogen; 4. ↑procalcitonin; 5. ↑D-dimer; 6. ↑ferritin; 7. ↑LDH; 8. ↑IL-6; 9. neutrophilia; 10. lymphopenia; 11. hypoalbuminemia	Elevated inflammation markers, including any of the following: 1. ↑ESR; 2. ↑CRP; 3. ↑procalcitonin
Link to SARS–CoV-2	Positive or negative by PCR	Current or recent findings of the following: 1. positive by PCR; 2. positive by serology; 3. positive by antigen test; *or* 4. COVID-19 exposure within prior 4 weeks	Evidence of COVID-19 by the following: 1. positive by PCR; 2. positive by antigen test; 3. positive by serology; *or* 4. likely COVID-19 contact
Exclusion	Other infections	No alternative diagnosis	No obvious microbial cause

* Case definitions of multisystem inflammatory syndrome in children (MIS-C) are adapted from recommendations from the World Health Organization (WHO) (8) and Centers for Disease Control and Prevention (CDC) (10) for MIS-C, as well as the Royal College of Paediatrics and Child Health (RCPCH) for pediatric inflammatory multisystem syndrome temporally associated with severe acute respiratory syndrome coronavirus 2 (SARS–Cov-2) (9). For laboratory parameters, ↑ indicates elevated levels. GI = gastrointestinal; CRP = C-reactive protein; ESR = erythrocyte sedimentation rate; LDH = lactate dehydrogenase; IL-6 = interleukin-6; PCR = polymerase chain reaction; COVID-19 = coronavirus disease 2019.

† In the RCPCH case definition, additional features include abdominal pain, confusion, conjunctivitis, cough, diarrhea, headache, lymphadenopathy, mucous membrane changes, neck swelling, rash, respiratory symptoms, sore throat, swollen hands and feet, syncope, and vomiting.

‡ In the WHO case definition, cardiac involvement is defined as the presence of myocardial dysfunction, pericarditis, valvulitis, or coronary abnormalities (including findings on echocardiogram or elevated levels of troponin/N-terminal pro–B-type natriuretic peptide).

encompassed all other scenarios. The votes of each Task Force member were counted equally and tallied. The results of the initial voting were distributed to the Task Force and reviewed during a 90-minute webinar on June 4, 2020. Statements that were rated as uncertain (median score 4–6) and/or characterized by moderate or low consensus were addressed first. The panelists were then encouraged to discuss the remaining statements.

Round 2. Input from the initial voting and discussion was incorporated (by LAH and JJM) into the draft guidance statements, and the document was redistributed to the entire Task Force for a second round of voting. Voting in this phase was conducted in the same manner as described above, and results were reviewed at a third webinar on June 10, 2020. Guidance statements that earned a median score of 7–9 with moderate or high levels of consensus were approved by the panel.

Guidance approval. Following the final webinar, approved statements were refined and, in some instances, combined to reduce redundancy. A preliminary guidance document was generated, and the entire Task Force was given an opportunity to review and edit the document. Approval was obtained from each panelist on June 14, 2020 and by the ACR Board of Directors on June 17, 2020 (12). After further review, the authors decided to include measurement of C-reactive protein (CRP) levels in the laboratory evaluation of hyperinflammation in severe COVID-19 (Table 7) and the entire Task Force then re-voted on the guidance statements and approved the modifications to this recommendation statement.

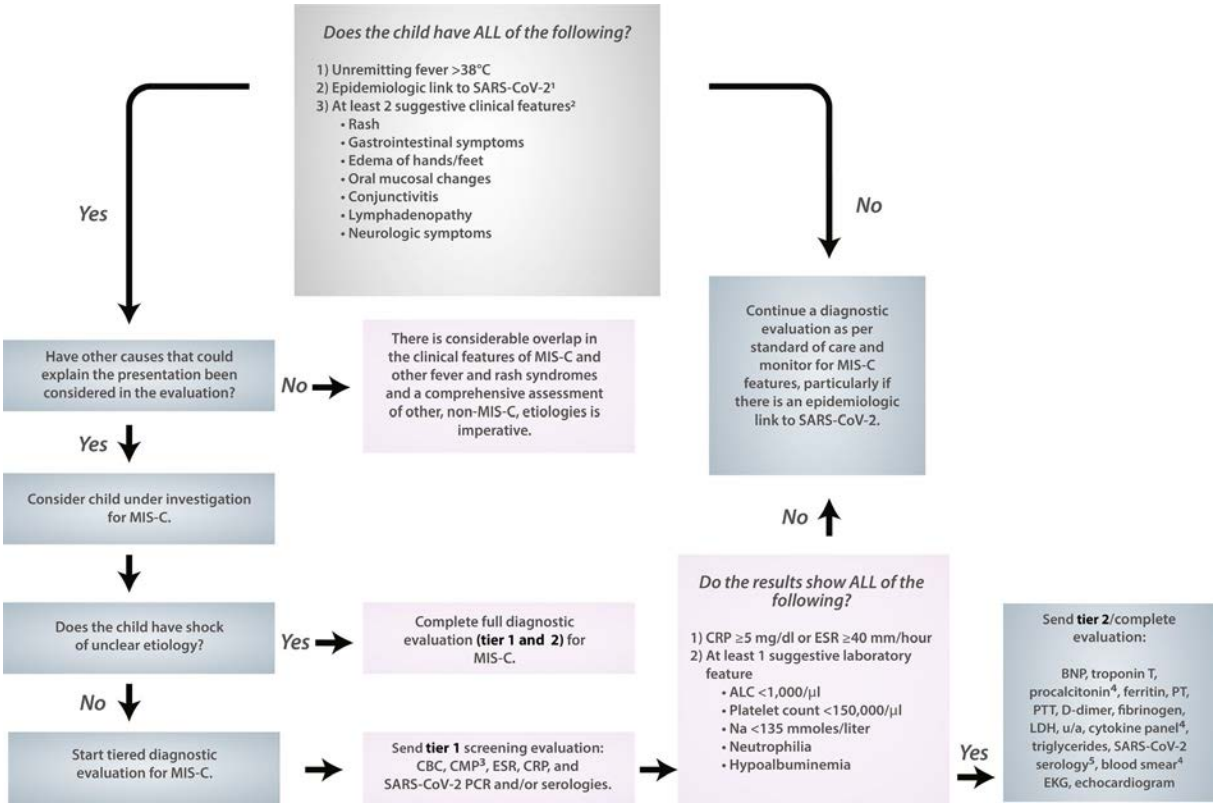

Figure 1. Diagnostic pathway for multisystem inflammatory syndrome in children (MIS-C). Moderate-to-high consensus was reached by the Task Force in the development of this diagnostic pathway for MIS-C associated with severe acute respiratory syndrome coronavirus 2 (SARS–CoV-2). [1]An epidemiologic link to SARS–CoV-2 infection is defined as a child with any of the following criteria: positive for SARS–CoV-2 by polymerase chain reaction (PCR), positive for SARS–CoV-2 by serology, preceding illness resembling coronavirus disease 2019 (COVID-19), or close contact with an individual with confirmed or suspected COVID-19 in the past 4 weeks. [2]Suggestive clinical features include rash (polymorphic, maculopapular, or petechial, but not vesicular), gastrointestinal symptoms (diarrhea, abdominal pain, or vomiting), oral mucosal changes (red and/or cracked lips, strawberry tongue, or erythema of the oropharyngeal mucosa), conjunctivitis (bilateral conjunctival infection without exudate), and neurologic symptoms (altered mental status, encephalopathy, focal neurologic deficits, meningismus, or papilledema). [3]The complete metabolic panel (CMP) includes measurement of sodium, potassium, carbon dioxide, chloride, blood urea nitrogen, creatinine, glucose, calcium, albumin, total protein, aspartate aminotransferase, alanine aminotransferase, alkaline phosphatase, and bilirubin. [4]Procalcitonin, cytokine panel, and blood smear test results should be sent, if available. [5]Serologic test results should be sent if not sent in tier 1 evaluation, and if possible, SARS–CoV-2 IgG, IgM, and IgA test results should be sent. CRP = C-reactive protein; ESR = erythrocyte sedimentation rate; ALC = absolute lymphocyte count; CBC = complete blood cell count; BNP = B-type natriuretic peptide; PT = prothrombin time; PTT = partial thromboplastin time; LDH = lactate dehydrogenase; u/a = urinalysis; EKG = electrocardiogram.

Figure 2. Algorithm for initial immunomodulatory treatment of multisystem inflammatory syndrome in children (MIS-C). Moderate-to-high consensus was reached by the Task Force in the development of this treatment algorithm for MIS-C associated with severe acute respiratory syndrome coronavirus 2. [1]Intravenous immunoglobulin (IVIG) dosing is 2 gm/kg based on ideal body weight. Cardiac function and fluid status should be assessed before IVIG is given. In some patients with cardiac dysfunction, IVIG may be given in divided doses (1 gm/kg daily over 2 days). [2]Methylprednisolone or another steroid at equivalent dosing may be used. [3]Refractory disease is defined as persistent fevers and/or ongoing and significant end-organ involvement. [4]Low-to-moderate–dose glucocorticoids (methylprednisolone 1–2 mg/kg/day) may be considered for first-line therapy in some MIS-C patients with concerning features (ill appearance, highly elevated B-type natriuretic peptide levels, unexplained tachycardia) who have not yet developed shock or organ-threatening disease. [5]If the patient was given low-to-moderate–dose glucocorticoids as first-line therapy, methylprednisolone IV dosing should be 10–30 mg/kg/day for intensification treatment.

Guidance revisions. For this subsequent version of the guidance, work group leaders were asked to identify guidance statements that should be modified based on clinical experience and newly available evidence in the literature. These revised statements along with the supporting literature were provided to the panelists before a webinar was held on October 13, 2020 to discuss the proposed changes. After the webinar, anonymous voting was conducted in the same manner as described above. Revised guidance statements that were voted as being appropriate (median score of 7–9) with a moderate or high degree of consensus were approved.

RESULTS

In the first round of voting, the Task Force evaluated a total of 125 statements that addressed the management of MIS-C and hyperinflammation in pediatric patients with COVID-19. Of these, 112 statements met the criteria for approval with a median score of 7–9 and moderate or high consensus, while 13 statements were rated as uncertain (median score of 4–6). After refining the statements based on the input from the initial phase, 128 guidance statements were approved in the second round of voting (see Supplementary Tables 1–4, available on the *Arthritis & Rheumatology* website at http://onlinelibrary.wiley.com/doi/10.1002/art.41616/abstract). These statements were organized into 40 final guidance statements as well as a flow diagram depicting the diagnostic pathway for MIS-C (Figure 1), which were approved by the entire Task Force and the ACR Board of Directors (12). For the second version of the guidance, the Task Force approved 22 revised statements (see Supplementary Table 5, available on the *Arthritis & Rheumatology* website at http://onlinelibrary.wiley.com/doi/10.1002/art.41616/abstract) as well as a second flow diagram (Figure 2). Topics covered in the guidance include

Table 2. Diagnostic evaluation of MIS-C*

Guidance statement	Level of consensus
The vast majority of children with COVID-19 present with mild symptoms and have excellent outcomes. MIS-C remains a rare complication of SARS–CoV-2 infections.	High
MIS-C is temporally associated with SARS–CoV-2 infections. Therefore, the prevalence of the virus in a given geographic location, which may change over time, should inform management decisions.	Moderate
The approach to testing for SARS–CoV-2 infections will evolve over the course of the COVID-19 pandemic, and it is therefore important to consider up-to-date testing methods and the prevalence of viral transmission in the community.	Moderate
A child "under investigation" for MIS-C should also be evaluated for other possible infections and non–infection-related conditions (e.g., malignancy) that may explain the clinical presentation.	High
Patients "under investigation" for MIS-C may require additional diagnostic studies (not described in Figure 1), including, but not limited to, imaging of the chest, abdomen, and/or central nervous system and lumbar puncture.	High
Outpatient evaluation for MIS-C may be appropriate for assessing well-appearing children with stable vital signs and for ensuring that physical examinations provide close clinical follow-up.	Moderate
Patients "under investigation" for MIS-C should be considered for admission to the hospital for further observation while the diagnostic evaluation is completed, especially if the patient displays any of the following symptoms: 1. abnormal vital signs (tachycardia, tachypnea); 2. respiratory distress of any severity; 3. neurologic deficits or change in mental status (including subtle manifestations); 4. evidence of even mild renal or hepatic injury; 5. marked elevations in inflammation markers (CRP ≥10 mg/dl); 6. abnormal EKG findings or abnormal levels of BNP or troponin T.	Moderate to high
Patients presenting with shock, significant respiratory distress, neurologic changes (altered mental status, encephalopathy, focal neurologic deficits, meningismus, papilledema), dehydration, or features of KD should be admitted for further evaluation, regardless of MIS-C status, in accordance with standard of care.	High
Children admitted to the hospital with MIS-C should be managed by a multidisciplinary team that includes pediatric rheumatologists, cardiologists, infectious disease specialists, and hematologists. Depending on the clinical manifestations, other subspecialties may need to be consulted as well; these include, but are not limited to, pediatric neurology, nephrology, hepatology, and gastroenterology.	Moderate to high

* MIS-C = multisystem inflammatory syndrome in children; COVID-19 = coronavirus disease 2019; SARS–CoV-2 = severe acute respiratory syndrome coronavirus 2; CRP = C-reactive protein; EKG = electrocardiogram; BNP = B-type natriuretic peptide; KD = Kawasaki disease.

the following: 1) diagnostic evaluation of MIS-C (Table 2 and Figure 1); 2) comparing and contrasting features of MIS-C and KD (Table 3); 3) cardiac management of MIS-C (Table 4); 4) treatment of MIS-C (Tables 5 and 6 and Figure 2); and 5) hyperinflammation in COVID-19 (Table 7).

Our understanding of SARS–CoV-2–related syndromes in the pediatric population continues to evolve. The recommendations provided by the Task Force reflect expert opinion and currently available evidence, which is of low quality and based on a limited number of case series and retrospective cohort studies. Thus, this

Table 3. Comparing and contrasting features of MIS-C and KD*

Guidance statement	Level of consensus
Patients with KD that is unrelated to SARS–CoV-2 will continue to require evaluation, diagnosis, and treatment during the SARS–CoV-2 pandemic.	High
MIS-C and KD unrelated to SARS–CoV-2 infections may share overlapping clinical features, including conjunctival infection, oropharyngeal findings (red and/or cracked lips, strawberry tongue), rash, swollen and/or erythematous hands and feet, and cervical lymphadenopathy.	Moderate to high
Several epidemiologic, clinical, and laboratory features of MIS-C may differ from KD unrelated to SARS–CoV-2 in the following ways: 1. There is an increased incidence of MIS-C in patients of African, Afro-Caribbean, and Hispanic descent, but a lower incidence in those of East Asian descent. 2. Patients with MIS-C encompass a broader age range, have more prominent GI and neurologic symptoms, present more frequently in a state of shock, and are more likely to display cardiac dysfunction (arrhythmias and ventricular dysfunction) than children with KD. 3. At presentation, patients with MIS-C tend to have lower platelet counts, lower absolute lymphocyte counts, and higher CRP levels than patients with KD.	Moderate to high
Epidemiologic studies of MIS-C suggest that younger children are more likely to present with KD-like features, while older children are more likely to develop myocarditis and shock.	Moderate
It is unknown if the incidence of CAAs is different in MIS-C compared to KD; however, MIS-C patients without KD features can develop CAAs.	Moderate to high

* MIS-C = multisystem inflammatory syndrome in children; KD = Kawasaki disease; SARS–CoV-2 = severe acute respiratory syndrome coronavirus 2; GI = gastrointestinal; CRP = C-reactive protein; CAAs = coronary artery aneurysms.

Table 4. Cardiac management of MIS-C*

Guidance statement	Level of consensus
Patients with MIS-C and abnormal BNP and/or troponin T levels at diagnosis should have these laboratory parameters trended over time until they normalize.	High
EKGs should be performed at a minimum of every 48 hours in MIS-C patients who are hospitalized and during follow-up visits. If conduction abnormalities are present, patients should be placed on continuous telemetry while in the hospital, and Holter monitors should be considered during follow-up.	Moderate to high
Echocardiograms conducted at diagnosis and during clinical follow-up should include evaluation of ventricular/valvular function, pericardial effusion, and coronary artery dimensions with measurements indexed to body surface area using z-scores.	High
Echocardiograms should be repeated at a minimum of 7–14 days and 4–6 weeks after presentation. For those patients with cardiac abnormalities occurring in the acute phase of their illness, an echocardiogram 1 year after MIS-C diagnosis could be considered. Patients with LV dysfunction and/or CAAs will require more frequent echocardiograms.	Moderate to high
Cardiac MRI may be indicated 2–6 months after MIS-C diagnosis in patients who presented with significant transient LV dysfunction in the acute phase of illness (LV ejection fraction <50%) or persistent LV dysfunction. Cardiac MRI should focus on myocardial characterization, including functional assessment, T1/T2-weighted imaging, T1 mapping and extracellular volume quantification, and late gadolinium enhancement.	High
Cardiac CT should be performed in patients with suspected presence of distal CAAs that are not well seen on echocardiogram.	Moderate

* MIS-C = multisystem inflammatory syndrome in children; BNP = B-type natriuretic peptide; EKGs = electrocardiograms; LV = left ventricular; CAAs = coronary artery aneurysms; MRI = magnetic resonance imaging; CT = computed tomography.

guidance is meant to be a "living document" and will be modified as additional data become available. The recommendations provided in the guidance document do not replace the importance of clinical judgment tailored to the unique circumstances of an individual patient.

Diagnostic evaluation of MIS-C. *Maintaining a broad differential diagnosis.* Multiple case definitions for MIS-C have been proposed (8–10), some of which are broader than others (Table 1). Common clinical features of MIS-C include fever, mucocutaneous findings (rash, conjunctivitis, edema of

Table 5. Immunomodulatory treatment in MIS-C*

Guidance statement	Level of consensus
Patients under investigation for MIS-C without life-threatening manifestations should undergo diagnostic evaluation for MIS-C as well as other possible infections and non–infection-related conditions before immunomodulatory treatment is initiated.	Moderate
Patients "under investigation" for MIS-C with life-threatening manifestations may require immunomodulatory treatment for MIS-C before the full diagnostic evaluation can be completed.	High
After evaluation by specialists with expertise in MIS-C, some patients with mild symptoms may only require close monitoring without immunomodulatory treatment. The panel noted uncertainty around the empiric use of IVIG to prevent CAAs in this setting.	Moderate
A stepwise progression of immunomodulatory therapies should be used to treat MIS-C with IVIG considered first-tier therapy. Glucocorticoids should be used as adjunctive therapy in patients with severe disease or as intensification therapy in patients with refractory disease.	High
IVIG should be given to MIS-C patients who are hospitalized and/or fulfill KD criteria.	High
High-dose IVIG (typically 2 gm/kg, based on ideal body weight) should be used for treatment of MIS-C.	High
Cardiac function and fluid status should be assessed in MIS-C patients before IVIG treatment is provided. Patients with depressed cardiac function may require close monitoring and diuretics with IVIG administration.	High
In some patients with cardiac dysfunction, IVIG may be given in divided doses (1 gm/kg daily over 2 days).	Moderate
Low-to-moderate–dose glucocorticoids (1–2 mg/kg/day) should be given with IVIG as adjunctive therapy for treatment of MIS-C patients with shock and/or organ-threatening disease.	Moderate
In patients who do not respond to IVIG and low-to-moderate–dose glucocorticoids, high-dose, IV pulse glucocorticoids (10–30 mg/kg/day) may be considered, especially if a patient requires high-dose or multiple inotropes and/or vasopressors.	Moderate
In patients with refractory MIS-C despite a single dose of IVIG, a second dose of IVIG is not recommended, given the risk of volume overload and hemolytic anemia associated with large doses of IVIG.	High
Low-to-moderate–dose steroids (1–2 mg/kg/day) may also be considered in patients with milder forms of MIS-C who are persistently febrile and symptomatic despite a single dose of IVIG.	Moderate
Anakinra (>4 mg/kg/day IV or SC) may be considered for treatment of MIS-C refractory to IVIG and glucocorticoids in patients with MIS-C and features of macrophage activation syndrome or in patients with contraindications to long-term use of glucocorticoids.	Moderate
Serial laboratory testing and cardiac assessment should guide immunomodulatory treatment response and tapering. Patients may require a 2–3-week, or even longer, taper of immunomodulatory medications.	High

* MIS-C = multisystem inflammatory syndrome in children; IVIG = intravenous immunoglobulin; CAAs = coronary artery aneurysms; SC = subcutaneous.

Table 6. Antiplatelet and anticoagulation therapy in MIS-C*

Guidance statement	Level of consensus
Low-dose aspirin (3–5 mg/kg/day; maximum 81 mg/day) should be used in patients with MIS-C and continued until the platelet count is normalized and normal coronary arteries are confirmed at ≥4 weeks after diagnosis. Treatment with aspirin should be avoided in patients with active bleeding, significant bleeding risk, and/or a platelet count of ≤80,000/μl.	Moderate
MIS-C patients with CAAs and a maximal z-score of 2.5–10.0 should be treated with low-dose aspirin. Patients with a z-score of ≥10.0 should be treated with low-dose aspirin and therapeutic anticoagulation with enoxaparin (factor Xa level 0.5–1.0) or warfarin.	Moderate to high
Patients with MIS-C and documented thrombosis or an EF of <35% should receive therapeutic anticoagulation with enoxaparin until at least 2 weeks after discharge from the hospital.	High
Indications for longer outpatient therapeutic enoxaparin dosing include the following: CAAs with a z-score of >10.0 (indefinite treatment), documented thrombosis (treatment for ≥3 months pending thrombus resolution), or ongoing moderate-to-severe LV dysfunction.	High
For MIS-C patients who do not meet the above criteria, the approach to antiplatelet and anticoagulation therapeutic management should be tailored to the patient's risk for thrombosis.	High

* MIS-C = multisystem inflammatory syndrome in children; KD = Kawasaki disease; CAAs = coronary artery aneurysms; EF = ejection fraction; LV = left ventricular.

the hands/feet, red/cracked lips, and strawberry tongue), myocardial dysfunction, cardiac conduction abnormalities, shock, gastrointestinal symptoms, and lymphadenopathy (2,4–7, 13–22). There are also increasing reports of neurologic involvement in select patients, manifesting as severe headache, altered mental status, cranial nerve palsies, or meningismus (5–7,13,14,19–22). These findings are nonspecific and can occur in other infections, as well as in non–infection-related conditions such as oncologic or inflammatory conditions. In the midst of the COVID-19 pandemic, there is potential for cognitive bias with anchoring on a diagnosis of MIS-C when children present with unexplained fevers. Therefore, it is imperative that a diagnostic evaluation for MIS-C include investigation for other possible causes, as deemed appropriate by the treating provider. MIS-C is temporally associated with SARS–CoV-2 infections, and clusters of cases have been reported in geographic areas with dense COVID-19 disease burden, typically being identified within 2–6 weeks after the peak incidence of acute, infectious COVID-19 (4,13,14,17,19–21). Thus, the prevalence and chronology of SARS–CoV-2 infection in a given location, which may change over time, should also inform the diagnostic evaluation.

The incidence of MIS-C is unknown; however, it appears to be a rare complication of SARS–CoV-2 infection, with some

Table 7. Hyperinflammation in COVID-19*

Guidance statement	Level of consensus
Medically complex children and those receiving immunosuppressive medications, including moderate-to-high–dose glucocorticoids, may be at higher risk for severe outcomes in COVID-19.	Moderate to high
Children and adults admitted to the hospital with COVID-19 present with similar symptoms, including fever, upper respiratory tract symptoms, abdominal pain, and diarrhea.	Moderate
Children with severe respiratory symptoms due to COVID-19 with any of the following should be considered for immunomodulatory therapy: ARDS, shock/cardiac dysfunction, substantial elevation in LDH, D-dimer, IL-6, IL-2R, CRP, and/or ferritin level, and depressed lymphocyte count, albumin level, and/or platelet count.	Moderate to high
Glucocorticoids should be used as first-tier immunomodulatory treatment in patients with COVID-19 and hyperinflammation.	High
Anakinra appears safe in severe infections and in children with hyperinflammatory syndromes. In children with COVID-19 and hyperinflammation, anakinra (>4 mg/kg/day IV or SC) should be considered for immunomodulatory therapy in patients with refractory disease despite glucocorticoid treatment or in patients with contraindications to steroids. Initiation of anakinra before invasive mechanical ventilation may be beneficial.	High
Children with COVID-19 treated with anakinra should be monitored for LFT abnormalities.	Moderate
Tocilizumab is not recommended for a majority of pediatric patients with COVID-19 and hyperinflammation, given the lack of benefit reported in randomized, double-blind, placebo-controlled trials in adults with COVID-19 pneumonia. In addition, the effects of tocilizumab are long-lasting, which leaves little recourse if a patient does not respond favorably to the medication.	Moderate to high
There is insufficient evidence to support the use of other immunomodulatory agents unless glucocorticoids and IL-1–blocking therapies are contraindicated or have failed.	Moderate

* COVID-19 = coronavirus disease 2019; ARDS = acute respiratory distress syndrome; LDH = lactate dehydrogenase; IL-6 = interleukin-6; IL-2R = interleukin-2 receptor; CRP = C-reactive protein; IV = intravenous; SC = subcutaneous; LFT = liver function test.

estimates indicating that MIS-C occurs in 2 of 200,000 individuals under the age of 21 years (20). The relative rarity of MIS-C should also be considered in the diagnostic approach.

Tier 1 screening. Based on our review of the literature and diagnostic algorithms that are publicly available, the Task Force chose to cast a broad net with respect to the evaluation of patients with possible MIS-C, while simultaneously balancing the need to reduce indiscriminate overtesting and to prevent unnecessary use of resources in the treatment of pediatric patients who have unrelated causes of fever (2,4,5,7,13–16,23,24). To date, there are no clear data indicating the pretest positive or negative predictive probabilities for each clinical symptom or laboratory value in diagnosing MIS-C. It should be noted that due to the paucity of data, our recommendations reflect a multidisciplinary consensus that is likely to be revised as these data become available.

Fever is a key manifestation of MIS-C, with affected children presenting with significantly higher temperatures and longer fever duration than children with other routine pediatric illnesses (25). Thus, children with unremitting fever, an epidemiologic link to SARS–CoV-2, and suggestive clinical symptoms should be considered "under investigation" for MIS-C, while alternative diagnoses that could explain the patient's clinical presentation are also explored (Figure 1). A tiered diagnostic approach is recommended in patients without life-threatening manifestations; this includes performing an initial screening evaluation (tier 1), and thereafter proceeding to a complete diagnostic evaluation (tier 2) only in patients with laboratory results from the tier 1 screening that are concerning. Tier 1 consists of laboratory studies that are easily obtained at most clinical facilities (complete blood cell count with manual differential, complete metabolic panel, erythrocyte sedimentation rate [ESR], CRP measurement, and testing for SARS–CoV-2 by polymerase chain reaction [PCR] or serology). Among MIS-C cases reported in the literature, the overwhelming majority involve elevated levels of inflammation markers, particularly CRP, as values higher than 10 mg/dl or even 20 mg/dl are common (2,4–6,13,14,17,19–22). Thus, to enter the second stage of testing, children should have elevated ESR and/or CRP levels and at least 1 other suggestive laboratory feature: lymphopenia, neutrophilia, thrombocytopenia, hyponatremia, or hypoalbuminemia (2,4–6,13,14,17,19–22).

Tier 2 evaluation. Tier 2 encompasses more complex testing that typically requires additional time to complete. Reports in the literature and unpublished observations by members of the panel both note that some patients with MIS-C can decompensate rapidly; however, the risk factors that predispose patients to such severe and progressive illness have not been identified (7,13). Accordingly, children with abnormal vital signs, concerning physical examination findings, significantly elevated levels of inflammation markers, or signs of cardiac involvement will need to be admitted to the hospital for supportive care while tier 2 testing is completed.

The panel also noted that MIS-C appears to be a continuum of disease that encompasses milder phenotypes that have not been fully described in the published literature (26). Some patients present with fever, rash, and systemic inflammation and no other organ damage. While these children require close monitoring, they do not always need to be hospitalized. Thus, in some cases, well-appearing children with reassuring vital signs and physical examination findings may be considered suitable for outpatient diagnostic evaluations as long as close clinical follow-up can be ensured.

Prominent cardiac involvement has been reported in a proportion of MIS-C patients in every retrospective cohort study published to date (2,4–6,13,14,17,19–22,27,28). These include left ventricular (LV) dysfunction, coronary artery dilation or coronary artery aneurysm (CAA), and electrical conduction abnormalities. Valvular dysfunction and pericardial effusion are less frequently described. Among the initial descriptions of MIS-C, LV dysfunction was present in 20–55% of cases, and coronary artery dilation or CAA in ~20% (2,4,13). Although the early reports may overestimate the incidence of cardiac features as they likely represent the most severe component of the MIS-C spectrum, these numbers nonetheless highlight the significant risk of cardiac involvement in MIS-C. While LV dysfunction and CAAs are salient and frequently described features of MIS-C, arrhythmias have been less well characterized. Recently, atrioventricular block was identified in up to 20% of children with MIS-C, including progression to second- and third-degree block in some (28).

For these reasons, EKG and echocardiogram are key components of the full diagnostic evaluation. The echocardiogram should include quantification of LV size and systolic function using end-diastolic volume (and z-score) and ejection fraction (EF) (29,30). Detailed evaluation of all coronary artery segments and normalization of coronary artery measurements to body surface area using z-scores is necessary (30,31). Cardiac laboratory values at the time of diagnosis, specifically levels of troponin T and B-type natriuretic peptide (BNP)/N-terminal proBNP (NT-proBNP), may help identify patients with cardiac sequelae from MIS-C (4–6,13,14,17). In particular, highly elevated BNP/NT-proBNP levels may be helpful in distinguishing between MIS-C patients with and those without LV dysfunction; however, mild and transient elevations in these laboratory parameters are likely to be nonspecific, and do not necessarily indicate cardiac involvement (14,32,33). BNP, in particular, is an acute-phase reactant, and therefore may be elevated in inflammatory conditions without cardiac involvement (32).

Tier 2 testing should also include further assessment for systemic inflammation. In addition to changes in the ESR and CRP level, MIS-C patients typically demonstrate other markers of inflammation, including high D-dimer levels, moderately elevated ferritin levels (often ranging from 500 to 2,000 ng/dl), profoundly increased procalcitonin levels in the absence of bacterial infection, and increased lactate dehydrogenase (LDH) levels (5–7,13,14,17). Cytokine panels, when available, can assist in the diagnostic evaluation, as levels of interleukin-6 (IL-6), tumor necrosis factor (TNF),

or IL-10 are often increased; however, cytokine levels measured in this manner should not dictate treatment choices and are not required to determine treatment plans (5,6,13,21,22,34–37). Along with systemic inflammation, endothelial dysfunction is a feature of MIS-C, and a peripheral blood smear can be used to identify microangiopathic changes in red blood cells, although the sensitivity and specificity of using a peripheral blood smear for the diagnosis of MIS-C is unknown (35).

Finally, a greater proportion of MIS-C patients have been found positive for SARS–CoV-2 by serologic testing (80–90%) than by PCR testing (20–40%), and both tests should be sent to evaluate the epidemiologic link to the infection (4–6,13,17,20,21). The use of serologic testing will become more complicated as the COVID-19 pandemic evolves, because seropositivity for SARS–CoV-2 IgG may not be indicative of a recent infection. It is important to interpret serologic testing in the context of the prevalence of viral transmission in the patient's community.

Comparing and contrasting features of MIS-C and KD. In an early sentinel report from Bergamo, the Italian epicenter of the COVID-19 pandemic, KD and KD-like illnesses were observed at a rate 30 times higher than that observed in the pre-pandemic era (4). Since this observation, the clinical symptoms of MIS-C have frequently been compared to those of KD given their similarity in profiles, which includes fevers, mucocutaneous features, and cardiac sequelae (2,4–7,13–17,21,29,34,38). However, a closer examination of the literature shows that only about one-quarter to one-half of patients with a reported diagnosis of MIS-C meet the full diagnostic criteria for KD (4–6,13,14,19,20,34).

Several epidemiologic, clinical, and laboratory features of MIS-C that differ from KD unrelated to SARS–CoV-2 are worthy of mention. First, while the incidence of KD is highest in Japan, MIS-C appears to be frequent in patients of African and Hispanic descent (2,5,6,14,19,20,22,39). It is unclear whether genetic or biologic factors could explain this racial/ethnic distribution of MIS-C or whether socioeconomic status, structural inequality, and risk of SARS–CoV-2 exposure are more causative.

Second, the age distribution of MIS-C is broad, with reports of MIS-C found in children ranging in age from 3 months to 20 years (2,4–7,13,14,17,19–21,34). In contrast, the majority of children with KD present with symptoms before age 5 years (4,14,21,34,40,41).

Third, as discussed above, the clinical presentations of LV dysfunction and shock that are characteristic of patients with MIS-C are considerably less common in patients with KD, with fewer than 10% of KD patients presenting with KD shock syndrome (42). Close to one-quarter of untreated KD patients develop CAAs (43). Coronary artery dilations or CAAs have been documented in up to 20% of MIS-C patients, and at least 3 patients have developed giant CAAs (2,4,13,14,17,19,20,34). It is unknown if the incidence or progression of CAAs differ between MIS-C and KD. Importantly, it is clear that MIS-C patients without KD symptoms can develop CAAs, highlighting the need for cardiac evaluation in all patients with MIS-C regardless of phenotypic features, and providing support for the treatment rationale discussed below (14).

Fourth, although gastrointestinal and neurologic symptoms are reported in KD patients, the panel agreed that these findings were more frequently encountered in the MIS-C population.

Finally, the laboratory parameters that have been found to differ in retrospective cohorts of MIS-C patients compared to historical cohorts of KD patients include a lower platelet count, lower absolute lymphocyte count, and higher CRP level in MIS-C patients (4,14,21,34). There is emerging evidence that age may impact the clinical phenotype of MIS-C. Epidemiologic studies suggest that younger children are more likely to present with KD-like features, while older children are more likely to develop myocarditis and shock (19,20).

Cardiac management of MIS-C. Children with MIS-C will need close clinical follow-up with cardiology. Extrapolating data from KD, another condition that can be complicated by CAA, the panel recommended that repeat echocardiograms be obtained from all children with MIS-C at a minimum of 7–14 days and then 4–6 weeks after the initial presentation (29). For those patients with cardiac involvement noted during the acute phase of illness, another echocardiogram at 1 year after MIS-C diagnosis could be considered. Children with LV dysfunction and CAAs will require more frequent echocardiograms.

Although LV function improves rapidly in most MIS-C patients, the long-term complications of myocardial inflammation in this syndrome are not known and may include myocardial fibrosis and scarring, representing features that have been seen in other forms of pediatric myocarditis (6,13,44). Cardiac magnetic resonance imaging at 2–6 months post–acute illness in those patients who had moderate-to-severe LV dysfunction will allow for evaluation of fibrosis and scarring. Electrical conduction abnormalities are increasingly noted in MIS-C patients and may develop after the initial presentation; therefore, EKGs should be obtained at a minimum of every 48 hours in patients who are hospitalized and at each follow-up visit (5,6,13,14,28). If conduction abnormalities are present, the patient should be placed on telemetry while in the hospital, and may need Holter monitoring at clinical follow-up.

Treatment of MIS-C. *Immunomodulatory treatment in MIS-C.* Goals of treatment in the MIS-C population are to stabilize patients with life-threatening manifestations such as shock, and to prevent long-term sequelae that may include CAAs, myocardial fibrosis/scarring, and fixed cardiac conduction abnormalities. There is no available literature that directly compares therapeutic approaches in MIS-C. Recommendations approved by the Task Force are derived from experience in managing MIS-C and higher quality data from other pediatric conditions with similar features. Initiation of treatment will often depend on the severity of the patient's presentation. There was

consensus among the panelists that patients under investigation for MIS-C without life-threatening manifestations should undergo a diagnostic evaluation for MIS-C as well as other possible infections and non–infection-related conditions before immunomodulatory treatment is initiated. This is to prevent the use of therapies that could be potentially harmful in patients who do not have MIS-C.

Further, a subgroup of patients with MIS-C will develop progressive cardiac involvement rapidly; therefore, hospital admission and sequential monitoring of inflammation markers, including BNP/NT-proBNP and troponin T levels, without instituting treatment can sometimes inform the diagnostic evaluation (7,13). Children with a life-threatening presentation such as shock will clearly require supportive care and may benefit from early initiation of immunomodulatory treatment, sometimes before a full diagnostic evaluation can be completed. In such cases, ongoing diagnostic evaluation should be pursued in parallel with treatment by a multidisciplinary team.

Finally, the current recommendations address the treatment of MIS-C that is uncomplicated by macrophage activation syndrome (MAS). Importantly, there is a subgroup of patients with MIS-C who may also develop overt MAS. The treatment of those patients may need to deviate from the recommendations presented herein (4).

Initial immunomodulatory therapy. A stepwise approach to immunomodulatory treatment in MIS-C is recommended, with intravenous immunoglobulin (IVIG) and/or glucocorticoids considered first-tier agents (Figure 2). Both IVIG and glucocorticoids are the most commonly used immunomodulatory medications in MIS-C patients reported to date (2,4–7,13–15,17,19–21,34). High-quality studies that compare the efficacy of IVIG and glucocorticoids in MIS-C, either alone or in combination, are not currently available. There is some evidence to suggest that faster initiation of IVIG and glucocorticoids in MIS-C is associated with a reduction in intensive care unit (ICU) admissions and length of hospital stay (45). In one retrospective and comparative cohort study, children with MIS-C and myocarditis who were treated with IVIG and methylprednisolone at 0.8 mg/kg/day had faster recovery of cardiac function and shorter time in the ICU than patients given IVIG monotherapy (46). Evidence for IVIG and glucocorticoids in MIS-C is also based on their use in KD and fulminant myocarditis, representing 2 conditions that resemble MIS-C in some aspects. IVIG at a dose of 2 gm/kg prevents CAAs in KD while the benefit of IVIG in myocarditis remains unclear; however, case reports have described the successful use of IVIG in patients with coronavirus-associated myocarditis (29,43,47–53). Glucocorticoids reduce the rates of CAA development when used in KD patients at high risk for IVIG resistance (54,55). Compared to historical KD cohorts, studies by Verdoni et al and Pouletty et al have demonstrated a high rate of IVIG resistance in KD patients who presented during the COVID-19 pandemic, which may suggest a role for glucocorticoids in MIS-C (4,21).

The Task Force recommended that IVIG be given to all MIS-C patients who require hospitalization, administered at a dose of 2 gm/kg based on ideal body weight. Low-to-moderate–dose glucocorticoids (1–2 mg/kg/day) should be used as adjunctive therapy with IVIG in patients with shock and/or organ-threatening disease. Glucocorticoids may also be added to IVIG as first-line therapy in patients who have not yet developed shock or severe end-organ involvement but present with concerning features such as ill appearance, highly elevated BNP levels, or unexplained tachycardia. Before IVIG is given, cardiac function and fluid status should be assessed. If abnormal, the rate of IVIG infusion may be slowed, the treatment may be given in divided doses over 2 days, and/or diuretics may be considered to avoid volume overload.

Intensification of immunomodulatory therapy. A patient with MIS-C is considered to have refractory disease when the child has persistent fevers and/or significant end-organ involvement despite initial immunomodulatory treatment. Compared to pre–COVID-19 pandemic KD, MIS-C patients display more cardiac dysfunction and require larger doses of IVIG due to the age and size of these patients. Thus, patients with MIS-C are at greater risk for IVIG complications such as hemolytic anemia and volume overload. Furthermore, MIS-C patients are more likely to decompensate rapidly and may benefit from faster intensification of therapy than children with non–SARS–CoV-2–related KD. Accordingly, a second dose of IVIG is not recommended in patients with refractory disease. Instead, glucocorticoids at low-to-moderate doses could be considered in children who are symptomatic despite a single dose of IVIG. In those patients who presented at disease onset with severe disease and were initially treated with a combination of IVIG and low-to-moderate–dose glucocorticoids, higher-dose steroids can be considered. Several panelists have found that some children with shock, requiring multiple inotropes and/or vasopressors, have responded best to high doses of intravenous glucocorticoids (10–30 mg/kg/day). High-dose intravenous glucocorticoids have been used safely in patients with KD and have been used successfully in small numbers of patients with MIS-C and shock (7,56–58). Adjunctive glucocorticoids have also been shown to shorten the duration of shock in patients with sepsis (59).

High-dose anakinra (recombinant human IL-1 receptor antagonist) (>4 mg/kg/day) can also be considered for MIS-C patients with refractory disease despite having received IVIG and steroid treatment. In addition, anakinra may also be considered as a steroid-sparing agent in patients with contraindications to long courses of glucocorticoids. These recommendations are based on the relative safety of anakinra in pediatric patients with hyperinflammatory syndromes and active infection, the experience of panel members in using anakinra to treat MIS-C patients, and case descriptions of a small number of MIS-C patients reported in the literature (13,14,17,19,21,22,34,60–63). In addition, anakinra has been used successfully in a small number of patients with

IVIG-resistant KD (64–66). Other biologic medications, such as infliximab, have been described in the literature for use in MIS-C; however, the panelists reported that such treatments were not used routinely in their clinical practice.

Tapering immunomodulatory therapy. Serial laboratory testing and cardiac assessment should guide decisions to decrease immunomodulatory treatment. Children with MIS-C require a prolonged course of immunomodulatory treatment that may need to extend for 2–3 weeks, or even longer, to avoid rebound inflammation.

Treatment of non-hospitalized patients. Treatment with immunomodulatory agents may not always be required in MIS-C. Whittaker et al reported that 22% of MIS-C patients recovered with supportive care (14). In close coordination with specialists who have expertise in MIS-C, some patients with mild symptoms may require only close monitoring, without the use of IVIG and/or glucocorticoids. The panel noted uncertainty around the empiric use of IVIG in this setting to prevent CAAs.

Antiplatelet and anticoagulation therapy in MIS-C. Published reports of patients with MIS-C describe marked abnormalities in the coagulation cascade, including prominent elevations in D-dimer and fibrinogen levels, a variable effect on the platelet count, and a high clot strength as determined by thromboelastography (2,4–6,13,14,19,20,22). An increased risk of thrombosis is a concern in patients with MIS-C, based on the data outlined above as well as the hypercoagulability noted in adults with COVID-19 (67–70). A recent report described a small number of MIS-C patients with deep vein thrombosis or pulmonary embolism, but the overall risk of thrombosis in this population is not known (19). Therefore, these recommendations are based on experience in analogous pediatric conditions, specifically KD and myocarditis, and the emerging data from adults with COVID-19.

Antiplatelet agents such as aspirin are recommended in patients with KD, because of the platelet activation, thrombocytosis, altered flow dynamics in abnormal coronary arteries, and endothelial damage characteristic of this disease (29). Accordingly, low-dose aspirin (3–5 mg/kg/day up to 81 mg once daily) is recommended in all MIS-C patients who are without active bleeding or significant bleeding risk. Aspirin should be continued until normalization of the platelet count is achieved and normal coronary arteries are confirmed at ≥4 weeks after diagnosis. Antiacid treatments should be used to prevent gastrointestinal complications in MIS-C patients who are receiving steroids and aspirin. The risk of coronary artery thrombosis is directly related to size of the CAA, with an exponentially increased probability of thrombosis occurring in coronary arteries with dimensions above a z-score of 10.0 (29,71,72). Thus, anticoagulation with enoxaparin (factor Xa level 0.5–1.0) or warfarin in MIS-C patients with a coronary artery z-score greater than 10.0 is advised. Patients with more-than-mild LV dysfunction are at risk for intracardiac thrombosis (73,74). Given the lack of clarity about the exact risk of hypercoagulability in MIS-C, the Task Force recommended considering anticoagulation therapy for MIS-C patients with moderate or severe LV dysfunction (EF <35%).

Hyperinflammation in children with COVID-19. *Severe COVID-19 in children.* The Task Force also addressed immunomodulatory treatment in severe COVID-19, a condition that panelists (given current information) deemed to be readily distinguishable from MIS-C. A vast majority of children with COVID-19 have mild symptoms in the acute, infectious phase of the disease, but a small minority of patients become severely ill (75–80). MIS-C patients who are often previously healthy may present with fever, inflammation, and multiorgan dysfunction that manifests late in the course of SARS–CoV-2 infection (most are positive for SARS–CoV-2 IgG). In contrast, children who develop severe COVID-19 during their initial infection often have a complex medical history (76–79). Shekerdemian and colleagues reported that 40% of patients admitted to the ICU for COVID-19 had developmental delay or a genetic anomaly, or were dependent on technological support (e.g., tracheostomy) for survival (77). There is no definitive evidence suggesting that children with rheumatic diseases treated with immunosuppression are also at risk of developing poor outcomes from COVID-19. Shekerdemian et al also observed that 23% of pediatric patients with COVID-19 who were admitted to the ICU were either immunosuppressed or had cancer, but did not specify if any of these patients had a rheumatic condition (77). Extrapolating from adults with inflammatory bowel disease and rheumatic conditions, glucocorticoid use may be associated with worse outcomes in COVID-19 while treatment with TNF inhibitors may actually be protective against severe COVID-19 (81,82). In addition, among cohorts of pediatric patients in this population receiving immunosuppressive medications, an increased risk of severe COVID-19 has not been identified (83–85).

Immunomodulatory treatment in children with hyperinflammation and COVID-19. Data to guide the treatment of pediatric patients with severe illness during the early phase of SARS–CoV-2 infection are limited. In adults, certain laboratory parameters associated with an exaggerated inflammatory response (hyperinflammation) portend worse outcomes in COVID-19, including elevated levels of LDH, D-dimer, IL-6, IL-2 receptor, CRP, and ferritin, and a decreased lymphocyte count, albumin level, and platelet count (86–89). In at least one case series of pediatric patients with COVID-19, increased CRP levels, elevated procalcitonin levels, and decreased platelet counts were significantly more common in children requiring ICU admission compared to those receiving floor-level hospital care; however, further studies are needed to identify laboratory parameters that could serve as predictors of poor outcomes in the pediatric population (90). These results suggest that patients with COVID-19 and hyperinflammation have poor outcomes, and that the host immune response to SARS–CoV-2 may contribute to disease severity. The panel agreed that children with severe COVID-19 manifesting as acute respiratory

distress syndrome (ARDS), shock, or signs of hyperinflammation (as measured by the laboratory parameters discussed above) should be considered for immunomodulatory therapy in addition to supportive care and antiviral medications.

Glucocorticoids are a readily available and inexpensive option for immunomodulation. Prior experience with adjunctive glucocorticoid therapy in ARDS unrelated to COVID-19 has been equivocal (91–93). Observational studies evaluating glucocorticoid treatment in other respiratory viral infections, such as influenza, suggest that this treatment is associated with increased mortality; however, these studies are difficult to interpret, due to confounding by indication (94,95). There are concerns that glucocorticoids given at high doses or early in the course of infection delay viral clearance (96,97). Glucocorticoid use in critically ill patients is also associated with increased neuropathy and myopathy (98). In SARS–CoV-2 infections, there is conflicting evidence about the impact of glucocorticoids on viral clearance (99,100). A small number of cohort studies have suggested a benefit from glucocorticoid treatment in patients with severe COVID-19 pneumonia (87,101). Importantly, results from a large randomized controlled trial (the RECOVERY trial) indicate that low-to-moderate–dose dexamethasone significantly reduced mortality in COVID-19 patients requiring mechanical ventilation (102). A meta-analysis of 7 randomized clinical trials that studied glucocorticoid treatment in adults with COVID-19 supports the results of the RECOVERY trial and also demonstrates a reduction in mortality in the treatment group (103). Based on these studies in adults, the Task Force achieved high consensus in recommending that glucocorticoids should be used as first-tier immunomodulatory treatment in pediatric patients with severe COVID-19 and signs of hyperinflammation.

Targeted neutralization of inflammatory cytokines is another approach that can be employed to reduce pathologic inflammation in COVID-19. In pediatric patients with severe COVID-19 and hyperinflammation who have refractory disease despite glucocorticoid administration, anakinra could be considered for treatment. In addition, anakinra is an option for patients with contraindications to steroids. Anakinra appears to be safe in severe infections, based on the results of a randomized controlled trial in patients with sepsis in whom there was no difference in the frequency of adverse events in the anakinra group compared to the placebo group (62). Furthermore, a re-analysis of data from this trial showed increased survival in patients with sepsis treated with anakinra who also had excessive inflammation manifested as hepatobiliary dysfunction and coagulopathy, which is commonly seen in COVID-19 (104). IL-1 blockade has also been used safely in children with inflammatory syndromes, including those with systemic juvenile idiopathic arthritis and those with MAS (60,61,63). In COVID-19, observations from case series provide evidence of the safety and efficacy of anakinra in patients with elevated inflammation marker levels and moderate-to-severe disease; however, most of those studies do not have a comparison group (105–109). In one retrospective cohort of patients with COVID-19–related moderate-to-severe ARDS, treatment with anakinra in addition to usual care significantly reduced mortality when compared to patients treated at the same center a week prior (110). The patients in this cohort received high-dose anakinra (10 mg/kg/day) and were not yet mechanically ventilated, suggesting that treatment before intubation is beneficial. Similar results were reported in the Ana-COVID study, in which a prospective cohort of patients treated with anakinra was compared to a historical cohort (111). Importantly, randomized controlled trials confirming the efficacy of anakinra in adults with COVID-19 have not yet been published.

Given the association between increased IL-6 levels and negative outcomes in COVID-19, IL-6 neutralization with tocilizumab may be an appealing therapy (86,87,89). Initially, observations from some case series, reported without a comparison group, suggested clinical improvement with tocilizumab treatment, while others have not observed any clinical improvement or have noted a high rate of bacterial and fungal infections (112–115). Cohort studies with comparison groups have demonstrated conflicting results, with one study showing safety and efficacy with tocilizumab, while another showing no improvement in clinical outcomes (116,117). In a study by Capra and colleagues, treatment with tocilizumab showed some benefit in COVID-19 patients who were not yet mechanically ventilated (116). Ultimately, randomized controlled trials of tocilizumab in adults with moderate and severe COVID-19 did not demonstrate a reduction in mortality at 28 days (118,119). Given these data, the Task Force did not recommend tocilizumab for the majority of pediatric patients with COVID-19.

DISCUSSION

There has been an evolution in our understanding of SARS–CoV-2 infections in children. Initially, it was believed that COVID-19 was almost entirely benign and of little consequence in the pediatric population. There has been a sudden reversal from this stance in the context of the emergence of MIS-C cases. The goal of this ACR Task Force was to synthesize available data and expert opinion to provide a resource for clinicians on the frontlines caring for children with inflammatory syndromes associated with recent or concurrent infections with SARS–CoV-2.

Recognizing the need to address the unique challenges facing children with inflammatory conditions triggered by SARS–CoV-2 infections, the ACR convened the Task Force to provide guidance in a short period of time. To accomplish this charge, a multidisciplinary panel was assembled that included clinicians from North America with expertise encompassing pediatric rheumatology, cardiology, infectious disease, and critical care. Well-established methodology in the form of the RAND/UCLA Appropriateness Method was used to achieve consensus.

There are limitations inherent in our approach. Given the need for expedited decision-making, we were unable to provide guidance on all topics of interest. In particular, the Task Force focused

its efforts on providing diagnostic and treatment recommendations for MIS-C instead of developing a new case definition for this condition. This choice was made because several case definitions of MIS-C exist, and the data needed to develop a sensitive and specific set of criteria are not yet available. The guidance provided in this document is targeted to clinicians with access to complex diagnostic tools and biologic treatments. Thus, some of the recommendations are not practical in less resource-rich settings. In addition, the work product of the Task Force is considered guidance, instead of formal treatment guidelines that must adhere to the strict methodology endorsed by the ACR.

The guidance provided in this document is supported by reports from the scientific literature and recommendations from public health institutions. Yet, the available data remain restricted to low-quality evidence that often must be extrapolated from the experience in adults. This approach is particularly problematic when confronting clinical questions regarding MIS-C, which, to date, has been reported primarily in children. This unique manifestation of COVID-19 in children and adolescents highlights the need to prioritize and fund rigorous research in the pediatric population. For now, our understanding of pediatric SARS–CoV-2 infections is rudimentary and will continue to change as higher-quality evidence becomes available. Thus, the recommendations contained in this document should be interpreted in the setting of this shifting landscape and will be modified prospectively as our understanding of COVID-19 improves. For these reasons, this guidance does not replace the critical role of clinical judgment that is essential to address the unique needs of individual patients.

As the SARS–CoV-2 pandemic continues to unfold, the ACR will support clinicians caring for children with COVID-19 by enabling this Task Force to continue the work of reviewing evidence and providing expert opinion through revised versions of this guidance document. It is the ultimate goal of both the ACR and the Task Force panelists to disseminate knowledge quickly in an effort to improve outcomes for children with SARS–CoV-2 infections.

AUTHOR CONTRIBUTIONS

All authors were involved in drafting the article or revising it critically for important intellectual content, and all authors approved the final version to be published. Dr. Henderson had full access to all of the data in the study and takes responsibility for the integrity of the data and the accuracy of the data analysis.

Study conception and design. Henderson, Friedman, Gorelik, Lapidus, Behrens, Ferris, Seo, Turner, Mehta.

Acquisition of data. Henderson, Canna, Gorelik, Lapidus, Bassiri, Behrens, Ferris, Kernan, Schulert, Seo, Tremoulet, Yeung, Karp, Mehta.

Analysis and interpretation of data. Henderson, Canna, Friedman, Gorelik, Lapidus, Bassiri, Kernan, Schulert, Seo, Son, Tremoulet, Yeung, Mudano, Karp, Mehta.

REFERENCES

1. Dong E, Du H, Gardner L. An interactive web-based dashboard to track COVID-19 in real time [letter]. Lancet Infect Dis 2020;20:533–4.
2. Riphagen S, Gomez X, Gonzalez-Martinez C, Wilkinson N, Theocharis P. Hyperinflammatory shock in children during COVID-19 pandemic [letter]. Lancet 2020;395:1607–8.
3. World Federation of Pediatric Intensive and Critical Care Societies. Statement to the media following the 2 May Pediatric Intensive Care-COVID-19 International Collaborative conference call. May 2020. URL: http://www.wfpiccs.org/wp-content/uploads/2020/05/Media-statement-Final.pdf.
4. Verdoni L, Mazza A, Gervasoni A, Martelli L, Ruggeri M, Ciuffreda M, et al. An outbreak of severe Kawasaki-like disease at the Italian epicentre of the SARS-CoV-2 epidemic: an observational cohort study. Lancet 2020;395:1771–8.
5. Toubiana J, Poirault C, Corsia A, Bajolle F, Fourgeaud J, Angoulvant F, et al. Kawasaki-like multisystem inflammatory syndrome in children during the covid-19 pandemic in Paris, France: prospective observational study. BMJ 2020;369:m2094.
6. Cheung EW, Zachariah P, Gorelik M, Boneparth A, Kernie SG, Orange JS, et al. Multisystem inflammatory syndrome related to COVID-19 in previously healthy children and adolescents in New York City [letter]. JAMA 2020;324:294–6.
7. Chiotos K, Bassiri H, Behrens EM, Blatz AM, Chang J, Diorio C, et al. Multisystem inflammatory syndrome in children during the COVID-19 pandemic: a case series. J Pediatric Infect Dis Soc 2020;9:393–8.
8. World Health Organization. Multisystem inflammatory syndrome in children and adolescents with COVID-19. May 2020. URL: https://www.who.int/publications/i/item/multisystem-inflammatory-syndrome-in-children-and-adolescents-with-covid-19.
9. Royal College of Paediatrics and Child Health. Guidance: paediatric multisystem inflammatory syndrome temporally associated with COVID-19. June 2020. URL: https://www.rcpch.ac.uk/resources/guidance-paediatric-multisystem-inflammatory-syndrome-temporally-associated-covid-19-pims.
10. Centers for Disease Control and Prevention. Emergency preparedness and response: health alert network. May 2020. URL: https://emergency.cdc.gov/han/2020/han00432.asp.
11. Brook R. US Agency for Health Care Policy and Research Office of the Forum for Quality and Effectiveness in Health Care clinical practice guideline development: methodology perspectives. In: McCormick K, Siegel R, editors. The RAND/UCLA Appropriateness Method. Rockville (MD): Agency for Healthcare Research and Quality; 1994: p. 59–70.
12. American College of Rheumatology. Clinical guidance for pediatric patients with multisystem inflammatory syndrome in children (MIS-C) associated with SARS–CoV-2 and hyperinflammation in COVID-19. June 2020. URL: https://www.rheumatology.org/Portals/0/Files/ACR-COVID-19-Clinical-Guidance-Summary-MIS-C-Hyperinflammation.pdf.
13. Belhadjer Z, Meot M, Bajolle F, Khraiche D, Legendre A, Abakka S, et al. Acute heart failure in multisystem inflammatory syndrome in children (MIS-C) in the context of global SARS-CoV-2 pandemic. Circulation 2020;142:429–36.
14. Whittaker E, Bamford A, Kenny J, Kaforou M, Jones CE, Shah P, et al. Clinical characteristics of 58 children with a pediatric inflammatory multisystem syndrome temporally associated with SARS-CoV-2. JAMA 2020;324:259–69.
15. Leon MP, Redzepi A, McGrath E, Abdel-Haq N, Shawaqfeh A, Sethuraman U, et al. COVID-19 associated pediatric multisystem inflammatory syndrome. J Pediatric Infect Dis Soc 2020;9:407–8.
16. Dallan C, Romano F, Siebert J, Politi S, Lacroix L, Sahyoun C. Septic shock presentation in adolescents with COVID-19 [letter]. Lancet Child Adolesc Health 2020;4:e21–3.
17. Capone CA, Subramony A, Sweberg T, Schneider J, Shah S, Rubin L, et al. Characteristics, cardiac involvement, and outcomes of

multisystem inflammatory disease of childhood (MIS-C) associated with SARS-CoV-2 infection. J Pediatr 2020;224:141–5.

18. Licciardi F, Pruccoli G, Denina M, Parodi E, Taglietto M, Rosati S, et al. SARS-CoV-2-induced Kawasaki-like hyperinflammatory syndrome: a novel COVID phenotype in children. Pediatrics 2020;146:e20201711.
19. Feldstein LR, Rose EB, Horwitz SM, Collins JP, Newhams MM, Son MB, et al. Multisystem inflammatory syndrome in US children and adolescents. N Engl J Med 2020;383:334–46.
20. Dufort EM, Koumans EH, Chow EJ, Rosenthal EM, Muse A, Rowlands J, et al. Multisystem inflammatory syndrome in children in New York State. N Engl J Med 2020;383:347–58.
21. Pouletty M, Borocco C, Ouldali N, Caseris M, Basmaci R, Lachaume N, et al. Paediatric multisystem inflammatory syndrome temporally associated with SARS-CoV-2 mimicking Kawasaki disease (Kawa-COVID-19): a multicentre cohort. Ann Rheum Dis 2020;79:999–1006.
22. Kaushik S, Aydin SI, Derespina KR, Bansal PB, Kowalsky S, Trachtman R, et al. Multisystem inflammatory syndrome in children associated with severe acute respiratory syndrome coronavirus 2 infection (MIS-C): a multi-institutional study from New York City. J Pediatr 2020;224:24–9.
23. Hennon TR, Abdul-Aziz R, Alibrahim OS, McGreevy MB, Prout AJ, Schaefer BA, et al. COVID-19 associated multisystem inflammatory syndrome in children (MIS-C) guidelines: a western New York approach. Prog Pediatr Cardiol 2020. E-pub ahead of print.
24. Children's Hospital of Philadelphia. Emergency Department, ICU, and inpatient clinical pathway for evaluation of possible multisystem inflammatory syndrome (MIS-C). May 2020. URL: https://www.chop.edu/clinical-pathway/multisystem-inflammatory-syndrome-mis-c-clinical-pathway.
25. Carlin RF, Fischer AM, Pitkowsky Z, Abel D, Sewell TB, Landau EG, et al. Discriminating MIS-C requiring treatment from common febrile conditions in outpatient settings. J Pediatr 2020. E-pub ahead of print.
26. Abrams JY, Godfred-Cato SE, Oster ME, Chow EJ, Koumans EH, Bryant B, et al. Multisystem inflammatory syndrome in children associated with severe acute respiratory syndrome coronavirus 2: a systematic review. J Pediatr 2020;226:45–54.
27. Grimaud M, Starck J, Levy M, Marais C, Chareyre J, Khraiche D, et al. Acute myocarditis and multisystem inflammatory emerging disease following SARS-CoV-2 infection in critically ill children. Ann Intensive Care 2020;10:69.
28. Dionne A, Mah DY, Son MB, Lee PY, Henderson L, Baker AL, et al. Atrioventricular block in children with multisystem inflammatory syndrome. Pediatr 2020;146:e2020009704.
29. McCrindle BW, Rowley AH, Newburger JW, Burns JC, Bolger AF, Gewitz M, et al. Diagnosis, treatment, and long-term management of Kawasaki disease: a scientific statement for health professionals from the American Heart Association [review]. Circulation 2017;135:e927–99.
30. Colan SD. The why and how of Z scores [editorial]. J Am Soc Echocardiogr 2013;26:38–40.
31. Lopez L, Colan SD, Frommelt PC, Ensing GJ, Kendall K, Younoszai AK, et al. Recommendations for quantification methods during the performance of a pediatric echocardiogram: a report from the Pediatric Measurements Writing Group of the American Society of Echocardiography Pediatric and Congenital Heart Disease Council. J Am Soc Echocardiogr 2010;23:465–95.
32. Yetkin O, Hacievliyagil SS, Gunen H. Assessment of B-type natriuretic peptide in patients with pneumonia. Int J Clin Pract 2008;62:488–91.
33. Melendez E, Whitney JE, Norton JS, Silverman M, Monuteaux MC, Bachur RG. A pilot study of the association of amino-terminal pro-B-type natriuretic peptide and severity of illness in pediatric septic shock. Pediat Crit Care Med 2019;20:e55–60.
34. Lee PY, Day-Lewis M, Henderson LA, Friedman K, Lo J, Roberts JE, et al. Distinct clinical and immunological features of SARS-COV-2-induced multisystem inflammatory syndrome in children. J Clin Invest 2020;130:5942–50.
35. Diorio C, Henrickson SE, Vella LA, McNerney KO, Chase JM, Burudpakdee C, et al. Multisystem inflammatory syndrome in children and COVID-19 are distinct presentations of SARS-CoV-2. J Clin Invest 2020;130:5967–75.
36. Carter MJ, Fish M, Jennings A, Doores KJ, Wellman P, Seow J, et al. Peripheral immunophenotypes in children with multisystem inflammatory syndrome associated with SARS-CoV-2 infection. Nat Med 2020;26:1701–7.
37. Gruber CN, Patel RS, Trachtman R, Lepow L, Amanat F, Krammer F, et al. Mapping systemic inflammation and antibody responses in multisystem inflammatory syndrome in children (MIS-C). Cell 2020;183:982–95.
38. Kawasaki T, Kosaki F, Okawa S, Shigematsu I, Yanagawa H. A new infantile acute febrile mucocutaneous lymph node syndrome (MLNS) prevailing in Japan. Pediatrics 1974;54:271–6.
39. Makino N, Nakamura Y, Yashiro M, Kosami K, Matsubara Y, Ae R, et al. Nationwide epidemiologic survey of Kawasaki disease in Japan, 2015–2016. Pediatr Int 2019;61:397–403.
40. Holman RC, Curns AT, Belay ED, Steiner CA, Schonberger LB. Kawasaki syndrome hospitalizations in the United States, 1997 and 2000. Pediatrics 2003;112:495–501.
41. Son MB, Gauvreau K, Ma L, Baker AL, Sundel RP, Fulton DR, et al. Treatment of Kawasaki disease: analysis of 27 US pediatric hospitals from 2001 to 2006. Pediatrics 2009;124:1–8.
42. Kanegaye JT, Wilder MS, Molkara D, Frazer JR, Pancheri J, Tremoulet AH, et al. Recognition of a Kawasaki disease shock syndrome. Pediatrics 2009;123:e783–9.
43. Newburger JW, Takahashi M, Burns JC, Beiser AS, Chung KJ, Duffy CE, et al. The treatment of Kawasaki syndrome with intravenous gamma globulin. N Engl J Med 1986;315:341–7.
44. Banka P, Robinson JD, Uppu SC, Harris MA, Hasbani K, Lai WW, et al. Cardiovascular magnetic resonance techniques and findings in children with myocarditis: a multicenter retrospective study. J Cardiovasc Magn Reson 2015;17:96.
45. Jonat B, Gorelik M, Boneparth A, Geneslaw AS, Zachariah P, Shah A, et al. Multisystem inflammatory syndrome in children associated with coronavirus disease 2019 in a children's hospital in New York City: patient characteristics and an institutional protocol for evaluation, management, and follow-up. Pediatr Crit Care Med 2020. E-pub ahead of print.
46. Belhadjer Z, Auriau J, Meot M, Oualha M, Renolleau S, Houyel L, et al. Addition of corticosteroids to immune globulins is associated with recovery of cardiac function in multi-inflammatory syndrome in children (MIS-C). Circulation 2020. E-pub ahead of print.
47. Furusho K, Kamiya T, Nakano H, Kiyosawa N, Shinomiya K, Hayashidera T, et al. High-dose intravenous gammaglobulin for Kawasaki disease. Lancet 1984;2:1055–8.
48. Newburger JW, Takahashi M, Gerber MA, Gewitz MH, Tani LY, Burns JC, et al. Diagnosis, treatment, and long-term management of Kawasaki disease: a statement for health professionals from the Committee on Rheumatic Fever, Endocarditis, and Kawasaki Disease, Council on Cardiovascular Disease in the Young, American Heart Association. Pediatrics 2004;114:1708–33.
49. Kociol RD, Cooper LT, Fang JC, Moslehi JJ, Pang PS, Sabe MA, et al. Recognition and initial management of fulminant myocarditis: a scientific statement from the American Heart Association. Circulation 2020;141:e69–92.
50. Dennert R, Velthuis S, Schalla S, Eurlings L, van Suylen RJ, van Paassen P, et al. Intravenous immunoglobulin therapy for patients with idiopathic cardiomyopathy and endomyocardial biopsy-proven high PVB19 viral load. Antivir Ther 2010;15:193–201.
51. Goland S, Czer LS, Siegel RJ, Tabak S, Jordan S, Luthringer D, et al. Intravenous immunoglobulin treatment for acute fulminant

inflammatory cardiomyopathy: series of six patients and review of literature. Can J Cardiol 2008;24:571–4.

52. Yen CY, Hung MC, Wong YC, Chang CY, Lai CC, Wu KG. Role of intravenous immunoglobulin therapy in the survival rate of pediatric patients with acute myocarditis: a systematic review and meta-analysis. Sci Rep 2019;9:10459.
53. Hu H, Ma F, Wei X, Fang Y. Coronavirus fulminant myocarditis saved with glucocorticoid and human immunoglobulin. Eur Heart J 2020. E-pub ahead of print.
54. Kobayashi T, Saji T, Otani T, Takeuchi K, Nakamura T, Arakawa H, et al. Efficacy of immunoglobulin plus prednisolone for prevention of coronary artery abnormalities in severe Kawasaki disease (RAISE study): a randomised, open-label, blinded-endpoints trial. Lancet 2012;379:1613–20.
55. Wardle AJ, Connolly GM, Seager MJ, Tulloh RM. Corticosteroids for the treatment of Kawasaki disease in children [review]. Cochrane Database Syst Rev 2017;1:CD011188.
56. Newburger JW, Sleeper LA, McCrindle BW, Minich LL, Gersony W, Vetter VL, et al. Randomized trial of pulsed corticosteroid therapy for primary treatment of Kawasaki disease. N Engl J Med 2007;356:663–75.
57. Inoue Y, Okada Y, Shinohara M, Kobayashi T, Kobayashi T, Tomomasa T, et al. A multicenter prospective randomized trial of corticosteroids in primary therapy for Kawasaki disease: clinical course and coronary artery outcome. J Pediatr 2006;149:336–41.
58. Ogata S, Ogihara Y, Honda T, Kon S, Akiyama K, Ishii M. Corticosteroid pulse combination therapy for refractory Kawasaki disease: a randomized trial. Pediatrics 2012;129:e17–23.
59. Venkatesh B, Finfer S, Cohen J, Rajbhandari D, Arabi Y, Bellomo R, et al. Adjunctive glucocorticoid therapy in patients with septic shock. N Engl J Med 2018;378:797–808.
60. Quartier P, Allantaz F, Cimaz R, Pillet P, Messiaen C, Bardin C, et al. A multicentre, randomised, double-blind, placebo-controlled trial with the interleukin-1 receptor antagonist anakinra in patients with systemic-onset juvenile idiopathic arthritis (ANAJIS trial). Ann Rheum Dis 2011;70:747–54.
61. Ter Haar NM, van Dijkhuizen EH, Swart JF, van Royen-Kerkhof A, el Idrissi A, Leek AP, et al. Treatment to target using recombinant interleukin-1 receptor antagonist as first-line monotherapy in new-onset systemic juvenile idiopathic arthritis: results from a five-year follow-up study. Arthritis Rheumatol 2019;71:1163–73.
62. Fisher CJ Jr, Dhainaut JF, Opal SM, Pribble JP, Balk RA, Slotman GJ, et al, for the Phase III rhIL-1ra Sepsis Syndrome Study Group. Recombinant human interleukin 1 receptor antagonist in the treatment of patients with sepsis syndrome: results from a randomized, double-blind, placebo-controlled trial. JAMA 1994;271:1836–43.
63. Eloseily EM, Weiser P, Crayne CB, Haines H, Mannion ML, Stoll ML, et al. Benefit of anakinra in treating pediatric secondary hemophagocytic lymphohistiocytosis. Arthritis Rheumatol 2020;72:326–34.
64. Kone-Paut I, Cimaz R, Herberg J, Bates O, Carbasse A, Saulnier JP, et al. The use of interleukin 1 receptor antagonist (anakinra) in Kawasaki disease: a retrospective cases series. Autoimmun Rev 2018;17:768–74.
65. Lind-Holst M, Hartling UB, Christensen AE. High-dose anakinra as treatment for macrophage activation syndrome caused by refractory Kawasaki disease in an infant. BMJ Case Rep 2019;12: e229708.
66. Guillaume MP, Reumaux H, Dubos F. Usefulness and safety of anakinra in refractory Kawasaki disease complicated by coronary artery aneurysm. Cardiol Young 2018;28:739–42.
67. Carsana L, Sonzogni A, Nasr A, Rossi RS, Pellegrinelli A, Zerbi P, et al. Pulmonary post-mortem findings in a series of COVID-19 cases from northern Italy: a two-centre descriptive study. Lancet Infect Dis 2020;20:1135–40.
68. Connors JM, Levy JH. Thromboinflammation and the hypercoagulability of COVID-19. J Thromb Haemost 2020;18:1559–61.
69. Klok FA, Kruip M, van der Meer NJ, Arbous MS, Gommers D, Kant KM, et al. Incidence of thrombotic complications in critically ill ICU patients with COVID-19. Thrombosis Res 2020;191:145–7.
70. Zhou B, She J, Wang Y, Ma X. Venous thrombosis and arteriosclerosis obliterans of lower extremities in a very severe patient with 2019 novel coronavirus disease: a case report. J Thromb Thrombolysis 2020;50:229–32.
71. Friedman KG, Gauvreau K, Hamaoka-Okamoto A, Tang A, Berry E, Tremoulet AH, et al. Coronary artery aneurysms in Kawasaki disease: risk factors for progressive disease and adverse cardiac events in the US population. J Am Heart Assoc 2016;5:e003289.
72. Tsuda E, Tsujii N, Hayama Y. Stenotic lesions and the maximum diameter of coronary artery aneurysms in Kawasaki disease. J Pediatr 2018;194:165–70.
73. Chen K, Williams S, Chan AK, Mondal TK. Thrombosis and embolism in pediatric cardiomyopathy. Blood Coagul Fibrinolysis 2013;24:221–30.
74. Giglia TM, Massicotte MP, Tweddell JS, Barst RJ, Bauman M, Erickson CC, et al. Prevention and treatment of thrombosis in pediatric and congenital heart disease: a scientific statement from the American Heart Association. Circulation 2013;128:2622–703.
75. Parri N, Lenge M, Buonsenso D, for the Coronavirus Infection in Pediatric Emergency Departments Research Group. Children with Covid-19 in pediatric emergency departments in Italy [letter]. N Engl J Med 2020;383:187–90.
76. Lu X, Zhang L, Du H, Zhang J, Li YY, Qu J, et al. SARS-CoV-2 infection in children [letter]. N Engl J Med 2020;382:1663–5.
77. Shekerdemian LS, Mahmood NR, Wolfe KK, Riggs BJ, Ross CE, McKiernan CA, et al. Characteristics and outcomes of children with coronavirus disease 2019 (COVID-19) infection admitted to US and Canadian pediatric intensive care units. JAMA Pediatr 2020;174:868–73.
78. Tagarro A, Epalza C, Santos M, Sanz-Santaeufemia FJ, Otheo E, Moraleda C, et al. Screening and severity of coronavirus disease 2019 (COVID-19) in children in Madrid, Spain [letter]. JAMA Pediatr 2020. E-pub ahead of print.
79. DeBiasi RL, Song X, Delaney M, Bell M, Smith K, Pershad J, et al. Severe COVID-19 in children and young adults in the Washington, DC metropolitan region. J Pediatr 2020;223:199–203.
80. Dong Y, Mo X, Hu Y, Qi X, Jiang F, Jiang Z, et al. Epidemiology of COVID-19 among children in China. Pediatrics 2020;145:e20200702.
81. Brenner EJ, Ungaro RC, Gearry RB, Kaplan GG, Kissous-Hunt M, Lewis JD, et al. Corticosteroids, but not TNF antagonists, are associated with adverse COVID-19 outcomes in patients with inflammatory bowel diseases: results from an international registry. Gastroenterology 2020;159:481–91.
82. Gianfrancesco M, Hyrich KL, Al-Adely S, Carmona L, Danila MI, Gossec L, et al. Characteristics associated with hospitalisation for COVID-19 in people with rheumatic disease: data from the COVID-19 Global Rheumatology Alliance physician-reported registry. Ann Rheum Dis 2020;79:859–66.
83. Marlais M, Wlodkowski T, Vivarelli M, Pape L, Tonshoff B, Schaefer F, et al. The severity of COVID-19 in children on immunosuppressive medication [letter]. Lancet Child Adolesc Health 2020;4:e17–8.
84. Turner D, Huang Y, Martin-de-Carpi J, Aloi M, Focht G, Kang B, et al. Coronavirus disease 2019 and paediatric inflammatory bowel diseases: global experience and provisional guidance (March 2020) from the Paediatric IBD Porto Group of European Society of Paediatric Gastroenterology, Hepatology, and Nutrition. J Pediatr Gastroenterol Nutr 2020;70:727–33.
85. Michelena X, Borrell H, Lopez-Corbeto M, Lopez-Lasanta M, Moreno E, Pascual-Pastor M, et al. Incidence of COVID-19 in a

cohort of adult and paediatric patients with rheumatic diseases treated with targeted biologic and synthetic disease-modifying antirheumatic drugs. Semin Arthritis Rheum 2020;50:564–70.

86. Zhou F, Yu T, Du R, Fan G, Liu Y, Liu Z, et al. Clinical course and risk factors for mortality of adult inpatients with COVID-19 in Wuhan, China: a retrospective cohort study. Lancet 2020; 395:1054–62.
87. Wu C, Chen X, Cai Y, Xia J, Zhou X, Xu S, et al. Risk factors associated with acute respiratory distress syndrome and death in patients with coronavirus disease 2019 pneumonia in Wuhan, China. JAMA Intern Med 2020;180:934–43.
88. Chen G, Wu D, Guo W, Cao Y, Huang D, Wang H, et al. Clinical and immunologic features in severe and moderate coronavirus disease 2019. J Clin Invest 2020;130:2620–9.
89. Huang C, Wang Y, Li X, Ren L, Zhao J, Hu Y, et al. Clinical features of patients infected with 2019 novel coronavirus in Wuhan, China. Lancet 2020;395:497–506.
90. Chao JY, Derespina KR, Herold BC, Goldman DL, Aldrich M, Weingarten J, et al. Clinical characteristics and outcomes of hospitalized and critically ill children and adolescents with coronavirus disease 2019 (COVID-19) at a tertiary care medical center in New York City. J Pediatr 2020;223:14–9.
91. Villar J, Ferrando C, Martinez D, Ambros A, Munoz T, Soler JA, et al. Dexamethasone treatment for the acute respiratory distress syndrome: a multicentre, randomised controlled trial. Lancet Respir Med 2020;8:267–76.
92. Seam N, Meduri GU, Wang H, Nylen ES, Sun J, Schultz MJ, et al. Effects of methylprednisolone infusion on markers of inflammation, coagulation, and angiogenesis in early acute respiratory distress syndrome. Crit Care Med 2012;40:495–501.
93. Yehya N, Servaes S, Thomas NJ, Nadkarni VM, Srinivasan V. Corticosteroid exposure in pediatric acute respiratory distress syndrome. Intensive Care Med 2015;41:1658–66.
94. Ni YN, Chen G, Sun J, Liang BM, Liang ZA. The effect of corticosteroids on mortality of patients with influenza pneumonia: a systematic review and meta-analysis. Crit Care 2019;23:99.
95. Lansbury LE, Rodrigo C, Leonardi-Bee J, Nguyen-van-Tam J, Lim WS. Corticosteroids as adjunctive therapy in the treatment of influenza: an updated Cochrane systematic review and meta-analysis. Crit Care Med 2020;48:e98–106.
96. Cao B, Gao H, Zhou B, Deng X, Hu C, Deng C, et al. Adjuvant corticosteroid treatment in adults with influenza A (H7N9) viral pneumonia. Crit Care Med 2016;44:e318–28.
97. Lee N, Chan KC, Hui DS, Ng EK, Wu A, Chiu RW, et al. Effects of early corticosteroid treatment on plasma SARS-associated Coronavirus RNA concentrations in adult patients. J Clin Virol 2004;31:304–9.
98. Yang T, Li Z, Jiang L, Xi X. Corticosteroid use and intensive care unit-acquired weakness: a systematic review and meta-analysis. Crit Care 2018;22:187.
99. Ling Y, Xu SB, Lin YX, Tian D, Zhu ZQ, Dai FH, et al. Persistence and clearance of viral RNA in 2019 novel coronavirus disease rehabilitation patients. Chin Med J (Engl) 2020;133:1039–43.
100. Fang X, Mei Q, Yang T, Li L, Wang Y, Tong F, et al. Low-dose corticosteroid therapy does not delay viral clearance in patients with COVID-19. J Infect 2020;81:147–78.
101. Fadel R, Morrison AR, Vahia A, Smith ZR, Chaudhry Z, Bhargava P, et al. Early short course corticosteroids in hospitalized patients with COVID-19. Clin Infect Dis 2020;71:2114–20.
102. Horby P, Lim WS, Emberson J, Mafham M, Bell J, Linsell L, et al. Dexamethasone in hospitalized patients with COVID-19: preliminary report. N Engl J Med 2020. E-pub ahead of print.
103. Sterne JA, Murthy S, Diaz JV, Slutsky AS, Villar J, Angus DC, et al, on behalf of the WHO Rapid Evidence Appraisal for COVID-19 Therapies (REACT) Working Group. Association between administration of systemic corticosteroids and mortality among critically ill patients with COVID-19: a meta-analysis. JAMA 2020;324:1330–41.
104. Shakoory B, Carcillo JA, Chatham WW, Amdur RL, Zhao H, Dinarello CA, et al. Interleukin-1 receptor blockade is associated with reduced mortality in sepsis patients with features of macrophage activation syndrome: reanalysis of a prior phase III trial. Crit Care Med 2016;44:275–81.
105. Franzetti M, Pozzetti U, Carugati M, Pandolfo A, Molteni C, Faccioli P, et al. Interleukin-1 receptor antagonist anakinra in association with remdesivir in severe coronavirus disease 2019: a case report. Int J Infect Dis 2020;97:215–8.
106. Filocamo G, Mangioni D, Tagliabue P, Aliberti S, Costantino G, Minoia F, et al. Use of anakinra in severe COVID-19: a case report. Int J Infect Dis 2020;96:607–9.
107. Dimopoulos G, de Mast Q, Markou N, Theodorakopoulou M, Komnos A, Mouktaroudi M, et al. Favorable anakinra responses in severe covid-19 patients with secondary hemophagocytic lymphohistiocytosis. Cell Host Microbe 2020;28:117–123.
108. Aouba A, Baldolli A, Geffray L, Verdon R, Bergot E, Martin-Silva N, et al. Targeting the inflammatory cascade with anakinra in moderate to severe COVID-19 pneumonia: case series [letter]. Ann Rheum Dis 2020;79:1381–2.
109. Pontali E, Volpi S, Antonucci G, Castellaneta M, Buzzi D, Tricerri F, et al. Safety and efficacy of early high-dose IV anakinra in severe COVID-19 lung disease [letter]. J Allergy Clin Immunol 2020;136:213–5.
110. Cavalli G, de Luca G, Campochiaro C, Della-Torre E, Ripa M, Canetti D, et al. Interleukin-1 blockade with high-dose anakinra in patients with COVID-19, acute respiratory distress syndrome, and hyperinflammation: a retrospective cohort study. Lancet Rheumatol 2020;2:e325–31.
111. Huet T, Beaussier H, Voisin O, Jouveshomme S, Dauriat G, Lazareth I, et al. Anakinra for severe forms of COVID-19: a cohort study. Lancet Rheumatol 2020;2:e393–400.
112. Luo P, Liu Y, Qiu L, Liu X, Liu D, Li J. Tocilizumab treatment in COVID-19: a single center experience. J Med Virol 2020;92:814–8.
113. Xu X, Han M, Li T, Sun W, Wang D, Fu B, et al. Effective treatment of severe COVID-19 patients with tocilizumab. Proc Natl Acad Sci U S A 2020;117:10970–5.
114. Morena V, Milazzo L, Oreni L, Bestetti G, Fossali T, Bassoli C, et al. Off-label use of tocilizumab for the treatment of SARS-CoV-2 pneumonia in Milan, Italy. Eur J Intern Med 2020;76:36–42.
115. Toniati P, Piva S, Cattalini M, Garrafa E, Regola F, Castelli F, et al. Tocilizumab for the treatment of severe COVID-19 pneumonia with hyperinflammatory syndrome and acute respiratory failure: a single center study of 100 patients in Brescia, Italy [review]. Autoimmun Rev 2020;19:102568.
116. Capra R, de Rossi N, Mattioli F, Romanelli G, Scarpazza C, Sormani MP, et al. Impact of low dose tocilizumab on mortality rate in patients with COVID-19 related pneumonia. Eur J Intern Med 2020;76:31–5.
117. Colaneri M, Bogliolo L, Valsecchi P, Sacchi P, Zuccaro V, Brandolino F, et al. Tocilizumab for treatment of severe COVID-19 patients: preliminary results from SMAtteo COvid19 REgistry (SMACORE). Microorganisms 2020;8:695.
118. Stone JH, Frigault MJ, Serling-Boyd NJ, Fernandes AD, Harvey L, Foulkes AS, et al. Efficacy of tocilizumab in patients hospitalized with Covid-19. N Engl J Med 2020. E-pub ahead of print.
119. Hermine O, Mariette X, Tharaux PL, Resche-Rigon M, Porcher R, Ravaud P, et al. Effect of tocilizumab vs usual care in adults hospitalized with COVID-19 and moderate or severe pneumonia: a randomized clinical trial. JAMA Intern Med 2020. E-pub ahead of print.